Carina Isabel Coelho Proença

Assessment of the antidiabetic activity of flavonoids: targeting key enzymes involved in type 2 diabetes pathophysiology

Tese do 3º Ciclo de Estudos Conducente ao Grau de Doutoramento em Ciências Farmacêuticas na Especialidade de Química Farmacêutica e Medicinal apresentada à Faculdade de Farmácia da Universidade do Porto

Trabalho realizado sob a orientação de:

Professora Doutora Eduarda Fernandes
Laboratório de Química Aplicada, Departamento de Ciências Químicas, Faculdade de Farmácia da Universidade do Porto

Professor Doutor Artur Silva
Departamento de Química, Universidade de Aveiro

Professor Doutor Pedro Fernandes
Departamento de Química e Bioquímica, Faculdade de Ciências da Universidade do Porto

abril de 2021

É AUTORIZADA A REPRODUÇÃO INTEGRAL DESTA TESE APENAS PARA EFEITOS DE INVESTIGAÇÃO, MEDIANTE DECLARAÇÃO ESCRITA DO INTERESSADO, QUE A TAL SE COMPROMETE.

Assinatura da autora,



“Remember to look up at the stars and not down at your feet”

Stephen Hawking

AGRADECIMENTOS

Sinto que ao fim destes quatro anos me tornei uma pessoa mais forte, mais madura e sobretudo mais confiante nas minhas capacidades. Foram várias as pessoas que estiveram presentes durante esta trajetória, e que contribuíram para que este duro (mas também gratificante) percurso se tornasse mais fácil. Sei que será impossível mencionar aqui todas essas pessoas, mas existem aquelas a quem eu não poderia de forma alguma deixar de agradecer:

À Professora Eduarda, a minha "mãe científica". Desde o primeiro dia em que entrei no seu gabinete, senti uma ligação imediata. Uma das primeiras coisas que me disse foi que o mais importante seria sermos felizes naquilo que fazemos. E eu sempre fui muito feliz a trabalhar na FRAU, sob a sua orientação. Mesmo nos momentos de desânimo e de cansaço, pude sempre contar com o seu apoio e conforto. Agradeço até os "puxões de orelhas", sempre certeiros e que me fizeram crescer e olhar para as situações de uma perspectiva diferente. Na verdade, o gabinete da Professora Eduarda foi muitas vezes palco de alegrias, conquistas, amizade e desabafos. A sua preocupação com todos os elementos do grupo é um grande alento para nos esforçarmos todos os dias a ser melhores. Não poderia deixar de salientar ainda a admiração que tenho pelo seu mérito científico, já mais que comprovado. O seu rigor e experiência, assim como a sua exigência, permitiram que aprendesse muito e desenvolvesse bastante o meu espírito crítico para que me tornasse cada vez mais autónoma. Gostaria ainda de referir que a Professora Eduarda colocou sempre à disposição todos os meios, recursos, equipamentos e reagentes necessários à realização desta tese. O seu apoio e incentivo na participação em congressos científicos nacionais e internacionais foram igualmente de enorme valor para o meu desenvolvimento na ciência. Por todos estes motivos, nunca me esquecerei de tudo o que fez por mim e pelo meu trabalho ao longo destes anos.

Ao Professor Artur Silva e ao Professor Pedro Fernandes, meus co-orientadores, agradeço pela constante disponibilidade e acompanhamento neste meu percurso. Agradeço ao Professor Artur e aos elementos do seu grupo, Sara Tomé e Joana Sousa, por providenciarem os compostos de síntese necessários à realização dos trabalhos experimentais. Agradeço também ao Professor Pedro Fernandes, assim como ao Eduardo, à Ana e à Matilde, o desenvolvimento e realização dos estudos in silico presentes nesta tese.

Ao Professor Félix Carvalho, pelo seu grande rigor e exigência científica, que em muito contribuíram para a evolução deste trabalho. Os conhecimentos transmitidos foram de grande importância para o meu crescimento científico. Não poderia deixar de referir as suas preciosas críticas às figuras realizadas para a tese, ajudando a que o resultado final fosse sempre o melhor possível.

Ao Professor Alberto Araújo, pelo seu auxílio na análise dos resultados das cinéticas enzimáticas. Agradeço pelas suas ideias inovadoras e disponibilidade constante na resolução de problemas, quer a nível de trabalho experimental quer a nível de esclarecimentos acerca do curso de Doutoramento em Ciências Farmacêuticas, do qual é diretor. Aproveito também para agradecer o seu apoio incansável na melhoria contínua de todos os aspetos relacionados ao Laboratório de Química Aplicada, do qual é responsável.

À Engenheira Manuela Barros e à Vânia Dias, agradeço pela boa disposição, simpatia, disponibilidade e esforço constante em satisfazerem os meus pedidos, assim como os do grupo FRAU. Não posso deixar de salientar o papel essencial que desempenham para o bom funcionamento do Laboratório de Química Aplicada. E não menos importante, o vosso bom humor, assim como a amizade que têm com todos os elementos, certamente contribuem para o bom ambiente do Laboratório.

Às enfermeiras e dadores de sangue do Centro Hospitalar Universitário do Porto, agradeço a ajuda e esforço na disponibilização de amostras, tão importantes para a realização de trabalhos experimentais efetuados para esta tese.

À Marisa e à Daniela, presenças constantes desde o primeiro instante em que tive o privilégio de integrar a FRAU. Receberam-me de "braços abertos" e foram sempre um pilar de apoio e aconchego. Com elas tive a oportunidade de aprender a ser melhor, quer na ciência quer como pessoa. Nunca me faltou uma palavra amiga e de incentivo, ou até um precioso momento de descontração na vossa companhia, para retomar o trabalho com mais força e ainda mais vontade. Sei que estarão sempre por cá para me aconselhar e discutir ciência com opiniões válidas e assertivas. Não me posso esquecer dos bons momentos passados e das confidências trocadas nas nossas viagens a congressos. Espero que possamos renovar memórias daqui para a frente. Um sincero e sentido muito obrigada.

Aos meus queridos colegas da FRAU: Miguel, Sónia, Adelaide, Mariane e Ana. Estas curtas palavras nunca serão suficientes para vos demonstrar o apreço e carinho que tenho por cada um de vocês. Vocês são uma das razões para que eu vá todos os dias para o laboratório com um sorriso no rosto. Sinto que o laço que nos une é tão forte... Tenho muita sorte por passar grande parte dos meus dias com pessoas tão boas, competentes e com tanta capacidade de trabalho. Não vejo a hora que acabe esta pandemia para que possamos trocar abraços e festejar com um merecido almoço de sushi...no restaurante.

À Sílvia, por todos os momentos de grande amizade. Juntas já passámos por tanto e por tantas ocasiões surreais que já lhes perdi a conta! Obrigada por estares comigo sempre, quer nas horas de alegria quer nas de desânimo. Não poderia pensar em melhor pessoa para partilhar cada confidência, lágrimas ou risos. Sabes que estarás sempre no meu coração, e

és das pessoas mais lutadoras, bondosas, genuínas e fortes que conheço. Tornaste-te uma umas das minhas melhores amigas, e sei que te levarei comigo para a vida.

À Liliana, por seres tão generosa e tão preocupada comigo. Mesmo no teus momentos mais difíceis, como foram estes últimos. Sempre fizeste de tudo para me fazer sentir melhor e esquecer os problemas. Sou privilegiada por ter uma amiga tão especial e honesta. Que esta amizade, já de tanto tempo, continue por muitos e muitos anos.

Aos meus amigos David, Ricardo, Daniela e Raquel. Amizades de longa data, e embora não tenhamos a disponibilidade para estarmos muitas vezes juntos, sei que posso contar convosco para o que for. Por vezes, uma simples chamada ou mensagem é tão importante e sabe tão bem. Às minhas primas do coração, Andreia, Catarina, Rita, Juliana e Ana. Cada uma à sua maneira me traz à memória momentos tão felizes durante esta caminhada!! Sei que cada instante que passo com cada uma de vocês é precioso.

À minha irmã, Anaïs, por seres uma das minhas pessoas favoritas. É tão raro ter uma conexão assim com alguém... As nossas conversas são quase telepáticas. És sem dúvida a pessoa que melhor me conhece. Obrigada por teres acrescentado tanto à minha vida desde o dia em que nasceste. Pelo amor, compreensão, companheirismo e até pelas discussões que terminam sempre em gargalhadas.

Aos meus pais, sem dúvida as pessoas mais importantes da minha vida. Agradeço pelo amor incondicional, apoio, aconchego e pelo enorme esforço que fizeram para que eu e a Anaïs tivéssemos a oportunidade de estudar. Obrigada por me transmitirem valores e educação tão importantes e valiosos. Obrigada por me mostrarem que o trabalho e o esforço depositado em tudo o que fazemos são imprescindíveis para o sucesso. É a vocês que devo tudo aquilo que sou hoje.

À memória dos meus avós, que infelizmente já partiram. Sempre fizeram questão de demonstrar o orgulho que têm em mim. Pois eu tenho muito orgulho por terem sido meus avós e pela vossa história de sacrifício e superação.

Agradeço ainda à Faculdade de Farmácia da Universidade do Porto, por me ter aceitado como estudante de Doutoramento. À FCT (Fundação para a Ciência e Tecnologia) e ao Fundo Social Europeu (FSE) através do programa POCH (Programa Opercional Capital Humano) agradeço o financiamento da bolsa de Doutoramento que me foi concedida (ref. SFRH/BD/116005/2016). Agradeço o apoio financeiro de fundos nacionais (FCT/MEC, Fundação para a Ciência e Tecnologia e Ministério da Educação e Ciência) no âmbito do financiamento UIDB/50006/2020, e da União Europeia (fundos FEDER através do COMPETE2020 POCI-01-0145-FEDER-029241) e de fundos nacionais (FCT) através do projeto PTDC/MED-QUI/29241/2017.


FCT
Fundação para a Ciência e a Tecnologia
MINISTÉRIO DA CIÊNCIA, TECNOLOGIA E ENSINO SUPERIOR




REPÚBLICA
PORTUGUESA


POCH


NORTE2020
PROGRAMA OPERACIONAL REGIONAL DO NORTE


COMPETE
2020


PORTUGAL
2020

ABSTRACT

Type 2 diabetes (T2D) is the most common form of diabetes (90 - 95 % of all cases), and encompasses individuals who have relative insulin deficiency and peripheral insulin resistance. The last decades have witnessed the introduction of many different classes of drugs to treat diabetes, with variable efficacy and side effects. The drug discovery process is therefore of extreme importance for the identification of new targets or molecules for the development of safer and effective agents for the treatment of this disease. Flavonoids have been explored as promising alternatives for both prevention and management of T2D, and as scaffolds for the synthesis and development of more potent and efficient antidiabetic drugs. As such, the work developed in the present PhD thesis aims to extend and rationalize the current knowledge on the alleged antidiabetic properties of flavonoids, either in targets already established in clinical practice or in other promising targets for the T2D therapy.

The first approach was based on the study of the inhibitory activity of a group of flavonoids against the carbohydrate hydrolysing enzyme, α-glucosidase. Inhibitory kinetic analysis and molecular docking calculations were applied for the most active compounds. It can be deduced by the most active flavonoid found (a competitive inhibitor), that the hydroxylation at 3-position of C ring, at 3'- and 4'-positions of B ring, and at 7- and 8-positions of A ring, is favourable for the intended effect.

Following the previous study, the second work was based on the *in vitro* evaluation of the modulation of α-amylase by flavonoids, with an inhibitory kinetic analysis and molecular docking calculations being performed for the most active molecules. By analysing the structure of the most effective flavonoid (a competitive inhibitor), it seems that besides the presence of hydroxyl groups at 3'- and 4'-positions of B ring and at 5- and 7-positions of A ring, the chlorine ion at 3-position of C ring has an important role for the inhibition of α-amylase.

In the third approach of this thesis, the inhibitory effect of flavonoids on protein tyrosine phosphatase 1B (PTP1B) was studied. PTP1B has emerged as a key negative regulator of insulin signalling pathway that leads to insulin resistance, making this enzyme a promising therapeutic target for the treatment of T2D. The most potent flavonoid, a mixed inhibitor, showed that the presence of methoxy and benzyloxy groups at A or B rings, as well as the presence of a hydroxyl group at 3-position of C ring, is beneficial for the inhibitory activity of flavonoids against PTP1B.

In the fourth work, the assessment of the inhibition of dipeptidyl peptidase-4 (DPP-4) by flavonoids was performed by *in vitro* and *ex vivo* approaches. Through the fluorometric method, and by the analysis of the best inhibitor (a noncompetitive inhibitor) it was possible

to observe that the hydroxylation at 3-position of C ring and at 5- and 7-positions of A ring, and especially the methoxylation at 3'- and 4´-positions of B ring are beneficial in what concerns the inhibitory activity against DPP-4. Subsequently, the most active flavonoids were tested in human blood and plasma, and interestingly did not show any inhibitory activity against DPP-4. Through the determination of plasma protein binding, it appears that the DPP-4 inhibition by flavonoids is hindered in blood and plasma matrices due to protein binding.

The fifth approach of this thesis concerned the inhibitory activity of flavonoids against fructose 1,6-bisphosphatase (FBPase), a well-known regulatory enzyme of the gluconeogenesis pathway, which has emerged as a valid therapeutic target to control hyperglycaemia. In sequence of the *in vitro* study, seven flavonoids were selected and evaluated by molecular dynamics simulations. The obtained result showed that the presence of hydroxy groups at A ring, in special at 5-, 7- and 8-positions, has an important role for the increase of FBPase inhibition. In addition, the hydroxylation at 3-position of C ring, and at 4'-position of B ring also showed to be favourable for this specific biological activity.

Finally, the α-glucosidase inhibition by flavonoids was studied in Caco-2/TC7 cellular model, through the assessment of the inhibition of sucrase-isomaltase. The selected group of flavonoids demonstrated promising inhibitory activity against both sucrase and maltase. The presence of -OH groups at 3-position of C ring, at 3'- and 4'-positions of B ring, and at 7- and 8-positions of A ring, seems to be highly favourable for the inhibition of this carbohydrate-hydrolysing enzyme.

The experimental studies performed in the present thesis allowed to conclude that different substituents present in the chemical structure of flavonoids are required to increase the inhibition of each target under study. This means that the antidiabetic effect of flavonoids should be selected according to the enzyme we intend to inhibit. Some flavonoid scaffolds showed a promising antidiabetic effect via a specific enzyme modulation, and their potential as alternative drugs to be used in the management of T2D should be explored. In this thesis, important conclusions were drawn for a better and deeper knowledge (through the establishment of the structure-activity relationship), in what concerns the synthesis and development of new molecules with improved antidiabetic activity.

Keywords: Type 2 diabetes; flavonoids; enzymatic targets; structure-activity relationship.

RESUMO

A diabetes tipo 2 (DT2) é a forma mais comum de diabetes (90 - 95% de todos os casos), e engloba indivíduos com deficiência relativa de insulina e resistência periférica à insulina. As últimas décadas testemunharam a introdução de várias classes diferentes de medicamentos para tratar a diabetes, com graus de eficácia e efeitos secundários variáveis. O processo de descoberta de fármacos baseado é assim de extrema importância na identificação de novos alvos ou moléculas para o desenvolvimento de agentes mais seguros e eficazes para o tratamento desta doença. Os flavonoides têm sido explorados como alternativas promissoras tanto para a prevenção como para o tratamento da DT2, e como modelos para a síntese e desenvolvimento de agentes antidiabéticos mais potentes e eficazes. Deste modo, o trabalho desenvolvido na presente tese de doutoramento visa alargar e racionalizar os conhecimentos atuais acerca das potenciais propriedades antidiabéticas dos flavonoides, quer em alvos já estabelecidos na prática clínica, quer em outros alvos promissores para a terapia da DT2.

A primeira abordagem baseou-se no estudo da capacidade de inibição de uma enzima responsável pela hidrólise de hidratos de carbono, a α-glicosidase, por um grupo de flavonoides. Foram aplicadas análises de inibição cinética e cálculos de acoplamento molecular para os compostos mais ativos. Pode deduzir-se, através do flavonoide mais ativo testado (um inibidor competitivo), que a hidroxilação na posição 3 do anel C, nas posições 3' e 4' do anel B, e nas posições 7 e 8 do anel A, é favorável para o efeito pretendido.

Na sequência do estudo anterior, o segundo trabalho baseou-se na avaliação *in vitro* da modulação da α-amilase por flavonoides, com uma análise de inibição cinética e cálculos de acoplamento molecular a serem realizados para as moléculas mais ativas. Analisando a estrutura do flavonoide mais eficaz (um inibidor competitivo), parece que para além da presença de grupos hidroxilo nas posições 3' e 4' do anel B e nas posições 5 e 7 do anel A, o substituinte cloro na posição 3 do anel C tem um papel importante para a inibição da α-amilase.

Na terceira abordagem desta tese, foi estudado o efeito inibitório dos flavonoides na proteína tirosina fosfatase 1B (PTF1B). A PTF1B emergiu como um regulador negativo da via de sinalização da insulina que conduz à resistência à insulina, tornando esta enzima num alvo terapêutico promissor para o tratamento da DT2. O flavonoide mais potente, um inibidor misto, demonstrou que a presença de grupos metoxilo e benziloxilo nos anéis A ou B, bem como a presença de um grupo hidroxilo na posição 3 do anel C, é benéfica para a inibição da PTF1B por flavonoides.

No quarto trabalho foi realizada a avaliação da inibição *in vivo* e *ex vivo* da enzima dipeptidil peptidase-4 (DPP-4) por flavonoides. Recorrendo a um método fluorimétrico com a enzima isolada, e pelo estudo do melhor inibidor (inibidor não competitivo) foi possível observar que a hidroxilação na posição 3 do anel C e nas posições 5 e 7 do anel A, e especialmente a metoxilação nas posições 3' e 4' do anel B são favoráveis no que diz respeito à inibição da DPP-4. Subsequentemente, os flavonoides mais ativos foram testados em sangue e plasma humanos, e, curiosamente, não demosntraram ter a capacidade de inibir DPP-4. Através da determinação da ligação das proteínas plasmáticas, a inibição da DPP-4 por flavonoides é possivelmente dificultada no sangue e nas matrizes plasmáticas devido à sua ligação às proteínas.

A quinta abordagem desta tese é focada na atividade inibitória de flavonoides na frutose 1,6-bisfosfatase (FBFase), uma conhecida enzima reguladora da via da gluconeogénese, que surgiu como um alvo terapêutico válido para controlar a hiperglicemia. Na sequência do estudo *in vitro*, sete flavonoides foram seleccionados e avaliados através de simulações de dinâmica molecular. Os resultados obtidos demonstraram que a presença de grupos hidroxilo no anel A, em especial nas posições 5, 7 e 8, tem um papel importante na inibição da FBFase. Adicionalmente, a hidroxilação na posição 3 do anel C, e na posição 4' do anel B também mostrou ser favorável a esta atividade biológica específica.

Finalmente, a inibição da α-glucosidase por flavonoides foi estudada usando Caco-2/TC7 como modelo celular, através da avaliação da inibição da sacarase-isomaltase. O grupo seleccionado de flavonoides demonstrou uma actividade inibitória promissora tanto na sacarase como na maltase. A presença dos grupos -OH na posição 3 do anel C, nas posições 3' e 4' do anel B, e nas posições 7 e 8 do anel A, parece ser bastante favorável à inibição desta enzima metabolizadora de hidratos de carbono.

Os estudos experimentais realizados nesta tese permitiram concluir que diferentes substituintes presentes na estrutura química dos flavonoides são necessários para aumentar a inibição de cada alvo em estudo. Isto significa que o efeito antidiabético dos flavonoides deve ser seleccionado de acordo com a enzima que pretendemos inibir. Alguns flavonoides demonstraram um efeito antidiabético promissor através de uma modulação enzimática específica, e o seu potencial como agentes alternativos a serem utilizados no tratamento da DT2 deve ser explorado. Nesta tese, obtiveram-se conclusões importantes para um maior conhecimento (através do estabelecimento da relação estrutura-atividade), no que diz respeito à síntese e desenvolvimento de novas moléculas com maior atividade antidiabética.

Palavras-chave: diabetes tipo 2; flavonoides; alvos enzimáticos; relação estrutura-atividade.

INDEX

AGRADECIMENTOS V

ABSTRACT IX

RESUMO XI

INDEX XIII

INDEX OF FIGURES XIV

INDEX OF TABLES XVIII

ABBREVIATIONS AND CHEMICAL SYMBOLS XXVIII

OUTLINE OF THE THESIS XXXIV

CHAPTER I. GENERAL INTRODUCTION 1

I.1. THEORETICAL BACKGROUND 1
I.1.1. Diabetes mellitus 1
I.1.2. Flavonoids as potential agents in the management of type 2 diabetes through the modulation of α-amylase and α-glucosidase activity: a review 24
I.1.3. A comprehensive review on the antidiabetic activity of flavonoids targeting PTP1B and DPP-4: a structure-activity relationship analysis 96
I.2. GENERAL AND SPECIFIC OBJECTIVES OF THE THESIS 154

CHAPTER II. ORIGINAL RESEARCH 1

II.1. A-GLUCOSIDASE INHIBITION BY FLAVONOIDS: AN *IN VITRO* AND *IN SILICO* STRUCTURE-ACTIVITY RELATIONSHIP STUDY 1
II.2. EVALUATION OF A FLAVONOIDS LIBRARY FOR INHIBITION OF PANCREATIC A-AMYLASE TOWARDS A STRUCTURE-ACTIVITY RELATIONSHIP 15
II.3. INHIBITION OF PROTEIN TYROSINE PHOSPHATASE 1B BY FLAVONOIDS: A STRUCTURE-ACTIVITY RELATIONSHIP STUDY 28
II.4. THE DIPEPTIDYL PEPTIDASE-4 INHIBITORY EFFECT OF FLAVONOIDS IS HINDERED IN PROTEIN RICH ENVIRONMENTS 37
II.5. STRUCTURAL SPECIFICITY OF FLAVONOIDS IN THE INHIBITION OF HUMAN FRUCTOSE 1,6-BISPHOSPHATASE 52
II.6. DEVELOPMENT OF A HUMAN SUCRASE-ISOMALTASE (A-GLUCOSIDASE) *IN VITRO* ASSAY IN CACO-2/TC7 CELLS, AND PROOF OF CONCEPT WITH THE INHIBITORY ACTIVITY OF FLAVONOIDS 65

CHAPTER III. DISCUSSION AND CONCLUSIONS 1

III.1. INTEGRATED DISCUSSION 1
III.2. CONCLUSIONS 11
III.3. FUTURE PERSPECTIVES 13
III.4. REFERENCES 14

INDEX OF FIGURES

CHAPTER I. General Information

I.1.1.

Figure 1. Schematic illustration depicting major signalling inputs in pancreatic β-cells....4

Figure 2. Chemical structure of metformin.....7

Figure 3. Chemical substructures of examples of 1st (chloropropamide, tolazamide and tolbutamide) and 2nd generation (glipizide, glimepiride and glyburide) sulfonylureas.....9

Figure 4. Chemical structures of examples of meglitinide: repaglinide and nateglinide...10

Figure 5. Chemical structures of examples of thiazolidinediones: rosiglitazone and pioglitazone.....11

Figure 6. Chemical structures of examples of DPP-4 inhibitors: sitagliptin, vildagliptin, saxagliptin, linagliptin and alogliptin.....13

Figure 7. Chemical structures of examples of SGLT2 inhibitors: canagliflozin, dapagliflozin and empagliflozin.....14

Figure 8. Chemical structures of examples of α-glucosidase inhibitors.....16

I.1.2.

Figure 1. Schematic representation of the hydrolysing α-glucosidases: maltase-glucoamylase (MGAM) and sucrase-isomaltase (SI).....29

Figure 2. Mechanism of action of α-amylase and α-glucosidase.....30

Figure 3. Basic chemical structure of flavonoids.....31

Figure 4. Schematic literature research methodology used in this review.....33

Figure 5. Representation of the possible substitutions that affect the inhibitory activity of flavonoids on α-amylase.....89

Figure 6. Representation of the possible substitutions that affect the inhibitory activity of flavonoids on α-glucosidase.....89

I.1.3.

Figure 1. Basic chemical structure of flavonoids and their subclasses: flavones, flavonols, biflavonoids, flavanones, isoflavones, isoflavanones, flavans, isoflavans and anthocyanidins.....98

Figure 2. Negative regulation of protein tyrosine phosphatase 1B (PTP1B) in insulin signalling pathway, through inhibition of insulin receptor (IR) and insulin receptor substrates (IRS).....100

Figure 3. Chemical structures of PTP1B inhibitors ertiprotafib, trodusquemine and JTT-551.....101

Figure 4. Mechanism of action of dipeptidyl peptidase-4 (DPP-4).....102

Figure 5. Scheme of literature search.....106

Figure 6. Chemical features of flavonoids that increase or decrease the inhibition of PTP1B.....147

Figure 7. Chemical features of flavonoids that increase or decrease the inhibition of DPP-4.....148

II.1

Figure 1. Chemical structures of the tested flavonoids.....4

Figure 2. Lineweaver-Burk double reciprocal plots of α-glucosidase inhibition by **A5** (A), **B3** (B), **C7** (C), **D8** (quercetin) (D), **D10** (E), **E3** (taxifolin) (F) and **acarbose** (G).....8

Figure 3. Predicted binding mode for **acarbose** (A) and flavones **A5** (B), **B1** and **B3** (C), **C7** (D), **D8** (quercetin) (E), **D10** (F) and **E3** (taxifolin) (G).....9

Figure 4. Potential flavonoids' substitution pattern that contributes to increase the α-glucosidase inhibition.....12

II.2.

Figure 1. Schematic representation of the pancreatic α-amylase and α-glucosidase activity.....17

Figure 2. Chemical structures of the studied flavonoids.....18

Figure 3. Predicted binding mode for **acarbose**.....22

Figure 4. (A) Predicted binding mode of flavonoid **A5**, occupying the -2 and -1 subsites with the more hydrophobic A-ring on the -2 subsite interacting with Leu162 and Val163. (B) the predicted binding mode for **B4** shows the C-ring carbonyl and A-ring hydroxyl hydrogen bonded to the catalytic residues Glu233, Asp300 and His299.....22

Figure 5. (A) The binding mode predicted for **C5** shows the C-ring carbonyl and –OH group interacting with the active site residues in a similar way as in **B4**. This requires the B-ring to be placed in the –1/–2 subsites, stabilized mostly by hydrophobic interactions with Tyr62, Val163 and Leu165. (B) The best tested inhibitor, flavonoid **D11**, and flavonoid **B4** binds very similarly to a-amylase. The most important difference seems to come from the 3–Cl substitution that interacts with Ile235 and Phe256.....23

Figure 6. Potential substitution pattern of flavonoids contributing to the improvement of α-amylase inhibition.....25

II.3.

Figure 1. Negative regulation of insulin signaling pathway by PTP1B.....30

Figure 2. Chemical structures of the tested flavonoids.....31

Figure 3. Lineweaver-Burk double reciprocal plots of PTP1B inhibition by flavonoids **C13** (A), morin (**D8**) (B) and the positive control, **ursolic acid** (C).....33

Figure 4. Potential pattern substitution of flavonoids that contributes to increase PTP1B inhibition.....35

II.4.

Figure 1. Schematic representation of the dipeptidyl peptidase-4 (DPP-4) monomer bound to the cell membrane.....39

Figure 2. Metabolic pathway of the dipeptidyl peptidase-4 (DPP-4).....39

Figure 3. Chemical structures of the DPP-4 inhibitors applied in the treatment of T2D....40

Figure 4. Chemical structures of the tested flavonoids.....41

II.5.

Figure 1. Gluconeogenesis process.....54

Figure 2. Chemical structures of the studied flavonoids.....55

Figure 3. Predominant interactions observed along the MD trajectories for the selected flavonoids.....59

Flavonoid 4. Potential flavonoid substituents that contribute to increase FBPase inhibition.....61

II.6.

Figure 1. Chemical structure of the studied flavonoids.....70

Figure 2. Viability (ability to reduce MTT) of Caco-2/TC7 cells treated with different concentrations of flavonoids.....75

Figure 3. Detection of human sucrase-isomaltase (SI) enzyme by western blot.....76

Figure 4. Optimization of assay parameters in Caco-2/TC7 cell extracts, using sucrose (green) and maltose (red) as substrates: dependence of added protein [A] [B], added substrate [C] [D] and time [E] [F].....77

Figure 5. Optimization of assay parameters in Caco-2/TC7 cells extracts, using *p*NPG as substrate: dependence of added protein [A], added substrate [B] and time [C].....79

III.1

Figure 1: Substitution pattern of the flavonoid that presented the best inhibitory activity against α-glucosidase, α-amylase, PTP1B, DPP-4 and FBPase.....9

INDEX OF TABLES

I.1.2.

Table 1. Available antidiabetic agents: examples, route of administration, mechanism of action, benefits and limitations.....27

Table 2. Chemical structure, examples, and natural sources of different subclasses of flavonoids.....32

Table 3. Experimental conditions used to evaluate the inhibitory effect of flavonoids against α-amylase.....34

Table 4. Flavonoids tested by Kim, Kwon and Sun (2000), and respective inhibitory activity on α-amylase (the most active flavonoids are highlighted).....35

Table 5. Flavonoids tested by Tadera et al. (2006), and respective inhibitory activity on α-amylase (the most active flavonoids are highlighted).....36

Table 6. Flavonoids tested by Mohamed (2008), and respective inhibitory activity on α-amylase (the most active flavonoids are highlighted).....37

Table 7. Flavonoids tested by Li et al. (2009), and respective inhibitory activity on α-amylase (the most active flavonoid is highlighted).....37

Table 8. Flavonoids tested by Yilmazer-Musa et al. (2012), and respective inhibitory activity on α-amylase (the most active flavonoid is highlighted).....38

Table 9. Flavonoids tested by Luyen et al. (2013), and respective inhibitory activity on α-amylase (the most active flavonoid is highlighted).....38

Table 10. Flavonoids tested by Ahmed et al. (2014), and respective inhibitory activity on α-amylase (the most active flavonoid is highlighted).....38

Table 11. Flavonoids tested by Asghari et al. (2015), and respective inhibitory activity on α-amylase (the most active flavonoid is highlighted).....39

Table 12. Flavonoids tested by Ibrahim et al. (2015), and respective inhibitory activity on α-amylase (the most active flavonoids are highlighted).....39

Table 13. Flavonoids tested by Meng et al. (2016), and respective inhibitory activity on α-amylase (the most active flavonoid is highlighted).....39

Table 14. Flavonoids tested by Milella et al. (2016), and respective inhibitory activity on α-amylase (the most active flavonoid is highlighted).....40

Table 15. Flavonoids tested by Tundis et al. (2016), and respective inhibitory activity on α-amylase (the most active flavonoid is highlighted).....41

Table 16. Flavonoids tested by Ibrahim et al. (2017), and respective inhibitory activity on α-amylase (the most active flavonoids are highlighted).....41

Table 17. Flavonoids tested by Sun et al. (2017), and respective inhibitory activity on α-amylase (the most active flavonoid is highlighted).....41

Table 18. Flavonoids tested by Zhang et al. (2017), and respective inhibitory activity on α-amylase (the most active flavonoid is highlighted).....42

Table 19. Flavonoids tested by Desseaux et al. (2018), and respective inhibitory activity on α-amylase (the most active flavonoids are highlighted).....42

Table 20. Flavonoids tested by Li, Yao, et al. (2018), and respective inhibitory activity on α-amylase (the most active flavonoid is highlighted).....43

Table 21. Flavonoids tested by Lim et al. (2019), and respective inhibitory activity on α-amylase (the most active flavonoids are highlighted).....43

Table 22. Flavonoids tested by Martinez-Gonzalez et al. (2019), and respective inhibitory activity on α-amylase (the most active flavonoid is highlighted).....44

Table 23. Flavonoids tested by Proença et al. (2019), and respective inhibitory activity on α-amylase (the most active flavonoids are highlighted).....45

Table 24. Flavonoids tested by Kaeswum et al. (2019), and respective inhibitory activity on α-amylase (the most active flavonoids are highlighted).....46

Table 25. Flavonoids tested by Ren et al. (2019), and respective inhibitory activity on α-amylase (the most active flavonoid is highlighted).....46

Table 26. Summary of the results obtained for the α-amylase inhibitory activity of flavonoids, in the analyzed research studies.....47

Table 27. Methodologies used to evaluate the inhibitory effect of flavonoids on α-glucosidase.....48

Table 28. Flavonoids tested by Aderogba et al. (2013), and respective inhibitory activity on α-glucosidase (the most active flavonoid is highlighted).....51

Table 29. Flavonoids tested by Cheng et al. (2014), and respective inhibitory activity on α-glucosidase (the most active flavonoids are highlighted).....51

Table 30. Flavonoids tested by Dendup et al. (2014), and respective inhibitory activity on α-glucosidase (the most active flavonoids are highlighted).....52

Table 31. Flavonoids tested by Wang, Cheng, et al. (2014), and respective inhibitory activity on α-glucosidase (the most active flavonoids are highlighted).....53

Table 32. Flavonoids tested by Chang, Ho, and Lee (2015), and respective inhibitory activity on α-glucosidase (the most active flavonoid is highlighted).....53

Table 33. Flavonoids tested by Costa et al. (2015), and respective inhibitory activity on α-glucosidase (the most active flavonoid is highlighted).....54

Table 34. Flavonoids tested by Flores-Bocanegra et al. (2015), and respective inhibitory activity on α-glucosidase (the most active flavonoid is highlighted).....54

Table 35. Flavonoids tested by Guo et al. (2015), and respective inhibitory activity on α-glucosidase (the most active flavonoids are highlighted).....55

Table 36. Flavonoids tested by Imran et al. (2015), and respective inhibitory activity on α-glucosidase (the most active flavonoid is highlighted).....56

Table 37. Flavonoids tested by Ma et al. (2015), and respective inhibitory activity on α-glucosidase (the most active flavonoid is highlighted).....56

Table 38. Flavonoids tested by Sheliya et al. (2015), and respective inhibitory activity on α-glucosidase (the most active flavonoid is highlighted).....57

Table 39. Flavonoids tested by Sun et al. (2015), and respective inhibitory activity on α-glucosidase (the most active flavonoid is highlighted).....57

Table 40. Flavonoids tested by Zhang et al. (2015), and respective inhibitory activity on α-glucosidase (the most active flavonoid is highlighted).....58

Table 41. Flavonoids tested by Chen et al. (2016), and respective inhibitory activity on α-glucosidase (the most active flavonoid is highlighted).....59

Table 42. Flavonoids tested by Imran et al. (2016), and respective inhibitory activity on α-glucosidase (the most active flavonoid is highlighted).....60

Table 43. Flavonoids tested by Shi et al. (2016), and respective inhibitory activity on α-glucosidase (the most active flavonoid is highlighted).....61

Table 44. Flavonoids tested by Silva et al. (2016), and respective inhibitory activity on α-glucosidase (the most active flavonoid is highlighted).....62

Table 45. Flavonoids tested by Zeng, Zhang, et al. (2016), and respective inhibitory activity on α-glucosidase (the most active flavonoids are highlighted).....62

Table 46. Flavonoids tested by Zeng, Chen, et al. (2016), and respective inhibitory activity on α-glucosidase (the most active flavonoid is highlighted).....62

Table 47. Flavonoids tested by Zhang et al. (2016), and respective inhibitory activity on α-glucosidase (the most active flavonoid is highlighted).....62

Table 48. Flavonoids tested by Amin et al. (2017), and respective inhibitory activity on α-glucosidase (the most active flavonoid is highlighted).....63

Table 49. Flavonoids tested by Boonsombat et al. (2017), and respective inhibitory activity on α-glucosidase (the most active flavonoid is highlighted).....63

Table 50. Flavonoids tested by Chen et al. (2017), and respective inhibitory activity on α-glucosidase (the most active flavonoid is highlighted).....63

Table 51. Flavonoids tested by Hmidene et al. (2017), and respective inhibitory activity on α-glucosidase (the most active flavonoids are highlighted).....63

Table 52. Flavonoids tested by Jeong and Kim (2017), and respective inhibitory activity on α-glucosidase (the most active flavonoid is highlighted).....64

Table 53. Flavonoids tested by Kim, Cho, et al. (2017), and respective inhibitory activity on α-glucosidase (the most active flavonoid is highlighted).....64

Table 54. Flavonoids tested by Kim, Jung, et al. (2017), and respective inhibitory activity on α-glucosidase (the most active flavonoid is highlighted).....64

Table 55. Flavonoids tested by Lee, Kim, and Whang (2017), and respective inhibitory activity on α-glucosidase (the most active flavonoid is highlighted).....65

Table 56. Flavonoids tested by Proença et al. (2017), and respective inhibitory activity on α-glucosidase (the most active flavonoid is highlighted).....65

Table 57. Flavonoids tested by Qin et al. (2017), and respective inhibitory activity on α-glucosidase (the most active flavonoid is highlighted).....66

Table 58. Flavonoids tested by Sarian et al. (2017), and respective inhibitory activity on α-glucosidase (the most active flavonoid is highlighted).....66

Table 59. Flavonoids tested by Şöhretoğlu et al. (2017), and respective inhibitory activity on α-glucosidase (the most active flavonoid is highlighted).....66

Table 60. Flavonoids tested by Song et al. (2017), and respective inhibitory activity on α-glucosidase (the most active flavonoid is highlighted).....67

Table 61. Flavonoids tested by Ye, Fan, and Ma (2017), and respective inhibitory activity on α-glucosidase (the most active flavonoid is highlighted).....67

Table 62. Flavonoids tested by Wang et al. (2017), and respective inhibitory activity on α-glucosidase (the most active flavonoid is highlighted).....67

Table 63. Flavonoids tested by Zhen et al. (2017), and respective inhibitory activity on α-glucosidase (the most active flavonoid is highlighted).....68

Table 64. Flavonoids tested by Zhou et al. (2017), and respective inhibitory activity on α-glucosidase (the most active flavonoid is highlighted).....71

Table 65. Flavonoids tested by Alhassan et al. (2018), and respective inhibitory activity on α-glucosidase (the most active flavonoids are highlighted).....72

Table 66. Flavonoids tested by Adhikari-Devkota et al. (2018), and respective inhibitory activity on α-glucosidase (the most active flavonoid is highlighted).....72

Table 67. Flavonoids tested by Ha et al. (2018), and respective inhibitory activity on α-glucosidase (the most active flavonoid is highlighted).....72

Table 68. Flavonoids tested by Li, Li et al. (2018), and respective inhibitory activity on α-glucosidase (the most active flavonoid is highlighted).....73

Table 69. Flavonoids tested by Shahinozzaman et al. (2018), and respective inhibitory activity on α-glucosidase (the most active flavonoid is highlighted).....73

Table 70. Flavonoids tested by Şöhretoğlu et al. (2018), and respective inhibitory activity on α-glucosidase (the most active flavonoid is highlighted).....73

Table 71. Flavonoids tested by Renda et al. (2018), and respective inhibitory activity on α-glucosidase (the most active flavonoid is highlighted).....73

Table 72. Flavonoids tested by Xu, Wang, et al. (2018), and respective inhibitory activity on α-glucosidase (the most active flavonoid is highlighted).....75

Table 73. Flavonoids tested by Xu, Xie, et al. (2018), and respective inhibitory activity on α-glucosidase (the most active flavonoid is highlighted).....75

Table 74. Flavonoids tested by Fan et al. (2019), and respective inhibitory activity on α-glucosidase (the most active flavonoids are highlighted).....76

Table 75. Flavonoids tested by Ghani et al. (2019) and Nur et al. (2019), and respective inhibitory activity on α-glucosidase (the most active flavonoid is highlighted).....77

Table 76. Flavonoids tested by Li, Kongstad, and Staerk (2019), and respective inhibitory activity on α-glucosidase (the most active flavonoid is highlighted).....78

Table 77. Flavonoids tested by Meesakul et al. (2019), and respective inhibitory activity on α-glucosidase (the most active flavonoid is highlighted).....79

Table 78. Flavonoids tested by Zhao, Liu, and Chen (2019), and respective inhibitory activity on α-glucosidase (the most active flavonoid is highlighted).....80

Table 79. Flavonoids tested by Cedeño et al. (2019), and respective inhibitory activity on α-glucosidase (the most active flavonoids are highlighted).....80

Table 80. Flavonoids tested by Liu et al. (2019), and respective binding constants on α-glucosidase (the most active flavonoid is highlighted).....80

Table 81. Flavonoids tested by Zhu et al. (2019), and respective inhibitory activity on α-glucosidase (the most active flavonoid is highlighted).....80

Table 82. Flavonoids tested by Jia et al. (2019), and respective inhibitory activity on α-glucosidase (the most active flavonoid is highlighted).....81

Table 83. Flavonoids tested by He et al. (2019), and respective inhibitory activity on α-glucosidase (the most active flavonoid is highlighted).....81

Table 84. Flavonoids tested by Li, Wang, et al. (2019), and respective inhibitory activity on α-glucosidase (the most active flavonoid is highlighted).....82

Table 85. Flavonoids tested by Li, Zhu, et al. (2019), and respective inhibitory activity on α-glucosidase (the most active flavonoid is highlighted).....84

Table 86. Summary of the results obtained for the inhibitory activity of flavonoids on α-glucosidase, in the analyzed research studies.....86

I.1.3.

Table 1. DPP-4 inhibitors currently available for clinical use.....104

Table 2. Experimental conditions applied in the analysed research studies concerning the inhibition of PTP1B by flavonoids.....107

Table 3. PTP1B inhibition by flavonoids tested by Chen et al. (2002).....109

Table 4. PTP1B inhibition by flavonoids tested by Li et al. (2005).....109

Table 5. PTP1B inhibition by flavonoids tested by Bae et al. (2006).....110

Table 6. PTP1B inhibition by flavonoids tested by Cui et al. (2006).....111

Table 7. PTP1B inhibition by flavonoids tested by Na et al. (2006).....112

Table 8. PTP1B inhibition by flavonoids tested by Cui et al. (2007).....113

Table 9. PTP1B inhibition by flavonoids tested by Cui et al. (2008).....114

Table 10. PTP1B inhibition by flavonoids tested by Jang et al. (2008).....115

Table 11. PTP1B inhibition by flavonoids tested by Cui et al. (2010).....115

Table 12. PTP1B inhibition by flavonoids tested by Li et al. (2010).....116

Table 13. PTP1B inhibition by flavonoids tested by Nguyen et al. (2011).....116

Table 14. PTP1B inhibition by flavonoids tested by Nguyen et al. (2012).....117

Table 15. PTP1B inhibition by flavonoids tested by Islam et al. (2013).....117

Table 16. PTP1B inhibition by flavonoids tested by Sun et al. (2013).....118

Table 17. PTP1B inhibition by flavonoids tested by Choi et al. (2014).....118

Table 18. PTP1B inhibition by flavonoids tested by Choi et al. (2014).....118

Table 19. PTP1B inhibition by flavonoids tested by Sasaki et al. (2014).....119

Table 20. PTP1B inhibition by flavonoids tested by Cai et al. (2015).....119

Table 21. PTP1B inhibition by flavonoids tested by Guo et al. (2015).....120

Table 22. PTP1B inhibition by flavonoids tested by Jeong et al. (2015).....121

Table 23. PTP1B inhibition by flavonoids tested by Jiang et al. (2015).....122

Table 24. PTP1B inhibition by flavonoids tested by Li et al. (2015).....122

Table 25. PTP1B inhibition by flavonoids tested by Nguyen et al. (2002).....123

Table 26. PTP1B inhibition by flavonoids tested by Quang et al. (2015).....124

Table 27. PTP1B inhibition by flavonoids tested by Wang et al. (2015).....124

Table 28. PTP1B inhibition by flavonoids tested by Wu et al. (2015).....125

Table 29. PTP1B inhibition by flavonoids tested by Na et al. (2016).....126

Table 30. PTP1B inhibition by flavonoids tested by Wang et al. (2016).....126

Table 31. PTP1B inhibition by flavonoids tested by Zhang et al. (2016).....127

Table 32. PTP1B inhibition by flavonoids tested by Zhao et al. (2016).....127

Table 33. PTP1B inhibition by flavonoids tested by Huang et al. (2017).....128

Table 34. PTP1B inhibition by flavonoids tested by Jung et al. (2017).....128

Table 35. PTP1B inhibition by flavonoids tested by Kim et al. (2017).....128

Table 36. PTP1B inhibition by flavonoids tested by Nguyen et al. (2017).....129

Table 37. PTP1B inhibition by flavonoids tested by Qin et al. (2017).....129

Table 38. PTP1B inhibition by flavonoids tested by Song et al. (2017).....129

Table 39. PTP1B inhibition by flavonoids tested by Trinh, Jager, and Staerk (2017).....130

Table 40. PTP1B inhibition by flavonoids tested by Proença et al. (2018).....131

Table 41. PTP1B inhibition by flavonoids tested by Qin et al. (2018).....132

Table 42. PTP1B inhibition by flavonoids tested by Xu et al. (2018).....133

Table 43. PTP1B inhibition by flavonoids tested by Xue et al. (2018).....133

Table 44. PTP1B inhibition by flavonoids tested by Zhang et al. (2018).....134

Table 45. PTP1B inhibition by flavonoids tested by Zhao et al. (2018).....134

Table 46. PTP1B inhibition by flavonoids tested by Ren et al. (2019).....136

Table 47. PTP1B inhibition by flavonoids tested by Xu et al. (2019).....136

Table 48. PTP1B inhibition by flavonoids tested by Zhao et al. (2019).....137

Table 49. Summary of the results obtained for the flavonoids with the best inhibitory activity against PTP1B, in the analyzed research studies.....138

Table 50. Experimental conditions applied in the research studies concerning the inhibition of DPP-4 by flavonoids.....140

Table 51. DPP-4 inhibition by flavonoids tested by Eidenberger, Selg, and Krennhuber (2013).....140

Table 52. DPP-4 inhibition by flavonoids tested by Fan et al. (2013).....141

Table 53. DPP-4 inhibition by flavonoids tested by Bower et al. (2014).....142

Table 54. DPP-4 inhibition by flavonoids tested by Morikawa et al. (2015).....142

Table 55. DPP-4 inhibition by flavonoids tested by Zhao et al. (2016).....143

Table 56. DPP-4 inhibition by flavonoids tested by Sarian et al. (2017).....143

Table 57. DPP-4 inhibition by flavonoids tested by Gupta et al. (2018).....144

Table 58. DPP-4 inhibition by flavonoids tested by Kim et al. (2018).....144

Table 59. DPP-4 inhibition by flavonoids tested by Proença et al. (2019).....145

Table 60. Summary of the results obtained for the flavonoids with the best inhibitory activity against DPP-4, in the analyzed research studies.....146

II.1.

Table 1. Structures and *in vitro* α-glucosidase inhibition by the studied flavonoids (IC_{50} μM, mean ± SEM).....6

Table 2. K_i values (mean ± SEM, μM) for the inhibition of yeast α-glucosidase by the selected flavonoids.....7

II.2.

Table 1. Inhibitory activity of flavonoids against porcine pancreatic α-amylase (IC_{50}, μM ± SEM).....20

Table 2. Type of inhibition and V_{max}, K_m, K_{ic} and K_{iu} values ± SD (μM) for the inhibition of α-amylase by the selected flavonoids.....21

II.3.

Table 1. Structure and in vitro PTP1B inhibitory activity of the tested flavonoids (IC_{50} μM ± SEM or % inhibition at the highest tested concentration).....32

Table 2. K_i values ± SEM (μM) for the inhibition of human recombinant PTP1B.....33

II.4.

Table 1. Inhibition of human DPP-4 by the flavonoids under study and the positive controls, applying the fluorometric method.....44

Table 2. Type of inhibition of flavonoid C11, sitagliptin and diprotin A and respective kinetic parameters values: Km, Vmax, Kic and/or Kiu (mean ± SD).....45

Table 3. Inhibition of DPP-4 activity by the positive controls sitagliptin and diprotin A and by the flavonoids under study in the human blood assay and in the human plasma assay....45

Table 4. Plasma protein binding (PPB) values of the flavonoids under study.....45

II.5.

Table 1. Inhibitory activity of tested flavonoids against human liver FBPase.....56

Table 2. Persistent hydrogen bonds between each inhibitor and the receptor, in terms of percentage of time held.....60

II.6.

Table 1. Inhibitory activity of flavonoids and positive controls against human sucrase and maltase (IC50 ± SEM or % inhibition ± SEM).....78

Table 2. Inhibitory activity of flavonoids and positive controls against sucrase-isomaltase (IC50 ± SEM or % inhibition ± SEM).....80

ABBREVIATIONS

AAG - α1-acid glycoprotein

ACE2 - angiotensin converting enzyme-2

ADA - American Diabetes Association

ADME - absorption-distribution-metabolism excretion

ADP - adenosine diphosphate

AGEs - advanced glycation end-products

AIC - Akaike information criterion

AMC - 7-amino-4-methylcoumarin

AMP - adenosine 5'-monophosphate

AMPK - AMP-activated protein kinase

ANOVA - analysis of variance

AS160 - Akt substrate of 160 kDa

ATP - adenosine triphosphate

BMI - body mass index

cAMP - cytoplasmic cyclic adenosine monophosphate

CBG - cytosolic β-glucosidase

CNP - 2-chloro nitrophenol

CNPG2 - 2-chloro- nitrophenyl-α-D-maltotrioside

CNPG3 - 2-chloro-4-nitrophenyl-α-D-maltotrioside

COMTs - catechol-*O*-methyltransferases

COVID-19 - coronavirus disease 2019

CPT-1 - carnitine palmitoyltransferase-1

CRPP - common rat plasma proteins

CVOTs - cardiovascular outcome trials

DAG - diacylglycerol

DM - diabetes *mellitus*

DMSO - dimethyl sulfoxide

DPP-4 - dipeptidyl peptidase-4

DTT - dithiothreitol

EDTA - ethylenediaminetetraacetic acid

EGP - endogenous glucose production

EPAC - exchange factor directly activated by cAMP

Epac2 - guanine nucleotide exchange factor

ER - endoplasmic reticulum

ERK - extracellular-signal regulated kinase

FAP - fibroblast activating protein

FBPase - fructose 1,6-bisphosphatase

FDA - Food and Drug Administration

FFA - free fatty acid

FGF - fibroblast growth factor

FOXO1 - forkhead box protein O1

G6Pase - glucose-6-phosphatase

GAP - GTPase activating protein

GD - gestational diabetes

GDP - guanosine diphosphate

GEP - cAMP-guanine nucleotide exchange factor

GH31 - glycoside hydrolase family 31

GIP - glucose-dependent insulinotropic polypeptide

GIPR - glucose-dependent insulinotropic polypeptide receptor

GK - glucokinase

GLP-1 - glucagon-like peptide-1

GLP-1R - glucagon-like peptide-1 receptor

GLUT - glucose transporter

GP-AMC - H-Gly-Pro-7-amino-4-methylcoumarin hydrobromide

GPPN - Gly-Pro-*p*-nitroanilide hydrochloride

GPCR - G protein coupled receptor

GSK-3 - glycogen synthase-3

GSV - GLUT4 storage vesicles

GTP - guanosine triphosphate

GWAs - genome-wide association studies

HbA1c - glycated haemoglobin

HDL - high-density lipoprotein

HPAEC - high-performance anion-exchange chromatography

HSA - human serum albumin

IAPP - hypersecretion of islet amyloid polypeptide

IC_{50} - half-maximal inhibitory concentration

IDF - International Diabetes Federation

IFG - fasting plasma glucose levels

IGT - impaired glucose tolerance

IKK - IκB kinase

IL - interleukin

IR - insulin receptor

IRS - insulin receptor substrate

K_{ATP} - ATP-sensitive K^+ channels

K_i - constant of inhibition

K_{ic} - inhibitor dissociation constant of enzyme-inhibitor (for competitive inhibition)

K_{iu} - inhibitor dissociation constant of enzyme-substrate inhibitor complexes (for uncompetitive inhibition)

K_{IR} - inwardly rectifying K^+ channels

K_m - Michaelis constant

KOH - potassium hydroxide

K_V - repolarizing voltage-gated K^+ channels

LDL - low-density lipoprotein

LIE - linear interaction energy

LPH - lactase phlorizin hydrolase

LPS - lipopolysaccharide

MD - molecular dynamics

MERS - Middle East respiratory syndrome

MGAM - maltase-glucoamylase

MMPs - matrix metalloproteases

$mTORC_2$ - mechanistic (or mammalian) target of rapamycin complex 2

NAD^+ - nicotinamide adenine dinucleotide

NADH - reduced nicotinamide adenine dinucleotide

NF - nuclear factor

PBS - Dulbecco's phosphate buffered saline

PC-1/3 - pro-hormone convertase 1/3

PDB - Protein Data Bank

PDK-1 - 3-phosphoinositide dependent protein kinase-1

PEP - phosphoenolpyruvate

PH - pleckstrin homology

P_i - inorganic phosphate

PI3K - phosphatidylinositol 3-kinase

PIP_2 - phosphatidylinositol 4,5-biphosphate

PIP_3 - phosphatidylinositol 3,4,5-triphosphate

PKA - protein kinase A

PKB (or Akt) - protein kinase B

PKC - protein kinase C

PLA2 - phospholipase A2

PLC - phospholipase C

*p*NPG - *p*-nitrophenyl-α-D-glucopyranoside

*p*NPP - *p*-nitrophenyl phosphate

PPAR - peroxisome proliferator-activated receptor

PPB - plasma protein binding

PPHG - postprandial hyperglycaemia

PTB - phosphotyrosine binding

PtdIns(4,5)P_2 - phosphatidylinositol 4,5-bisphosphate

PTKs - protein tyrosine kinases

PTP1B - protein tyrosine phosphatase 1B

PTPs - protein tyrosine phosphatases

QPP - quiescent cell proline dipeptidase

RMSD - root mean square deviation

RNS - reactive nitrogen species

ROS - reactive oxygen species

SAR - structure-activity relationship

SARS-CoV-2- severe acute respiratory syndrome coronavirus 2

SD - standard deviation

SEM - standard error of the mean

SGLT - sodium/glucose co-transporter

SI - sucrase-isomaltase

SIRT1 - sirtuin 1

SNPs - single-nucleotide polymorphisms

ST8SIS - α-*N*-acetylneuramide α-2,8-sialyltransferase

T1D - type 1 diabetes

T2D - type 2 diabetes

TCPTP - T-cell protein tyrosine phosphatase

tmAC - transmembrane adenylyl cyclase

TNF - tumour necrosis factor

UGTs - glucuronosyl transferases

UV - ultraviolet

VDCCs - voltage-dependent Ca^{2+} channels

V_{max} - maximum velocity

WHO - World Health Organization

OUTLINE OF THE THESIS

The present thesis is organized in three main chapters (I., II., III.):

Chapter I - General Introduction

This chapter is divided in two sections (I.1., I.2.):

I.1. Theoretical background

This section is divided in three subsections. The first subsection (I.1.1.) is an overview of the pathophysiology of type 2 diabetes, the mechanisms involved, the current pharmaceutical approach, as well as the recent major advances and future perspectives related to this disease. The sub-subsection I.1.1.1. contains the references corresponding to the subsection I.1.1. The second subsection (I.1.2.) is a review article that provides a deep overview of the scientific literature regarding inhibitory activity of flavonoids against α-amylase and α-glucosidase (covering a totality of 500 compounds), including, whenever possible, their type of inhibition, and the respective conclusions in what concerns the structure-activity relationship. The third subsection (I.1.3.) is a review article that provides a deep analysis of the published scientific literature about the inhibition of PTP1B and DPP-4 by flavonoids, and whenever possible their type of inhibition, covering a totality of 351 compounds, and to establish the most important aspects of the respective structure-activity relationship.

I.2. General and specific objectives of the thesis

This section provides the general and specific objectives of the thesis.

Chapter II - Original Research

This chapter is divided in six sections corresponding to published (II.1., II.2., II.3., II.4., II.5.) or submitted (II.6) original manuscripts, as the result of experimental studies performed with the purpose of answering the questions raised in the general and specific objectives of this thesis. In this chapter, I performed all the experimental studies, except the molecular docking calculations and the molecular dynamics simulations.

Chapter III - Integrated Discussion and Conclusions

This chapter is divided in four sections. The first section (III.1.) comprises an integrated discussion of the performed original research; the second section (III.2.) contains the general conclusions of the thesis, the third section (III.3.) is focused on future perspectives on the study of flavonoids as therapeutic agents in T2D, and the fourth section (III.4.) contains the references.

CHAPTER I. GENERAL INTRODUCTION

I.1. Theoretical background

I.1.1. Diabetes *mellitus*

In general, the term "diabetes" describes a group of metabolic disorders characterized by hyperglycaemia, in the absence of treatment. The heterogeneous etiopathology includes defects in insulin secretion or/and insulin production, and abnormalities in carbohydrate, fat and protein metabolism. The long-term specific effects of diabetes are retinopathy, nephropathy, neuropathy, among other complications (1). Since the 1980s the worldwide prevalence of diabetes has grown dramatically and is currently reaching epidemic proportions (2, 3). Between 2000 and 2019, deaths from diabetes increased 70 % worldwide, with an 80 % rise in deaths among males (4). Due to the easy access to energy-dense foods and increasingly sedentary lifestyles, obesity and diabetes are major health and socio-economic problems in the 21st century (3).

The main characteristic symptoms of diabetes include thirst, polyuria, blurred vision and weight loss, while genital infections are also frequent. The most severe clinical manifestations are ketoacidosis, or a non-ketonic hyperosmolar state that can cause dehydration, coma, and even death, in case of the absence of effective treatment (1). According to American Diabetes Association (ADA), diabetes can be classified into the following general categories: type 1 diabetes (T1D), type 2 diabetes (T2D), gestational diabetes (GD) and specific types of diabetes due to other causes (5). T1D is caused by β-cell destruction, usually leading to absolute insulin deficiency; T2D is the result of a progressive loss of adequate β-cell insulin secretion normally on the background of insulin resistance; GD is diabetes diagnosed in the second or third trimester of pregnancy that was not clearly overt diabetes before gestation; specific types of diabetes due to other causes can be attributed to genetic defects of the β-cells, genetic defects in insulin action, diseases of the exocrine pancreas, endocrinopathies, drug- or chemical-induced diabetes, infections, among others. T1D and T2D are the most common forms of diabetes, representing approximately 5-10 % and 90-95 % of all patients with diabetes, respectively (5, 6).

T1D is a chronic illness characterized by insulin deficiency as the result of pancreatic β-cell loss, leading to hyperglycaemia. Although the age of symptomatic onset is observed during childhood or adolescence, in some cases, symptoms can develop much later. The aetiology of T1D is not totally understood but the pathogenesis of this disease is thought to involve T cell-mediated destruction of β-cells. Islet-targeting autoantibodies that target insulin, which are proteins associated with secretory granules in β-cells, also function as biomarkers of

T1D-autoimmunity that are found months to years before symptomatic onset (7). The pathogenesis of T1D can be divided in different stages related to the detection of autoantibodies and progress to β-cell destruction, dysglycaemia, and lastly, symptoms associated with hyperglycaemia. Nowadays, the aetiology of β-cell targeted autoimmunity remains undefined, but probably includes a combination of environmental and genetic factors that trigger or allow the autoimmune response against pancreatic β-cells (8). The cure of T1D is not available, and patients depend on lifelong insulin injections although novel approaches to insulin treatment, namely insulin pumps, continuous glucose monitoring, and hybrid closed loops are already available or in development. The intensive glycaemic control has decreased the development of micro- and macrovascular damage, although the majority of T1D patients are still developing these complications (7).

The focus of this thesis is the search and study of possible new flavonoid-based molecules for the treatment of T2D, so this form of diabetes will be more deeply described.

I.1.1.2. Type 2 diabetes

Hyperglycaemia is preceded by prediabetes, a condition that predisposes individuals to the development of T2D. Prediabetes is characterized by one of the following situations: impaired fast glucose levels (IFG) (fasting plasma glucose levels higher than normal but do not meet the criteria for the diagnosis of diabetes), impaired glucose tolerance (IGT), or increased glycated haemoglobin (HbA1c) levels. At the time of diagnosis, many T2D patients are asymptomatic, while others manifest severe hyperglycaemia or even diabetic ketoacidosis (9). However, T2D symptoms are usually less severe than TD1 symptoms, owing to the slow pace at which the hyperglycaemia is worsening (1). Screening in at-risk individuals is extremely important, since according to International Diabetes Federation (IDF), 1 in 2 adults with diabetes are undiagnosed, corresponding to 232 million people (10). Prevention of T2D requires identification of individuals with prediabetes and intervention with lifestyle modifications and administration of antidiabetic agents. As T2D is a complex metabolic disorder, strategies to normalize blood glucose levels, lipid profiles and blood pressure are the continuous medical care, patient self-management for control of blood glucose levels, and multifactorial risk reduction measures. These actions are of high importance for minimization of acute and long-term microvascular (namely retinopathy, nephropathy, and neuropathy) and macrovascular complications (namely heart attack and stroke). It is extremely important that T2D is viewed and treated as a heterogeneous disorder with multiple pathophysiological abnormalities, with variations in susceptibility to complications and response to therapeutic intervention (9). It is important to mention that in addition to diabetes, insulin resistance has several manifestations including obesity,

hypertension, dyslipidaemia, ovarian hyperandrogenism and premature adrenarche, non-alcoholic fatty liver disease and systemic inflammation (11). In fact, insulin resistance is mainly attributed to obesity, caused by poor dietary and lifestyle habits (12). The determinants for the development of T2D consist of a matrix of genetic, epigenetic and lifestyle factors that interact with each other the larger physical-cultural environment. In this way, the main risk factors of T2D are older age, non-white ancestry, family history of T2D, low socio-economic status, genetic factors, components of the metabolic syndrome, overweight or obesity, unhealthy dietary factors, cigarette smoking, sedentary lifestyle, history of GD, and psychosocial stress and depression (13).

Islets of Langerhans are specialized micro-organs located in the pancreas and have a crucial role in the tight regulation of blood glucose levels through the coordinated release of hormones (14). In human islets, β-cells constitute around 60 % of cells, while glucagon-producing α-cells, somatostatin-producing δ-cells, and pancreatic polypeptide-producing cells constitute approximately 30 %, 10 % and 1 %, respectively (9, 15). The β-cells rapidly sense rising blood glucose concentrations after a meal and release adequate amounts of insulin, thereby enabling glucose uptake in liver and other peripheral tissues. Upon reduction of blood glucose levels, β-cells respond by finishing insulin secretion. In turn, α-cells release glucagon that stimulates hepatic gluconeogenesis and glycogenolysis, increasing blood glucose levels and avoiding hypoglycaemia. Inhibition of insulin and glucagon secretion is mediated through negative feedback by a third islet hormone, somatostatin, secreted by δ-cells. These synchronized and balanced processes maintain the normal glucose concentration in healthy human adults (≈ 74 - 106 mg/dL) (14).

Upon entry into the β-cell, glucose undergoes glycolysis and oxidative phosphorylation, leading to an increase in adenosine triphosphate (ATP) production. The rise in ATP: adenosine diphosphate (ADP) ratio results in a closure of ATP-sensitive K^+ channels (K_{ATP}), followed by depolarization of membrane and Ca^{2+} influx through voltage-dependent Ca^{2+} channels (VDCCs). Increased intracellular Ca^{2+} levels lead to an activation of the exocytotic machinery to promote the fusion of insulin-containing granules with the cell membrane and the consequent release of insulin into blood circulation. Other pathways also contribute to regulation of insulin release: cyclic adenosine monophosphate (cAMP), protein kinase A (PKA), protein kinase C (PKC), phospholipase C (PLC), extracellular-signal regulated kinase (ERK) and β-arrestin (16-19) (Figure 1).

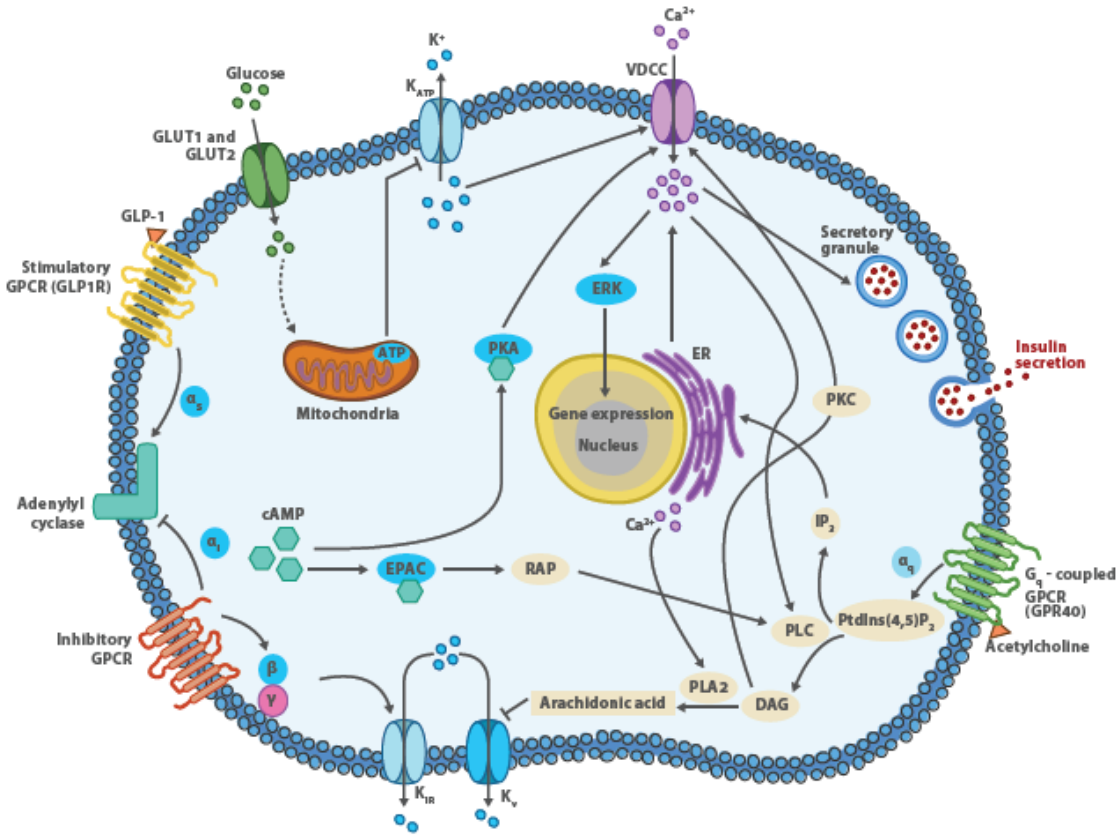


Figure 1: Schematic illustration depicting major signaling inputs in pancreatic β-cells. Glucose is the most important stimulator of insulin secretion. Glucose is taken up by the glucose transporters (GLUT)1 and 2 of β-cells and undergoes the glycolysis/Krebs cycle/oxidative phosphorylation pathways. This process results in the increase of intracellular adenosine triphosphate (ATP) at the expense of adenosine diphosphate (ADP), leading to closure of ATP-sensitive K^+ (K_{ATP}) channel, triggering membrane depolarization, and initiating β-cell electrical activity. This activates voltage-dependent calcium channel (VDCC) allowing influx of Ca^{2+}, which in turn drives pulsatile insulin exocytosis. Ca^{2+} oscillations are facilitated by repolarizing voltage-gated K^+ (K_v) channels and inwardly rectifying K^+ (K_{IR}) channels. Other potentiators of insulin secretion exert their effects by two main pathways from G protein-coupled receptor (GPCR)-mediated responses. The first involves G protein-mediated stimulation of adenylyl cyclase and increase of cyclic adenosine monophosphate (cAMP) levels. This results in activation of protein kinase A (PKA) and exchange factor directly activated by cAMP (EPAC). Agents such as glucagon-like peptide -1 (GLP-1) act by enhancing cAMP. The second mechanism is through activation of the phosphoinositide pathway. This involves G protein-mediated activation of phospholipase C (PLC), which cleaves phosphatidylinositol 4,5-bisphosphate [$PtdIns(4,5)P_2$] to produce the signaling molecules inositol triphosphate (IP_3) and diacylglycerol (DAG). IP_3 binds to its receptor in the endoplasmic reticulum (ER) to liberate intracellular Ca^{2+}, while DAG primarily acts via activation of protein kinase C (PKC). DAG is hydrolyzed by phospholipase A2 (PLA2) into arachidonic acid, which negatively regulates K_v channels, prolonging stimulus-induced depolarization of the β-cell plasma membrane and thereby amplifying insulin secretion. Agents such acetylcholine stimulate insulin secretion by activating the PLC/PKC pathway.
αi - Giα subunit; αq - Gqα subunit; αs - Gsα subunit; βγ - G βγ complex; ERK - extracellular-signal-regulated kinase; GLP1R - GLP-1 receptor; RAP - Ras-related protein 1.

Insulin resistance is the earliest detectable characteristic in individuals with T2D, although T2D only occurs when β-cells are unable to secrete enough insulin to counterbalance insulin resistance. Within the islets, β-cells form sparce subclusters with functional connectivity through gap junctions (9). Gap junctions are extremely important for β-cell-β-cell communication since it was previously described that loss of normal gap junctions signalling has been shown to disrupt Ca^{2+} dynamics and insulin secretion (16) Each islet

contains about 100 - 500 μU of insulin, which means that the whole exocrine pancreas (≈ 1 million islets) has 10 days' worth of supply for a healthy adult. β-Cells communicate with each other and with the other islet endocrine cells by means of connexin proteins and other cell-cell adhesion complexes and, in addition, endocrine cells can influence each other through hormones released into the blood. Lastly, non-hormonal endocrine cell products, including ATP and zinc, and neurotransmitters affect β-cell function (9, 15). Notably, β-cell subpopulations display variations in maturity, proliferation, metabolism, Ca^{2+} signalling and insulin secretion, with their proportions changing with age and T2D status. Previous surface antigen analysis identified four different β-cell subpopulations (termed β1-4) on the basis of differential expression of the surface antigen marker, α-N-acetylneuraminide α-2,8-sialyltransferase (ST8SIS). Interestingly, the β3 and β4 subpopulations can be distinguished from the β1 and β2 subpopulations, which exhibit lower glucose responsiveness and are increased in proportion during diabetes (16).

In individuals with T2D, β-cell mass is reduced between 25 to 60 %, which is believed to occur via apoptosis and dysregulated autophagy, while vascular disarray and amyloid deposition contribute to impaired cytoarchitecture in T2D islets. Free fatty acids might elicit endoplasmic reticulum (ER) stress and thereby impair β-cell function and survival. It was also suggested that accelerated β-cell ageing and senescence occurs in T2D (20). The loss of β-cells is not counterbalanced with new β-cells since the human pancreas does not seem to be able to renew these cells after 30 years of age (21). The quantitative functional impact of these structural modifications is not completely defined. Insulin resistance is the result of the increase of β-cells secretion of insulin at any serum level of glucose. The rise of insulin secretion is stimulated by its substrates (glucose, free fatty acids, arginine, fructose and amino acids), hormones and nerve endings to adjust insulin release in response of modified demands such as fasting-feeding cycles, exercise and stress, with the purpose to maintain blood glucose levels (9). In that sense, it is possible that the absolute insulin secretion in response to an oral glucose challenge is normal or even increased in T2D, with the exception of a long-standing and poorly controlled diabetes, in which absolute insulin secretion is decreased. Nevertheless, when the insulin release rates are plotted against the concomitant blood glucose levels, T2D patients secrete considerably less insulin than the controls without diabetes. The reduction in β-cell glucose sensing occurs progressively from normoglycaemia in prediabetes to decompensated diabetes, and constitutes an efficient predictor of diabetes (9, 20). Although less studied, dysregulated secretion of glucagon by α-cells, which demonstrates as increased concentrations of fasting glucagon and failure to adequately supress glucagon secretion, also contributes to the development of hyperglycaemia. It is known that islet blood flows from β-cells to α-cells, and then to

somatostatin-producing δ-cells, so it can explain that high concentrations of insulin bathing α-cells are capable of supress glucagon release during the development of T2D (21).

As mentioned before, insulin resistance precedes T2D, and is not only present in muscle and liver but also in adipose, kidney, gastrointestinal tract, vasculature and brain tissues, and pancreatic β-cells. Obesity is tightly related to insulin resistance, and obese individuals have more adipose tissues, being associated to higher secretion of hormones and other substances that may increase the fluctuation of insulin sensitivity. Circulating non-esterified fatty acids in obese people is also related to insulin resistance since an increased fatty acid environment with hyperglycaemic conditions can lead to reduced insulin gene expression. Impaired function of cholesterol transporter destroys β-cells by means of sterol accumulation and inflammation of islets, while lipoprotein fractions and cholesterol metabolism contribute to β-cell failure (12, 22). The low-density lipoprotein (LDL) that undergo oxidation is able to reduce the pre-proinsulin expression in β-cells and very low-density lipoprotein can induce β-cell apoptosis. In turn, it was described that high-density lipoprotein (HDL) has a beneficial role on glucose homeostasis, by increasing β-cells function and plasma glucose disposal. In addition, lipids interact with incretin hormones by down regulating their receptors and modifying the downstream cAMP signalling, and consequently having a negative impact on incretin signalling that promotes insulin release and survival of β-cells (12, 22).

Systemic inflammation is a well-known contributor to insulin resistance, with increased levels of pro-inflammatory cytokines such as interleukin (IL)-6 and tumour necrosis factor (TNF) and increased number of macrophages and other inflammatory cells being found in adipose tissue, liver and sera of insulin-resistant patients (9, 21). It was verified that lifestyle modifications and pharmacological therapy improve markers of inflammation and have been associated with improvements in β-cell function in patients with T2D. Direct effects of inflammation of β-cells occur from activation of the intraislet immune response. Glucose and fatty acids are responsible for the increase of IL-1β production in islets, and the balance and regulation of the action of IL-1β in islets and other tissues is performed by naturally occurring antagonists, specially IL-1 receptor antagonist. Circulating levels of IL-1β and IL-1 receptor antagonist are increased in diabetic patients, thus intervention to reduce inflammation might lead to maintenance of improved β-cell function. Hypothalamic inflammation can also contribute to central leptin resistance and weight gain (21). In addition, saturated fatty acids activate Toll-like receptor, which in turn mediates insulin resistance-associated inflammation by upregulating the expression of IκB kinase (Ikk), nuclear-factor (NF)-κB transcription factors and pro-inflammatory mediators in

macrophages from adipose tissue. Altogether, inflammation is clearly involved in the pathogenesis of diabetes (12).

I.1.1.3. Therapeutic approaches

The increasing prevalence of T2D worldwide has caused the need of developing several approaches to treat this disorder and improve hyperglycaemia. The purpose of these therapies is to decrease and maintain glucose levels as close to normal for as long as possible after the diagnosis and thus avoiding the development of complications. The mode of action for most of the antidiabetic agents has been described. Nevertheless, individual responses to these agents can significantly differ, eventually as the result of the heterogeneous nature of T2D physiopathology (21). When compared to lifestyle changes alone, each pharmacological agent used as monotherapy multiplied by 2 - 3 folds the number of diabetic patients who reached HbA1c target levels below 7 %. Furthermore, due to poor diabetes control, most patients would require multiple therapies to achieve an improved control of blood glucose levels. Several factors should be taken into consideration before the selection of an antidiabetic agent, such as cost, potential side effects, potential benefits and glucose lowering efficacy (12). Further description of the currently available antidiabetic agents is provided below.

I.1.1.3.1. Biguanides

The discovery of biguanide and its derivatives started in the middle ages, when the herbaceous plant *Galega officinalis* was found to contain guanidine, galegine and biguanide, which reduced blood glucose levels (23). Metformin (Figure 2) is a biguanide and it is considered the first line antidiabetic agent, if not contraindicated and tolerated, and is the most prescribed drug for the treatment of T2D across all age groups (12, 24, 25).

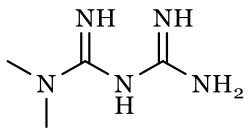


Figure 2: Chemical structure of metformin.

It is specially used in overweight and obese diabetic patients. Metformin can modify the composition of gut microbiota and activate AMP-activated protein kinase (AMPK) that preserve the intestinal barrier integrity. These effects, in addition to the activation of AMPK

in hepatocytes, seem to be the mechanism that lead to the decrease of lipopolysaccharide (LPS) levels in circulation and the liver (24, 26). In liver, metformin promotes hepatic uptake of glucose and inhibits gluconeogenesis via complex effects on the mitochondrial enzymes. Metformin is effective, safe and inexpensive, and has low risk of hypoglycaemia and low chances of weight gain. Additionally, it improves insulin sensitivity through the activation of insulin receptor expression. It was also suggested that metformin decreases plasma lipid levels through a peroxisome-activated receptor (PPAR)-α pathway, reducing the risk of cardiovascular disease. The possible reducing weight loss of metformin may be caused by glucagon-like peptide (GLP-1)-mediated actions, decreasing the food intake (23, 26). However, gastrointestinal side effects are common in patients treated with metformin and it was also found that long-term users of metformin may develop vitamin B_{12} deficiency (25). Metformin is highly efficient when there is enough production of insulin by β-cells, but when T2D reaches the state of β-failure, this antidiabetic agent loses its efficacy (23).

I.1.1.3.2. Sulfonylureas

Sulfonylureas (Figure 3) are currently prescribed as second-line or add-on options for the treatment of T2D. They enhance insulin by acting on the special receptor (SUR1 of Kir.6/SUR complex) in pancreatic β-cells thereby inhibiting the ATP-dependent K^+ channels that regulate the β-cells potential, leading to the opening of Ca^{2+} channels and promoting the exocytosis of insulin-loaded vesicles (12, 24, 26-28). Furthermore, these agents limit gluconeogenesis in liver. Sulfonylureas reduce the breakdown of lipids to fatty acids and decrease the clearance of insulin in liver (23, 27). They are divided in two groups: the first-generation agents (e.g. chloropropamide, tolazamide and tolbutamide) and second-generation agents (e.g. glipizide, glimepiride and glyburide).

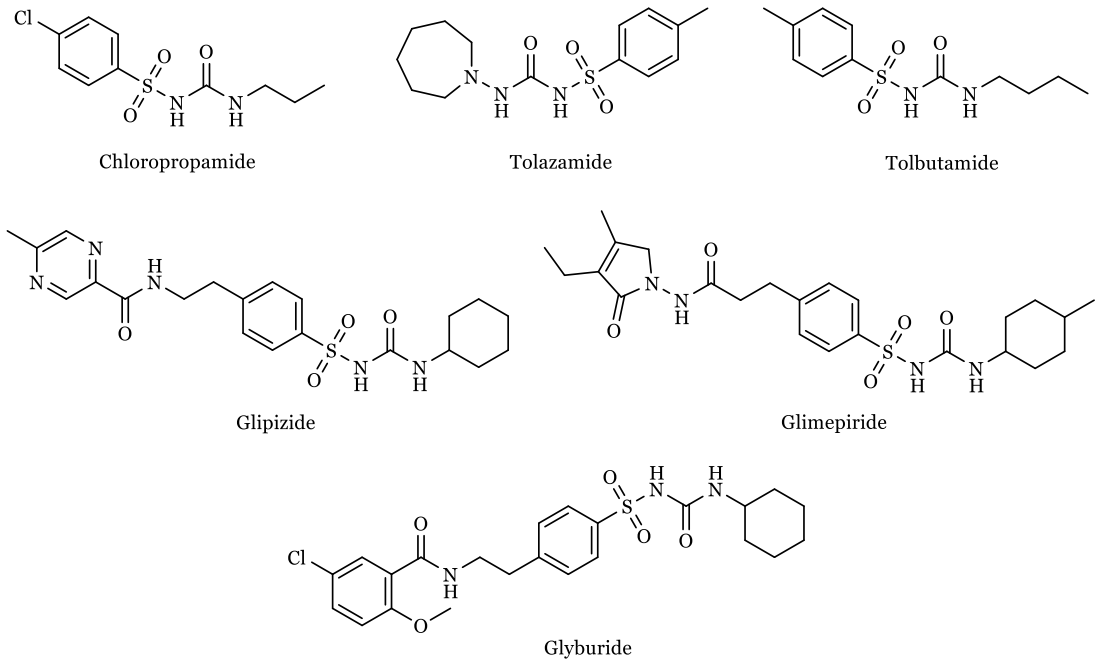


Figure 3: Chemical substructures of examples of 1st (chloropropamide, tolazamide and tolbutamide) and 2nd generation (glipizide, glimepiride and glyburide) sulfonylureas.

Comparing with second-generation agents, first-generation agents are found to have longer half-lives, higher risk of hypoglycaemia, and slower onset of action, so second-generation agents are preferred in clinical practice. Moreover, first-generation sulfonylureas produced cardiovascular advert events with many studies concluding the same for second-generation molecules but with lesser frequency (27). All sulfonylureas present hypoglycaemia and increased body weight as the major side effects, but some minor side effects are also common, such as headache, dizziness, nausea, hypersensitivity reactions and weight gain (23, 26).

I.1.1.3.3. Meglitinides

Meglitinides (Figure 4) were approved for the management of T2D in 1997, and are non-sulfonylurea insulin secretagogues.

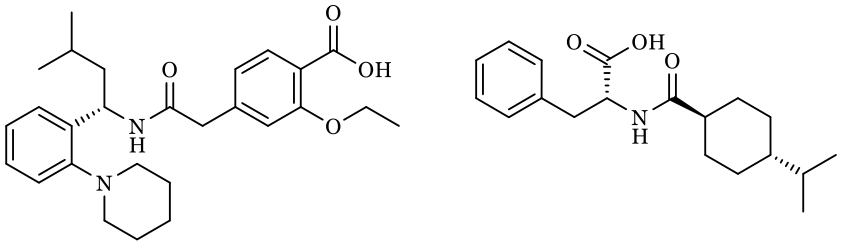


Figure 4: Chemical structures of examples of meglitinide: repaglinide and nateglinide.

They share a similar mechanism of action of sulfonylureas, but they do not bind to SUR1/Kir.6 rather a distinct receptor (27). Meglitinides are considered short-acting insulin secretagogues since the binding of meglitinide to the receptor is weaker than sulfonylurea. These agents are rapidly absorbed, showing an insulin release within minutes, being also rapidly metabolized in the liver and excreted primarily in bile. This gives to meglitinides flexibility in its administration. Although they are less effective than sulfonylureas because higher blood sugar levels are needed before they can stimulate the insulin secretion from β-cells, in most cases meglitinides are a better option than sulfonylureas and are also prescribed in patients whom metformin is contraindicated. Meglitinides, as short-acting secretagogues, can be used in the place of sulfonylureas in patients with irregular meal schedules or in patients that develop late postprandial hyperglycaemia (PPHG) using sulfonylureas. They also show a good combination with other oral antidiabetic agents, such as metformin and thiazolidinediones, and even with insulin. In combination with the α-glucosidase inhibitor, voglibose, meglitinides have shown to be very effective in preventing PPHG and related atherosclerosis and cardiovascular problems (23, 27).

I.1.1.3.4. Thiazolidinediones

Rosiglitazone and pioglitazone (Figure 5) are representative agents of thiazolidinediones and are responsible for increasing insulin action.

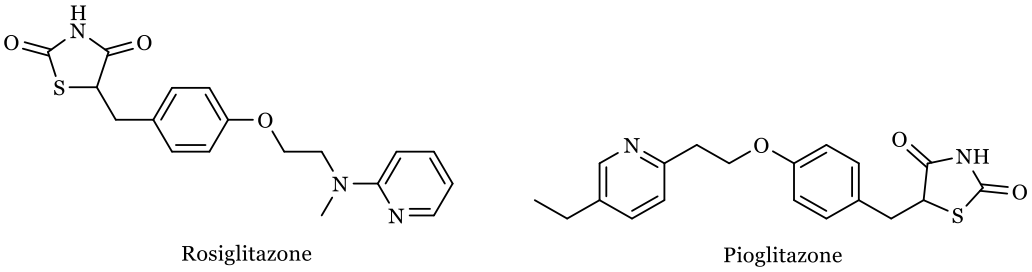


Figure 5: Chemical structures of examples of thiazolidinediones: rosiglitazone and pioglitazone.

These antidiabetic agents act by modulating the PPAR-γ receptor as their selective agonists. Among the tree types of PPARs (PPAR-α, PPAR-δ and PPAR-γ), PPAR-γ is located primarily in adipocytes. Thus, when activated by thiazolidinediones, the PPAR-γ forms a dimer with retinoid X receptor (RXR), modulating the corresponding gene expression. PPAR-γ has demonstrated to be responsible for adipocyte differentiation (12, 26, 27). Thiazolidinediones reduce peripheral insulin resistance and improve β-cell exhaustion through reduction of free fatty acid (FFA) accumulation, decrease in inflammatory cytokines, increase of adiponectin levels, and preservation of β-cell integrity and function. They also increase GLUT4 mediated enhanced glucose utilization in muscle tissue and decrease hepatic glucose output. Thiazolidinediones were found to remodel adipocytes by producing new, small adipocytes which are more sensitive to insulin and promote the apoptosis of old adipocytes (23, 26, 27). Despite this, important concerns are attributed to the use of thiazolidinediones, being associated with cardiac events and increased heart failure. Another serious adverse effect related to the use of thiazolidinediones is fluid retention, leading to increased vascular retention and trans-endothelial permeability. For this reason, these antidiabetic agents are not selected as first-line therapy or even step-up treatment (12, 23, 27, 29).

I.1.1.3.5. Incretin mimetics

Targeting the incretin system has become a significant therapeutic approach for T2D management. The concept “incretin effect” was first recognized in 1960s and is defined as the difference in insulin secretory response from an oral glucose load comparing to an intravenous administration of glucose (30). The incretin effect reduces between 50 % and 70 % the total secretion of insulin after oral glucose intake. In T2D individuals, the incretin effect is reduced or even absent. The naturally occurring incretin hormones are glucagon-like peptide-1 (GLP-1) and glucose-dependent insulinotropic polypeptide (GIP). Both incretins have short half-lives since they are rapidly hydrolysed by the enzyme dipeptidyl peptidase-4 (DPP-4). Incretins have several physiological roles, including glucose-

dependent stimulation of insulin and suppression of glucagon release, insulin biosynthesis and gene transcription activation, increasing of β-cell growth and apoptosis inhibition, gastric emptying reduction, enhancement of glucose uptake and glycogen synthesis in muscle, liver and adipose tissues (23, 27, 30). Diabetic patients demonstrate impaired GLP-1 postprandial secretion, which may explain the defects in insulin response. GIP levels are normal or increased in patients with T2D but the insulinotropic effect is impaired, possibly due to the downregulation of GIP receptor expression as the result of hyperglycaemia (31). The two subclasses of antidiabetic drugs acting on the incretin effect are GLP-1 receptor agonists and DPP-4 inhibitors.

GLP-1 receptor agonists

Efforts have been made to identify new peptides that have similar structure to incretin hormones but are not degraded by DPP-4. Specifically, researchers and pharmaceutical companies have paid attention to structural features of GLP-1, since GLP-1 and not GIP, has relatively preserved insulinotropic activity in patients with T2D. The first GLP-1 receptor agonist was exenatide is a exendin-4 mimetic that presents about 53 % of sequence homology to native GLP-1, and was approved in 2005 by FDA (26, 30). This antidiabetic agent is currently administrated as a single drug or in combination with metformin/sulfonylurea. Exenatide is well tolerated in general but can cause mild to moderate gastrointestinal adverse effects. Currently, the available GLP-1 receptor agonists available are the peptides exenatide, liraglutide, albiglutide, dulaglutide, lixisenatide, and semaglutide. Newer drugs, except lixisenatide have over 90 % of amino acid sequence identity to native human GLP-1 which leads to a lower risk of antibody formation to these peptide medications. Recent studies have demonstrated that GLP-1 receptor agonists can further replace rapid-acting insulin in basal insulin therapy with cost-saving benefits, effective glycaemic control, and reduced risk of weight gain and hypoglycaemia in patients with T2D uncontrolled using basal insulin therapy. Despite their inconvenient route of administration, these drugs are in general well tolerated but can cause mild to moderate gastrointestinal adverse effects, or possible slight effects as nausea, diarrhea, and minor hypoglycaemia (23, 26, 27, 30).

DPP-4 inhibitors

DPP-4 (lymphocyte cell surface protein CD26), detected in endothelium and in blood circulation, is an endopeptidase found in several tissues, including gut, lymphocyte, liver, lungs, and endothelial cells. As mentioned above, this enzyme is responsible for the rapid

degradation of its substrates GLP-1 and GIP, thus DPP-4 inhibition increases the time of action of incretins leading to an increase in insulin secretion (12, 24, 26-28). Since the first DPP-4 inhibitor, sitagliptin, has been released on the market in 2006, several pharmaceutical companies have developed new inhibitors, such as saxagliptin, vildagliptin, linagliptin and alogliptin (Figure 6) (26, 30).

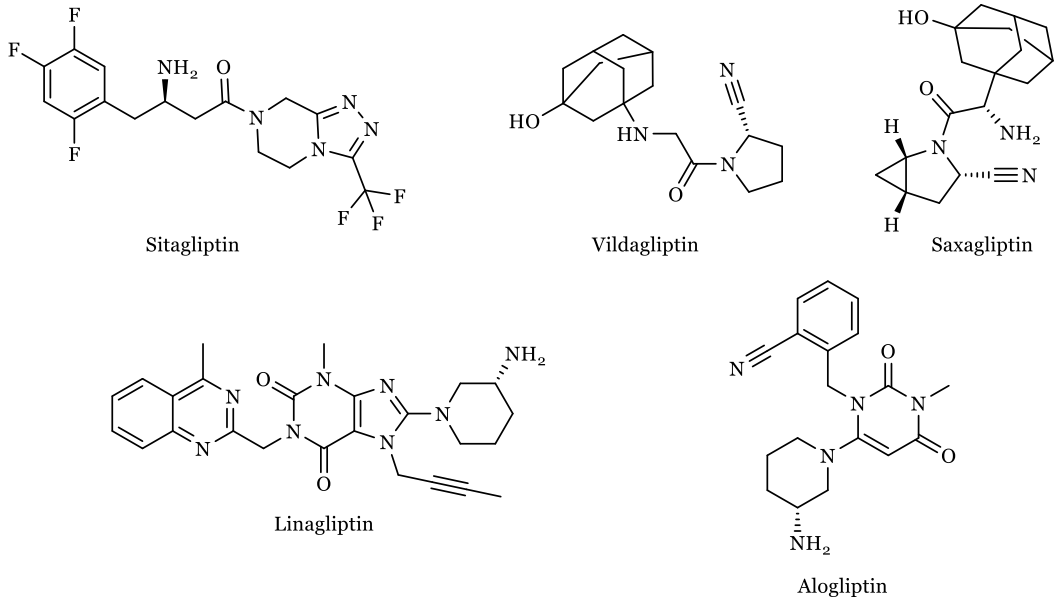


Figure 6: Chemical structures of examples of DPP-4 inhibitors: sitagliptin, vildagliptin, saxagliptin, linagliptin and alogliptin.

They can be used as monotherapy or in combination with metformin, sulfonylureas and thiazolidinediones. DPP-4 inhibitors have a positive effect on PPHG, good tolerability and favourable safety profiles. The tree most common adverse effects associated with the use of DPP-4 inhibitors are nasopharyngitis, upper respiratory tract infection, and headache. Acute pancreatitis was observed in a fraction of diabetic patients using sitagliptin. As a result of their neutral effect on body weight and a recent clinical outcomes trial report on increased risk of hospitalization due to heart failure with the use of saxagliptin, ADA recommends preferred consideration of GLP-1 receptor agonists over DPP-4 inhibitors in patients with cardiovascular diseases or weight-related problems. However, DPP-4 inhibitors are still attractive second-line pharmaceutical options since they are orally available leading to increased patient compliance in comparison with GLP-1 receptor agonists which are administrated by subcutaneous injection (23, 26, 27, 30).

I.1.1.3.6. SGLT2 inhibitors

Glucose is transported across the cell membrane by two major processes, passive and active transport. Passive transport is mediated through the GLUT family of glucose transporters, while active transport takes place in the presence of sodium-driven electrochemical gradient through sodium-glucose cotransporters (SGLTs). SGLTs are mainly found in gastrointestinal tract and kidney, being SGLT1 (primarily found in small intestine) and SGLT2 (mostly found in kidney) the most studied members (26, 27). SGLT2 is the most prevalent subtype at the early proximal tubules of kidney, accounting for more than 90 % of renal glucose reabsorption in normoglycaemic conditions. Nevertheless, high blood glucose levels induce the growth of proximal tubules and SGLT2 expression, leading to increased and undesirable glucose reabsorption (24, 30, 31). In this sense, induction of glycosuria through SGLT2 inhibition has been considered a key mechanism of renal glucose homeostasis (12). SGLT2 inhibitors are among the most recent antidiabetic drugs available in clinical practice, and some examples are canagliflozin, dapagliflozin and empagliflozin (Figure 7). SGLT2 inhibitors block glucose reabsorption in the proximal renal tubule through inhibition of SGLT2, providing insulin-independent glucose reduction. Since these drugs present a glucose-independent mechanism of action, they can be effective in advanced stages of T2D, when a large number of β-cells are permanently lost. The use of SGLT2 inhibitors does not promote weight gain or hypoglycaemia, which are common side effects in conventional antidiabetic drugs. The main side effects that occur with the use of these antidiabetic agents are urinary tract and genital infections. Since SGLT2 inhibitors were recently marketed, compared with other drugs used for the treatment of T2D, the evaluation of efficacy and safety of these agents in several clinical settings has not been yet fully established (23, 24, 27, 30).

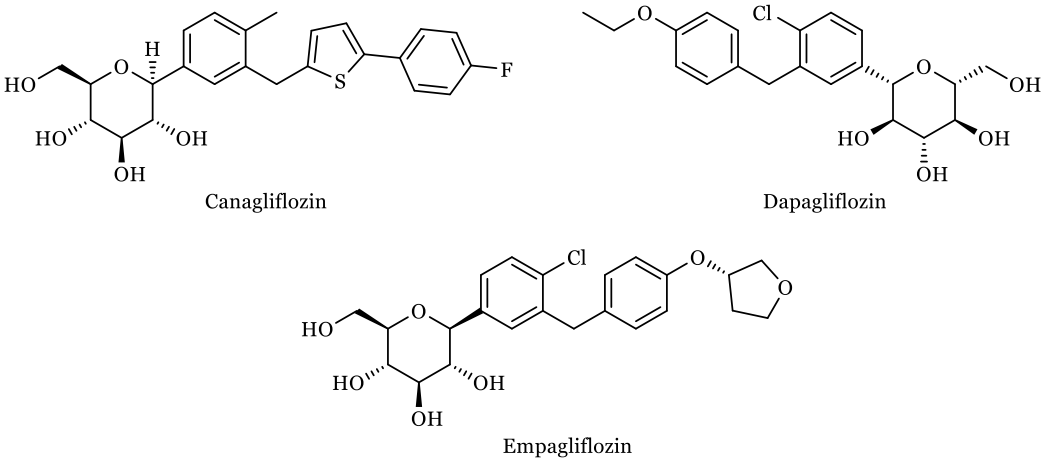


Figure 7: Chemical structures of examples of SGLT2 inhibitors: canagliflozin, dapagliflozin and empagliflozin.

I.1.1.3.7. Insulin

Therapy with insulin must be introduced in newly diagnosed individuals with T2D that present severe symptoms, such as ketosis, and/or very elevated blood glucose (≥ 300 - 350 mg/dL) or HbA1c (≥ 10 -12 %) levels. However, insulin therapy is administrated in most patients during the course of the disease. Insulin therapy has advanced significantly in the last years, for instance by discontinuation of animal forms and introduction of human forms. The alterations of insulin have focused on changing its pharmacokinetics to provide either a more rapid action (to better stimulate the postprandial release of insulin) or more prolonged, in order to reduce the need for twice-daily administration and a more flexible dosing (21).

Basal insulin is the initial insulin regimen and is usually added to metformin and possibly one additional non-insulin agent, and normally covers the long or intermediate acting insulin. If basal insulin promotes acceptable blood glucose levels but HbA1c levels are persistently high, rapid-acting insulin analogue should be used and administrated just before meals. These analogues are sometimes administrated in addition to basal insulin, and are used due to their prompt onset of action. To avoid multiple injections, insulin pump (continuous subcutaneous insulin infusion) may be used (23, 27). In fact, according to the onset of action by synthetic insulin, these analogues have been classified in rapid-acting insulin (e.g. glulisine, lispro and aspart); short-acting insulin (e.g. Humulin R and Novolin R); intermediate-acting insulin (e.g. Humulin N and Novolin N); long-acting insulin (e.g. detemir and glargine); and ultra-long acting insulin (e.g. Degludec) (24, 27). Other areas of research have been focused on the formulation of insulin for delivery by other routes and to reduce the risk of hypoglycaemia. Inhaled insulin (Technosphere insulin-inhalation system, Afrezza) is also currently available for prandial use but requires pulmonary function testing before and after starting therapy. Although inhaled insulin was expected to be revolutionary, some difficulties were found in the development of practical delivery devices and a possible higher risk of developing lung carcinoma mostly hindered the pursuit of this approach. Patients with asthma or other lung diseases must also avoid inhaled insulin therapy (12, 21, 23). The development of oral insulin formulations are equally challenging due to the need to avoid destruction of insulin by intestinal secretions and, at the same time, deliver a predictable amount of insulin to plasma from the intestinal tract (12, 21). In the absence of an adequate treatment, prolonged hyperglycaemia can cause glucose toxicity than can progressively cause impaired insulin secretion. Thus, the initiation of insulin therapy is crucial to reverse the toxic effects of high glucose levels in pancreas. Once continuous glucose control is achieved, insulin therapy can be stopped and replaced with oral antidiabetic agents. It is also known that at some point in the management of T2D, β-cells reserves are exhausted with phenotypical reversal to a T1D kind of pathological

situation and need for continued reliance on insulin therapy is common. Insulin therapy is frequently associated with weight gain and with lipohyperthrophy due to failure to change the subcutaneous injections, leading to poor insulin absorption and suboptimal glycaemic control (23).

Currently, "smart insulins", that are dependent on ambient glucose concentration, are being developed due to the emergence of treatment approaches that aggressively reduce blood glucose levels. These formulations become active when the levels of glucose are increased, so the raised glucose competes with glycosylated insulin for binding to a lectin and consequently freeing insulin (this effect is not observed in normal levels of glucose). This technology is still under development but could be a promising alternative if successful in clinical research (21).

I.1.1.3.8. α-Glucosidase inhibitors

This class of antidiabetic agents inhibits the absorption of carbohydrates from the small intestine reducing the amount of glucose absorbed in the blood. Examples of this class are acarbose, voglibose and miglitol (Figure 8), which competitively and reversibly inhibit the α-glucosidases sucrase-isomaltase (SI) and maltase-glucoamylase (MGAM) present at the brush border of the gut which hydrolyse the oligosaccharides into smaller components which easily enter into the systemic circulation (32, 33).

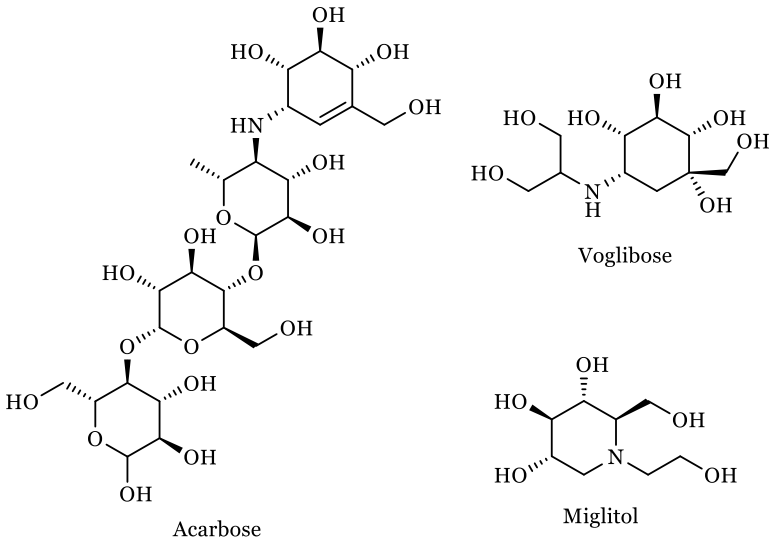


Figure 8: Chemical structures of examples of α-glucosidase inhibitors.

Following the oral administration of α-glucosidase inhibitors, the postprandial glucose absorption is reduced, leading to attenuation of glucose-mediated insulin secretion (24, 26, 27, 29). Since there is a reduction of postprandial raise in glucose and insulin levels, the triglyceride uptake into adipocytes and hepatic lipogenesis are also decreased, showing a protective metabolic effect. Studies in animal models have demonstrated a decrease in urinary glucose loss and prevention of GLUT4 receptor loss in skeletal muscles, after the use of acarbose. In addition, AGE were also reduced, as well as all glycaemic parameters. α-Glucosidase inhibitors can be a good option as first-line therapy since they reduce PPHG in most patients and HbA1c levels in about 52 % of patients. An additional advantage associated with the use of these antidiabetic agents is the negligible hypoglycaemia and no advert effect of weight gain. Miglitol has shown to improve vascular functions in humans, with increased IL-6 inhibition which is a marker of cardiovascular disease (27). However, the use of α-glucosidase inhibitors is commonly related with severe gastrointestinal effects such as flatulence, diarrhoea and abdominal distention, leading with possible incompliance in about 25 % to 45 % of patients to this therapeutic approach (26, 29, 34).

I.1.1.3.9. Amylin analogue

Amylin, also known as islets amyloid polypeptide, is a neuroendocrine hormone synthesized in pancreatic β-cells and co-secreted along with insulin and shares the same processing enzymes with insulin. Amylin is also released in a nutrient responsive manner, similarly to insulin. Amylin has two forms, non-glycosylated (the active form) and glycosylated form. This hormone acts both in carbohydrate absorption and its disposal and is mainly eliminated through renal metabolism (24, 27, 35). It accelerates the muscle glycogenolysis, although inducing glycogen formation in liver. One of the major activities of amylin is mediated by delaying the gastric emptying and inhibiting postprandial glucagon secretion, leading to satiety and reduction of food intake, in a more potent way than GLP-1. The only amylin analogue currently available in clinical practice is Pramlintide (Symlin by Amylin Pharmaceuticals) which is used by subcutaneous administration in combination with mealtime insulin in diabetic patients who fail to respond to insulin. The use of amylin analogue is also associated with reduction of diurnal glucose fluctuations, decrease of insulin dose and improvement of HbA1c levels. The major adverse effect found using amylin analogue is nausea (24, 27, 36).

I.1.1.4. Future perspectives in therapeutic targets

Conventional therapies used for the management of T2D have been very beneficial but are frequently associated with adverse events leading to market withdrawals (27). The complex pathophysiology of T2D provide a variety of therapeutic targets that enable drugs with different mechanisms of action to act in combination to improve glycaemic control. In fact, the combination of antidiabetic agents can achieve a similar or a better efficacy than the use of only one agent, frequently with less adverse effects (37). The growing availability of fixed-dose oral and fixed-injectable combination therapy makes combination therapy easier by reducing the pill/injection burden, and consequently increasing therapeutic adherence. Despite the advantages of early, effective, and continued control of blood glucose levels in T2D being well-known, a large proportion of patients (about 30 - 60 % of occidental societies) fail to achieve or maintain glycaemic control. For this reason, the occurrence of complications remains significantly high, which signifies the need of develop new glucose-lowering agents and strategies to address poor adherence to treatment by patients (37). Given the complexity of T2D, nanotechnology-based approaches could be a good therapeutic option, as it comes with added advantage of site-specific drug delivery with higher bioavailability and reduced dosage regimen. To date, several nanotools have proven to be promising drug carriers for treatment of T2D. These advances in nanotechnology might offer appealing prospects regarding the development of efficient glucose lowering therapy (33).

Despite the meaningful progress in the management of metabolic diseases, the prevalence of TD2 and obesity is still growing. This increase demonstrates the importance of accelerating the translation of basic research achievements to safe and effective new drugs, following the rationale of combination therapy. For example, the pharmacological treatment with long-acting GLP-1 receptor agonists provides a clear weight loss and improves T2D management. However, the dose-dependent adverse gastrointestinal effects are a limiting factor in the maximal efficacy that can be achieved with these agonists. Thus, the combination of GLP-1 with another hormone analogue can provide the delivery of amplified metabolic benefits without compromising safety. To achieve this goal, a natural starting point would be the combination of GLP-1 with other endocrine factors that robustly suppress appetite and/or improve glycaemic control, such as cholecystokinin, peptide YY, glucagon, gastrin, fibroblast growth factor (FGF)21, among others. It has becoming evident that coordinated targeting of multiple pathways is required for the pharmaceutical treatment of metabolic disorders, controlling food intake, energy expenditure and glucose metabolism (38). In fact, with no widely effective treatment, and rates of T2D continuing to rise alongside costs, the toll of this disease seems to be unyielding. Several new potential therapeutic approaches for insulin sensitization have been under intensive study (39). Apart

from the combination of therapies to achieve good and continuous glycaemic control, novel pipeline candidates include G protein coupled receptor (GPCR)40 agonists, glucokinase (GK) activators, glycogen synthase-3 (GSK-3) inhibitors, and GPCR21 inhibitors, with the potential to be used in the near future. Another example would be the administration of FGF1, which is produced in ependymal cells of the central nervous system, and interacts with tanycytes, astrocytes and glucose-sensing neurons of the hypothalamus to influence feeding and glycaemic control (39). Other different therapeutic targets are being developed, including free fatty acid receptor (FFAR)1 and GPCR119 to increase β-cell secretory function; liver-derived proteins such as betatrophin, and forkhead box protein O1 (FOXO1) to increase β-cell mass; glucagon-receptor antagonists and glucagon antibodies, and oxyntomodulin to decrease the effect of glucagon; targeting glucose 6-phosphatase, fructose 1,6-bisphosphatase (FBPase), glycogen phosphorylase, and carnitine palmitoyltransferase-1 (CPT-1) to reduce hepatic production of glucose; adenosine monophosphate (AMP) kinase, sirtuin 1 (SIRT1), and protein tyrosine phosphatase 1B (PTP1B), to increase insulin action; IκB kinase β (IKKβ)-NF-κB pathway, and IL-1β receptor agonists and IL-1β antibodies to decrease cellular inflammation; and 11β-hydroxysteroid dehydrogenase type 1 (11β-HSD1) to reduce cortisol production (21). Protein tyrosine phosphatase 1B (PTP1B) (subsections I.1.3.a and II.3) and fructose 1,6-bisphosphatase (FBPase) (subsection II.5) are further described in this thesis. In this sense, the search of novel antidiabetic molecules targeting those approaches, such as natural products, is an important topic of research for promising and effective future therapeutics that could lead towards the hope of the better management of T2D in our society (27) .

Another alternative to finding new agents is to evaluate existing drugs for their potential utility in the treatment of T2D. Colesvelam and bromocriptine, which were previously approved by the FDA for other indications, have been further indicated for T2D management. Colesvelam, a bile acid sequestrant traditionally used for the treatment of hyperlipidaemia, also delays or alters absorption of glucose from the intestine. The main side effects associated with colesvelam are gastrointestinal adverse effects and increased triglyceride levels (29, 40). Bromocriptine, a dopamine-2 receptor agonist, was shown to reduce HbA1c levels. The use of this agent has been associated with cardiovascular events, and the main side effects include nausea, vomiting, fatigue, dizziness, and hypotension. The administration of both drugs is not frequently recommended, not only due to their adverse effects, but also because they are not highly effective in reducing blood glucose levels (29, 41).

Due to progressive loss of insulin-producing β-cells, some remarkable advances have been made in generating β-cells to mitigate the aberrant glucose homeostasis manifested in

diabetes. The approaches studied in this field include human stem cell differentiation to enable the generation of mature β-cells with dynamic insulin secretion and metabolic properties similar to primary β-cells. In addition to β-cells, differentiation of other hormone-expressing islet cell types is under study. In addition, transdifferentiation of endogenous non-β-cells to insulin-producing cells is being explored as an alternative strategy to enhance the level of functional β-cells (12, 14, 42).

In spite of the advances in the field of T2D, the interaction of genes with the environment that cause progressive loss of β-cell function is still unclear. Understanding the genetics and additional metabolic markers in T2D is important to better recognize the pathophysiology of T2D and the heterogeneity of responses to different glucose-lowering therapies (15, 21).

I.1.1.5. References

1. World Health Organization. Classification of diabetes mellitus 2019 [Available from: https://www.who.int/publications/i/item/classification-of-diabetes-mellitus].

2. Barrès R, Zierath JR. The role of diet and exercise in the transgenerational epigenetic landscape of T2DM. Nat Rev Endocrinol. 2016;12(8):441-51.

3. Canfora EE, Meex RCR, Venema K, Blaak EE. Gut microbial metabolites in obesity, NAFLD and T2DM. Nat Rev Endocrinol. 2019;15(5):261-73.

4. World Health Organization. The top 10 causes of death 2020 [Available from: https://www.who.int/news-room/fact-sheets/detail/the-top-10-causes-of-death].

5. American Diabetes Association. 2. Classification and diagnosis of diabetes: standards of medical care in diabetes - 2020. Diabetes Care. 2020;43(Supplement 1):S14-S31.

6. American Diabetes Association. Diagnosis and classification of diabetes mellitus. Diabetes Care. 2014;37(Suppl 1):S81-S90.

7. Katsarou A, Gudbjörnsdottir S, Rawshani A, Dabelea D, Bonifacio E, Anderson BJ, et al. Type 1 diabetes mellitus. Nat Rev Dis Primers. 2017;3(17016):1-17.

8. Rewers M, Ludvigsson J. Environmental risk factors for type 1 diabetes. Lancet. 2016;387(10035):2340-8.

9. DeFronzo RA, Ferrannini E, Groop L, Henry RR, Herman WH, Holst JJ, et al. Type 2 diabetes mellitus. Nat Rev Dis Primers. 2015;1(15019):1-22.

10. International Diabetes Federation. IDF Diabetes Atlas 9th edition. 2019.

11. Kharroubi AT, Darwish HM. Diabetes mellitus: the epidemic of the century. World J Diabetes. 2015;6(6):850-67.

12. Tan SY, Mei Wong JL, Sim YJ, Wong SS, Mohamed Elhassan SA, Tan SH, et al. Type 1 and 2 diabetes mellitus: A review on current treatment approach and gene therapy as potential intervention. Diabetes Metab Syndr. 2019;13(1):364-72.

13. Zheng Y, Ley SH, Hu FB. Global aetiology and epidemiology of type 2 diabetes mellitus and its complications. Nat Rev Endocrinol. 2018;14(2):88-98.

14. Nair GG, Tzanakakis ES, Hebrok M. Emerging routes to the generation of functional β-cells for diabetes mellitus cell therapy. Nat Rev Endocrinol. 2020;16(9):506-18.

15. Krentz NAJ, Gloyn AL. Insights into pancreatic islet cell dysfunction from type 2 diabetes mellitus genetics. Nat Rev Endocrinol. 2020;16(4):202-12.

16. Frank JA, Broichhagen J, Yushchenko DA, Trauner D, Schultz C, Hodson DJ. Optical tools for understanding the complexity of β-cell signalling and insulin release. Nat Rev Endocrinol. 2018;14(12):721-37.

17. Jacobson DA, Weber CR, Bao S, Turk J, Philipson LH. Modulation of the pancreatic islet β-cell-delayed rectifier potassium channel Kv2.1 by the polyunsaturated fatty acid arachidonate. J Biol Chem. 2007;282(10):7442-9.

18. Arrojo e Drigo R, Ali Y, Diez J, Srinivasan DK, Berggren P-O, Boehm BO. New insights into the architecture of the islet of Langerhans: a focused cross-species assessment. Diabetologia. 2015;58(10):2218-28.

19. Rorsman P, Ashcroft FM. Pancreatic β-cell electrical activity and insulin secretion: of mice and men. Physiol Rev. 2018;98(1):117-214.

20. Eizirik DL, Pasquali L, Cnop M. Pancreatic β-cells in type 1 and type 2 diabetes mellitus: different pathways to failure. Nat Rev Endocrinol. 2020;16(7):349-62.

21. Kahn SE, Cooper ME, Del Prato S. Pathophysiology and treatment of type 2 diabetes: perspectives on the past, present, and future. Lancet. 2014;383(9922):1068-83.

22. Yaribeygi H, Farrokhi FR, Butler AE, Sahebkar A. Insulin resistance: Review of the underlying molecular mechanisms. J Cell Physiol. 2019;234(6):8152-61.

23. Chaudhury A, Duvoor C, Reddy Dendi VS, Kraleti S, Chada A, Ravilla R, et al. Clinical review of antidiabetic drugs: implications for type 2 diabetes mellitus management. Front Endocrinol (Lausanne). 2017;8(6):1-12.

24. Marín-Peñalver JJ, Martín-Timón I, Sevillano-Collantes C, del Cañizo-Gómez FJ. Update on the treatment of type 2 diabetes mellitus. World J Diabetes. 2016;7(17):354-95.

25. Chamberlain JJ, Herman WH, Leal S, Rhinehart AS, Shubrook JH, Skolnik N, et al. Pharmacologic therapy for type 2 diabetes: synopsis of the 2017 American Diabetes Association Standards of Medical Care in Diabetes. Ann Intern Med. 2017;166(8):572-8.

26. Tahrani AA, Barnett AH, Bailey CJ. Pharmacology and therapeutic implications of current drugs for type 2 diabetes mellitus. Nat Rev Endocrinol. 2016;12(10):566-92.

27. Kumar A, Bharti SK, Kumar A. Therapeutic molecules against type 2 diabetes: what we have and what are we expecting? Pharmacol Rep. 2017;69(5):959-70.

28. Nasykhova YA, Tonyan ZN, Mikhailova AA, Danilova MM, Glotov AS. Pharmacogenetics of type 2 diabetes-progress and prospects. Int J Mol Sci. 2020;21(18):1-26.

29. Mazzola N. Review of current and emerging therapies in type 2 diabetes mellitus. Am J Manag Care. 2012;18(1 Suppl):S17-S26.

30. Heo CU, Choi CI. Current progress in pharmacogenetics of second-line antidiabetic medications: towards precision medicine for type 2 diabetes. J Clin Med. 2019;8(3):1-28.

31. Libianto R, Ekinci EI. New agents for the treatment of type 2 diabetes. Crit Care Clin. 2019;35(2):315-28.

32. Sim L, Willemsma C, Mohan S, Naim HY, Pinto BM, Rose DR. Structural basis for substrate selectivity in human maltase-glucoamylase and sucrase-isomaltase N-terminal domains. J Biol Chem. 2010;285(23):17763-70.

33. Padhi S, Nayak AK, Behera A. Type II diabetes mellitus: a review on recent drug based therapeutics. Biomed Pharmacother. 2020;131(110708):1-23.

34. Derosa G, Maffioli P. α-Glucosidase inhibitors and their use in clinical practice. Arch Med Sci. 2012;8(5):899-906.

35. Schmitz O, Brock B, Rungby J. Amylin agonists: A novel approach in the treatment of diabetes. Diabetes. 2004;53(suppl 3):S233-8.

36. Hoogwerf BJ, Doshi KB, Diab D. Pramlintide, the synthetic analogue of amylin: physiology, pathophysiology, and effects on glycemic control, body weight, and selected biomarkers of vascular risk. Vasc Health Risk Manag. 2008;4(2):355-62.

37. Bailey CJ, Day C. The future of new drugs for diabetes management. Diabetes Res Clin Pract. 2019;155(107785):1-27.

38. Clemmensen C, Finan B, Müller TD, DiMarchi RD, Tschöp MH, Hofmann SM. Emerging hormonal-based combination pharmacotherapies for the treatment of metabolic diseases. Nat Rev Endocrinol. 2019;15(2):90-104.

39. Gasser E, Moutos CP, Downes M, Evans RM. FGF1 — a new weapon to control type 2 diabetes mellitus. Nat Rev Endocrinol. 2017;13(10):599-609.

40. Ooi CP, Loke SC. Colesevelam for type 2 diabetes mellitus: an abridged Cochrane review. Diabet Med. 2014;31(1):2-14.

41. Reda E, Hassaneen S, El-Abhar HS. Novel trajectories of bromocriptine antidiabetic action: leptin-IL-6/ JAK2/p-STAT3/SOCS3, p-IR/p-AKT/GLUT4, PPAR-γ/adiponectin, Nrf2/PARP-1, and GLP-1. Front Pharmacol. 2018;9(771):1-12.

42. Wang P, Fiaschi-Taesch NM, Vasavada RC, Scott DK, García-Ocaña A, Stewart AF. Diabetes mellitus—advances and challenges in human β-cell proliferation. Nat Rev Endocrinol. 2015;11(4):201-12.

I.1.2. Flavonoids as potential agents in the management of type 2 diabetes through the modulation of α-amylase and α-glucosidase activity: a review

Version of record from Critical Reviews in Food Science and Nutrition

Copyright © (2021) with kind permission of Taylor & Francis

"A fixed version of a journal article that has been made available by Taylor & Francis, a publisher by formally and exclusively declaring the article 'published'."

CRITICAL REVIEWS IN FOOD SCIENCE AND NUTRITION
https://doi.org/10.1080/10408398.2020.1862755

Taylor & Francis
Taylor & Francis Group

REVIEW

Check for updates

Flavonoids as potential agents in the management of type 2 diabetes through the modulation of α-amylase and α-glucosidase activity: a review

Carina Proença, Daniela Ribeiro, Marisa Freitas, and Eduarda Fernandes

LAQV, REQUIMTE, Laboratory of Applied Chemistry, Department of Chemical Sciences, Faculty of Pharmacy, University of Porto, Porto, Portugal

ABSTRACT

Type 2 diabetes (T2D) is one of the most prevalent metabolic diseases worldwide and is characterized by increased postprandial hyperglycemia (PPHG). α-Amylase and α-glucosidase inhibitors have been shown to slow the release of glucose from starch and oligosaccharides, resulting in a delay of glucose absorption and a reduction in postprandial blood glucose levels. Since current α-glucosidase inhibitors used in the management of T2D, such as acarbose, have been associated to strong gastrointestinal side effects, the search for novel and safer drugs is considered a hot topic of research. Flavonoids are phenolic compounds widely distributed in the Plant Kingdom and important components of the human diet. These compounds have shown promising antidiabetic activities, including the inhibition of α-amylase and α-glucosidase. The aim of this review is to provide an overview on the scientific literature concerning the structure-activity relationship of flavonoids in inhibiting α-amylase and α-glucosidase, including their type of inhibition and experimental procedures applied. For this purpose, a total of 500 compounds is covered in this review. Available data may be considered of high value for the design and development of novel flavonoid derivatives with effective and potent inhibitory activity against those carbohydrate-hydrolyzing enzymes, to be possibly used as safer alternatives for the regulation of PPHG in T2D.

KEYWORDS

Antidiabetic agents; diabetes *mellitus*; digestive hydrolyzing enzymes; inhibitory activity; phenolic compounds

Introduction

Diabetes comprises a group of metabolic disorders characterized by chronic hyperglycemia. This disease results from the impairment of insulin secretion, insulin action or a combination of both. Insulin deficiency and resistance to insulin action on target tissues lead to disturbances in carbohydrate, fat and protein metabolism (Kahn, Cooper, and Del Prato 2014; Kharroubi and Darwish 2015; Eizirik, Pasquali, and Cnop 2020). Diabetes is associated with numerous acute and long-term complications. Acute complications, with a substantial short-term risk of morbidity and mortality, encompass diabetic ketoacidosis, hyperosmolar hyperglycemic state, and malignant hyperthermia-like syndrome with rhabdomyolysis (Pinhas-Hamiel and Zeitler 2007; Forbes and Cooper 2013). Long-term complications include hypertension, nephropathy, retinopathy, dyslipidemia, nonalcoholic fatty liver disease, neuropathy, cardiovascular and atherosclerotic complications (Pinhas-Hamiel and Zeitler 2007; Forbes and Cooper 2013). The most common symptoms of hyperglycemia are polyuria, polydipsia, unexplained weight loss, polyphagia and blurred vision (American Diabetes Association 2014). According to the American Diabetes Association (ADA), diabetes can be classified as type 1 diabetes (T1D) (resulting from the autoimmune destruction of pancreatic β-cells), type 2 diabetes (T2D) (progressive loss of insulin secretion from β-cells, usually on the background of resistance to insulin), gestational diabetes (GD) (diagnosed in the second or third trimester of pregnancy that was not clearly diagnosed as diabetes prior to gestation) and specific types of diabetes, due to other causes (American Diabetes Association 2018). The International Diabetes Federation (IDF) estimated that, in 2019, about 463 million adults had diabetes, and predicts that, in 2054, 700 million adults across the globe will suffer from this metabolic disease. T2D is the most common type of diabetes, accounting for around 90% of all diabetes cases (International Diabetes Federation 2019). Due to the variable and progressive pathophysiological changes associated to T2D, pharmacological compounds acting in different targets are available for different stages of the disease (Tahrani et al. 2011).

However, many of these treatments have several side effects, and long-term efficacy is difficult to achieve without regular adjustment and combination therapy. Thus, the search for novel, effective and safer drugs is considered a hot topic of research. In fact, several research studies have revealed a promising inhibitory activity of α-amylase and α-glucosidase by flavonoids. The purpose of this review is to provide an overview on the scientific literature concerning the structure-activity relationship (SAR) of flavonoids in inhibiting α-amylase and α-glucosidase activities, including their type of inhibition and experimental procedures applied,

CONTACT Eduarda Fernandes egracas@ff.up.pt LAQV, REQUIMTE, Laboratory of Applied Chemistry, Department of Chemical Sciences, Faculty of Pharmacy, University of Porto, Rua de Jorge Viterbo Ferreira n.° 228, 4050-313 Porto, Portugal.

© 2021 Taylor & Francis Group, LLC

covering a total of 500 compounds. For this purpose, this manuscript provides a small appraisal on T2D and the available antidiabetic agents, with special focus on their inhibitory activity against α-amylase and α-glucosidase activity. This is followed by the definition, classification and metabolism of flavonoids, ending with the analysis of the available studies on the inhibitory effect of flavonoids against those carbohydrate-hydrolyzing enzymes.

Type 2 diabetes

T2D is characterized by impairment of carbohydrate, lipid, and protein metabolism, leading to high glucose levels in blood. The main cause of T2D is the progressive reduction of insulin secretion from pancreatic β-cells, frequently upon a background of preexisting resistance of insulin in skeletal muscle, liver and adipose tissue (DeFronzo et al. 2015).

The core defects of insulin resistance in liver, muscle and adipocytes, and progressive β-cell failure are present virtually in all T2D patients. In addition to these abnormalities, five other pathophysiologic conditions are responsible for glucose intolerance in T2D: chronic exposure to non-esterified fatty acids (lipotoxicity); decreased incretin [glucagon-like peptide-1 (GLP-1) and glucose-dependent insulinotropic polypeptide (GIP)] effect as a result of impaired GLP-1 secretion, as well as β-cell resistance to stimulatory effect of incretin hormones; increased glucagon secretion by α-cells and increased hepatic sensitivity to glucagon, resulting in an increase in hepatic glucose production and its impaired suppression by insulin; enhanced renal glucose reabsorption by the sodium/glucose transporter-2 (SGLT2), leading to a maintenance in high blood glucose levels; central nervous system resistance to the appetite-suppressive effects of insulin and impaired neurosynaptic hormone secretion, contributing to appetite dysregulation and weight gain, which exacerbate the underlying resistance (DeFronzo et al. 2015).

In addition, genome-wide association studies (GWAs) reported more than 100 common genetic variants associated with T2D, including single-nucleotide polymorphisms (SNPs) in *TCF7L2*, *SLC30A8*, *FTO*, *CDKAL1*, *CDKN2A*, and *CDKN2B*, among others (DeFronzo et al. 2015). However, the currently identified genetic variants only increase around 10% to 20% the risk of T2D. Thus, the described SNPs do not explain the majority of the heritability (≈ 85%), and other alternatives have been raised: the heterogeneity of the disease, gene-environment interactions and epigenetic mechanisms (Kahn, Cooper, and Del Prato 2014; DeFronzo et al. 2015). Environmental factors play a key role in the rapid increase in prevalence of T2D, and include the increase in caloric intake, decrease in energy expenditure, obesity, nutrient composition (specifically increased amount of dietary fat, regular consumption of red meat and sugary beverages), cigarette smoking and drug- or chemical-induced diabetes (such as in the treatment of HIV/AIDS or after organ transplantation). Furthermore, a reduction of responsiveness of β-cells to carbohydrate partly underlies the reduction in glucose tolerance with ageing (Kahn, Cooper, and Del Prato 2014; DeFronzo et al. 2015). Other multiple factors are related to an increased risk of β-cell failure, such as incretin hormone resistance and/or deficiency, lipotoxicity, glucotoxicity, hypersecretion of islet amyloid polypeptide (IAPP), oxidative/nitrosative stress and inflammation (Donath and Shoelson 2011; Pitocco et al. 2013; DeFronzo et al. 2015; Donath 2016). Inflammation plays an important role in the pathophysiology of T2D, resulting in altered levels of specific cytokines and chemokines, alterations in the number and activation state of different populations of leukocytes, and increased leukocyte apoptosis and tissue fibrosis (Donath and Shoelson 2011; Donath 2016).

It is well known that T2D is responsible for numerous microvascular and macrovascular complications, depending on the severity and duration of hyperglycemia. Microvascular complications result from hyperglycemia promoted by the activation of major pathological pathways as: enhanced polyol pathway flux, raised generation of advanced glycation end products (AGEs), increased AGE receptor expression, activation of protein kinase C (PKC) isoforms, increased hexosamine flux and high production of reactive oxygen (ROS) and nitrogen species (RNS) (DeFronzo et al. 2015). The mechanisms that contribute for the microvascular complications, also contribute to the macrovascular complications. The major microvascular complications include retinopathy, nephropathy and neuropathy (Forbes and Cooper 2013). Accelerated cardiovascular disease, resulting in myocardial infarction and congestive heart failure, and cerebrovascular disease, manifesting as strokes, are significantly increased in T2D and also constitute one of the major macrovascular complications. Moreover, hypertension is 2-fold enhanced in T2D, and largely contributes to the macrovascular complications observed in those patients (Forbes and Cooper 2013; DeFronzo et al. 2015). Other chronic complications associated to diabetes are depression, dementia and sexual dysfunction (Forbes and Cooper 2013).

The current available drugs used in the management of T2D are biguanide, sulphonylureas, meglitinides, α-glucosidase inhibitors, thiazolidinediones, GLP-1 receptor agonists, dipeptidyl pedptidase-4 (DPP-4) inhibitors, SGLT2 inhibitors, amylin analogues, and insulin. These antidiabetic agents, their route of administration, mechanism of action, benefits and limitations are summarized in Table 1.

α-Amylase and α-glucosidases

In humans, the enzymes α-amylase and α-glucosidase are involved in the breakdown of dietary starch and sugars into glucose. α-1,4-Glucan-4-glucanohydrolases (EC 3.2.1.1.), commonly known as α-amylases, belong to the family 13 of glycoside hydrolases (GH), and can be found in saliva and pancreatic juice (Butterworth, Warren, and Ellis 2011; Patel et al. 2017). Both isozymes, salivary and pancreatic α-amylase, are expressed from genes AMY1 and AMY2, respectively, and are composed by 496 amino acids in a single polypeptide chain. They possess three different domains (A, B and C) and a common calcium-binding site responsible for the stabilization of the interface between the central A

Table 1. Available antidiabetic agents: examples, route of administration, mechanism of action, benefits and limitations.

Class of antidiabetic agents	Examples	Administration	Primary mechanism of action	Benefits	Limitations	References
Biguanide	Metformin	Oral	Inhibition of hepatic gluconeogenesis Increase of insulin sensitivity in liver and muscle Interference with glucose and lactate in the intestine	- HbA_{1c} reduction of up to 1.5% as monotherapy - No weight gain - Low risk of hypoglycaemia - Improves atherogenic lipid profiles and reduces CV event rates and mortality - Low cost	- Common gastrointestinal side-effects - Possible lactic acidosis when renal clearance is limited - Avoid use in deteriorating renal function or hypoxaemic states	(Barnett and Grice 2011; Tahrani et al. 2011; Wright and Tylee 2016; Chaudhury et al. 2017; Kumar, Bharti, and Kumar 2017; Chikara et al. 2018; Davies et al. 2018)
Sulphonylureas	Gliclazide Glipizide Glimepiride Glibenclamide	Oral	Stimulation of insulin secretion by binding to sulphonylurea receptors 1 in β-cells, leading to depolarization and calcium influx	- Rapid onset of action and almost immediate effects on blood glucose - HbA_{1c} reduction of up to 1.5% as monotherapy - Low cost	- Weight gain - Risk of hypoglycaemia - Possible need of self-monitoring of blood glucose levels	(Barnett and Grice 2011; Tahrani et al. 2011; Wright and Tylee 2016; Chikara et al. 2018; Davies et al. 2018)
Meglitinides	Nateglinide Repaglinide	Oral	Stimulation of insulin secretion by binding to sulphonylurea receptors 1 in β-cells (but in a different site of sulphonylureas), resulting in a faster and shorter insulin response	- Rapid onset of action - Suitable for prandial use - Repaglinide associated with HbA_{1c} reduction of up to 1.5% as monotherapy	- Weight gain - Risk of hypoglycaemia - Multiple daily dosing required	(Barnett and Grice 2011; Tahrani et al. 2011; Chaudhury et al. 2017; Chikara et al. 2018; Davies et al. 2018)
α-Glucosidase inhibitors	Acarbose Voglibose Miglitol	Oral	Inhibition of polysaccharides and oligosaccharides degradation in small intestine, delaying glucose absorption	- Low risk of hypoglycaemia - No weight gain - HbA_{1c} reduction of 0.5–0.8% as monotherapy - Acarbose has shown benefits on CV outcomes beyond glycaemic control - Low cost	- Gastrointestinal side-effects (e.g., flatulence, diarrhea, bloating) - Must be taken with meals containing digestible carbohydrates	(Barnett and Grice 2011; Tahrani et al. 2011; Joshi et al. 2015; Kumar, Bharti, and Kumar 2017; Chikara et al. 2018; Davies et al. 2018)
Thiazolidinediones	Pioglitazone Rosiglitazone	Oral	Increase of insulin sensitivity in muscle, liver and adipose tissue Peroxisome proliferator activated receptor γ agonists that act mainly in the adipose tissue to enhance subcutaneous adipogenesis and decrease release of free fatty acids	- HbA_{1c} reduction of up to 1.5% as monotherapy - Low risk of hypoglycaemia - Preservation of markers of β-cell function - Sustained long-term glycaemic control	- Slow onset of action - Common weight gain - Fluid retention may lead to oedema, and new or worsening heart failure - Rosiglitazone is not recommended in patients with ischemic heart disease - Increased risk of distal bone fracture	(Tahrani et al. 2011; Wright and Tylee 2016; Chaudhury et al. 2017; Kumar, Bharti, and Kumar 2017; Chikara et al. 2018; Davies et al. 2018)
GLP-1 receptor agonists	Exenatide Liraglutide	Subcutaneous injection	Stimulation of glucose-dependent insulin secretion and inhibition of glucagon release, delay of gastric emptying and appetite suppression, by binding to GLP-1 receptor	- Weight loss - Low risk of hypoglycaemia (unless combined with sulphonylureas) - Possible effect on preservation or even restore of β-cell function	- Unconfirmed association with pancreatitis and medullary cell carcinoma - Gastrointestinal side-effects - Avoid use in renal failure	(Barnett and Grice 2011; Tahrani et al. 2011; Chaudhury et al. 2017; Scheen 2017; Chikara et al. 2018; Libianto and Ekinci 2019)

(*continued*)

Table 1. Continued.

Class of antidiabetic agents	Examples	Administration	Primary mechanism of action	Benefits	Limitations	References
DPP-4 inhibitors	Sitagliptin Vildagliptin Saxagliptin	Oral	Since DPP-4 rapidly inactivates GLP-1 and GIP, its inhibition results in an increased half-life of these incretin hormones leading to stimulation of glucose-dependent insulin secretion and inhibition of glucagon release	- Low risk of hypoglycaemia (unless when combined with sulphonylureas) - No weight gain - Possible effect on β-cell survival and function	- Possible increased risk of CV events - Unconfirmed association with pancreatitis	(Barnett and Grice 2011; Tahrani et al. 2011; Bonora and Cigolini 2016; Wright and Tylee 2016; Chaudhury et al. 2017; Kumar, Bharti, and Kumar 2017; Scheen 2017; Chikara et al. 2018; Davies et al. 2018; Ahrén 2019; Libianto and Ekinci 2019)
SGLT2 inhibitors	Canagliflozin Dapagliflozin Empagliflozin	Oral	Reduction of renal tubular glucose reabsorption, which facilitates its excretion in urine, reducing blood glucose levels without stimulating insulin release	- Weight loss - Reduction of blood pressure - HbA_{1c} reduction of 0.5–1.0%	- Increased risk of genital mycotic infections, urinary tract infections and osmotic diuresis - Possible episodes of ketoacidosis	(Chao and Henry 2010; Angelopoulos and Doupis 2014; Wright and Tylee 2016; Chaudhury et al. 2017; Scheen 2017; Chikara et al. 2018; Libianto and Ekinci 2019)
Amylin analogue	Pramlintide	Subcutaneous injection	Reduces PPHG by centrally mediated satiety, resulting in inhibition of postprandial glucagon release and delay of gastric emptying	- Weight loss - HbA_{1c} reduction of 0.5–0.8% - β-Cell not required for glucose-lowering effect so can be used in patients with advanced disease	- Nausea - High risk of hypoglycaemia - Only used with insulin	(Barnett and Grice 2011; Tahrani et al. 2011; Chaudhury et al. 2017; Kumar, Bharti, and Kumar 2017; Davies et al. 2018)
Insulin	Aspart and Glargine (long acting) Actrapid® (short acting) Insulatard® (intermediate acting)	Subcutaneous injection	Direct activation of insulin receptor, reducing hepatic glucose output and lipolysis	- Sustained long-term glycaemic control compared with other drugs	- Weight gain - Risk of hypoglycaemia - Fluid retention - Need for self-monitoring of blood glucose levels	(Tahrani et al. 2011; Wright and Tylee 2016; Chaudhury et al. 2017; Kumar, Bharti, and Kumar 2017; Chikara et al. 2018; Davies et al. 2018)

CV – Cardiovascular; DPP-4 – dipeptidyl-peptidase-4; HbA_{1C} – glycated hemoglobin; GIP – glucose-dependent insulinotropic polypeptide; GLP-1 – glucagon-like peptide-1; PPHG – postprandial hyperglycemia; SGLT2 – sodium-glucose transporter-2.

domain and the variable B domain. The catalytic triad (Asp, Asp, Glu) is located in the A domain and the active site is found in a long cleft between the carboxyl end of both A and B domains. The C domain has a β-sheet structure linked to the A domain by a simple polypeptide chain (Sales et al. 2012; Liu et al. 2017; Martinez-Gonzalez et al. 2017).

Starch represents the major source of energy in the human diet. Before being absorbed, starch is sequentially hydrolyzed by salivary and pancreatic α-amylases, in the mouth and small intestine, respectively (Brayer et al. 2000; Butterworth, Warren, and Ellis 2011; Dhital et al. 2017). These isozymes catalyze the initial hydrolysis of starch and other carbohydrate polymers into smaller oligomers, such as maltose and maltotriose, as well as α-limit dextrins, through cleavage of 1-4-α-D-glycosidic linkages. The salivary isozyme provides an initial partial cleavage into smaller oligomers (10–30%) (Martinez-Gonzalez et al. 2017). Once the partially digested saccharides reach the gut, they are then extensively hydrolyzed into smaller oligosaccharides, by pancreatic amylase synthesized in the pancreas and excreted into the lumen (Brayer et al. 2000).

The α-amylase products are further hydrolyzed into glucose units in the small intestinal lumen by the combination of the brush border exohydrolases, maltase-glucoamylase (MGAM; EC 3.2.1.20 and 3.1.2.3) and sucrase-isomaltase (SI; EC 3.2.1.48 and 3.2.1.10), commonly known as α-glucosidases (Nichols et al. 2003; Butterworth, Warren, and Ellis 2011; Williamson 2013; Dhital et al. 2017). MGAM and SI have two duplicated catalytic domains: a N-terminal membrane-proximal domain – ntMGAM and ntSI – and a C-terminal luminal domain – ctMGAM and ctSI. The domains are anchored to brush-border membrane of the small intestine through a *O*-glycosylated stalk stemming from the N-terminal domain (Sim et al. 2010). The N-terminal domains of MGAM and SI are more similar to one another in sequence, as are the C-terminal domains (≈

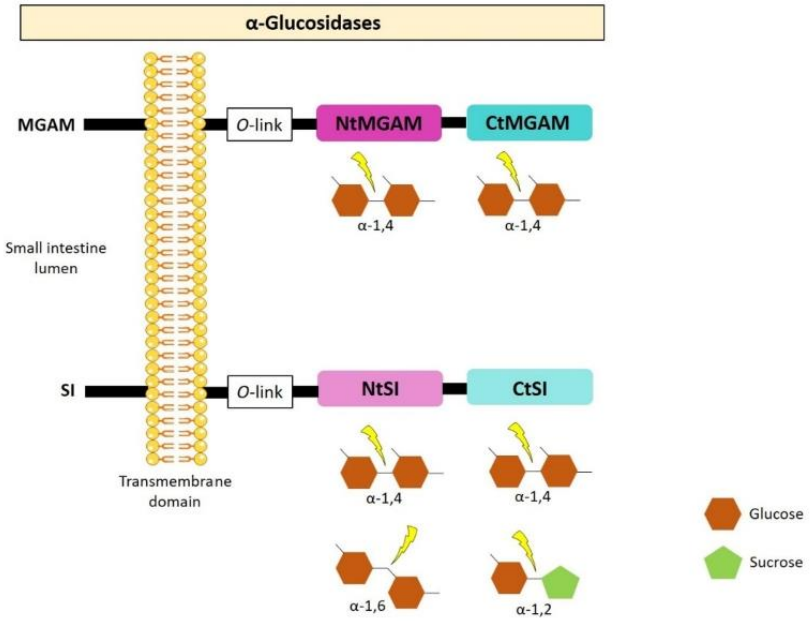


Figure 1. Schematic representation of the hydrolyzing α-glucosidases: maltase-glucoamylase (MGAM) and sucrase-isomaltase (SI). MGAM and SI are membrane-bound enzymes which contain two catalytic subunits: N-terminal subunit (NtMGAM and NtSI) and a C-terminal subunit (CtMGAM and CtSI). MGAM and SI display overlapping terminal starch digesting activities as both enzymes cleave the α-1,4 linkages of linear dextrin molecules. SI possesses an additional substrate specificity as its NtSI catalytic subunit acts on α-1,6-linkages of isomaltose, and its CtSI catalytic subunit acts on α-1,2-linkages of sucrose. Nevertheless, as starch is the main component of the human diet, the predominant SI substrates are α-1,4 linked glucose oligomers. In addition, SI is more abundant than MGAM, but MGAM displays higher hydrolytic activity.

60% sequence identity), compared to the N- and C-terminal domains associated with the same enzyme (≈ 40% sequence identity). This happens because MGAM and SI genes arose from duplication and divergence of an ancestral gene, which itself has been subjected of duplication. N- and C-terminal MGAM and SI domains are members of the GH 31 family. The four domains are responsible for the hydrolysis of the nonreducing ends of (1-4)-α-glycosidic linkages, but display different specificities for malto-oligosaccharides of various lengths (Nichols et al. 2003; Butterworth, Warren, and Ellis 2011; Williamson 2013; Dhital et al. 2017). MGAM has a preference α-1,4-oligossacharides and shows the ability to hydrolyze increasing lengths up to glucohexaose efficiently. The regiochemistry is relevant since α-1,6 glycosidic bonds are hydrolyzed at only 2% of the rate of α-1,4-glycosidic linkages. In addition, there is small amount α-1,2- and α-1,3-hydrolyzing activity. The glycosidic bonds preferences of MGAM and SI are represented in Figure 1. In turn, SI accounts for about 80% of the overall intestinal maltase (α-1,4 glycosidic bonds) activity and the almost all the sucrase (α-1,2 glycosidic bonds) activity present in the small intestine. SI also shows the capacity the hydrolyze α-1,6 glycosidic linkages present in isomaltose, as well as some α-1,3- hydrolyzing activity (Sim et al. 2010; Elferink et al. 2020).

Glucose is then absorbed from the intestinal mucosa into the bloodstream by glucose transporter (GLUT)-2 and sodium/glucose cotransporter-1 (SGLT1), leading to postprandial hyperglycemia (PPHG) (Williamson 2013) (Figure 2).

Increased PPHG constitutes a common feature in T2D, significantly contributing to the development of chronic diabetes complications, even more than fasting hyperglycemia (Brás et al. 2018). Of all available antidiabetic drugs, α-glucosidase inhibitors, such as acarbose, voglibose and miglitol, are the most effective in reducing PPHG. Acarbose, a pseudotetrasaccharide obtained from the fermentation of *Actinoplanes utahensis*, was approved in 1990 and is the most prescribed α-glucosidase inhibitor, being commercially available in 117 countries. Miglitol was launched in 1996 and is approved in 10 countries, while voglibose is commercially available since 1994 (in Japan) and is approved in only 3 countries (Joshi et al. 2015). These agents also inhibit α-amylase but have no effect on *β*-glucosidases such as lactase. However, α-amylase and α-glucosidase inhibitors used on therapy are associated with gastrointestinal adverse effects, including flatulence, diarrhea, and bloating. Moreover, a few cases of hepatitis have been reported with the use of acarbose (Derosa and Maffioli 2012). For this reason, the search and development of new effective and safer α-amylase and α-glucosidase inhibitors is of utmost importance in the management of PPHG in T2D. As it is already known, α-glucosidase inhibitors also inhibit α-amylase. As such, it was also previously suggested that it is recommended only a mild inhibition of α-amylase with the purpose to avoid gastrointestinal side effects as a result of excessive bacterial fermentation of carbohydrates in colon (Etxeberria et al. 2012).

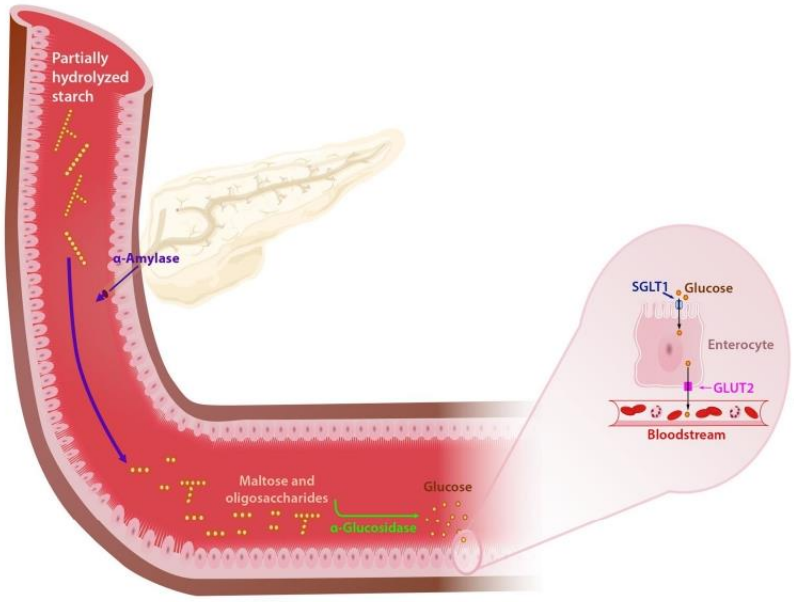


Figure 2. Mechanism of action of α-amylase and α-glucosidase (adapted from Proença et al. (2019)). After a meal, starch (amylose and amylopectin), partially hydrolyzed by salivary α-amylase, is hydrolyzed by pancreatic α-amylase. This enzyme catalyzes the hydrolysis of α-1,4 linkages, resulting in the formation of intermediate unbranched (e.g., maltose and maltotriose) and branched (α-limit dextrins) oligosaccharides. The brush border enzyme α-glucosidase is responsible for the conversion of disaccharides and oligosaccharides into glucose, which is then transported by sodium/glucose cotransporter-1 (SGLT1) from the intestinal lumen to the cytosol of enterocytes. Finally, glucose is transported from enterocytes to blood via facilitated diffusion, by glucose transporter 2 (GLUT2).

Flavonoids

Definition, classification and metabolism

Flavonoids (from the Latin *flavus*, which means yellow, their color in nature) represent a range of heterocyclic phenolic compounds ubiquitous in the Plant Kingdom and widely present in the human diet (e.g., fruits, vegetables, grains, herbs and beverages) (Cassidy and Minihane 2017; Slamova, Kapesova, and Valentova 2018). Flavonoids are secondary plant metabolites, and together with other plant phenols, share the common origin from the amino acid phenylalanine. As result, these phenols derive from a common building block in their skeleton, known as the phenylpropanoid unit (C_6-C_3) (Hollman 2004). Flavonoids are based upon a fifteen-carbon skeleton (C_6-C_3-C_6) consisting in two benzene rings (A and B rings) linked through a heterocyclic pyran ring (C ring) (Figure 3) (Kumar and Pandey 2013).

These plant secondary metabolites, can be generally found in the form of various glycosides, and are responsible for several biological functions, including the protection against ultraviolet (UV) radiation and phytopathogens, signaling during nodulation, auxin transport and the coloration of flowers to attract pollinators (Ferreyra, Rius, and Casati 2012; Petrussa et al. 2013). Due to the structural complexity of flavonoids, these compounds have been subclassified as flavones (2-phenyl-4H-chromen-4-one), flavonols (3-hydroxy-2-phenyl-4H-chromen-4-one), flavanones (2-phenyl-2,3-dihydro-4H-chromen-4-one), isoflavones (3-phenyl-4H-chromene-4-one), flavans (2-phenyl-2-chromane), and anthocyanidins (2-phenylchromenylium) (Table 2) (Cassidy and Minihane 2017). In mammals, flavonoids have recognized biological effects, including antioxidant (Heim, Tagliaferro, and Bobilya 2002), anti-inflammatory (Ribeiro et al. 2015), antimicrobial (Xie et al. 2015), antitumoral (Menezes et al. 2016) and antidiabetic (Alkhalidy, Wang, and Liu 2018).

In what concerns metabolism, flavonoids are substrates for conjugating and hydrolyzing enzymes in the small intestine, liver and colon. These compounds are all conjugated to *O*-glucuronides, sulfate esters and *O*-methyl esters and practically no aglycones are present in the plasma. Conjugation of flavonoids first occurs in the small intestine and then in the liver, and the generated glucuronides and sulfate derivatives facilitate their excretion via urine and bile (Thilakarathna and Rupasinghe 2013). The biliary excreted glucuronide derivatives undergo enterohepatic circulation or are hydrolyzed by the microbiota to aglycones. Aglycones are then catabolized to low molecular weight compounds that are ready to be absorbed. Flavonoids that are not absorbed in the intestine also suffer structural modifications by intestinal microflora (Thilakarathna and Rupasinghe 2013).

Absorption of flavonoids vary drastically among different classes as well as among different conjugates of the same compound in a specific class. As such, absorption of some flavonoids can be very rapid, while for others it can be very slow, which directly affects the bioavailability. Interestingly, α-glucosidase inhibitors are only minimally absorbed and are rarely associated with hypoglycemia and weight gain (Wyne and Bakris 2007). Acarbose, the most prescribed α-glucosidase inhibitor, acts locally in the gastrointestinal tract on the surface of enterocytes, and only 2% of an oral dose of this antidiabetic agent is systemically absorbed (Schmeltz and Metzger 2007).

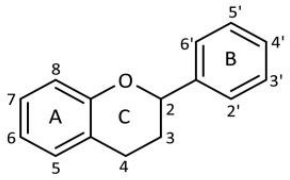


Figure 3. Basic chemical structure of flavonoids.

Modulatory effect of flavonoids against α-amylase and α-glucosidase activity

Literature search methods

The data about the antidiabetic activity of isolated flavonoids on both enzymes, α-amylase and α-glucosidase, were searched in databases such as PubMed, Science Direct, ResearchGate and Google Scholar, up to January 1st of 2020. The keywords used were "alpha-amylase," "alpha-glucosidase" and "flavonoids". From the 716 articles found for α-amylase and the 868 articles found for α-glucosidase, 22 and 70 articles were included, respectively (Figure 4). The criteria used for inclusion were the selection of the papers focusing in T2D, that tested pure compounds and the papers that studied more than one flavonoid, in order to allow the establishment of a SAR. Taking into account the large number of published papers about the inhibition of α-glucosidase by flavonoids (Xiao et al. 2013), in the present work the studies mentioned will be those published from 2013 (inclusive), while the research studies concerning the α-amylase inhibition by flavonoids include articles published from 2000.

α-Amylase inhibition by flavonoids

Methodologies used to evaluate the inhibitory activity of flavonoids against α-amylase

Several methodologies have been used to evaluate the inhibitory activity of flavonoids against α-amylase, which brings difficulties in the interpretation of SAR and in the comparison among the published papers. In fact, the variability found in the results of the α-amylase inhibitory activity by flavonoids could be explained by the different experimental conditions applied in each study, such as the source and the concentration of the enzyme, the type and concentration of the substrate, the time of incubation, the pH and the temperature (Table 3).

The values of the results exhibited below are exactly the ones presented by the authors in the research articles. As such, in some cases, the associated error values are not available. For the evaluation of the inhibitory activity of flavonoids against the α-amylase, the present review was organized in the following order: flavonoids evaluated and establishment of the SAR; tables presenting the corresponding chemical structure of the flavonoid and its inhibitory activity; table presenting the summarized results of all the articles analyzed; and an integrated discussion of the results for the enzyme under study.

Comprehensive structure-activity relationship analysis concerning the α-amylase inhibition by flavonoids

Kim and coworkers (Kim, Kwon, and Son 2000) tested a panel of 21 flavonoids, including flavones, biflavones and isoflavones (Table 4), for their ability to inhibit porcine pancreatic α-amylase. It was found that luteolin (**1**) was the most active compound (IC_{50} value in the range of 50 to 500 µg/mL), followed by kaempferol-3-*O*-[6″-*O*-(3-hydroxy-3-methylglutaroyl)glucoside] (**13**) and luteolin-7-*O*-glucoside (**4**), both showing total inhibitory activity of α-amylase at the concentration of 5 mg/mL. Nevertheless, the mentioned flavonoids were less active than the positive control acarbose (IC_{50} value in the range from 5 to 50 µg/mL). This study indicated that the presence of -OH groups together at 3′- and 4′- positions of B ring and at 5- and 7- positions of A ring increases the inhibition of α-amylase by flavonoids.

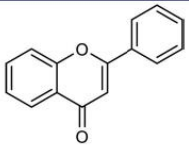
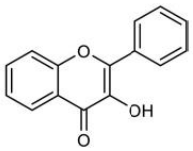
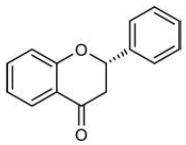
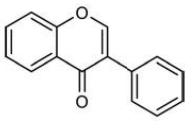
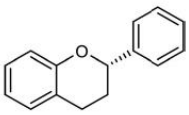
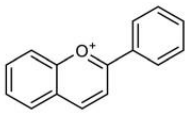
Tadera et al. (Tadera et al. 2006) tested the inhibitory activity of 16 flavonoids, from the following subclasses: flavones, flavonols, flavanones, isoflavones, flavanols or anthocyanidins, against porcine pancreatic α-amylase (Table 5). Their potency to inhibit α-amylase was, in a descending order: luteolin (**1**) ≈ myricetin (**24**) and quercetin (**25**), confirming the high potency of luteolin (Kim, Kwon, and Son 2000; Tadera et al. 2006). Here, the linkage of the C ring at the 3-position (by comparing isoflavones with the flavonoids from other subclasses), the C2 = C3 double bond, as well as the hydroxylation at 5-position of A ring and at 4′-position of B ring of flavonoids, enhanced their inhibitory activity. On the other hand, the addition of an -OH group at 3-position of C ring seems to slightly decrease the intended effect, since luteolin (**1**) was more active than quercetin (**25**).

Inhibition of α-amylase was also tested for flavonoids isolated from *Allium cepa* L. (Table 6) (Mohamed 2008). By comparing compounds **36** (inhibition = 87.7%) and **37** (inhibition = 56.4%), it was possible to observe that the substitution of an -OH for a glucose at 4′-position of B ring decrease the inhibitory effect.

Li et al. (2009) studied the interaction between α-amylase and three flavonoids isolated from tartary buckwheat bran, rutin (**5**), quercetin (**25**) and isoquercetin (**38**) (Table 7), was studied by fluorescence spectroscopy and enzyme kinetics. The tested flavonoids were effective inhibitors of α-amylase. The sequence of binding constants was isoquercetin (**38**) > quercetin (**25**) > rutin (**5**), indicating in this work that the replacement of the -OH at 3-position of C ring by an indicant is advantageous to its binding to α-amylase than quercetin (**25**) itself. It was also found that the flavonoids under study presented a competitive mechanism of inhibition.

Yilmazer-Musa et al. (2012) evaluated the human salivary α-amylase inhibitory activity of plant-based extracts, namely grape seed, and their isolated catechins. Catechin (**30**), epicatechin (**31**), epigallocatechin (**32**), epigallocatechin gallate (**33**), gallocatechin gallate (**39**) and epicatechin gallate (**40**) (Table 8) were considerably less potent than acarbose. These results are in agreement with the work of Tadera et al. (2006), in which the tested catechins were weak inhibitors of α-amylase, even though a different source of enzyme was used. According to

Table 2. Chemical structure, examples, and natural sources of different subclasses of flavonoids.

Subclass	Chemical structure	Examples	Natural sources	Reference
Flavones		Luteolin Chrysin Apigenin	Parsley Celery Chicory Oregano	(Egert and Rimbach 2011; Kumar and Pandey 2013; Kozlowska and Szostak-Wegierek 2014; Hostetler, Ralston, and Schwartz 2017)
Flavonols		Quercetin Galangin Kaempferol	Onion Rocket lettuce Capers Radish	(Egert and Rimbach 2011; Kumar and Pandey 2013; Kozlowska and Szostak-Wegierek 2014)
Flavanones		Naringenin Eriodictyol Taxifolin	Artichokes Orange Lemon Grapefruit	(Egert and Rimbach 2011; Kumar and Pandey 2013; Kozlowska and Szostak-Wegierek 2014)
Isoflavones		Prunetin Daidzein Genistein	Soy flour Soybeans Soymilk	(Egert and Rimbach 2011; Kumar and Pandey 2013)
Flavans		Catechin Epicatechin Epigallocatechin	Chocolate Green tea Beans Blackberry	(Egert and Rimbach 2011; Kumar and Pandey 2013; Kozlowska and Szostak-Wegierek 2014)
Anthocyanidins		Cyanidin Petunidin Malvidin	Elderberry Aubergine Blackberry Chickpeas	(Egert and Rimbach 2011; Kumar and Pandey 2013; Kozlowska and Szostak-Wegierek 2014)

Yilmazer-Musa et al. (2012), the lack of activity of catechins is likely due to the lack of an unsaturated C ring with a 4-keto group in flavanols, and the lack of specific of A and B rings' -OH groups in the correct stereospecific orientation to effectively interact with the catalytic site of the enzyme.

Luyen et al. (2013) studied the α-amylase (from *Aspergillus oryzae*) inhibition by three flavonoids (**41–43**) (Table 9). The three flavonoids tested showed to be more active than acarbose (IC_{50} = 732.4 ± 41.6 μM). Buddleoside (**43**) was the most promising compound with an IC_{50} value of 112.5 ± 15.7 μM, followed by eriodictyol (**41**) (IC_{50}= 318.2 ± 26.9 μM) and acacetin-7-*O*-*β*-D-glucoside (**42**) (IC_{50}= 337.1 ± 28.2 μM). This study indicates that the replacement of a glucose by a rhamnose at 7-position of A ring significantly increases the inhibitory activity, by comparing buddleoside (**43**) and acacetin 7-*O*-*β*-D-glucoside (**42**).

The flavonoids luteolin (**1**), geraldone (**44**), and isookanin (**45**) (Table 10), isolated from the stem bark of *Albizzia Lebbeck Benth* plant, were tested for their capacity to inhibit α-amylase from *Bacillus subtilis* (Ahmed et al. 2014). These flavonoids showed a higher inhibition % comparing to acarbose (37.65 ± 0.94%), with values of 93.98 ± 1.02%, 84.36 ± 0.60% and 90.10 ± 0.58%, respectively. However, it was not specified at which concentrations the compounds were tested, making it difficult to draw conclusions from these results.

Asghari et al. (2015) studied the α-amylase (from porcine pancreas type VI) inhibition by the flavonoids luteolin-7-*O*-glucoside (**4**), luteolin-7-*O*-glucuronide (**46**), diosmetin-7-*O*-glucuronide (**47**) and salvigenin (**48**) (Table 11), isolated from the aerial parts of *Salvia chloroleuca*. Flavonoids luteolin-7-O-glucoside (**4**), luteolin-7-*O*-glucuronide (**46**) and diosmetin-7-*O*-glucuronide (**47**) presented IC_{50} values of 81.7 μM, 61.5 μM and 76.3 μM, while salvigenin (**48**) has an IC_{50} value higher than 100 μM. By the obtained results, it was concluded that a sugar moiety on A ring are more favorable for the inhibitory activity than -OCH_3 groups. It was also observed that the substitution of a -OCH_3 group for a -OH group at 4′ position of B ring increased the α-amylase inhibition, as already postulated by Tadera et al. (2006).

Ibrahim et al. (2015) evaluated the inhibition of α-amylase by flavonoids isolated from *Targetes minuta* L.: minutaside A (**49**), axillarin-7-*O*-*β*-D-glucoside (**50**), quercetagetin-3,7-dimethoxy-6-*O*-*β*-D -glucoside (**51**), quercetagetin-7-methoxy-6-*O*-*β*-D-glucoside (**52**), and quercetagetin-6-*O*-*β*-D-glucoside (**53**)

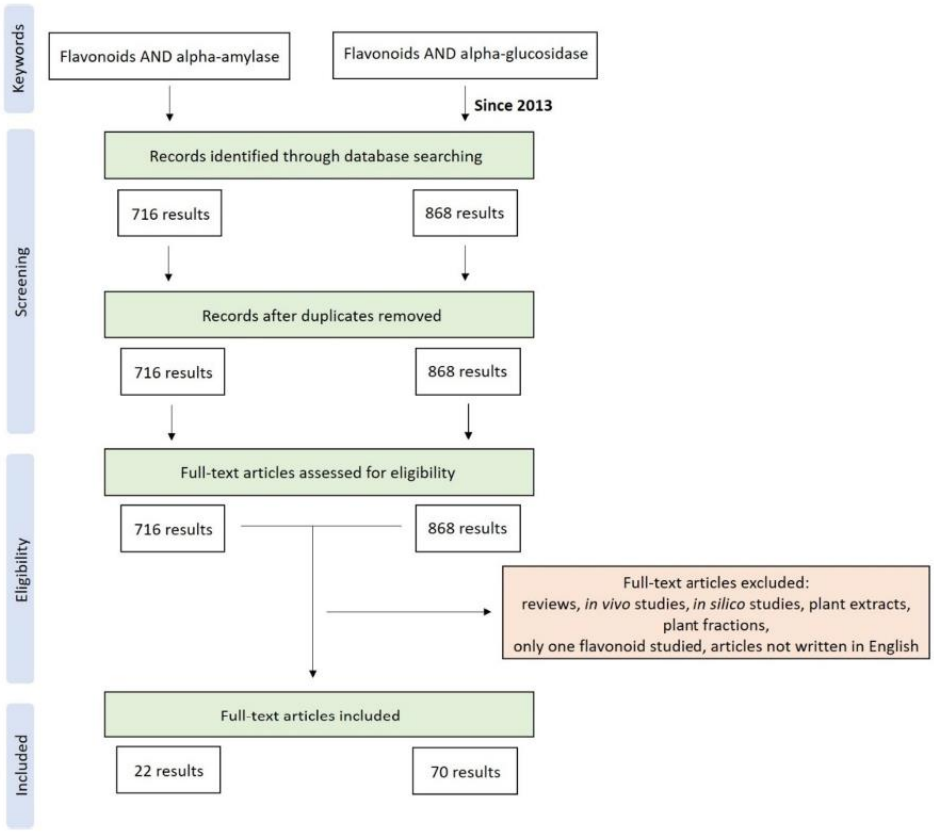


Figure 4. Schematic literature research methodology used in this review.

(Table 12). The most active flavonoid was quercetagetin-6-O-*β*-D-glucoside (**53**) and minutaside A (**49**), with inhibition % of 93.26 and 90.89 at 10 µL/50 µg respectively, comparable with acarbose (inhibition of 100% at 10 µL/50 µg). From the results, the authors concluded that the presence of -OH groups at 5- and 7-positions of A ring in the flavonoid scaffold increases the α-amylase inhibitory activity, by comparing the most active flavonoids with axillarin-7-*O*-*β*-D -glucoside (**50**) (71.41% of inhibition), quercetagetin-3,7-dimethoxy-6-*O*-*β*-D-glucoside (**51**) (68.92% of inhibition) and quercetagetin-7-methoxy-6-*O*-*β*-D-glucoside (**52**) (81.35% of inhibition). On the other hand, the methylation of the -OH groups at 3-position of C ring or/and at 7-position of A ring decreased the binding affinity of flavonoids to α-amylase.

The pancreatic α-amylase inhibitory effect of myricetin (**24**) and quercetin (**25**) (Table 13) from *Hovenia dulcis* was also studied (Meng et al. 2016). As it was verified by Tadera et al. (2006), myricetin (**24**) presented a slightly higher inhibitory activity than quercetin (**25**). Both have shown to be competitive inhibitors, these results being in agreement with the work of Li et al. (2009), who also verified that quercetin (**25**) has a competitive inhibition type. As such, the addition of a -OH group at 5-position of A ring seems to increase the ability of flavonoids to inhibit α-amylase.

Milella et al. (2016) tested the inhibitory activity of flavonoids isolated from *Arcytophyllum thymifolium*: (2S)-7-prenyloxyeriodictyol (**54**), hyperin (**3**), rhamnetin (**55**) and kaempferol-3-*O*-*β*-D -glucosyl-(1→2)-*β*-D -galactoside (**56**) (Table 14) against α-amylase from hog pancreas. (2S)-7-Prenyloxyeriodictyol (**54**) and hyperin (**3**), presented no effect, while kaempferol 3-*O*-*β*-D-glucosyl-(1-2)-*β*-D-galactoside (**56**) had an IC_{50} value around 27-fold higher than the one found for rhamnetin (**55**). The obtained results demonstrate that the sugar moiety at 3-position of C ring is not favorable for the inhibition of α-amylase, in comparison with the -OH group at this position.

The inhibition of α-amylase (from porcine pancreas) by the main flavonoids identified in *Poncirus trifoliata* was investigated (Tundis et al. 2016). The flavanones glycosides tested were: narirutin (**57**), poncirin (**58**), didymin (**59**), naringin (**60**), hesperidin (**14**) and neoeriocitrin (**61**) (Table 15). The compound with the higher inhibitory activity was neoeriocitrin (**61**), with an IC_{50} value of 4.69 ± 0.9 µM, a value almost 17-fold lower than the one found for acarbose (IC_{50} = 77.45 ± 1.8 µM). The obtained results indicate that the catechol group at B ring significantly enhance the inhibition of α-amylase, in comparison with flavanones with only an -OH group at 4′-position of B ring, such as narirutin

Table 3. Experimental conditions used to evaluate the inhibitory effect of flavonoids against α-amylase.

α-Amylase source	α-Amylase concentration	Substrate	Substrate concentration	Preincubation of flavonoids with α-amylase	Time of enzymatic reaction	pH	Temperature (°C)	Positive control activity	Reference
Porcine pancreas	100 U/mL	*p*-Nitrophenyl-α-D-maltopentoglycoside	NM	5 min	5 min	7.0	RT	Acarbose IC_{50}= 5–50 μg/mL	(Kim, Kwon, and Son 2000)
	0.1 mg/mL	Blocked *p*-nitrophenyl-α-D-maltoheptaoside			10 min [b]	6.9	37	NM	(Tadera et al. 2006)
EnzCheck[a]	NM	NM		NM	60 min		RT	Acarbose Inhibition (%) = 100% at 5 mg/mL	(Mohamed 2008)
Bacillus subtilis	2.0×10^{-5} mol/L	Starch		NM	NM	6.8		NM	(Li et al. 2009)
Human saliva	2.5 mU/mL	DQ™ starch	5 μg/mL	30 min		6.0		Acarbose: IC_{50}= 6.9 ± 0.8 μg/mL	(Yilmazer-Musa et al. 2012)
Aspergillus oryzae	5 μg/mL	Potato starch	4.9 mg/mL	NM	15 min [c]	7.0 (before the addition of HCl)	37	Acarbose: IC_{50} = 732.4 ± 41.6 μM	(Luyen et al. 2013)
Bacillus subtilis	NM	Starch	0.2% (w/v)		5 min [d]	6.7		Acarbose: % Inhibition= 37.65 ± 0.94	(Ahmed et al. 2014)
Porcine pancreas	25.0 U/mL		6 mg/mL		30 min [d]	6.8		Acarbose: IC_{50}= 53.4 ± 3.1 μM	(Asghari et al. 2015)
EnzCheck[a]	NM	NM	NM	5 min	30 min	6.9		Acarbose % Inhibition =100% at 5 mg/mL	(Ibrahim et al. 2015)
Porcine pancreas	0.54 U/mL	Starch	1%	NM	3 min [d]		25	NM	(Meng et al. 2016)
Hog pancreas	50 U/mL			10 min	10 min [d]			Acarbose: IC50 = 26.3 ± 1.2 μM	(Milella et al. 2016)
Porcine pancreas	0.2 g/L	Potato starch	5 g/L	NM	5 min [d]			Acarbose: 77.45 ± 1.8 μM	(Tundis et al. 2016)
EnzCheck [a]	NM	NM	NM	5 min	30 min		37	Acarbose % Inhibition =100% at 5 mg/mL	(Ibrahim et al. 2017)
Hog pancreas	25 mU	2-Chloro-4-nitrophenyl-α-D-maltotrioside	0.5 mM	NM		6.0		Acarbose: IC50 = 2.21 μM	(Sun et al. 2017)
Porcine pancreas	0.1 U/mL	Starch	0.4% (w/v)		10 min	7.0		Acarbose IC_{50} = 5.3 ± 3.1 μM	(Zhang et al. 2017)
	Amylose: 0.2 nM Maltopentose: 1 nM	Amylose Maltopentose	Amylose: 0.02 to 0.16 g/L Maltopentose: 25 to 600 μM		5 min d	6.9		NM	(Desseaux et al. 2018)
	5 U/mL	Starch	1%	20 min	20 min d			Acarbose: IC50 = 678.43 ± 16.52 μg/mL	(Li, Yao, et al. 2018)
	1% (w/v)	Maltopentaose	1% (w/v)	15 min	15 min d	NM		NM	(Lim et al. 2019)
	1 μM	*p*-Nitrophenyl maltopentaoside	0.3–2.7 mM	NM	120 min	7.0		Acarbose: Ki= 9.48 ± 1.65 mM	(Martinez-Gonzalez et al. 2019)
	0.2 U/mL	2-chloro-4-nitrophenyl-α-D-maltotrioside	0.5 mM	10 min	30 min	6.8		Acarbose: IC50 = 1.3 ± 0.2 μM	(Proença et al. 2019)
	1.51 U (≈ 100 pM)	2-chloro-4-nitrophenyl-4-*O*-β-galactosyl maltoside	0–2 mM	NM	NM	6.1		Acarbose: IC50 = 0.02 ± 0.1 μM	(Kaeswurm et al. 2019)
	300 U/mL	Starch	1.0 g/mL	10 min	5 min d	6.8		NM	(Ren, Li, and Liu 2019)

DNS – 3,5-Dinitrosalicylic acid; IC_{50} – concentration of drug or compound required for 50% inhibition; NM – Not mentioned; RT – Room temperature.
[a]The method was based on the EnzCheck®- Ultra Amylase Assay Kit, from ThermoFisher.
[b]Boiling H_2O to stop the reaction.
[c]HCl 1.0 M to stop the reaction.
[d]Dinitrosalicylic acid reagent was added to stop the reaction.

Table 4. Flavonoids tested by Kim, Kwon, and Son (2000), and respective inhibitory activity on α-amylase (the most active flavonoids are highlighted).

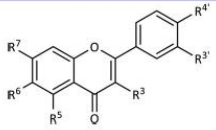
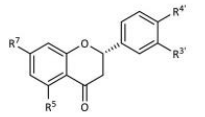
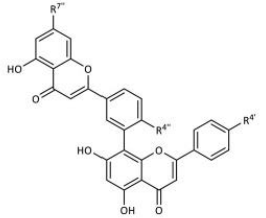
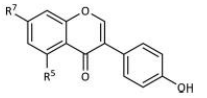
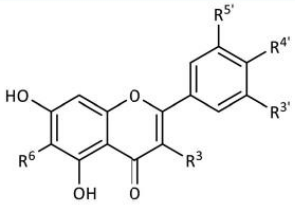
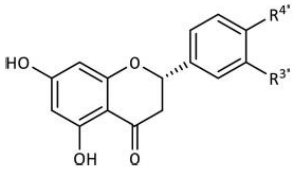
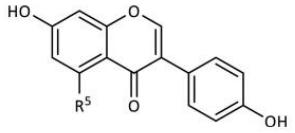
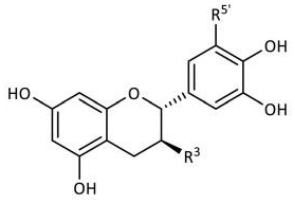
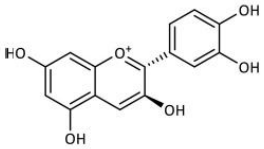
Flavonoid	Structure	R^3	$R^{3'}$	$R^{4'}$	R^5	R^6	R^7	$R^{4''}$	$R^{7''}$	% Inhibition at 5 mg/mL
Luteolin (**1**)		H	OH	OH	OH	H	OH	–	–	≈**100**
Astraglin (**2**)		glucose	H	OH	OH	H	OH	–	–	≈ 50
Hyperin (**3**)		galactose	OH	OH	OH	H	OH	–	–	≈ 60
Luteolin 7-*O*-glucoside (**4**)		H	OH	OH	OH	H	glucose	–	–	≈ **100**
Rutin (**5**)		rutinose	OH	OH	OH	H	OH	–	–	≈ 20
Isorhamnetin 3-O-rutinoside (**6**)		rutinose	OCH_3	OH	OH	H	OH	–	–	≈ 70
Linarin (**7**)		H	H	OCH_3	OH	H	rutinose	–	–	< 10
Pectolinarin (**8**)		H	H	OCH_3	OH	OH	rutinose	–	–	< 10
Quercetrin (**9**)		rhamnose	OH	OH	OH	H	OH	–	–	≈ 30
Lonicerin (**10**)		H	OH	OH	OH	H	rhamnose	–	–	≈ 50
Rhoifolin (**11**)		H	H	OH	OH	H	rhamnose	–	–	≈ 60
Baicalin (**12**)		H	H	H	OH	OH	glucuronide	–	–	< 10
Kaemperol-3-*O*-[6″-*O*-(3-hydroxy-3-methylglutaroyl)glucose (**13**)		6″-*O*-(3-hydroxy-3-methylglutaroyl) glucose	H	OH	OH	H	OH	–	–	≈ **100**
Hesperidin (**14**)		–	OH	OCH_3	OH	–	rutinose	–	–	≈ 10
Amentoflavone (**15**)		–	–	OH	–	–	–	OH	OH	< 10
Bilobetin (**16**)		–	–	OCH_3	–	–	–	OH	OH	≈ 30
Ginkgetin (**17**)		–	–	OH	–	–	–	OCH_3	OCH_3	< 10
Isoginkgetin (**18**)		–	–	OCH_3	–	–	–	OCH_3	OCH_3	< 10
Genistein (**19**)		–	–	–	OH	–	OH	–	–	≈ 20
Daidzein (**20**)		–	–	–	H	–	OH	–	–	≈ 50
Genistin (**21**)		–	–	–	OH	–	glucose	–	–	≈ 20
Positive control **Acarbose**	–	–	–	–	–	–	–	–	–	≈ 100

Table 5. Flavonoids tested by Tadera et al. (2006), and respective inhibitory activity on α-amylase (the most active flavonoids are highlighted).

Flavonoid	Structure	R^3	$R^{3'}$	$R^{4'}$	$R^{5'}$	R^5	R^6	IC_{50} (mM)
Luteolin (**1**)		H	OH	OH	H	OH	H	**0.36**
Apigenin (**22**)		H	H	OH	H	OH	H	> 0.50
Baicalein (**23**)		H	H	H	H	OH	OH	> 0.50
Myricetin (**24**)		OH	OH	OH	OH	OH	H	**0.38**
Quercetin (**25**)		OH	OH	OH	H	OH	H	0.50
Kaempferol (**26**)		OH	H	OH	H	OH	H	> 0.50
Fisetin (**27**)		OH	OH	OH	H	H	H	> 0.50
Naringenin (**28**)		–	H	OH	–	–	–	> 0.50
Hesperetin (**29**)		–	OH	OCH_3	–	–	–	> 0.50
Daidzein (**19**)		–	–	–	–	OH	–	> 0.50
Genistein (**20**)		–	–	–	–	H	–	> 0.50
(+)-Catechin (**30**)		OH	–	–	H	–	–	> 0.50
(-)-Epicatechin (**31**)		OH	–	–	H	–	–	> 0.50
(-)-Epigallocatechin (**32**)		OH	–	–	OH	–	–	> 0.50
(-)-Epigallocatechin gallate (**33**)		gallate	–	–	OH	–	–	> 0.50
Cyanidin (**34**)		–	–	–	–	–	–	> 0.50

(**57**) (IC_{50} = 70.80 ± 2.5 μM) and naringin (**60**) (IC_{50} = 36.35 ± 1.9 μM), or with a -OCH_3 group at the referred position, such as poncirin (**58**) (IC_{50} = 39.19 ± 1.3 μM) and didymin (**59**) (IC_{50} = 31.62 ± 2.8 μM).

The inhibition of α-amylase by nine isoflavones isolated from *Iris germanica* rhizomes was evaluated: irilone-4′-methyl ether (**62**), irilone (**63**), irilone-4′-*O*-*β*-D -glucoside (**64**), irisolidone (**65**), irigenin S (**66**), irigenin (**67**), iridin S (**68**), iridin (**69**), and iridin A (**70**) (Table 16) (Ibrahim et al. 2017). The most active compounds were irisolidone (**65**), irigenin (**67**) and iridin A (**70**). The authors mentioned that the % of inhibition were comparable to the one found for the positive control acarbose, but the tested concentrations were not mentioned. It was concluded that the hydroxylation at 7- or at 8-position of A ring increase the α-amylase inhibition. The same effect was observed when the number of -OH groups is increased in A- and B rings. On the other hand, the glycosylation of isoflavones decreased their inhibitory activity.

Sun and colleagues (Sun et al. 2017) tested the inhibition of hog pancreas α-amylase by flavanones naringenin (**28**), 8-prenylnaringenin (**71**) and 8-geranylnaringenin (**72**) (Table 17). Naringenin (**28**) and 8-prenylnaringenin (**71**) did not show inhibitory activity, while 8-geranylnaringenin (**72**) presented an IC_{50} value of 15.38 μM. These results suggest that the addition or the substitution of a prenyl group for a geranyl group at 8-position of A ring significantly increase the ability of flavanones to inhibit α-amylase.

Porcine pancreatic α-amylase inhibition by a panel of 16 flavonoids (Table 18) was evaluated (Zhang et al. 2017). The most effective flavonoid was apigenin (**22**), with an IC_{50} value of 146.8 ± 7.1 μM, while the IC_{50} value for the positive control acarbose was 5.3 ± 3.1 μM. Comparing apigenin (**22**) with chrysin (**73**), it is possible to conclude that the -OH group at 4′-position of B ring increased the inhibition of the enzyme under study. On the other hand, the presence of a -OH group at 3-position of C ring as well as the absence of the C2 = C3 double bond led to a reduction in α-amylase

Table 6. Flavonoids tested by Mohamed (2008), and respective inhibitory activity on α-amylase (the most active flavonoids are highlighted).

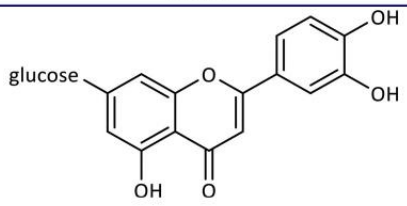
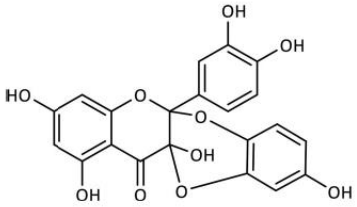
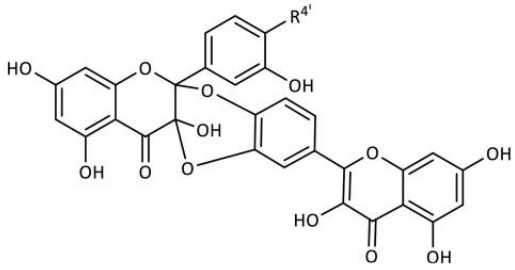
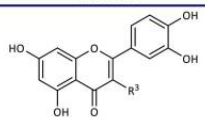
Flavonoid	Structure	$R^{4'}$	% Inhibition
Luteolin 7-*O*-glucoside (**4**)			82.8
Alliuocide G (**35**)		–	**96.5**
36		OH	87.7
37		glucose	56.4
Positive control **Acarbose**	–	–	100

Table 7. Flavonoids tested by Li et al. (2009), and respective inhibitory activity on α-amylase (the most active flavonoid is highlighted). Ki – inhibition constant.

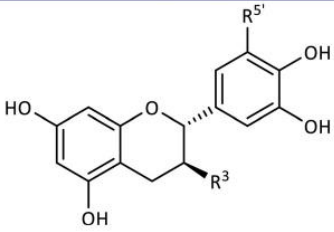
Flavonoid	Structure	R^3	$Ki/10^{-5}$ (mol/L)
Rutin (**5**)		rutinose	0.535
Quercetin (**25**)		OH	0.636
Isoquercetin (**38**)		glucose	**0.896**

inhibition. This conclusion results from the comparison of apigenin (**22**) (IC_{50} = 146.8 ± 7.1 μM) with kaempferol (**26**) and naringenin (**28**), which presented IC_{50} values higher than 400 μM.

The inhibitory effect of six flavans was tested on the activity of porcine pancreatic α-amylase under steady-state kinetic conditions, where both amylose and maltopentose were used as substrates (representing the initial and final stages of starch digestion) (Desseaux et al. 2018). The tested flavanols were: catechin (**30**), epicatechin (**31**), catechin gallate (**77**), epicatechin gallate (**40**), gallocatechin gallate (**39**) and epigallocatechin gallate (**33**) (Table 19). All flavanols were competitive inhibitors of amylose hydrolysis by α-amylase, except gallocatechin gallate (**39**), which was a mixed type inhibitor. The most active compounds in both substrates were epigallocatechin gallate (**33**) and catechin gallate (**77**). The presence of a galloyl group led to a moderate decrease in the constant of inhibition (Ki) values and the *cis*-flavanols epicatechin (**31**), epicatechin gallate (**40**) and epigallocatechin gallate (**33**) and the *trans*-flavanols catechin (**30**), catechin gallate (**77**) and gallocatechin gallate (**39**) had similar activities, regarding α-amylase inhibition. With maltopentaose as a substrate, the presence of a galloyl group led to an increase in the flavanol inhibition of α-amylase. However, as verified with amylose, also in the maltopentaose hydrolysis by α-amylase the cis/trans isomerism had no noticeable effect on the inhibitory activity of flavanols.

Li et al. (2018) evaluated the inhibitory effect on porcine pancreatic α-amylase by baicalin (**12**), apigenin (**22**), baicalein (**23**), scutellarin (**74**), chrysin (**73**), apigenin-7-*O*-glucuronide (**78**), chrysin-7-*O*-glucuronide (**79**) and isocarthamidin-7-*O*-glucuronide (**80**) (Table 20), isolated from *Scutellaria baicalensis* shoots. The most active flavonoids were apigenin (**22**) and baicalein (**23**), with IC_{50} values of 287.53 ± 5.39 μg/mL and 336.22 ± 6.31 μg/mL, respectively; and presented a better inhibitory activity than the positive control, acarbose (IC_{50} = 678.43 ± 16.52 μg/mL). Following an assign – score method refined for the assessment of SAR of flavonoids, it was verified that, as observed in other studies (Asghari et al. 2015; Ibrahim et al. 2015; Tundis et al. 2016; Zhang et al. 2017; Li, Yao, et al. 2018; Lim et al. 2019), the C2 = C3 double bond as well as the

Table 8. Flavonoids tested by Yilmazer-Musa et al. (2012), and respective inhibitory activity on α-amylase (the most active flavonoid is highlighted).

Flavonoid	Structure	R^3	$R^{5'}$	IC_{50} (μg/mL ± SD)
(+)-Catechin (**30**)		OH	H	160 ± 67
(-)-Epicatechin (**31**)		OH	H	ND
(-)-Epigallocatechin (**32**)		gallate	OH	ND
(-)-Epigallocatechin gallate (**33**)		gallate	OH	≈ 27
(-)-Gallocatechin gallate (**39**)		gallate	OH	≈ 24
(-)-Epicatechin gallate (**40**)		gallate	H	≈ **17**
Positive control **Acarbose**	–	–	–	6.9 ± 0.8

ND – Not determined.

Table 9. Flavonoids tested by Luyen et al. (2013), and respective inhibitory activity on α-amylase (the most active flavonoid is highlighted).

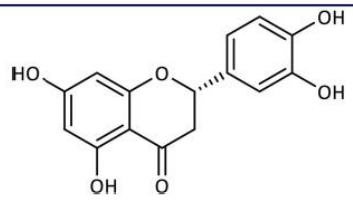
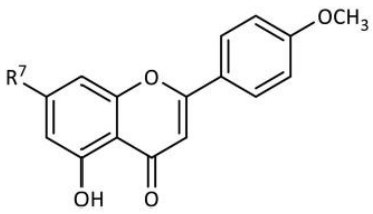
Flavonoid	Structure	R^7	IC_{50} (μM ± SD)
Eriodictyol (**41**)		–	318.2 ± 26.9
Acacetin 7-O-β-D-glucoside (**42**)		glucose	337.1 ± 28.2
Buddleoside (**43**)		rhamnose	**112.5 ± 15.7**
Positive control **Acarbose**	–	–	732.4 ± 41.6

Table 10. Flavonoids tested by Ahmed et al. (2014), and respective inhibitory activity on α-amylase (the most active flavonoid is highlighted).

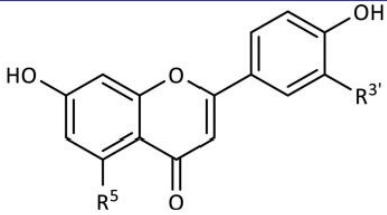
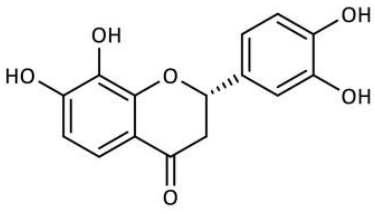
Flavonoid	Structure	$R^{3'}$	R^5	% Inhibition ± SD
Luteolin (**1**)		OH	OH	90.10 ± 0.58
Geraldone (**44**)		OCH_3	H	**93.98 ± 1.02**
Isookanin (**45**)		–	–	84.36 ± 0.60
Positive control **Acarbose**	–	–	–	37.65 ± 0.94

Table 11. Flavonoids tested by Asghari et al. (2015), and respective inhibitory activity on α-amylase (the most active flavonoid is highlighted).

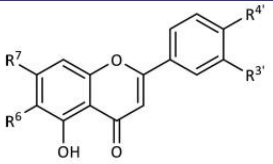
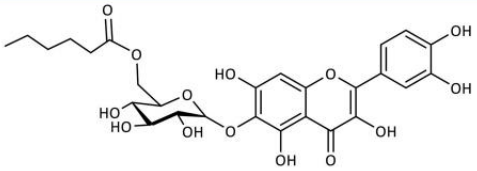
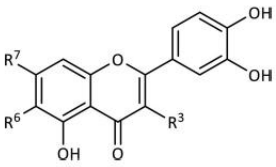
Flavonoid	Structure	$R^{3'}$	$R^{4'}$	R^6	R^7	IC_{50} (μM ± SD)
Luteolin 7-*O*-glucoside (**4**)		OH	OH	H	glucose	81.7 ± 2.3
Luteolin 7-*O*-glucuronide (**46**)		OH	OH	H	glucuronide	**61.5 ± 1.4**
Diosmetin 7-*O*-glucuronide (**47**)		OH	OCH_3-	H	glucuronide	76.3 ± 0.6
Salvigenin (**48**)		H	OCH_3	OCH_3	OCH_3	> 100
Positive control **Acarbose**	–	–	–	–	–	53.4 ± 3.1

Table 12. Flavonoids tested by Ibrahim et al. (2015), and respective inhibitory activity on α-amylase (the most active flavonoids are highlighted).

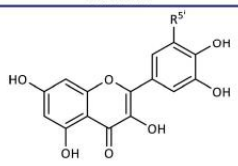
Flavonoid	Structure	R^3	R^6	R^7	Inhibition % at 10 μL/50 μg
Minutaside A (**49**)		–	–	–	**90.89**
Axillarin 7-*O*-β-D-glucoside (**50**)		OCH_3	OCH_3	glucose	71.41
Quercetagetin 3,7-dimethoxy-6-*O*-β-D-glucoside (**51**)		OCH_3	glucose	OCH_3	68.92
Quercetagetin 7-methoxy-6-*O*-β-D-glucoside (**52**)		OH	glucose	OCH_3	81.35
Quercetagetin 6-*O*-β-D-glucoside (**53**)		OH	glucose	OH	**93.26**
Positive control **Acarbose**	–	–	–	–	100

presence of -OH groups at 6- and 7- positions of A ring and at 4′-position of B ring enhanced the α-amylase inhibition. In turn, a sugar moiety on the flavonoid structure reduced their inhibitory capacity.

A high-performance anion-exchange chromatography (HPAEC) method was used to evaluate the inhibitory activity of luteolin (**1**), quercetin (**25**) and eriodictyol (**41**) (Table 21) on porcine pancreatic α-amylase (Lim et al. 2019). The obtained results indicate that, as abovementioned, the lack of the C2 = C3 double bond significantly decreased the α-amylase inhibition, since eriodictyol (**41**) presented a Ki value of 5.10 mM, comparing with luteolin (**1**) (Ki= 0.22 mM)

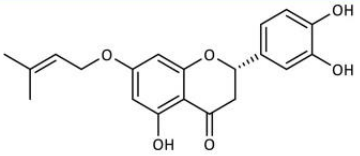
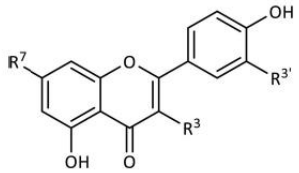
In 2019, Martinez-Gonzalez et al. (2019) studied the inhibitory activity of porcine pancreas α-amylase type I-A by luteolin (**1**), quercetin (**25**), rutin (**5**), hesperetin (**29**) and catechin (**30**) (Table 22). The following order of potency was quercetin (**25**) > luteolin (**1**) > hesperetin (**29**). No α-amylase inhibition was found for rutin (**5**) and catechin (**30**). As stated before (Tadera et al. 2006; Zhang et al. 2017), it is possible to conclude that the C2 = C3 double bond, the catechol structure in B ring and the planarity of C ring, increase the activity of flavonoids. In addition, these results are in agreement with the work of Li et al. (2009), in which quercetin (**25**) was more effective than rutin (**5**).

Table 13. Flavonoids tested by Meng et al. (2016), and respective inhibitory activity on α-amylase (the most active flavonoid is highlighted).

Flavonoid	Structure	$R^{5'}$	IC_{50} (μg/mL)
Myricetin (**24**)		OH	**662**
Quercetin (**25**)		H	770

Proença et al. (2019) evaluated a panel of 40 flavonoids concerning their ability to inhibit α-amylase from porcine pancreas, most of them tested for the first time. Among these compounds, a group of chlorinated flavonoids (**102–106**), parents of luteolin (**1**) and quercetin (**25**), were studied (Table 23). The most active compound was the chlorinated flavonoid 3-chloro-3′,4′,5,7-tetrahydroxyflavone (**102**). The most important conclusions obtained from the establishment of the SAR were: the replacement of the -OH group at 3-position of C ring for a -Cl ion increases the α-amylase inhibition [e.g., quercetin (**25**) vs. **102**], as well as the presence of an -OH group at 5-position of A ring [e.g., luteolin (**1**) vs. **96**] and the C2 = C3 double bond [e.g., quercetin (**25**) vs. taxifolin (**111**)], as mentioned above. On the other hand, the

Table 14. Flavonoids tested by Milella et al. (2016), and respective inhibitory activity on α-amylase (the most active flavonoid is highlighted).

Flavonoid	Structure	R^3	$R^{3'}$	R^7	IC_{50} (μM ± SD)
(2*S*)-7-Prenyloxyeriodictyol (**54**)		–	–	–	NA
Hyperin (**3**)		galactose	OH	OCH_3	NA
Rhamnetin (**55**)		OH	OH	OCH_3	**73.9 ± 5.9**
Kaempferol 3-*O*-*β*-D-glucosyl-(1-2)-*β*-D-galactoside] (**56**)		glucosyl-(1-2)-*β*-D-galactose	H	OH	≈ 2000
Positive control **Acarbose**	–	–	–	–	26.3 ± 1.2

NA – Not active.

presence of -OCH_3 groups in the flavonoid scaffold is not favorable for the inhibitory activity of the tested compounds.

The α-amylase (porcine pancreas) inhibition by flavans epicatechin (**31**) and epigallocatechin gallate (**33**) and anthocyanin malvidin-3-glucoside (**113**) was evaluated (Table 24) (Kaeswurm et al. 2019). The better inhibitor was epigallocatechin gallate (**33**), presenting an IC_{50} value of 66 ± 3 μM (using a substrate concentration of 10^3 μmol) and a mixed type of inhibition. It is suggested, by the obtained results, that the galloyl group at 3-position of C ring and the addition of an -OH group at 5′-position of B ring increases the ability of flavonoids to inhibit α-amylase. The conclusions are made considering the specific chemical structure of the tested flavonoids and the present substituents, in the assay conditions performed.

Rutin (**5**), quercetin (**25**) and catequin (**30**) (Table 25) were studied concerning their ability to inhibit α-amylase from porcine pancreas (Ren, Li, and Liu 2019). Quercetin (**25**) was the most active flavonoid, with an IC_{50} value of 0.67 mg/mL), followed by catechin (**30**) (IC_{50} = 1.17 mg/mL) and rutin (**5**) (IC_{50} = 1.71 mg/mL). It can be concluded that the substitution of a rutinose by an -OH group at 3-position of C ring increase the inhibitory activity, since quercetin (**25**) was a better inhibitor than rutin (**5**). The results also indicate that the C2 = C3 double bond in conjugation with the 4-keto group are important for the enhancement of α-amylase inhibition, by comparing quercetin (**25**) with catechin (**30**).

The results of the analyzed research studies on α-amylase inhibition by flavonoids are summarized in the Table 26.

α-Glucosidase inhibition by flavonoids

Methodologies used to evaluate the inhibitory activity of flavonoids against α-glucosidase

The variability of the results obtained for the α-glucosidase inhibitory activity of flavonoids, also depends on the experimental conditions applied in each study, such as the source and the concentration of the enzyme, the type and concentration of the substrate, the time of incubation, the pH and the temperature (Table 27).

The values of the results exhibited below are exactly the ones presented by the authors in the research articles. As such, in some cases, the associated error values are not available. For the evaluation of the inhibitory activity of flavonoids against the α-amylase, the present review was organized in the following order: flavonoids evaluated and establishment of the SAR; tables presenting the corresponding chemical structure of the flavonoid and its inhibitory activity; table presenting the summarized results of all the articles analyzed; and an integrated discussion of the results for the enzyme under study.

Comprehensive structure-activity relationship analysis concerning the α-glucosidase inhibition by flavonoids

Aderogba and coworkers (Aderogba et al. 2013) studied the ability of flavonoids isolated from *Croton menyharthii* [myricitrinquercetrin (**9**), quercetin (**25**) and myricitrin-3-*O*-rhamnoside (**113**)] (Table 28) to inhibit α-glucosidase from *Saccharomyces cerevisiae*. The most active compound was quercetin (**25**), followed by myricitrin (**113**) and quercetrin (**9**), with IC_{50} values of 30.9 ± 8.4, 79.0 ± 4.3 and 122.7 ± 1.6 μg/mL, respectively. Both quercetin (**9**) and myricitrin-3-*O*-rhamnoside (**113**) presented higher inhibitory activity than acarbose (IC_{50} = 103.3 ± 9.3 μg/mL). These results indicate that the -OH group at 3-position of the C ring is more favorable than the presence of a rhamnose at this position. In addition, in the presence of a rhamnose at 3-position of C ring, an additional -OH group at 5′-position of the B ring seems to increase the α-glucosidase inhibition. In turn, glycosylation at 3-position of the C ring is not favorable for the intended effect.

Luyen et al. (2013) evaluated the inhibition of α-glucosidase from *Saccharomyces cerevisiae* by eriodictyol (**41**), acacetin-7-*O*-*β*-D-glucoside (**42**) and buddleoside (**43**) (see the chemical structures in Table 9). Eriodictyol (**41**) did not show any inhibitory activity, possibly due to the lack of C2 = C3 double bond, while acacetin-7-*O*-*β*-D-glucoside (**42**)

Table 15. Flavonoids tested by Tundis et al. (2016), and respective inhibitory activity on α-amylase (the most active flavonoid is highlighted).

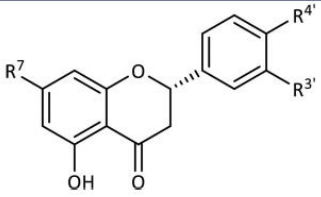
Flavonoid	Structure	$R^{3'}$	$R^{4'}$	R^7	IC_{50} (μM ± SD)
Hesperidin (**14**)		OH	OCH_3	rutinose	26.04 ± 1.7
Narirutin (**57**)		H	OH	rutinose	70.80 ± 2.5
Poncirin (**58**)		H	OCH_3	neohesperidose	39.19 ± 1.3
Didymin (**59**)		H	OCH_3	rutinose	31.62 ± 2.8
Naringin (**60**)		H	OH	neohesperidose	36.35 ± 1.9
Neoeriocitrin (**61**)		OH	OH	neohesperidose	**4.69 ± 0.9**
Positive control **Acarbose**	–	–	–	–	77.45 ± 1.8

Table 16. Flavonoids tested by Ibrahim et al. (2017), and respective inhibitory activity on α-amylase (the most active flavonoids are highlighted).

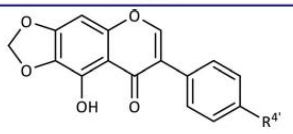
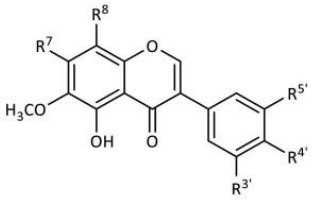
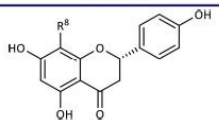
Flavonoid	Structure	$R^{3'}$	$R^{4'}$	$R^{5'}$	R^7	R^8	% Inhibition ± SD
Irilone 4′-methylether (**62**)		–	OCH_3	–	–	–	44.2 ± 0.10
Irilone (**63**)		–	OH	–	–	–	51.7 ± 0.13
Irilone 4′-*O*-β-D-glucoside (**64**)		–	glucose	–	–	–	32.8 ± 0.11
Irisolidone (**65**)		H	OH	H	OH	H	**70.8 ± 0.19**
Irigenin S (**66**)		OCH_3	OCH_3	OH	OCH_3	H	56.9 ± 0.41
Irigenin (**67**)		OCH_3	OCH_3	OH	OH	H	**67.5 ± 0.32**
Iridin S (**68**)		OCH_3	OCH_3	OCH_3	glucose	H	34.1 ± 0.08
Iridin (**69**)		OCH_3	OCH_3	OH	glucose	H	38.7 ± 0.22
Iridin A (**70**)		OCH_3	OCH_3	OH	glucose	OH	**70.5 ± 0.32**
Positive control **Acarbose**	–	–	–	–	–	–	100

Table 17. Flavonoids tested by Sun et al. (2017), and respective inhibitory activity on α-amylase (the most active flavonoid is highlighted).

Flavonoid	Structure	R^8	IC_{50} (μM)
Naringenin (**28**)		H	> 100
8-Prenylnaringenin (**71**)		prenyl	> 100
8-Geranylnaringenin (**72**)		geranyl	**15.38**
Positive control **Acarbose**	–	–	2.21

and buddleoside (**43**) had IC_{50} values of 451.8 ± 36.4 and 362.5 ± 35.1 μM, respectively, being more active than the positive control acarbose (IC_{50} = 1907 ± 156 μM). The replacement of a glucose by a rhamnose at 7-position of A ring increased the α-glucosidase inhibition.

Luteolin (**1**), geraldone (**44**) and isookanin (**45**) were evaluated concerning their ability to inhibit α-glucosidase from *Saccharomyces cerevisiae* (see the chemical structures in Table 10) (Ahmed et al. 2014). The tested flavonoids presented a % inhibition higher than acarbose (43.77 ± 1.67%), although the authors did not mention the tested concentrations of the compounds. In fact, the most effective compounds were geraldone (**44**) and luteolin (**1**), presenting inhibition % of 93.91 ± 1.21% and 92.59 ± 1.36%, respectively. These results suggest that the absence of a C2 = C3 double bond reduce the inhibitory activity of the enzyme under study.

Several derivatives (**115–126**) have been synthesized based on luteolin (**1**), apigenin (**22**), chrysin (**73**) and diosmetin (**114**) scaffolds, and their α-glucosidase (from *Saccharomyces cerevisiae*) inhibitory activity was evaluated (Table 29) (Cheng et al. 2014). The most potent derivatives were $O^{3'}$,O^7-dibutyl diosmetin (**122**) and $O^{3'}$,O^7-dihexyl diosmetin (**123**) with IC_{50} values of 2.940 ± 0.051 μmol/L and 2.406 ± 0.101 μmol/L, respectively. These synthesized flavonoids were generally more active than their precursors, except the luteolin derivatives, and presented increased inhibitory activity comparing with the positive controls, acarbose (IC_{50} = 563.601 ± 40.492 μmol/L) and 1-deoxynojirimycin (IC_{50} = 226.912 ± 12.573 μmol/L). From a SAR perspective, it was found that replacing the hydrogen of the -OH group, at 3′- and 4′-positions of B ring and at 7-position of A ring, by various alkyl chains were the critical factors in enhancing the ability of flavonoids to inhibit α-glucosidase activity.

A group of isoflavones and isoflavanones (**127–140**) (Table 30) was isolated from the roots of *Mucuna pruriens* and tested regarding their inhibitory activity of α-glucosidase from *Saccharomyces cerevisiae* (Dendup et al. 2014). The most effective flavonoid was parvisoflavone B (**133**) presenting an IC_{50} value of 12.19 ± 0.14 μM, but still with less

Table 18. Flavonoids tested by Zhang et al. (2017), and respective inhibitory activity on α-amylase (the most active flavonoid is highlighted).

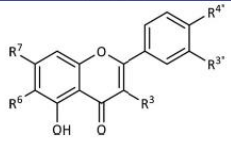
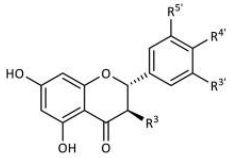
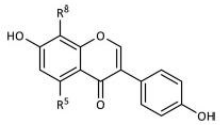
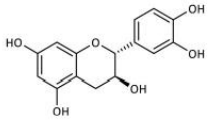
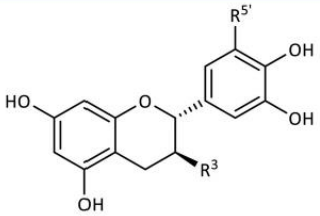
Flavonoid	Structure	R^3	$R^{3'}$	$R^{4'}$	$R^{5'}$	R^5	R^6	R^7	R^8	IC_{50} (μM ± SD)
Luteolin (**1**)		H	OH	OH	–	–	H	OH-	–	> 400
Rutin (**5**)		rutinose	OH	OH	–	–	H	OH-	–	> 400
Baicalin (**12**)		H	H	H	–	–	OH	glucuronide	–	> 400
Apigenin (**22**)		H	H	OH	–	–	H	OH	–	**146.8 ± 7.1**
Baicalein (**23**)		H	H	H	–	–	OH	OH	–	446.4 ± 23.9
Quercetin (**25**)		OH	OH	OH	–	–	H	OH	–	> 400
Kaempferol (**26**)		OH	H	OH	–	–	H	OH	–	> 400
Chrysin (**73**)		H	H	H		–	H	OH	–	> 400
Scutellarin (**74**)		H	H	OH	–	–	OH	glucuronide	–	> 400
Naringenin (**28**)		H	H	OH	H	–	–	–	–	> 400
Hesperetin (**29**)		H	OH	OCH_3	H	–	–	–	–	> 400
Dihydromyricetin (**75**)		OH	OH	OH	OH	–	–	–	–	> 400
Genistein (**19**)		–	–	–	–	OH	–	–	H	> 400
Daidzein (**20**)		–	–	–	–	H	–	–	H	> 400
Puerarin (**76**)		–	–	–	–	H	–	–	glucose	394.2 ± 17.1
(+)-Catechin (**30**)		–	–	–	–	–	–	–	–	> 400
Positive control **Acarbose**	–	–	–	–	–		–	–		5.3 ± 3.1

Table 19. Flavonoids tested by Desseaux et al. (2018), and respective inhibitory activity on α-amylase (the most active flavonoids are highlighted).

				K_i (μM ± SD)	
Flavonoid	Structure	R^3	$R^{5'}$	Amylose	Maltopentaose
(+)-Catechin (**30**)		OH	H	19 ± 3	NA
(-)-Epicatechin (**31**)		OH	H	23 ± 4	NA
(-)-Epigallocatechin gallate (**33**)		galloyl	OH	**11 ± 2**	**36 ± 5**
(-)-Gallocatechin gallate (**39**)		galloyl	OH	34 ± 5	**28 ± 4**
(-)-Epicatechin gallate (**40**)		galloyl	H	14 ± 2	**29 ± 6**
(-)-Catechin gallate (**77**)		galloyl	H	**7 ± 2**	**33 ± 5**

NA – Not active.

inhibitory activity than acarbose (IC_{50} = 7.96 ± 1.68 μM). By comparing with the other tested flavonoids, it can be concluded that the C2 = C3 double bond [parvisoflavone B (**133**) *vs.* **127**], as well as the presence of -OH groups at 2′- and 4′-positions of B ring (**127** *vs.* **128**), increased the activity under study.

Wang and coworkers (Wang, Cheng, et al. 2014) synthesized five series of apigenin (**22**) and chrysin (**73**) and nitric oxide (NO) derivatives (**141–155**) (Table 31) and evaluated their α-glucosidase (from *Saccharomyces cerevisiae*) inhibitory activity. All the tested derivatives demonstrated to be better inhibitors than their precursors, apigenin (**22**) (IC_{50} = 16.780 ± 0.257 μmol/L) and chrysin (**73**) (IC_{50} = 77.730 ± 3.490 μmol/L) and much better inhibitors than the positive controls, acarbose (IC_{50} = 563.601 ± 40.492 μmol/L) and 1-deoxynojirimycin (IC_{50} = 226.912 ± 12.573 μmol/L). In fact, the most active compound was flavonoid (**145**), which presented an IC_{50} value of 2.333 ± 0.123 μmol/L). The obtained results indicate that -OH groups at 5-position of A ring (e.g., **149** *vs.* **152**) and carboxyl groups on the coupling chain of derivatives act as H-bond receptors [e.g., chrysin (**73**) *vs.* **141**] , increasing the inhibitory activity of the derivatives toward α-glucosidase. In addition, hydrophobicity can be used to change the α-glucosidase inhibition by flavonoids.

The inhibitory activity of flavonoids isolated from *Salvia chloroleuca* – luteolin-7-*O*-glucoside (**4**), luteolin-7-*O*-glucuronide (**46**), diosmetin-7-*O*-glucuronide (**47**) and salvigenin (**48**) (see the chemical structures in Table 11) – toward α-glucosidase from *Saccharomyces cerevisiae*, was studied by Asghari et al. (2015). Among the tested flavonoids, luteolin-

Table 20. Flavonoids tested by Li, Yao, et al. (2018), and respective inhibitory activity on α-amylase (the most active flavonoid is highlighted).

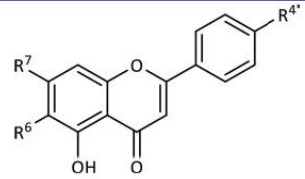
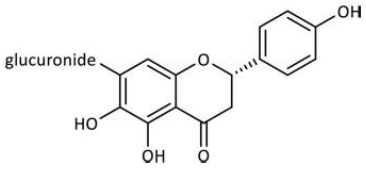
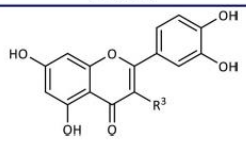
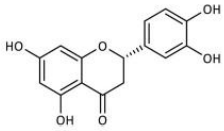
Flavonoid	Structure	$R^{4'}$	R^6	R^7	IC_{50} (μg/mL ± SD)
Baicalin (**12**)		H	OH	glucuronide	658.67 ± 16.38
Apigenin (**22**)		OH	H	OH	**287.53 ± 5.39**
Baicalein (**23**)		H	OH	OH	336.22 ± 6.31
Chrysin (**73**)		H	H	OH	450.16 ± 10.45
Scutellarin (**74**)		OH	OH	glucuronide	369.52 ± 8.43
Apigenin 7-*O*-glucuronide (**78**)		OH	H	glucuronide	653.98 ± 15.28
Chrysin 7-*O*-glucuronide (**79**)		H	H	glucuronide	980.73 ± 18.34
Isocarthamidin 7-*O*-glucuronide (**80**)		–	–	–	2941.25 ± 62.12
Positive control **Acarbose**	–	–	–	–	678.43 ± 16.52

Table 21. Flavonoids tested by Lim et al. (2019), and respective inhibitory activity on α-amylase (the most active flavonoids are highlighted).

Flavonoid	Structure	R^3	K_i (mM)
Luteolin (**1**)		H	**0.22**
Quercetin (**25**)		OH	**0.18**
Eriodictyol (**41**)		–	5.10

7-*O*-glucuronide (**46**) was the most effective (IC_{50} = 14.7 ± 2.1 μM), presenting similar activity to acarbose (16.1 ± 0.8 μM). The results suggest that the -OH substitution on the B ring as well as the presence of a sugar moiety on A ring improved the α-glucosidase inhibition.

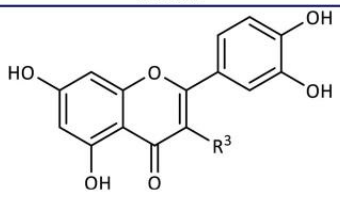
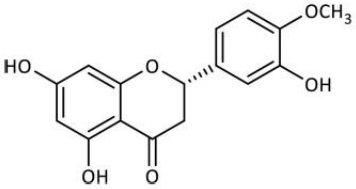
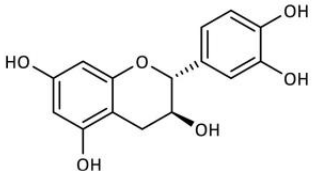
Chang and colleagues isolated seventeen flavonoids (Table 32) from *Tinospora crispa* leaf and studied their ability to inhibit α-glucosidase from *Bacillus stearothermophilus* (Chang, Ho, and Lee 2015). Among the isolated compounds, isovitexin 2″-(*E*)-*p*-coumarate (**161**) showed the best activity with an IC_{50} value of 4.3 ± 1.4 μM. By comparing flavonoid **161** with isoorientin 2″-(*E*)-*p*-coumarate (**160**) (IC_{50} = 35.7 ± 5.7 μM), it can be observed that the addition of a -OH group at 3′-position of B ring decreased the inhibitory activity. On the other hand, the presence of a -OH group at 4′-position of B ring is more favorable than the presence of a glucose at this position, since luteolin (**1**) was a better inhibitor than luteolin 4′-*O*-*β*-glucoside (**156**).

Costa et al. (2015) isolated the following *C*-glycosylflavonoids from *Passiflora bogotensis*: isoorientin (**157**), isovitexin (**158**), isovitexin-2″-*O*-rhamnoside (**169**), isoorientin-2″-*O*-rhamnoside (**170**), apigenin-6-*C*-α-L-rhamnosyl-(1➔2)-(6″-*O*-acetyl)-*β*-D -glucoside (**171**) and luteolin 6-*C*-α-L-rhamnosyl-(1➔2)-(6″-*O*-acetyl)-*β*-D -glucoside (**172**) (Table 33). The decreasing order of inhibitory activity of α-glucosidase (from *Saccharomyces cerevisiae*) by the tested flavonoids is **171** > **172** > **157** > **158** > **170** > **169**, suggesting that the acetyl group in the C(6″)-position has a crucial and favorable influence in the inhibitory effect, since flavonoids **171** and **172** have the lowest IC_{50} values, 19 ± 0.01 μM and 25 ± 0.04 μM, respectively.

Flavonoids from the aerial parts of *Vauquelinia corymbose* were isolated and their inhibitory activity on yeast and mammalian α-glucosidases was studied (Flores-Bocanegra et al. 2015). The tested flavonoids were quercetrin (**9**), quercetin (**25**), epicatechin (**31**), isoquercetin (**38**), hyperoside (**173**), and quercetin-3-*O*-(6″-benzoyl)-*β*-galactoside (**174**) (Table 34). The most effective compound was the mixed-type inhibitor quercetin-3-*O*-(6″-benzoyl)-*β*-galactoside (**174**), with IC_{50} values of 0.03 ± 0.006 mM for the yeast enzyme and 0.43 ± 0.03 mM for the mammalian α-glucosidase. Acarbose presented IC_{50} values of 0.50 ± 0.23 mM and 0.10 ± 0.03 mM, for yeast (*Saccharomyces cerevisiae*) and mammalian enzymes, respectively. The results suggested that benzoylation at 6″-position of the sugar moiety of flavonoids significantly increase their ability to inhibit α-glucosidase, comparing with the other tested compounds. Furthermore, the nature of the sugar moiety seemed to influence the inhibitory activity, since flavonoid glucoside, isoquercetin (**38**), was more active than flavonoid galactoside, hyperoside (**173**), and flavonoid rhamnoside, quercetrin (**9**). Interestingly, with the exception of quercetrin (**9**), all flavonoids presented a better activity in inhibiting yeast α-glucosidase than the mammalian enzyme.

Guo et al. (2015) isolated four flavones [4′,7-dihydroxyflavone (**93**), licoflavone A (**178**), licoflavone C (**179**) and licoflavone B (**180**)], five isoflavones [genistein (**19**), formononetin (**137**), eurycarpin A (**175**), luteone (**176**) and glabrone (**177**)], two flavanones [liquiritigenin (**181**) and glabrol (**182**)] and one flavan [glabridin (**183**)] (Table 35) from licorice, *Glycyrrhiza uralensis* Fish. Based on the results, it was concluded that the -OH groups and the prenyl groups

Table 22. Flavonoids tested by Martinez-Gonzalez et al. (2019), and respective inhibitory activity on α-amylase (the most active flavonoid is highlighted).

Flavonoid	Structure	R^3	IC_{50} (μM ± SD)
Luteolin (**1**)		H	18.00 ± 1.00
Rutin (**5**)		rutinose	NA
Quercetin (**25**)		OH	**12.70 ± 1.20**
Hesperetin (**29**)		–	20.10 ± 0.70
(+)-Catechin (**30**)		–	NA
Positive control **Acarbose**	–	–	14.60 ± 1.70

NA – Not active.

play a crucial role on the flavonoids' activity, as the flavonoids with these substituents presented the lowest IC_{50} values. Moreover, flavonoids with more than one -OH and/or prenyl groups, presented IC_{50} values lower than 0.1 μM, being even better inhibitors than the other tested compounds.

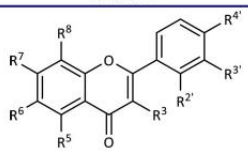
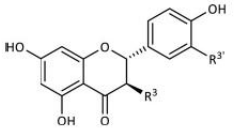
Imran et al. (2015) synthesized thirty derivatives of flavone hydrazones (Table 36) and screened their α-glucosidase (from *Saccharomyces cerevisiae*) inhibitory activity. It was observed that the additional functional group on *N*-benzylidene moiety generally increased the flavonoids' inhibitory effect. Flavonoid **187**, a 2″,4″,6″-trihydroxy substituted compound, was the most active, suggesting that the addition of -OH groups in *N*-benzylidene moiety increase the α-glucosidase inhibition, when compared with the 2″,4″-dihydroxy substituted compound **189** (IC_{50} = 27.3 ± 0.36 μM) or 2″-hydroxy substituted compound **192** (IC_{50} = 37.4 ± 0.5 μM). Other strong α-glucosidase inhibitors are those having chlorine (**203–205**), fluorine (**209–211**) and nitro substituents (**206–208**). In turn, flavonoids with methoxy (**195–198, 212, 213**), pyridine (**214–216**), and methyl (**200–202**) substituents presented a lower capacity to inhibit the enzyme under study.

Ma et al. (2015) tested the inhibitory activity of flavonoids, from flowers of *Edgeworthia gardneri*, against α-glucosidase (Table 37). The most active compound was quercetin (**25**), with an IC_{50} value of 5.0 ± 0.3 μg/mL. It was observed that the substitution of an -OH group by a sugar at 3-position of C ring decrease the α-glucosidase inhibition, by comparing quercetin (**25**) with astraglin (**2**), rutin (**5**), and isoquercetin (**38**). Moreover, by comparing quercetin (**25**) with kaempferol (**26**) (IC_{50} = 56.2 ± 4.1 μg/mL), it was found that the addition of an -OH group at 3′-position of B ring increased considerably the effect under study. Glycosylated flavonoids [astraglin (**2**), rutin (**5**), isoquercetin (**38**), tiliroside (**217**) and nicotiflorin (**218**)] were less active than their respective aglycones, quercetin (**25**) and kaempferol (**26**).

Quercetrin (**9**), dimethoxy quercetrin (**219**), hirtacoumaroflavonoside (**220**) and hirtaflavonoside B (**221**) (Table 38) were isolated from *Euphorbia hirta* by Sheliya et al. (2015), and their inhibitory activity toward α-glucosidase from *Saccharomyces cerevisiae* was evaluated. The best inhibitor was hirtacoumaroflavonoside (**220**), with an IC_{50} value of 22 μM, followed by hirtaflavonoside B (**221**) (IC_{50} = 0.071 mM), quercetrin (**9**) (IC_{50} = 0.151 mM) and dimethoxy quercetrin (**219**) (IC_{50} = 0.182 μM). From these results, it appears that the prenylation of flavonoids, as in hirtacoumaroflavonoside (**220**) and hirtaflavonoside B (**221**) makes them best inhibitors. It was also suggested that the *p*-coumaroyl substitution at 7-position of A ring increased α-glucosidase inhibition, although none of the tested flavonoids can be directly compared with hirtacoumaroflavonoside (**220**). On the other hand, the presence of -OCH_3 groups at 5- and 7- positions of A ring seems to reduce the inhibitory activity of flavonoids.

Sun et al. (2015) synthesized a series of geranylated and/or prenylated isoflavones and flavones (Table 39), and evaluated their inhibitory effect on α-glucosidase from

Table 23. Flavonoids tested by Proença et al. (2019), and respective inhibitory activity on α-amylase (the most active flavonoids are highlighted).

Flavonoid	Structure	$R^{2'}$	R^3	$R^{3'}$	$R^{4'}$	R^5	$R^{5'}$	R^6	R^7	R^8	IC_{50} (μM ± SEM) or % Inhibition at 200 μM
81		H	H	H	H	H	H	H	H	H	< 20%
82		H	H	OH	H	H	H	H	H	H	< 20%
83		H	H	H	OH	H	H	H	H	H	< 20%
84		H	H	OH	OH	H	H	H	H	H	46 ± 2%
85		H	OH	OH	OH	H	H	H	H	H	31 ± 3%
86		H	OH	OCH_3	OCH_3	H	H	H	H	H	< 20%
87		H	H	H	H	OH	H	H	H	H	< 20%
88		H	H	OH	H	OH	H	H	H	H	< 20%
89		H	H	H	OH	OH	H	H	H	H	< 20%
90		H	H	OH	OH	OH	H	H	H	H	148 ± 5 μM
91		H	H	H	H	H	H	H	OH	H	< 20%
92		H	H	OH	H	H	H	H	OH	H	28 ± 3%
93		H	H	H	OH	H	H	H	OH	H	36 ± 3%
94		H	OH	OH	H	H	H	H	OH	H	34 ± 3%
95		H	OH	H	H	H	H	H	OH	H	59 ± 4 μM
96		H	H	OH	OH	H	H	H	OH	H	131 ± 1 μM
97		H	OH	OCH_3	H	H	H	H	OCH_3	H	< 20%
98		H	OH	H	OCH_3	H	H	H	OCH_3	H	< 20%
Chrysin (**73**)		H	H	H	H	OH	H	H	OH	H	22 ± 3%
Galangin (**99**)		H	OH	H	H	H	H	H	OH	H	< 20%
Baicalein (**23**)		H	H	H	H	OH	H	OH	OH	H	< 20%
100		H	H	OH	H	OH	H	H	OH	H	≈ 200 μM
Apigenin (**22**)		H	H	H	OH	OH	H	H	OH	H	122 ± 7 μM
Kaempferol (**26**)		H	OH	H	OH	OH	H	H	OH	H	118 ± 7 μM
Luteolin (**1**)		H	H	OH	OH	OH	H	H	OH	H	78 ± 3 μM
Quercetin (**25**)		H	OH	OH	OH	OH	H	H	OH	H	138 ± 5 μM
Myricetin (**24**)		H	OH	OH	OH	OH	OH	H	OH	H	107 ± 6 μM
Morin (**101**)		OH	OH	H	OH	OH	H	H	OH	H	23 ± 1%
102		H	Cl	OH	OH	OH	H	H	OH	H	**44 ± 3 μM**
103		H	H	OH	OH	OH	H	Cl	OH	H	≈ 200 μM
104		H	H	OH	OH	OH	H	H	OH	Cl	173 ± 5 μM
105		H	Cl	OH	OH	OH	H	H	OH	Cl	82 ± 4 μM
106		H	H	OH	OH	OH	H	Cl	OH	Cl	98 ± 3 μM
Chrysoeriol (**107**)		H	H	OCH_3	OH	OH	H	H	OH	H	192 ± 7 μM
Acacetin (**108**)		H	H	H	OCH_3	OH	H	H	OH	H	< 20%
Hispidulin (**109**)		H	H	H	OH	OH	H	OCH_3	OH	H	33 ± 3%
110		H	H	OCH_3	OCH_3	OH	H	H	OH	H	< 20%
Rutin (**5**)		H	rutinose	OH	OH	OH	H	H	OH	H	< 20%
Naringenin (**28**)		–	H	H	–	–	–	–	–	–	< 20%
Eriodictyol (**41**)		–	H	OH	–	–	–	–	–	–	< 20%
Taxifolin (**111**)		–	OH	OH	–	–	–	–	–	–	< 20%
Positive control **Acarbose**		–	–	–	–	–		–	–	–	1.3 ± 0.2 μM

Saccharomyces cerevisiae. Among all the tested flavonoids, 8-geranylquercetin (**229**) was the best α-glucosidase inhibitor, exhibiting an IC_{50} value of 1.15 μM. From the group of isoflavones, the most active compound was the mixed-type inhibitor lespedeza E_1 (**223**) with a geranyl side chain (IC_{50} = 6.26 μM), being 8 – fold more active than the unsubstituted isoflavone genistein (**19**) (IC_{50} = 50.05 μM) and acarbose (IC_{50} = 51.32 μM), suggesting that the geranyl side chain improves the enzyme's inhibition. Regarding the group of flavones, it was possible to observe that the competitive inhibitor 8-geranyl quercetin (**229**) was almost 10-fold more active than quercetin (**25**) (IC_{50} = 10.98 μM), which is consistent with the above-mentioned considerations about the geranyl side chain. In turn, the di- [lupiwighteone (**222**) *vs.* **226** and lespedeza E_1 (**223**) *vs.* **227**] and trimethylation [lupiwighteone (**222**) *vs.* **224** and lespedeza E_1 (**223**) *vs.* **225**] of the -OH groups led to a significant decrease in the inhibitory activity, suggesting that the free -OH in the flavonoid's structure is crucial for the desired activity.

Flavonoids were isolated from the root barks of *Morus alba* var. *tatarica* (Table 40) and their capacity to inhibit α-glucosidase was evaluated (Zhang et al. 2015). Mortatarin D (**233**) and albanin D (**235**) were the best α-glucosidase inhibitors, with IC_{50} values of 5.0 ± 0.3 μM and 5.9 ± 0.2 μM, respectively. Being albanin D (**235**) (IC_{50} = 5.9 ± 0.2 μM) among the most active compounds, it was suggested that a geranyl group at 6-position of A ring enhances the inhibitory effect comparing with the presence of prenyl groups at other positions of the flavonoid skeleton. Moreover, by comparing albanin D (**235**) with albanin E (**236**) (IC_{50} = 11.5 ± 0.7 μM), it was verified that the addition of an -OH group at 2′-position of B ring reduced the desired activity. Genistein (**19**), with an IC_{50} value of 17.8 ± 1.1 μM, was used as positive control.

Chen et al. (2016) studied the α-glucosidase inhibition (from *Saccharomyces cerevisiae*) by flavonoids isolated from leaves and stems of *Ampelopsis grossedentata*: myricetin (**24**), dihydromyricetin (**76**), myricitrin (**113**) and flavonoids

Table 24. Flavonoids tested by Kaeswurm et al. (2019), and respective inhibitory activity on α-amylase (the most active flavonoids are highlighted).

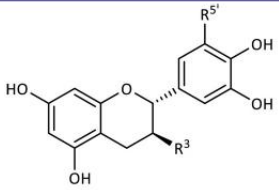
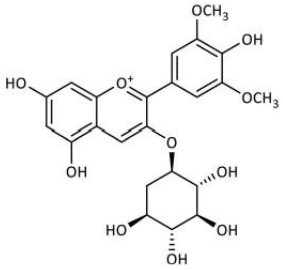
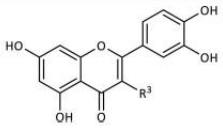
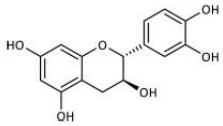
Flavonoid	Structure	R^3	$R^{5'}$	IC_{50} (μM ± SD) [S] μmol 10	100	10^3	10^6
(-)-Epicatechin (**31**)		OH	H	90 ± 37	108 ± 413	177 ± 48	231 ± 45
(-)-Epigallocatechin gallate (**33**)		galloyl	OH	**128 ± 23**	**98 ± 8**	**66 ± 3**	**58 ± 4**
Malvidin 3-glucoside (**113**)		–	–	71 ± 16	83 ± 10	121 ± 21	147 ± 50
Positive control **Acarbose**	–	–	–	0.41 ± 0.35	0.06 ± 0.01	0.02 ± 0.01	0.02 ± 0.01

Table 25. Flavonoids tested by Ren et al. (2019), and respective inhibitory activity on α-amylase (the most active flavonoid is highlighted).

Flavonoid	Structure	R^3	IC_{50} (mg/mL)
Rutin (**5**)		rutinose	1.71
Quercetin (**25**)		OH	**0.67**
(+)-Catechin (**30**)		–	1.17
Positive control **Acarbose**	–	–	14.60 ± 1.70

242–247 (Table 41). Results indicate that the introduction of some polyethylene glycol at 4′-position of B ring cause an increased inhibitory activity of flavonoids, by comparing for example myricetin (**24**) (IC_{50} = 319 ± 22.9 μM) with compound **243** (IC_{50} = 43.8 ± 1.5 μM). The most active flavonoid was **247**, a competitive inhibitor, with an IC_{50} value of 9.3 ± 0.4 μM, and also presented better inhibitory activity than the positive control acarbose, which had an IC_{50} value of 720.3 ± 57.5 μM. As such, it was observed that the introduction of a *N*-tosyl group in B ring was favorable for the intended effect, forming hydrogen bonds with the Lys155 and Ser244 in the enzyme's active site.

Imran and colleagues (Imran et al. 2016) synthesized 13 new flavone ethers and evaluated their in vitro and *in silico* capacity to inhibit the α-glucosidase from *Saccharomyces cerevisiae*. Flavonoids presenting fluorine substituents – **250, 252, 253,** and **258** – demonstrated high inhibitory activity (Table 42). Flavonoid **252**, a 2,5-trifluoromethyl-substituted compound, was the most potent flavonoid, with an IC_{50} value of 1.26 ± 0.01 μM, a value 30-fold lower than the one of acarbose (IC_{50} = 38.25 ± 0.12 μM). On the other hand, flavonoids that are *para*-substituted with nitro (**248**), nitrile (**254** and **260**), *tert*-butyl (**251**), methoxy (**255**) and methyl (**259**) substituents were weak α-glucosidase inhibitors, presenting higher IC_{50} values than acarbose.

Myricetin (**24**) and quercetin (**25**) (see the chemical structures in Table 13) were isolated from *Hovenia dulcis* and their inhibitory activity on α-glucosidase was studied (Meng et al. 2016). These flavonoids presented IC_{50} values of 3 μg/mL and 32 μg/mL, respectively; and both compounds demonstrated a noncompetitive inhibition. These values suggest that the addition of a -OH group at 5′-position of B ring increases the inhibition of α-glucosidase.

Milella et al. (2016) tested the inhibitory activity of flavonoids isolated from *Arcytophyllum thymifolium* on α-glucosidase (from *Saccharomyces cerevisiae*) (see the chemical structures in Table 14). It was found that the most active compound was flavanone **54**, with an IC_{50} value of 28.1 ± 2.6 μM), being almost 15 times more active than acarbose (402.7 ± 15.5 μM). These results suggest that the presence of a prenyloxy group at 7-position of A ring is advantageous for the intended effect.

Some flavones and isoflavones isolated from *Ficus hispida* were evaluated for their ability to inhibit α-glucosidase from *Saccharomyces cerevisiae* (Table 43) (Shi et al. 2016). The most active flavonoid was the isoflavone 3′-(3-methylbut-2-en-1-yl) biochanin A (**266**), with an IC_{50} value of 22.1 ± 7.6 μM. The -OCH_3 group present at 4′-position of B ring in flavonoid **266** increased the inhibitory activity in

Table 26. Summary of the results obtained for the α-amylase inhibitory activity of flavonoids, in the analyzed research studies.

Class	Tested concentrations	Most active flavonoid	Inhibitory activity	Type of inhibition	Positive control	Relative coefficient to Acarbose	Reference
Flavones	5000 μg/mL	Luteolin (**1**)	IC_{50} = 50–500 μg/mL	NT	Acarbose (IC_{50} = 5 - 50 μg/mL)	10.00	(Kim, Kwon, and Son 2000)
	0 - 500 μM		IC_{50} = 360 μM		NM	NM	(Tadera et al. 2006)
	NM	Isoquercetin (**38**)	Ki = 0.535×10^{-5} mol/L	Competitive			(Li et al. 2009)
		Buddleoside (**43**)	IC_{50} = 112.5 ± 15.7 μM	NT	Acarbose (IC_{50} = 732.4 ± 41.6 μM)	0.15	(Luyen et al. 2013)
		Geraldone (**44**)	% Inhibition = 93.98 ± 1.02	Competitive	Acarbose (% Inhibition = 37.65 ± 0.94)	0.40	(Ahmed et al. 2014)
	12.5–150 μM	Luteolin-7-*O*-glucuronide (**46**)	IC_{50} = 61.5 ± 1.4 μM	NT	Acarbose (IC_{50} = 53.4 ± 3.1 μM)	1.15	(Asghari et al. 2015)
	NM	Apigenin (**22**)	IC_{50} = 146.8 ± 7.1 μM		Acarbose (IC_{50} = 5.3 ± 3.1 μM)	27.70	(Zhang et al. 2017)
	0–2000 μg/mL		IC_{50} = 287.53 ± 5.39 μg/mL		Acarbose (IC_{50} = 678.43 ± 16.52 μg/mL)	0.42	(Li, Yao, et al. 2018)
	NM	Luteolin (**1**)	IC_{50} = 12.70 ± 1.20 μM	Mixed	Acarbose (IC_{50} = 14.60 ± 1.70 μM)	0.87	(Martinez-Gonzalez et al. 2019)
	0–200 μM	Flavonoid **102**	IC_{50} = 44 ± 3 μM	Competitive	Acarbose (IC_{50} = 1.3 ± 0.2 μM)	33.85	(Proença et al. 2019)
Flavonols	5 mg/mL	Quercetagetin-6-*O*-β-D-glucoside (**53**)	% Inhibition = 93.26%$^{10\ \mu L/50\ \mu g}$		Acarbose (% Inhibition = 100%$^{5\ mg/mL}$)	1.07	(Ibrahim et al. 2015)
	NM	Myricetin (**24**)	IC_{50} = 662 $\mu g/mL^{-1}$		NM	NM	(Meng et al. 2016)
	NM	Rhamnetin (**55**)	IC_{50} = 73.9 ± 5.9 μM	NT	Acarbose (IC_{50} = 26.3 ± 1.2 μM)	2.81	(Milella et al. 2016)
	31.25–750 μM	Quercetin (**25**)	Quercetin: Ki= 180 μM	Competitive	NM	NM	(Lim et al. 2019)
	0.2–1.0 mg/mL	Quercetin (**25**) Rutin (**5**)	Quercetin (24): 1.28 mg/L Rutin (5): 1.29 mg/mL	Noncompetitive			(Ren, Li, and Liu 2019)
Flavanones	5000 μg/mL	Alliuocide G (**34**)	% Inhibition$_{5000\ \mu g/mL}$= 96.5	NT	Acarbose (% Inhibition$_{5000\ \mu g/mL}$= 100)	1.03	(Mohamed 2008)
	NM	Neoeriocitrin (**61**)	IC_{50} = 4.69 ± 0.9 μM		Acarbose (IC_{50} = 77.45 ± 0.9 μM)	0.06	(Tundis et al. 2016)
		8-Geranylnaringenin (**72**)	IC_{50} = 15.38 μM		Acarbose (IC_{50} = 2.21 μM)	6.96	(Sun et al. 2017)
Flavans	0.5–500 μg/mL	Gallocatechin gallate (**39**)	IC_{50} = ~ 17 μg/mL		Acarbose (IC_{50} = 6.9 ± 0.8 μg/mL)	2.46	(Yilmazer-Musa et al. 2012)
	0–200 μM	Amylose (substrate): Catechin gallate (**77**) Maltopentaose (substrate): Gallocatechin gallate (**39**)	Catechin gallate (amylose): Ki = 7 ± 2 μM Gallocatechin gallate (maltopentaose): Ki = 28 ± 4 μM	Catechin gallate (amylose): competitive Gallocatechin gallate (maltopentaose): mixed	NM	NM	(Desseaux et al. 2018)
	50–250 μM	Epigallocatechin gallate (**33**)	IC_{50} = 66 ± 3 μM	Uncompetitive	Acarbose (IC_{50} = 0.02 ± 0.01 μM)	3300	(Kaeswurm et al. 2019)
Isoflavones	NM	Irisolidone (**65**) and iridin A (**70**)	% Inhibition: Irisolidone – 70.8 ± 0.19 Iridin A – 70.5 ± 0.32	NT	Acarbose (% Inhibition = 100%)	Irisolidone: 1.41 Iridin A: 1.42	(Ibrahim et al. 2017)

comparison of the presence of an -OH group in this position, as structurally related isoflavones isowighteone (**265**) and lupiwighteone (**222**) did not inhibit α-glucosidase.

Silva et al. (2016) studied the α-glucosidase (from *Saccharomyces cerevisiae*) inhibition by flavonoids isolated from *Eremanthus crotonoides*, namely luteolin (**1**), quercetin (**25**), *trans*-tiliroside (**270**) and quercetin 3-methyl ether (**271**) (Table 44). The flavonoid that showed the best inhibitory activity was quercetin (**25**) (IC_{50} = 7.19 ± 0.06 μM), which was almost 120-fold more active than acarbose (IC_{50} = 859.79 ± 0.09 μM). Comparing quercetin (**25**) with luteolin (**1**) (IC_{50} = 59.64 ± 1.32 μM), it appears the hydroxylation at 3-position of C ring significantly increased the inhibition of α-glucosidase.

The main flavonoids identified in *Poncirus trifoliata* were investigated for their α-glucosidase inhibitory activity: hesperidin (**14**), narirutin (**57**), poncirin (**58**), didymin (**59**), naringin (**60**) and neoeriocitrin (**61**) (see the chemical structures in Table 15) (Tundis et al. 2016). As didymin (**59**) was the most active compound (IC_{50} = 4.20 ± 0.6 μM), it seems that in comparison with the other tested flavanones, the presence of a rutinose at 7-position of A ring, together with

Table 27. Methodologies used to evaluate the inhibitory effect of flavonoids on α-glucosidase.

α-Glucosidase source	α-Glucosidase concentration	Substrate	Substrate concentration	Preincubation of flavonoids with α-glucosidase	Time of enzymatic reaction	pH	Temperature (°C)	Positive control activity	Reference
Yeast	0.1 U/mL	*p*NPG	0.375 mM	10 min	40 min [a]	6.8 (before the addition of Na_2CO_3)	37	Acarbose $IC_{50} = 103.3 \pm 9.3$ μg/mL	(Aderogba et al. 2013)
Saccharomyces cerevisiae	0.5 U/mL		5.0 mM	5 min	30 min	7.0		Acarbose $IC_{50} = 1907 \pm 156$ μM	(Luyen et al. 2013)
	0.8 U/mL			15 min	15 min [a]	6.8 (before the addition of Na_2CO_3)		Acarbose $IC_{50} = 43.77 \pm 1.67$ μM	(Ahmed et al. 2014)
	0.3 U/mL		10.0 mmol/L	10 min	20 min [b]	6.8 After the addition of Na_2CO_3: 9.8		Acarbose $IC_{50} = 563.601 \pm 40.492$ μM 1-Deoxynojirimycin $IC_{50} = 226.912 \pm 12.573$ μM	(Cheng et al. 2014)
	0.04 U/mL	NM	0.5 mM	30 min	5 min [c]			Acarbose $IC_{50} = 7.96$ μM	(Dendup et al. 2014)
	1.0×10^{-6} mol/L	*p*NPG	NM	NM	10 min	6.8	NM	Acarbose $IC_{50} = 563.601 \pm 40.492$ μM 1-Deoxynojirimycin $IC_{50} = 226.912 \pm 12.573$ μM	(Wang, Cheng, et al. 2014)
	0.5 U/mL		5.0 mM	15 min	15 min [a]	6.9 (before the addition of Na_2CO_3)	37	Acarbose $IC_{50} = 16.1 \pm 0.8$ μM	(Asghari et al. 2015)
Bacillus stearothermophilus	3.0 U/mL		20.0 mM	10 min	35 min	6.5		Acarbose $IC_{50} = 33$ nM	(Chang, Ho, and Lee 2015)
Saccharomyces cerevisiae	1.0 U/mL		11.3 mM	NM	45 min	6.8		Acarbose $IC_{50} = 15 \pm 0.01$ μM	(Costa et al. 2015)
Yeast and Mammalian	Yeast: 0.4 U/mL Mammalian: 40 mg		5.0 mM		20 min	7.4		Acarbose Yeast: 0.50 ± 0.23 mM Mammalian: 0.10 ± 0.003 mM	(Flores-Bocanegra et al. 2015)
Saccharomyces cerevisiae	2.0 U/mL		10.0 mM	5 min	30 min [d]	6.8 (before the addition of Na_2CO_3)		Acarbose $IC_{50} = 5.42$ μM	(Guo et al. 2015)
	NM		5.0 mM		NM	6.8	NM	Acarbose $IC_{50} = 860.23 \pm 6.10$ μM	(Imran et al. 2015)
	0.1 U/mL		1.0 mM	10 min	30 min [d]	6.7 (before the addition of Na_2CO_3)	37	Acarbose $IC_{50} = 465 \pm 37$ μM	(Ma et al. 2015)
NM			2.5 mM		20 min [a]	6.8 (before the addition of Na_2CO_3)		Acarbose $IC_{50} = 92$ μM	(Sheliya et al. 2015)
Saccharomyces cerevisiae	0.04 U/mL		0.5 mM	NM	30 min	6.8		Acarbose $IC_{50} = 51.32$ μM	(Sun et al. 2015)
NM	3.0 U/mL		1.0 mM	30 min				Genistein $IC_{50} = 17.8 \pm 1.1$ μM	(Zhang et al. 2015)
Saccharomyces cerevisiae	0.1 U/mL			10 min	30 min [d]	6.7 (before the addition of Na_2CO_3)		Acarbose $IC_{50} = 720.3 \pm 57.5$ μM	(Chen et al. 2016)
	NM		5.0 mM	5 min	5 min	6.8	NM	Acarbose $IC_{50} = 38.25 \pm 0.12$ μM	(Imran et al. 2016)
NM	35.0 U/mL		2.02×10^{-4} mol/L	NM	10 min		37	–	(Meng et al. 2016)
Saccharomyces cerevisiae	0.28 U/mL		2.5 mM			7.0		Acarbose $IC_{50} = 402.7 \pm 15.5$ μM	(Milella et al. 2016)
	0.0125 U/mL		1.0 mM	15 min	NM	6.8		Acarbose $IC_{50} = 347.1 \pm 68.6$ μM	(Shi et al. 2016)
	NM		10.0 mM	10 min	35 min	NM		Acarbose $IC_{50} = 859.79 \pm 0.09$ μM	(Silva et al. 2016)
	1.0 U/mg	Maltose	0.04 g/mL	NM	30 min [e]			Acarbose $IC_{50} = 54.99 \pm 1.3$ μM	(Tundis et al. 2016)
	4.5 U/mL	*p*NPG	8.0 mM	10 min	10 min [c]	6.8 (before the addition of Na_2CO_3)		Acarbose $IC_{50} = > 250$ μM	(Zeng, Chen, et al. 2016)
	NM		4.55×10^{-4} mol/L	120 min	NM	NM			(Zeng, Zhang, et al. 2016)

(*continued*)

Table 27. Continued.

α-Glucosidase source	α-Glucosidase concentration	Substrate	Substrate concentration	Preincubation of flavonoids with α-glucosidase	Time of enzymatic reaction	pH	Temperature (°C)	Positive control activity	Reference
								Acarbose $IC_{50} = 3.04 \pm 0.04 \times 10^{-4}$ mol/L	
Yeast	0.1 U/mL		5.0 mM	10 min	5 min	6.9	25	Acarbose $IC_{50} = 168.95 \pm 12.25$ μM	(Zhang et al. 2016)
Saccharomyces cerevisiae	0.2 U/mL		0.29 mM		30 min [a]	6.8 (before the addition of Na_2CO_3)	37	Acarbose $IC_{50} = 260$ μM	(Amin et al. 2017)
	0.4 U/mL		3.0 mM	30 min	60 min [c]	NM		Acarbose $IC_{50} = 6.54 \pm 0.04$ μM	(Boonsombat et al. 2017)
Yeast	0.5 U/mL		5.0 mM	20 min	20 min [f]	6.8 (before the addition of Na_2CO_3)		–	(Chen et al. 2017)
Mammalian maltase and sucrase	Prepared from rat 100 mg intestinal acetone powder in 3 mL of 0.9% acetone solution	Maltose and sucrose	Maltose: 5.0 mM Sucrose: 56.0 mM	NM	15 min [g]	6.8 (before the addition of Tris-HCl)		Acarbose % Maltase inhibition: 62.5 ± 0.5 % Sucrase inhibition: 56.1 ± 0.6	(Hmidene et al. 2017)
NM	0.02 U/mL	*p*NPG	1.0 mM		20 min [h]	7.0 (before the addition of NaOH)	37.5	Acarbose $IC_{50} = 310.2 \pm 3.6$ μM	(Jeong and Kim 2017)
Saccharomyces cerevisiae	0.16 U/mL		2.5 mM		NM	6.8	37	Acarbose $IC_{50} = 119.2 \pm 3.7$ μM	(Kim, Cho, et al. 2017)
Yeast	0.2 U/mL				15 min [a]	6.8 (before the addition of Na_2CO_3)		Acarbose $IC_{50} = 101.16 \pm 3.69$ μM	(Kim, Jung, et al. 2017)
Saccharomyces cerevisiae								Acarbose $IC_{50} = 172 \pm 17$ μM	(Lee, Kim, and Whang 2017)
	0.05 U/mL		0.6 mM	5 min	30 min	6.8		Acarbose $IC_{50} = 607 \pm 56$ μM	(Proença et al. 2017)
	2.0 U/mL		10.0 mM		30 min [d]	6.8 (before the addition of Na_2CO_3)		Acarbose $IC_{50} = 2.68 \pm 0.07$ μM	(Qin et al. 2017)
	NM		NM		15 min [i]	6.5 (before the addition of glycine) 10.0 (after the addition the glycine)	RT	Quercetin $IC_{50} = 4.30 \pm 1.06$ μg/mL	(Sarian et al. 2017)
	0.5 U/mL		5.0 mM	15 min	10 min	6.9	25	Acarbose $IC_{50} = 31.92 \pm 0.17$ μg/mL	(Şöhretoğlu et al. 2017)
	0.45 U/mL		0.15 mM	NM	15 min	6.8	37	Voglibose $IC_{50} = 24.5 \pm 1.2$ μM	(Song et al. 2017)
	4.0 mU/mL		0.075 mM		30 min			Acarbose $IC_{50} = 51.30$ μM	(Sun et al. 2017)
Bacillus steathermophilus	0.4 U/mL		2.0 mM		20 min	7.0		Acarbose $EC_{50} = 0.1$ μg/mL	(Ye, Fan, and Ma 2017)
Saccharomyces cerevisiae	0.1 U/mL		2.5 mM	15 min	15 min [a]	6.8 (before the addition of Na_2CO_3)		Acarbose $IC_{50} = 1998.79$ μM	(Wang et al. 2017)
Mammalian maltase and sucrase	Enzyme solution: 0.002 U/mL	Maltose and sucrose	Maltose: 9.0 mM Sucrose: 27.0 mM		30 min [j]	NM		Acarbose Maltase: $IC_{50} = 0.4 \pm 0.1$ μM Sucrase: $IC_{50} = 1.2 \pm 0.3$ μM	(Zhang et al. 2017)
Saccharomyces cerevisiae	1.0 U/mL	*p*NPG	5.0 mM		30 min [a]	6.8 (before the addition of Na_2CO_3)		–	(Zhen et al. 2017)
NM	0.5 U/mL				NM	6.8		Acarbose $IC_{50} = 11.8 \pm 0.08$ μM	(Zhou et al. 2017)
Saccharomyces cerevisiae	0.7 U/mL			5 min	5 min	7.0	RT	–	(Alhassan et al. 2019)
	1.0 U/mL		4.0 mM		12 min	6.8	37	Acarbose $IC_{50} = 607.9$ μM	(Adhikari-Devkota et al. 2019)
	5.0 μg/mL		6.0 mM	NM	NM	7.0		Acarbose $IC_{50} = 620.2 \pm 7.2$ μM	(Ha et al. 2018)
	0.15 U/mL		5.0 mM	5 min	60 min	7.4		Acarbose $IC_{50} = 385.2 \pm 18.6$ μM	(Li, Li, et al. 2018)
	1.0 U/mL		2.0 mM	10 min	120 min	6.8		Acarbose $IC_{50} = 996.02 \pm 21.34$ μM	(Li, Yao, et al. 2018)
	0.25 U/mL		5.0 mM	15 min	15 min	6.9	RT	Acarbose $IC_{50} = 57.49 \pm 0.25$ μM	(Renda et al. 2018)
Yeast	0.0073 U/mL		0.7 mM	10 min	NM	6.8	37		

(*continued*)

Table 27. Continued.

α-Glucosidase source	α-Glucosidase concentration	Substrate	Substrate concentration	Preincubation of flavonoids with α-glucosidase	Time of enzymatic reaction	pH	Temperature (°C)	Positive control activity	Reference
								Quercetin $IC_{50} = 6.65$ μM	(Shahinozzaman et al. 2018)
Saccharomyces cerevisiae	0.5 U/mL		5.0 mM		10 min	6.9	RT	Acarbose $IC_{50} = 50.58 \pm 0.25$ μM	(Şöhretoğlu et al. 2018)
Yeast	2.0 U/mL		10.0 mM	5 min	30 min [d]	6.8 (before the addition of Na_2CO_3)	37	Acarbose $IC_{50} = 5.90 \pm 0.98$ μM	(Xu, Wang, et al. 2018)
Saccharomyces cerevisiae	0.5 U/mL		1.0 mM	10 min				Acarbose $IC_{50} = 356.26$ μM	(Xu, Xie, et al. 2018)
Bacillus stearothermophilus	0.4 U/mL		2.0 mM	NM	20 min	7.0		Acarbose $IC_{50} = 0.04$ μg/mL	(Fan et al. 2019)
Saccharomyces cerevisiae	0.04 U/mL		0.7 mM	15 min	NM	6.8		Acarbose Ki = 4.72 ± 0.38 μM	(Ghani et al. 2019)
	2.0 U/mL		10.0 mM	10 min	35 min	7.5	28	Acarbose $IC_{50} = 266.1 \pm 0.01$ μM	(Li, Kongstad, and Staerk 2019)
Mammalian maltase and sucrase	10.0% (w/v)	Maltose	2.5% (w/v)	NM	15 min	6.9	37	–	(Lim et al. 2019)
Saccharomyces cerevisiae	0.4 U/mL	*p*NPG	3.0 mM	30 min	60 min [c]	NM		Acarbose $IC_{50} = 170.7$ μM	(Meesakul et al. 2019)
	0.04 U/mL		0.7 mM	15 min	NM	6.8		Acarbose % Inhibition = $98.7 \pm 0.9^{50\ \mu M}$	(Nur et al. 2019)
Aspergillus niger	1.0 mg/mL		0.8 mM	NM	2 min	7.0		Acarbose $IC_{50} = 320.1$ μM	(Zhao, Liu, and Chen 2019)
Yeast	60 U/mL		5.0 mM	10 min	30 min [a]	6.8		–	(Ren, Li, and Liu 2019)
Saccharomyces cerevisiae	0.15 U/mL			5 min	60 min	7.4		Acarbose $IC_{50} = 700$ μM	(Cedeño et al. 2019)
	0.1 U/mL	NM	NM	3 min	NM	NM	NM	–	(Liu et al. 2020)
NM	0.2 U/mL	*p*NPG	3.0 mM	NM	30 min [c]		37	Acarbose $IC_{50} = 214.8$ μM	(Zhu et al. 2019)
Saccharomyces cerevisiae	NM		NM		NM		NM	Acarbose $IC_{50} = 0.59 \pm 0.14$ μM	(Jia et al. 2019)
	0.2 U/mL		1.0 mM	10 min	20 min [k]		37	Acarbose	(He et al. 2019)
NM					20 min	6.8		Acarbose $IC_{50} = 1727.07$ μM	(Li, Wang, et al. 2019)
Saccharomyces cerevisiae	0.5 U/mL		5.0 mM	5 min	30 min			Acarbose $IC_{50} = 172.3 \pm 14.7$ μM	(Li, Zhu, et al. 2019)

IC_{50} – concentration of a drug or compound that is required for 50% inhibition in vitro. NM – Not mentioned; NT – Not tested; *p*NPG – 4-Nitrophenyl *β*-D-glucuronide; RT – Room temperature.
[a]Addition of Na_2CO_3 0.2 M to stop the reaction.
[b]Addition of Na_2CO_3 10 mmol/L to stop the reaction.
[c]Addition of Na_2CO_3 0.1M to stop the reaction.
[d]Addition of Na_2CO_3 1 M to stop the reaction.
[e]Addition of $HClO_4$ to stop the reaction.
[f]Addition of Na_2CO_3 0.4 M to stop the reaction.
[g]Addition of Tris-HCl 2 M to stop the reaction.
[h]Addition of NaOH 2 M to stop the reaction.
[i]Addition of glycine to stop the reaction.
[j]Incubation at 100 °C to stop the reaction.
[k]Addition of 1 mL of ethanol to stop the reaction.

Table 28. Flavonoids tested by Aderogba et al. (2013), and respective inhibitory activity on α-glucosidase (the most active flavonoid is highlighted).

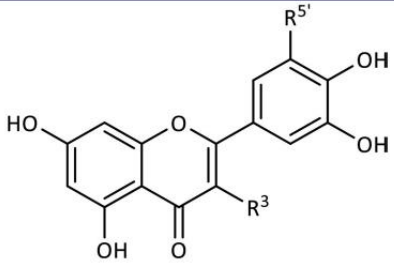
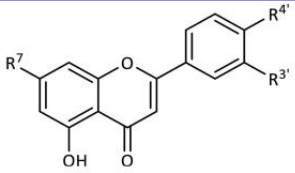
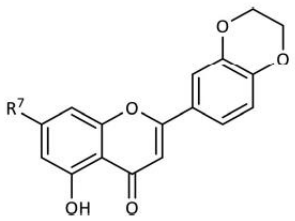
Flavonoid	Structure	R^3	$R^{5'}$	IC_{50} (μg/mL ± SD)
Quercetrin (**9**)		rhamnose	H	122.7 ± 1.6
Quercetin (**25**)		OH	H	**30.9 ± 8.4**
Myricitrin (**113**)		rhamnoses	OH	79.0 ± 4.3
Positive control **Acarbose**	–	–		103.3 ± 9.3

Table 29. Flavonoids tested by Cheng et al. (2014), and respective inhibitory activity on α-glucosidase (the most active flavonoids are highlighted).

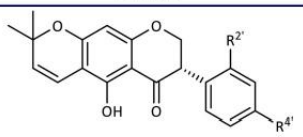
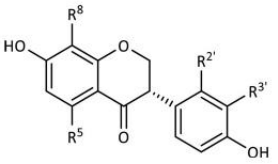
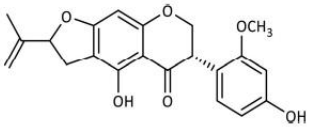
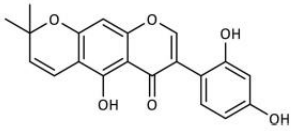
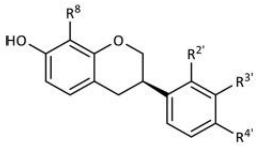
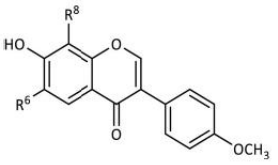
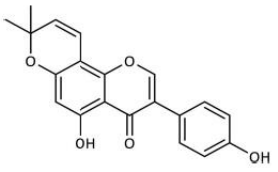
Flavonoid	Structure	$R^{3'}$	$R^{4'}$	R^7	IC_{50} (μmol/L ± SD)
Luteolin (**1**)		OH	OH	OH	3.652 ± 0.077
Apigenin (**22**)		H	OH	OH	16.780 ± 0.257
Chrysin (**73**)		H	H	OH	77.730 ± 3.490
Diosmetin (**114**)		OH	OCH_3	OH	22.764 ± 3.503
O^7-Ethyl chrysin (**115**)		H	H	OC_2H_5	24.396 ± 0.665
O^7-Butyl chrysin (**116**)		H	H	OC_4H_9	7.040 ± 1.634
O^7-Hexyl chrysin (**117**)		H	H	OC_6H_{13}	4.476 ± 1.109
$O^{4'}$, O^7-Diethyl apigenin (**118**)		H	OC_2H_5	OC_2H_5	7.350 ± 0.998
$O^{4'}$, O^7-Dibutyl apigenin (**119**)		H	OC_4H_9	OC_4H_9	6.897 ± 0.263
$O^{4'}$, O^7-Dihexyl apigenin (**120**)		H	OC_6H_{13}	OC_6H_{13}	4.426 ± 0.281
$O^{3'}$, O^7-Diethyl diosmetin (**121**)		OC_2H_5	OCH_3	OC_2H_5	22.051 ± 3.596
$O^{3'}$, O^7-Dibutyl diosmetin (**122**)		OC_4H_9	OCH_3	OC_4H_9	**2.940 ± 0.051**
$O^{3'}$, O^7-Dihexyl diosmetin (**123**)		OC_6H_{13}	OCH_3	OC_6H_{13}	**2.406 ± 0.101**
O^7-Ethyl- $O^{3'}$, $O^{4'}$-ethylidene luteolin (**124**)		–	–	OC_2H_5	15.952 ± 1.013
O^7-Butyl- $O^{3'}$, $O^{4'}$-ethylidene luteolin (**125**)		–	–	OC_4H_9	13.733 ± 0.299
O^7-Hexyl- $O^{3'}$, $O^{4'}$-ethylidene luteolin (**126**)		–	–	OC_6H_{13}	5.180 ± 0.451
Positive control **Acarbose**	–	–	–	–	563.601 ± 40.492
Positive control **1-Deoxynojirimycin**	–	–	–	–	226.912 ± 12.573

the presence of a -OCH_3 group at 4′-position of B ring enhance the α-glucosidase inhibition.

Flavones apigenin (**22**), luteolin (**1**) and buddleoside (**43**), as well as flavanones naringenin (**28**), eriodictyol (**41**), isosakuranetin (**272**), didymin (**59**) and hesperidin (**14**) (Table 45), were isolated from *Clinopodium chinense* (Benth.) (Zeng, Chen, et al. 2016). The inhibitory activity of these flavonoids was tested on α-glucosidase from *Saccharomyces cerevisiae*. Luteolin (**1**) and eriodictyol (**41**) were the flavonoids with the best activity, with IC_{50} values of 2.0 ± 1.8 μM and 1.4 ± 3.4 μM, respectively, suggesting that the addition of an -OH group at 3′-position of B ring enhances significantly the intended activity, when compared to apigenin (**22**) and naringenin (**28**), respectively. Furthermore, the remarkable reduction of the inhibitory activity of didimyn (**59**) (IC_{50} > 60 μM) when compared with isosakuranetin (**272**) (IC_{50} = 31.2 ± 2.8 μM) revealed the importance of the OH group at 7-position of A ring for the inhibition of α-glucosidase. In turn, the glycosylation of flavonoids leads to a reduction of the inhibitory activity.

The inhibitory activity of apigenin (**22**), morin (**101**) and myricetin (**24**) (Table 46) was studied on α-glucosidase from *Saccharomyces cerevisiae*, presenting IC_{50} values of (10.5 ± 0.05) × 10^{-6} mol L^{-1}, (4.48 ± 0.04) × 10^{-6} mol L^{-1} and (2.25 ± 0.05) × 10^{-6} mol L^{-1}, respectively (Zeng, Zhang, et al. 2016). All three flavonoids were more effective than acarbose, with an IC_{50} value of (3.04 ± 0.04) × 10^{-4} mol L^{-1}. The higher inhibitory activity of myricetin (**24**) might be due to the increased number of -OH groups in B ring. Compared to myricetin (**24**) and morin (**101**), the IC_{50} value of apigenin (**22**) was the highest, which may be mainly due to the

Table 30. Flavonoids tested by Dendup et al. (2014), and respective inhibitory activity on α-glucosidase (the most active flavonoids are highlighted).

Flavonoid	Structure	$R^{2'}$	$R^{3'}$	$R^{4'}$	R^5	R^6	R^8	IC_{50} (μM ± SD)
127		OH	–	OH	–	–	–	58.43 ± 1.47
128		OCH_3	–	OH	–	–	–	115.01 ± 0.57
129 (*3R*)		H	H	–	H	–	OCH_3	NA
130 (*3S*)		OCH_3	OCH_3	–	OH	–	H	NA
131 (*3S*)		OCH_3	OCH_3	–	H	–	H	NA
132		–	–	–	–	–	–	NA
Parvisoflavone (**133**)		–	–	–	–	–	–	**12.19 ± 0.14**
134		OH	H	OCH_3	–	–	H	32.96 ± 0.45
135		OCH_3	OCH_3	OH	–	–	H	NA
136		OH	H	OCH_3	–	–	OCH_3	51.88 ± + 1.10
Formononetin (**137**)		–	–	–	–	H	H	NA
Afrormosin (**138**)		–	–	–	–	OCH_3	H	NA
8-*O*-Methylretusin (**139**)		–	–	–	–	H	OCH_3	NA
Derrone (**140**)		–	–	–	–	–	–	NA
Positive control **Acarbose**	–	–	–	–	–	–	–	7.96 ± 1.68

NA – Not active.

lower number of -OH groups, comparing with the other tested flavonoids.

In the work of Zhang et al. (2016), the ability of isoquercetin/quercetin-3-*O*-glucoside (**38**), rhamnazin (**273**) and rhamnetin (**55**) (Table 47) to inhibit α-glucosidase from *Saccharomyces cerevisiae* was studied. The obtained IC_{50} values were of 22.38 ± 1.73 μM, > 3000 μM and 432.04 ± 10.17 μM for flavonoids **38, 273**, and **55**, respectively. These results indicate that the presence of -OCH_3 groups at 7-position of A ring and at 3′-position of B ring of flavones leads to a reduction in their activity.

In the work of Amin et al. (2017), α-glucosidase (from *Saccharomyces cerevisiae*) inhibition by pectolinarigenin (**274**) and pectolinarine (**275**) (Table 48), two flavonoids isolated from *Kickxia ramosissima*, was tested. Pectolinarigenin (**274**) (IC_{50} = 0.23 mM) was more active than pectolinarine (**275**) (48% of inhibition, at 2 mM), indicating that the glycosylation of at 7-position of A ring significantly reduced the inhibitory activity. Pectolinarigenin (**274**) also presented an IC_{50} value similar to the positive control, acarbose (IC_{50} = 0.26 mM).

The inhibitory activity of some isoflavones, isolated from *Butea superba*, on α-glucosidase (from *Saccharomyces*

Table 31. Flavonoids tested by Wang, Cheng, et al. (2014), and respective inhibitory activity on α-glucosidase (the most active flavonoids are highlighted).

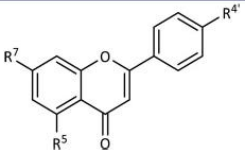
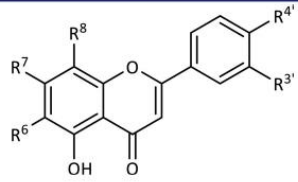
Flavonoid	Structure	$R^{4'}$	R^5	R^7	IC_{50} (μmol/L ± SD)
Apigenin (**22**)		OH	OH	OH	16.780 ± 0.257
Chrysin (**73**)		H	OH	OH	77.730 ± 3.490
141		$O(CH_2)_2ONO_2$	OH	$O(CH_2)_2ONO_2$	7.779 ± 1.230
142		$O(CH_2)_4ONO_2$	OH	$O(CH_2)_4ONO_2$	5.045 ± 0.527
143		$O(CH_2)_6ONO_2$	OH	$O(CH_2)_6ONO_2$	4.594 ± 0.528
144		$OCH_2COO(CH_2)_2ONO_2$	OH	$OCH_2COO(CH_2)_2ONO_2$	3.714 ± 0.426
145		$OCH_2COO(CH_2)_4ONO_2$	OH	$OCH_2COO(CH_2)_4ONO_2$	**2.333 ± 0.123**
146		$OCH_2COO(CH_2)_6ONO_2$	OH	$OCH_2COO(CH_2)_6ONO_2$	**2.567 ± 0.070**
147		H	OH	$O(CH_2)_2ONO_2$	30.040 ± 6.630
148		H	OH	$O(CH_2)_4ONO_2$	18.700 ± 0.220
149		H	OH	$O(CH_2)_6ONO_2$	20.960 ± 1.620
150		H	CH_3COO	$O(CH_2)_2ONO_2$	> 100
151		H	CH_3COO	$O(CH_2)_4ONO_2$	> 100
152		H	CH_3COO	$O(CH_2)_6ONO_2$	> 100
153		H	OH	$OCH_2COO(CH_2)_2ONO_2$	23.980 ± 4.660
154		H	OH	$OCH_2COO(CH_2)_4ONO_2$	14.100 ± 3.980
155		H	OH	$OCH_2COO(CH_2)_6ONO_2$	3.390 ± 3.860
Positive control **Acarbose**	–	–	–	–	563.601 ± 40.492
Positive control **1-Deoxynojirimycin**	–	–	–	–	226.912 ± 12.573

Table 32. Flavonoids tested by Chang, Ho, and Lee (2015), and respective inhibitory activity on α-glucosidase (the most active flavonoid is highlighted).

Flavonoid	Structure	$R^{3'}$	$R^{4'}$	R^6	R^7	R^8	IC_{50} (μM ± SD)
Luteolin (**1**)		OH	OH	H	OH	H	86.1 ± 4.3
Luteolin 7-*O*-*β*-glucoside (**4**)		OH	OH	H	glucose	H	*
Apigenin (**22**)		H	OH	H	OH	H	34.6 ± 3.9
Chrysoeriol (**107**)		OCH_3	OH	H	OH	H	*
Luteolin 4′-*O*-*β*-glucoside (**156**)		OH	glucose	H	OH	H	*
Isoorientin (**157**)		OH	OH	glucose	OH	H	1525.7 ± 3.7
Isovitexin (**158**)		H	OH	glucose	OH	H	61.2 ± 2.5
159		OH	OH	glucosyl-2″-(*E*)-sin	OH	H	*
Isoorientin 2″-(*E*)-*p*-coumarate (**160**)		OH	OH	glucosyl-2″-(*E*)-*p*-cou	OH	H	35.7 ± 5.7
Isovitexin 2″-(*E*)-*p*-coumarate (**161**)		H	OH	glucosyl-2″-(*E*)-*p*-cou	OH	H	**4.3 ± 1.4**
Orientin (**162**)		OH	OH	H	OH	glucose	*
Apigenin 7-*O*-*β*-glucoside/ Cosmosiin (**163**)		H	OH	H	glucose	H	*
Cosmosiin 6′′-(*E*)-ferulate (**164**)		H	OH	H	glucosyl-6″-(*E*)-fer	H	8.8 ± 2.9
Cosmosiin 6-(*E*)-*p*-coumarate (**165**)		H	OH	H	glucosyl-6″-(*E*)-*p*-cou	H	14.6 ± 4.8
Cosmosiin 6-(*Z*)-*p*-coumarate (**166**)		H	OH	H	glucosyl-6″-(*Z*)-*p*-cou	H	10.1 ± 3.5
Cosmosiin 6-(*E*)-*p*-cinnamate (**167**)		H	OH	H	glucosyl-6″-(*E*)-*p*-cin	H	11.3 ± 2.0
Luteolin 7-*O*-*β*-glucosyl-6″-(*E*)-*p*-cinnamate (**168**)		OH	OH	H	glucosyl-6″-(*E*)-*p*-cin	H	*
Positive control **Acarbose**	–	–	–	–	–	–	0.033 ± 0.006

*Showed no inhibition at 10 μg/mL and their IC_{50} values were not obtained due to the limited amount of material.

cerevisiae) was studied (Boonsombat et al. 2017). The most effective flavonoid was biochanin A (**276**), which bears an -OH group at 5- and 7- positions of A ring and a -OCH_3 group at 4′-position of B ring (Table 49), with an IC_{50} value of 12.35 ± 0.36 μM. The results showed that the presence of a -OCH_3 (**277, 278, 286,** and **287**), an allyl (**279**), a propagyl (**280**) or a prenyl (**282**) group at 7-position of A ring significantly decreased the α-glucosidase inhibition, since the isoflavones with the mentioned substituents were not active.

The importance of the addition of -OH groups in B ring was once again pronounced in the study of Chen et al. (2017), where the inhibitory activity of quercetin (**25**) (IC_{50} = 66.8 μg/mL) and kaempferol (**26**) (IC_{50} = 109 μg/mL) (Table 50) on yeast α-glucosidase was evaluated. As mentioned above, the catechol group in B ring seems to be favorable for the α-glucosidase inhibition.

The sucrase and maltase inhibition from rat intestinal powder was studied, testing flavonoids quercetin (**25**), rhamnetin (**55**), rhamnazin (**273**), tamarixetin (**289**), kaempferol (**25**), quercetin 3-*O*-*β*-D-glucuronide (**290**), quercetin 3-*O*-*β*-D-glucuronide methyl ester (**291**), kaempferol 3-*O*-*β*-D-glucuronide (**292**) and kaempferol 3-*O*-*β*-D-glucuronide methyl ester (**293**) (Table 51) (Hmidene et al. 2017). Concerning the inhibition of sucrase activity, the flavonoids

Table 33. Flavonoids tested by Costa et al. (2015), and respective inhibitory activity on α-glucosidase (the most active flavonoid is highlighted).

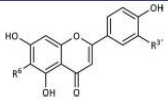
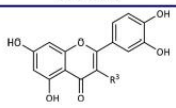
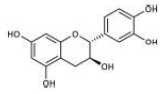
Flavonoid	Structure	$R^{3'}$	R^6	IC_{50} (μM ± SD)
Isoorientin (**157**)		OH	glucose	29 ± 0.03
Isovitexin (**158**)		H	glucose	32 ± 0.04
Isovitexin 2″-*O*-rhamnoside (**169**)		H	glucosyl-2″O-rhamnose	35 ± 0.03
Isoorientin 2″-*O*-rhamnoside (**170**)		OH	glucosyl-2″O-rhamnose	34 ± 0.02
Apigenin 6-*C*-α-L-rhamnosyl-(1-2)-(6″-*O*-acetyl)-β-D-glucoside (**171**)		H	rhamnosyl-(1-2)-(6″-O-acetyl)-b-D-glucose	**19 ± 0.01**
Luteolin 6-*C*-α-L-rhamnosyl-(1-2)-(6″-*O*-acetyl)-β-D-glucoside (**172**)		OH	rhamnosyl-(1-2)-(6″-O-acetyl)-b-D-glucose	25 ± 0.04
Positive control **Acarbose**	–	–		15 ± 0.01

Table 34. Flavonoids tested by Flores-Bocanegra et al. (2015), and respective inhibitory activity on α-glucosidase (the most active flavonoid is highlighted).

			IC_{50} (mM ± SD)	
Flavonoid	Structure	R^3	Yeast	Rat Small Intestine
Quercetrin (**9**)		rhamnose	45.0% [10 mM]	3.34 ± 0.38
Quercetin (**25**)		OH	0.03*	0.216*
Isoquercetin (**38**)		glucose	0.06 ± 0.005	1.63 ± 0.11
Hyperoside (**173**)		galactose	0.40 ± 0.02	1.98 ± 0.15
Quercetin 3-*O*-(6″-benzoyl)-β-galactoside (**174**)		6″-benzoyl-β-galactose	**0.03 ± 0.006**	**0.43 ± 0.03**
(-)-Epicatechin (**31**)		–	0.30 ± 0.02	15.2% [10 mM]
Positive control **Acarbose**	–	–	0.50 ± 0.23	0.10 ± 0.03

*Values taken from reference (Yin et al. 2014) by the authors.

under study showed a lower activity than acarbose (56.1 ± 0.6%), at the highest tested concentration (100 μM). Regarding the inhibition of maltase, the most active flavonoids, **290** (inhibition % = 62.0 ± 0.1) and **291** (inhibition % = 75.3 ± 0.5), both noncompetitive inhibitors, presented similar activity to acarbose (62.5 ± 0.5%, at 100 μM). For the inhibition of mammalian α-glucosidase, particularly maltase, the results suggest that the substitution of the -OH group at 3-position of C ring with a glucuronic acid and its methyl ester enhance the activity of flavonoids toward α-glucosidase.

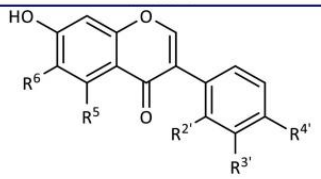
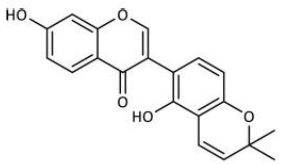
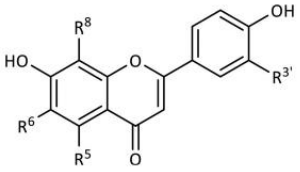
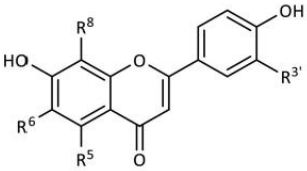
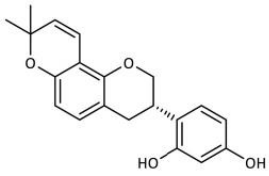
In the work of Jeong and Kim (2017), rutin (**5**) was exposed to γ-ray and produced 3 new hydroxymethylated products in the C ring: radiorutinol (**294**), isoradiorutinol (**295**) and radiorutindiol (**296**). The inhibitory activity of those compounds, including the precursor rutin (**5**), against α-glucosidase was evaluated (Table 52). All the new hydroxymethylated flavonoids were more active than rutin (**5**) (IC_{50} > 500 μM) and acarbose (IC_{50} = 310.2 ± 3.6 μM). Isoradiorutinol (**295**) was the most active (IC_{50} = 11.2 ± 0.7 μM). These results suggest that the replacement and stereochemistry of the hydroxymethyl group at 2-position of C ring in dihydroflavonol skeleton may increase α-glucosidase inhibition.

Four flavanones isolated from the roots of *Sophora flavescens* [kushenol A (**297**), kushenol E (**298**), kushenol B (**299**) and kushenol L (**300**)] (Table 53) were evaluated for their inhibitory activity on α-glucosidase from *Saccharomyces cerevisiae* (Kim, Cho, et al. 2017). The most effective flavonoid was kushenol B (**299**), an uncompetitive inhibitor, with an IC_{50} value of 11.0 ± 0.3 μM. This may indicate that the presence of a lavandulyl group at 8-position and a prenyl group at 6-position of A ring increases α-glucosidase inhibition. In accordance, the substitution of the lavandulyl for a prenyl group at 8-position of A ring [kushenol E (**298**)] led to a decrease in the inhibitory effect (IC_{50} = 24.6 ± 0.8 μM).

Icaritin (**301**), icariside II (**302**), icariin (**303**), epimedin A (**304**), epimedin B (**305**), and epimedin C (**306**) (Table 54) were isolated from *Epimedium koreanum*, and their ability to inhibit α-glucosidase from *Saccharomyces cerevisiae* was evaluated (Kim, Jung, et al. 2017). Icaritin (**301**), with an IC_{50} value of 74.42 ± 0.01 and a noncompetitive inhibition type, was found to be the most active compound. In addition, the glycosylation of flavonoids at 7-position of A ring and at 3-position of C ring significantly decreased the intended effect, when compared with the presence of -OH groups at these positions.

Kaempferol 3-*O*-β-D-glucosyl-7-*O*-α-L-rhamnoside (**307**), quercetrin (**9**), afzelin (**308**) and isoscutellarein 8-*O*-rhamnoside (**309**) (Table 55), isolated from *Smilax china* L. stem, were tested (Lee, Kim, and Whang 2017). The compound with better inhibition of α-glucosidase was afzelin (**308**), with an IC_{50} value of 31.7 ± 1.6 μM, while quercetrin (**9**), kaempferol 3-*O*-β-D-glucosyl-7-*O*-α-L-rhamnoside (**307**) and isoscutellarein 8-*O*-rhamnoside (**309**) presented IC_{50} values of 135 ± 13 μM, 609 ± 32 μM and 45.1 ± 2.6 μM, respectively. By comparing afzelin (**308**) with quercetrin (**9**), it can be found that the -OH group at 3′-position of B ring significantly decreases the inhibition of α-glucosidase. Besides that, by comparing afzelin (**308**) with isoscutellarein 8-*O*-rhamnoside (**309**), the presence of the rhamnose at 3-position of C ring is more favorable for the intended effect than the presence of this sugar at 8-position of A ring. The positive control acarbose presented an IC_{50} value of 172 ± 17 μM. In the work of Torres-Naranjo et al. (2016), afzelin (**308**) (IC_{50} = 3.56 μM) was also more active than quercetrin (**9**) (IC_{50} = 7.77 μM).

Table 35. Flavonoids tested by Guo et al. (2015), and respective inhibitory activity on α-glucosidase (the most active flavonoids are highlighted).

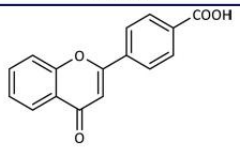
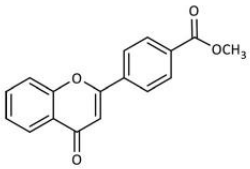
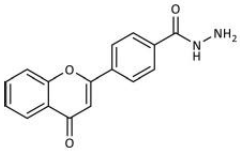
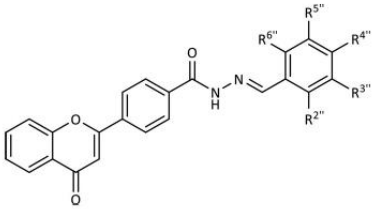
Flavonoid	Structure	$R^{2'}$	$R^{3'}$	$R^{4'}$	R^5	R^6	R^7	R^8	IC_{50} (μM)
Genistein (**19**)		H	H	OH	OH	H	–	–	0.74
Formononetin (**137**)		H	H	OCH_3	H	H	–	–	> 50
Eurycarpin A (**175**)		OH	prenyl	OH	H	H	–	–	**< 0.10**
Luteone (**176**)		OH	H	OH	OH	prenyl	–	–	**< 0.10**
Glabrone (**177**)		–	–	–	–	–	–	–	> 50
93		–	H	–	H	H	–	H	**< 0.10**
Licoflavone A (**178**)		–	H	–	H	prenyl	–	H	> 50
Licoflavone C (**179**)		–	H	–	OH	H	–	prenyl	0.30
Licoflavone B (**180**)		–	prenyl	–	H	prenyl	–	H	**< 0.10**
Liquiritigenin (**181**)		–	H	–	–	–	OH	H	> 50
Glabrol (**182**)		–	prenyl	–	–	–	OH	prenyl	**< 0.10**
Glabridin (**183**)		–	–	–	–	–	–	–	46.42
Positive control **Acarbose**	–	–	–	–	–	–	–	–	5.42

Proença et al. (2017) studied a panel of 44 structurally related flavonoids regarding their inhibitory effect on α-glucosidase from *Saccharomyces cerevisiae*. The most active flavonoid found was **310** (Table 56), with an IC_{50} value of 7.6 ± 0.4 μM, which is almost 80 times lower than the IC_{50} of acarbose (IC_{50} = 607 ± 56 μM). These results suggest that the presence of two catechol groups (at 7- and 8- positions of A ring, and at 3′- and at 4′-positions of B ring) in the flavonoid structure is crucial for the inhibition of α-glucosidase. It was also observed that the methoxylation and benzoxylation of flavonoids did not favor the inhibitory activity, since flavonoids **315** and **316** presented low or no inhibitory effect against the target under study. The second most active flavonoid was quercetin (**25**), with an IC_{50} value of 15 ± 3 μM. The presence of an -OH group at 3-position of C ring seems to be advantageous for the intended activity, since luteolin (**1**), with no substituents at this position, presented a higher IC_{50} value (46 ± 6 μM).

The ability of flavonoids isolated from *Silybum marianum,* taxifolin (**111**), dihydrokaempferol (**317**), dihydroquercetin 4′-methyl ether (**318**), naringenin (**28**), naringenin 7-*O*-β-D-glucoside (**319**) and kaempferol (**25**) (Table 57), to inhibit α-glucosidase from *Saccharomyces cerevisiae* was evaluated in the work of Qin et al. (2017). It was shown that the presence of a glucosyl group at 7-position of A ring increased the studied effect, since naringenin 7-*O*-β-D-glucoside (**319**) was the most active flavonoid (IC_{50} = 1.44 ± 0.01 μM); being more effective than its parent compound, naringenin (**28**), which presented a higher IC_{50} value (37.21 ± 1.12 μM). In addition, by comparing taxifolin (**111**) (IC_{50} = > 100 μM) and dihydroquercetin 4′-methyl ether (**318**) (IC_{50} = 41.43 ± 0.21 μM), it was possible to observe that the substitution of an -OH group to a -OCH_3 group at 4′-position of B ring enhanced the inhibitory activity.

A panel of flavonoids was selected for the evaluation of the inhibitory activity toward α-glucosidase from

Table 36. Flavonoids tested by Imran et al. (2015), and respective inhibitory activity on α-glucosidase (the most active flavonoid is highlighted).

Flavonoid	Structure	$R^{2''}$	$R^{3''}$	$R^{4''}$	$R^{5''}$	$R^{6''}$	IC_{50} (μM ± SEM)
184		–	–	–	–	–	802.6 ± 1.34
185		–	–	–	–	–	NA
186		–	–	–	–	–	730 ± 0.50
187		OH	H	OH	H	OH	**15.4 ± 0.22**
188		OH	OH	H	H	H	16.9 ± 0.65
189		OH	H	OH	H	H	27.3 ± 0.36
190		OH	H	H	OH	H	37.8 ± 0.44
191		H	OH	OH	H	H	17.2 ± 1.21
192		OH	H	H	H	H	37.4 ± 0.50
193		H	OH	H	H	H	86.3 ± 0.98
194		H	H	OH	H	H	27.4 ± 1.46
195		OH	H	OCH_3	H	H	29.4 ± 0.32
196		H	OH	OCH_3	H	H	34.4 ± 1.18
197		OH	H	H	OCH_3	H	37.4 ± 0.33
198		H	OCH_3	H	OCH_3	H	623.1 ± 0.61
199		Br	H	OH	H	H	587.4 ± 1.42
200		CH_3	H	H	H	H	487.4 ± 1.08
201		H	CH_3	H	H	H	497.4 ± 0.70
202		H	H	CH_3	H	H	367.4 ± 0.54
203		Cl	H	H	H	H	29.6 ± 0.26
204		H	Cl	H	H	H	64.5 ± 2.08
205		H	H	Cl	H	H	38.3 ± 0.34
206		NO_2	H	H	H	H	123.4 ± 1.69
207		H	NO_2	H	H	H	98.0 ± 1.10
208		H	H	NO_2	H	H	88.4 ± 0.97
209		Fl	H	H	H	H	17.1 ± 0.24
210		H	Fl	H	H	H	22.8 ± 1.23
211		H	H	Fl	H	H	19.4 ± 0.20
212		H	OCH_3	H	H	H	680.5 ± 1.27
213		H	H	OCH_3	H	H	690.3 ± 2.04
214		Pyr	H	H	H	H	487.4 ± 1.36
215		H	Pyr	H	H	H	520.7 ± 0.80
216		H	H	Pyr	H	H	430.2 ± 0.28
Positive control Acarbose	–	–	–	–	–	–	860.23 ± 6.10

NA – Not active.

Table 37. Flavonoids tested by Ma et al. (2015), and respective inhibitory activity on α-glucosidase (the most active flavonoid is highlighted).

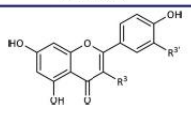
Flavonoid	Structure	R^3	$R^{3'}$	IC_{50} (μg/mL ± SEM)
Astraglin (**2**)		glucose	H	179 ± 9.2
Rutin (**5**)		rutinose	OH	272 ± 15
Quercetin (**25**)		OH	OH	**5.1 ± 0.3**
Kaempferol (**26**)		OH	H	56.2 ± 4.1
Isoquercetin (**38**)		glucose	OH	1233 ± 87
Tiliroside (**217**)		(6″-*O*-*p*-coumaroyl)-glucose	H	202 ± 12
Nicotiflorin (**218**)		rutinose	H	253 ± 19
Positive control **Acarbose**	–	–	–	465 ± 37

Table 38 Flavonoids tested by Sheliya et al. (2015), and respective inhibitory activity on α-glucosidase (the most active flavonoid is highlighted).

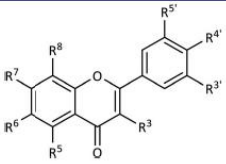
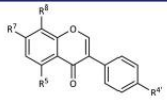
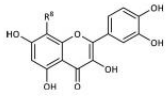
Flavonoid	Structure	R^3	$R^{3'}$	$R^{4'}$	R^5	$R^{5'}$	R^6	R^7	R^8	IC_{50} (mM)
Quercetrin (**9**)		rhamose	OH	OH	OH	H	H	OH	H	0.151
Dimethoxyquercetrin (**219**)		rhamnose	OH	OH	OCH_3	H	H	OCH_3	H	0.182
Hirtacoumaroflavonoside (**220**)		glucosyl-(2''-1'')-*O*-α-L-rhamnose	H	OH	OH	H	prenyl	*p*-cou	H	**0.022**
Hirtaflavonoside B (**221**)		glucose	OH	H	OH	OH	prenyl	OH	isobutenyl	0.071
Positive control **Acarbose**	–	–	–	–	–	–	–	–	–	0.092

Table 39. Flavonoids tested by Sun et al. (2015), and respective inhibitory activity on α-glucosidase (the most active flavonoid is highlighted).

Flavonoid	Structure	$R^{4'}$	R^5	R^7	R^8	IC_{50} (μM)
Genistein (**19**)		OH	OH	OH	H	50.05
Lupiwighteone (**222**)		OH	OH	OH	prenyl	> 100
Lespedeza E_1 (**223**)		OH	OH	OH	geranyl	6.26
224		OCH_3	OCH_3	OCH_3	prenyl	> 100
225		OCH_3	OCH_3	OCH_3	geranyl	> 100
226		OCH_3	OH	OCH_3	prenyl	> 100
227		OCH_3	OH	OCH_3	geranyl	> 100
Quercetin (**25**)		–	–	–	H	10.98
8-Prenylquercetin (**228**)		–	–	–	prenyl	4.38
8-Geranylquercetin (**229**)		–	–	–	geranyl	**1.15**
Positive control **Acarbose**	–	–	–	–	–	51.32

Saccharomyces cerevisiae (Table 58) (Sarian et al. 2017). Quercetin (**25**) was the most active compound, with an IC_{50} value of 4.92 ± 7.06 μg/mg. The obtained results indicate that the presence of -OCH_3 [wogonin methyl ether (**321**), techtochrysin (**323**) and **324**] and -acetate groups [wogonin acetate (**322**) and norwogonin acetate (**326**)], as well as the lack of the C2 = C3 double bond [catechin (**30**) and epicatechin (**31**)], decrease the inhibitory activity. On the other hand, the presence of a catechol group in B ring enhance the α-glucosidase inhibition by flavonoids, as can be seen by comparing quercetin (**25**) with kaempferol (**26**) (IC_{50} = 12.19 ± 4.63 μM).

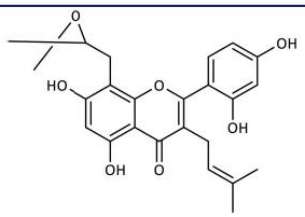
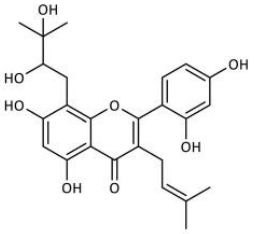
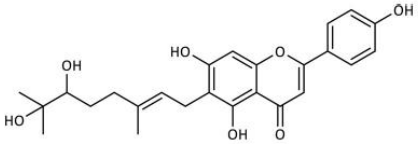
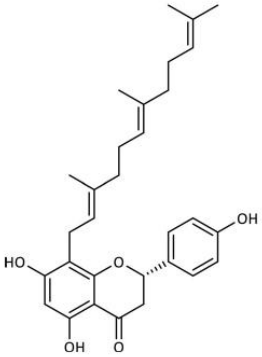
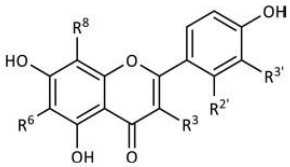
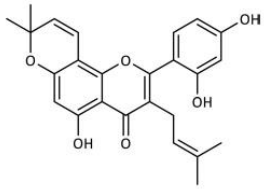
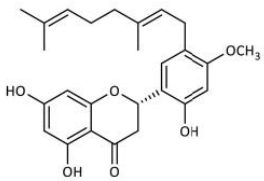
α-Glucosidase (from *Saccharomyces cerevisiae*) inhibition by isoflavones prunetin 5-*O*-*β*-glucoside (**329**) and genistein 5-*O*-*β*-glucoside (**330**) isolated from *Potentilla astracanica*, as well as their aglycone parent compounds prunetin (**331**) and genistein (**19**) was evaluated (Table 59) (Şöhretoğlu et al. 2017). The flavonoid aglycones were found to be more active. The uncompetitive inhibitor, genistein (**19**) was the most effective compound (IC_{50} = 1.47 ± 0.11 μg/mL). Furthermore, it was also observed that the replacement of the -OH group by a -OCH_3 group at 7-position of A ring decreased the inhibitory activity, as seen by comparing genistein (**19**) with prunetin (**331**) (IC_{50} = 31.87 ± 0.16 μg/mL). In addition, it seems that the replacement of an -OH group for a glucose at 5-position of A ring, since genistein (**19**) was more active than genistein 5-*O*-*β*-glucoside (**330**), which presented an IC_{50} value of 43.24 ± 0.16 μM.

Geranylated flavanones isolated from *Paulownia tomentosa* were studied regarding their inhibitory effect on α-glucosidase from *Saccharomyces cerevisiae* (Song et al. 2017). The isolated flavonoids were mimulone (**332**), 3′-*O*-methyldiplacone (**333**), 4′-*O*-methyldiplacone (**334**), **335**, 3′-*O*-methyl-5′-*O*-methyldiplacone (**336**), 3′-*O*-methyldiplacol (**337**), 4′-*O*-methyldiplacol (**338**) and **339** (Table 60) (Song et al. 2017). Among the tested compounds, flavonoid **339** was the most active (IC_{50} = 2.2 ± 0.2 μM), with a noncompetitive inhibition type. The positive control voglibose was about 11-fold less effective, with an IC_{50} value of 24.5 ± 1.2 μM. The results showed that a better inhibition was observed when there were two free -OH groups at 3′- and 5′- positions on B ring, in replacement of -OCH_3 groups at these positions, as it can be seen by comparing flavonoid **335** (IC_{50} = 6.5 ± 0.5 μM) with 3′-*O*-methyl-5′-*O*-methyldiplacone (**336**) (IC_{50} = 78.9 ± 2.1 μM). On the other hand, once again, it can be observed that the presence of an -OH group at 3-position of C ring is favorable for the intended effect, since flavonoid **339** was more active than flavonoid **335**.

Sun et al. (2017) studied the α-glucosidase (from *Saccharomyces cerevisiae*) inhibition by naringenin (**28**), 8-prenylnaringenin (**71**) and 8-geranylnaringenin (**72**) (see the chemical structures in Table 17). Flavonoid 8-geranylnaringenin (**72**) was the most active, (IC_{50} value of 3.77 μM) presenting a competitive inhibition type. In addition, flavonoid (**72**) was more than 13-fold more effective than acarbose (IC_{50} = 51.30 μM). The obtained results indicate that the geranyl group at 8-position of A ring plays an important role for the inhibition of α-glucosidase.

α-Glucosidase (from *Bacillus stearothermophilus*) inhibition by flavonoids isolated from *Glycyrrhiza uralensis* leaves was tested, as well as their parent compounds luteolin (**1**), quercetin (**25**), isoquercetin (**38**), rutin (**5**), eriodictyol (**41**) and taxifolin (**111**) (Table 61) (Ye, Fan, and Ma 2017). It

Table 40. Flavonoids tested by Zhang et al. (2015), and respective inhibitory activity on α-glucosidase (the most active flavonoid is highlighted).

Flavonoid	Structure	$R^{2'}$	R^3	$R^{3'}$	R^6	R^8	IC_{50} (μM ± SD)
Mortatarin A (**230**)		–	–	–	–	–	81.5 ± 5.6
Mortatarin B (**231**)		–	–	–	–	–	94.9 ± 4.3
Mortatarin C (**232**)		–	–	–	–	–	> 100
Mortatarin D (**233**)		–	–	–	–	–	**5.0 ± 0.3**
Kwanon T (**234**)		OH	prenyl	prenyl	H	H	12.7 ± 1.9
Albanin D (**235**)		H	H	H	geranyl	H	**5.9 ± 0.2**
Albanin E (**236**)		OH	H	H	geranyl	H	11.5 ± 0.7
Kwanon C (**237**)		OH	prenyl	H	H	prenyl	16.9 ± 2.1
Albanin A (**238**)		OH	prenyl	H	H	H	40.5 ± 5.1
Morusin (**239**)		–	–	–	–	–	> 100
Kwanon U (**240**)		–	–	–	–	–	7.5 ± 0.5

(*continued*)

Table 40. Continued.

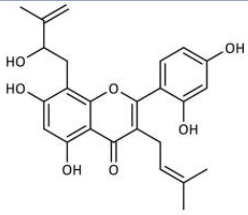
Flavonoid	Structure	$R^{2'}$	R^3	$R^{3'}$	R^6	R^8	IC_{50} (μM ± SD)
Mornigrol F (**241**)		–	–	–	–	–	35.7 ± 2.7
Positive control **Genistein**	–	–		–	–	–	17.8 ± 1.1

Table 41. Flavonoids tested by Chen et al. (2016), and respective inhibitory activity on α-glucosidase (the most active flavonoid is highlighted).

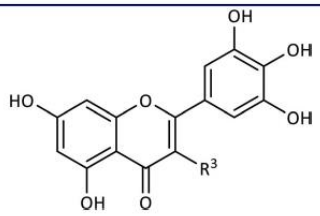
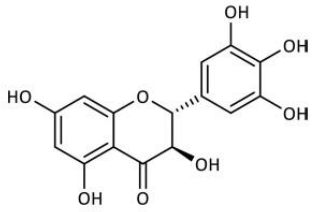
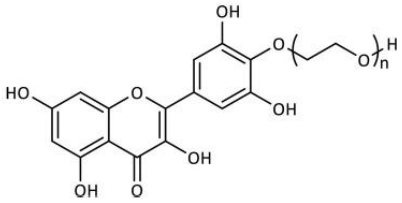
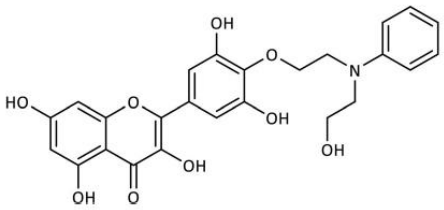
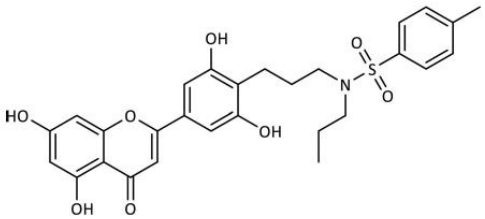
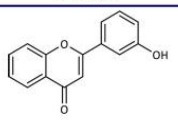
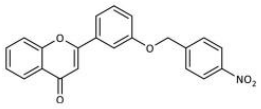
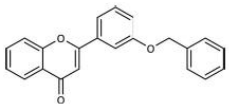
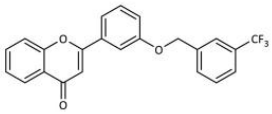
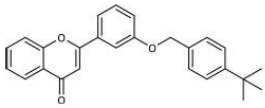
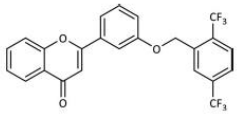
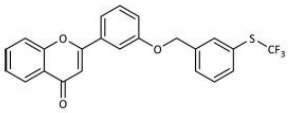
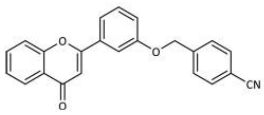
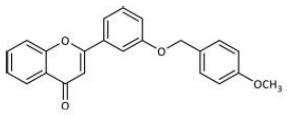
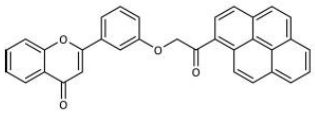
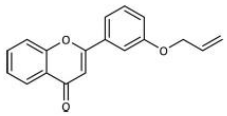
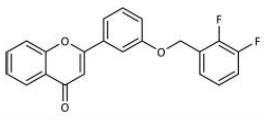
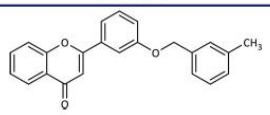
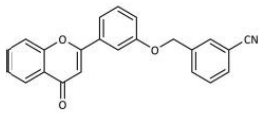
Flavonoid	Structure	R^3	n	IC_{50} (μM ± SEM)
Myricetin (**24**)		OH	–	319.3 ± 22.9
Myricitrin (**113**)		rhamnose	–	837.7 ± 22.0
Dihydromyricetin (**76**)		–	–	633.9 ± 24.9
242		–	1	84.5 ± 8.6
243		–	2	43.8 ± 1.5
244		–	3	233.1 ± 12.0
245		–	4	463.1 ± 15.8
246		–	–	41.1 ± 2.3
247		–	–	**9.3 ± 0.4**
Positive control **Acarbose**	–	–	–	720.3 ± 57.5

Table 42 Flavonoids tested by Imran et al. (2016), and respective inhibitory activity on α-glucosidase (the most active flavonoid is highlighted).

Flavonoid	Structure	IC_{50} (μM ± SEM)
82		34.66 ± 0.28
248		36.44 ± 0.031
249		59.66 ± 0.21
250		5.45 ± 0.08
251		49.54 ± 0.61
252		**1.26 ± 0.01**
253		8.66 ± 0.08
254		34.69 ± 0.28
255		35.35 ± 0.31
256		NA
257		NA
258		3.49 ± 0.05

(*continued*)

Table 42 Continued.

Flavonoid	Structure	IC_{50} (μM ± SEM)
259		88.66 ± 1.20
260		38.64 ± 0.34
Positive control – **Acarbose**		38.25 ± 0.12

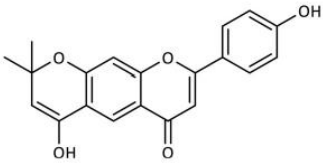
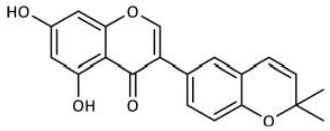
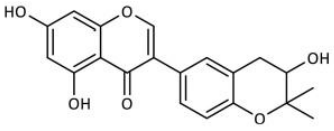
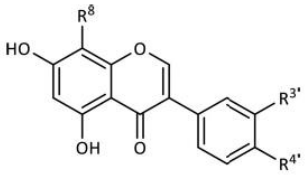
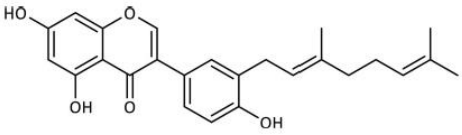
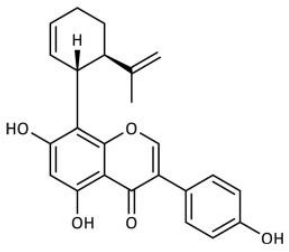
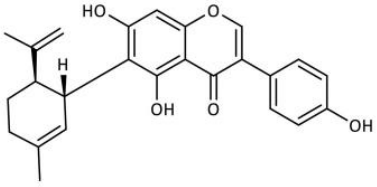
NA – Not active.

was found that the most active flavonoid was 5′-prenylquercetin (**341**), presenting an IC_{50} value of 2.3 μg/mL. The results indicate that the presence of a prenyl group at 5′-position of B ring is important, as quercetin (**25**) was 11 times less effective (25.8 μg/mL). In turn, as already suggested, the presence of an -OH group at 3-position of C ring is also favorable for the intended effect, since luteolin (**1**) (IC_{50} > 100 μg/mL) was less active than quercetin (**25**). Furthermore, it was also verified that the C2 = C2 double ring increased the inhibitory activity of α-glucosidase, by comparing quercetin (**25**) with taxifolin (**111**) (IC_{50} = 84.7 μg/mL). Finally, the glycosylation of flavonoids did not favor the α-glucosidase inhibition, as observed by the lack of activity of isoquercetin (**38**) and rutin (**5**) (IC_{50} > 100 μg/mL), when compared with quercetin (**25**).

Isoflavones daidzein (**20**), puerarin (**77**), daidzin (**345**) and ononin (**346**) (Table 62) isolated from *Pueraria lobata* were tested regarding their inhibitory activity on α-glucosidase from *Saccharomyces cerevisiae* (Wang et al. 2017). The flavonoid with best inhibitory activity was daidzein (**20**), a noncompetitive inhibitor, with an IC_{50} value of 23.01 μM, and almost 87-fold more active than acarbose (IC_{50} = 1998.79 μM). The results indicate that the replacement of the glucose by an -OH group at 7-position of A ring is important for the increase of α-glucosidase inhibition, by comparing daidzein (**20**) with daidzin (**345**) (IC_{50}= 253.78 μM). Moreover, it was also observed the substitution of the -OH by an -OCH_3 group at 4′-position of B ring reduce the inhibitory effect, since ononin (**346**) (IC_{50} = 422.89 μM) was less active than daidzin (**345**) (IC_{50} = 253.78 μM).

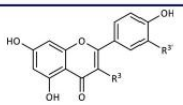
Zhang and coauthors (Zhang et al. 2017) tested the inhibitory activity of 16 flavonoids on mammalian sucrase and maltase (see the chemical structures in Table 18). For the maltose-hydrolyzing activity, baicalein (**23**) showed the strongest inhibition, with an IC_{50} value of 74.1 ± 5.6 μM, while acarbose presented an IC_{50} of 0.4 ± 0.1 μM. Quercetin (**25**) and luteolin (**1**) showed weaker inhibition than baicalein, with IC_{50} values of 282.1 ± 19.2 μM and 339.4 ± 16.3 μM, respectively. The IC_{50} for the other tested flavonoids were higher than 400 μM. For the sucrose-hydrolyzing activity, the IC_{50} value for acarbose was 1.2 ± 0.3 μM. Once again, baicalein (**23**) showed the strongest inhibition

Table 43. Flavonoids tested by Shi et al. (2016), and respective inhibitory activity on α-glucosidase (the most active flavonoid is highlighted).

Flavonoid	Structure	$R^{3'}$	$R^{4'}$	R^{8}	IC_{50} (μM ± SD)
261		–	–	–	NA
Carpachromene (**262**)		–	–	–	NA
Isoderrone (**263**)		–	–	–	108.1 ± 10.8
Ficuisoflavone (**264**)		–	–	–	NA
Lupiwighteone (**222**)		H	OH	prenyl	NA
Isowighteone (**265**)		prenyl	OH	H	NA
[3′-(3-Methylbut-2-en1-yl) biochanin A (**266**)		prenyl	OCH_3	H	**22.1 ± 7.6**
Myrsininone A (**267**)		–	–	–	50.5 ± 3.7
Ficusin A (**268**)		–	–	–	80.1 ± 8.1
269		–	–	–	30.7 ± 6.9
Positive control **Acarbose**	–	–	–	–	347.1 ± 68.6

NA – Not active.

Table 44. Flavonoids tested by Silva et al. (2016), and respective inhibitory activity on α-glucosidase (the most active flavonoid is highlighted).

Flavonoid	Structure	R^3	$R^{3'}$	IC_{50} (μM ± SD)
Luteolin (**1**)		H	OH	59.64 ± 1.32
Quercetin (**25**)		OH	OH	**7.19 ± 0.06**
trans-Tiliroside (**270**)		(6″-*O*-(*Z*)-*p*-cou)-*β*-D-glucose	H	NA
Quercetin 3-methyl ether (**271**)		OCH_3	OH	20.36 ± 1.30
Positive control **Acarbose**	–	–	–	859.79 ± 0.09

NA – Not active.

Table 45. Flavonoids tested by Zeng, Zhang, et al. (2016), and respective inhibitory activity on α-glucosidase (the most active flavonoids are highlighted).

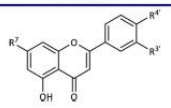
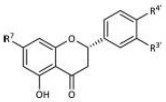
Flavonoid	Structure	$R^{3'}$	$R^{4'}$	R^7	IC_{50} (μM ± SD)
Luteolin (**1**)		OH	OH	OH	**2.0 ± 1.8**
Apigenin (**22**)		H	OH	OH	15.4 ± 2.3
Buddleoside (**43**)		H	OCH_3	rhamnose	14.6 ± 2.2
Hesperidin (**14**)		OH	OCH_3	rutinose	> 60
Naringenin (**28**)		H	OH	OH	57.1 ± 2.1
Eriodictyol (**41**)		OH	OH	OH	**1.4 ± 3.4**
Didymin (**59**)		H	OCH_3	rutinose	> 60
Isosakuranetin (**272**)		H	OCH_3	OH	31.2 ± 2.8
Positive control **Acarbose**	–	–	–		> 250

Table 46. Flavonoids tested by Zeng, Chen, et al. (2016), and respective inhibitory activity on α-glucosidase (the most active flavonoid is highlighted).

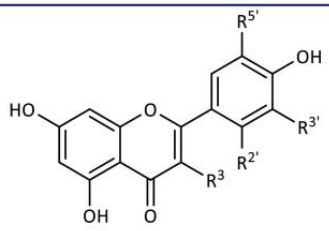
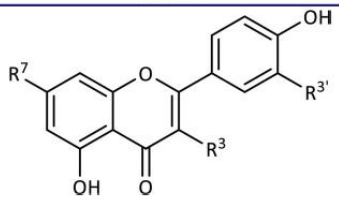
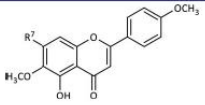
Flavonoid	Structure	$R^{2'}$	R^3	$R^{3'}$	$R^{5'}$	IC_{50} (mol L^{-1} ± SD)
Apigenin (**22**)		H	H	H	H	(10.5 ± 0.05) x 10^{-6}
Myricetin (**24**)		H	OH	OH	OH	**(2.25 ± 0.05) x 10^{-6}**
Morin (**101**)		OH	OH	H	H	(4.48 ± 0.04) x 10^{-6}
Positive control **Acarbose**	–	–	–	–	–	(3.04 ± 0.04) x 10^{-4}

Table 47. Flavonoids tested by Zhang et al. (2016), and respective inhibitory activity on α-glucosidase (the most active flavonoid is highlighted).

Flavonoid	Structure	R^3	$R^{3'}$	R^7	IC_{50} (μM ± SD)
Isoquercetin (**38**)		glucose	OH	OH	**22.38 ± 1.73**
Rhamnetin (**55**)		OH	OH	OCH_3	432.04 ± 10.17
Rhamnazin (**273**)		OH	OCH_3	OCH_3	> 3000
Positive control **Acarbose**	–	–	–	–	168.95 ± 12.27

among the flavonoids under study, with an IC_{50} value of 14.6 ± 2.7 μM, while the other flavonoids had IC_{50} values higher than 400 μM. The inhibition of both maltase and sucrase by the tested flavonoids seems to be different. Although baicalein (**23**) was the best inhibitor for both enzymes, this flavonoid had higher capacity to inhibit sucrase than maltase. On the other hand, it was observed that quercetin (**25**) presented a higher inhibitory activity

Table 48. Flavonoids tested by Amin et al. (2017), and respective inhibitory activity on α-glucosidase (the most active flavonoid is highlighted).

Flavonoid	Structure	R^7	IC_{50} (mM)
Pectolinarigenin (**274**)		OH	**0.23**
Pectolinarin (**275**)		glucose(1″-6″)-rhamnose(1‴-6″)	> 2*
Positive control **Acarbose**	–	–	0.26

* Inhibition of 48% at 2 mM.

Table 49. Flavonoids tested by Boonsombat et al. (2017), and respective inhibitory activity on α-glucosidase (the most active flavonoid is highlighted).

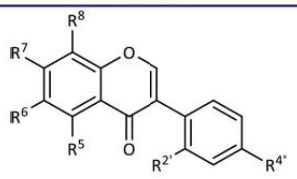
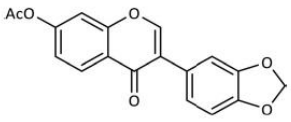
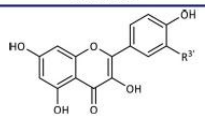
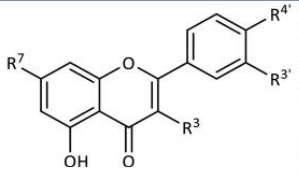
Flavonoid	Structure	$R^{2'}$	$R^{4'}$	R^5	R^6	R^7	R^8	% Inhibition at 100 μM
Formononetin (**137**)		H	OCH_3	H	H	OH	H	< 10%
Afrormosin (**138**)		H	OCH_3	H	OCH_3	OH	H	12.22 ± 1.11
8-*O*-Methylretusin (**139**)		H	OCH_3	H	H	OH	OCH_3	19.86 ± 0.98
Biochanin A (**276**)		H	OCH_3	OH	H	OH	H	**75.45 ± 1.05** (IC_{50} = 12.35 ± 0.36 μM)
277		H	OCH_3	OH	H	OCH_3	H	< 10%
278		H	OCH_3	OCH_3	H	OCH_3	H	< 10%
279		H	OCH_3	OH	H	allyl	H	< 10%
280		H	OCH_3	OH	H	propagyl	H	< 10%
281		H	OCH_3	OH	H	prenyl	H	< 10%
282		H	OCH_3	OH	H	prenyl	prenyl	< 10%
Cajanin (**283**)		OH	OH	OH	H	OCH_3	H	< 10%
284		OCH_3	OH	H	OCH_3	OH	H	< 10%
285		H	OCH_3	H	H	AcO	H	36.83 ± 1.04
286		AcO	AcO	OH	H	OCH_3	H	< 10%
287		OH	AcO	OH	H	OCH_3	H	< 10%
288		–	–	–	–	–	–	15.58 ± 0.44
Positive control **Acarbose**	–							83.13 ± 0.72 (IC_{50} = 6.54 ± 0.04 μM)

Table 50. Flavonoids tested by Chen et al. (2017), and respective inhibitory activity on α-glucosidase (the most active flavonoid is highlighted).

Flavonoid	Structure	$R^{3'}$	IC_{50} (μg/mL)
Quercetin (**25**)		OH	**66.8**
Kaempferol (**26**)		H	109

against maltase than against sucrase. Considering the SAR, for the inhibition of maltase, the presence of an -OH group at 6-position of A ring seems to have an important role, since baicalein (**23**) was more active than chrysin (**73**). In addition, by comparing baicalein (**23**) with baicalin (**12**), the replacement of the -OH by a glucuronic acid is not favorable for the intended effect. The same conclusions can be drawn considering the inhibition of sucrase. Regarding again the maltase inhibition, the presence of a rutinose at 3-pos-

Table 51. Flavonoids tested by Hmidene et al. (2017), and respective inhibitory activity on α-glucosidase (the most active flavonoids are highlighted).

						% Inhibition at 100 μM	
Flavonoid	Structure	R^3	$R^{3''}$	$R^{4'}$	R^7	Sucrase	Maltase
Quercetin (**25**)		OH	OH	OH	OH	21.8 ± 0.5	20.2 ± 1.5
Kaempferol (**26**)		OH	H	OH	OH	9.2 ± 0.5	19.1 ± 0.5
Rhamnetin (**55**)		OH	OH	OH	OCH_3	**29.5 ± 0.5**	23.7 ± 1.2
Rhamnazin (**273**)		OH	OCH_3	OH	OCH_3	17.5 ± 0.4	19.6 ± 1.7
Tamarixetin (**289**)		OH	OH	OCH_3	OH	20.9 ± 1.2	20.7 ± 0.2
Quercetin 3-*O*-β-D-glucuronide (**290**)		glucuronide	OH	OH	OH	**27.8 ± 0.5**	**62.0 ± 0.1**
Quercetin 3-*O*-β-D-glucuronide methyl ester (**291**)		glucuronide-OCH_3	OH	OH	OH	**30.9 ± 2.2**	**75.3 ± 0.5**
Kaempferol 3-*O*-β-D-glucuronide (**292**)		glucuronide	H	OH	OH	11.2 ± 1.5	31.7 ± 1.1
Kaempferol 3-*O*-β-D-glucuronide methyl ester (**293**)		glucuronide-OCH_3	H	OH	OH	16.7 ± 1.3	33.5 ± 1.1
Positive control **Acarbose**	–	–	–	–	–	56.1 ± 0.6	62.5 ± 0.5

ition of C ring instead of an -OH group, significantly decrease the inhibitory activity of flavonoids, as observed by comparing rutin (**5**) with quercetin (**25**).

Zhen et al. (2017) synthesized and screened novel flavonoid alkaloids (Table 63) for their inhibitory activity of α-glucosidase from *Saccharomyces cerevisiae*. Among the tested flavonoids, **369** exhibited the lowest IC_{50} value, 4.1 μM, with a noncompetitive inhibition type. Naringenin (**28**) was used as positive control, presenting an IC_{50} value of 77 μM. The flavan derivatives (**353, 354**) did not show inhibitory activity at the highest tested concentration (500 μM), underlying the importance of the carbonyl group at 4-position of C ring. The introduction of a tertiary amine appears to provide improved inhibitory activity compared to the secondary amine group, effect seen by comparing for example flavonoids **347** (IC_{50} = 249.4 μM) and **355** (IC_{50} = 82.8 μM). Moreover, the attachment of hydrophobic groups at A ring of flavonoids, as well as the addition of an extra hydrogen bond acceptor at the side end of the attached moiety may increase the α-glucosidase inhibition. This can be observed by comparing flavonoid **369** with **363** (IC_{50} = 521.0 μM) and **366** (IC_{50} = 65.1 μM).

Flavonoids were isolated from Ying De tea and their ability to inhibit α-glucosidase was evaluated (Table 64) (Zhou et al. 2017). It was observed that flavones were more active than isoflavones, since amelliaone A (**370**) (IC_{50} = 10.2 ± 0.04 μM) and amelliaone B (**371**) (IC_{50} = 25.3 ± 0.05 μM) presented lower IC_{50} values than amelliaone D (**373**) (IC_{50} = 75.3 ± 1.22 μM) and amelliaone E (**374**) (IC_{50} = 89.7 ± 0.09 μM). In fact, amelliaone A (**370**) presented a slightly higher inhibitory activity than acarbose (IC_{50} = 11.8 ± 0.08 μM). Amelliaone B (**371**) was more effective than amelliaone C (**372**) (IC_{50} = 58.2 ± 0.03 μM), suggesting that the presence of an -OH group at 4′-position of B ring is favorable for the intended effect. α-Glucosidase inhibition by epigallocatechin gallate (**32**), gallocatechin gallate (**39**) and epicatechin (**30**) was also studied, and it was found that their inhibitory activity was similar, presenting IC_{50} values of 25.0 ± 0.09 μM, 30.2 ± 0.53 μM and 32.1 ± 0.56 μM, respectively, indicating that the presence of -OH or gallate at 3-position of C ring did not bring difference in inhibitory activity of flavans against α-glucosidase.

Table 52. Flavonoids tested by Jeong and Kim (2017), and respective inhibitory activity on α-glucosidase (the most active flavonoid is highlighted).

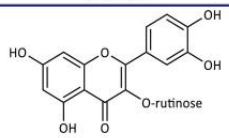
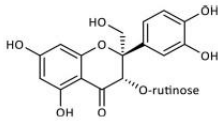
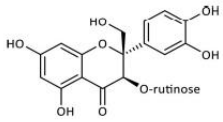
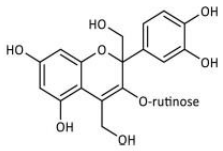
Flavonoid	Structure	IC_{50} (μM ± SD)
Rutin (**5**)		> 500
Radiorutinol (**294**)		23.1 ± 1.2
Isoradiorutinol (**295**)		**11.2 ± 0.7**
Radiorutindiol (**296**)		56.2 ± 3.5
Positive control **Acarbose**	–	310.2 ± 3.6

Table 53. Flavonoids tested by Kim, Cho, et al. (2017), and respective inhibitory activity on α-glucosidase (the most active flavonoid is highlighted).

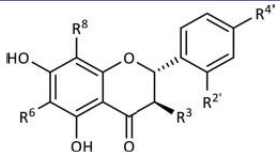
Flavonoid	Structure	$R^{2'}$	R^3	$R^{4'}$	R^6	R^8	IC_{50} (μM ± SD)
Kushenol A (**297**)		OH	H	H	H	lavandulyl	50.6 ± 1.3
Kushenol E (**298**)		OH	H	OH	prenyl	prenyl	24.6 ± 0.8
Kushenol B (**299**)		OH	H	OH	prenyl	lavandulyl	**11.0 ± 0.3**
Kushenol L (**300**)		H	OH	OH	prenyl	prenyl	32.6 ± 1.8
Positive control **Acarbose**	–	–	–	–	–	–	119.2 ± 3.7

Table 54. Flavonoids tested by Kim, Jung, et al. (2017), and respective inhibitory activity on α-glucosidase (the most active flavonoid is highlighted).

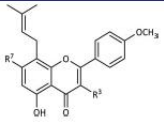
Flavonoid	Structure	R^3	R^7	IC_{50} (μM ± SEM)
Icaritin (**301**)		OH	OH	**74.42 ± 0.01**
Icariside II (**302**)		rhamnose	OH	106.59 ± 0.44
Icariin (**303**)		rhamnose	glucose	> 300
Epimedin A (**304**)		rhamnosylglucose	glucose	> 300
Epimedin B (**305**)		rhamnosylxylose	glucose	> 300
Epimedin C (**306**)		rhamnosylrhamnose	glucose	> 300
Positive control **Acarbose**	–	–	–	101.16 ± 3.69

Table 55. Flavonoids tested by Lee, Kim, and Whang (2017), and respective inhibitory activity on α-glucosidase (the most active flavonoid is highlighted).

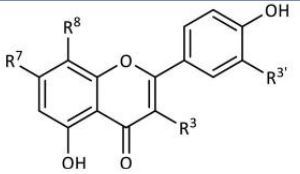
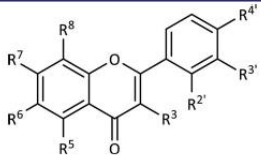
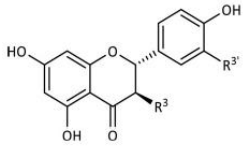
Flavonoid	Structure	R^3	$R^{3'}$	R^7	R^8	IC_{50} (μM ± SD)
Quercetrin (**9**)		rhamnose	OH	OH	H	135 ± 13
Kaempferol 3-*O*-*β*-D-glucosyl-7-*O*-*β*-D-L-rhamnoside (**307**)		glucose	H	rhamnose	H	609 ± 32
Afzelinn (**308**)		rhamnose	H	OH	H	**31.7 ± 1.6**
Isoscutellarein 8-*O*-rhamnoside (**309**)		H	H	OH	rhamnose	45.1 ± 2.6
Positive control **Acarbose**	–	–	–	–	–	172 ± 17

Table 56. Flavonoids tested by Proença et al. (2017), and respective inhibitory activity on α-glucosidase (the most active flavonoid is highlighted).

Flavonoid	Structure	$R^{2'}$	R^3	$R^{3'}$	$R^{4'}$	R^5	R^6	R^7	R^8	IC_{50} (μM ± SEM) or % Inhibition at 200 μM
81		H	H	H	H	H	H	H	H	< 20%
82		H	H	OH	H	H	H	H	H	< 20%
83		H	H	H	OH	H	H	H	H	< 20%
84		H	H	OH	OH	H	H	H	H	32 ± 4%
85		H	OH	OH	OH	H	H	H	H	54 ± 3 μM
86		H	OH	OCH_3	OCH_3	H	H	H	H	< 20%*
87		H	H	H	H	OH	H	H	H	< 20%
88		H	H	OH	H	OH	H	H	H	31 ± 4%
89		H	H	H	OH	OH	H	H	H	66 ± 2 μM
90		H	H	OH	OH	OH	H	H	H	66 ± 7 μM
91		H	H	H	H	H	H	OH	H	< 20%
92		H	H	OH	H	H	H	OH	H	53 ± 4 μM
93		H	H	H	OH	H	H	OH	H	≈ 200 μM
94		H	OH	OH	H	H	H	OH	H	42 ± 4 μM
95		H	OH	H	H	H	H	OH	H	96 ± 10 μM
96		H	H	OH	OH	H	H	OH	H	95 ± 7 μM
310		H	OH	OH	OH	H	H	OH	OH	**7.6 ± 0.4 μM**
311		H	OH	OCH_3	H	H	H	OCH_3	H	22 ± 2%*
312		H	OH	H	OCH_3	H	H	OCH_3	H	< 20%
313		H	OH	OH	OH	H	H	OCH_3	OCH_3	86 ± 6 μM
314		H	OH	OCH_3	OCH_3	H	H	OH	OH	31 ± 3%
315		H	OH	OBn	OBn	H	H	OCH_3	OCH_3	< 20%
316		H	OH	OCH_3	OCH_3	H	H	OBn	OBn	32 ± 3%
Chrysin (**73**)		H	H	H	H	OH	H	OH	H	< 20%**
Galangin (**99**)		H	OH	H	H	H	H	OH	H	21 ± 3%
Baicalein (**23**)		H	H	H	H	OH	OH	OH	H	44 ± 3 μM
100		H	H	OH	H	OH	H	OH	H	89 ± 3 μM
Apigenin (**22**)		H	H	H	OH	OH	H	OH	H	82 ± 6 μM
Kaempferol (**26**)		H	OH	H	OH	OH	H	OH	H	32 ± 3 μM
Luteolin (**1**)		H	H	OH	OH	OH	H	OH	H	46 ± 6 μM
Quercetin (**25**)		H	OH	OH	OH	OH	H	OH	H	15 ± 3 μM
Morin (**101**)		OH	OH	H	OH	OH	H	OH	H	32 ± 2 μM
102		H	Cl	OH	OH	OH	H	OH	H	21 ± 2 μM
103		H	H	OH	OH	OH	Cl	OH	H	≈ 200 μM
104		H	H	OH	OH	OH	H	OH	Cl	55 ± 2 μM
105		H	Cl	OH	OH	OH	H	OH	Cl	43 ± 3 μM
106		H	H	OH	OH	OH	Cl	OH	Cl	34 ± 3 μM
Chrysoeriol (**107**)		H	H	OCH_3	OH	OH	H	OH	H	156 ± 5 μM
Acacetin (**108**)		H	H	H	OCH_3	OH	H	OH	H	≈ 200 μM
110		H	H	OCH_3	OCH_3	OH	H	OH	H	< 20%
Rutin (**5**)		H	rutinose	OH	OH	OH	H	OH	H	< 20%
Naringenin (**28**)		–	H	H	–	–	–	–	–	45 ± 3%
Eriodictyol (**41**)		–	H	OH	–	–	–	–	–	35 ± 4%
Taxifolin (**111**)		–	OH	OH	–	–	–	–	–	≈ 200 μM
Positive control **Acarbose**		–	–	–	–	–	–	–	–	607 ± 56 μM

5,7-Dihydroxyflavone-*O*-8-sulfate (**375**), techtochrysin (**323**), wogonin (**320**), norwogonin (**325**), kaempferol (**26**) and quercetin (**25**) were isolated from *Tetracera indica* leaves and their inhibitory activity toward α-glucosidase (*Saccharomyces cerevisiae*) was studied (Table 65) (Alhassan et al. 2019). The most active flavonoids were quercetin (**25**)

Table 57. Flavonoids tested by Qin et al. (2017), and respective inhibitory activity on α-glucosidase (the most active flavonoid is highlighted).

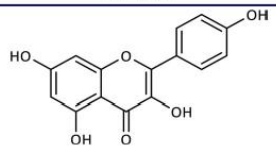
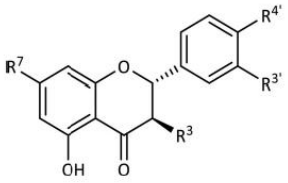
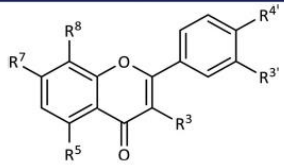
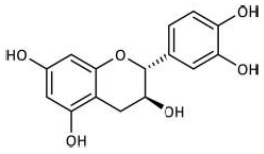
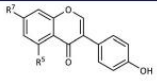
Flavonoid	Structure	R^3	$R^{3'}$	$R^{4'}$	R^7	IC_{50} (μM ± SD)
Kaempferol (**26**)		–	–	–	–	5.64 ± 0.29
Naringenin (**28**)		H	H	OH	OH	37.21 ± 1.12
Taxifolin (**111**)		OH	OH	OH	OH	> 100
Dihydrokaempferol (**317**)		OH	H	OH	OH	> 100
Dhydroquercetin 4′-methyl ether (**318**)		OH	OH	OCH_3	OH	41.43 ± 0.21
Naringenin 7-*O*-β-D-glucoside (**319**)		H	H	OH	glucose	**1.44 ± 0.01**
Positive control **Acarbose**	–	–	–	–	–	2.68 ± 0.07

Table 58. Flavonoids tested by Sarian et al. (2017), and respective inhibitory activity on α-glucosidase (the most active flavonoid is highlighted).

Flavonoid	Structure	R^3	$R^{3'}$	$R^{4'}$	R^5	R^7	R^8	IC_{50} (μg/mg ± SEM)
Quercetin (**25**)		OH	OH	OH	OH	OH	H	**4.92 ± 7.06**
Kaempferol (**26**)		OH	H	OH	OH	OH	H	12.19 ± 4.63
Chrysin (**73**)		H	H	H	OH	H	OH	> 100
Wogonin (**320**)		H	H	H	OH	OH	OCH_3	> 100
Wogonin methyl ether (**321**)		H	H	H	OCH_3	OCH_3	OCH_3	NA
Wogonin acetate (**322**)		H	H	H	AcO	AcO	OCH_3	> 100
Techtochrysin (**323**)		H	H	H	OH	OCH_3	H	> 100
324		H	H	H	H	OCH_3	OH	> 100
Norwogonin (**325**)		H	H	H	OH	OH	OH	> 100
Norwogonin acetate (**326**)		H	H	H	AcO	AcO	AcO	NA
Isoscutellarein (**327**)		H	H	OH	OH	OH	OH	7.15 ± 0.96
Hypolaetin (**328**)		H	OH	OH	OH	OH	OH	48.42 ± 9.71
(+)-Catechin (**30**)		–	–	–	–	–	–	NA
(-)-Epicatechin (**31**)		–	–	–	–	–	–	NA
Positive control **Quercetin** (commercial)	–	–	–	–			–	4.30 ± 1.06

NA – Not active.

Table 59. Flavonoids tested by Şöhretoğlu et al. (2017), and respective inhibitory activity on α-glucosidase (the most active flavonoid is highlighted).

Flavonoid	Structure	R^5	R^7	IC_{50} (μg/mL ± SD)
Genistein (**19**)		OH	OH	**1.47 ± 0.11**
Prunetin 5-*O*-β-glucoside (**329**)		glucose	OCH_3	56.05 ± 0.06
Genistein 5-O-β-glucoside (**330**)		glucose	OH	43.24 ± 0.16
Prunetin (**331**)		OH	OCH_3	31.87 ± 0.16
Positive control **Acarbose**	–	–	–	31.92 ± 0.17

and kaempferol (**26**), showing IC_{50} values of 61.86 ± 2.40 μM and 68.46 ± 3.50 μM, respectively. These values indicate that the presence of -OH groups at 3′- and/or at 4′- positions of B ring is responsible for the higher ability of flavonoids to inhibit α-glucosidase. It was also observed that the presence of a sulfate group at 8-position of A ring (**375**) (IC_{50} = 133.57 ± 5.25 μM) is beneficial for the intended effect, since the substitution of this group for a -OH [norwogonin (**325**), IC_{50} = > 500 μM] or an OCH_3 group [wogonin (**320**), IC_{50} = > 500 μM] reduced the inhibitory activity.

Adhikari-Devkota et al. (2019) tested the α-glucosidase inhibition by hesperidin (**14**), hesperetin (**29**), rutin (**5**), quercetin (**25**), nicotiflorin (**218**), eriocitrin (**376**) and narirutin (**57**) (Table 66). The compound with the best inhibitory

Table 60. Flavonoids tested by Song et al. (2017), and respective inhibitory activity on α-glucosidase (the most active flavonoid is highlighted).

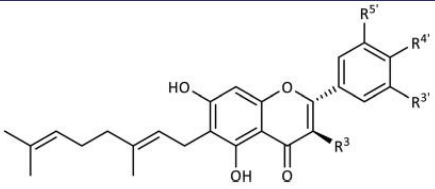
Flavonoid	Structure	R^3	$R^{3'}$	$R^{4'}$	$R^{5'}$	IC_{50} (μM ± SD)
Mimulone (**332**)		H	H	OH	H	30.7 ± 1.5
3′-*O*-Methyldiplacone (**333**)		H	OCH_3	OH	H	18.4 ± 0.9
4′-*O*-Methyldiplacone (**334**)		H	OH	OCH_3	H	19.6 ± 1.1
335		H	OH	OCH_3	OH	6.5 ± 0.5
3′-*O*-Methyl-5′-*O*-methyldiplacone (**336**)		H	OCH_3	OH	OCH_3	78.9 ± 2.1
3′-*O*-Methyldiplacol (**337**)		OH	OCH_3	OH	H	17.8 ± 1.1
4′-*O*-Methyldiplacol (**338**)		OH	OH	OCH_3	H	25.8 ± 1.2
339		OH	OH	OCH_3	OH	**2.2 ± 0.2**
Positive control **Voglibose**	–	–	–	–	–	24.5 ± 1.2

Table 61. Flavonoids tested by Ye, Fan, and Ma (2017), and respective inhibitory activity on α-glucosidase (the most active flavonoid is highlighted).

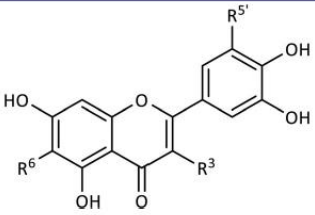
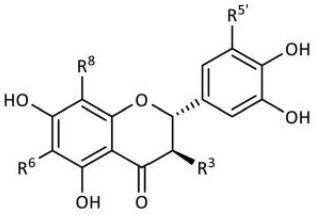
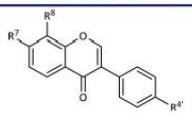
Flavonoid	Structure	R^3	$R^{5'}$	R^6	R^8	IC_{50} (μg/mL)
Luteolin (**1**)		H	H	H	H	> 100
Rutin (**5**)		rutinose	H	H	H	> 100
Quercetin (**25**)		OH	H	H	H	25.8
Isoquercetin (**38**)		glucose	H	H	H	> 100
Quercetin 3-methyl ether (**271**)		OCH_3	H	H	H	24.5
6-Prenylquercetin 3-methyl ether (**340**)		OCH_3	H	prenyl	H	21.3
5′-Prenylquercetin (**341**)		OH	prenyl	H	H	**2.3**
Eriodictyol (**41**)		H	H	H	H	> 100
Taxifolin (**111**)		OH	H	H	OH	84.7
6-Prenyleriodictyol (**342**)		H	H	prenyl	H	31.2
5′-Prenyleriodictyol (**343**)		H	prenyl	H	OH	57.4
8-[(*E*)-3-Hydroxymethyl-2-butenyl]eriodictyol (**344**)		H	OH	OH	[(*E*)-3-hydroxymethyl -2-butenyl	> 100
Positive control **Acarbose**	–	–	–	–	–	EC_{50} = 0.1

Table 62. Flavonoids tested by Wang et al. (2017), and respective inhibitory activity on α-glucosidase (the most active flavonoid is highlighted).

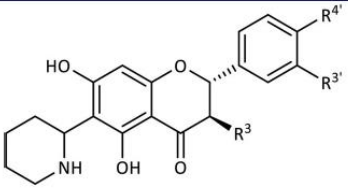
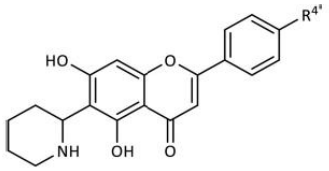
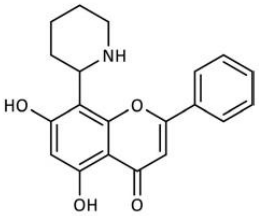
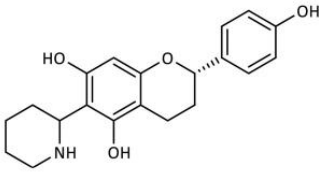
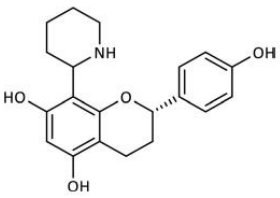
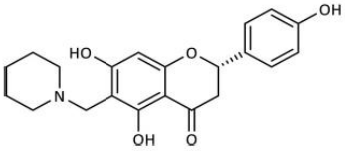
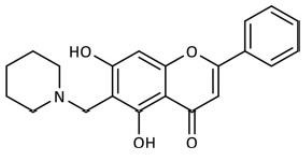
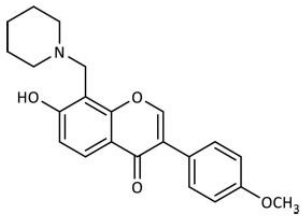
Flavonoid	Structure	$R^{4'}$	R^7	R^8	IC_{50} (μM)
Daidzein (**20**)		OH	OH	H	**23.01**
Puerarin (**77**)		OH	OCH_3	glucose	524.08
Daidzin (**345**)		OH	glucose	H	253.78
Ononin (**346**)		OCH_3	glucose	H	422.89
Positive control **Acarbose**	–	–	–	–	1998.79

activity was quercetin (**25**), with an IC_{50} value of 10.6 μM, and almost 60-fold more active than acarbose (IC_{50} = 607.9 μM). It was observed that the glycosylation of flavonoids clearly decreases the inhibition of the enzyme under study, namely at 3-position of C ring or at 7-position of A ring, by comparing quercetin (**25**) with rutin (**5**) (not active), and hesperetin (**29**) (IC_{50} = 35.2 μM) with hesperidin (**14**) (not active).

Flavans were isolated from the seeds of *Vigna nakashimae* (Table 67) and their α-glucosidase (from *Saccharomyces cerevisiae*) inhibitory activity was evaluated (Ha et al. 2018). Luteoliflavan 7-*O*-glucoside (**378**), catechin 7-*O*-glucoside (**379**), gambiriin D (**377**) and catechin (**30**) showed dose-dependent inhibition and their IC_{50} values were 40.4 ± 4.6 μM, 150.3 ± 3.5 μM, 36.8 ± 2.3 μM and 125.4 ± 5.6 μM, respectively. These values suggest that the presence of a -OH group at 3-position of C ring in flavans may reduce α-glucosidase inhibition.

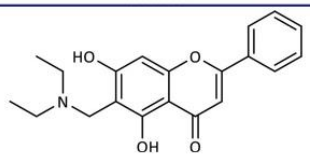
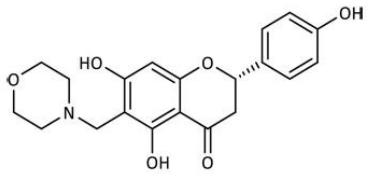
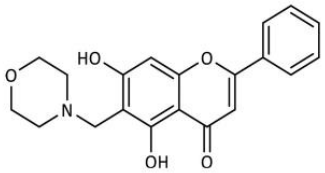
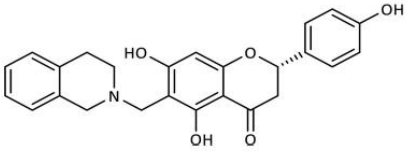
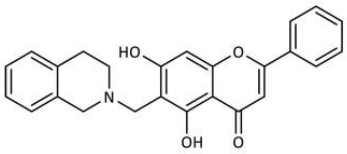
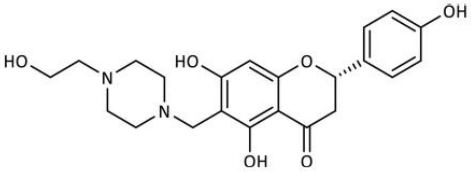
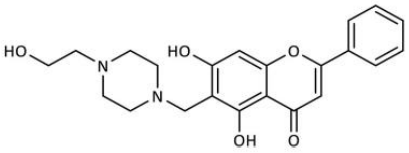
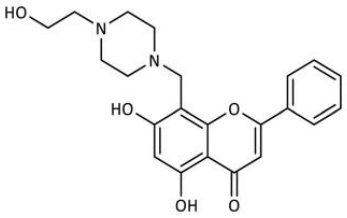
Several flavonoids (Table 68) were isolated from *Panax ginseng* flower buds and tested for their ability to inhibit α-glucosidase from *Saccharomyces cerevisiae* (Li, Li, et al. 2018). Afzelin (**308**) was found to be the most active compound, with an IC_{50} value of 5.48 ± 1.05 μM, a value about 70-fold lower than the one found for acarbose (IC_{50} = 385.2 ± 18.6 μM). In this study, the presence of a rhamnose at 3-position of C ring instead of the presence of this sugar at 7-position of A ring significantly increased the inhibitory activity, as seen by comparing afzelin (**308**) with kaempferol-7-*O*-α-L-rhamnoside (**384**) (IC_{50} =482.1 ± 26.6 μM). Moreover, the replacement of the rhamnose at 3-position of C ring for a galactose [trifolin (**383**)] at the same position (IC_{50} = 18.2 ± 3.2 μM), decreased the intended effect. However, the galactose is more favorable than a glucosylgalactose at 3-position of C ring, since trifolin (**383**) was more active than panasenoside (**381**) (IC_{50} = 103.2 ± 14.7 μM).

Table 63. Flavonoids tested by Zhen et al. (2017), and respective inhibitory activity on α-glucosidase (the most active flavonoid is highlighted).

Flavonoid	Structure	R^3	$R^{3'}$	$R^{4'}$	IC_{50} (μM)
347		H	H	OH	249.4
348		H	OH	OCH_3	> 500
349		OH	OH	OH	> 500
350		–	–	H	> 500
351		–	–	OH	293.3
352		–	–	–	> 500
353		–	–	–	> 500
354		–	–	–	> 500
355		–	–	–	82.8
356		–	–	–	> 500
357		–	–	–	> 500

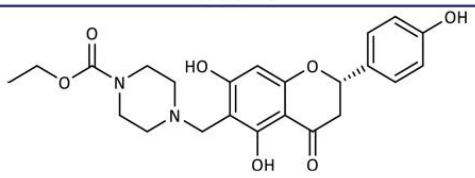
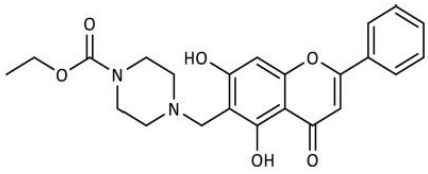
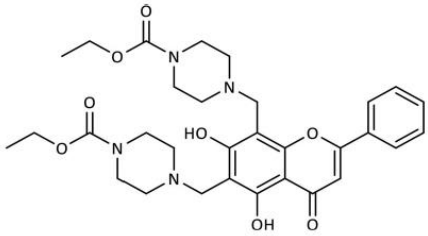
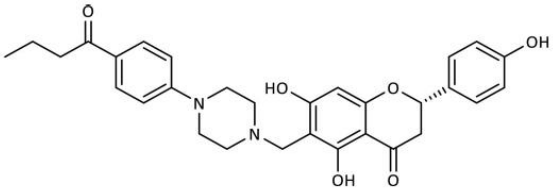
(*continued*)

Table 63. Continued.

Flavonoid	Structure	R^3	$R^{3'}$	$R^{4'}$	IC_{50} (μM)
358		–	–	–	217.0
359		–	–	–	202.5
360		–	–	–	> 500
361		–	–	–	23.4
362		–	–	–	> 500
363		–	–	–	521.0
364		–	–	–	> 500
365		–	–	–	> 500

(*continued*)

Table 63. Continued.

Flavonoid	Structure	R^3	$R^{3'}$	$R^{4'}$	IC_{50} (μM)
366		–	–	–	65.1
367		–	–	–	> 500
368		–	–	–	> 500
369		–	–	–	**4.1**
Positive control **Naringenin**	–	–	–	–	77

Li, Yao, et al. (2018) tested flavonoid isolated from *Scutellaria baicalensis* (see the chemical structures in Table 20) for their inhibitory activity on α-glucosidase (*Saccharomyces cerevisiae*). It was observed that the glycosylation of flavonoids at 7-position of A ring reduced the α-glucosidase inhibition, as seen by comparing baicalein (**23**) (IC_{50} = 277.94 ± 6.21 μg/mL) with baicalin (**12**) (IC_{50} = 591.58 ± 12.21 μg/mL); apigenin (**22**) (IC_{50} = 231.13 ± 5.35 μg/mL) with apigenin-7-*O*-glucuronide (**78**) (IC_{50} = 543.28 ± 11.41 μg/mL); and chrysin (**73**) (IC_{50} = 422.67 ± 9.37 μg/mL) with chrysin-7-*O*-glucuronide (**79**) (IC_{50} = 612.13 ± 15.34 μg/mL). Additionally, the presence of -OH groups at 6- position of A ring [baicalein (**23**) vs chrysin (**73**)] and at 4′-position of B ring [apigenin (**22**) vs. chrysin (**73**)] enhanced the inhibitory activity of flavonoids.

Five flavonoids were isolated from *Okinawa propolis* – nymphaeol A (**385**), nymphaeol B (**386**), nymphaeol C (**387**), isonymphaeol B (**388**) and 3′-geranylnaringenin (**389**) (Table 69) – and tested regarding their ability to inhibit α-glucosidase from *Saccharomyces cerevisiae* (Shahinozzaman et al. 2018). The compound with best inhibitory activity was nymphaeol-A (**385**), with a geranyl group at 6-position of A ring, which presented an IC_{50} value of 3.77 μM. The presence of the geranyl group at this position increased the inhibitory activity, comparing to its presence at 2′- or at 5′- position of A ring, as seen in nymphaeol B (**386**) (IC_{50} = 5.66 μM) and isonymphaeol-B (**388**) (IC_{50} = 5.12 μM). Quercetin (**25**) was used as positive control and showed an IC_{50} value of 6.65 μM.

The inhibition of α-glucosidase (from *Saccharomyces cerevisiae*) by kaempferol (**26**) and quercetin (**25**) derivatives was tested (Table 70) (Şöhretoğlu et al. 2018). The most active flavonoids were quercetin-3-*O*-(3″-*O*-galloyl)-*β*-galactoside (**392**) and quercetin-3-*O*-(6″-*O*-galloyl)-*β*-glucoside (**393**), presenting IC_{50} values of 0.97 ± 0.02 μM and 1.35 ± 0.06 μM, respectively, and proved to be approximately 52 and 37-fold more potent than acarbose (IC_{50} = 50.58 ± 0.25 μM), respectively. The comparison of the IC_{50} value of quercetin (**25**) (IC_{50} = 77.42 ± 0.91 μM) to those of quercetin-3-*O*-(6″-*O*-galloyl)-*β*-galactoside (**391**) (IC_{50} = 27.84 ± 2.19 μM), quercetin-3-*O*-(3″-*O*-galloyl)-*β*-galactoside (**392**) and quercetin-3-*O*-(6″-*O*-galloyl)-*β*-glucoside (**393**),

Table 64. Flavonoids tested by Zhou et al. (2017), and respective inhibitory activity on α-glucosidase (the most active flavonoid is highlighted).

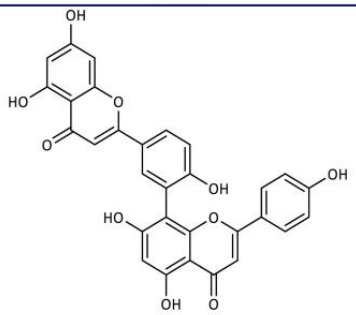
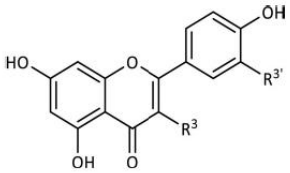
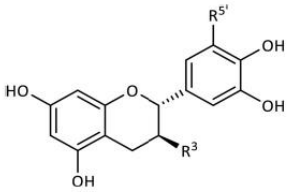
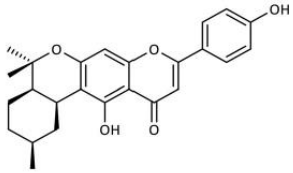
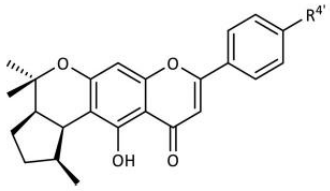
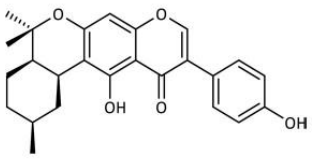
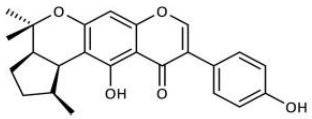
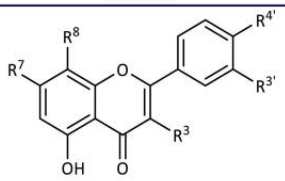
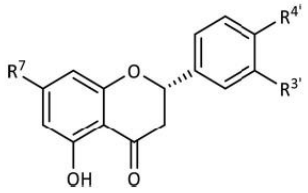
Flavonoid	Structure	R^3	$R^{3'}$	$R^{4'}$	$R^{5'}$	IC_{50} (μM ± SD)
Amentoflavone (**15**)		H	H	H	H	45.2 ± 0.67
Apigenin (**22**)		H	H	–	H	39.3 ± 0.22
Quercetin (**25**)		OH	OH	–		34.6 ± 0.05
(-)-Epicatechin (**30**)		OH	–	–	H	32.1 ± 0.56
(-)-Epigallocatechin gallate (**32**)		gallate	–	–	OH	25.0 ± 0.09
(-)-Gallocatechin gallate (**39**)		gallate	–	–	OH	30.2 ± 0.53
Amelliaone A (**370**)		–	–	–	–	**10.2 ± 0.04**
Amelliaone B (**371**)		–	–	OH	–	25.3 ± 0.05
Amelliaone C (**372**)		–	–	–	–	58.2 ± 0.03
Amelliaone D (**373**)		–	–	–	–	75.3 ± 1.22
Amelliaone E (**374**)		–	–	–	–	89.7 ± 0.09
Positive control **Acarbose**	–	–	–	–	–	11.8 ± 0.08

Table 65. Flavonoids tested by Alhassan et al. (2019), and respective inhibitory activity on α-glucosidase (the most active flavonoids are highlighted).

Flavonoid	Structure	R^3	$R^{3'}$	$R^{4'}$	R^7	R^8	IC_{50} (μM ± SD)
Quercetin (**25**)		OH	OH	OH	OH	H	**61.86 ± 2.40**
Kaempferol (**26**)		OH	H	OH	OH	H	**68.46 ± 3.50**
Wogonin (**320**)		H	H	H	OH	OCH_3	> 500
Techtochrysin (**323**)		H	H	H	OCH_3	H	NA
Norwogonin (**325**)		H	H	H	OH	OH	> 500
375		H	H	H	OH	sulphate	133.57 ± 5.25

NA – Not active

Table 66. Flavonoids tested by Adhikari-Devkota et al. (2019), and respective inhibitory activity on α-glucosidase (the most active flavonoid is highlighted).

Flavonoid	Structure	R^3	$R^{3'}$	$R^{4'}$	R^7	IC_{50} (μM)
Rutin (**5**)		rutinose	OH	–	–	NA
Quercetin (**25**)		OH	OH	–	–	**10.6**
Nicotiflorin (**218**)		rutinose	H	–	–	NA
Hesperidin (**14**)		–	OH	OCH_3	rutinose	NA
Hesperetin (**29**)		–	OH	OCH_3	OH	35.2
Narirutin (**57**)		–	H	OH	rutinose	NA
Eriocitrin (**376**)		–	OH	OH	rutinose	NA
Positive control **Acarbose**	–	–	–	–	–	607.9

NA – Not active.

Table 67. Flavonoids tested by Ha et al. 2018), and respective inhibitory activity on α-glucosidase (the most active flavonoids are highlighted).

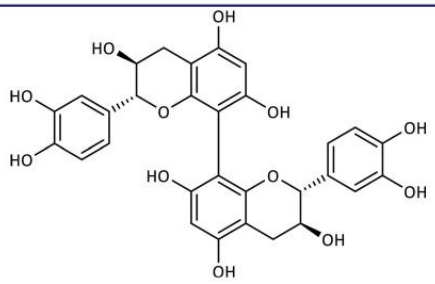
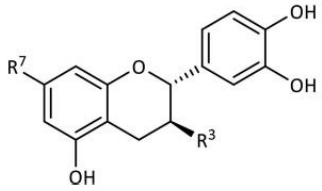
Flavonoid	Structure	R^3	R^7	IC_{50} (μM ± SD)
Gambiriin D (**377**)		–		**36.8 ± 2.3**
(+)-Catechin (**30**)		OH	OH	125.4 ± 5.6
Luteoliflavan 7-*O*-glucoside (**378**)		H	glucose	**40.4 ± 4.6**
(+)-Catechin 7-*O*-glucoside (**379**)		OH	glucose	150.3 ± 3.5
Positive control **Acarbose**	–	–		620.2 ± 7.2

Table 68. Flavonoids tested by Li, Li, et al. (2018), and respective inhibitory activity on α-glucosidase (the most active flavonoid is highlighted).

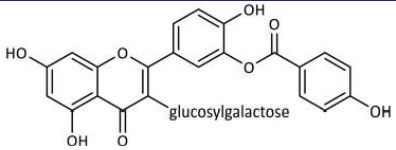
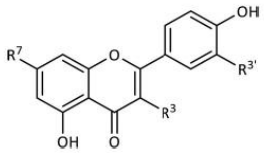
Flavonoid	Structure	R^3	$R^{3'}$	R^7	IC_{50} (μM ± SD)
Floralpanasenoside A (**380**)		–	–	–	62.4 ± 10.8
Afzelin (**308**)		rhamnose	H	OH	**5.48 ± 1.05**
Panasenoside (**381**)		glucosylgalactose	H	OH	103.2 ± 14.7
Quercetin 3-*O*-(2″-*β*-D-glucosyl)-*β*-D-galactoside (**382**)		2″-*β*-D-glucosyl-*β*-D-galactose	OH	OH	463.4 ± 28.3
Trifolin (**383**)		galactose	H	OH	18.2 ± 3.2
Kaempferol 7-*O*-α-L-rhamnoside (**384**)		OH	H	rhamnose	482.1 ± 26.6
Positive control **Acarbose**	–	–	–	–	385.2 ± 18.6

Table 69. Flavonoids tested by Shahinozzaman et al. (2018), and respective inhibitory activity on α-glucosidase (the most active flavonoid is highlighted).

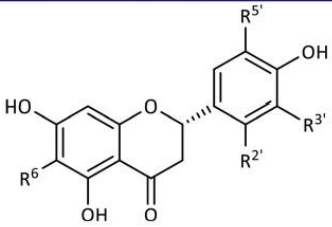
Flavonoid	Structure	$R^{2'}$	$R^{3'}$	$R^{5'}$	R^6	IC_{50} (μM)
Nymphaeol-A (**385**)		H	OH	H	geranyl	**3.77**
Nymphaeol-B (**386**)		geranyl	OH	H	H	5.66
Nymphaeol-C (**387**)		geranyl	OH	H	prenyl	4.09
Isonymphaeol-B (**388**)		H	OH	geranyl	H	5.12
3′-Geranyl naringenin (**389**)		H	geranyl	H	H	5.40
Positive control **Quercetin**	–	–	–	–	–	6.65

Table 70. Flavonoids tested by Şöhretoğlu et al. (2018), and respective inhibitory activity on α-glucosidase (the most active flavonoid is highlighted).

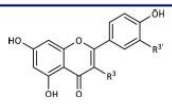
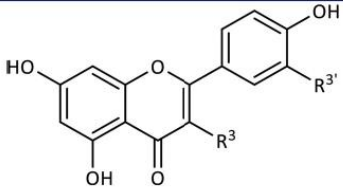
Flavonoid	Structure	R^3	$R^{3'}$	IC_{50} (μM ± SD)
Astraglin (**2**)		glucose	H	> 100
Hyperin (**3**)		galactose	OH	> 100
Quercetin (**25**)		OH	OH	77.42 ± 0.91
Kaempferol (**26**)		OH	H	8.97 ± 0.88
Isoquercetin (**38**)		glucose	OH	> 100
Isorhamnetin 3-O-*β*-glucoside (**390**)		glucose	OCH_3	> 100
Quercetin 3-*O*-(6″-*O*-galloyl)-*β*-galactoside (**391**)		(6″-O-galloyl)-*β*-galactose	OH	27.84 ± 2.19
Quercetin 3-*O*-(3″-*O*-galloyl)-*β*-galactoside (**392**)		(3″-O-galloyl)-*β*-galactose	OH	**0.97 ± 0.02**
Quercetin 3-*O*-(6″-*O*-galloyl)-*β*-glucoside (**393**)		(6″-O-galloyl)-*β*-glucose	OH	1.35 ± 0.06
Kaempferol 3-*O*-vicianoside (**394**)		vicianose	H	> 100
Quercetin 3-*O*-vicianoside (**395**)		vicianose	OH	> 100
Positive control **Acarbose**	–	–	–	50.58 ± 0.25

Table 71. Flavonoids tested by Renda et al. (2018), and respective inhibitory activity on α-glucosidase (the most active flavonoid is highlighted).

Flavonoid	Structure	R^3	$R^{3'}$	IC_{50} (μM ± SD)
Quercetrin (**9**)		rhamnose	OH	74.51 ± 4.70
Quercetin 3-*O*-*β*-D-glucuronide (**290**)		glucuronide	OH	62.55 ± 2.85
Afzelin (**308**)		rhamnose	H	**29.92 ± 1.07**
Kaempferol 3-*O*-α-arabinofuranoside (**396**)		arabinofuranose	H	57.10 ± 1.75
Quercetin 3-*O*-α-rhamnofuranoside (**397**)		rhamnofuranose	OH	52.54 ± 0.45
Positive control **Acarbose**	–	–	–	57.49 ± 0.25

showed that the substitution at 3-position of C ring with (*O*-galloyl)glucose or (*O*-galloyl)galactose significantly increased the inhibitory effect due to galloyl moieties including three -OH groups. Moreover, the addition of a galactose unit at 3″-position of the galloyl moiety enhanced the α-glucosidase inhibition, compared to its presence at 6″-position [quercetin-3-*O*-(6″-*O*-galloyl)-*β*-galactoside]. Finally, the galactosylation, glucosylation or the addition of a vicianose at 3-position of C ring reduced the intended activity, by comparing quercetin (**25**) with hyperin (**3**), isoquercetin (**38**) and quercetin 3-*O*-vicianoside (**395**).

Renda and coworkers (Renda et al. 2018) evaluated the inhibitory activity of flavonoids isolated from *Geranium asphodeloides* (Table 71) on α-glucosidase from *Saccharomyces cerevisiae*. The flavonoid that presented the lowest IC_{50} value was afzelin (**308**) (IC_{50} = 29.92 ± 1.07 μM), being almost 2-fold lower that the one found for acarbose (IC_{50} = 57.49 ± 0.25 μM). Comparing the activity of this compound with quercetrin (**9**), it can be seen that the addition of a -OH group at 3′-position of B ring decreased the inhibitory activity. Furthermore, the sugar rhamnose led to a better effect than the sugar arabinofuranose at 3-position of C ring, through comparison of afzelin (**308**) with kaempferol 3-*O*-α-arabinofuranoside (**396**) (IC_{50} = 57.10 ± 1.75 μM).

Inhibitory activity on yeast α-glucosidase by flavonoids isolated from acorn leaves (Table 72) was studied (Xu, Wang, et al. 2018). Among the tested compounds, quercetin (**25**), kaempferol (**26**) and myricetin (**24**) were the most actives, presenting IC_{50} values of 1.61 ± 0.06 μM, 2.73 ± 0.33 μM and 0.52 ± 0.09 μM, respectively. The positive control acarbose had an IC_{50} value of 5.90 ± 0.98 μM. The results indicate that a higher number of -OH groups at B ring may strengthen the inhibitory activity. Moreover, the results showed that flavonoid aglycones were better inhibitors than flavonoids glycosides, by comparing for example myricetin (**24**) with myricetin 3-*O*-L-rhamnoside (**400**) (IC_{50} = 49.37 ± 5.21 μM), quercetin (**25**) with isoquercetin (**38**) (IC_{50} = 53.98 ± 3.09 μM), and kaempferol (**26**) with kaempferol 3-*O*-(2′′,3′′-diol acetonide)-α-L-rhamnoside (**398**) (IC_{50} = 60.52 ± 4.19 μM). Besides that, it was found that quercetin-3-*O*-(2″-*O*-galloyl)-*β*-galactoside (**399**), with an IC_{50} value of 8.59 ± 1.52 μM, was more effective than other flavonoids glycosides without a galloyl group, namely hyperin (**3**) (IC_{50} = 52.17 ± 5.91 μM).

Xu, Xie, et al. (2018) isolated anthocyanins from berry fruits (strawberry, raspberry, blueberry, mulberry, bayberry and cranberry) (Table 73) and tested their inhibitory activity of α-glucosidase (*Saccharomyces cerevisiae*). The most effective flavonoid was pelargonidin-3-*O*-rutinoside (**403**), with an IC_{50} value of 1.69 μM, while acarbose presented an IC_{50} value of 356.26 μM. From a SAR perspective, it was observed that the order of inhibitory activity for both anthocyanins' aglycones and glycosides was pelargonidin > malvidin > peonidin > delphinidin > petunidin > cyanidin. For the glycosyl groups the order of activity was as follows: arabinose > rutinose > glucose > galactose > sambubiose.

A panel of 13 flavonoids (Table 74) was isolated from *Glycyrrhiza uralensis* leaves and their inhibitory activity on α-glucosidase was studied (Fan et al. 2019). It was observed that 5′-prenylquercetin (**341**) and 6-prenylquercetin (**420**) were the best inhibitors, presenting IC_{50} values of 3.9 μg/mL and 3.7 μg/mL, respectively. The obtained results suggest that the prenylation of quercetin at 5′-position of B ring or at 6-position of A ring, as improve the α-glucosidase inhibition. In addition, flavones were more actives than flavanones. On the other hand, the presence of -OCH_3 groups in flavonoids is not favorable for the intended effect, by comparing 6-prenylquercetin (**420**) with 6-prenylquercetin 3-methyl ether (**340**) (IC_{50} = 21.3 μg/mL). These results are in agreement with the work of Ye, Fan, and Ma (2017), who also tested isolated compounds from *Glycyrrhiza uralensis*.

Ghani et al. (2019) evaluated the α-glucosidase (from *Saccharomyces cerevisiae*) inhibition by flavones and isoflavones isolated from *Retama raetam* plant (Table 75). All the compounds carried substitutions at 6- or 8- position of A ring, in which -OH or -CH_3 groups terminally flank as side groups. The most potent inhibitor was retamasin H (**428**) (Ki= 12.06 μM ± 0.57), an isoflavone with a *γ*-lactone substituent at 6-position of A ring, that noncompetitively inhibited α-glucosidase. The potent activity of this flavonoid appears to be related to the presence of the *γ*-lactone side chain. Erysubin B (**430**), which bears a dihydropyran group at 6-position of A ring, presented a Ki value of 71.7 ± 0.64 μM. Its activity increased more than 4-fold when its substitution at 6-position of A ring is replaced by a lactone group carrying a -OH group, as verified in Erysubin A (**429**) (Ki= 16.42 ± 0.18 μM). Therefore, it seems that the presence of a lactone group at 6-position of A ring in the isoflavone moiety contributes to the potent inhibition of α-glucosidase. Similar conclusions were found in a preliminary work where flavonoids isolated from *Retama raetam* plant were studied (Table 75) (Nur et al. 2019). Table 75 exhibited the results obtained for both Ghani et al. (2019) and Nur et al. (2019) studies.

Dicoumaroylated flavonoids rhamnosides (**431–438**) (Table 76) were isolated from *Machilus litseifolia* and their capacity to inhibit α-glucosidase (*Saccharomyces cerevisiae*) was evaluated (Li, Kongstad, and Staerk 2019). The most active compound was 4′-*O*-methyl-2″,4″-di-(*Z*)-*p*-coumaroylafzelin (**435**), with an IC_{50} value of 5.9 ± 0.01 μM, a value about 45-fold lower than the one found for acarbose (IC_{50} = 266.1 ± 0.01 μM). 4′-Methylkaempferol/afzelin analogues (flavonoids **435–438**) showed stronger inhibitory activity than quercetin and kaempferol analogues (flavonoids **431–434**). Moreover, in the 4′-methyl kaempferol analogues series, it was found that the presence of one or two *Z*-*p*-coumaroyl units favored the α-glucosidase inhibition compared to *E*-*p*-coumaroyl units. Interestingly, the presence of a *Z*-*p*-coumaroyl unit at 4″-position of the rhamnose seemed to be more important for the intended effect than its presence at 2″-position, as it can be seen by comparing flavonoids **432**/**433** and flavonoids **436**/**437**.

Lim et al. (2019) studied the α-glucosidase inhibition by luteolin (**1**), quercetin (**25**) and eriodictyol (**41**) (see the chemical structures in Table 21), through the analysis of starch digested product by HPAEC method. The most active

Table 72. Flavonoids tested by Xu, Wang, et al. (2018), and respective inhibitory activity on α-glucosidase (the most active flavonoid is highlighted).

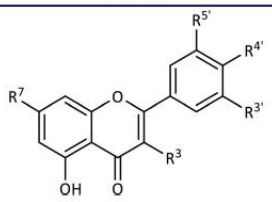
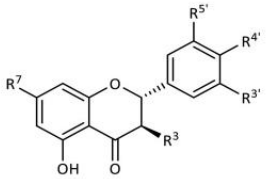
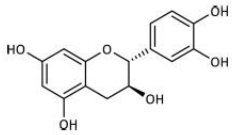
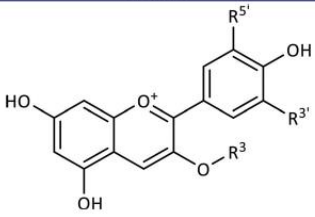
Flavonoid	Structure	R^3	$R^{3'}$	$R^{4'}$	$R^{5'}$	R^7	IC_{50} (μM ± SD)
Hyperin (**3**)		galactose	OH	OH	H	OH	52.17 ± 5.91
Rutin (**5**)		rutinose	OH	OH	H	OH	25.33 ± 5.19
Quercetrin (**9**)		rhamnose	OH	OH	H	OH	52.09 ± 4.65
Myricetin (**24**)		OH	OH	OH	OH	OH	**0.52 ± 0.09**
Quercetin (**25**)		OH	OH	OH	H	OH	1.61 ± 0.06
Kaempferol (**26**)		OH	H	OH	H	OH	2.73 ± 0.33
Isoquercetin (**38**)		glucose	OH	OH	H	OH	53.98 ± 3.09
Nicotiflorin (**218**)		rutinose	H	OH	H	OH	30.06 ± 3.19
Afzelin (**308**)		rhamnose	H	OH	H	OH	59.11 ± 5.06
Kaempferol 3-*O*-(2″,3″-diol acetonide)-α-L-rhamnoside (**398**)		(2″,3″-diol acetonide)-α-L-rhamnose	H	OH	H	OH	60.52 ± 4.19
Quercetin 3-*O*-(2″-galloyl)-*β*-galactoside (**399**)		(2″-galloyl)-*β*-galactose	OH	OH	H	OH	8.59 ± 1.52
Myricetin 3-*O*-L-rhamnoside (**400**)		rhamnose	OH	OH	OH	OH	49.37 ± 5.21
401		H	H	OCH_3	H	OCH_3	> 100
Naringenin (**28**)		H	H	OH	H	OH	10.96 ± 1.78
Hesperetin (**29**)		H	OH	OCH_3	H	OH	15.28 ± 1.77
Dihydromyricetin (**76**)		OH	OH	OH	OH	OH	7.56 ± 1.99
402		H	H	OH	H	rhamnosyl glucose	69.38 ± 5.81
(+)-Catechin (**30**)		–	–	–	–	–	63.93 ± 5.12
Positive control **Acarbose**	–	–	–	–	–	–	5.90 ± 0.98

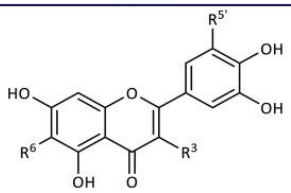
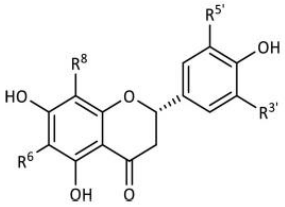
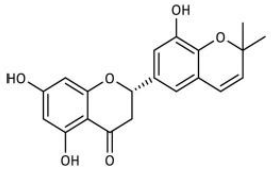
Table 73. Flavonoids tested by Xu, Xie, et al. (2018), and respective inhibitory activity on α-glucosidase (the most active flavonoid is highlighted).

Flavonoid	Structure	R^3	$R^{3'}$	$R^{5'}$	IC_{50} (μM)
Malvidin 3-*O*-glucoside (**112**)		glucose	OCH_3	OCH_3	116.77
Pelargonidin 3-*O*-rutinoside (**403**)		rutinose	H	H	**1.69**
Pelargonidin 3-*O*-glucoside (**404**)		glucose	H	H	10.35
Cyanidin 3-*O*-rutinoside (**405**)		rutinose	OH	H	608.69
Cyanidin 3-*O*-glucoside (**406**)		glucose	OH	H	1025.32
Cyanidin 3-*O*-sambubinoside (**407**)		sambubinose	OH	H	> 4000
Delphinidin 3-*O*-arabinoside (**408**)		arabinose	OH	OH	22.70
Delphinidin 3-*O*-rutinoside (**409**)		rutinose	OH	OH	69.82
Delphinidin 3-*O*-glucoside (**410**)		glucose	OH	OH	142.68
Delphinidin 3-*O*-galactoside (**411**)		galactose	OH	OH	148.20
Delphinidin 3-*O*-sambubinoside (**412**)		sambubinose	OH	OH	> 4000
Petunidin 3-*O*-arabinoside (**413**)		arabinose	OCH_3	OH	81.47
Petunidin 3-*O*-glucoside (**414**)		glucose	OCH_3	OH	158.65
Petunidin 3-*O*-galactoside (**415**)		galactose	OCH_3	OH	234.40
Malvidin 3-*O*-arabinoside (**416**)		arabinose	OCH_3	OCH_3	11.32
Malvidin 3-*O*-galactoside (**417**)		galatose	OCH_3	OCH_3	139.64
Peonidin 3-*O*-arabinoside (**418**)		arabinose	OCH_3	H	18.75
Peonidin 3-*O*-galactoside (**419**)		galatose	OCH_3	H	143.31
Positive control **Acarbose**	–	–	–	–	356.26

flavonoid was quercetin (**25**), with a Ki value 0.12 mM, revealing that the presence of the double C2 = C3 bond as well as the presence of a -OH group at 3-position of C ring increase the intended effect, as inferred by comparing quercetin (**25**) with eriodictyol (**41**) (Ki = 2.59 mM) and luteolin (**1**) (Ki = 2.63 mM).

In the work of Meesakul et al. (2019), the α-glucosidase (*Saccharomyces cerevisiae*) inhibitory activity of flavonoids from the leaf and twig extracts of *Desmos cochinchinensis* (Table 77) was tested. The most active compounds were desmosconchiflavone A (**439**), desmosconchiflavone B (**440**) and dichamanetin (**443**), presenting IC_{50} values of 0.9, 0.9 and 0.2 μM, respectively. The IC_{50} of acarbose was 170.7 μM. These results suggest that the presence of a benzyl group mono- or dihydroxylated at 6- or/and 8-positions of A ring is responsible for a significant increase in the α-glucosidase inhibition. This effect can be also seen by comparing desmosconchiflavone A (**439**) and B (**440**) with chrysin

Table 74. Flavonoids tested by Fan et al. (2019), and respective inhibitory activity on α-glucosidase (the most active flavonoids are highlighted).

Flavonoid	Structure	R^3	$R^{3'}$	$R^{5'}$	R^6	R^8	IC_{50} (μg/mL)
Quercetin (**25**)		OH	–	H	H	–	26.7
Quercetin 3-methyl ether (**271**)		OCH_3	–	H	H	–	26.2
6-Prenylquercetin 3-methyl ether (**340**)		OCH_3	–	H	prenyl	–	21.3
5′-Prenylquercetin (**341**)		OH	–	prenyl	H	–	**3.9**
6-Prenylquercetin (**420**)		OH	–	H	prenyl		**3.7**
Naringenin (**28**)		–	H	H	H	H	> 100
Eriodictyol (**41**)		–	OH	H	H	H	> 100
6-Prenyleriodictyol (**342**)		–	OH	H	prenyl	H	27.5
5′-Prenyleriodictyol (**343**)		–	OH	prenyl	H	H	53.4
8-[(E)-3-hydroxymethyl-2butenyl]eriodictyol (**344**)		–	OH	H	H	(E)-3-hydroxymethyl-2-butenyl	> 100
6-Prenylnaringenin (**421**)		–	H	H	prenyl	H	15.4
3′-Prenylnaringenin (**422**)		–	prenyl	H	H	H	> 100
Sigmoidin C (**423**)		–	–	–	–	–	> 100
Positive control **Acarbose**	–	–	–	–	–	–	0.04

(**73**), which do not possess the aromatic ring at the referred position and presents an IC_{50} value of 4.9 μM. The same conclusion can be drawn by comparing the flavanones dichamanetin (**443**) with isochamanetin (**441**) (IC_{50} = 2.9 μM), where it can be observed that the lack of the benzyl group at 8-position of A ring decreased the intended effect.

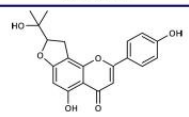
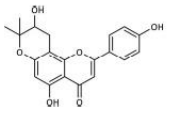
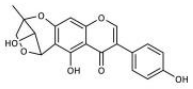
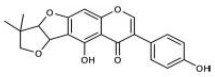
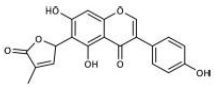
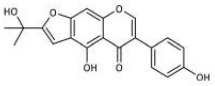
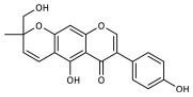
Zhao, Liu, and Chen (2019) evaluated the α-glucosidase (*Aspergillus niger*) inhibition by a group of natural flavonoids (Table 78). The most effective compound was isoflavone genistein (**19**), with an IC_{50} value of 0.5 mM. By comparing genistein (**19**) with daidzein (**20**), which presented an IC_{50} value of 1.66 mM, the lack of an -OH group at 5-position of A ring, leads to a reduction in the activity. Furthermore, the inhibitory effect of formononetin (**137**) (IC_{50} = 2.82 mM) decreased when compared to daidzein (**20**), possibly due to the replacement of the -OH group at 4′-position of B ring by a $-OCH_3$ substituent. This effect can also be seen by comparing genistein (**19**) with biochanin A (**276**) (IC_{50} = 0.69 mM).

Ren, Li, and Liu (2019) evaluated the yeast α-glucosidase inhibitory activity by rutin (**5**), quercetin (**25**) and catechin (**30**) (see the chemical structures in Table 25). With an IC_{50} value of 0.44 mg/mL, quercetin (**25**) was the most active compound, presenting a competitive inhibition type. Although the authors did not present the standard errors associated to the IC_{50} values, the comparison of quercetin (**25**) with rutin (**5**) (IC_{50} = 0.57 mg/mL), suggests that the replacement of the -OH group by a rutinose at 3-position of C ring reduces the intended effect. In addition, the absence of the C2 = C3 double bond and the 4-keto group also seems to decrease the α-glucosidase inhibition, by comparing quercetin (**25**) with catechin (**30**) (IC_{50} = 0.76 mg/mL).

α-Glucosidase (from *Saccharomyces cerevisiae*) inhibition by flavonoids isolated from leaves and flowers of *Gaiadendron punctatum*, was studied (Table 79) (Cedeño et al. 2019). The compounds which presented higher inhibition of α-glucosidase were rutin (**5**) and hecpatrin (**446**) with IC_{50} values of 7.53 ± 1.08 and 9.66 ± 1.04, 16.87 ± 1.02, respectively. The results indicate that the presence of an -OH group at 3′-position of B ring has a significant role for the inhibition under study, since rutin (**5**) was more active than nicotiflorin (**218**) (IC_{50} = 159.09 ± 9.54 μM). Moreover, the nature of the sugar substitution at 3-position of C ring is important, as seen by comparing gaiadendrin (**447**) with puchiktirin (**448**), which was not active at the higher tested concentration (220.26 μM).

The effect of eriodictyol (**41**) and eriocitrin (**376**) (Table 80) on α-glucosidase, from *Saccharomyces cerevisiae*, was tested (Liu et al. 2020). The obtained results indicated that both compounds could quench the intrinsic fluorescence of the enzyme, showing binding constants, at 298 K, of $(4.57 \pm 0.16) \times 10^4$ L mol^{-1} and $(6.01 \pm 0.22) \times 10^4$ L/mol^{-1} for eriodictyol (**41**) and eriocitrin (**376**), respectively. These findings suggest that eriocitrin (**376**) has higher binding affinity for α-glucosidase than eriodictyol (**41**). In this sense, the presence of a rutinose at 7-position of A ring seems to improve the inhibitory effect, compared with the presence of an -OH group at this position.

Table 75. Flavonoids tested by Ghani et al. (2019) and Nur et al. (2019), and respective inhibitory activity on α-glucosidase (the most active flavonoid is highlighted).

Flavonoid	Structure	K_i (μM ± SEM)*	% Inhibition at 50 μM**
Retamasin C (**424**)		19.93 ± 0.77	62.9 ± 1.9
Retamasin D (**425**)		39.17 ± 0.86	43.6 ± 0.4
Retamasin F (**426**)		14.45 ± 0.83	33.2 ± 1.6
Retamasin G (**427**)		56.61 ± 0.95	61.0 ± 0.6
Retamasin H (**428**)		**12.06 ± 0.57**	**96.3 ± 0.2**
Erysubin A (**429**)		16.42 ± 0.18	67.9 ± 0.7
Erysubin B (**430**)		71.17 ± 0.64	46.7 ± 0.9
Positive control **Acarbose**	–	4.72 ± 0.38	98.7 ± 0.9

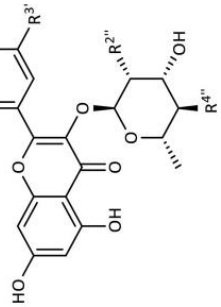
*Results from the study of Ghani et al. (2019); ** Results from the study of Nur et al. (2019).

Flavonoids isolated from the seeds of *Psoralea corylifolia* (Table 81) were evaluated regarding their ability to inhibit α-glucosidase (Zhu et al. 2019). The better inhibitor was bavachinone B (**451**), with an IC_{50} value of 28.0 μM, followed by compounds **450** (IC_{50} = 32.7 μM) and **449** (IC_{50} = 41.2 μM). It was observed that the tested flavanones were clearly more active than the isoflavones, corylifols E (**452**) and corylifols D (**453**), which presented IC_{50} values of 157.5 μM and 179.4 μM, respectively.

The inhibition of α-glucosidase (*Saccharomyces cerevisiae*) by 27 dietary flavonoids (Table 82) was studied in the work of Jia et al. (2019). The most potent compound was myricetin (**24**), with an IC_{50} value of 11.63 ± 0.36 μM. This result indicates that the addition of an -OH group at 5′-position of B ring has a crucial role for the intended effect, since myricetin (**23**) has an IC_{50} value around 10-fold lower than the one found for quercetin (**25**) (IC_{50} = 115.14 ± 2.19 μM). Additionally, in general, flavonoids glycosides were weaker α-glucosidase inhibitors than their respective aglycones. This can be observed by comparing, for example, myricetin (**24**) with myricitrin (**113**) (IC_{50} = 309.28 ± 2.40 μM), and luteolin (**1**) (IC_{50} = 82.73 ± 2.51 μM) with luteolin 7-glucoside (**4**) (IC_{50} = 431.22 ± 3.03 μM). Moreover by comparing luteolin (**1**) with eriodictyol (**41**) (IC_{50} = 1033.48 ± 4.74 μM), as well as quercetin (**25**) and taxifolin (**111**) (IC_{50} = 2946.97 ± 4.91 μM), it is possible to corroborate that the lack of the C2 = C3 double bond significantly reduces the inhibitory activity, which might be caused by the decreased planarity of C ring. In what concerns the tested flavans, it seems that the addition of an -OH group at 5′-position of B ring as well as the presence of a galloyl group at 3-position of C ring enhances the inhibition of yeast α-glucosidase, as seen by comparing catechin (**30**) and epigallocatechin gallate (**33**), with IC_{50} values of 16244.26 ± 12.74 μM and 97.52 ± 1.35 μM, respectively.

He et al. (2019) evaluated the inhibitory activity of a series of flavonoids on α-glucosidase from Saccharomyces cerevisiae (Table 83). Myricetin (**24**) was the best inhibitor, presenting an IC_{50} value of 2.09 μg/mL. Thus, once again it was observed that the presence of an -OH group at 3-position of C ring and at 5′-position of B ring (together with the catechol at 3′- and 4′-positions of B ring, and the presence of an -OH group at 5- and 7-positions of A ring) increased the inhibitory activity, by comparing of myricetin (**24**) with luteolin (**1**) (IC_{50} = 27.22 μg/mL) and quercetin (**25**) (IC_{50} = 6.10 μg/mL), respectively. In addition, as mentioned above, compared with flavonoid aglycones [luteolin (**1**), baicalein (**23**), myricetin (**24**), quercetin (**25**) and chrysin (**73**)], the flavonoid glycosides [rutin (**5**) and baicalin (**12**)] are poor α-glucosidase inhibitors, possibly due to

Table 76. Flavonoids tested by Li, Kongstad, and Staerk (2019), and respective inhibitory activity on α-glucosidase (the most active flavonoid is highlighted).

Flavonoid	Structure	R^3	$R^{4'}$	$R^{2''}$	$R^{4''}$	IC_{50} (μM ± SD)
Tamarixetin 3-*O*-(2″-*E*-*p*-coumaroyl,4″-*Z*-*p*-coumaroyl)-α-L-rhamnoside (**431**)		OH	OCH_3	*E*-*p*-cou	*Z*-*p*-cou	28.2 ± 0.00
Kaempferol 3-*O*-(2″-*E*-*p*-coumaroyl,4″-*Z*-*p*-coumaroyl)-α-L-rhamnoside (**432**)		H	OH	*E*-*p*-cou	*Z*-*p*-cou	16.1 ± 0.01
Kaempferol 3-*O*-(2″-*Z*-*p*-coumaroyl,4″-*E*-*p*-coumaroyl)-α-L-rhamnoside (**433**)		H	OH	*Z*-*p*-cou	*E*-*p*-cou	35.3 ± 0.02
Kaempferol 3-*O*-(2″, 4″-di-*E*-*p*-coumaroyl)-α-L-rhamnoside (**434**)		H	OH	*E*-*p*-cou	*E*-*p*-cou	12.9 ± 0.00
4′-*O*-Methyl-2″,4″-di-(*Z*)-*p*-coumaroylafzelin (**435**)		H	OCH_3	*Z*-*p*-cou	*Z*-*p*-cou	**5.9 ± 0.01**
4′-*O*-Methyl-(2″-*E*-*p*-coumaroyl,4″-*Z*-*p*-coumaroyl)afzelin (**436**)		H	OCH_3	*E*-*p*-cou	*Z*-*p*-cou	6.8 ± 0.00
4′-*O*-Methyl-(2″-*Z*-*p*-coumaroyl,4″-*E*-*p*-coumaroyl)afzelin (**437**)		H	OCH_3	*Z*-*p*-cou	*E*-*p*-cou	10.1 ± 0.00
4′-*O*-Methyl-2″,4″-di-(*E*)-*p*-coumaroylafzelin (**438**)		H	OCH_3	*E*-*p*-cou	*E*-*p*-cou	26.9 ± 0.01
Positive control						266.1 ± 0.01
Acarbose						

the large molecular size of flavonoids glycosides which hindered their access to the enzyme. Furthermore, -OH groups at B ring had a beneficial effect on this specific biological activity, which might be due to the B ring of flavonoids pointing to the inside of the active center of the enzyme. Finally, it was also found that the absence of the C2 = C3 double bond drastically reduced the inhibition of α-glucosidase, as it can be observed by comparing, for example, myricetin (**24**) with dihydromyricetin (**75**) (IC_{50} = 85.95 μg/mL).

Flavonoids isolated from the seeds of *Hippophae rhamnoses* subsp. *Sinensis* and their capacity to inhibit α-glucosidase (Table 84) (Li, Wang, et al. 2019). The compound with best inhibitory activity was flavonoid hippophin M (**465**), presenting an IC_{50} value of 8.30 μM. This compound was followed by flavonoids **463, 466, 464** and hippophin K (**462**), with IC_{50} values of 53.20 μM, 89.74 μM, 103.36 μM and 112.11 μM, respectively, while the other tested compounds showed no inhibitory activity up to 5000 μM. These results indicate that the α-glucosidase inhibition by flavonoids [hippophin K (**462**) – **466**] might be due to the presence of only one side chain, since compounds hippophin F (**467**) – hippophin C (**470**), with no inhibitory activity, possess two side chain groups. Besides, flavonoids hippophin N (**458**) – hippophin P (**460**) were also not active, suggesting that different connections of sugars may be not negligible.

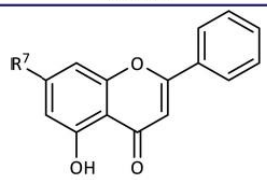
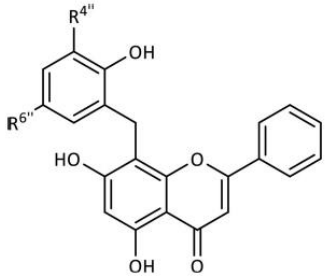
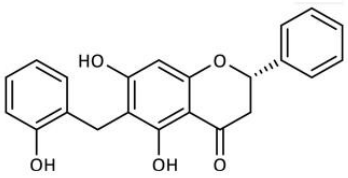
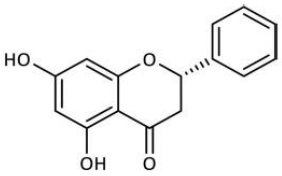
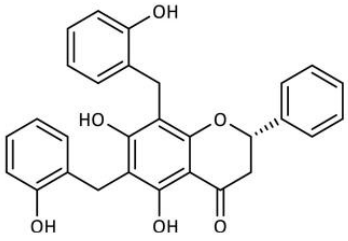
A series of 30 flavanones (Table 85) were isolated from the rhizomes of *Matteuccia intermedia* and their α-glucosidase (*Saccharomyces cerevisiae*) inhibitory activity was studied (Li, Zhu, et al. 2019). Farreol (**481**) – cyrtominetin (**486**) were effective inhibitors, being cyrtominetin (**486**) the most active compound with an IC_{50} value of 12.4 ± 2.66 μM. By comparing this flavonoid, which has two -OH groups in B ring, with methoxymatteucin (**484**) (IC_{50} = 69.7 ± 7.86 μM) and 3′-hydroxymatteucinol (**485**) (IC_{50} = 43.6 ± 3.96 μM), it can be observed that the presence of just one -OH group together with one-OCH_3 group in B ring decreased the α-glucosidase inhibition. In this study, all flavanones that presented an effective α-glucosidase inhibition have an -OH group at 7-position of A ring, while the tested flavanones, which have a glucose at this position, [matteflavonid H (**472**) – matteurinate E (**479**) and demethoxymateucinol 7-*O*-glucoside (**488**) – matteuorienate K (**500**)] were not active. This suggests that the glycosylation of an -OH group at 7-position of A ring reduces the intended effect. These findings are in accordance with the conclusions mentioned above. Moreover, flavonoids having a -CH_3 at 6- and 8-positions of A ring, together with an -OH group or a -OCH_3 group in B ring [farrerol (**481**) – cyrtometin (**486**)], showed a stronger inhibitory activity than the other flavanones aglycones [demethylmatteucinol (**471**), demethoxymatteucinol (**480**) and flavonoid (**487**)]. As such, these features may be important for the effect under study.

The results of the analyzed research studies are summarized in the Table 86.

Discussion

The high variability concerning the experimental conditions of the enzyme assays lead to different ranges of IC_{50} values

Table 77. Flavonoids tested by Meesakul et al. (2019), and respective inhibitory activity on α-glucosidase (the most active flavonoid is highlighted).

Flavonoid	Structure	$R^{4''}$	$R^{6''}$	R^7	IC_{50} (μM)
Chrysin (**73**)		–	–	OH	4.9
Techtochrysin (**323**)		–	–	OCH_3	158.2
Desmoscochinflavone A (**439**)		OH	H	–	0.9
Desmoscochinflavone B (**440**)		H	OH	–	0.9
Isochamanetin (**441**)		–	–	–	2.9
Pinocembrin (**442**)		–	–	–	4.3
Dichamanetin (**443**)		–	–	–	**0.2**
Positive control **Acarbose**		–	–	–	170.7

found for flavonoids in different studies. Although the analyzed publications allow the establishment of a SAR, and consequently the features on the chemical structure of flavonoids that are responsible for a higher or lower inhibition of the target, standardization of the experimental parameters would be desirable. The main factors that must be considered for the optimization of enzyme assays are temperature, time assay and time of incubation with tested compounds, pH, ionic strength, and the proper concentrations of the essential components, like substrate and enzyme, as well as their source (Bisswanger 2014). Regarding α-amylase and α-glucosidase, the specific enzyme and substrate sources dictate different assay conditions. In what concerns the different ranges of tested concentrations (nM to mM) of flavonoids among different studies, their bioavailability and toxicity should be taken into consideration in case of further developments with the most promising compounds. Flavonoids are present in the daily human diet, and are considered safe and having low toxicity, although the toxicological studies cannot be excluded (Hernández-Rodríguez, Baquero, and Larrota 2019). It is well known that the bioavailability of flavonoids is highly variable, depending on

Table 78. Flavonoids tested by Zhao, Liu, and Chen (2019), and respective inhibitory activity on α-glucosidase (the most active flavonoid is highlighted).

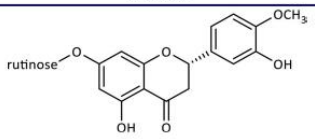
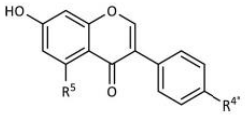
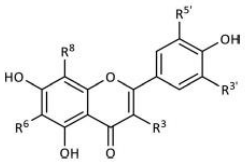
Flavonoid	Structure	R^3	$R^{3'}$	$R^{4'}$	R^5	$R^{5'}$	R^6	R^8	IC_{50} (mM)
Hesperidin (**14**)		–	–	–	–	–	–	–	2.24
Genistein (**19**)		–	–	OH	OH	–	–	–	**0.50**
Daidzein (**20**)		–	–	OH	H	–	–	–	1.66
Formononetin (**137**)		–	–	OCH_3	H	–	–	–	2.82
Biochanin A (**276**)		–	–	OCH_3	OH	–	–	–	0.69
Myricetin (**24**)		OH	OH	–	–	OH	H	H-	3.63
Isoschaftoside (**444**)		H	H	–	–	H	arabinose	glucose	1.10
Schaftoside (**445**)		H	H	–	–	OH	glucose	arabinose	1.86
Positive control **Acarbose**		–	–	–	–	–	–	–	0.32

Table 79. Flavonoids tested by Cedeño et al. (2019), and respective inhibitory activity on α-glucosidase (the most active flavonoids are highlighted).

Flavonoid	Structure	R^3	$R^{3'}$	$R^{4'}$	IC_{50} (μM ± SEM)
Rutin (**5**)		rutinose	OH	OH	**7.53 ± 1.08**
Nicotiflorin (**218**)		rutinose	H	OH	159.09 ± 9.54
Hecpatrin (**446**)		OH	OH	2-*O*-β-rhamnosyl-6-β-glucose	**9.66 ± 1.04**
Gaiadendrin (**447**)		2,6-di-*O*-β, β-rhamnosyl-β-glucose	OH	OH	16.87 ± 1.02
Puchiktrin (**448**)		2,6-di-*O*-β, β-rhamnosyl-α-mannose	OH	OH	NA
Positive control **Acarbose**	–	–	–	–	300–700

NA – Not active at the maximum tested concentration (220.26 μM).

Table 80. Flavonoids tested by Liu et al. (2020), and respective binding constants on α-glucosidase (the most active flavonoid is highlighted).

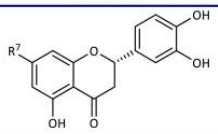
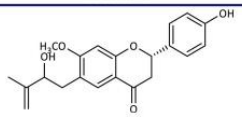
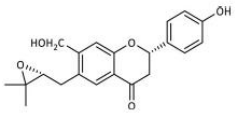
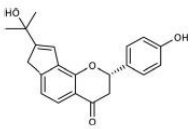
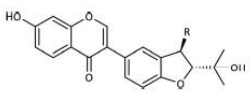
Flavonoid	Structure	R^7	K_b (L mol^{-1} ± SD)
Eriodictyol (**41**)		OH	(4.57 ± 0.16) x 10^4
Eriocitrin (**376**)		rutinose	**(6.01 ± 0.22) x 10^4**

Table 81. Flavonoids tested by Zhu et al. (2019), and respective inhibitory activity on α-glucosidase (the most active flavonoid is highlighted).

Flavonoid	Structure	R	IC_{50} (μM)
449		–	41.2
450		–	32.7
Bavachinone B (**451**)		–	**28.0**
Corylifols E (**452**)		OH	157.5
Corylifols D (**453**)		H	179.4
Positive control **Acarbose**	–	–	214.8

their subclass and substituents, but also revealed specific bioactive properties in the gastrointestinal tract (Hollman 2004; Gonzales et al. 2015). One way to improve the bioavailability and, hence, the therapeutic benefits of flavonoids, is the application of nanotechnology (Mignet, Seguin, and Chabot 2013; Wang, Su, et al. 2014). Noteworthy, the α-glucosidase inhibitors available for the treatment of T2D are poorly absorbed, acting on the surface of enterocytes (Schmeltz and Metzger 2007).

General conclusions observed through the analysis of the several studies, concerning the SAR of flavonoids inhibitory activity against α-amylase and α-glucosidase are discussed below.

Table 82. Flavonoids tested by Jia et al. (2019), and respective inhibitory activity on α-glucosidase (the most active flavonoid is highlighted).

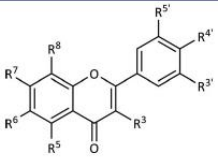
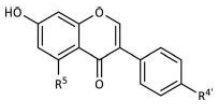
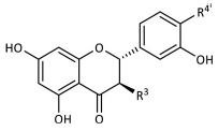
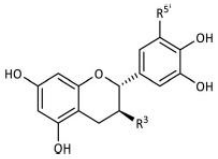
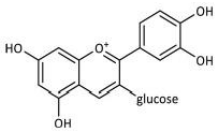
Flavonoid	Structure	R^3	$R^{3'}$	$R^{4'}$	R^5	$R^{5'}$	R^6	R^7	R^8	IC_{50} (μM ± SD)
Luteolin (**1**)		H	OH	OH	OH	H	H	OH	H	82.73 ± 2.51
Luteolin 7-glucoside (**4**)		H	OH	OH	OH	H	H	glucose	H	431.22 ± 3.03
Rutin (**5**)		rutinose	OH	OH	OH	H	H	OH	H	173.58 ± 1.23
Isorhamnetin 3-rutinoside (**6**)		rutinose	OCH_3	OH	OH	H	H	OH	H	539.76 ± 2.78
Apigenin (**22**)		H	H	OH	OH	H	H	OH	H	597.56 ± 5.26
Baicalein (**23**)		H	H	H	H	H	OH	OH	OH	259.56 ± 3.15
Myricetin (**24**)		OH	OH	OH	OH	OH	H	OH	H	**11.63 ± 0.36**
Quercetin (**25**)		OH	OH	OH	OH	H	H	OH	H	115.14 ± 2.19
Kaempferol (**26**)		OH	H	OH	OH	H	H	OH	H	153.39 ± 1.79
Fisetin (**27**)		OH	OH	OH	H	H	H	OH	H	46.39 ± 0.34
Galangin (**99**)		OH	H	H	OH	H	H	OH	H	415.91 ± 5.92
Myricitrin (**113**)		rhamnose	OH	OH	OH	OH	H	OH	H	309.28 ± 2.40
Apigenin 7-*O*-β-glucoside/Cosmosiin (**163**)		H	H	OH	OH	H	H	glucose	H	22.80 ± 0.24
Isoschaftoside (**444**)		H	H	OH	OH	H	arabinose	OH	glucose	387.88 ± 3.68
Isorhamnetin (**454**)		OH	OCH_3	OH	OH	H	H	OH	H	676.71 ± 7.42
Vitexin (**455**)		H	H	OH	OH	H	H	OH	glucose	356.12 ± 3.28
Vitexin 4′-glucoside (**456**)		H	H	glucose	OH	H	H	OH	glucose	442.50 ± 3.41
Kaempferol 7-glucoside (**457**)		OH	H	OH	OH	H	H	glucose	H	204.47 ± 3.15
Genistein (**19**)		–	–	OH	OH	–	–	–	–	642.21 ± 3.66
Formononetin (**137**)		–	–	OH	OH	–	–	–	–	747.83 ± 2.73
Hesperetin (**29**)		OH	–	OCH_3	–	–	–	–	–	1903.27 ± 5.51
Eriodictyol (**41**)		H	–	OH	–	–	–	–	–	1033.48 ± 4.74
Taxifolin (**111**)		OH	–	OH	–	–	–	–	–	2946.97 ± 4.91
(+)-Catechin (**30**)		OH	–	–	–	H	–	–	–	16244.26 ± 12.74
(-)-Epigallocatechin gallate (**33**)		gallate	–	–	–	OH	–	–	–	97.52 ± 1.35
Cyanidin 3-*O*-glucoside (**406**)		–	–	–	–	–	–	–	–	63.50 ± 0.26
Positive control **Acarbose**										0.59 ± 0.14

Table 83. Flavonoids tested by He et al. (2019), and respective inhibitory activity on α-glucosidase (the most active flavonoid is highlighted).

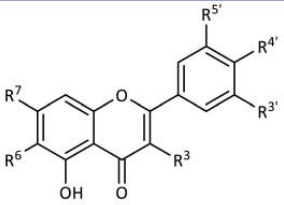
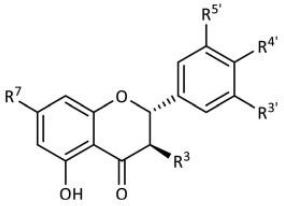
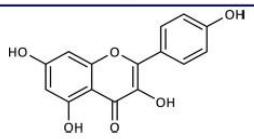
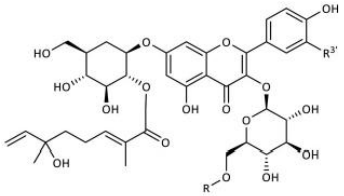
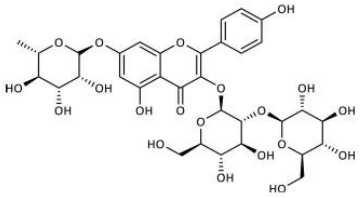
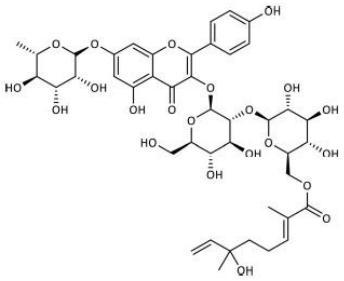
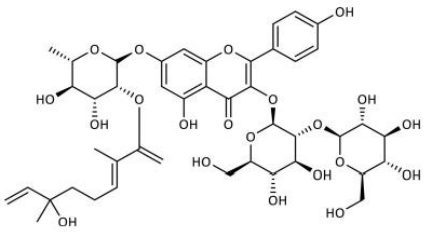
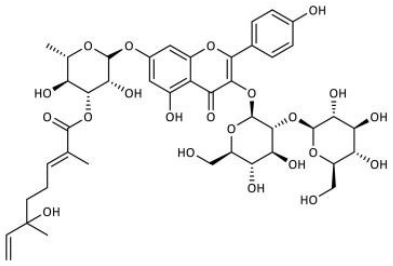
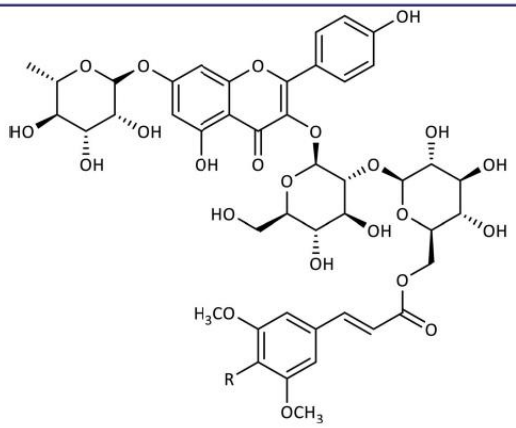
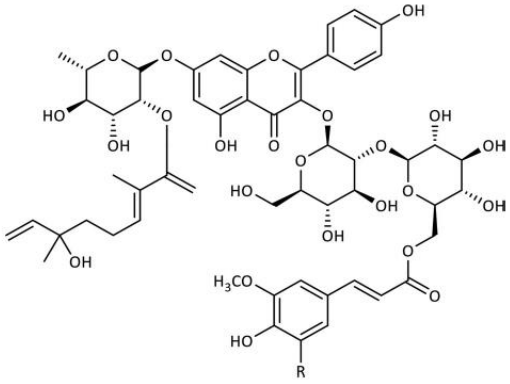
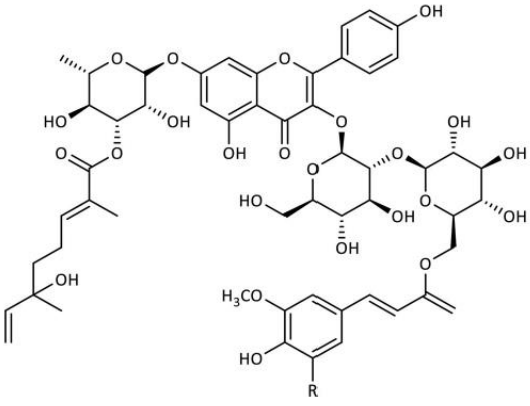
Flavonoid	Structure	R^3	$R^{3'}$	$R^{4'}$	$R^{5'}$	R^6	R^7	IC_{50} (μg/mL)
Luteolin (**1**)		H	OH	OH	H	H	OH	27.22
Rutin (**5**)		rutinose	OH	OH	H	H	OH	> 500
Baicalin (**12**)		H	H	H	H	OH	glucuronide	> 500
Baicalein (**23**)		H	H	H	H	OH	OH	6.75
Myricetin (**24**)		OH	OH	OH	OH	H	OH	**2.09**
Quercetin (**25**)		OH	OH	OH	H	H	OH	6.10
Fisetin (**26**)		OH	OH	OH	H	H	OH	5.50
Chrysin (**73**)		H	H	H	H	H	OH	70.07
Hesperidin (**14**)		H	OH	OCH_3	H	–	rutinose	> 500
Hesperetin (**29**)		H	OH	OCH_3	H	–	OH	286.60
Naringin (**60**)		H	H	OH	H	–	rutinose	> 500
Dihydromyricetin (**75**)		OH	OH	OH	OH	–	OH	85.95

Table 84. Flavonoids tested by Li, Wang, et al. (2019), and respective inhibitory activity on α-glucosidase (the most active flavonoid is highlighted).Structure

Flavonoid	R	$R^{3'}$	IC_{50} (μM)	
Kaempferol (**26**)		–	–	23.98
Hippophin N (**458**)		rhamnose	H	> 5000
Hippophin O (**459**)		rhamnose	OCH_3	> 5000
Hippophin P (**460**)		H	H	> 5000
461		–	–	> 5000
Hippophin K (**462**)		–	–	112.11
463		–	–	53.20
464		–	–	103.36

(*continued*)

Table 84. Continued.

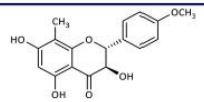
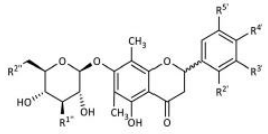
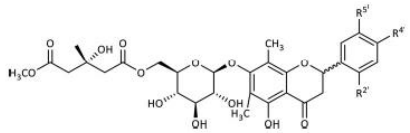
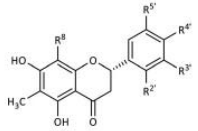
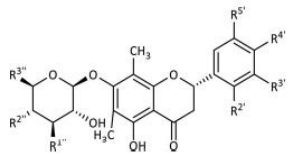
Flavonoid	R	$R^{3'}$	IC_{50} (μM)	
Hippophin M (**465**)		OCH_3	–	**8.30**
466		OH	–	89.74
Hippophin F (**467**)		H	–	> 5000
Hippophin D (**468**)		OCH_3	–	> 5000
Hippophin E (**469**)		H	–	> 5000
Hippophin C (**470**)		OCH_3	–	> 5000
Positive control **Acarbose**	–	–	–	1727.07

α-Amylase inhibition by flavonoids

The analysis of the published studies on the inhibition of α-amylase by flavonoids allows a good understanding of the respective SAR (Figure 5).

In general, the chemical features in flavonoids that are favorable for the α-amylase inhibition are the presence of the 4-keto group and the C2 = C3 double bond, as well as the hydroxylation at 3′- and 4′- positions of B ring and at 5-, 6- and 7-positions of A ring. Moreover, the replacement of

Table 85. Flavonoids tested by Li, Zhu, et al. (2019), and respective inhibitory activity on α-glucosidase (the most active flavonoid is highlighted).

Flavonoid	Structure	$R^{2'}$	$R^{3'}$	$R^{4'}$	$R^{5'}$	R^{8}	$R^{1''}$	$R^{2''}$	$R^{3''}$	IC_{50} (μM ± SD)
Demethylmatteucinol (**471**)		–	–	–	–	–	–	–	–	> 200
Matteflavoside H (**472**)		H	OH	OCH_3	H	–	OH	OH	–	> 200
Matteflavoside I (**473**)		OH	H	OCH_3	H	–	OH	OH	–	> 200
Matteflavoside J (**474**)		OH	H	H	H	–	OH	OH	–	> 200
Matteuinterate A (**475**)		H	OH	OCH_3	H	–	OH	(S)-3-hydroxy-3-methylglutaroyl	–	> 200
Matteuinterate B (**476**)		H	H	OH	H	–	OH	(S)-3-hydroxy-3-methylglutaroyl	–	> 200
Matteuinterate C (**477**)		OH	H	H	OCH_3	–	(S)-3-hydroxy-3-methylglutaroyl	OH	–	> 200
Matteuinterate D (**478**)		H	–	OH	H	–	–	–	–	> 200
Matteuinterate E (**479**)		OH	–	H	OCH_3	–	–	–	–	> 200
Demethoxymateucinol (**480**)		H	H	H	H	CH_3	–	–	–	> 200
Farrerol (**481**)		H	H	OH	H	CH_3	–	–	–	44.1 ± 0.42
Matteucin (**482**)		OH	H	H	H	CH_3	–	–	–	37.6 ± 2.67
Matteucinol (**483**)		H	H	OCH_3	H	CH_3	–	–	–	28.0 ± 3.56
Methoxymatteucin (**484**)		OH	H	H	OCH_3	CH_3	–	–	–	69.7 ± 7.86
3'Hydroxymatteucinol (**485**)		H	OH	OCH_3	H	CH_3	–	–	–	43.6 ± 3.96
Cyrtominetin (**486**)		H	OH	OH	H	CH_3	–	–	–	**12.4 ± 2.66**
487		H	H	OCH_3	H	H	–	–	–	> 200
Demethoxymateucinol 7-*O*-glucoside (**488**)		H	H	H	H	–	OH	OH	OH	> 200
Farrerol 7-*O*-glucoside (**489**)		H	H	OH	H	–	OH	OH	OH	> 200
Matteucinol 7-*O*-glucoside (**490**)		H	H	OCH_3	H	–	OH	OH	OH	> 200
Myrclacitrin II (**491**)		OH	H	H_3	OCH_3	–	OH	OH	OH	> 2001
Matteflavoside G (**492**)		H	OH	OCH_3	OH	–	OH	OH	OH	> 200
Matteuorienate A (**493**)		H	H	OCH_3	H	–	OH	OH	(S)-3-hydroxy-methylglutarolyl	> 200
Matteuorienate B (**494**)		H	H	H	H	–	OH	OH	(S)-3-hydroxy-methylglutarolyl	> 200
Matteuorienate D (**495**)		H	H	OCH_3	H	–	OH	(S)-3-hydroxy-methylglutaroyl-	OH	> 200
Matteuorienate F (**496**)		H	H	OCH_3	H	–	(S)-3-hydroxy-methylglutaroyl-	OH	OH	> 200
Matteuorienate H (**497**) (*2S*)		OH	H	OCH_3	H	–	OH	OH	(S)-3-hydroxy-methylglutaroyl-	> 200
Matteuorienate I (**498**) (*2R*)		OH	H	OCH_3	H	–	OH	OH	(S)-3-hydroxy-methylglutaroyl	> 200

(*continued*)

Table 85. Continued.

Flavonoid	Structure	$R^{2'}$	$R^{3'}$	$R^{4'}$	$R^{5'}$	R^{8}	$R^{1''}$	$R^{2''}$	$R^{3''}$	IC_{50} (μM ± SD)
Matteuorienate J (**499**)		OH	H	H	OCH_3	–	OH	OH	(S)-3-hydroxy-methylglutaroyl	> 200
Matteuorienate K (**500**)		OH	H	H	H	–	OH	OH	(S)-3-hydroxy-methylglutaroyl	> 200
Positive control **Acarbose**		–	–	–	–	–	–	–	–	172.3 ± 14.7

a prenyl group for a geranyl group at 8-position of A ring, or an -OH group for a -Cl ion at 3-position of C ring, are responsible for an increase in the intended effect. On the other side, the methylation and glycosylation of -OH groups in A and B rings, and the presence of a -OH group at 3-position of C ring, reduce the inhibitory activity of the compounds under study on α-amylase.

α-Glucosidase inhibition by flavonoids

The analysis of the studies published since 2013 on the inhibition of α-glucosidase by flavonoids, also allows a good understanding of the respective SAR (Figure 6).

In general, the chemical features in flavonoids that are favorable for the α-glucosidase inhibition are: the carbonyl group at 4-position of C ring, the C2 = C3 double bond, as well as the presence of -OH groups at 3-position of C ring, at 3′-, 4′- and/or 5′- positions of B ring, and at 5-, 6-, 7- and/or at 8-positions of A ring. Furthermore, the 2, 4, 6-trihydroxylation on *N*-benzylidene ring of flavone hydrazine derivatives improves the α-glucosidase inhibition, as well as the presence of other substituents, such as chlorine, fluorine and nitro. In addition, prenylation of flavonoids at 5- and/or 6-positions of A ring, and at 5′-position of B ring; geranylation at 6- and/or 8-position of A ring; and lavandulylation at 7-position of A ring, also enhance the inhibitory activity. Other substitutions also seem to have a beneficial effect for the inhibition of the enzyme under study, including the presence of a *N*-tosyl group at 4′-position of B ring, or a 2,5-trifluoromethyl substitution in flavone ethers; a Y -lactone chain at 6-position of A ring; a prenyloxy group at 7-position of A ring; or a benzyl group at 8-position of the same ring. Moreover, the replacement of -OH and $-OCH_3$ groups by a sulfate group at 8-position of A ring or the replacement of the catechol at 3′- and 4′-positions of B ring by alkyl chains seems to increase the inhibition of α-glucosidase. In isoflavones, it was suggested that the presence of -OH groups at 2′- and 4′-positions of B ring, and the addition of a pyran ring was favorable for the intended effect.

Through the analysis of the numerous research studies, it was also found that flavones are better α-glucosidase inhibitors than isoflavones. In general, flavonoid aglycones presented a higher ability to inhibit α-glucosidase than the corresponding glycosides. Nevertheless, among the flavonoid glycosides, it was observed that some substitutions improved the intended effect, such as the replacement of glucose by a rhamnose at 7-position of A ring or the replacement of arabinose by a rhamnose at 3-position of C ring. The benzoylation of flavonoids at 6″-position of the sugar moiety, the presence of galloyl groups specially at 3″-position of galactose, or the presence of *Z*-*p*-coumaroyl units in flavonoids glycosides also seem to be favorable for the inhibitory activity.

As mentioned before, the glycosylation of flavonoids reduced their inhibitory effect, in special at 3-position of C ring and at 7-position of A ring. In fact, it was verified that both glycosylation or methylation of -OH groups are not beneficial for the intended effect. Following this rationale,

Table 86. Summary of the results obtained for the inhibitory activity of flavonoids on α-glucosidase, in the analyzed research studies.

Class	Tested concentrations	Most active flavonoid	Inhibitory activity	Type of inhibition	Positive control	Relative coefficient to positive control	Reference
Flavonols	NM	Quercetin (25)	IC_{50} = 30.9 ± 8.4 μg/mL	NT	Acarbose (IC_{50} = 103.3 ± 9.3 μg/mL)	0.30	(Aderogba et al. 2013)
			IC_{50} = 5.1 ± 0.3 μg/mL		Acarbose (IC_{50} = 465 ± 37 μg/mL)	91.18	(Ma et al. 2015)
		8-Geranylquercetin (229)	IC_{50} = 1.15 μM	Competitive	Acarbose IC_{50} = 51.32 μM	0.02	(Sun et al. 2015)
		Flavonoid 247	IC_{50} = 9.3 ± 0.4 μM	Competitive	Acarbose (IC_{50} = 720.3 ± 57.5 μM)	0.01	(Chen et al. 2016)
		Myricetin (24)	IC_{50} = 3 μg/mL	Noncompetitive	NM	NM	(Meng et al. 2016)
		Quercetin (25)	IC_{50} = 7.19 ± 0.06 μM	NT	Acarbose (IC_{50} = 859.79 ± 0.09 μM)	0.008	(Silva et al. 2016)
		Myricetin (24)	IC_{50} = 2.25 ± 0.05 μmol/L	Competitive	Acarbose (IC_{50} = 3.04 ± 0.04 μM)	0.74	(Zeng, Zhang, et al. 2016)
		Quercetin (25)	IC_{50} = 66.8 μg/mL	Mixed	NM	NM	(Chen et al. 2017)
	20–300 μM	Icaritin (301)	IC_{50} = 74.42 ± 0.01 μM	NT	Acarbose (IC_{50} = 101.16 ± 3.69 μM)	0.74	(Kim, Jung, et al. 2017)
	0–200 μM	Flavonoid 310	IC_{50} = 7.6 ± 0.4 μM	Competitive	Acarbose (IC_{50} = 607 ± 56 μM)	0.01	(Proença et al. 2017)
	NM	Quercetin (25)	IC_{50} = 4.92 ± 7.06 μM	NT	Quercetin (commercial) (IC_{50} = 4.30 ± 1.06 μM)	1.14	(Sarian et al. 2017)
		5'-Prenylquercetin (341)	IC_{50} = 2.3 μg/mL		Acarbose (EC_{50} = 0.1 μg/mL)	23	(Ye, Fan, and Ma 2017)
	0.0078–1 mg/mL	Quercetin (25)	IC_{50} = 61.86 ± 2.40 μM		NM	NM	(Alhassan et al. 2019)
	NM		IC_{50} = 10.6 μM		Acarbose (IC_{50} = 607.9 μM)	0.02	(Adhikari-Devkota et al. 2019)
		Myricetin (24)	IC_{50} = 0.52 ± 0.09 μM		Acarbose (IC_{50} = 5.90 ± 0.98 μM)	0.09	(Xu, Wang, et al. 2018)
		5'-Prenylquercetin (341)	IC_{50}:		Acarbose	5'-Prenylquercetin (339): 97.5	(Fan et al. 2019)
		6-Prenylquercetin (420)	5'-Prenylquercetin (341): 3.9 μg/mL 6-Prenylquercetin (420): 3.7 μg/mL		IC_{50} = 0.04 μg/mL	6-Prenylquercetin (416): 92.5	
	31.25–750 μM	Quercetin (25)	Ki = 120 μM	Competitive	NM	NM	(Lim et al. 2019)
	0.2–1 mg/mL	Hecpatrin (446)	IC_{50} = 0.44 mg/mL	Competitive			(Ren, Li, and Liu 2019)
	0–280 μM		IC_{50} = 1.04 μM	Competitive	Acarbose IC_{50} = 700 μM	0.001	(Cedeño et al. 2019)
	NM	Myricetin (24)	IC_{50} = 11.63 ± 0.36 μM	NT	Acarbose IC_{50} = 0.59 ± 0.14 μM	19.71	(Jia et al. 2019)
Flavones		Buddleoside (43)	IC_{50} = 2.09 μg/mL		NM	NM	(He et al. 2019)
			IC_{50} = 362.5 ± 35.1 μM		Acarbose (IC_{50} = 1907 ± 156 μM)	0.19	(Luyen et al. 2013)
		Geraldone (44)	% Inhibition:		Acarbose	0.47	(Ahmed et al. 2014)
		Luteolin (1)	Geraldone (44) – 93.91 ± 1.21 Luteolin (1) – 92.59 ± 1.36		(IC_{50} = 43.77 ± 1.67%)		
		$O^{[N^1,N^3]}$-Dihexyl diosmetin (122)	IC_{50} = 2.406 ± 0.101 μmol/L		Acarbose (IC_{50} = 563.601 ± 40.492 μmol/L 1-Deoxynojirimycin (IC_{50} = 226.912 ± 12.573 μmol/L)	Acarbose 0.004 1-Deoxynojirimycin 0.01	(Cheng et al. 2014)
		Flavonoid 144	IC_{50} = 2.333 ± 0.123 μmol/L		Acarbose (IC_{50} = 563.601 ± 40.492 μmol/L) 1-Deoxynojirimycin (IC_{50} = 226.912 ± 12.573 μmol/L)	Acarbose 0.0002 1-Deoxynojirimycin 0.0005	(Wang, Cheng, et al. 2014)
	(5–50 μM)	Luteolin 7-O-glucuronide (46)	IC_{50} = 14.7 ± 2.1 μM		Acarbose (IC_{50} = 16.1 ± 0.8 μM)	0.91	(Asghari et al. 2015)
	(0.12–100 μg/mL)	Isovitexin 2''-(E)-p-coumarate (161)	IC_{50} = 43 ± 1.4 μM		Acarbose (IC_{50} = 0.033 ± 0.006 μM)	130.30	(Chang, Ho, and Lee 2015)
	NM	Apigenin 6-C-α-L-rhamnosyl-(1 → 2)-6''-O-acetyl)-β-D-glucoside (171)	IC_{50} = 19 ± 0.01 μM		Acarbose (IC_{50} = 15 ± 0.01 μM)	1.27	(Costa et al. 2015)

	Quercetin-3-O-(6′′-benzoyl)-β-galactoside (174)	IC_{50}: Yeast enzyme: 30 ± 6 μM Mammalian enzyme: 437 ± 30 μM	Mixed	Acarbose IC_{50}: Yeast enzyme: 500 ± 230 μM Mammalian enzyme: 100 ± 3 μM	Yeast enzyme: 0.06 Mammalian enzyme: 4.37	(Flores-Bocanegra et al. 2015)		
	Flavonoid 93 Licoflavone B (180)	IC_{50} = < 0.1 μM	NT	Acarbose (IC_{50} = 5.42 μM)	< 0.01	(Guo et al. 2015)		
	Flavonoid 187	IC_{50} = 15.4 ± 0.22 μM		Acarbose (IC_{50} = 860.23 ± 6.10 μM)	0.02	(Imran et al. 2015)		
	Hirtacoumaroflavonoside (220)	IC_{50} = 0.022 mM	Noncompetitive	Acarbose (IC_{50} = 0.092 mM)	0.24	(Shellya et al. 2015)		
	Mortatarin D (233)	IC_{50} = 5.0 ± 0.3 μM	NT	Genistein (IC_{50} = 17.8 ± 1.1 μM)	0.28	(Zhang et al. 2015)		
	Flavonoid 252	IC_{50} = 1.26 ± 0.01 μM		Acarbose (IC_{50} = 38.25 ± 0.12 μM)	0.03	(Imran et al. 2016)		
	Luteolin (1)	IC_{50} = 2.0 ± 1.8 μM		Acarbose (IC_{50} = > 250 μM)	< 0.008	(Zeng, Chen, et al. 2016)		
	Isoquercetin (38)	IC_{50} = 22.38 ± 1.73 μM		Acarbose (IC_{50} = 168.95 ± 12.27 μM)	0.13	(Zhang et al. 2016)		
0.062–1 mM	Pectolinarigenin (274)	IC_{50} = 0.23 mM		Acarbose (IC_{50} = 0.26 mM)	0.88	(Amin et al. 2017)		
NM	Quercetin 3-O-β-D-glucuronide methyl ester (291)	Sucrase inhibition: 30.9 ± 2.2% $^{100\ \mu M}$ Maltase inhibition: 75.3 ± 0.5% $^{100\ \mu M}$	Noncompetitive	Acarbose (Sucrase inhibition: 56.1 ± 0.6% $^{100\ \mu M}$ Maltase inhibition: 62.5 ± 0.5% $^{100\ \mu M}$)	Sucrase: 1.81 Maltase: 0.83	(Hmidene et al. 2017)		
1–1000 μM	Afzelin (308)	IC_{50} = 31.7 ± 1.6 μM	NT	Acarbose (IC_{50} = 172 ± 17 μM)	0.18	(Lee, Kim, and Whang 2017)		
NM	Baicalein (23)	IC_{50}: Maltase: 74.1 ± 5.6 μM Sucrase: 14.6 ± 2.7 μM	Noncompetitive	Acarbose IC_{50}: Maltase: 0.4 ± 0.1 μM Sucrase: 1.2 ± 0.3 μM	Maltase: 185.25 Sucrase: 12.17	(Zhang et al. 2017)		
	Amelliaone A (370)	IC_{50} = 10.2 ± 0.04 μM	NT	Acarbose (IC_{50} = 11.8 ± 0.08 μM)	0.86	(Zhou et al. 2017)		
	Afzelin (308)	IC_{50} = 5.48 ± 1.05 μM		Acarbose (IC_{50} = 385.2 ± 18.6 μM)	0.01	(Li, Li, et al. 2018)		
	Apigenin (22)	IC_{50} = 231.13 ± 5.35 μM		Acarbose (IC_{50} = 996.02 ± 21.34 μM)	0.23	(Li, Yao, et al. 2018)		
	Afzelin (308)	IC_{50} = 29.92 ± 1.07 μM	Competitive	Acarbose (IC_{50} = 57.49 ± 0.25 μM)	0.52	(Renda et al. 2018)		
	Quercetin 3-O-β-(3′′-O-galloyl)-β-galactoside (392)	IC_{50} = 0.97 ± 0.02 μM	Noncompetitive	Acarbose (IC_{50} = 50.58 ± 0.25 μM)	0.02	(Şöhretoğlu et al. 2018)		
	4′-O-Methyl-2′′,4′′-di-(Z)-P-coumaroylafzelin (435)	IC_{50} = 5.9 ± 0.01 μM	NT	Acarbose (IC_{50} = 266.1 ± 0.01 μM)	0.02	(Li, Kongstad, and Staerk 2019)		
0–280 μM	Rutin (5) Galadendrin (447)	IC_{50}: Rutin (5): 1.08 μM Galadendrin (447): 1.02 μM	Noncompetitive	Acarbose (IC_{50} = 700 μM)	Rutin (5): 0.002 Galadendrin (447): 0.001	(Cedeño et al. 2019)		
NM	Hippophin M (465)	IC_{50} = 8.30 μM	NT	Acarbose (IC_{50} = 1727.07 μM)	0.005	(Li, Wang, et al. 2019)		
NM	Parvisoflavone B (133)	IC_{50} = 12.19 ± 0.14 μM	NT	Acarbose (IC_{50} = 7.96 ± 1.68 μM)	1.53	(Dendup et al. 2014)		
	Eurycarpin A (175) Luteone (176)	IC_{50} = < 0.1 μM		Acarbose (IC_{50} = 5.42 μM)	< 0.02	(Guo et al. 2015)		
0.3–300 μM	3′-(3-Methylbut-2-en-1-yl) Biochanin A (266)	IC_{50} = 22.1 ± 7.6 μM		Acarbose (IC_{50} = 347.1 ± 68.6 μM)	0.06	(Shi et al. 2016)		
NM	Biochanin A (276)	IC_{50} = 12.35 ± 0.36 μM		Acarbose IC_{50} = 6.54 ± 0.04 μM	1.89	(Boonsombat et al. 2017)		
0.5–100 μg/mL	Genistein (19)	IC_{50} = 1.47 ± 0.11 μg/mL	Uncompetitive	Acarbose (IC_{50} = 31.92 ± 0.17 μM)	0.05	(Şöhretoğlu et al. 2017)		
	Daidzein (20)	IC_{50} = 23.01 ± 1.05 μM	Noncompetitive	Acarbose (IC_{50} = 1998.79 ± 26.22 μM)	86.87	(Wang et al. 2017)		
	Retamasin H (428)	Ki = 12.06 ± 0.57 μM)	Noncompetitive	Acarbose	2.56	(Ghani et al. 2019)		
	Retamasin H (428)	% Inhibition = 96.3 ± 0.2 $^{50\ \mu M}$	NT	Acarbose (% Inhibition = 98.7 ± 0.9 $^{50\ \mu M}$)	1.02	(Nur et al. 2019)		
	Genistein (19)	IC_{50} = 500 μM		Acarbose (IC_{50} = 320.1 μM)	1.56	(Zhao, Liu, and Chen 2019)		

(continued)

Table 86. Continued.

Class	Tested concentrations	Most active flavonoid	Inhibitory activity	Type of inhibition	Positive control	Relative coefficient to positive control	Reference
Flavanones	NM	Glabrol (182)	$IC_{50} = < 0.1$ μM	NT	Acarbose ($IC_{50} = 5.42$ μM)	< 0.02	(Guo et al. 2015)
		(2S)-7-Prenyloxyeriodictyol (54)	$IC_{50} = 28.1 \pm 2.6$ μM		Acarbose ($IC_{50} = 402.7 \pm 15.5$ μM)	0.07	(Milella et al. 2016)
		Didymin (59)	$IC_{50} = 4.20 \pm 0.6$ μM		Acarbose ($IC_{50} = 54.99 \pm 1.3$ μM)	0.08	(Tundis et al. 2016)
		Eriodictyol (41)	$IC_{50} = 1.4 \pm 3.4$ μM		Acarbose ($IC_{50} = > 250$ μM)	< 0.006	(Zeng, Chen, et al. 2016)
		Isoradiorutinol (295)	$IC_{50} = 11.2 \pm 0.7$ μM		Acarbose ($IC_{50} = 310.2 \pm 3.6$ μM)	0.04	(Jeong and Kim 2017)
		Kushenol B (299)	$IC_{50} = 11.1 \pm 0.3$ μM	Uncompetitive	Acarbose ($IC_{50} = 119.2 \pm 3.7$ μM)	0.09	(Kim, Cho, et al. 2017)
		Naringenin 7-*O*-β-D-glucoside (319)	$IC_{50} = 1.44 \pm 0.01$ μM	NT	Acarbose ($IC_{50} = 2.68 \pm 0.07$ μM)	0.54	(Qin et al. 2017)
		Flavonoid 339	$IC_{50} = 2.2 \pm 0.2$ μM	Noncompetitive	Voglibose ($IC_{50} = 24.5 \pm 1.2$ μM)	0.09	(Song et al. 2017)
		8-Geranylnaringenin (72)	$IC_{50} = 3.77$ μM	NT	Acarbose ($IC_{50} = 51.30$ μM)	13.61	(Sun et al. 2017)
		Flavonoid 369	$IC_{50} = 4.1$ μM	Noncompetitive	Naringenin (77 μM)	18.78	(Zhen et al. 2017)
		Nymphaeol A (385)	$IC_{50} = 3.77$ μM	NT	Quercetin ($IC_{50} = 6.65$ μM)	1.76	(Shahinozzaman et al. 2018)
		Dichamanetin (443)	$IC_{50} = 0.2$ μM		Acarbose ($IC_{50} = 170.7$ μM)	853.50	(Meesakul et al. 2019)
		Eriocitrin (376)	Kb = $(6.01 \pm 0.22) \times 10^4$ L mol^{-1} at 298 K		–	–	(Liu et al. 2020)
		Bavachinone (451)	$IC_{50} = 28.0$ μM		Acarbose $IC_{50} = 214.8$ μM	0.13	(Zhu et al. 2019)
		Cyrtominetin (486)	$IC_{50} = 12.4 \pm 2.66$ μM		Acarbose 172.3 ± 14.7 μM	0.07	(Li, Zhu, et al. 2019)
Flavans	NM	Gambiriin D (377); Luteoliflavan 7-*O*-glucoside (378)	Gambiriin D (377): $IC_{50} = 36.8 \pm 2.3$ μM Luteoliflavan 7-*O*-glucoside (378): $IC_{50} = 40.4 \pm 4.6$ μM	NT	Acarbose ($IC_{50} = 620.2 \pm 7.2$ μM)	16.85 15.35	(Ha et al. 2018)
Anthocyanins	0.1–10,000 μM	Pelargonidin 3-*O*-rutinoside (403)	$IC_{50} = 1.69$ μM	Mixed	Acarbose $IC_{50} = 356.26$ μM	210.80	(Xu, Xie, et al. 2018)

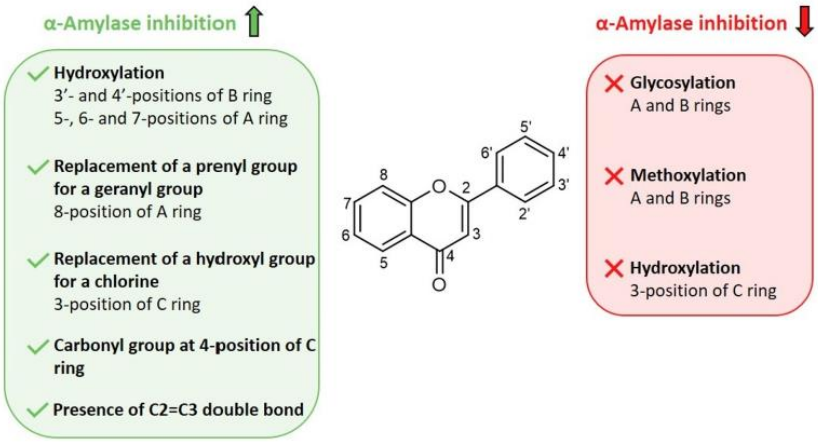


Figure 5. Representation of the possible substitutions that affect the inhibitory activity of flavonoids on α-amylase.

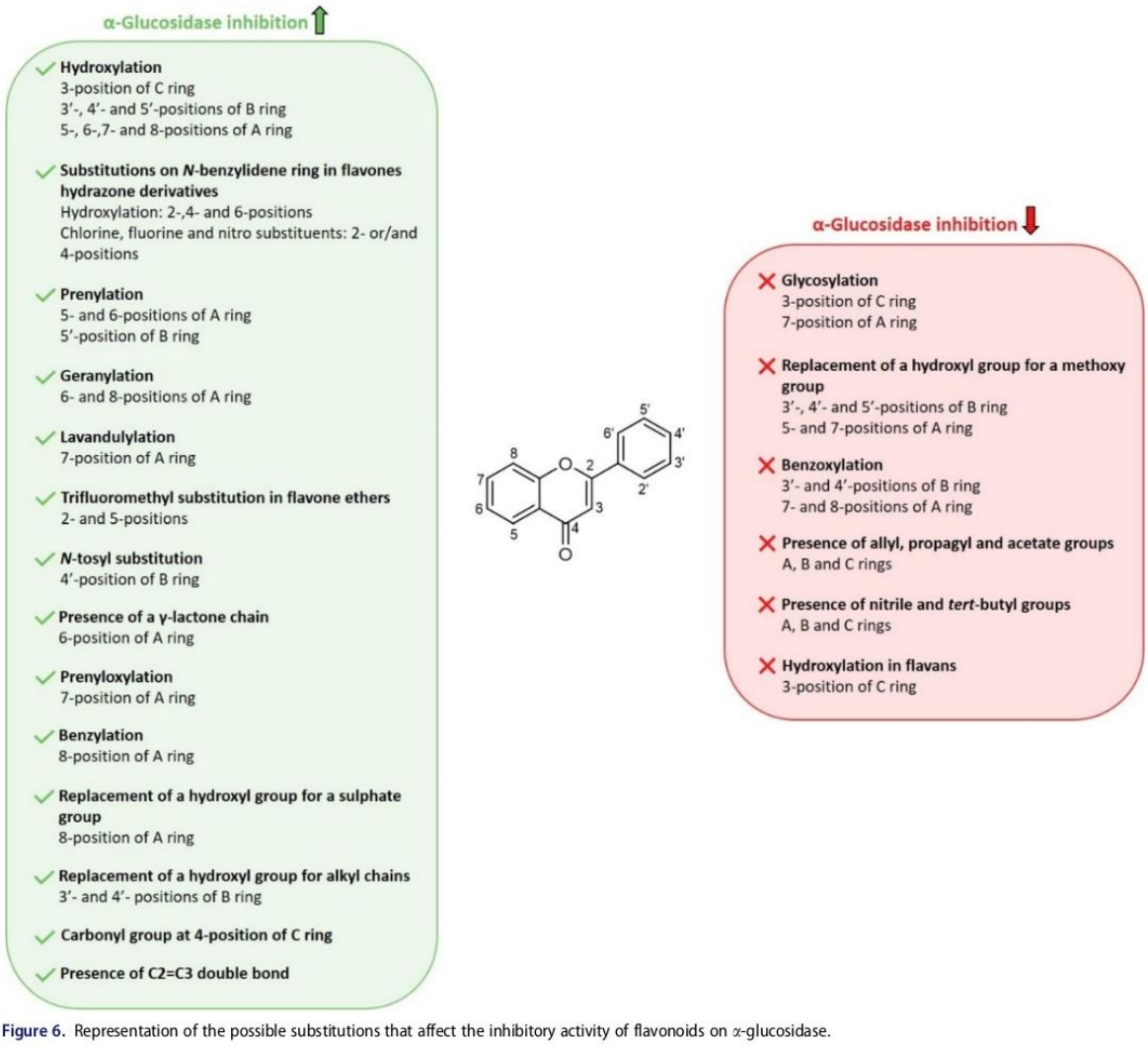


Figure 6. Representation of the possible substitutions that affect the inhibitory activity of flavonoids on α-glucosidase.

he reduction in the inhibitory activity of flavonoids on α-glucosidase is more pronounced when -OH groups are substituted by -OCH_3 groups at 3′- ,4′- and 5′- positions of B ring, and at 5- and 7- positions of A ring. Besides the presence of -OCH_3 groups, the presence of allyl, propagyl, acetate and benzoxy groups reduce the α-glucosidase inhibition. The *para*-substitution with nitrile and tert-butyl groups also seems not to be favorable for the inhibition of the enzyme under study. Interestingly, it was suggested that the presence of a -OH group at 3-position of catechins is also responsible for a reduction in the inhibitory activity. Finally, the methylation of flavonoids at 6- and/or at 8-positions of A ring seems to improve this specific biological activity.

Conclusion

The present review allowed a deep analysis regarding the inhibitory effect of flavonoids on α-amylase and α-glucosidase, covering a total of about 500 natural or synthetic compounds. The variability of the experimental conditions, such as the source and concentration of the enzyme, the source and concentration of the substrates, the times of incubation and the temperature, make it difficult to compare all the results. Despite that difficulties, it was established, whenever possible, a SAR and significant conclusions were obtained in what regards the important features in the chemical structure of flavonoids, that favor their ability to modulate the inhibition of α-amylase and α-glucosidase.

Based on the current review, it is possible to verify that flavonoids are molecules with promising antidiabetic activity through the modulation of α-amylase and α-glucosidase. The main purpose of this review is to rise new perspectives on the treatment of T2D, through the design, synthesis and development of novel molecules based on the flavonoid scaffold with improved and more potent inhibitory activity on two important T2D targets for the management of PPHG, α-amylase and α-glucosidase.

Acknowledgements

The work was supported by UIDB/50006/2020 with funding from Fundação para a Ciência e Tecnologia (FCT)/Ministério da Ciência, Tecnologia e Ensino Superior (MCTES) through national funds, and "Programa Operacional Competitividade e Internacionalização" (COMPETE) (POCI-01-0145-FEDER-029241). CP acknowledges FCT the financial support for the PhD grant (SFRH/BD/116005/2016), in the ambit of "QREN – POPH – Tipologia 4.1 – Formação Avançada," co-sponsored by Fundo Social Europeu (FSE) and by national funds of MCTES. DR and MF acknowledge the financial support from the European Union (FEDER funds through COMPETE) (POCI-01-0145-FEDER-029253 and POCI-01-0145-FEDER-029248, respectively).

Declaration of interest statement

No potential conflict of interest was reported by the authors.

Abbreviations

ADA	American Diabetes Association
AGEs	advanced glycation end-products
DPP-4	dipeptidyl peptidase-4
GD	gestational diabetes
GH	glycoside hydrolases
GIP	glucose-dependent insulinotropic polypeptide
GLP-1	glucagon-like peptide-1
GLUT-2	glucose transporter-2
GWAs	genome-wide association studies
HPAEC	high-performance anion-exchange chromatography
IAPP	hypersecretion of islet amyloid polypeptide
IDF	International Diabetes Federation
Ki	constant of inhibition
MGAM	maltase-glucoamylase
NO	nitric oxide
PKC	protein kinase C
PPHG	postprandial hyperglycemia
RNS	reactive nitrogen species
ROS	reactive oxygen species
SAR	structure-activity relationship
SGLT1	sodium/glucose transporter-1
SGLT2	sodium/glucose transporter-2
SI	sucrase-isomaltase
SNPs	single-nucleotide polymorphisms
T1D	type 1 diabetes
T2D	type 2 diabetes

ORCID

Carina Proença http://orcid.org/0000-0003-0859-6526
Daniela Ribeiro http://orcid.org/0000-0001-9733-7934
Marisa Freitas http://orcid.org/0000-0001-9114-9967
Eduarda Fernandes http://orcid.org/0000-0001-6424-0976

References

Aderogba, M. A., A. R. Ndhlala, K. R. Rengasamy, and J. Van Staden. 2013. Antimicrobial and selected in vitro enzyme inhibitory effects of leaf extracts, flavonols and indole alkaloids isolated from *Croton menyharthii*. *Molecules* 18 (10):12633–44. doi: 10.3390/molecules181012633.

Adhikari-Devkota, A., S. M. I. Elbashir, T. Watanabe, and H. P. Devkota. 2019. Chemical constituents from the flowers of *Satsuma mandarin* and their free radical scavenging and α-glucosidase inhibitory activities. *Natural Product Research* 33 (11):1670–4. doi: 10.1080/14786419.2018.1425856.

Ahmed, D., V. Kumar, M. Sharma, and A. Verma. 2014. Target guided isolation, in-vitro antidiabetic, antioxidant activity and molecular docking studies of some flavonoids from *Albizzia Lebbeck Benth.* bark. *BMC Complementary and Alternative Medicine* 14 (155):155. doi: 10.1186/1472-6882-14-155.

Ahrén, B. 2019. DPP-4 inhibition and the path to clinical proof. *Frontiers in Endocrinology* 10 (376):376. doi: 10.3389/fendo.2019.00376.

Alhassan, A. M., Q. U. Ahmed, J. Latip, and S. A. A. Shah. 2019. A new sulphated flavone and other phytoconstituents from the leaves of *Tetracera indica* Merr. and their alpha-glucosidase inhibitory activity. *Natural Product Research* 33 (1):1–8. doi: 10.1080/14786419.2018.1437427.

Alkhalidy, H., Y. Wang, and D. Liu. 2018. Dietary flavonoids in the prevention of T2D: An overview. *Nutrients* 10 (4):438. doi: 10.3390/nu10040438.

American Diabetes Association. 2014. Diagnosis and classification of diabetes mellitus. *Diabetes Care* 37 (Suppl 1):S81–S90. doi: 10.2337/dc14-S081.

American Diabetes Association. 2018. 2. Classification and diagnosis of diabetes: Standards of medical care in diabetes – 2018. *Diabetes Care* 41 (Supplement 1):S13–S27. doi: 10.2337/dc18-S002.

Amin, A., E. Tuenter, K. Foubert, J. Iqbal, P. Cos, L. Maes, V. Exarchou, S. Apers, and L. Pieters. 2017. *In vitro* and *in silico* antidiabetic and antimicrobial evaluation of constituents from *Kickxia ramosissima* (*Nanorrhinum ramosissimum*). *Frontiers in Pharmacology* 8 (232):232. doi: 10.3389/fphar.2017.00232.

Angelopoulos, T. P., and J. Doupis. 2014. Sodium-glucose linked transporter 2 (SGLT2) inhibitors-fighting diabetes from a new perspective. *Advances in Therapy* 31 (6):579–91. doi: 10.1007/s12325-014-0127-7.

Asghari, B., P. Salehi, A. Sonboli, and S. Nejad Ebrahimi. 2015. Flavonoids from *Salvia chloroleuca* with α-amylase and α-glucosidase inhibitory effect. *Iranian Journal of Pharmaceutical Research* 14 (2): 609–15.

Barnett, A. H., and J. Grice. 2011. *New mechanisms in glucose control*. 1st ed. Hoboken, NJ: Blackwell Publishing, Ltd.

Bisswanger, H. 2014. Enzyme assays. *Perspectives in Science* 1 (1-6): 41–55. doi: 10.1016/j.pisc.2014.02.005.

Bonora, E., and M. Cigolini. 2016. DPP-4 inhibitors and cardiovascular disease in type 2 diabetes mellitus. Expectations, observations and perspectives. *Nutrition, Metabolism, and Cardiovascular Diseases* 26 (4):273–84. doi: 10.1016/j.numecd.2016.03.002.

Boonsombat, J., V. Prachyawarakorn, A. Pansanit, C. Mahidol, S. Ruchirawat, and S. Thongnest. 2017. Superbanone, a new 2-aryl-3-benzofuranone and other bioactive constituents from the tube roots of *Butea superba*. *Chemistry & Biodiversity* 14:1–9. doi: 10.1002/cbdv.201700044.

Brás, N. F., D. Santos-Martins, P. A. Fernandes, and M. J. Ramos. 2018. Mechanistic pathway on human α-glucosidase maltase-glucoamylase unveiled by QM/MM calculations. *The Journal of Physical Chemistry. B* 122 (14):3889–99. doi: 10.1021/acs.jpcb.8b01321.

Brayer, G. D., G. Sidhu, R. Maurus, E. H. Rydberg, C. Braun, Y. Wang, N. T. Nguyen, C. M. Overall, and S. G. Withers. 2000. Subsite mapping of the human pancreatic alpha-amylase active site through structural, kinetic, and mutagenesis techniques . *Biochemistry* 39 (16):4778–91. doi: 10.1021/bi9921182.

Butterworth, P. J., F. J. Warren, and P. R. Ellis. 2011. Human α-amylase and starch digestion: An interesting marriage. *Starch – Stärke* 63 (7):395–405. doi: 10.1002/star.201000150.

Cassidy, A., and A.-M. Minihane. 2017. The role of metabolism (and the microbiome) in defining the clinical efficacy of dietary flavonoids. *The American Journal of Clinical Nutrition* 105 (1):10–22. doi: 10.3945/ajcn.116.136051.

Cedeño, H., S. Espinosa, J. M. Andrade, L. Cartuche, and O. Malagon. 2019. Novel flavonoid glycosides of quercetin from leaves and flowers of *Gaiadendron punctatum* G.Don. (Violeta de Campo), used by the Saraguro Community in Southern Ecuador, inhibit alpha-glucosidase enzyme. *Molecules* 24 (4267):1–17. doi: 10.3390/molecules24234267.

Chang, C. C., S. L. Ho, and S. S. Lee. 2015. Acylated glucosylflavones as α-glucosidase inhibitors from *Tinospora crispa* leaf. *Bioorganic & Medicinal Chemistry* 23 (13):3388–96. doi: 10.1016/j.bmc.2015.04.053.

Chao, E. C., and R. R. Henry. 2010. SGLT2 inhibition-a novel strategy for diabetes treatment. *Nature Reviews. Drug Discovery* 9 (7):551–9. doi: 10.1038/nrd3180.

Chaudhury, A., C. Duvoor, V. S. Reddy Dendi, S. Kraleti, A. Chada, R. Ravilla, A. Marco, N. S. Shekhawat, M. T. Montales, K. Kuriakose, et al. 2017. Clinical review of antidiabetic drugs: Implications for type 2 diabetes mellitus management. *Frontiers in Endocrinology* 8 (6):6–12. doi: 10.3389/fendo.2017.00006.

Chen, H., K. Ouyang, Y. Jiang, Z. Yang, W. Hu, L. Xiong, N. Wang, X. Liu, and W. Wang. 2017. Constituent analysis of the ethanol extracts of *Chimonanthus nitens* Oliv. leaves and their inhibitory effect on α-glucosidase activity. *International Journal of Biological Macromolecules* 98:829–36. doi: 10.1016/j.ijbiomac.2017.02.044.

Chen, J., Y. Wu, J. Zou, and K. Gao. 2016. α-Glucosidase inhibition and antihyperglycemic activity of flavonoids from *Ampelopsis grossedentata* and the flavonoid derivatives. *Bioorganic & Medicinal Chemistry* 24 (7):1488–94. doi: 10.1016/j.bmc.2016.02.018.

Cheng, N., W. B. Yi, Q. Q. Wang, S. M. Peng, and X. Q. Zou. 2014. Synthesis and α-glucosidase inhibitory activity of chrysin, diosmetin, apigenin, and luteolin derivatives. *Chinese Chemical Letters* 25 (7): 1094–8. doi: 10.1016/j.cclet.2014.05.021.

Chikara, G., P. Kumar Sharma, P. Dwivedi, J. Charan, S. Ambwani, and S. Singh. 2018. A narrative review of potential future antidiabetic drugs: Should we expect more? *Indian Journal of Clinical Biochemistry* 33 (2):121–31. doi: 10.1007/s12291-017-0668-z.

Costa, G. M., P. A. Cardenas, A. C. Gazola, D. M. Aragon, L. Castellanos, F. H. Reginatto, F. A. Ramos, and E. P. Schenkel. 2015. Isolation of C-glycosylflavonoids with α-glucosidase inhibitory activity from *Passiflora bogotensis Benth* by gradient high-speed counter-current chromatography. *Journal of Chromatography. B* 990:104–10. doi: 10.1016/j.jchromb.2015.03.015.

Davies, M. J., D. A. D'Alessio, J. Fradkin, W. N. Kernan, C. Mathieu, G. Mingrone, P. Rossing, A. Tsapas, D. J. Wexler, and J. B. Buse. 2018. Management of hyperglycemia in type 2 diabetes, 2018. A consensus report by the American Diabetes Association (ADA) and the European Association for the Study of Diabetes (EASD). *Diabetes Care* 41 (12):2669–701. doi: 10.2337/dci18-0033.

DeFronzo, R. A., E. Ferrannini, L. Groop, R. R. Henry, W. H. Herman, J. J. Holst, F. B. Hu, C. R. Kahn, I. Raz, G. I. Shulman, et al. 2015. Type 2 diabetes mellitus. *Nature Reviews. Disease Primers* 1 (15019): 15019. doi: 10.1038/nrdp.2015.19.

Dendup, T., V. Prachyawarakorn, A. Pansanit, C. Mahidol, S. Ruchirawat, and P. Kittakoop. 2014. α-Glucosidase inhibitory activities of isoflavanones, isoflavones, and pterocarpans from *Mucuna pruriens*. *Planta Medica* 80 (7):604–8. doi: 10.1055/s-0034-1368427.

Derosa, G., and P. Maffioli. 2012. α-Glucosidase inhibitors and their use in clinical practice. *Archives of Medical Science* 8 (5):899–906. doi: 10.5114/aoms.2012.31621.

Desseaux, V., P. Stocker, P. Brouant, and E. H. Ajandouz. 2018. The mechanisms of alpha-amylase inhibition by flavan-3-ols and the possible impacts of drinking green tea on starch digestion. *Journal of Food Science* 83 (11):2858–65. doi: 10.1111/1750-3841.14353.

Dhital, S., F. J. Warren, P. J. Butterworth, P. R. Ellis, and M. J. Gidley. 2017. Mechanisms of starch digestion by α-amylase-structural basis for kinetic properties. *Critical Reviews in Food Science and Nutrition* 57 (5):875–92. doi: 10.1080/10408398.2014.922043.

Donath, M. Y. 2016. Multiple benefits of targeting inflammation in the treatment of type 2 diabetes. *Diabetologia* 59 (4):679–82. doi: 10.1007/s00125-016-3873-z.

Donath, M. Y., and S. E. Shoelson. 2011. Type 2 diabetes as an inflammatory disease. *Nature Reviews. Immunology* 11 (2):98–107. doi: 10.1038/nri2925.

Egert, S., and G. Rimbach. 2011. Which sources of flavonoids: Complex diets or dietary supplements? *Advances in Nutrition* 2 (1): 8–14. doi: 10.3945/an.110.000026.

Eizirik, D. L., L. Pasquali, and M. Cnop. 2020. Pancreatic *β*-cells in type 1 and type 2 diabetes mellitus: Different pathways to failure. *Nature Reviews. Endocrinology* 16 (7):349–62. doi: 10.1038/s41574-020-0355-7.

Elferink, H., J. P. J. Bruekers, G. H. Veeneman, and T. J. Boltje. 2020. A comprehensive overview of substrate specificity of glycoside hydrolases and transporters in the small intestine: "A gut feeling". *Cellular and Molecular Life Sciences* 77 (23):4799–826. doi: 10.1007/s00018-020-03564-1.

Etxeberria, U., A. L. de la Garza, J. Campion, J. A. Martinez, and F. I. Milagro. 2012. Antidiabetic effects of natural plant extracts via inhibition of carbohydrate hydrolysis enzymes with emphasis on pancreatic alpha amylase. *Expert Opinion on Therapeutic Targets* 16 (3):269–97. doi: 10.1517/14728222.2012.664134.

Fan, Y.-H., R. Ye, H.-Y. Xu, X.-H. Feng, and C.-M. Ma. 2019. Structures and in vitro antihepatic fibrosis activities of prenylated dihydrostilbenes and flavonoids from *Glycyrrhiza uralensis* leaves. *Journal of Food Science* 84 (5):1224–30. doi: 10.1111/1750-3841.14592.

Ferreyra, M. L. F., S. Rius, and P. Casati. 2012. Flavonoids: Biosynthesis, biological functions, and biotechnological applications. *Frontiers in Plant Science* 3 (222):222. doi: 10.3389/fpls.2012.00222.

Flores-Bocanegra, L., A. Perez-Vasquez, M. Torres-Piedra, R. Bye, E. Linares, and R. Mata. 2015. α-Glucosidase inhibitors from *Vauquelinia corymbosa*. *Molecules* 20 (8):15330–42. doi: 10.3390/molecules200815330.

Forbes, J. M., and M. E. Cooper. 2013. Mechanisms of diabetic complications. *Physiological Reviews* 93 (1):137–88. doi: 10.1152/physrev.00045.2011.

Ghani, U., M. Nur-e-Alam, M. Yousaf, Z. Ul-Haq, O. M. Noman, and A. J. Al-Rehaily. 2019. Natural flavonoid α-glucosidase inhibitors from *Retama raetam*: Enzyme inhibition and molecular docking reveal important interactions with the enzyme active site. *Bioorganic Chemistry* 87:736–42. doi: 10.1016/j.bioorg.2019.03.079.

Gonzales, G. B., G. Smagghe, C. Grootaert, M. Zotti, K. Raes, and J. Van Camp. 2015. Flavonoid interactions during digestion, absorption, distribution and metabolism: A sequential structure-activity/property relationship-based approach in the study of bioavailability and bioactivity. *Drug Metabolism Reviews* 47 (2):175–90. doi: 10.3109/03602532.2014.1003649.

Guo, Z., X. Niu, T. Xiao, J. Lu, W. Li, and Y. Zhao. 2015. Chemical profile and inhibition of α-glycosidase and protein tyrosine phosphatase 1B (PTP1B) activities by flavonoids from licorice (*Glycyrrhiza uralensis Fisch*). *Journal of Functional Foods* 14:324–36. doi: 10.1016/j.jff.2014.12.003.

Ha, T. J., S. Bo Song, J. Ko, C.-H. Park, J.-M. Ko, M.-E. Choe, D.-Y. Kwak, and J. H. Lee. 2018. Isolation and identification of α-glucosidase inhibitory constituents from the seeds of *Vigna nakashimae*: Enzyme kinetic study with active phytochemical. *Food Chemistry* 266:483–9. doi: 10.1016/j.foodchem.2018.06.039.

He, C., X. Liu, Z. Jiang, S. Geng, H. Ma, and B. Liu. 2019. Interaction mechanism of flavonoids and alpha-glucosidase: Experimental and molecular modelling studies. *Foods* 8 (355):1–9. doi: 10.3390/foods8090355.

Heim, K. E., A. R. Tagliaferro, and D. J. Bobilya. 2002. Flavonoid antioxidants: Chemistry, metabolism and structure-activity relationships. *The Journal of Nutritional Biochemistry* 13 (10):572–84. doi: 10.1016/s0955-2863(02)00208-5.

Hernández-Rodríguez, P., L. P. Baquero, and H. R. Larrota. 2019. Chapter 14 – Flavonoids: Potential therapeutic agents by their antioxidant capacity. In *Bioactive compounds*, ed. M. R. S. Campos, 265–88. Cambridge, United Kingdom: Woodhead Publishing.

Hmidene, A. B., A. Smaoui, C. Abdelly, H. Isoda, and H. Shigemori. 2017. Effect of *O*-methylated and glucuronosylated flavonoids from *Tamarix gallica* on α-glucosidase inhibitory activity: Structure-activity relationship and synergistic potential. *Bioscience, Biotechnology, and Biochemistry* 81 (3):445–8. doi: 10.1080/09168451.2016.1254538.

Hollman, P. C. H. 2004. Absorption, bioavailability, and metabolism of flavonoids. *Pharmaceutical Biology* 42 (sup1):74–83. doi: 10.3109/13880200490893492.

Hostetler, G. L., R. A. Ralston, and S. J. Schwartz. 2017. Flavones: Food sources, bioavailability, metabolism, and bioactivity. *Advances in Nutrition* 8 (3):423–35. doi: 10.3945/an.116.012948.

Ibrahim, S., A. Al-Ahdal, A. Khedr, and G. Mohamed. 2017. Antioxidant α-amylase inhibitors flavonoids from *Iris germanica* rhizomes. *Revista Brasileira de Farmacognosia* 27 (2):170–4. doi: 10.1016/j.bjp.2016.10.001.

Ibrahim, S. R. M., G. A. Mohamed, M. M. M. Abdel-Latif, S. M. El-Messery, N. M. Al Musayeib, and I. A. Shehata. 2015. Minutaside A, new α-amylase inhibitor flavonol glucoside from *Tagetes minuta*: Antidiabetic, antioxidant, and molecular modeling studies. *Starch – Stärke* 67 (11-12):976–84. doi: 10.1002/star.201500068.

Imran, S., M. Taha, N. H. Ismail, S. M. Kashif, F. Rahim, W. Jamil, M. Hariono, M. Yusuf, and H. Wahab. 2015. Synthesis of novel flavone hydrazones: *In-vitro* evaluation of α-glucosidase inhibition, QSAR analysis and docking studies. *European Journal of Medicinal Chemistry* 105:156–70. doi: 10.1016/j.ejmech.2015.10.017.

Imran, S., M. Taha, N. H. Ismail, S. M. Kashif, F. Rahim, W. Jamil, H. Wahab, and K. M. Khan. 2016. Synthesis, in vitro and docking studies of new flavone ethers as α-glucosidase inhibitors. *Chemical Biology & Drug Design* 87 (3):361–73. doi: 10.1111/cbdd.12666.

International Diabetes Federation. 2019. IDF diabetes atlas. https://www.diabetesatlas.org/upload/resources/2019/IDF_Atlas_9th_Edition_2019.pdf.

Jeong, G. H., and T. H. Kim. 2017. Hydroxymethylation of rutin induced by radiolysis as novel α-glucosidase inhibitors. *Chemical & Pharmaceutical Bulletin* 65 (7):678–82. doi: 10.1248/cpb.c17-00190.

Jia, Y., Y. Ma, G. Cheng, Y. Zhang, and S. Cai. 2019. Comparative study of dietary flavonoids with different structures as α-glucosidase inhibitors and insulin sensitizers. *Journal of Agricultural and Food Chemistry* 67 (37):10521–33. doi: 10.1021/acs.jafc.9b04943.

Joshi, S. R., E. Standl, N. Tong, P. Shah, S. Kalra, and R. Rathod. 2015. Therapeutic potential of α-glucosidase inhibitors in type 2 diabetes mellitus: An evidence-based review. *Expert Opinion on Pharmacotherapy* 16 (13):1959–81. doi: 10.1517/14656566.2015.1070827.

Kaeswurm, J. A. H., B. Claasen, M. P. Fischer, and M. Buchweitz. 2019. Interaction of structurally diverse phenolic compounds with porcine pancreatic α-amylase. *Journal of Agricultural and Food Chemistry* 67 (40):11108–18. doi: 10.1021/acs.jafc.9b04798.

Kahn, S. E., M. E. Cooper, and S. Del Prato. 2014. Pathophysiology and treatment of type 2 diabetes: Perspectives on the past, present, and future. *Lancet* 383 (9922):1068–83. doi: 10.1016/S0140-6736(13)62154-6.

Kharroubi, A. T., and H. M. Darwish. 2015. Diabetes mellitus: The epidemic of the century. *World Journal of Diabetes* 6 (6):850–67. doi: 10.4239/wjd.v6.i6.850.

Kim, D. H., H. A. Jung, H. S. Sohn, J. W. Kim, and J. S. Choi. 2017. Potential of icariin metabolites from *Epimedium koreanum Nakai* as antidiabetic therapeutic agents. *Molecules* 22 (6):986. doi: 10.3390/molecules22060986.

Kim, J. H., C. W. Cho, H. Y. Kim, K. T. Kim, G.-S. Choi, H.-H. Kim, I. S. Cho, S. J. Kwon, S.-K. Choi, J.-Y. Yoon, et al. 2017. α-Glucosidase inhibition by prenylated and lavandulyl compounds from *Sophora flavescens* roots and in silico analysis. *International Journal of Biological Macromolecules* 102 (2017):960–9. doi: 10.1016/j.ijbiomac.2017.04.092.

Kim, J. S., C. S. Kwon, and K. H. Son. 2000. Inhibition of alpha-glucosidase and amylase by luteolin, a flavonoid. *Bioscience, Biotechnology, and Biochemistry* 64 (11):2458–61. doi: 10.1271/bbb.64.2458.

Kozlowska, A., and D. Szostak-Wegierek. 2014. Flavonoids—food sources and health benefits. *Roczniki Panstwowego Zakladu Higieny* 65 (2):79–85.

Kumar, A., S. K. Bharti, and A. Kumar. 2017. Therapeutic molecules against type 2 diabetes: What we have and what are we expecting? *Pharmacological Reports* 69 (5):959–70. doi: 10.1016/j.pharep.2017.04.003.

Kumar, S., and A. K. Pandey. 2013. Chemistry and biological activities of flavonoids: An overview. *The Scientific World Journal* 2013:1–16. doi: 10.1155/2013/162750.

Lee, H. E., J. A. Kim, and W. K. Whang. 2017. Chemical constituents of *Smilax china* L. stems and their inhibitory activities against glycation, aldose reductase, α-glucosidase, and lipase. *Molecules* 22 (3):451. doi: 10.3390/molecules22030451.

Li, K., S. Li, F. Xu, G. Cao, and X. Gong. 2020. A novel acylated quercetin glycoside and compounds of inhibitory effects on α-glucosidase from *Panax ginseng* flower buds. *Natural Product Research* 34 (18):2559–7. doi: 10.1080/14786419.2018.1543685.

Li, K., F. Yao, Q. Xue, H. Fan, L. Yang, X. Li, L. Sun, and Y. Liu. 2018. Inhibitory effects against α-glucosidase and α-amylase of the flavonoids-rich extract from *Scutellaria baicalensis* shoots and interpretation of structure-activity relationship of its eight flavonoids by a refined assign-score method. *Chemistry Central Journal* 12 (1):82. doi: 10.1186/s13065-018-0445-y.

Li, R., Q. Wang, M. Zhao, P. Yang, X. Hu, and D. Ouyang. 2019. Flavonoid glycosides from seeds of Hippophae rhamnoides subsp. Sinensis with α-glucosidase inhibition activity . *Fitoterapia* 137 (104248):104248. doi: 10.1016/j.fitote.2019.104248.

Li, T., K. T. Kongstad, and D. Staerk. 2019. Identification of α-glucosidase inhibitors in *Machilus litseifolia* by combined use of high-

resolution α-glucosidase inhibition profiling and HPLC-PDA-HRMS-SPE-NMR. *Journal of Natural Products* 82 (2):249–58. doi: 10.1021/acs.jnatprod.8b00609.

Li, X., L. J. Zhu, J. P. Chen, C. Y. Shi, L. T. Niu, X. Zhang, and X. S. Yao. 2019. C-Methylated flavanones from the rhizomes of *Matteuccia intermedia* and their α-glucosidase inhibitory activity . *Fitoterapia* 136 (104147):104147. doi: 10.1016/j.fitote.2019.04.002.

Li, Y., F. Gao, F. Gao, F. Shan, J. Bian, and C. Zhao. 2009. Study on the interaction between 3 flavonoid compounds and α-amylase by fluorescence spectroscopy and enzymatic kinetics. *Journal of Food Science* 74 (3):C199–203. doi: 10.1111/j.1750-3841.2009.01080.x.

Libianto, R., and E. I. Ekinci. 2019. New agents for the treatment of type 2 diabetes. *Critical Care Clinics* 35 (2):315–28. doi: 10.1016/j.ccc.2018.11.007.

Lim, J., X. Zhang, M. G. Ferruzzi, and B. R. Hamaker. 2019. Starch digested product analysis by HPAEC reveals structural specificity of flavonoids in the inhibition of mammalian α-amylase and α-glucosidases. *Food Chemistry* 288:413–21. doi: 10.1016/j.foodchem.2019.02.117.

Liu, D., H. Gao, W. Tang, and S. Nie. 2017. Plant non-starch polysaccharides that inhibit key enzymes linked to type 2 diabetes mellitus. *Annals of the New York Academy of Sciences* 1401 (1):28–36. doi: 10.1111/nyas.13430.

Liu, J. L., Y. C. Kong, J. Y. Miao, X. Y. Mei, S. Y. Wu, Y. C. Yan, and X. Y. Cao. 2020. Spectroscopy and molecular docking analysis reveal structural specificity of flavonoids in the inhibition of α-glucosidase activity. *International Journal of Biological Macromolecules* 152: 981–9. doi: 10.1016/j.ijbiomac.2019.10.184.

Luyen, N. T., L. H. Tram, T. T. H. Hanh, P. T. Binh, N. H. Dang, C. V. Minh, and N. T. Dat. 2013. Inhibitors of α-glucosidase, α-amylase and lipase from *Chrysanthemum morifolium*. *Phytochemistry Letters* 6 (3):322–5. doi: 10.1016/j.phytol.2013.03.015.

Ma, Y. Y., D. G. Zhao, A. Y. Zhou, Y. Zhang, Z. Du, and K. Zhang. 2015. α-Glucosidase inhibition and antihyperglycemic activity of phenolics from the flowers of *Edgeworthia gardneri*. *Journal of Agricultural and Food Chemistry* 63 (37):8162–9. doi: 10.1021/acs.jafc.5b03081.

Martinez-Gonzalez, A. I., A. G. Diaz-Sanchez, L. A. de la Rosa, I. Bustos-Jaimes, and E. Alvarez-Parrilla. 2019. Inhibition of α-amylase by flavonoids: Structure activity relationship (SAR). *Spectrochimica Acta. Part A, Molecular and Biomolecular Spectroscopy* 206:437–47. doi: 10.1016/j.saa.2018.08.057.

Martinez-Gonzalez, A. I., A. G. Diaz-Sanchez, L. A. Rosa, C. L. Vargas-Requena, I. Bustos-Jaimes, and A. E. Alvarez-Parrilla. 2017. Polyphenolic compounds and digestive enzymes: In vitro non-covalent interactions. *Molecules* 22 (4):669. doi: 10.3390/molecules22040669.

Meesakul, P., C. Richardson, S. G. Pyne, and S. Laphookhieo. 2019. α-Glucosidase inhibitory flavonoids and oxepinones from the leaf and twig extracts of *Desmos cochinchinensis*. *Journal of Natural Products* 82 (4):741–7. doi: 10.1021/acs.jnatprod.8b00581.

Menezes, J. C., B. Orlikova, F. Morceau, and M. Diederich. 2016. Natural and synthetic flavonoids: Structure-activity relationship and chemotherapeutic potential for the treatment of leukemia. *Critical Reviews in Food Science and Nutrition* 56 (Suppl 1):S4–s28. doi: 10.1080/10408398.2015.1074532.

Meng, Y., A. Su, S. Yuan, H. Zhao, S. Tan, C. Hu, H. Deng, and Y. Guo. 2016. Evaluation of total flavonoids, myricetin, and quercetin from *Hovenia dulcis* Thunb. as inhibitors of α-amylase and α-glucosidase. *Plant Foods for Human Nutrition* 71 (4):444–9. doi: 10.1007/s11130-016-0581-2.

Mignet, N., J. Seguin, and G. G. Chabot. 2013. Bioavailability of polyphenol liposomes: A challenge ahead. *Pharmaceutics* 5 (3):457–71. doi: 10.3390/pharmaceutics5030457.

Milella, L., S. Milazzo, M. De Leo, M. B. Vera Saltos, I. Faraone, T. Tuccinardi, M. Lapillo, N. D. Tommasi, and A. Braca. 2016. α-Glucosidase and α-amylase inhibitors from *Arcytophyllum thymifolium*. *Journal of Natural Products* 79 (8):2104–12. doi: 10.1021/acs.jnatprod.6b00484.

Mohamed, G. A. 2008. Alliuocide G, a new flavonoid with potent α-amylase inhibitory activity from *Allium cepa L. Arkivoc* 2008 (11): 202–9. doi: 10.3998/ark.5550190.0009.b20.

Nichols, B. L., S. Avery, P. Sen, D. M. Swallow, D. Hahn, and E. Sterchi. 2003. The maltase-glucoamylase gene: Common ancestry to sucrase-isomaltase with complementary starch digestion activities. *Proceedings of the National Academy of Sciences of the United States of America* 100 (3):1432–7. doi: 10.1073/pnas.0237170100.

Nur, E., M. Alam, M. Yousaf, I. Parveen, R. M. Hafizur, U. Ghani, S. Ahmed, A. Hameed, M. D. Threadgill, and A. J. Al-Rehaily. 2019. New flavonoids from the Saudi Arabian plant *Retama raetam* which stimulates secretion of insulin and inhibits α-glucosidase. *Organic & Biomolecular Chemistry* 17 (5):1266–76. doi: 10.1039/c8ob02755b.

Patel, H., P. G. Royall, S. Gaisford, G. R. Williams, C. H. Edwards, F. J. Warren, B. M. Flanagan, P. R. Ellis, and P. J. Butterworth. 2017. Structural and enzyme kinetic studies of retrograded starch: Inhibition of α-amylase and consequences for intestinal digestion of starch. *Carbohydrate Polymers* 164 (2017):154–61. doi: 10.1016/j.carbpol.2017.01.040.

Petrussa, E., E. Braidot, M. Zancani, C. Peresson, A. Bertolini, S. Patui, and A. Vianello. 2013. Plant flavonoids-biosynthesis, transport and involvement in stress responses. *International Journal of Molecular Sciences* 14 (7):14950–73. doi: 10.3390/ijms140714950.

Pinhas-Hamiel, O., and P. Zeitler. 2007. Acute and chronic complications of type 2 diabetes mellitus in children and adolescents. *Lancet* 369 (9575):1823–31. doi: 10.1016/S0140-6736(07)60821-6.

Pitocco, D., M. Tesauro, R. Alessandro, G. Ghirlanda, and C. Cardillo. 2013. Oxidative stress in diabetes: Implications for vascular and other complications. *International Journal of Molecular Sciences* 14 (11):21525–50. doi: 10.3390/ijms141121525.

Proença, C., M. Freitas, D. Ribeiro, E. F. T. Oliveira, J. L. C. Sousa, S. M. Tome, M. J. Ramos, A. M. S. Silva, P. A. Fernandes, and E. Fernandes. 2017. α-Glucosidase inhibition by flavonoids: An *in vitro* and *in silico* structure-activity relationship study. *Journal of Enzyme Inhibition and Medicinal Chemistry* 32 (1):1216–28. doi: 10.1080/14756366.2017.1368503.

Proença, C., M. Freitas, D. Ribeiro, S. M. Tomé, E. F. T. Oliveira, M. F. Viegas, A. N. Araújo, M. J. Ramos, A. M. S. Silva, P. A. Fernandes, et al. 2019. Evaluation of a flavonoids library for inhibition of pancreatic α-amylase towards a structure-activity relationship. *Journal of Enzyme Inhibition and Medicinal Chemistry* 34 (1): 577–88. doi: 10.1080/14756366.2018.1558221.

Qin, N. B., C. C. Jia, J. Xu, D. H. Li, F. X. Xu, J. Bai, Z. L. Li, and H. M. Hua. 2017. New amides from seeds of *Silybum marianum* with potential antioxidant and antidiabetic activities. *Fitoterapia* 119: 83–9. doi: 10.1016/j.fitote.2017.04.008.

Ren, L., L. Z. Li, J. Huang, L. Z. Huang, J. H. Li, Y. M. Li, and S. Y. Tang. 2020. New compounds from the seeds of *Psoralea corylifolia* with their protein tyrosine phosphatase 1B inhibitory activity. *Journal of Asian Natural Products Research* 22 (8):732–6. doi: 10.1080/10286020.2019.1621852.

Ren, S., K. Li, and Z. Liu. 2019. Research on the influences of five food-borne polyphenols on *in vitro* slow starch digestion and the mechanism of action. *Journal of Agricultural and Food Chemistry* 67 (31):8617–25. doi: 10.1021/acs.jafc.9b01724.

Renda, G., S. Sari, B. Barut, M. Şoral, T. Liptaj, B. Korkmaz, A. Özel, İ. Erik, and D. Şöhretoğlu. 2018. α-Glucosidase inhibitory effects of polyphenols from *Geranium asphodeloides*: Inhibition kinetics and mechanistic insights through in vitro and in silico studies. *Bioorganic Chemistry* 81:545–52. doi: 10.1016/j.bioorg.2018.09.009.

Ribeiro, D., M. Freitas, J. L. Lima, and E. Fernandes. 2015. Proinflammatory pathways: The modulation by flavonoids. *Medicinal Research Reviews* 35 (5):877–936. doi: 10.1002/med.21347.

Sales, P. M., P. M. Souza, L. A. Simeoni, and D. Silveira. 2012. α-Amylase inhibitors: A review of raw material and isolated compounds from plant source. *Journal of Pharmacy & Pharmaceutical Sciences* 15 (1):141–83. doi: 10.18433/j35s3k.

Sarian, M. N., Q. U. Ahmed, S. Z. Mat So'ad, A. M. Alhassan, S. Murugesu, V. Perumal, S. N. A. Syed Mohamad, A. Khatib, and J. Latip. 2017. Antioxidant and antidiabetic effects of flavonoids: A

structure-activity relationship based study. *BioMed Research International* 2017:1–14. doi: 10.1155/2017/8386065.

Scheen, A. J. 2017. Pharmacological management of type 2 diabetes: What's new in 2017? *Expert Review of Clinical Pharmacology* 10 (12):1383–94. doi: 10.1080/17512433.2017.1376652.

Schmeltz, L., and B. Metzger. 2007. 6.19—Diabetes/Syndrome X. In *Comprehensive medicinal chemistry II*, ed. J. B. Taylor and D. J. Triggle, 417–58. Oxford: Elsevier.

Shahinozzaman, M., N. Taira, T. Ishii, M. A. Halim, M. A. Hossain, and S. Tawata. 2018. Anti-Inflammatory, anti-diabetic, and anti-Alzheimer's effects of prenylated flavonoids from *Okinawa Propolis*: An investigation by experimental and computational studies. *Molecules* 23 (10):2479. doi: 10.3390/molecules23102479.

Sheliya, M. A., B. Rayhana, A. Ali, K. K. Pillai, V. Aeri, M. Sharma, and S. R. Mir. 2015. Inhibition of α-glucosidase by new prenylated flavonoids from *Euphorbia hirta* L. herb. *Journal of Ethnopharmacology* 176:1–8. doi: 10.1016/j.jep.2015.10.018.

Shi, Z. F., C. Lei, B. W. Yu, H. Y. Wang, and A. J. Hou. 2016. New alkaloids and α-glucosidase inhibitory flavonoids from *Ficus hispida*. *Chemistry & Biodiversity* 13 (4):445–50. doi: 10.1002/cbdv.201500142.

Silva, E. L., J. F. Lobo, J. M. Vinther, R. M. Borges, and D. Staerk. 2016. High-resolution α-glucosidase inhibition profiling combined with HPLC-HRMS-SPE-NMR for identification of antidiabetic compounds in *Eremanthus crotonoides* (Asteraceae). *Molecules* 21 (6): 782. doi: 10.3390/molecules21060782.

Sim, L., K. Jayakanthan, S. Mohan, R. Nasi, B. D. Johnston, B. M. Pinto, and D. R. Rose. 2010. New glucosidase inhibitors from an ayurvedic herbal treatment for type 2 diabetes: Structures and inhibition of human intestinal maltase-glucoamylase with compounds from *Salacia reticulata*. *Biochemistry* 49 (3):443–51. doi: 10.1021/bi9016457.

Slamova, K., J. Kapesova, and K. Valentova. 2018. "Sweet flavonoids": Glycosidase-catalyzed modifications. *International Journal of Molecular Sciences* 19 (2126):1–19. doi: 10.3390/ijms19072126.

Şöhretoğlu, D., S. Sari, B. Barut, and A. Özel. 2018. Discovery of potent α-glucosidase inhibitor flavonols: Insights into mechanism of action through inhibition kinetics and docking simulations. *Bioorganic Chemistry* 79:257–64. doi: 10.1016/j.bioorg.2018.05.010.

Şöhretoğlu, D., S. Sari, A. Özel, and B. Barut. 2017. α-Glucosidase inhibitory effect of *Potentilla astracanica* and some isoflavones: Inhibition kinetics and mechanistic insights through in vitro and in silico studies. *International Journal of Biological Macromolecules* 105 (Pt 1):1062–70. doi: 10.1016/j.ijbiomac.2017.07.132.

Song, Y. H., Z. Uddin, Y. M. Jin, Z. Li, M. J. Curtis-Long, K. D. Kim, J. K. Cho, and K. H. Park. 2017. Inhibition of protein tyrosine phosphatase (PTP1B) and α-glucosidase by geranylated flavonoids from *Paulownia tomentosa*. *Journal of Enzyme Inhibition and Medicinal Chemistry* 32 (1):1195–202. doi: 10.1080/14756366.2017.1368502.

Sun, H., Y. Li, X. Zhang, Y. Lei, W. Ding, X. Zhao, H. Wang, X. Song, Q. Yao, Y. Zhang, et al. 2015. Synthesis, α-glucosidase inhibitory and molecular docking studies of prenylated and geranylated flavones, isoflavones and chalcones. *Bioorganic & Medicinal Chemistry Letters* 25 (20):4567–71. doi: 10.1016/j.bmcl.2015.08.059.

Sun, H., D. Wang, X. Song, Y. Zhang, W. Ding, X. Peng, X. Zhang, Y. Li, Y. Ma, R. Wang, et al. 2017. Natural prenylchalconaringenins and prenylnaringenins as antidiabetic agents: α-glucosidase and α-amylase inhibition and in vivo antihyperglycemic and antihyperlipidemic effects. *Journal of Agricultural and Food Chemistry* 65 (8): 1574–81. doi: 10.1021/acs.jafc.6b05445.

Tadera, K., Y. Minami, K. Takamatsu, and T. Matsuoka. 2006. Inhibition of α-glucosidase and α-amylase by flavonoids. *Journal of Nutritional Science and Vitaminology* 52 (2):149–53. doi: 10.3177/jnsv.52.149.

Tahrani, A. A., C. J. Bailey, S. Del Prato, and A. H. Barnett. 2011. Management of type 2 diabetes: New and future developments in treatment. *The Lancet* 378 (9786):182–97. doi: 10.1016/S0140-6736(11)60207-9.

Thilakarathna, S. H., and H. P. V. Rupasinghe. 2013. Flavonoid bioavailability and attempts for bioavailability enhancement. *Nutrients* 5 (9):3367–87. doi: 10.3390/nu5093367.

Torres-Naranjo, M., A. Suarez, G. Gilardoni, L. Cartuche, P. Flores, and V. Morocho. 2016. Chemical constituents of *Muehlenbeckia tamnifolia* (Kunth) Meisn (Polygonaceae) and its in vitro α-amylase and α-glucosidase inhibitory activities. *Molecules* 21 (11):1461. doi: 10.3390/molecules21111461.

Tundis, R., M. Bonesi, V. Sicari, T. M. Pellicanò, M. C. Tenuta, M. Leporini, F. Menichini, and M. R. Loizzo. 2016. *Poncirus trifoliata* (L.) Raf.: Chemical composition, antioxidant properties and hypoglycaemic activity via the inhibition of α-amylase and α-glucosidase enzymes. *Journal of Functional Foods* 25:477–85. doi: 10.1016/j.jff.2016.06.034.

Wang, Q. Q., N. Cheng, W. B. Yi, S. M. Peng, and X. Q. Zou. 2014. Synthesis, nitric oxide release, and α-glucosidase inhibition of nitric oxide donating apigenin and chrysin derivatives. *Bioorganic & Medicinal Chemistry* 22 (5):1515–21. doi: 10.1016/j.bmc.2014.01.038.

Wang, S., R. Su, S. Nie, M. Sun, J. Zhang, D. Wu, and N. Moustaid-Moussa. 2014. Application of nanotechnology in improving bioavailability and bioactivity of diet-derived phytochemicals. *The Journal of Nutritional Biochemistry* 25 (4):363–76. doi: 10.1016/j.jnutbio.2013.10.002.

Wang, X.-L., F.-R. Jiao, M. Yu, L.-B. Lin, J. Xiao, Q. Zhang, L. Wang, D.-Z. Duan, and G. Xie. 2017. Constituents with potent α-glucosidase inhibitory activity from *Pueraria lobata* (Willd.) *ohwi*. *Bioorganic & Medicinal Chemistry Letters* 27 (9):1993–8. doi: 10.1016/j.bmcl.2017.03.013.

Williamson, G. 2013. Possible effects of dietary polyphenols on sugar absorption and digestion. *Molecular Nutrition & Food Research* 57 (1):48–57. doi: 10.1002/mnfr.201200511.

Wright, J. J., and T. S. Tylee. 2016. Pharmacologic therapy of type 2 diabetes. *The Medical Clinics of North America* 100 (4):647–63. doi: 10.1016/j.mcna.2016.03.014.

Wyne, K., and G. L. Bakris. 2007. Chapter 90—Control of blood glucose and insulin resistance. In *Comprehensive hypertension*, ed. G. Y. H. Lip and J. E. Hall, 1105–12. Philadelphia: Mosby.

Xiao, J., G. Kai, K. Yamamoto, and X. Chen. 2013. Advance in dietary polyphenols as α-glucosidases inhibitors: A review on structure-activity relationship aspect. *Critical Reviews in Food Science and Nutrition* 53 (8):818–36. doi: 10.1080/10408398.2011.561379.

Xie, Y., W. Yang, F. Tang, X. Chen, and L. Ren. 2015. Antibacterial activities of flavonoids: Structure-activity relationship and mechanism. *Current Medicinal Chemistry* 22 (1):132–49. doi: 10.2174/0929867321666140916113443.

Xu, J., X. Wang, J. Yue, Y. Sun, X. Zhang, and Y. Zhao. 2018. Polyphenols from acorn leaves (*Quercus liaotungensis*) protect pancreatic beta cells and their inhibitory activity against α-glucosidase and protein tyrosine phosphatase 1B. *Molecules* 23 (9):2167. doi: 10.3390/molecules23092167.

Xu, Y., L. Xie, J. Xie, Y. Liu, and W. Chen. 2018. Pelargonidin-3-*O*-rutinoside as a novel α-glucosidase inhibitor for improving postprandial hyperglycemia. *Chemical Communications* 55 (1):39–42. doi: 10.1039/c8cc07985d.

Ye, R., Y. H. Fan, and C. M. Ma. 2017. Identification and enrichment of α-glucosidase-inhibiting dihydrostilbene and flavonoids from *Glycyrrhiza uralensis* leaves. *Journal of Agricultural and Food Chemistry* 65 (2):510–5. doi: 10.1021/acs.jafc.6b04155.

Yilmazer-Musa, M., A. M. Griffith, A. J. Michels, E. Schneider, and B. Frei. 2012. Grape seed and tea extracts and catechin 3-gallates are potent inhibitors of α-amylase and α-glucosidase activity. *Journal of Agricultural and Food Chemistry* 60 (36):8924–9. doi: 10.1021/jf301147n.

Yin, Z., W. Zhang, F. Feng, Y. Zhang, and W. Kang. 2014. α-Glucosidase inhibitors isolated from medicinal plants. *Food Science and Human Wellness* 3 (3-4):136–74. doi: 10.1016/j.fshw.2014.11.003.

Zeng, B., K. Chen, P. Du, S. S. Wang, B. Ren, Y. L. Ren, H. S. Yan, Y. Liang, and F. H. Wu. 2016. Phenolic compounds from *Clinopodium chinense* (Benth.) O. Kuntze and their inhibitory effects on

α-glucosidase and vascular endothelial cells injury. *Chemistry & Biodiversity* 13 (5):596–601. doi: 10.1002/cbdv.201500187.

Zeng, L., G. Zhang, S. Lin, and D. Gong. 2016. Inhibitory mechanism of apigenin on α-glucosidase and synergy analysis of flavonoids. *Journal of Agricultural and Food Chemistry* 64 (37):6939–49. doi: 10.1021/acs.jafc.6b02314.

Zhang, B. W., X. Li, W. L. Sun, Y. Xing, Z. L. Xiu, C. L. Zhuang, and Y. S. Dong. 2017. Dietary flavonoids and acarbose synergistically inhibit α-glucosidase and lower postprandial blood glucose. *Journal of Agricultural and Food Chemistry* 65 (38):8319–30. doi: 10.1021/acs.jafc.7b02531.

Zhang, L., Z-c Tu, T. Yuan, H. Wang, X. Xie, and Z-f Fu. 2016. Antioxidants and α-glucosidase inhibitors from *Ipomoea batatas* leaves identified by bioassay-guided approach and structure-activity relationships. *Food Chemistry* 208:61–7. doi: 10.1016/j.foodchem.2016.03.079.

Zhang, Y. L., J. G. Luo, C. X. Wan, Z. B. Zhou, and L. Y. Kong. 2015. Four new flavonoids with α-glucosidase inhibitory activities from *Morus alba* var. tatarica. *Chemistry & Biodiversity* 12 (11):1768–76. doi: 10.1002/cbdv.201500005.

Zhao, H.-H., Y.-Q. Liu, and J. Chen. 2019. Screening of α-glucosidase inhibitors from natural flavonoids by an in-capillary assay combining PMMA and EMMA. *Analytical Methods* 11 (10):1371–8. doi: 10.1039/C8AY02232A.

Zhen, J., Y. Dai, T. Villani, D. Giurleo, J. E. Simon, and Q. Wu. 2017. Synthesis of novel flavonoid alkaloids as α-glucosidase inhibitors. *Bioorganic & Medicinal Chemistry* 25 (20):5355–64. doi: 10.1016/j.bmc.2017.07.055.

Zhou, H., H.-M. Li, Y.-M. Du, R.-A. Yan, S.-Y. Ou, T.-F. Chen, Y. Wang, L.-X. Zhou, and L. Fu. 2017. C-geranylated flavanones from YingDe black tea and their antioxidant and α-glucosidase inhibition activities. *Food Chemistry* 235:227–33. doi: 10.1016/j.foodchem.2017.05.034.

Zhu, G., Y. Luo, X. Xu, H. Zhang, and M. Zhu. 2019. Anti-diabetic compounds from the seeds of Psoralea corylifolia. *Fitoterapia* 139:104373. doi: 10.1016/j.fitote.2019.104373.

I.1.3. A comprehensive review on the antidiabetic activity of flavonoids targeting PTP1B and DPP-4: a structure-activity relationship analysis

Version of record from Critical Reviews in Food Science and Nutrition

Copyright © (2021) with kind permission of Taylor & Francis

"A fixed version of a journal article that has been made available by Taylor & Francis, a publisher by formally and exclusively declaring the article 'published'."

CRITICAL REVIEWS IN FOOD SCIENCE AND NUTRITION
https://doi.org/10.1080/10408398.2021.1872483

Taylor & Francis
Taylor & Francis Group

REVIEW

Check for updates

A comprehensive review on the antidiabetic activity of flavonoids targeting PTP1B and DPP-4: a structure-activity relationship analysis

Carina Proença[a], Daniela Ribeiro[a], Marisa Freitas[a], Félix Carvalho[b], and Eduarda Fernandes[a]

[a]LAQV, REQUIMTE, Laboratory of Applied Chemistry, Department of Chemical Sciences, Faculty of Pharmacy, University of Porto, Porto, Portugal; [b]UCIBIO, REQUIMTE, Laboratory of Toxicology, Department of Biological Sciences, Faculty of Pharmacy, University of Porto, Porto, Portugal

ABSTRACT

Type 2 diabetes (T2D) is an expanding global health problem, resulting from defects in insulin secretion and/or insulin resistance. In the past few years, both protein tyrosine phosphatase 1B (PTP1B) and dipeptidyl peptidase-4 (DPP-4), as well as their role in T2D, have attracted the attention of the scientific community. PTP1B plays an important role in insulin resistance and is currently one of the most promising targets for the treatment of T2D, since no available PTP1B inhibitors were still approved. DPP-4 inhibitors are among the most recent agents used in the treatment of T2D (although its use has been associated with possible cardiovascular adverse events). The antidiabetic properties of flavonoids are well-recognized, and include inhibitory effects on the above enzymes, although hitherto not therapeutically explored. In the present study, a comprehensive review of the literature of both synthetic and natural isolated flavonoids as inhibitors of PTP1B and DPP-4 activities is made, including their type of inhibition and experimental conditions, and structure-activity relationship, covering a total of 351 compounds. We intend to provide the most favorable chemical features of flavonoids for the inhibition of PTP1B and DPP-4, gathering information for the future development of compounds with improved potential as T2D therapeutic agents.

KEYWORDS

Diabetes; protein tyrosine phosphatase 1B; dipeptidyl peptidase-4; inhibitory activity; phenolic compounds; flavonoids; antidiabetic agents

Introduction

Flavonoids

Flavonoids are a class of heterocyclic phenolic compounds widely distributed in nature and are present in a variety of plant-based common foods in the human diet (Balentine et al. 2015). In 1930, Rusznyak and Szent-Gyorgyi (Rusznyák and Szent-Györgyi 1936) extracted a substance containing a mixture of flavonoids from Hungarian peppers, which had an action on vascular permeability, and named this mixture vitamin P. The further advances in flavonoids research led to the discover of many other structures, developments in their chemical characterization and the study of their biological activities. Flavonoids are frequently referred as nutraceuticals (Alkhalidy, Wang, and Liu 2018). "Nutraceutical" is a hybrid term resulting from the combination of nutrients and pharmaceuticals, and firstly defined by Stephen DeFelice as "a food or parts of food that provide medical or health benefits, including the prevention or treatment of disease" (De Felice 1992).

These compounds are synthesized in plants as secondary metabolites, from phenylalanine (Alkhalidy, Wang, and Liu 2018). Flavonoids share the basic chemical structure of a common three ring moiety (A, B and C rings) with 15 carbon atoms (C_6-C_3-C_6) (Figure 1) (Alkhalidy, Wang, and Liu 2018). Flavonoids are synthesized through the phenylpropanoid pathway, where phenylalanine is transformed into 4-coumaroyl CoA, which subsequently enters the flavonoid biosynthesis pathway. The first specific enzyme involved in the flavonoid biosynthesis is chalcone synthase, resulting in the production of chalcone scaffolds from which all flavonoids derive. Depending on the plant species, several enzymes, such as isomerases, reductases, hydroxylases, and Fe^{2+}/2-oxoglutarate-dependent dioxygenases, modify the basic flavonoid skeleton and can originate different flavonoid subclasses (Ferreyra, Rius, and Casati 2012; Atmani et al. 2009). It is well-known that flavonoids can be subclassified in flavones, flavonols, flavanones, isoflavanones, flavans, isoflavans, isoflavones, biflavonoids [dimers formed by the covalent bond (C–C or C–O–C) between two monoflavonoids, example in Figure 1] and anthocyanidins (Figure 1) (Abbas et al. 2017; Gontijo, Dos Santos, and Viegas 2017).

It is important to refer that, in humans, bioavailability of flavonoids is generally low, which may limit its clinical use (Teng and Chen 2019). However, it is hoped that appropriate formulations may be developed in the near future to overcome such limitation, using nanotechnology approaches to increase the absorption and protect these compounds from metabolism (Annunziata et al. 2020; Yang et al. 2020).

CONTACT Eduarda Fernandes egracas@ff.up.pt LAQV, REQUIMTE, Laboratory of Applied Chemistry, Department of Chemical Sciences, Faculty of Pharmacy, University of Porto, Rua de Jorge Viterbo Ferreira n.° 228, 4050-313 Porto, Portugal.

© 2021 Taylor & Francis Group, LLC

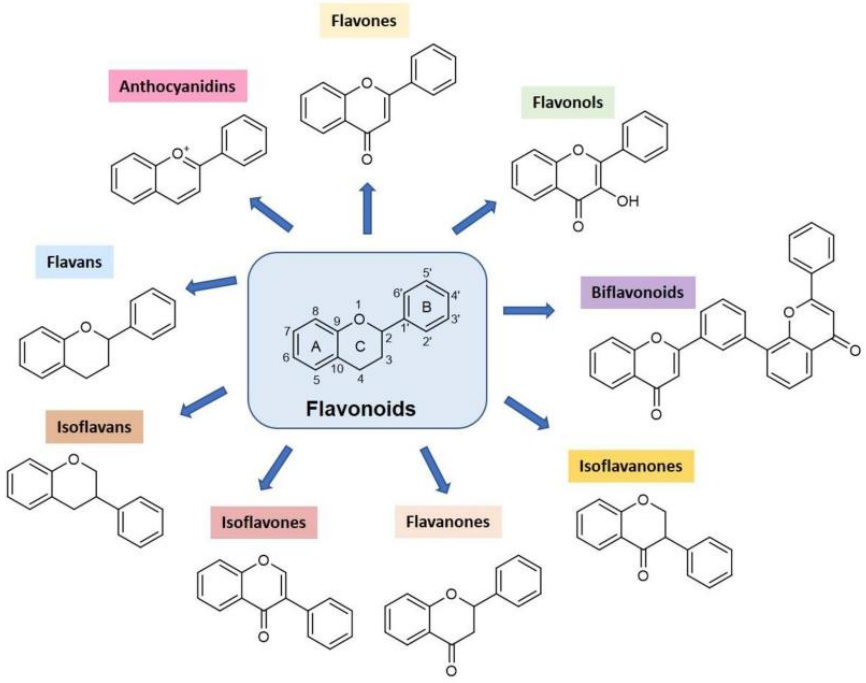


Figure 1. Basic chemical structure of flavonoids and their subclasses: flavones, flavonols, biflavonoids, flavanones, isoflavones, isoflavanones, flavans, isoflavans and anthocyanidins.

In nature, the antioxidant properties of flavonoids protect plants from desiccation, oxidation and ultraviolet damage. These phenolic compounds also have an important role in plant growth and in plant defense systems against microbial invasion (Alkhalidy, Wang, and Liu 2018). The biological activities may vary according to the flavonoids' structural subclass, degree of hydroxylation, other substitutions and conjugations, and degree of polymerization (Kumar and Pandey 2013).

Numerous studies have demonstrated the high antidiabetic potential of flavonoids, targeting various cellular signaling pathways in pancreas, liver, skeletal muscle and white adipose tissue (Babu, Liu, and Gilbert 2013). Other studies, using insulin-releasing cell lines, isolated pancreatic islets, as well as animal models of diabetes, also support the idea that flavonoids can preserve the function and survival of β-cells (Ghorbani, Rashidi, and Shafiee-Nick 2019). The antidiabetic effect of flavonoids has been substantiated by the modulation of blood sugar transporters in tissues, at pancreatic β-cells by increasing insulin secretion, reducing apoptosis, and promoting proliferation, and in muscle, by reducing inflammation, insulin resistance and oxidative stress (van Dam, Naidoo, and Landberg 2013; Kawser et al. 2016; Soares et al. 2017). Prophylactically, the consumption of dietary total flavonoids is associated with a reduced risk of develop T2D, as indicated in a meta-analysis of prospective cohort studies (Liu et al. 2014).

Furthermore, it was found that flavonoids have the capacity to modulate a large number of enzymatic diabetic targets, including α-amylase (Proença, Freitas, Ribeiro, Tomé, Oliveira, et al. 2019; Zhu et al. 2019), α-glucosidase (Proença et al. 2017; Zhu et al. 2019), aldose reductase (Nicolle et al. 2011), fructose 1,6-bisphosphatase (FBPase) (Proença et al. 2020), protein tyrosine phosphatase 1B (PTP1B) (Proença et al. 2018), and dipeptidyl peptidase-4 (DPP-4) (Proença, Freitas, Ribeiro, Tomé, Araújo, et al. 2019).

As such, the main purpose of the present review is to explore and establish a reliable structure-activity relationship concerning the flavonoids' inhibition of the promising therapeutic target PTP1B, and one of the most recent targets used in T2D therapeutic, DPP-4. In this work, the role of both PTP1B and DPP-4 in diabetes physiopathology, as well as the analysis of published articles regarding the inhibitory effect of flavonoids against those targets, are explored.

Protein tyrosine phosphatase 1B (PTP1B)

T2D used to be considered an "adult- or maturity-onset" diabetes, but is currently becoming more prevalent throughout the population, including children. This situation illustrates that therapeutic options for the management of T2D are ineffective in many cases, and further approaches to counter this metabolic disorder are urgently needed. In this sense, the ability to modulate signal transduction pathways holds enormous potential (Krishnan et al. 2018).

Protein tyrosine phosphorylation is a key post-translational mechanism involved in several cellular processes. Phosphorylation states are regulated by the dynamic and opposing actions of protein tyrosine kinases (PTKs) – which are responsible for tyrosine phosphorylation – and protein

tyrosine phosphatases (PTPs) – which induce dephosphorylation. For this reason, a dysregulation of protein tyrosine phosphorylation is tightly related to several diseases, including diabetes (Chen et al. 2015).

A total of 125 PTPs enzymes have been determined in the human genome. The PTP superfamily has a highly conserved catalytic domain, composed of around 240 amino acids. This superfamily is categorized into class I, II and III depending on their protein tyrosine specificities. Class I comprises the classical PTPs, being this class further subclassified in two major subgroups, based on the enzyme cellular location: receptor-like and cytosolic PTPs (Abdelsalam et al. 2019). Cytosolic PTPs, also known as non-receptor like PTPs, are divided in classical tyrosine-specific phosphatases and dual-specific phosphatases. Tyrosine-specific phosphatases can dephosphorylate phosphotyrosine-containing proteins, while dual-specific phosphatases are able to hydrolyze proteins containing phosphotyrosine, as well as phosphoserine and phosphothreonine. PTP1B (EC 3.1.3.48) is an intracellular ubiquitous enzyme. It has 435 amino acids and a molecular size of 50 kDa. PTP1B was first isolated from the human placenta in 1988 and is one of the most studied PTPs (Abdelsalam et al. 2019).

PTP1B constitutes an abundant and widely expressed non-receptor phosphatase encoded by the protein tyrosine phosphatase non-receptor type 1 (*PTPN1*). This enzyme consists of a N-terminal catalytic domain, two proline-rich sequences and a C-terminal hydrophobic region (Feldhammer et al. 2013). PTP1B contains numerous interaction domains that play critical roles in defining their location, stability and function. After being synthesized, PTP1B gets anchored to the endoplasmic reticulum (ER) with the C-terminus 35 amino acids residues. These 35 residues are hydrophobic, which helps in directing the enzyme toward the cytoplasmic face of the ER membrane. In addition to the localization of PTP1B at the ER surface, some mechanisms are known to regulate this enzyme, including phosphorylation, oxidation, sumoylation, and proteolysis (calpain cleavage) (Yip, Saha, and Chernoff 2010; Fueller et al. 2015).The location of PTP1B imposes topological constraint of this enzyme to access substrates. As such, besides the key catalytic domain, PTP1B has a C-terminal side extension that controls the access of PTP1B to substrates and hence plays a role in the regulation of its function (Bakke and Haj 2015; Chen et al. 2015; Abdelsalam et al. 2019). Some other possibilities were described as ways to facilitate the access of PTP1B to its substrates despite its localization: activated receptors can be internalized via vesicle-mediated endocytosis, bringing them into close proximity to the ER for dephosphorylation by PTP1B; ER-bound PTP1B might interact with and dephosphorylate the substrate during its biosynthesis; PTP1B can reside in a dynamic or "stretchable" form; ER membrane that is in constant contact with substrates located at the plasma membrane; and PTP1B and substrates interactions might be facilitated by adaptor proteins which physically link PTP1B to its substrates (Yip, Saha, and Chernoff 2010; Fueller et al. 2015; Feldhammer et al. 2013).

PTP1B is an established metabolic and a pharmacological regulator for obesity and T2D (Bakke and Haj 2015). In fact, PTP1B is associated to the negative regulation of insulin signaling, through dephosphorylation of insulin receptor (IR) and insulin receptor substrates (IRS). It is well known that insulin, secreted from pancreatic β-cells, plays a crucial role in the metabolism of carbohydrates and lipids in liver, skeletal muscle and adipose tissue. Insulin acts as a major regulator of glucose homeostasis through a complex and integrated signaling network (Feldhammer et al. 2013). Insulin signaling is performed through multiple pathways that act at different vesicle trafficking steps to redistribute glucose transporter-4 (GLUT4) and enhance glucose uptake in fat and muscle cells.

In adipocytes and muscle cells, insulin binds to the α-subunit of its receptor, leading to the activation of IR by autophosphorylation, followed by rapid phosphorylation of IRS (Feldhammer et al. 2013; Boucher, Kleinridders, and Kahn 2014). The amino acids terminus of IRS has one phosphotyrosine binding (PTB) domain and a pleckstrin homology (PH) domain. The PH domain is necessary for IRS tyrosine phosphorylation after insulin stimulation, and PTB domain seems to be crucial for high-affinity interactions between IRS and insulin receptor (Farhang-Fallah et al. 2002; Boucher, Kleinridders, and Kahn 2014). Tyrosine phosphorylation of IRS induces recruitment and activation of phosphatidylinositol-3-kinase (PI3K), resulting in the activation of the catalytic subunit, which rapidly leads to phosphorylation of phosphatidylinositol 4,5-bisphosphate (PIP_2) to form the lipid second messenger phosphatidylinositol 3,4,5-triphosphate (PIP_3) in plasma membrane, but only IRS1 is required for signal transmission toward GLUT4 translocation (Boucher, Kleinridders, and Kahn 2014; Jaldin-Fincati et al. 2017). PI3K activation, and consequent PIP_3 generation, constitutes a point of bifurcation of insulin signaling, activating two separate cascades typified by activation of the serine/threonine kinase Akt and the Rho family small GTPase Rac1, which in parallel promote GLUT4 traffic (Boucher, Kleinridders, and Kahn 2014; Klip et al. 2014; Jaldin-Fincati et al. 2017).

PIP_3 is associated to Akt at plasma membrane, where Akt is activated by phosphatidylinositol-dependent kinase-1 (PDK1) and mammalian target of rapamycin complex 2 (mTORC2) on Th308 and S473, respectively (Govers 2014; Jaldin-Fincati et al. 2017). AS160 (for Akt substrate of 160 kDa), a 160 kDa protein, has a Rab GAP (GTPase-activating protein) domain that is phosphorylated on multiple sites by the activated Akt. As such, through a variety of effects on vesicular traffic, Rab GTPases coordinate the translocation of GLUT4 from GLUT4 storage vesicles (GSV) to the plasma membrane in order to facilitate glucose transport (Figure 2) (Miinea et al. 2005; Klip et al. 2014; Jaldin-Fincati et al. 2017).

As mentioned above, PTP1B is involved in the dephosphorylation of IR and IRS, leading to the attenuation of the insulin signal. It was found that in PTP1B$^{-/-}$ mice, an enhanced insulin sensitivity and increased phosphorylation of the IR in liver and muscle tissue after insulin injection

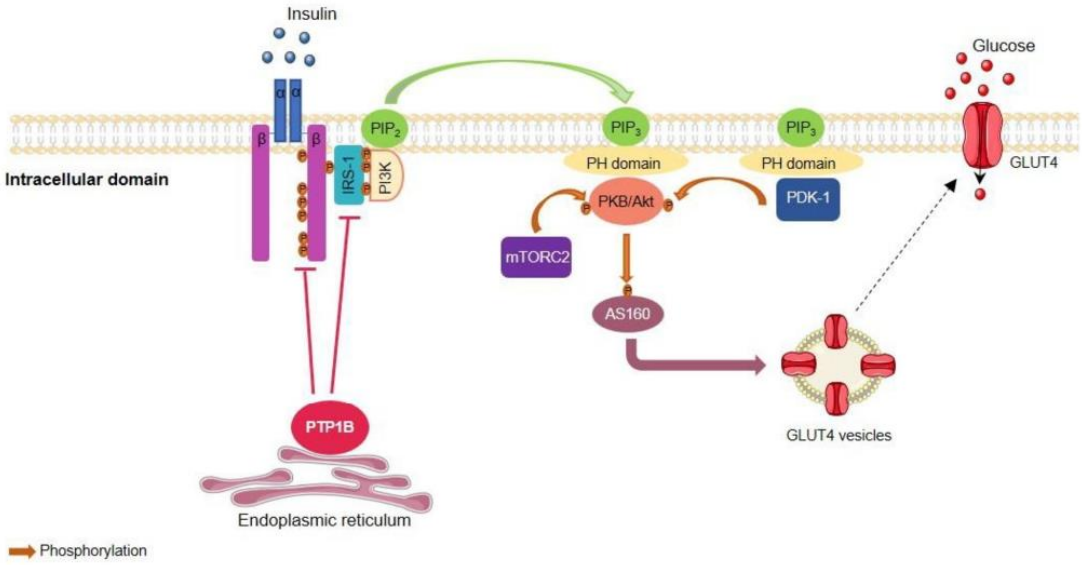


Figure 2. Negative regulation of protein tyrosine phosphatase 1B (PTP1B) in insulin signaling pathway, through inhibition of insulin receptor (IR) and insulin receptor substrates (IRS). In adipocytes and muscle cells, insulin binds to its receptor, leading to the activation of IR by autophosphorylation. Tyrosine phosphorylation of IRS induces binding to phosphatidylinositol-3-kinase (PI3K), which converts phosphatidylinositol 4,5-bisphosphate (PIP_2) to the lipid second messenger phosphatidylinositol 3,4,5-triphosphate (PIP_3). This promotes the recruitment of 3-phosphoinositide dependent protein kinase-1 (PDK-1) to the plasma membrane, which phosphorylates the protein kinase B (PKB)/Akt. The PKB-Thr308 complex leads to an improved activity of the mechanistic (or mammalian) target of rapamycin complex 2 (mTORC2), which in turn phosphorylates PKB, and induces fully activation of PKB/Akt. PKB/Akt phosphorylates its substrate AS160 (160 kDa), promoting the translocation of glucose transporter 4 (GLUT4) from intracellular storage vesicles to plasma membrane and results in a glucose uptake in cell. PTP1B, bounded to endoplasmic reticulum deactivates IR and IRS, through dephosphorylation. This deactivation prevents the PI3K and PKB/Akt activation and consequently, the translocation of GLUT4 does not occur, causing a reduction of glucose transport into the cell.

was observed in comparison to $PTP1B^{+/+}$ mice (Elchebly et al. 1999). In addition, Zabolotny et al. (Zabolotny et al. 2004) found that, in overexpressed PTP1B mice muscle, the phosphorylation of IR tyrosine stimulated by insulin decreased 35% and the activity of PI3K decreased about 40–60%. Further studies corroborated these results, demonstrating the role of PTP1B in insulin resistance (Salmeen et al. 2000; Bento et al. 2004; Haj et al. 2005; Sugiyama et al. 2017; Yang et al. 2019).

Thus, changes in the expression levels or activity of PTP1B can affect insulin signaling and contribute to the insulin resistance observed in T2D patients.

PTP1B inhibitors

Currently, PTP1B is considered a potential drug target and can provide a new approach for the treatment of T2D (Kennedy and Ramachandran 2000; Feldhammer et al. 2013; Panzhinskiy, Ren, and Nair 2013; Sun et al. 2016). In this context, although several PTP1B inhibitors have been studied, the highly conserved and polar nature of the PTP1B catalytic site makes it a challenge for PTP1B inhibitors to achieve selectivity and cell permeability. Up to now, at least 4 drug candidates that hinder PTP1B activity have reached clinical trials: ertiprotafib, trodusquemine, JTT-551 (Figure 3) and the antisense oligonucleotide IONIS-PTP1BRx (Tang et al. 2018). Ertiprotafib was considered an effective inhibitor of PTP1B, and through the reduction of plasma glucose and insulin levels in diabetic animal models, and progressed to phase 2 clinical trials. However, it failed at this stage in 2002 due to poor clinical efficacy and undesirable side effects due to its tendency to cause aggregation of PTP1B (He et al. 2012; Kumar, Page, and Peti 2020). Trodusquemine (MSI-1436), a steroid-based sulfonic acid, has shown promising efficacy, and was well-tolerated in preclinical and phase 1 clinical studies. Nevertheless, phase 2 clinical trials with T2D patients have not been conducted (He and Zhang 2016). JTT-551 was also a promising PTP1B inhibitor, which has shown to improve glucose metabolism through enhancement of insulin signaling, but unfortunately phase 1 clinical trials were discontinued in 2007 (AdInsight 2007; Ito et al. 2014). The antisense oligonucleotide IONIS-PTP1BRx targets the mRNA of PTP1B and has entered phase 2 clinical trials for diabetes. In this phase, compared with placebo, IONIS-PTP1BRx treatment for 26 weeks resulted in prolonged reductions in glycated hemoglobin (HbA_{1c}), enhanced medium-term glycaemic parameters, decreased leptin and increased adiponectin levels, and produced a body weight-reducing effect. To the best of our knowledge, no more studies were made with this compound (Digenio et al. 2018; Luo et al. 2018). Taking this into account, the development of highly effective, selective and safe PTP1B inhibitors still remains a challenge (Thareja et al. 2012; Tamrakar, Maurya, and Rai 2014).

Dipeptidyl peptidase-4 (DPP-4)

DPP-4 (EC 3.4.14.5), also known as CD26, was discovered in 1966 as a new aminopeptidase (Mulvihill and Drucker

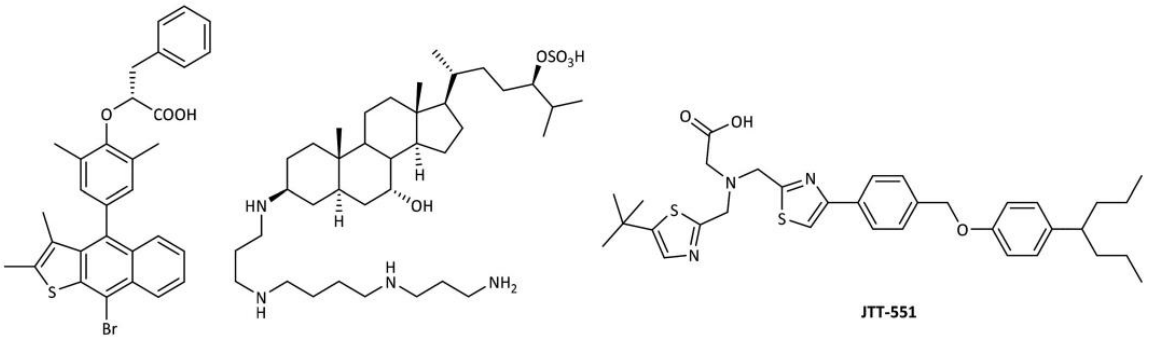


Figure 3. Chemical structures of PTP1B inhibitors ertiprotafib, trodusquemine and JTT-551.

2014). DPP-4 is a member of the prolyl oligopeptidase family, which besides prolyl oligopeptidase proteins, also contains exopeptidases, namely quiescent cell proline dipeptidase (QPP) and attractin. Within this family, the DPP-4 gene family belongs to the subclass S9B and includes six proteins: fibroblast activation protein (FAP), DPP-4, DPP-8 and DPP-9, which are enzymatically active but also exert protein-protein interactions effects, and DPP-6 and DPP-10, which are catalytically inactive, and their effects are focused on the modulation of voltage-gated potassium channels (Gall and Gorrell 2017; Deacon 2019). DPP-4 is 110 kDa amino-peptidase with 766 amino acids and liberates a dipeptide from the N-terminal of its substrate. Like the other members of the family, DPP-4 has more affinity for proline or alanine in the penultimate position, but can also cleave other peptides with other residues in the same position, although more slowly (Deacon 2019). This enzyme is an integral membrane protein, ubiquitously distributed, being expressed in several tissues, such as intestinal and renal brush border, vascular endothelium, liver, pancreas, glandular epithelial cells, and cells from the immune system (where DPP-4 is also known as the T-cell differentiation antigen, CD26) (Gall and Gorrell 2017). DPP-4 comprises a large extracellular domain, a transmembrane domain and a short intracellular domain (De et al. 2019). The extracellular domain is anchored to the cell membrane by a flexible segment coupled to the transmembrane sequence, with a short intracellular tail at the N-terminus. However, DPP-4 can be cleaved by metalloproteases in a process known by shedding, to release the extracellular domain which circulates in the plasma as soluble DPP-4 (sDPP-4) (aa 49-766) but can also be found in the seminal and cerebrospinal fluids (Röhrborn, Wronkowitz, and Eckel 2015; De et al. 2019).

The extracellular domain contains the catalytic site residues in the C-terminal region. However, the extracellular part of the protein also contains a cysteine-rich region and a region rich in glycosylation and it is believed that these regions are involved in many of the non-enzymatic functions of DPP-4, interacting with other proteins. DPP-4 is secreted as a mature monomer but for proteolytic activity, it forms a dimer (De et al. 2019).

Besides its catalytic activity, DPP-4 displays many other functions, being described as a receptor or ligand of numerous molecules and consequently allowing the interaction between cells and the extracellular matrix, cell migration, and proliferation. In addition, DPP-4/CD26 is one of the several proteins involved in amplifying the signal derived from the interaction with an antigen, leading to T-cell activation (Cahn, Cernea, and Raz 2016; Deacon 2019).

Among the numerous physiological functions of DPP-4, the most noted is its ability to inactivate the incretin hormones glucagon-like peptide-1 (GLP-1) and glucose-dependent insulinotropic polypeptide (GIP) (Gall and Gorrell 2017). As such, regarding metabolic effects, the best characterized substrates of DPP-4 are GLP-1 and GIP. Both incretin hormones play an important role in the maintenance of glucose blood levels.

GLP-1 production results from the post-translational processing of the pro-glucagon gene product by pro-hormone convertase 1/3 (PC-1/3) in the L cells of the lower intestine and colon. Pro-glucagon processing generates a 31-amino acids peptide, GLP (7-37), which can be amidated at the C-terminal glycine residue to give the second form, GLP (7-36)NH_2. In humans, most of the peptide released from L cells is in the amidated form, due to an efficient amidation process. In what concerns GIP, it is a hormone with 42amino acids secreted from K cells of the upper small intestine, as the result of PC-1/3 processing of pro-GIP (Seino, Fukushima, and Yabe 2010; Opinto, Natalicchio, and Marchetti 2013). In the intestinal entero-endocrine cells, GLP-1 and GIP are stored as intact peptides within secretory granules until their secretion. Both hormones, in special GLP-1, display numerous functions in pancreatic β-cells: both increase the meal-stimulated release of insulin in a glucose-dependent manner (incretin effect), stimulate all stages of biosynthesis of insulin, and have a protective effect on β-cell function. The incretin effect is a phenomenon where oral glucose leads to a higher stimulation of insulin secretion than an intravenous glucose administration even when the same plasma glucose concentrations are achieved, being this effect attributed to the release of the incretin hormones (Nauck and Meier 2018). However, GLP-1 and GIP have multiple functions in addition to those involved in the

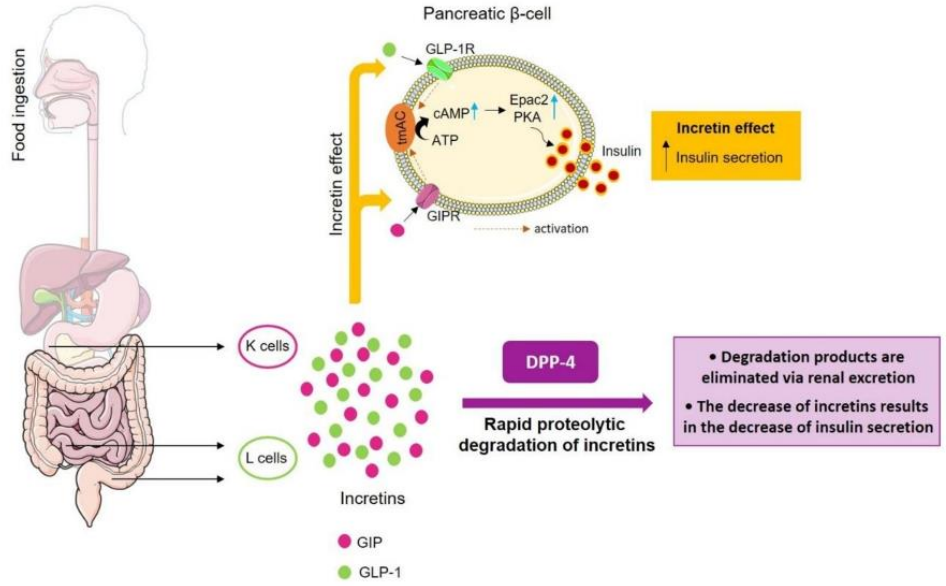


Figure 4. Mechanism of action of dipeptidyl peptidase-4 (DPP-4). After food ingestion, glucose-insulinotropic polypeptide (GIP) and glucagon-like peptide-1 (GLP-1) are released from K cells (duodenum and proximal jejunum) and L cells (ileum and colon), respectively. In pancreatic β-cells, GIP and GLP-1 bind to their respective receptors, GIPR and GLP-1R, leading to the stimulation of cyclic adenosine monophosphate (cAMP), catalyzed by the action of transmembrane adenylyl cyclase (tmAC). The improved production of cAMP results in the activation of the guanine nucleotide exchange factor (Epac2) and protein kinase A (PKA) to stimulate the insulin secretion in a glucose-dependent manner, through exocytosis of insulin-containing granules. The incretin effect is affected by the short half-lives of GIP and GLP-1, due to their rapid proteolytic degradation by the enzyme DPP-4. The inactivated incretins are excreted through the kidneys.

maintenance of glucose homeostasis. GLP-1 and GIP exert their effects via activation of their specific G protein-coupled receptors by binding to their specific receptors - GLP-1 receptor (GLP-1R) and GIP receptor (GIPR) - directly in pancreatic β cells, leading to the activation of adenylate cyclase and enhancement of intracellular cyclic adenosine monophosphate (cAMP), and consequently activate protein kinase A (PKA) and exchange protein activated by cAMP2 (EPAC2)/cAMP-guanine nucleotide exchange factor (GEF) II(Seino, Fukushima, and Yabe 2010). PKA and EPAC2 are involved in numerous intracellular events, namely altered ion channel activity, increased cytosolic calcium levels and enhanced exocytosis of insulin-containing granules. This contributes to the stimulation of insulin in a glucose-dependent manner, evidencing the insulinotropic actions of GLP-1 and GIP (Drucker 2006; Seino, Fukushima, and Yabe 2010).

By employing synthetic human GIP, it was confirmed the inability of GIP to exert insulinotropic responses in T2D patients, not leading to a significant stimulation of insulin secretion. Regarding GLP-1, the situation is different, since this hormone still exert its insulinotropic effect in T2D subjects, meaning that the stimulation of insulin secretion as well as suppression of glucagon secretion with GLP-1 is enough to lead to a significant reduction in plasma glucose levels. Moreover, it was found that co-administration of GLP-1 and GIP in patients with T2D does not stimulate insulin secretion more than GLP-1 alone (Nauck and Meier 2018).

In addition, the beneficial effects associated to the action of GLP-1 and GIP are limited due to their short plasma half-lives, as the result of their rapid deactivation by DPP-4 (Figure 4). The cleavage of incretin hormones operated by this enzyme results in a half-life of 7.3 minutes for GLP-1 and 1-2 minutes for GIP (De et al. 2019). Since DPP-4 plays an extremely important role in the degradation of incretin hormones, the idea arose that blocking this metabolism pathway can raise the levels of intact biologically active peptides. This should therefore enhance their insulinotropic effect and hence, glucose-lowering effects, giving the rationale for targeting DPP-4 as means of controlling hyperglycaemia in T2D patients.

DPP4 inhibitors

DPP-4 inhibitors constitute an established and successful class of oral antidiabetic agents. These antidiabetic agents are small molecules that act as reversible competitive inhibitors and are associated with at least 70% inhibition of plasma DPP-4 catalytic activity, when used at the appropriate therapeutic dose. As mentioned above, the reduction of plasma glucose concentration by DPP-4 inhibitors is mediated via enhancing the levels of endogenous DPP-4 substrates, particularly GLP-1, since the inhibitors themselves do not present any inherent glucose-lowering effect. The degree of DPP-4 inhibition reached in vivo is enough to rise circulating levels of intact incretin hormones by 2- to 4-fold, with subsequent improved glycaemic control (Cahn, Cernea, and Raz 2016).

In 2004, it was found that the administration of vildagliptin, a DPP-4 inhibitor, in patients with inadequate glycaemic

control with metformin monotherapy, not only prevented the deterioration in glycaemic control seen in the placebo group, but also improved fasting and postprandial plasma glucose levels, leading to a noteworthy reduction in HbA_{1c} levels (Ahrén 2019). Importantly, the improvements in glucose homeostasis in these clinical studies were not accompanied by an increase in hypoglycaemia. These results, in combination with other studies testing numerous DPP-4 inhibitors, demonstrated that DPP-4 inhibition effectively improves glycaemic control without causing hypoglycaemia and has a neutral effect on body weight, even in patients with longstanding T2D and poor β-cell function (Ahrén 2019). There is no increased risk of hypoglyacemia, since the DPP-4 inhibition effects in decreasing glucose levels are self-limiting. The insulin secretion is only stimulated when glucose concentration rises above fasting levels, being the action of incretins glucose-dependent (Deacon 2019). The first DPP-4 inhibitor was launched in 2006, and DPP-4 inhibitors are antidiabetic agents currently used with success for T2D therapy, with at least 12 drugs approved in different parts of the world (Table 1) (Cahn, Cernea, and Raz 2016; Deacon 2018).

DPP-4 inhibitors are frequently used as second-line therapy for the management of T2D. Since 2007, the use of DPP-4 inhibitors nearly tripled and in 2011, in Japan, these antidiabetic agents were the most prescribed in the first month of T2D treatment. Sitagliptin (either as single pill or in combination with metformin) is the most widely sold DPP-4 inhibitor worldwide, reaching sales of 6.358 million US dollars in a 2014 with a predicted rise of 7.525 US dollars in 2020. Furthermore, sitagliptin was the second leading antidiabetic agent 2014, after insulin glargine, being predicted to be the leading product by 2020 (Cahn, Cernea, and Raz 2016).

Regarding the adverse effects associated with the T2D treatment with DPP-4 inhibitors and given the role of DPP-4/CD26 in the regulation of T-cell activity, there had been some initial doubts whether DPP-4 inhibition might compromise immune function. Nevertheless, it was found that neither the innate nor the adaptative immune systems are affected by the use of DPP-4 inhibitors, meaning that the catalytic activity of this enzyme is not necessary for the co-stimulatory role of CD26 in T-cell activation (Deacon 2019). Unexpectedly, several previous meta-analyses have studied the association of the use of DPP-4 inhibitors and hospitalizations for heart failure (Scirica et al. 2013; Monami, Dicembrini, and Mannucci 2014; Kundu et al. 2016; Li et al. 2016; Elgendy et al. 2017; Rehman et al. 2017; Verma et al. 2017; Alfayez et al. 2019; Sano 2019; Sesti et al. 2019). It was suggested that this increased risk is not associated with DPP-4 inhibition, *per se*, but the cause is still unexplained (Fiorentino and Sesti 2016; Deacon 2019). Other short preliminary data suggest potential cardioprotective effects of GLP-1 based therapy in patients with heart failure and myocardial infarction. On the other hand, large-randomized trials including diabetic patients with preexisting heart failure and myocardial infarction demonstrated that the treatment with saxagliptin or alogliptin did not decrease cardiovascular events or mortality. Despite the controversial results from different studies, the US Food and Drug Administration (FDA) has ordered to add a warning of heart failure on the labels of medicines containing saxagliptin and alogliptin (Kumar, Bharti, and Kumar 2017; Libianto and Ekinci 2019). However, long-term studies are needed to evaluate the impact of the use of DPP-4 inhibitors on cardiovascular diseases in diabetic subjects (Fiorentino and Sesti 2016). The results are inconsistent, and some studies suggested a trending toward increased hospitalization events while other studies did not find an increase of heart failure hospitalizations but obtained a significant heterogeneity associated with this finding.

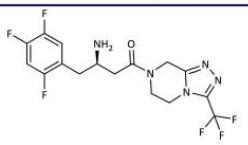
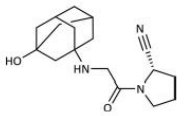
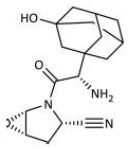
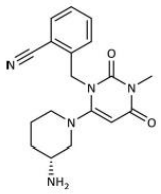
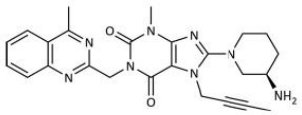
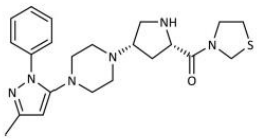
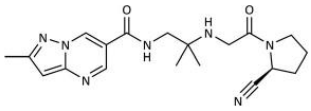
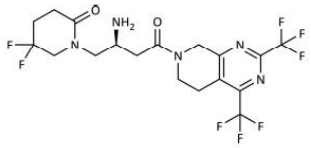
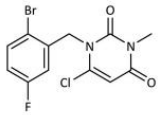
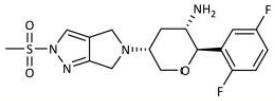
Some other adverse events were also observed with the treatment with DPP-4 inhibitors, including infections, headaches and gastrointestinal problems, and, the most frequent, nasopharyngitis and skin lesions (Ahrén 2019; Gallwitz 2019). Bullous pemphigoid, a rare autoimmune skin disease, was shown to be associated with the use of DPP-4 inhibitors in a study with more than 9000 patients treated in Japan, performed from 2009 to 2017 (Gallwitz 2019). It was further reported that the treatment with sitagliptin increased the risk of pancreatitis by 6-fold while the rate of pancreatic cancer raised 2.9-fold, in comparison with patients treated with other antidiabetic agents. For this reason, FDA included a label warning of possible adverse effect of acute pancreatitis and precancer pancreatic alterations along with severe joint pain in some patients with T2D, treated with DPP-4 inhibitors (Kumar, Bharti, and Kumar 2017).

The association of DPP-4 inhibitors with the overall adverse events described above are probably due to the action of DPP-4 in cleaving several bioactive peptides besides GLP-1 and GIP, namely neuropeptide Y, substance P and numerous chemokines. Since peptides are also inactivated by other pathways, the DPP-4 activity is not as important for their inactivation as it is for incretin hormones. Nevertheless, longer follow-up studies are required for safety analysis of these glucose-lowering agents (Ahrén 2019).

Further studies have been focused on the potential combination of DPP-4 inhibitors with sodium/glucose transporter 2 (SGLT2) inhibitors (which reduce plasma glucose levels by inhibiting renal reabsorption of glucose). It was suggested that this combination is a promising early-glucose lowering treatment of T2D due to their complementary mechanisms of action. It was also observed that this combination promotes an enhancement of glucose-lowering action with low risk of hypoglycaemia and without weight increase (Molina-Vega et al. 2018; Ahrén 2019).

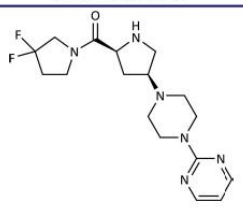
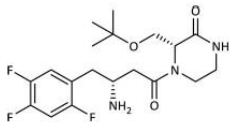
Historically, natural products have played a crucial role in providing multiple health benefits. Therefore, several modern drugs represent plant-derived agents for the treatment of T2D, including acarbose (α-glucosidase inhibitor), phlorizin-derived compounds (SGLT2 inhibitors), and galegine, which contributed to the discovery of biguanides (metformin) (Moradi-Marjaneh, Paseban, and Sahebkar 2019; Sun et al. 2020). Advantages of natural products-based discovery are evidenced by the biodiversity of resources, structural and chemical diversity, biocompatibility and biological validation (Sun et al. 2020). As mentioned above, among natural products, flavonoids have raised attention in

Table 1. DPP-4 inhibitors currently available for clinical use [adapted from Cahn et al. (Cahn, Cernea, and Raz 2016)].

Name	Chemical structure	Company	Year first launched	Countries approved
Sitagliptin		Merck	2006	Worldwide
Vildagliptin		Novartis	2007	Worldwide, excluding US
Saxagliptin		Bristol-Myers Squibb; AstraZeneca	2009	Worldwide
Alogliptin		Takeda	2010	Worldwide
Linagliptin		Boehringer Ingelheim; Lily	2011	Worldwide
Teneligltiptin		Mitsubishi Tanabe Pharma	2012	Japan, South Korea and India
Anagliptin		Sanwa Kagaku Kenkyusho	2012	Japan
Gemigliptin		LG Life Sciences; Double-Crane Pharmaceutical; Nobel Ilac	2012	South Korea and India
Trelagliptin		Takeda	2015	Japan
Omarigliptin		Merck	2015	Japan

(*continued*)

Table 1. Continued.

Name	Chemical structure	Company	Year first launched	Countries approved
Gosogliptin		Pfizer -SatRx	2016	Russian Federation
Evogliptin		Dong-A Pharmaceutical	2016	South Korea

scientific community in the last years, due to their very promising antidiabetic activity through the modulation of target signaling networks, thereby improving glucose metabolism, glucose transport or aldose reductase by carbohydrate metabolic pathway in pancreatic β-cells, hepatocytes, adipocytes and muscle tissues (Al-Ishaq et al. 2019; Hussain et al. 2020).

DPP-4 inhibitors are among the most recent antidiabetic agents available in the clinical practice, being associated with some possible severe adverse effects, as mentioned in the DPP-4 section. On the other hand, PTP1B currently constitutes one of the most promising therapeutic targets for T2D therapy, although none of the studied molecules has been launched in the market, due to safety concerns and poor clinical efficacy. These issues require further studies on potential inhibitors from other chemical families. The present review is focused on the potential of flavonoids as inhibitors of PTP1B and DPP-4, providing new insights for possible therapeutic intervention against T2D in near future.

Methodology

Literature search

The literature data about the antidiabetic effect of synthetic and natural flavonoids on the therapeutic targets under study were searched in the following scientific databases: PubMed, Science Direct, ResearchGate and Google Scholar, up to April 1st of 2020. The keywords used were "PTP1B", "DPP-4" (and "DPP-IV") and "flavonoids". From the 128 articles found for PTP1B and 39 articles found for DPP-4, 39 and 9 articles were included, respectively (Figure 5). The criteria used for inclusion were the selection of research papers focusing in *in vitro* inhibition of PTP1B or/and DPP-4 by flavonoids, that use pure compounds and the papers that studied more than one flavonoid, in order to allow the establishment, whenever possible, of a structure-activity relationship.

PTP1B inhibitory effect of flavonoids

Methodologies used to evaluate the PTP1B inhibitory activity of flavonoids

Currently published studies display a wide variability of experimental conditions. This variability frequently leads to different results among the research studies, as different IC_{50} values for positive controls and flavonoids. Table 2 comprises all the experimental conditions found in the analyzed studies, showing differences in the concentration of PTP1B, type and concentration of substrate, times of incubation applied before and after the addition of the substrate (*p*-nitrophenyl phosphate, *p*NPP), temperature and pH.

The subclasses of flavonoids studied in the present review are: flavones, flavonols, isoflavones, flavans, isoflavans, flavanones, isoflavanones, anthocyanidins, and biflavonoids. The values of the results exhibited below are the ones presented by the authors of the research articles. As such, in some cases, the associated standard deviations (SD) or standard errors of mean (SEM) are not shown, as they were not available. For the evaluation of the inhibitory activity of flavonoids against the targets under study, the present review was organized in the following order: flavonoids studied and establishment of the structure-activity relationship; tables presenting the corresponding flavonoid chemical structure and inhibitory activity; table presenting the summarized results of all the articles analyzed; and an integrated discussion of the results for the target under study.

Inhibitory activity of flavonoids against PTP1B

In 2002, Chen et al (Chen et al. 2002) tested the inhibition of PTP1B by flavonoids isolated from *Broussonetia papyrifera* (Table 3). From the obtained results, it was possible to conclude that the most active flavonoid was compound **1**, presenting an IC_{50} value of 4.3 μM. It was also observed that flavonols (**1**, **3** and **4**) were better inhibitors than the flavans (**2**). In addition, it was found that more nonpolar substituents at the flavonol skeleton increased their inhibitory activity, as observed by flavonoid **1** (two isoprenyl substituents) and flavonoid **4** (one isoprenyl substituent) (IC_{50}= 21.5 μM).

Li and coworkers (Li et al. 2005) evaluated the inhibition of PTP1B by flavonoids isolated from *Ardisia Japonica* (Table 4). The only flavonoid able to inhibit the enzyme under study was quercetin (**3**), with an IC_{50} value of 28.12 μM. It was possible to verify that the flavonol structure is more favorable for the intended effect than the flavan structure. Additionally, it was observed that the glycosylation

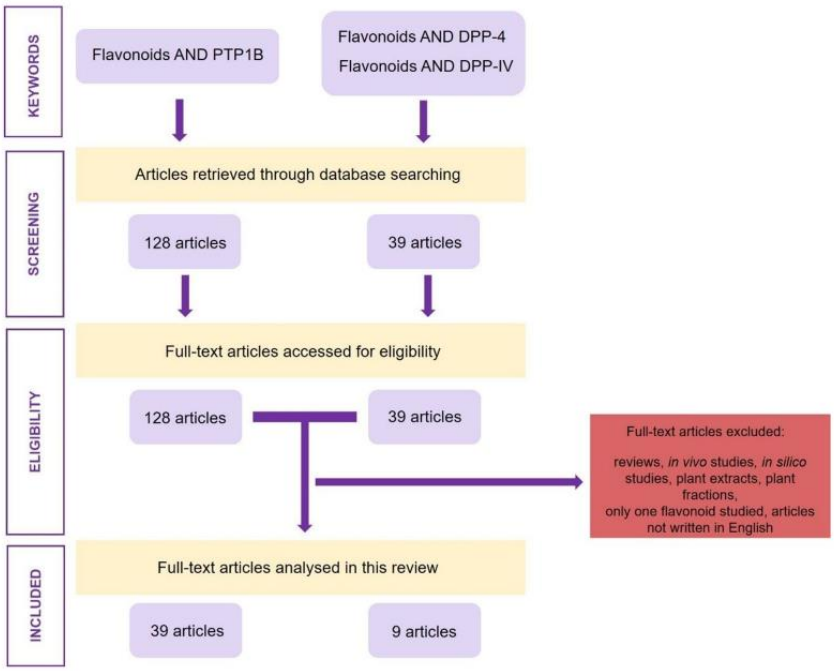


Figure 5. Scheme of literature search.

at the 3-position of C ring and/or at 7-position of A ring (**5** - **9**) significantly decreased the ability of flavonoids to inhibit human PT1B.

In 2006, prenylated isoflavones were isolated from the stem bark of *Erythrina addisionae* (Table 5) (Bae et al. 2006). The flavonoid with higher ability to inhibit PTP1B was isoflavone **15** (IC_{50} = 2.6 ± 0.5 μM), followed by **16** (IC_{50} = 4.1 ± 0.2 μM), **11** (IC_{50} = 10.1 ± 0.3 μM), **13** (IC_{50} = 42.5 ± 2.8 μM), and **12** and **14** (IC_{50} > 150 μM). These results demonstrate that both isoflavones **15** and **16**, which bear a prenyl group and a dimethylpyran moiety in the A ring were stronger inhibitors than compound **11**, which has two prenyl groups and two -OH groups in the A ring. This suggests that cyclization between an -OH group and one of the prenyl groups in the A ring might increase the PTP1B inhibition. Moreover, it was found that the presence of two -OH groups at 2′- and 4′- positions of B ring of isoflavones are favorable for the inhibition of PTP1B, comparing with isoflavones with only one -OH group at 4′-position of this ring. Finally, it was verified that the presence of the C2 = C3 double bond seems to decrease the inhibitory activity of isoflavones against PTP1B.

Flavonoids sanggenon G (**17**) and kwanon L (**18**) (Table 6), from the Chinese crude drug "Sang-Bai-Pi" (*Morus* root bark), were tested regarding their capacity to inhibit human PTP1B, presenting IC_{50} values of 1.6 ± 0.3 μM and 16.9 ± 1.1 μM, respectively (Cui et al. 2006). In fact, the mixed-type inhibitor sanggenon G (**17**) was more active than the positive control RK-682 (IC_{50} = 4.5 ± 0.5 μM). Considering the obtained results, it can be concluded that the substitution with a cyclohexene derivative at 6-position of A ring improved about 10-fold the PTP1B inhibition comparing with the presence of the cyclohexene derivative at 3′-position of B ring.

Na and colleagues (Na et al. 2006) tested the PTP1B inhibition by flavanones and isoflavones isolated from *Erythrina mildbraedii* (Table 7). The flavonoid with better activity was abyssinone IV (**22**), presenting an IC_{50} value of 16.0 ± 1.1 μM. It was found that the replacement of an -OH group for a -OCH_3 group at 4′-position of B ring decreases the ability of flavonoids to inhibit PTP1B, by comparing abyssinone IV (**22**) with abyssinone IV 4′-*O*-methyl ether (**19**) (IC_{50} = 21.2 ± 1.6 μM). Moreover, it can be observed that the presence of an -OH group at 5-position of A ring seems to reduce the inhibition of the enzyme under study, by comparing abyssinone V (**21**) (IC_{50} = 39.7 ± 2.5 μM) with abyssinone IV (**22**), and abyssinone IV 4′-*O*-methyl ether (**19**) with abyssinone V 4′-*O*-methyl ether (**20**) (IC_{50} = 26.3 ± 1.5 μM).

The PTP1B inhibition by flavanones isolated from the stem bark of *Erythrina abyssinica* was evaluated (Table 8) (Cui et al. 2007). The flavonoids with best activity were sigmoidin F (**32**) and sigmoidin A (**36**), with IC_{50} values of 14.2 ± 1.7 μM and 14.4 ± 0.8 μM, respectively. By comparing sigmoidin F (**32**) with sigmoidin C (**28**) (IC_{50} > 60 μM), it was found that the addition of a prenyl group at 2′-position of B ring significantly increases the inhibition of PTP1B. Furthermore, it can be observed that abyssinin I (**29**) (IC_{50} = 18.2 ± 1.4 μM), which bears a -OCH_3 group at 3′-position

Table 2. Experimental conditions applied in the analyzed research studies concerning the inhibition of PTP1B by flavonoids.

PTP1B (source, concentration)	*p*NPP concentration	Preincubation of flavonoids with PTP1B	Time of enzymatic reaction	pH	Temperature (°C)	Positive control(s) activity	Reference
Human, 100 nM	10 mM	NM	NM	NM	NM	Na_3VO_4 ($IC_{50} = 2$ μM)	(Chen et al. 2002)
Human, NM	NM			7.6	RT	NM	(Li et al. 2005)
				NM	NM	Ursolic acid ($IC_{50} = 2.5 \pm 0.2$ μM)	(Bae et al. 2006)
Human, 0.05 - 1 μg	2 mM		30 min	6.0*	37	RK-682 ($IC_{50} = 4.5 \pm 0.5$ μM)	(Cui et al. 2006; Cui et al. 2010)
						RK-682 ($IC_{50} = 4.5 \pm 0.5$ μM)	(Na et al. 2006; Cui et al. 2007; Cui et al. 2008; Jang et al. 2008)
						Ursolic acid ($IC_{50} = 3.6 \pm 0.2$ μM)	
Human, 0.05 μg						RK-682 ($IC_{50} = 4.4 \pm 0.1$ μM)	(Li et al. 2010)
Human, NM	NM		NM		NM	Ursolic acid ($IC_{50} = 3.6 \pm 0.2$ μM)	(Nguyen et al. 2011)
Human, 0.05 - 1 μg	2 mM		30 min		37	Ursolic acid ($IC_{50} = 3.6 \pm 0.2$ μM)	(Nguyen et al. 2012)
Human, 0.5 U		10 min	20 min			Ursolic acid ($IC_{50} = 2.57 \pm 0.71$ μg/mL)	(Islam et al. 2013)
Human, 30 nM		NM	NM	6.5	30	Ursolic acid ($IC_{50} = 3.20 \pm 0.31$ μM)	(Sun et al. 2013)
Human, 0.5 U		10 min	20 min	6.0*	37	Ursolic acid ($IC_{50} = 5.99 \pm 0.22$ μM)	(Choi, Islam, Ali, Kim, Kim, et al. 2014)
						Ursolic acid ($IC_{50} = 8.20 \pm 0.55$ μM)	(Choi, Islam, Ali, Kim, Park, et al. 2014)
NM, NM		NM	30 min			RK-682 ($IC_{50} = 4.49 \pm 0.15$ μM)	(Sasaki et al. 2014)
Human*, NM	NM		NM	NM	RT	Suramin ($IC_{50} = 11 \pm 1$ μM)	(Cai, Zhao, and Tao 2015)
Human, NM	10 mM	10 min	20 min	7.5	37	$NaVO_4$ ($IC_{50} = 29.10$ μM)	(Guo et al. 2015)
Human, 0.05 - 0.1 μg	2 mM			6.0*	37/20	RK-682 ($IC_{50} = 4.5 \pm 0.1$ μM)	(Jeong et al. 2015)
NM, NM	35 mM	5 min	30 min	NM**	RT	- ($IC_{50} = 1.97 \pm 0.5$ μM)	(Jiang et al. 2015)
	2 mM	NM	3 min	6.5	30	Oleanolic acid ($IC_{50} = 1.17 \pm 0.13$ μM)	(Li et al. 2015)
Human, NM		10 min	20 min	6.0*	37/20	RK-682 ($IC_{50} = 4.5 \pm 0.2$ μM)	(Nguyen et al. 2015)
	1 mM	NM	30 min		37.5	Ursolic acid ($IC_{50} = 3.8 \pm 0.4$ μM)	(Quang et al. 2015)
NM, 30 nM	2 mM		3 min	6.5	30	Oleanolic acid ($IC_{50} = 2.98 \pm 0.35$ μM)	(Wang et al. 2015)
Human, NM		10 min	20 min	6.0*	37/20	RK-682 ($IC_{50} = 4.47 \pm 0.03$ μM)	(Na et al. 2016)
Human, 1 μg/mL	4 mM		30 min	7.5	37	Ursolic acid ($IC_{50} = 15.5 \pm 0.9$ μM)	(Wang et al. 2016)
Human, 0.05 - 0.1 μg/200 μL	2 mM	NM		6.0*		Ursolic acid ($IC_{50} = 1.21 \pm 0.18$ μM)	(Zhao et al. 2016)
NM, 0.5 U		10 min	20 min			Ursolic acid ($IC_{50} = 5.4 \pm 0.30$ μM)	(Jung et al. 2017)
Human, 0.5 U		NM					(Kim et al. 2017)

(*continued*)

Table 2. Continued.

PTP1B (source, concentration)	*p*NPP concentration	Preincubation of flavonoids with PTP1B	Time of enzymatic reaction	pH	Temperature (°C)	Positive control(s) activity	Reference
						Ursolic acid (IC_{50} = 8.24 ± 0.30 μM)	
Human, NM		10 min	30 min	6.0***		Ursolic acid (IC_{50} = 9.43 ± 0.14 μM)	(Nguyen et al. 2017)
	NM	NM		6.0*		Oleanolic acid (IC_{50} = 8.35 ± 0.21 μM)	(Qin et al. 2017)
Human, 1 μg/mL	4 mM	10 min		7.5		Na_3VO_4 (IC_{50} = 32.6 ± 1.5 μM)	(Song et al. 2017)
Human, 0.05 μg/180 μL	1.5 mM	NM	10 min	7.0	25	RK682 (IC_{50} = 10.4 ± 1.6 μM)	(Trinh, Jager, and Staerk 2017)
Human, 4 μg/mL	2 mM	5 min	30 min	6.0	37	Ursolic acid (IC_{50} = 7.1 ± 0.9 μM)	(Proença et al. 2018)
Human, NM	4 mM	NM		6.0*		Ursolic acid (IC_{50} = 3.52 ± 0.10 μM)	(Qin et al. 2018)
	10 mM	10 min		7.5****		Na_3VO_4 (IC_{50} = 28.91 ± 2.78 μM)	(Xu et al. 2018)
NM, 0.2 μM	0.1 M	35 min		7.2****		–	(Zhang et al. 2018)
Human, NM	1.5 mM	NM	10 min	7.0	25	RK-682 (IC_{50} = 13.27 ± 1.00 μM)	(Zhao et al. 2018)
Human, 20 μg/mL	100 mM	5 min		6.0	30	$NaVO_4$ (% Inhibition = 56.58 ± 4.86 $^{20\,\mu M}$)	(Chen et al. 2019)
NM, 0.05 – 0.1 μg/100 μL	2 mM	NM	30 min	6.0*****	37	RK-682 (IC_{50} = 4.7 ± 0.6 μM)	(Ren et al. 2019)
NM, 1 μg/mL	3 mM	15 min	NM	7.0*		Ursolic acid (IC_{50} = 3.1 ± 0.4 μM)	(Xu et al. 2019)
Human, NM	1.5 mM	NM	10 min	7.0	25	RK-682 (IC_{50} = 14.5 ± 0.2 μM)	(Zhao et al. 2019)

NM – not mentioned; *p*NPP – *p*-nitrophenyl phosphate (substrate); RT - room temperature; Na_3VO_4 - sodium orthovanadate.
*NaOH 10 M to stop the reaction.
**NaOH 3 M to stop the reaction).
***NaOH 1 N to stop the reaction.
****NaOH 2 M to stop the reaction.
*****NaOH 1 M to stop the reaction.

of B ring, is more active than abyssinoflavone V (**27**) and sigmoidin C (**28**), suggesting that the hydroxylation or the absence of substituents at this position is not favorable for the intended effect. However, it was suggested that the presence of a catechol group at 3′- and 4′-positions of B ring favors PTP1B inhibition, by comparison of sigmoidin B (**33**) (IC_{50} = 19.4 ± 2.3) with 3′-prenylnaringenin (**37**) (IC_{50} = 26.7 ± 1.2 μM).

In the continuous interest in constituents of the stem bark of *Erythrina abyssinica*, Cui and coauthors (Cui et al. 2008) isolated and performed the structural elucidation of 12 new and 4 known flavanones (Table 9) and tested their ability to inhibit PTP1B. By the obtained results, it was seen that 8 flavonoids inhibited PTP1B activity in a dose-dependent manner, with IC_{50} values ranging from 13.9 ± 2.1 μM (flavonoid **38**) to 21.6 ± 2.1 μM [burttinonedehydrate (**53**)]. The other tested 8 flavanones – **39**, **43**, **46**, **47**, **48**, sigmoidin G (**49**), **50** and sigmoidin D (**51**) – in which prenyl and/or -OCH_3 groups are absent, presented no inhibitory activity against PTP1B. Following this rationale, all compounds with prenyl groups in their structure exhibited strong inhibitory activity, indicating the significant role of prenyl moiety in the intended effect. Flavanones **40** and **42**, both bearing a –OCH_3 group at 5′-position of B ring, were also effective PTP1B inhibitors. Therefore, the presence of a lipophilic group, namely prenyl and –OCH_3 groups, are important for the inhibition of the enzyme under study. On the other hand, the presence of a polar moiety, such as an –OH group, does not seem to improve this biological activity.

It was previously described the PTP1B inhibition by flavonoids isolated from the ethyl acetate soluble extract of the root bark of *Erythrina mildbraedii*, demonstrating the significant role of prenyl groups in the biological activity under study, as above mentioned (Na et al. 2006). The further study of the same research group (Jang et al. 2008) is based on the evaluation of the PTP1B inhibition of flavonoids isolated from the same plant (Table 10).

The best inhibitor was flavonoid **56**, with an IC_{50} value of 5.5 ± 0.3 μM, similar to the ones found for the positive controls RK-682 (IC_{50} = 4.5 ± 0.5 μM) and ursolic acid (IC_{50} = 3.6 ± 0.2 μM). Interestingly, the isoflavan structure (**56**) was more favorable for the intended effect than isoflavones (**55**, **57** and **58**) and flavanones (**54** and **34**). Another conclusion that can be drawn is that the replacement of a -OCH_3 group by a -OH group at 4′-position and a hydrogen by a -OCH_3 group at 3′-position reduce PTP1B inhibition by flavonoids, as seen by the inhibitory activities of compound **54**, with an IC_{50} value of 29.6 ± 2.5 μM, and abyssinin II (**34**), with an IC_{50} value of 40.5 ± 1.9 μM.

Table 3. PTP1B inhibition by flavonoids tested by Chen et al (Chen et al. 2002).

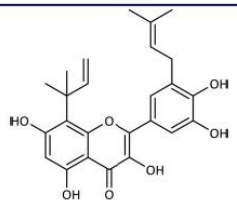
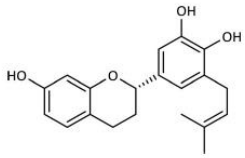
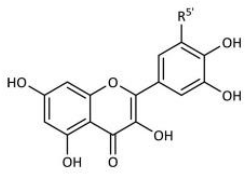
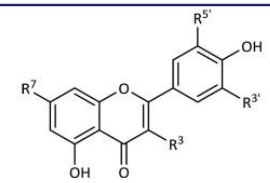
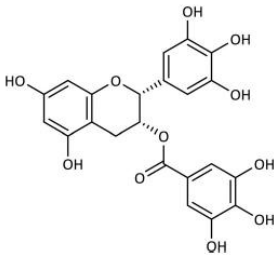
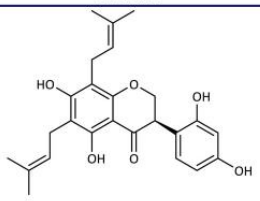
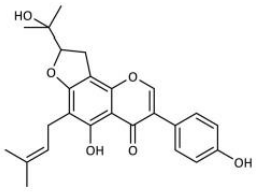
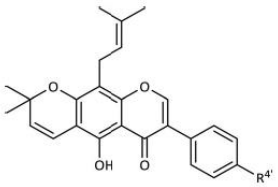
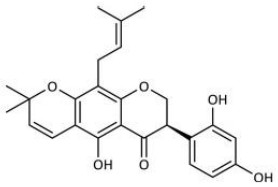
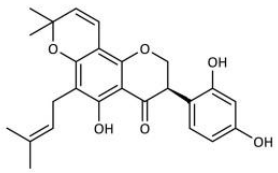
Flavonoid	Structure	$R^{5'}$	IC_{50} (μM)
1		–	**4.3**
2		–	41.5
Quercetin (**3**)		H	23.3
Uralenol (**4**)		prenyl	21.5
Positive control Na_3VO_4	–	–	2

Table 4. PTP1B inhibition by flavonoids tested by Li et al (Li et al. 2005).

Flavonoid	Structure	R^3	$R^{3'}$	$R^{5'}$	R^7	IC_{50} (μM)
Quercetin (**3**)		OH	OH	H	OH	**28.12**
Quercetrin (**5**)		rhamnose	OH	H	OH	NA
Myricitrin (**6**)		rhamnose	OH	OH	OH	NA
Afzelin (**7**)		rhamnose	H	H	OH	NA
Rutin (**8**)		rutinose	OH	H	OH	NA
Kaempferitrin (**9**)		rhamnose	H	H	rhamnose	NA
Epigallocatechin gallate (**10**)		–	–	–	–	NA

NA – Not active.

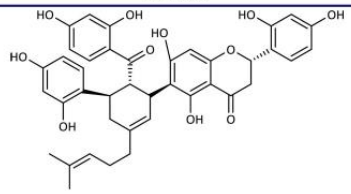
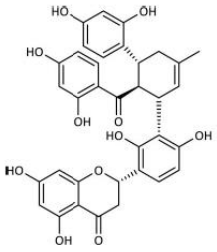
Table 5. PTP1B inhibition by flavonoids tested by Bae et al (Bae et al. 2006).

Flavonoid	Structure	$R^{4'}$	IC_{50} (μM ± SD)
Orientanol E (**11**)		–	10.1 ± 0.3
Senegalensin (**12**)		–	>150
Warangalone (**13**) Warangalone 4′-methyl ether (**14**)		OH OCH_3	42.5 ± 2.8 >150
2,3-Dihydroauriculatin (15)		–	**2.6 ± 0.5**
16		–	4.1 ± 0.2
Positive Control Ursolic acid		–	2.5 ± 0.2

As part of the continuous interest of Cui and colleagues in the constituents of stem bark of *Erythrina abyssinica* (Cui et al. 2007; Cui et al. 2008), 6 new dihydrofuran flavanones and 2 known flavanones were isolated and structurally elucidated (Cui et al. 2010) (Table 11). The flavonoids that presented a dose-dependent effect were **59**, **60**, **61**, **64**, **65** and **66**, with IC_{50} values of 15.2 ± 1.2 μM, 17.9 ± 2.6 μM, 16.1 ± 1.1 μM, 18.3 ± 1.6 μM, 16.2 ± 1.1 μM and 19.6 ± 2.3 μM, respectively. The significant role of -OCH_3 and prenyl groups in the flavonoid structure was emphasized one more time, since flavanones without any of these substituents (compounds **62** and **63**) were weak inhibitors (IC_{50} > 60 μM). It was also observed that flavonoids **65** (IC_{50} = 16.2 ± 1.1 μM) and **66** (IC_{50} = 19.6 ± 2.3 μM), without the dihydrofuran system, also presented inhibitory activity against PTP1B, suggesting that this system is not determinant for the inhibition of the enzyme under study.

Glycyrrhisoflavone (**67**), glisoflavone (**68**), cycloglyrrhisoflavone (**69**), licoflavone A (**70**), apigenin (**71**) and isokaempferide (**72**) (Table 12) were isolated from the roots of *Glycyrrhiza uralensis* and evaluated regarding their capacity to inhibit human PTP1B (Li et al. 2010). The most active flavonoid was glisoflavone (**68**), a mixed-type inhibitor with an IC_{50} value of 27.9 ± 1.4 μM. By comparing this isoflavone with glycyrrhisoflavone (**67**) (IC_{50} = 58.7 ± 1.4 μM), it is observed that the replacement of an -OH group by a –OCH_3 group at 5-position of A ring improves the inhibition of PTP1B. The cyclization of glycyrrhisoflavone (**67**), giving cycloglyrrhisoflavone (**69**), significantly reduced the inhibitory activity of flavonoids since this isoflavone presented less than 30% of PTP1B inhibition at 100 μM. Regarding the inhibitory effect of flavones licoflavone A (**70**), apigenin (**71**) and isokaempferide (**72**), the most active compound was licoflavone A, with an IC_{50} value of

Table 6. PTP1B inhibition by flavonoids tested by Cui et al (Cui et al. 2006).

Flavonoid	Structure	IC_{50} (μM ± SD)
Sanggenon G (**17**)		**1.6 ± 0.3**
Kwanon L (**18**)		16.9 ± 1.1
Positive Control RK-682		4.5 ± 0.5

54.5 ± 2.1 μM. These results highlight the importance of the prenylation of flavonoids, as well as the unfavorable effect of the hydroxylation at 5-position of A ring for this specific biologic activity.

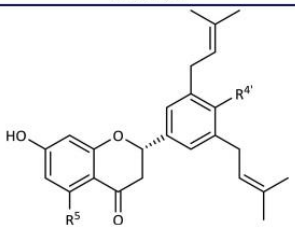
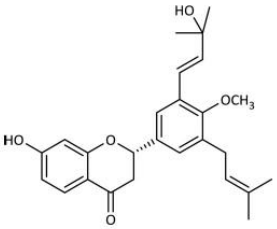
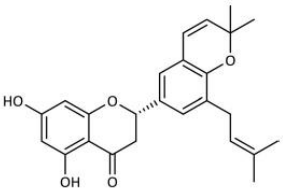
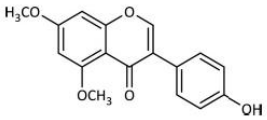
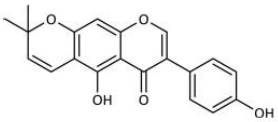
Nguyen et al. (2011) tested the inhibition of PTP1B of 13 flavonoids (Table 13). Among the tested flavonoids, isoflavanones erythribyssin E (**73**) and erythribyssin J (**75**), as well as the flavanone **64**, were the most promising inhibitors of PTP1B. These compounds bear a prenyl and a -OCH_3 group in B ring. The importance of prenylation or methoxylation of flavonoids can also be seen by comparing abyssinone II (**77**) (IC_{50} = 29.2 ± 2.7 μM) and liquiritigenin 5′-*O*-methyl ether (**79**) (IC_{50} = 98.1 ± 11.3 μM) with liquiritigenin (**78**) (IC50 = > 100 μM). However, it can also be seen that the presence of a prenyl group at 3′-position of B ring is more favorable for PTP1B inhibition than the presence of a -OCH_3 group at this position. As mentioned above (Cui et al. 2010), the prenylation at 5′-position of B ring has also a significant role for the enhancement of the enzyme's inhibition as it can be observed by the inhibitory activity of 5-deoxyabyssinin II (**35**) and flavanone **64**, with IC_{50} values of 19.2 ± 1.4 μM and 16.5 ± 1.1 μM, respectively. Interestingly, flavanone **64** was also studied by Cui et al (Cui et al. 2010), and presented a similar IC_{50} value (18.3 ± 1.6 μM). On the other hand, the aldehyde group and the 3-hydroxy-2,2-methylpyrano ring, found in erythribyssin K (**76**) and erythribyssin I (**83**), respectively, are not beneficial for the effect under study.

The capacity of some isoflavones and isoflavanones (Table 14) to inhibit PTPB was evaluated by Nguyen et al. (2012). The best inhibitor was erythraddison III (**87**), presenting an IC_{50} value of 4.6 ± 0.3 μM. As already mentioned above, the presence of prenyl and -OCH_3 groups in B ring is crucial for the inhibition of the enzyme under study. However, cyclization between the prenyl group with an –OH to form the 2,2-dimethylpyrano ring on the B ring, flavonoid erythraddison IV (**88**) (IC_{50} = 13.8 ± 1.8 μM), reduced the inhibitory activity even though a -OCH_3 was presented at 2′-position of B ring. Echrenon b10 (**89**), with one prenyl at 8-position of A ring, a -OH group at 5-position of the same ring, and a 1-hydroxy-1-methyldihydrofuran moiety fused at 6- and 7-positions of the A ring, exhibited higher activity than erythraddison I (**84**). This reduction in PTP1B inhibition showed by erythraddisson I (**84**) might be due to the lack of a prenyl group at 8-position of A ring, which was substituted by a polar group, and also to the different structural fused ring at 6 and 7 positions. Moreover, the presence of a conjugated -OH group at 5-position of A ring may also be responsible for this decrease. To conclude the remarks on structure-activity relationship, it was once again verified that the lack of lipophilic groups in the flavonoid structure, the cyclization, and/or modification of the prenyl moiety showed to have an important role in the reduction of PTP1B inhibition by the flavonoids under study.

Several constituents were isolated from *Artemisia capillaris*, including flavonoids (Table 15), and their inhibitory activity against PTP1B was studied (Islam et al. 2013). The most active flavonoid found was quercetin (**3**), which presented an IC_{50} value of 20.35 ± 7.56 μM. Nevertheless, the substitution of the -OH group of quercetin (**3**) by a galactose significantly decreased the inhibition of PTP1B as hyperoside (**93**) was not active. Interestingly, by comparing quercetin (**3**) with isorhamnetin (**92**), it was observed that the presence of -OCH_3 group in replacement of an -OH group at 3′-position of B ring reduced the effect under study. Regarding isorhamnetin (**92**), it was observed that its two glycosides, isorhamnetin 3-glucoside (**94**) and isorhamnetin 3-robinbioside (**95**), were not active at the tested concentrations. Taking that into account, glycosylation of flavonoids is not favorable for the inhibition of PTP1B.

In the study of Sun and coworkers (Sun et al. 2013), a series of 5,7-dihydroxyflavanones derivatives substituted in the B ring with halogens (–F, –Cl and –Br) or alkoxyl group, was designed and synthesized (Table 16). The flavonoids with best inhibitory activity against PTP1B were **99** (2.66 ± 0.23 μM), **107** (IC_{50} = 2.37 ± 0.37 μM) and **103** (IC_{50} = 2.40 ± 0.22 μM). Comparing flavonoid **99** with flavonoids **97** (IC_{50} = 9.06 ± 2.12 μM) and **98** (IC_{50} = 7.98 ± 0.91 μM), it seems that the presence of a fluorine substituent at 4′-position of B ring is more favorable for the intended effect than its presence at 2′- or 3′- positions of B ring. The high activity of flavonoids **107** and **103** also suggests that the –CF_3 group at 3′-position or –Cl substitution at 2′- and 4′-positions of B ring increases the inhibition of the enzyme under study. Both flavanones were better inhibitors than the positive control ursolic acid, which presented an IC_{50} value of 3.20 ± 0.31 μM. Furthermore, compound **107**, a competitive inhibitor, showed a 3.7-fold higher selectivity for PTP1B than for T-cell protein tyrosine phosphatase (TCPTP) and could cross the cellular membrane. TCPTP has high homology (74% amino acids sequence) but clearly fulfill different biological functions. TCPTP is a phosphatase abundantly

Table 7. PTP1B inhibition by flavonoids tested by Na et al (Na et al. 2006).

Flavonoid	Structure	$R^{4'}$	R^5	IC_{50} (μM ± SD)
Abyssinone IV 4′-methyl ether (**19**)		OCH_3	H	21.2 ± 1.6
Abyssinone V 4′-methyl ether (**20**)		OCH_3	OH	26.3 ± 1.5
Abyssinone V (**21**)		OH	OH	39.7 ± 2.5
Abyssinone IV (**22**)		OH	H	**16.0 ± 1.1**
23		–	–	>60
Sigmoidin E (**24**)		–	–	39.2 ± 1.9
25		–	–	>60
Alpinumisoflavone (**26**)		–	–	41.5 ± 2.4
Positive Control		–	–	4.5 ± 0.5
RK-682				3.6 ± 0.2
Ursolic acid				

expressed in hematopoietic cells and is implicated in the regulation of T-cell activation. As such, simultaneous inhibition of PTP1B and TCPTP is unsuitable, and selective inhibition of PTP1B over TCPTP is one of the most challenging aspects on drug discovery, due to their high homology (Li, Wang, and Shi 2016).

Concerning the structure-activity relationship, it seems that B ring of flavanones might be important for the inhibition of PTP1B, since pinocembrin (**108**), with no substituents in B ring, was the weakest inhibitor (IC_{50} = 36.73 ± 7.16 μM). It was also found that the position of the substituent on the B ring significantly influenced the PTP1B inhibition, with an activity order of *para*-F > *meta*-F > *ortho*-F for fluorinated flavonoids; *para*-Br > *ortho*-Br > *meta*-Br for brominated flavonoids; and 2′,4′-Cl > *para*-Cl ≈ *meta*-Cl > *ortho*-Cl for chlorinated compounds. Moreover, compound **107**, trifluorinated at 3′-position of B ring, (IC_{50} = 2.37 ± 0.37 μM) was around 6-fold more active than the flavonoid **109**, methylated at 4′-position of B ring (IC_{50} = 14.09 ± 1.38 μM). These results suggest that increasing the lipophilicity moiety of the B ring enhanced the ability of flavonoids to inhibit PTP1B.

PTP1B inhibition of vitexin (**111**), isovitexin (**112**) and apigenin (**71**) was evaluated (Table 17), presenting IC_{50} values of 7.62 ± 0.21 μM, 17.76 ± 0.53 μM and 24.76 ± 2.17 μM, respectively (Choi, Islam, Ali, Kim, Kim, et al. 2014). Interestingly, in this study it was concluded that glycosylation at 8- or at 6-position of A ting leads to an increase in PTP1B inhibition, by comparing with the hydroxylation present in apigenin (**71**). Quercetin (IC_{50} = 81.15 ± 3.85 μM) and ursolic acid (IC_{50} = 5.99 ± 0.22 μM) were used as positive controls.

Choi, Islam, Ali, Kim, Park, et al. (2014) studied the inhibitory activity of luteolin (**113**), isoorientin (**114**) and

Table 8. PTP1B inhibition by flavonoids tested by Cui et al (Cui et al. 2007).

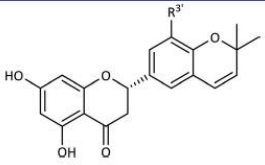
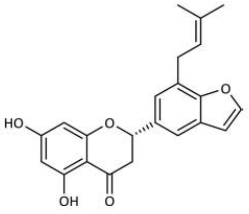
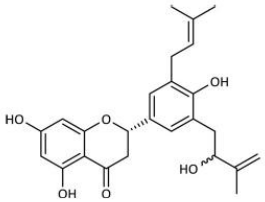
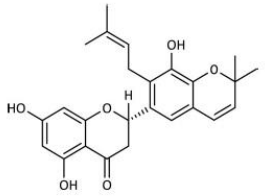
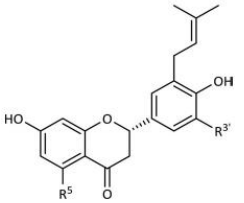
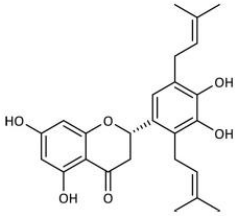
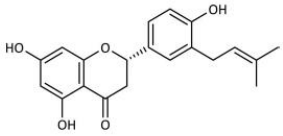
Flavonoid	Structure	$R^{3'}$	R^5	IC_{50} (μM ± SD)
Abyssinoflavanone V (**27**)		H	–	>60
Sigmoidin C (**28**)		OH	–	>60
Abyssinin I (**29**)		OCH_3	–	18.2 ± 1.4
Abyssinoflavanone VI (**30**)		–	–	18.9 ± 1.9
Abyssinoflavanone VII (**31**)		–	–	15.7 ± 0.4
Sigmoidin F (32)		–	–	**14.2 ± 1.7**
Sigmoidin B (**33**)		OH	OH	19.4 ± 2.3
Abyssinin II (**34**)		OCH_3	OH	17.3 ± 1.4
5-Deoxyabyssinin II (**35**)		OCH_3	H	19.2 ± 1.1
Sigmoidin A (**36**)		–	–	**14.4 ± 0.8**
3′-Prenylnaringenin (**37**)		–	–	26.7 ± 1.2
Positive Control		–	–	4.5 ± 0.5
RK-682				3.6 ± 0.2
Ursolic acid				

Table 9. PTP1B inhibition by flavonoids tested by Cui et al (Cui et al. 2008).

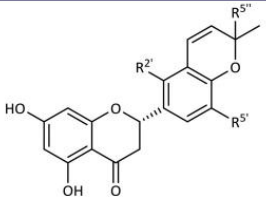
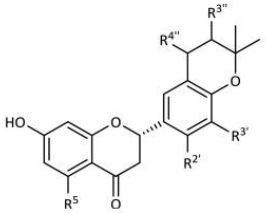
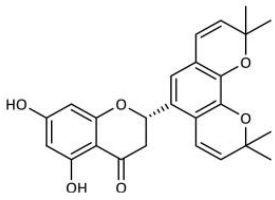
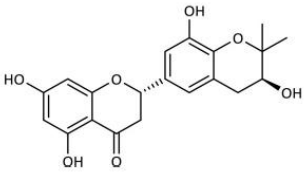
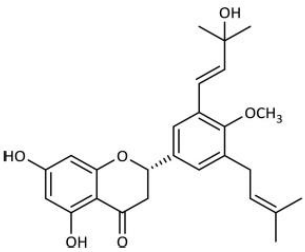
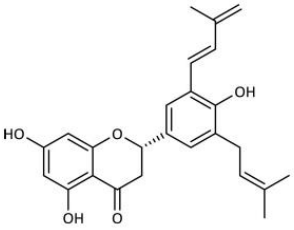
Flavonoid	Structure	$R^{2'}$	$R^{3'}$	$R^{3''}$	$R^{4''}$	R^{5}	$R^{5'}$	$R^{5''}$	IC_{50} (μM ± SD)
38		prenyl	–	–	–	–	OH	CH_3	**13.9 ± 2.1**
39		H	–	–	–	–	OH	CH_2OH	>60
40		H	–	–	–	–	OCH_3	CH_2OH	17.9 ± 1.7
41		H	prenyl	OH	H	OH	–	–	**14.9 ± 1.6**
42		H	OCH_3	OH	H	OH	–	–	18.2 ± 2.1
43		H	H	OH	OH	OH	–	–	>60
44		H	prenyl	OH	OH	OH	–	–	19.0 ± 1.8
45		prenyl	OH	OH	OH	OH	–	–	18.2 ± 1.2
46		H	OH	H	=O	OH	–	–	>60
47		H	OH	OH	H	H	–	–	>60
48		H	OH	OH	OH	H	–	–	>60
Sigmoidin G (**49**)		H	OH	OH	OH	OH	–	–	>60
50		–	–	–	–	–	–	–	>60
Sigmoidin D (**51**)		–	–	–	–	–	–	–	>60
Buttinone (**52**)		–	–	–	–	–	–	–	18.9 ± 1.3
Burttinonedehydrate (**53**)		–	–	–	–	–	–	–	21.6 ± 2.1
Positive control	–	–	–	–	–	–	–	–	4.7 ± 0.5
RK-682									3.6 ± 0.2
Ursolic acid									

Table 10. PTP1B inhibition by flavonoids tested by Jang et al (Jang et al. 2008).

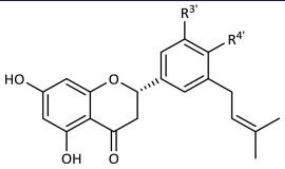
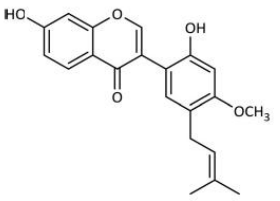
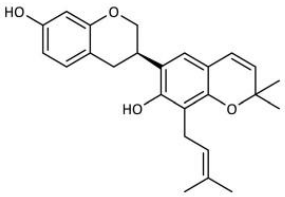
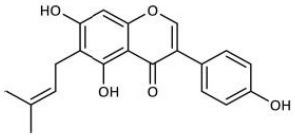
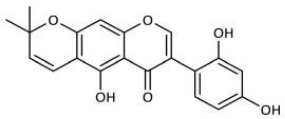
Flavonoid	Structure	$R^{3'}$	$R^{4'}$	IC_{50} (μM ± SD)
Abyssinin II (**34**)		OCH_3	OH	40.5 ± 1.9
54		H	OCH_3	29.6 ± 2.5
55		–	–	21.3 ± 1.3
56		–	–	**5.5 ± 0.3**
Erythrinin B (**57**)		–	–	>100
Parvisoflavone B (**58**)		–	–	42.6 ± 2.4
Positive Control		–	–	4.5 ± 0.5
RK-682				3.6 ± 0.2
Ursolic acid				

Table 11. PTP1B inhibition by flavonoids tested by Cui et al (Cui et al. 2010).

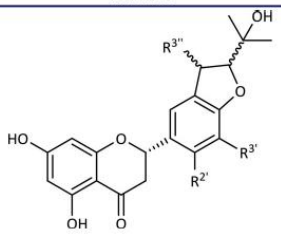
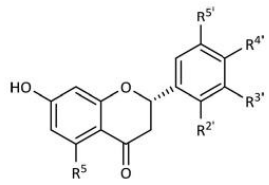
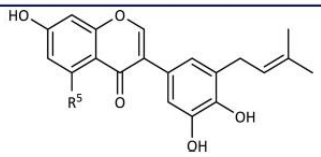
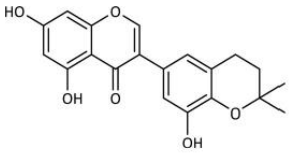
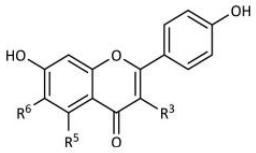
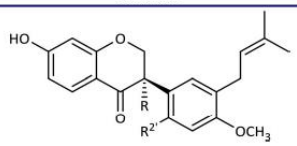
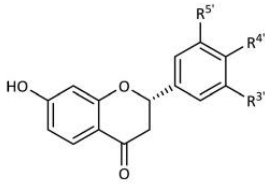
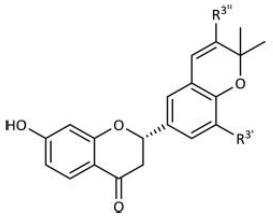
Flavonoid	Structure	$R^{2'}$	$R^{3'}$	$R^{3''}$	$R^{4'}$	R^{5}	$R^{5'}$	IC_{50} (μM ± SD)
59		H	prenyl	H	–	–	–	**15.2 ± 1.2**
60		H	prenyl	OH	–	–	–	**17.9 ± 2.6**
61		H	OCH_3	H	–	–	–	**16.1 ± 1.1**
62		H	OH	H	–	–	–	>60
63		H	OH	OH	–	–	–	>60
64		prenyl	OH	OH	–	–	–	18.3 ± 1.6
65		H	OH	–	OCH_3	H	prenyl	**16.2 ± 1.1**
66		prenyl	prenyl	–	OH	OH	OH	19.6 ± 2.3
Positive Control		–	–	–	–	–	–	4.7 ± 0.5
RK-682								

Table 12. PTP1B inhibition by flavonoids tested by Li et al (Li et al. 2010).

Flavonoid	Structure	R^3	R^5	R^6	IC_{50} (μM ± SD)
Glycyrrhisiflavone (**67**)		–	OH	–	58.7 ± 1.4
Glisoflavone (**68**)		–	OCH_3	–	**27.9 ± 1.4**
Cycloglyrrhisoflavone (**69**)		–	–	–	<30 % $^{100\,\mu M*}$
Licoflavone A (**70**)		H	H-	prenyl	54.5 ± 2.1
Apigenin (**71**)		H	OH	H	<30 % $^{100\,\mu M*}$
Isokaempferide (**72**)		OCH_3	OH	H	<30 % $^{100\,\mu M*}$
Positive Control RK-682	–	–	–	–	4.4 ± 0.1

*Less than 30% of inhibitory activity at the highest tested concentration (100 μM).

Table 13. PTP1B inhibition by flavonoids tested by Nguyen et al (Nguyen et al. 2011).

Flavonoid	Structure	R	$R^{2'}$	$R^{3'}$	$R^{3''}$	$R^{4'}$	$R^{5'}$	IC_{50} (μM ± SD)
Erythribyssin E (**73**)		H	OCH_3	–	–	–	–	**15.2 ± 0.9**
Prostatol C (**74**)		H	OH	–	–	–	–	17.2 ± 1.6
Erythribyssin J (**75**)		OH	OH	–	–	–	–	**14.9 ± 1.6**
5-Deoxyabyssinin II (**35**)		–	–	OCH_3	–	OH	prenyl	19.2 ± 1.4
64		–	–	OH	–	OCH_3	prenyl	**16.5 ± 1.1**
Erythribyssin K (**76**)		–	–	CHO	–	OH	H	>100
Abyssinone II (**77**)		–	–	prenyl	–	OH	H	29.2 ± 2.7
Liquiritigenin (**78**)		–	–	H	–	OH	H	>100
Liquiritigenin 5'-methyl ether (**79**)		–	–	OCH_3	–	OH	H	98.1 ± 11.3
80		–	–	H	H	–	–	72.9 ± 9.7
81		–	–	prenyl	H	–	–	22.6 ± 2.3
Erythribyssin G (**82**)		–	–	prenyl	OH	–	–	35.8 ± 5.2
Erythribyssin I (**83**)		–	–	H	OH	–	–	>100
Positive Control Ursolic acid	–	–	–	–	–	–	–	3.6 ± 0.2

orientin (**115**) (Table 18) against human PTP1B. Contrary to what was described for apigenin (**71**) (Choi, Islam, Ali, Kim, Kim, et al. 2014), glycosylation of luteolin (**115**) at either 6- or 8-position of A ring, seems to decrease the inhibition of the enzyme. Thus, the IC_{50} value found for luteolin (**113**) was 6.70 ± 0.03 μM, while isoorientin (**114**) and orientin (**115**) showed IC_{50} values of 24.54 ± 0.48 μM and 57.11 ± 0.69, respectively. By the obtained results, the effect seems to be more pronounced in the case of glycosylation at 6-position compared to 8-position of A ring. Luteolin (**113**) presented better activity than the positive control ursolic acid (IC_{50} = 8.20 ± 0.55 μM).

The inhibition of PTP1B of lavandulyl flavonoids isolated from the roots of *Sophora flavescens*: norkurarinone (**116**), kurarinone (**117**), 2′-methoxykurarinone (**118**) and kushenol T (**119**) was studied (Table 19) (Sasaki et al. 2014). The

Table 14. PTP1B inhibition by flavonoids tested by Nguyen et al (Nguyen et al. 2012).

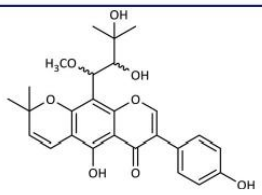
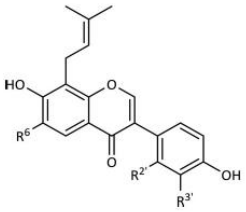
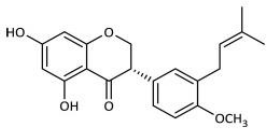
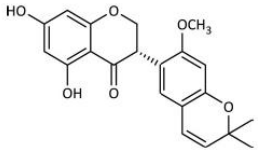
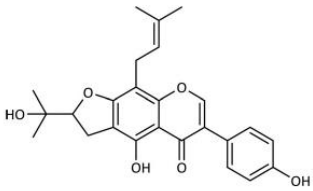
Flavonoid	Structure	$R^{2'}$	$R^{3'}$	R^{6}	IC_{50} (μM ± SD)
Erythraddison I (**84**)		–	–	–	>30
Erythraddison II (**85**)		OH	H	prenyl	17.4 ± 1.1
Erysubin F (**86**)		H	prenyl	H	7.8 ± 0.5
Erythraddison III (87)		–	–	–	**4.6 ± 0.3**
Erythraddison IV (**88**)		–	–	–	13.8 ± 1.8
Echrenon b10 (**89**)		–	–	–	24.2 ± 2.1
Positive Control RK-682	–	–	–	–	3.6 ± 0.2

Table 15. PTP1B inhibition by flavonoids tested by Islam et al (Islam et al. 2013).

Flavonoid	Structure	$R^{2'}$	R^{3}	$R^{4'}$	$R^{5'}$	R^{6}	R^{7}	IC_{50} (μM ± SD)
Quercetin (3)		H	OH	OH	OH	H	OH	**20.35 ± 7.56**
Arcapillin (**90**)		OH	H	OH	OCH_3	OCH_3	OCH_3	86.67 ± 4.12
Cirsilineol (**91**)		H	H	OH	OCH_3	OCH_3	OCH_3	206.78 ± 58.12
Isorhamnetin (**92**)		H	OH	OH	OCH_3	H	OH	43.88 ± 2.26
Hyperoside (**93**)		H	galactose	OH	OH	H	OH	NA
Isorhamnetin 3-glucoside (**94**)		H	glucose	OH	OCH_3	H	OH	NA
Isorhamnetin 3-robinbioside (**95**)		H	robinbiose	OH	OCH_3	H	OH	NA
Linarin (**96**)		H	H	H	OCH_3	H	rutinose	NA
Positive Control Ursolic acid	–	–	–	–				3.6 ± 0.2

NA - not active.

flavonoid with best inhibitory activity was 2′-methoxykurarinone (**118**), with an IC_{50} value of 5.26 ± 0.24 μM, being a similar value found for the positive control RK-682 (IC_{50} = 4.49 ± 0.15 μM). The presence of a -OCH_3 group at 2′-position of B ring appears to play an important role for PTP1B inhibition, since kurarinone (**117**) (IC_{50} = 41.68 ± 0.11 μM), which is hydroxylated at this position, presented a reduced capacity to inhibit the enzyme under study. Norkurarinone (**116**), kurarinone (**117**) and 2′-methoxykurarinone (**118**) also exhibited different selectivity against four homologous protein tyrosine phosphatases and increased the insulin-stimulated Akt phosphorylation level in human HepG2 cells.

Table 16. PTP1B inhibition by flavonoids tested by Sun et al (Sun et al. 2013).

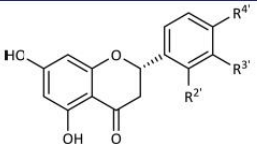
Flavonoid	Structure	$R^{2'}$	$R^{3'}$	$R^{4'}$	IC_{50} (μM ± SD)
97		F	H	H	9.06 ± 2.12
98		H	F	H	7.98 ± 0.91
99		H	H	F	**2.66 ± 0.23**
100		Cl	H	H	10.23 ± 2.45
101		H	Cl	H	4.18 ± 0.94
102		H	H	Cl	3.60 ± 0.41
103		Cl	H	Cl	**2.40 ± 0.22**
104		Br	H	H	4.90 ± 0.98
105		H	Br	H	7.33 ± 1.25
106		H	H	Br	3.48 ± 0.19
107		H	CF_3	H	**2.37 ± 0.37**
Pinocembrin (**108**)		H	H	H	36.73 ± 7.16
109		H	H	CH_3	14.09 ± 1.38
110		H	H	OCH_3	13.12 ± 1.25
Positive control Ursolic acid	–	–	–	–	3.20 ± 0.31

Table 17. PTP1B inhibition by flavonoids tested by Choi et al (Choi, Islam, Ali, Kim, Kim, et al. 2014).

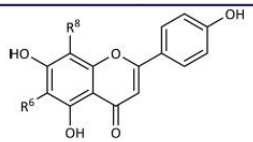
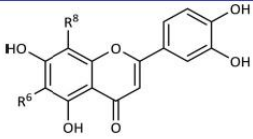
Flavonoid	Structure	R^6	R^8	IC_{50} (μM ± SD)
Apigenin (**71**)		H	H	24.76 ± 2.17
Vitexin (**111**)		H	glucose	**7.62 ± 0.21**
Isovitexin (**112**)		glucose	H	17.76 ± 0.53
Positive control	–	–	–	81.15 ± 3.85
Quercetin				5.99 ± 0.22
Ursolic acid				

Table 18. PTP1B inhibition by flavonoids tested by Choi et al (Choi, Islam, Ali, Kim, Park, et al. 2014).

Flavonoid	Structure	R^6	R^8	IC_{50} (μM ± SD)
Luteolin (**113**)		H	H	**6.70 ± 0.03**
Isoorientin (**114**)		glucose	H	24.54 ± 0.48
Orientin (**115**)		H	glucose	57.11 ± 0.69
Positive control Ursolic acid	–	–	–	8.20 ± 0.55

Flavonoids from *Anoectochilus chapaensis* were evaluated regarding their ability to inhibit PTP1B (Table 20) (Cai, Zhao, and Tao 2015). As observed above, the presence of a -OCH_3 group at 3′-position of B ring, in substitution of an -OH group, increases the PTP1B inhibition by comparing quercetin (**3**) with isorhamnetin (**92**), which presented IC_{50} values of 5.63 ± 0.04 μM and 1.75 ± 0.02 μM, respectively. It was not found a significant difference in inhibitory activity of glycosylated flavonoids at 3-position of C ring by observing IC_{50} values of isorhamnetin 3-glucoside (**94**) (IC_{50} = 1.16 ± 0.03 μM) and isorhamnetin 3-rutinoside (**120**) (IC_{50} = 1.20 ± 0.05 μM).

A series of isoflavones (**121** − **125**), flavones (**70** and **126** − **128**), flavanones (**78** and **129**), and a isoflavan (**130**) (Table 21) were studied by Guo et al (Guo et al. 2015) concerning their inhibitory inhibition against PTP1B. Among the tested compounds, isoflavones and flavanones were weak inhibitors, with IC_{50} values higher than 100 μM. Regarding the group of flavones, the best inhibitor was licoflavone B (**128**) (IC_{50} = 15.62 μM), followed by licoflavone C (**127**) (IC_{50} = 46.43 μM), being licoflavone B most active than the positive control $NaVO_4$ (IC_{50} = 29.10 μM). Two prenyl groups at 3′-position of B ring and at 6-position of A ring in the flavonoid structure seem to increase PTP1B inhibition, by comparing licoflavone B (**128**) with licoflavone A (**70**) (IC_{50} = > 100 μM).

Flavanone naringin (**131**), isoflavone puerarin (**132**) and flavan euonymalatus (**133**) (Table 22) were isolated *from Euonymus alatus* and their capacity to inhibit PTP1B was evaluated (Jeong et al. 2015). Naringin (**131**) and puerarin (**132**), both glycosylated, had IC_{50} values higher than 30 μM. On the other hand, flavan euonymalatus (**133**), a noncompetitive inhibitor, presented an IC_{50} value of 13.7 ± 0.2 μM.

Inhibition of PTP1B was tested on flavonoids isolated from *Hypericum scabrum*: 3,8″-bisapigenin (**134**), quercetin (**3**), peltatoside (**135**), quercetrin (**5**), isoquercetin (**136**), hyperoside (**93**), (−)-epicatechin (**137**) and (+)-catechin (**138**) (Table 23) (Jiang et al. 2015). As described before (Islam et al. 2013), glycosylation at 3-position of C ring appears not to be favorable for the intended effect as

Table 19. PTP1B inhibition by flavonoids tested by Sasaki et al (Sasaki et al. 2014).

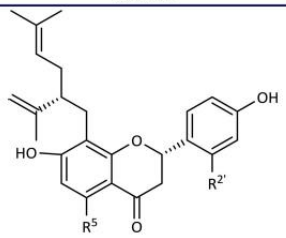
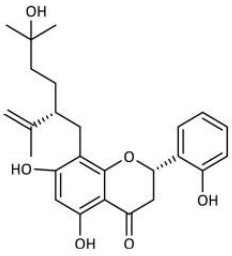
Flavonoid	Structure	$R^{2'}$	R^5	IC_{50} (μM ± SD)
Norkurarinone (**116**)		OH	OH	28.94 ± 0.23
Kurarinone (**117**)		OH	OCH_3	41.68 ± 0.11
2′-Methoxykurarinone (**118**)		OCH_3	OCH_3	**5.26 ± 0.24**
Kushenol T (**119**)		–	–	49.59 ± 0.16
Positive control RK-682	–	–	–	4.49 ± 0.15

Table 20. PTP1B inhibition by flavonoids tested by Cai et al (Cai, Zhao, and Tao 2015).

Flavonoid	Structure	R^3	$R^{3'}$	IC_{50} (μM ± SD)
Quercetin (**3**)		OH	OH	5.63 ± 0.04
Isorhamnetin (**92**)		OH	OCH_3	1.75 ± 0.02
Isorhamnetin 3-glucoside (**94**)		glucose	OCH_3	**1.16 ± 0.03**
Isorhamnetin 3-rutinoside (**120**)		rutinose	OCH_3	**1.20 ± 0.05**
Positive control Suramin	–	–	–	11 ± 1

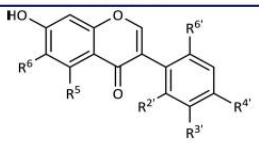
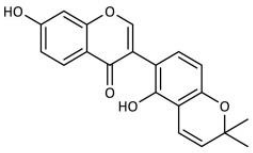
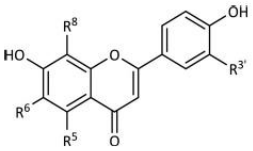
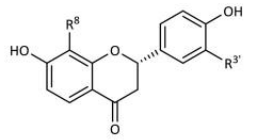
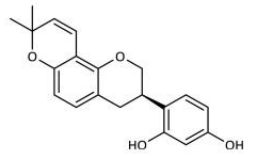
compared to hydroxylation at this position, since glycosylated flavonoids (**135**, **136**, **93**, and **5**) were weak inhibitors ($IC_{50} = > 50$ μM) and quercetin (**3**) presented an IC_{50} value of 2.19 ± 0.2 μM. Flavans, (−)-epicatechin (**137**) and (+)-catechin (**138**), were also effective PTP1B inhibitors, presenting similar IC_{50} values: 2.03 ± 0.1 μM and 2.16 ± 0.1 μM, respectively. It was also observed that the PTP1B inhibitor used as positive control had an IC_{50} value (1.97 ± 0.5 μM) comparable to the ones found for quercetin (**3**), (−)-epicatechin (**137**) and (+)-catechin (**138**).

Glycosylated flavonoids were tested regarding their ability to inhibit human PTP1B (Table 24) (Li et al. 2015). Among the tested flavonoids – isoquercetin (**136**), hyperoside (**93**), cynaroside (**139**) and guaijaverin (**140**) - only isoquercetin (**136**) inhibited PTP1B, with an IC_{50} value of 17.49 ± 3.31 μg/mL. This suggests that the presence of galactose at 3-position of C ring is more important for the intended activity than the presence of glucose or arabinose at this position. Interestingly, in the study of Jiang et al. (2015), isoquercetin (**136**) was a weak inhibitor of PTP1B ($IC_{50} > 50$ μM). These different results can be justified by the different experimental conditions applied, such as the times of incubation, as well as the concentrations of PTP1B and *p*NPP used.

The inhibitory effect of biflavonoids against PTP1B was tested by Nguyen and colleagues (Nguyen et al. 2015) (Table 25). 3,8″-Bisapigenin (**134**) was the most active compound, presenting an IC_{50} value of 4.5 ± 0.1 μM, like the values found for positive controls ursolic acid ($IC_{50} = 3.4 \pm 0.1$ μM) and RK-682 ($IC_{50} = 4.5 \pm 0.2$ μM). By the obtained results, it was suggested that the linkage of two apigenin structures is more favorable for PTP1B inhibition at 3-position of C ring and at 8″-position of A ring. The linkage of two apigenin structures at other positions led to a decrease in the inhibitory activity, as observed for amentoflavone (**142**) ($IC_{50} = 7.4 \pm 0.5$ μM), flavonoids **143** ($IC_{50} = 6.2 \pm 0.1$ μM) and **144** ($IC_{50} = 9.6 \pm 0.3$ μM).

The evaluation of inhibition of PTP1B by flavonoids isolated from the roots of *Cudrania tricuspidata* was performed by Quang et al. (2015) (Table 26). Cudraflavanone D (**149**) had an IC_{50} value of 5.7 ± 1.5 μM, suggesting that the presence of more lipophilic substituents, such as prenyl groups at 5′-position of B ring and at 6-position of A ring, is beneficial for the intended effect. For example,

Table 21. PTP1B inhibition by flavonoids tested by Guo et al (Guo et al. 2015).

Flavonoid	Structure	$R^{2'}$	$R^{3'}$	$R^{4'}$	R^5	R^6	R^8	IC_{50}
Genistein (**121**)		H	H	OH	OH	H	–	>100
Formononetin (**122**)		H	H	OCH_3	H	H	–	>100
Eurycarpin A (**123**)		OH	prenyl	OH	H	H	–	>100
Luteone (**124**)		OH	H	OH	OH	prenyl	–	>100
Glabrone (**125**)		–	–	–	–	–	–	>100
Licoflavone A (**70**)		–	H	–	H	prenyl	H	>100
126		–	H	–	H	H	H	>100
Licoflavone C (**127**)		–	H	–	OH	H	prenyl	46.43
Licoflavone B (128)		–	prenyl	–	H	prenyl	H	**15.62**
Liquiritigenin (**78**)		–	H	–	–	–	H	>100
Glabrol (**129**)		–	prenyl	–	–	–	prenyl	>100
Glabridin (**130**)		–	–	–	–	–	–	>100
Positive control $NaVO_4$	–	–	–					29.10

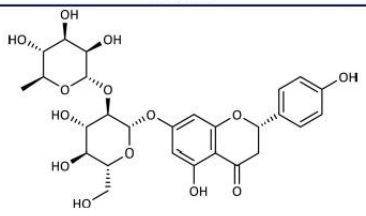
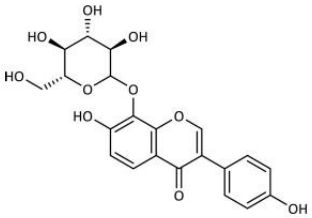
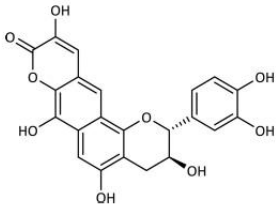
dihydrokaempferol (**146**) and steppogenin (**147**), which are only substituted with -OH groups, and cudraflavanone B (**148**), which has -OH groups and only one prenyl group at 6-position of A ring, were not active. Cudraflavone C (**151**) and kwanon C (**152**) presented IC_{50} values of 9.4 ± 2.9 μM and 13.6 ± 3.3 μM, respectively, and it seems that the second prenyl group is slightly more important for the intended effect at 6-position of A ring than at 8-position of the same ring.

Flavonoids isolated from *Morus laevigata* were tested regarding their capacity to inhibit PTP1B activity (Table 27) (Wang et al. 2015). The most active compound was hultenin (**154**), with an IC_{50} value of 1.04 ± 0.16 μM, being a better inhibitor than the positive control, oleanolic acid (IC_{50} = 2.98 ± 0.35 μM). The replacement of an -OH group by a $-OCH_3$ group at 3-position of C ring increase PTP1B inhibition, by comparing hultenin (**154**) with taxifolin (**153**) (IC_{50} = 5.30 ± 0.63 μM).

Wu et al (Wu et al. 2015) evaluated the inhibitory activity of flavonoids isolated from *Ficus tikoua* against human PTP1B (Table 28). Alpinumisoflavone (**26**) was the best inhibitor (IC_{50} = 11.16 ± 1.88 μM), indicating that the pyrano ring linked at 6- and 7-positions of A ring of the isoflavone structure enhances the inhibitory activity. This effect can be confirmed by comparing alpinumisoflavone (**26**) with derrone (**157**) (IC_{50} = 24.64 ± 0.57 μM), which has the pyrano ring linked at 7- and 8-positions of A ring. Moreover, the presence of a prenyl group at 3′-position of B ring and the replacement of an -OH group for a $-OCH_3$ group at 4′-position of B ring seems to lead to an increase of PTP1B inhibition, since 3′-(3-methylbut-2-enyl)biochanin A (**160**) (IC_{50} = 18.55 ± 0.74 μM) was a better inhibitor than genistein (**121**) (not active).

Glycosylated flavonoids were isolated from *Agrimonia pilosa* (Table 29) and their inhibitory activity against PTP1B was evaluated by Na et al. (2016). The presence of an -OH group at 3-position of C ring in replacement of a rhamnose at this position led to a decrease in the effect under study, as it can be seen by comparing kaempferol (**164**) (IC_{50} = 42.93 ± 2.36 μM) with afzelin (**7**) (IC_{50} = 12.16 ± 0.02 μM). In addition, tiriloside (**162**) was a weak inhibitor, with an IC_{50} value higher than 50 μM, suggesting that a 6′′-*p*-coumaroyl glucose at 3-position of C ring does not have a beneficial effect for PTP1B inhibition, by comparing this

Table 22. PTP1B inhibition by flavonoids tested by Jeong et al (Jeong et al. 2015).

Flavonoid	Structure	IC_{50} (μM ± SD)
Naringin (**131**)		>30
Puerarin (**132**)		>30
Euonymalatus (133)		**13.7 ± 0.2**
Positive control RK-682	–	4.5 ± 0.1

compound with afzelin (**7**) and kaempferol (**164**). In addition, the presence of a glucose at 3-position of C ring is more favorable for PTP1B inhibition than the presence of a glucose at 7-position of A ring, since isoquercetin (**136**) (IC_{50} = 27.73 ± 1.54 μM) is more active than quercetin 7-*O*-*β*-D-glucoside (**163**) (IC_{50} > 50 μM).

Wang et al. (2016) studied the PTP1B inhibition by flavonoids from *Flemingia philippinensis* (Table 30). 6,8-Diprenylorobol (**166**) (IC_{50} = 2.4 ± 0.3 μM) was the best inhibitor, with an IC_{50} value about 6-fold lower than the one found for the positive control ursolic acid (IC_{50} = 15.5 ± 0.9 μM). Interestingly, by the obtained results, it can be observed that in this work the presence of an -OH group at 3'position is responsible for an increase in the effect under study, when compared with the presence of a -OCH_3 group or no substitutions at this position. This effect can be observed by comparing 6,8-diprenylrobol (**166**) with flavonoid **168**, with an IC_{50} value of 17.4 ± 0.2 μM, and with 8-*γ*,*γ*-dimethylallylwighteone (**167**), with an IC_{50} value of 9.3 ± 0.7 μM.

The inhibitory activity against human PTP1B by geranylated flavonoids isolated from *Macaranga denticulate* was tested (Table 31) (Zhang et al. 2016). Both bonanniol A (**171**) and bonannione A (**172**) presented a similar ability to inhibit the enzyme under study, with IC_{50} values of 15.2 ± 2.8 μM and 14.0 ± 1.2 μM, respectively. Macarangin (**170**) (IC_{50} = 22.7 ± 4.7 μM) was slightly less active than bonanniol A (**171**) and bonannione A (**172**), indicating that the presence of the C2 = C3 double bond is not essential for the intended effect.

Zhao et al. (2016) evaluated the PTP1B inhibition by flavonoids isolated from the leaves of *Smilax china* (Table 32). Regarding the group of flavones and flavonols, quercetin 4′-*O*-*β*-D-glucoside (**176**) presented the highest inhibitory effect, with an IC_{50} value of 0.92 ± 0.19 μM, which was similar to the IC_{50} value found for the positive control ursolic acid (IC_{50} = 1.21 ± 0.18 μM). Concerning kaempferol (**164**) and kaempferol derivatives, it was observed that a rhamnose at 7-position of A ring significantly contributed for the intended effect in comparison with an -OH group at this position and with the replacement or addition of a rhamnose at 3-position of C ring, since the order of inhibitory activity is kaempferol 7-*O*-α-L-rhamnoside (**175**) > kaempferol (**164**) > kaempferide (**173**) > afzelin (**7**) and kaempferitrin (**9**). In addition, by comparing kaempferol (**164**) (IC_{50} = 42.85 ± 0.73 μM) with morin (**174**) (7.62 ± 0.99 μM), it was seen that the addition of an -OH group at 2′-position of B ring increases the inhibition of human PTP1B.

Regarding the group of isoflavones, the addition of a glucose seems not to be favorable for the intended effect, since both puerarin (**132**) and smilachinin (**180**) were less actives than pratensein (**179**).

PTP1B inhibition by flavonoids from *Morus alba* (Table 33) was evaluated by Huang et al. (2017). By the obtained results, it was possible to found that prenylation at 8-position of A ring has a crucial role in the inhibitory

Table 23. PTP1B inhibition by flavonoids tested by Jiang et al (Jiang et al. 2015).

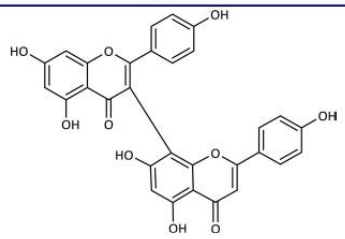
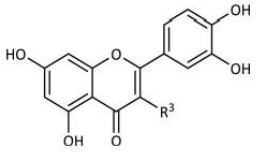
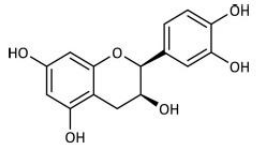
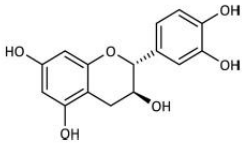
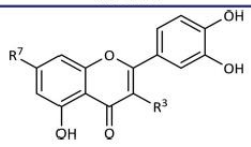
Flavonoid	Structure	R^3	IC_{50} (μM ± SD)
3-8″-Bisapigenin (**134**)		–	>50
Quercetin (3)		OH	**2.19 ± 0.12**
Quercetrin (**5**)		rhamnose	>50
Hyperoside (**93**)		arabinofuranose	>50
Peltatoside (**135**)		glucose	>50
Isoquercetin (**136**)		galactose	>50
(-)-Epicatechin (137)		–	**2.03 ± 0.1**
(+)-Catechin (138)		–	**2.16 ± 0.1**
Positive control 3-(3,5-dibromo-4-hydroxy-benzoyl)-2-ethyl-benzofuran-6-sulfonicacid-(4-(thiazol-2ylsulfamyl)-phenyl)-amide	–	–	1.97 ± 0.5

Table 24. PTP1B inhibition by flavonoids tested by Li et al (Li et al. 2015).

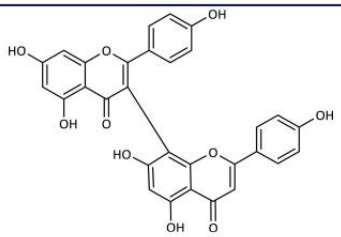
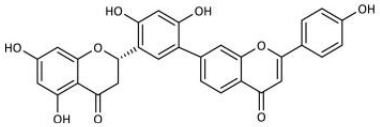
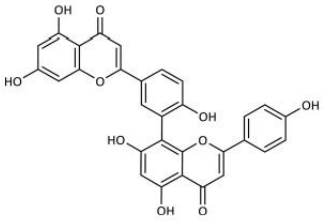
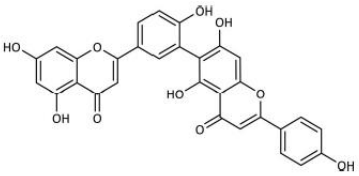
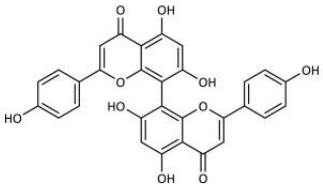
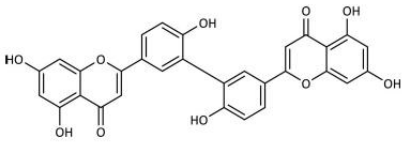
Flavonoid	Structure	R^3	R^7	IC_{50} (μg/mL ± SD)
Hyperoside (**93**)		glucose	OH	NA
Isoquercetin (**136**)		galactose	OH	**17.49 ± 3.31**
Cynaroside (**139**)		H	glucose	NA
Guaijaverin (**140**)		arabinose	OH	NA
Positive control Oleanolic acid	–	–	–	1.17 ± 0.13

NA – not active.

effect, since kwanon C (**152**) presented an IC_{50} value of 2.20 ± 0.83 μM and albanin A (**183**) was not active. Albasin D (**182**), with an IC_{50} value of 3.04 ± 0.67 μM, was also a much better inhibitor than albanin A (**183**), demonstrating that the cyclization at 7- and 8- positions of A ring, without the presence of the –OH at 5-position of the same ring is favorable for this biological activity. The positive control oleanolic acid had an IC_{50} value of 3.31 ± 0.02 μM.

Flavanones naringenin (**181**), prunin (**184**), naringin (**131**) and narirutin (**185**) were tested concerning their capacity to inhibit PTP1B (Table 34) (Jung et al. 2017). Considering the obtained results for these compounds, it was verified that the substitutions at 7-position of A ring have different contribution for the intended effect, since the order of positive influence of these substituents on the flavonoids' inhibitory activity is glucose > rutinose > neohesperidose > OH. Therefore, prunin (**184**), narirutin (**185**), naringin (**131**) and naringenin (**181**) displayed IC_{50} values of 17.5 ± 2.6 μM, 56.5 ± 0.12 μM, 91.8 ± 0.65 μM and 130.1 ± 0.47 μM, respectively.

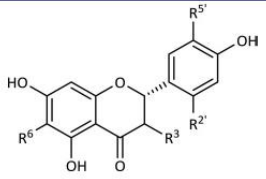
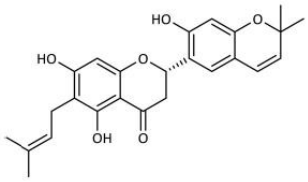
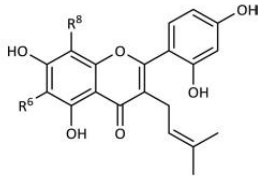
Table 25. PTP1B inhibition by flavonoids tested by Nguyen et al (Nguyen et al. 2015).

Flavonoid	Structure	IC_{50} (μM ± SD)
3-8′′-Bisapigenin (134)		**4.5 ± 0.1**
Selariscinin E (**141**)		9.8 ± 0.6
Amentoflavone (**142**)		7.4 ± 0.5
143		6.2 ± 0.1
144		9.6 ± 0.3
145		5.4 ± 0.2
Positive controls	–	3.4 ± 0.1
Ursolic acid		4.5 ± 0.2
RK-682		

The potential inhibitory activity of flavonoids isolated from *Epimedium koreanum* was studied (Table 35) (Kim et al. 2017). Icaritin (**186**) and icariside II (**187**) exhibited similar activities, with IC_{50} values of 11.59 ± 1.39 μM and 9.94 ± 0.15 μM, respectively. Since the other tested compounds were not active (IC_{50} > 300 μM), it was possible to observe that the presence of an -OH group at 7-position of A ring has an important role for the effect under study, in comparison with the presence of a glucose at this position.

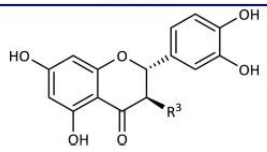
Nguyen et al. (2017) tested the PTP1B inhibition by flavonoids isolated from the aerial parts of *Agrimonia pilosa* (Table 36). Considering the apigenin derivatives, the most effective flavonoid was apigenin 7-*O*-*β*-D-glucuronide (**198**) (IC_{50} = 7.14 ± 1.75 μM), indicating that the glucuronic acid at 7-position of A ring displays a significant role for the inhibition of the enzyme. The same conclusion can be made for kaempferol and luteolin derivatives, since the best inhibitors were kaempferol 7-*O*-*β*-D-glucuronide (**195**) (IC_{50} = 48.34 ± 0.07 μM) and luteolin 7-*O*-*β*-D-glucuronide (**200**)

Table 26. PTP1B inhibition by flavonoids tested by Quang et al (Quang et al. 2015).

Flavonoid	Structure	$R^{2'}$	R^3	$R^{5'}$	R^6	R^8	IC_{50} (μM ± SD)
Dihydrokaempferol (**146**)		H	OH	H	H	–	NA
Steppagenin (**147**)		OH	H	H	H	–	NA
Cudraflavanone B (**148**)		OH	H	H	prenyl	–	NA
Cudraflavanone D (**149**)		OH	H	prenyl	prenyl	–	**5.7 ± 1.5**
Euchrestaflavanone C (**150**)		–	–	–	–	–	12.3 ± 2.2
Cudraflavone C (**151**)		–	–	–	prenyl	H	9.4 ± 2.9
Kwanon C (**152**)		–	–	–	H	prenyl	13.6 ± 3.3
Positive control Ursolic acid	–	–	–	–	–	–	3.8 ± 0.4

NA - not active.

Table 27. PTP1B inhibition by flavonoids tested by Wang et al (Wang et al. 2015).

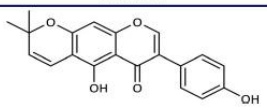
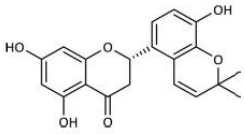
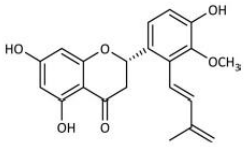
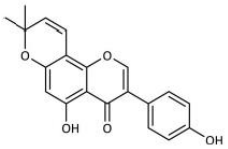
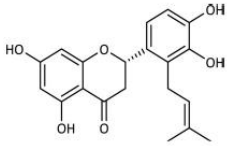
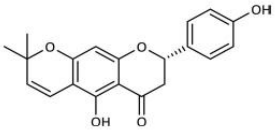
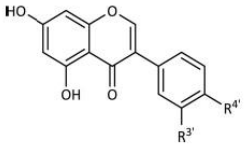
Flavonoid	Structure	R^3	IC_{50} (μM ± SD)
Taxifolin (**153**)		OH	5.30 ± 0.63
Hultenin (**154**)		OCH_3	**1.04 ± 0.16**
Positive control Oleanolic acid	–	–	2.98 ± 0.35

(IC_{50} = 38.08 ± 2.34 μM). Regarding the quercetin derivatives, it was found that the replacement of a glucose at 3-position of C ring or at 3′-position of B ring by an -OH group significantly increases the inhibitory activity, since quercetin (**3**) presented an IC_{50} value of 40.94 ± 0.46 μM, and isoquercetin (**136**) and quercetin 3′-*O*-*β*-D-glucoside (**199**) had an IC_{50} value higher than 100 μM.

Qin et al. (2017) isolated and evaluated the inhibitory activity of flavonoids, from seeds of *Silybum marianum*, against PTP1B (Table 37). Interestingly, from the obtained results, it can be concluded that replacement of an -OH group for an -OCH_3 group at 4′-position of B ring had no effect in PTP1B inhibition, effect seen by comparing taxifolin (**153**) (IC_{50} = 24.23 ± 1.69 μM) with dihydroquercetin 4′-methyl ether (**204**) (IC_{50} = 21.30 ± 2.16 μM). In addition, the replacement of an -OH group for a glucose at 7-position of A ring in the tested flavanones, also did not show any effect in the inhibitory activity under study, since both naringenin (**181**) and prunin (**184**) had an IC_{50} higher than 50 μM. Finally, it was suggested that the C2 = C3 double bond is important for the biological effect under study, since kaempferol (**164**) presented an IC_{50} value of 6.79 ± 0.22 μM and dihydrokaempferol (**146**) of 27.83 ± 1.34 μM. Kaempferol (**164**), the most active compound, was a better inhibitor than the positive control oleanolic acid (IC_{50} = 8.35 ± 0.21 μM).

Geranylated flavonoids were isolated from *Paulownia tomentosa* (Table 38) and their inhibitory activity against PTP1B was tested (Song et al. 2017). All tested flavonoids were active and with IC_{50} values lower than 10 μM, being better inhibitors than the positive control $NaVO_4$ (IC_{50} = 32.6 ± 1.5 μM). Bonannione A (**172**) was the compound with best PTP1B inhibition (IC_{50} = 1.9 ± 0.1 μM) and, contrary to what was observed in other studies (Cui et al. 2008; Cui et al. 2010; Cai, Zhao, and Tao 2015), it was suggested that the -OCH_3 group at 3′-position of B ring decreases the activity of the tested compounds, since 3′-*O*-methyldiplacol (**209**) presented an IC_{50} value of 4.9 ± 0.5 μM. However, by comparing 3′-*O*-methyldiplacone (**205**) (IC_{50} = 3.9 ± 0.3 μM) with 4′-*O*-methyldiplacone (**206**) (IC_{50} = 7.8 ± 0.6 μM), it seems that the presence of the -OCH_3 group at 3′-position of B ring is more favorable for the intended effect than its presence at 4′-position of B ring. Interestingly, it was also found that the addition of a -OH group at 5-position of A ring slightly increases PTP1B inhibition, as observed by comparing 4′-*O*-methyldiplacone (**206**) with flavonoid **207** (IC_{50} = 5.9 ± 0.4 μM). On the other hand, the addition of a -OCH_3 group at 5′-position of B ring does not affect the inhibitory activity of flavonoids, since 3′-*O*-methyldiplacone (**205**) and 3′-*O*-methyl-5′-*O*-methyldiplacone (**208**) (IC_{50} =

Table 28. PTP1B inhibition by flavonoids tested by Wu et al (Wu et al. 2015).

Flavonoid	Structure	$R^{3'}$	$R^{4'}$	IC_{50} (μM ± SD)
Alpinumisoflavone (26)		–	–	**11.16 ± 1.88**
Ficustikousin A (**155**)		–	–	40.37 ± 4.66
Ficustikousin B (**156**)		–	–	16.33 ± 1.47
Derrone (**157**)		–	–	24.64 ± 0.57
158		–	–	19.27 ± 3.26
(*S*)-Paratocarpin K (**159**)		–	–	25.12 ± 2.28
Genistein (**121**) 3′-3-Methylbut-2-enyl) biochanin A (**160**)		H prenyl	OH OCH_3	NA 18.55 ± 0.74
Positive control Oleanolic acid	–	–	–	2.61 ± 0.59

NA – not active.

3.8 ± 0.3 μM) have similar IC_{50} values. Furthermore, the addition of an -OH group at 3-position of C ring also seems not to have effect of the inhibitory activity, as seen by comparing 3′-*O*-methyldiplacone (**205**) with 3′-*O*-methyldiplacol (**209**) (IC_{50} = 4.9 ± 0.5 μM), 4′-*O*-methyldiplacone (**206**) with 4′-*O*-methyldiplacol (**210**) (IC_{50} = 8.2 ± 0.6 μM), and flavanone **207** with flavanonol **211** (IC_{50} = 6.6 ± 0.5 μM). Overall, and considering the obtained results, it is possible that the very good inhibitory activity of all tested flavonoids is due to the presence of the lipophilic group at 6-position of A ring.

PTP1B inhibition by isolated flavonoids from Vietnamese plants was evaluated (Table 39) (Trinh, Jager, and Staerk 2017). Mucusisoflavone B (**213**), an isoflavone dimer derivative, significantly inhibited PTP1B presenting an IC_{50} value of 2.5 ± 0.2 μM, a value about 4-fold lower than the one found for the positive control RK682 (IC_{50} = 10.4 ± 1.4 μM). Concerning the other tested isoflavones, derrone (**157**) presented an IC_{50} value of 12.6 ± 1.6 μM, indicating that the presence of the 2,2-dimethylpyran ring system at 7- and 8-positions of A ring enhances the intended effect; more than the presence of this system at 3′- and 4′-positions of B ring or at 6- and 7-positions of A ring. This effect can be observed by comparing derrone (**157**) with the flavonoids isoderrone (**212**) (IC_{50} = 22.7 ± 1.7 μM) and alpinumisoflavone (**26**) (IC_{50} = 21.2 ± 3.8 μM), respectively.

In the work of the group of Proença et al. (2018), a wide range of flavonoids was evaluated regarding their ability to

Table 29. PTP1B inhibition by flavonoids tested by Na et al (Na et al. 2016).

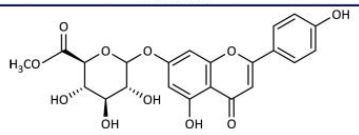
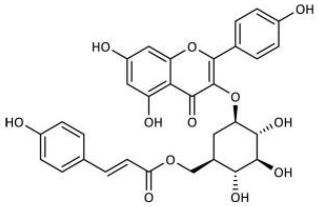
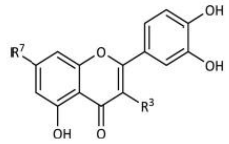
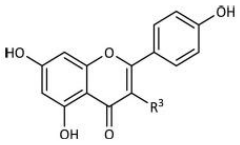
Flavonoid	Structure	R^3	R^7	IC_{50} (μM ± SD)
Apigenin 7-*O*-*β*-D-glucuronide-6′′-methyl ester (**161**)		–	–	14.35 ± 0.76
Tiriloside (**162**)		–	–	>50
Isoquercetin (**136**)		glucose	OH	27.73 ± 1.54
Quercetin 7-*O*-*β*-D-glucoside (**163**)		OH	glucose	>50
Afzelin (7)		rhamnose	–	**12.16 ± 0.02**
Kaempferol (**164**)		OH	–	42.93 ± 2.36
Positive control RK-682	–	–	–	4.47 ± 0.03

Table 30. PTP1B inhibition by flavonoids tested by Wang et al (Wang et al. 2016).

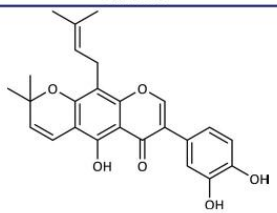
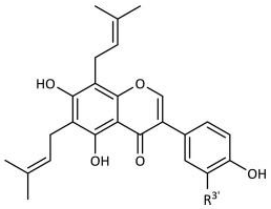
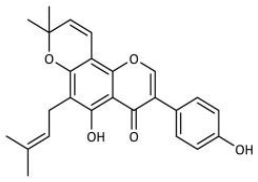
Flavonoid	Structure	$R^{3'}$	IC_{50} (μM ± SD)
Auriculasin (**165**)		–	3.6 ± 0.1
6,8-Diprenylorobol (166)		OH	**2.4 ± 0.3**
8-*γ*,*γ*-Dimethylallylwighteone (**167**)		H	9.3 ± 0.7
168		OCH_3	17.4 ± 0.2
Osajin (**169**)		–	23.6 ± 0.5
Positive control RK-682	–	–	15.5 ± 0.9

Table 31. PTP1B inhibition by flavonoids tested by Zhang et al (Zhang et al. 2016).

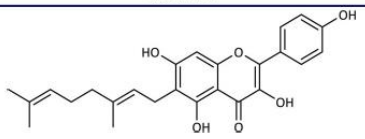
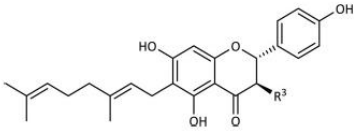
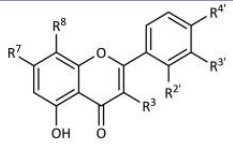
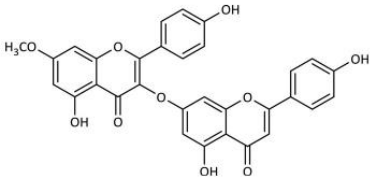
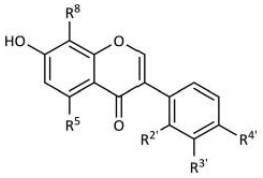
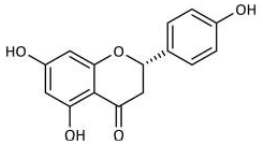
Flavonoid	Structure	R^3	IC_{50} (μM ± SD)
Macarangin (**170**)		–	22.7 ± 4.6
Bonanniol A (171)		OH	**15.2 ± 2.8**
Bonannione A (172)		H	**14.0 ± 1.2**
Positive controls RK-682	–	–	2.6 ± 0.6

Table 32. PTP1B inhibition by flavonoids tested by Zhao et al (Zhao et al. 2016).

Flavonoid	Structure	$R^{2'}$	R^3	$R^{3'}$	$R^{4'}$	R^5	R^7	R^8	IC_{50} (μM ± SD)
Afzelin (**7**)		H	rhamnose	H	OH	–	OH	H	>100
Rutin (**8**)		H	rutinose	OH	OH	–	OH	H	>100
Kaempferitrin (**9**)		H	rhamnose	H	OH	–	rhamnose	H	>100
Vitexin (**111**)		H	H	H	OH	–	OH	glucose	>100
Kaempferol (**164**)		H	OH	H	OH	–	OH	H	42.85 ± 0.73
Kaempferide (**173**)		H	OH		OCH_3	–	OH	H	67.06 ± 0.82
Morin (**174**)		OH	OH	H	OH	–	OH	H	7.62 ± 0.99
Kaempferol 7-*O*-α-L-rhamnoside (**175**)		H	OH	H	OH	–	rhamnose	H	10.80 ± 0.03
Quercetin 4′-*O*-β-D-glucoside (**176**)		H	OH	OH	glucose	–	OH	H	**0.92 ± 0.19**
Lepidoside (**177**)		H	rhamnose	H	OH	–	xylose	H	>100
Bismilachinone (**178**)		–	–	–	–	–	–	–	2.68 ± 0.18
Puerarin (**132**)		H	–	H	OH	H	–	glucose	53.01 ± 1.29
Pratensein (**179**)		H	–	OH	OCH_3	OH	–	H	9.77 ± 0.98
Smilachinin (**180**)		glucose	–	H	OCH_3	OH	–	H	35.28 ± 0.49
Naringenin (**181**)		–	–	–	–	–	–	–	63.25 ± 0.49
Positive control Ursolic acid	–	–	–	–	–	–	–	–	1.21 ± 0.18

inhibit human PTP1B activity (Table 40). Regarding the group of flavonoids **214**–**220**, they presented no or low inhibitory activity at the highest tested concentration, 200 μM. From the group of flavones **220**–**223** , all with an -OH group at 5-position of A ring, it was found that the presence of an -OH group at 4′-position of B ring slightly improved PTP1B inhibition. In accordance, flavonoid **223** was the most active with an IC_{50} value of 184 ± 13 μM, while it was not possible to determine the IC_{50} values of the other flavonoids of the group.

The group of flavonoids with different substitutions at 3-position of C ring, at 3′- and 4′-positions of B ring, and at 7- and 8-positions of A ring, has the two most potent flavonoids found, **234** and **235**, with IC_{50} values of 10 ± 1 μM and 16 ± 2 μM. In fact, the IC_{50} value of compound **234** did not significantly differ from the IC_{50} value of the positive control ursolic acid (IC_{50} = 7.1 ± 0.9 μM). The obtained results indicate that, as mentioned above, less polar substituents such as -OBn and -OCH_3 groups, increase PTP1B inhibition by flavonoids. Considering the other tested flavonoids

from this group, with exception of flavonoids **226** (IC_{50} = 153 ± 16 μM) and **231** (IC_{50} = 182 ± 15 μM), it was not possible to calculate the IC_{50} up to 200 μM, the maximum tested concentration.

From the group of flavonoids with -OH groups at 5- and 7-positions of A ring and different substituents at other positions, the most effective compound was morin (**174**), which presented an IC_{50} value of 37 ± 3 μM. By comparing morin (**174**) with kaempferol (**164**), which had no inhibitory effect up to 200 μM, it was observed that the lack of an -OH group at 2′-position of B ring considerably decreased the ability of flavonoids to inhibit PTP1B. Regarding flavonoids with $-OCH_3$ groups, it was clear that the replacement of an –OH group at 4′-position of B ring by a $-OCH_3$ group enhances the intended effect, by comparing apigenin (**71**) (IC_{50} = 159 ± 20 μM) and acacetin (**239**) (IC_{50} = 91 ± 7 μM).

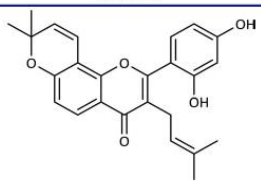
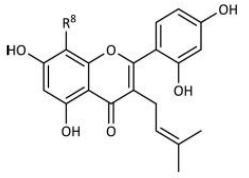
In what concerns the group of flavanones, it seems that the lack of C2 = C3 double bond weakened the inhibition of PTP1B since the tested compounds did not inhibit the enzyme under study. This conclusion can be made by comparing, for instance, the inhibitory activities of taxifolin (**153**) and quercetin (**3**) (IC_{50} = 37 ± 3 μM).

PTP1B inhibition by flavonoids from *Silybum marianum* seeds was evaluated (Table 41) (Qin et al. 2018), andthe most promising compounds were the noncompetitive inhibitors silybin A (**241**) (IC_{50} = 1.54 ± 0.22 μM) and isosylibin B (**244**) (IC_{50} = 1.37 ± 0.22 μM), which were more active than the positive control ursolic acid (IC_{50} = 3.52 ± 0.10 μM). Silybin A (**241**) was a better inhibitor than silybin B (**242**) (IC_{50} = 5.65 ± 0.20 μM), and isosylibin B (**244**) was a better inhibitor than isosylibin A (**243**) (IC_{50} = 2.65 ± 0.13 μM), suggesting that the absolute configurations at 7′′- and 8′′-positions have an important role for the biological activity under study. Moreover, by comparing the inhibitory activities of silychristin A (**245**) (IC_{50} = 5.58 ± 0.33 μM) and silychristin B (**246**) (IC_{50} = 23.87 ± 2.25 μM), it was observed that stereochemistry has an even more pronounced effect than in the silybin derivatives.

Additionally, the inhibitory activities of isosilychristin A (**247**) and dehydrosilychristin A (**248**), with IC_{50} values of 6.55 ± 0.09 μM and 7.18 ± 0.12 μM, respectively, suggest that the C2 = C3 double bond does not significantly affect the inhibition of PTP1B.

Xu et al. (2018) studied the ability of a panel of flavonoids isolated from acorn leaves (*Quercus liaotungensis*) to inhibit PTP1B (Table 42). By the obtained results, it was observed that the nature of glycosylation of flavonoids at 3-position of C ring significantly affect their inhibitory activity, since quercetin 3-*O*-(2′′-galloyl)-*β*-galactoside (**250**),

Table 33. PTP1B inhibition by flavonoids tested by Huang et al (Huang et al. 2017).

Flavonoid	Structure	R^8	IC_{50} (μM ± SD)
Albasin D (**182**)		–	3.04 ± 0.67
Kwanon C (152)		prenyl	**2.20 ± 0.83**
Albanin A (**183**)		H	NA
Positive control Oleanolic acid	–	–	3.31 ± 0.02

NA – not active.

Table 34. PTP1B inhibition by flavonoids tested by Jung et al (Jung et al. 2017).

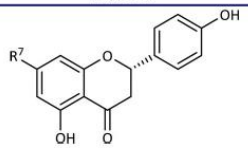
Flavonoid	Structure	R^7	IC_{50} (μM ± SD)
Naringin (**131**)		neohesperidose	91.8 ± 0.65
Naringenin (**181**)		OH	130.1 ± 0.47
Prunin (184)		glucose	**17.5 ± 2.6**
Narirutin (**185**)		rutinose	56.5 ± 0.12
Positive control Ursolic acid	–	–	5.4 ± 0.30

Table 35. PTP1B inhibition by flavonoids tested by Kim et al (Kim et al. 2017).

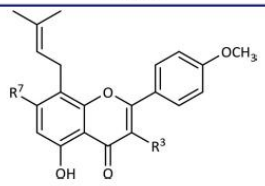
Flavonoid	Structure	R^3	R^7	IC_{50} (μM ± SD)
Icaritin (**186**)		OH	OH	11.59 ± 1.39
Icariside II (**187**)		rhamnose	OH	**9.94 ± 0.15**
Icariin (**188**)		rhamnose	glucose	> 300
Epimedin A (**189**)		rhamnose-glucose	glucose	> 300
Epimedin B (**190**)		rhamnose-xylose	glucose	> 300
Epimedin C (**191**)		rhamnose-rhamnose	glucose	> 300
Positive control Ursolic acid	–		–	8.24 ± 0.30

Table 36. PTP1B inhibition by flavonoids tested by Nguyen et al (Nguyen et al. 2017).

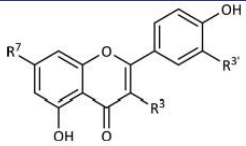
Flavonoid	Structure	R^3	$R^{3'}$	R^7	IC_{50} (μM ± SD)
Quercetin (**3**)		OH	OH	OH	40.94 ± 0.46
Apigenin (**71**)		H	H	OH	>100
Isoquercetin (**136**)		glucose	OH	OH	>100
Cynaroside (**139**)		H	OH	glucose	71.56 ± 0.53
Agriflavone (**192**)		H	H	arabinuronide methyl ester (2″-1″)-*O*-*β*-D-glucose	>100
Kaempferol 3-*O*-[(*S*)-3-hydroxy-3-methylglutaroyl (1-6)]-*β*-D-glucoside (**193**)		(*S*)-3-hydroxy-3-methylglutaroyl (1-6)]-*β*-D-glucose	H	OH	>100
Kaempferol 7-*O*-*β*-D-glucoside (**194**)		OH	H	glucose	>100
Kaempferol 7-*O*-*β*-D-glucuronide (**195**)		OH	H	glucuronic acid	48.34 ± 0.07
Astraglin (**196**)		glucose	H	OH	60.70 ± 0.96
Apigenin 7-*O*-*β*-D-glucoside (**197**)		H	H	glucose	>100
Apigenin 7-*O*-*β*-D-glucuronide (**198**)		H	H	glucuronic acid	**7.14 ± 1.75**
Quercetin 3′-*O*-*β*-D-glucoside (**199**)		OH	glucose	OH	>100
Luteolin 7-*O*-*β*-D-glucuronide (**200**)		H	OH	glucuronic acid	38.08 ± 2.34
Luteolin 7-*O*-*β*-D-glucuronide methyl ester (**201**)		H	OH	glucuronic acid methyl ester	49.09 ± 0.08
Luteolin 7-*O*-*β*-D-glucuronide butyl ester (**202**)		H	OH	glucuronic acid butyl ester	>100
Luteolin 3′-*O*-*β*-D-glucoside (**203**)		H	glucose	OH	>100
Positive control Ursolic acid	–	–	–	–	9.43 ± 0.14

Table 37. PTP1B inhibition by flavonoids tested by Qin et al (Qin et al. 2017).

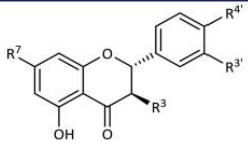
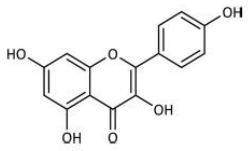
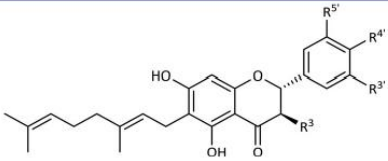
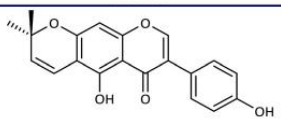
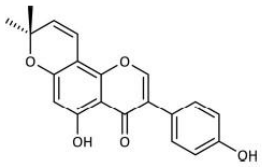
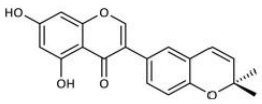
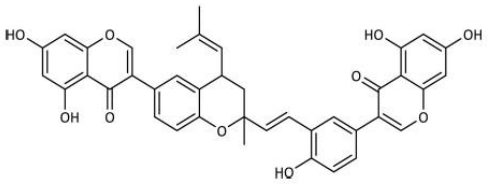
Flavonoid	Structure	R^3	$R^{3'}$	$R^{4'}$	R^7	IC_{50} (μM ± SD)
Dihydrokaempferol (**146**)		OH	H	OH	OH	27.83 ± 1.34
Taxifolin (**153**)		OH	OH	OH	OH	24.23 ± 1.69
Naringenin (**181**)		H	H	OH	OH	>50
Prunin (**184**)		H	H	OH	glucose	>50
Dihydroquercetin 4′-methyl ether (**204**)		OH	OH	OCH_3	OH	21.30 ± 2.16
Kaempferol (164)		–	–	–	–	**6.79 ± 0.22**
Positive control Ursolic acid	–		–			8.35 ± 0.21

Table 38. PTP1B inhibition by flavonoids tested by Song et al (Song et al. 2017).

Flavonoid	Structure	R^3	$R^{3'}$	$R^{4'}$	$R^{5'}$	IC_{50} (μM ± SD)
Bonannione A (**172**)		OH	H	OH	H	**1.9 ± 0.1**
3′-O-Methyldiplacone (**205**)		H	OCH_3	OH	H	3.9 ± 0.3
4′-*O*-Methyldiplacone (**206**)		H	OH	OCH_3	H	7.8 ± 0.6
207		H	OH	OCH_3	OH	5.9 ± 0.4
3′,5′-O-Dimethyldiplacone (**208**)		H	OCH_3	OH	OCH_3	3.8 ± 0.3
3′-O-Methyldiplacol (**209**)		OH	OCH_3	OH	H	4.9 ± 0.5
4′-O-Methyldiplacol (**210**)		OH	OH	OCH_3	H	8.2 ± 0.6
211		OH	OH	OCH_3	OH	6.6 ± 0.5
Positive control $NaVO_4$	–	–	–	–	–	32.6 ± 1.5

with an IC_{50} value of 5.56 ± 0.38 μM, was a better inhibitor than rutin (**8**) (IC_{50} = 20.56 ± 2.01 μM), isoquercetin (**136**) (IC_{50} = 82.87 ± 8.61 μM) and quercetrin (**5**) (IC_{50} = 81.59 ± 7.09 μM). Among flavonoids glycosides, besides the presence of a galactose at 3-position of C ring, the addition of a galloyl group also seems to be favorable for PTP1B inhibition, since quercetin 3-*O*-(2′′-galloyl)-*β*-galactoside (**250**) was the glycoside with the best inhibition, with an IC_{50} value of 5.56 ± 0.38. Furthermore, the replacement of the sugar at 3-position of C ring by an -OH group increased the inhibitory effect, as suggested by the activities of quercetin (**3**) (IC_{50} = 4.16 ± 0.56 μM), kaempferol (**164**) (3.92 ± 0.36 μM) and myricetin (**252**) (IC_{50} = 3.53 ± 0.92 μM), which were more active than their respective glycosides (**5**, **93**, **136** and **250**; **7**, **249** and **251**; and **6**, respectively). Moreover, the lack of the C2 = C3 double

Table 39. PTP1B inhibition by flavonoids tested by Trinh et al (Trinh, Jager, and Staerk 2017).

Flavonoid	Structure	IC_{50} (μM ± SD)
Alpinumisoflavone (**26**)		22.7 ± 1.7
Derrone (**157**)		12.6 ± 1.6
Isoderrone (**212**)		21.2 ± 3.8
Mucusisoflavone B (213)		**2.5 ± 0.2**
Positive control RK-682	–	10.4 ± 1.6

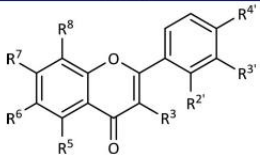
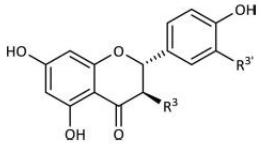
bond slightly decreased the intended effect, as seen by comparing myricetin (**252**) with dihydromyricetin (**255**) (IC_{50} = 9.58 ± 1.82 μM). It was also observed that the substitution of the -OH group by a rutinose at 7-position of A ring reduced the ability of flavonoids to inhibit PTP1B, since flavanone **254** (IC_{50} = 89.56 ± 7.06 μM) was a weak inhibitor, when compared with naringenin (**181**) (IC_{50} = 15.38 ± 2.76 μM).

PTP1B inhibition by flavans from *Broussonetia kazinoki* was studied by Xue and coauthors (Table 43) (Xue et al. 2018). In this study, the chiral analysis of broukazinol A was performed. It indicated the presence of an enantiomeric pair with the approximate ratio 2:1. After chiral resolution, (−)-broukazinol A (**257**)/(+)-broukazinol A (**262**) were obtained with opposite specific rotations, where the absolute configuration were assigned as 2*S* for (−)-broukazinol A (**257**) and 2*R* for (+)-broukazinol A (**262**). The mixture of flavonoids (+)-broukazinol A (**262**)/(−)-broukazinol A (**257**) was the most active, with an IC_{50} value of 20.00 ± 1.85 μM, followed by the mixture of flavonoids **263**/**268**, with an IC_{50} value of 27.20 ± 3.61 μM. These results suggest an -OH group at one aromatic domain and a prenyl group at another aromatic domain increase flavans ability to inhibit PTP1B. On the other hand, compounds without prenyl groups - broussoside F (**265**), demethylbroussin (**259**)/tupichinol C (**264**), **260** and **261** - showed weak or no inhibitory activity at the highest tested concentration.

A series of azolyl flavonoids were synthesized and screened for their potential PTP1B inhibitory activities (Table 44) (Zhang et al. 2018). The best inhibitor was flavonoid **270**, which presented an IC_{50} value of 1.6 ± 0.9 μM, and demonstrated a competitive type of inhibition. The obtained results suggest that the substitution of triazole with 2-methyl-5-nitroimidazole, 4-nitroimidazole, 5-methyl tetrazole or thiol-imidazole group which yielded flavonoids **266** (IC_{50} = 4.0 ± 1.7 μM), **268** (IC_{50} = 5.0 ± 1.2 μM), **272** (7.9 ± 0.3 μM) and **274** (IC_{50} = 3.0 ± 0.04 μM) resulted in lower PTP1B inhibition comparing with flavonoid **270**. This seems to indicate that the existence of triazole moiety in the tested flavonoids might be of special importance in the PTP1B inhibition profiles. Additionally, in general, long-chain alkyl derivatives presented less inhibitory activities than the short chains. Thus, the inhibition of PTP1B should be closely related to azole ring and alkyl chain lengths. For the compounds under study, azole moieties contributed for PTP1B inhibition in the following descendent order: triazole > imidazole-thiol > 2-methyl-5-nitroimidazole > 4-nitroimidazole > 5-methyl tetrazole derivatives.

The PTP1B inhibition by flavonoids isolated from the crude root bark of *Morus alba* leaves were studied (Table 45) (Zhao et al. 2018). The compound with best inhibitory activity was moracenin A (**277**), with an IC_{50} value of 4.04 ± 0.38 μM. This suggest that the addition of a prenyl group in the flavonoid skeleton increases the inhibitory activity, as observed by comparing moracenin A (**277**) with moracenin B (**276**), which presented an IC_{50} value of 13.07 ± 1.74 μM. Moreover the results showed that the presence of a prenyl group at 3′-position of B ring is more favorable for the intended effect than the presence of this group at 8-position of A ring, as seen by comparing kwanon T (**279**) (IC_{50} = 9.83 ± 0.36 μM) with kwanon C (**152**) (IC_{50} = 17.48 ± 2.52 μM). The positive control RK682 presented an IC_{50} value of 13.27 ± 1.00 μM, which means that

Table 40. PTP1B inhibition by flavonoids tested by Proença et al (Proença et al. 2018).

Flavonoid	Structure	$R^{2'}$	R^3	$R^{3'}$	$R^{4'}$	R^5	R^6	R^7	R^8	IC_{50} (μM ± SEM) or % Inhibition at 200 μM
Flavone (**214**)		H	H	H	H	H	H	H	H	<20 %
215		H	H	OH	H	H	H	H	H	<20 %
216		H	H	H	OH	H	H	H	H	<20 %
217		H	H	OH	OH	H	H	H	H	27 ± 4 %
218		H	OH	OH	OH	H	H	H	H	<20 %
219		H	OH	OCH_3	OCH_3	H	H	H	H	<20 %
220		H	H	H	H	OH	H	H	H	29 ± 1 %
221		H	H	OH	H	OH	H	H	H	39 ± 5 %
222		H	H	H	OH	OH	H	H	H	184 ± 13 μM
223		H	H	OH	OH	OH	H	H	H	<20 %
224		H	H	H	H	H	H	OH	H	<20 %
225		H	H	OH	H	H	H	OH	H	<20 %
126		H	H	H	OH	H	H	OH	H	<20 %
226		H	OH	OH	H	H	H	OH	H	153 ± 16 μM
227		H	OH	H	OH	H	H	OH	H	<20 %
228		H	H	OH	OH	H	H	OH	H	<20 %
229		H	OH	OH	OH	H	H	OH	OH	36 ± 3 %
230		H	OH	OCH_3	H	H	H	OCH_3	H	27 ± 6 %
231		H	OH	H	OCH_3	H	H	OCH_3	H	182 ± 15 μM
232		H	OH	OH	OH	H	H	OCH_3	OCH_3	<20 %
233		H	OH	OCH_3	OCH_3	H	H	OH	OH	<20 %
234		H	OH	OBn	OBn	H	H	OCH_3	OCH_3	16 ± 2 μM
235		H	OH	OCH_3	OCH_3	H	H	OBn	OBn	**10 ± 1 μM**
Quercetin (**3**)		H	OH	OH	OH	OH	H	OH	H	37 ± 3 μM
Rutin (**8**)		H	rutinose	OH	OH	OH	H	OH	H	<20 %
Apigenin (**71**)		H	H	H	OH	OH	H	OH	H	<20 %
Luteolin (**113**)		H	H	OH	OH	OH	H	OH	H	26 ± 1 %
Kaempferol (**164**)		H	OH	H	OH	OH	H	OH	H	<20 %
Morin (**174**)		OH	OH	H	OH	OH	H	OH	H	91 ± 7 μM
Chrysin (**236**)		H	H	H	H	OH	H	OH	H	<20 %
Galangin (**237**)		H	OH	H	H	OH	H	OH	H	<20 %
Baicalein (**238**)		H	H	H	H	OH	OH	OH	H	159 ± 20
Acacetin (**239**)		H	H	H	OCH_3	OH	H	OH	H	<20 %
Taxifolin (**153**)		–	OH	OH	–	–	–	–	–	<20 %
Naringenin (**181**)		–	H	H	–	–	–	–	–	<20 %
Eriodictyol (**240**)		–	H	OH	–	–	–	–	–	<20 %
Positive control Ursolic acid	–	–	–	–	–	–	–	–	–	7.1 ± 0.9 μM

moracenin A (**277**), kwanon F (**280/281**), kwanon T (**279**), kwanon M (**282**), sanggenon G (**17**) and moracenin B (**276**) were best PTP1B inhibitors than the tested positive control.

Ren et al. (2019) evaluated the inhibitory activity of flavonoids isolated from the seeds of *Psoralea corylifolia* against PTP1B (Table 46). The most active flavonoid was flavanone **284** (IC_{50} = 10.3 ± 0.9 μM). By comparing compound **284** with bavachin (**285**) (IC_{50} = 25.1 ± 1.6 μM), it was possible to observe that the cyclic oxidized prenylated aromatic moiety is responsible for the enhancement of PTP1B inhibition.

Biflavonoids from *Selaginella uncinata* were studied concerning their ability to inhibit PTP1B (Table 47) (Xu et al. 2019). Presenting an IC_{50} value of 4.6 ± 0.5 μM, compound **295** was one of the most effective PTP1B inhibitor among the tested flavonoids, demonstrating that the presence of methyl groups at 6- and 6″-positions increases the intended effect. (2″S)Chrysocauloflavone (**293**) (IC_{50} = 5.5 ± 0.7 μM) and delicaflavone (**294**) (IC_{50} = 6.2 ± 0.5 μM), with the C-O-C linkage, were also among the best PTP1B inhibitors. Compound **291** (IC_{50} = 16.1 ± 0.5 μM), amentoflavone (**142**) (IC_{50} = 10.6 ± 0.3 μM) and bilobetin (**292**) (IC_{50} = 14.6 ± 0.8 μM), all with the 3′-8″ linkage, were less active. These results suggest that the linkage between two flavonoid skeletons may influence the inhibitory activity. On the other hand, linkage of flavonoids in 3-4‴ (flavonoids **293** and **294**), as well as flavonoids linked in 3′- 4‴ (flavonoid **295**) seem to promote a higher inhibitory activity against PTP1B. In addition, it was verified that the presence of a -OCH_3 at 4′-position of B ring or at 7-position of A ring had no effect in the inhibitory activity, since robustoflavone 4′-methyl ether (**289**) and robustoflavone 7-methyl ether (**290**) presented similar IC_{50} values: 9.2 ± 0.4 μM and 9.8 ± 0.5 μM, respectively. The absence of the double bond appears to slightly decrease the PTP1B inhibition, as seen by comparing flavonoids **291** and **142**, and flavonoids **293** and **294**.

Inhibitory activity against PTP1B of flavonoids isolated from *Eremophila bignoniiflora* was evaluated (Table 48) (Zhao et al. 2019). Interestingly, the tested flavanones were not active at the highest tested concentration, 100 μM, suggesting that the C2 = C3 double bond might have a significant role in inhibition of PTP1B. Regarding the tested

Table 41. PTP1B inhibition by flavonoids tested by Qin et al (Qin et al. 2018).

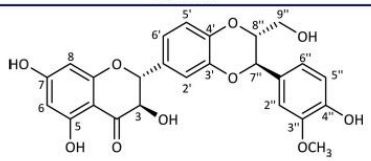
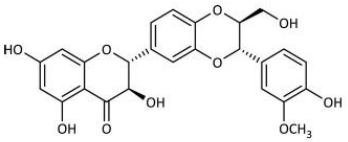
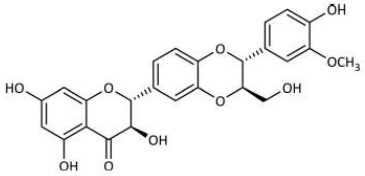
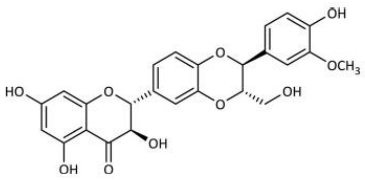
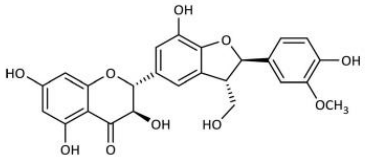
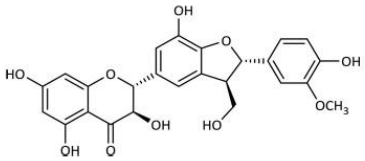
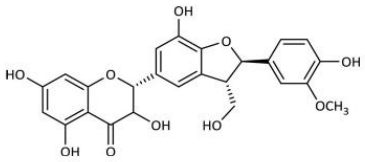
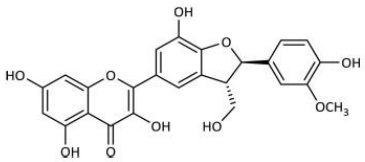
Flavonoid	Structure	IC_{50} (μM ± SD)
Silybin A (241)		**1.54 ± 0.22**
Silybin B (**242**)		5.65 ± 0.20
Isosilybin A (**243**)		2.65 ± 0.13
Isosilybin B (**244**)		**1.37 ± 0.22**
Silychristin A (**245**)		5.58 ± 0.33
Silychristin B (**246**)		23.87 ± 2.25
Isosilychristin A (**247**)		6.55 ± 0.09
Dehydrosilychristin A (**248**)		7.18 ± 0.12
Positive control Ursolic acid	–	3.52 ± 0.10

Table 42. PTP1B inhibition by flavonoids tested by Xu et al (Xu et al. 2018).

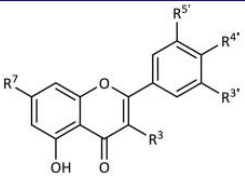
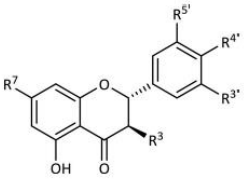
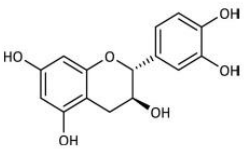
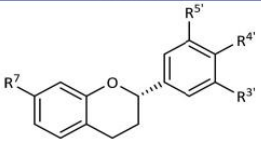
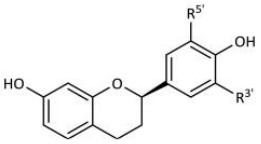
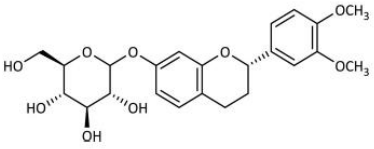
Flavonoid	Structure	R^3	$R^{3'}$	$R^{4'}$	$R^{5'}$	R^7	IC_{50} (μM ± SD)
Quercetin (3)		OH	OH	OH	H	OH	**4.16 ± 0.56**
Quercetrin (**5**)		rhamnose	OH	OH	H	OH	81.59 ± 7.09
Myricitrin (**6**)		rhamnose	OH	OH	OH	OH	70.52 ± 5.25
Afzelin (**7**)		rhamnose	H	OH	H	OH	98.01 ± 8.21
Rutin (**8**)		rutinose	OH	OH	H	OH	20.56 ± 2.01
Hyperoside (**93**)		galactose	OH	OH	H	OH	78.42 ± 6.15
Isoquercetin (**136**)		glucose	OH	OH	H	OH	82.87 ± 8.61
Kaempferol (**164**)		OH	H	OH	H	OH	**3.92 ± 0.36**
Kaempferol 3-*O*-(2″,3″-diol acetonide)-α-L-rhamnoside (**249**)		(2″,3″-diol acetonide)-α-L-rhamnose	H	OH	H	OH	80.19 ± 5.28
Quercetin 3-*O*-(2″-galloyl)-β-galactoside (**250**)		(2″-galloyl)-β-galactose	OH	OH	H	OH	5.56 ± 0.38
Nicotiflorin (**251**)		rutinose	H	OH	H	OH	24.89 ± 2.39
Myricetin (**252**)		OH	OH	OH	OH	OH	**3.53 ± 0.92**
253		H	H	OCH_3	H	OCH_3	>100
Naringenin (**181**)		H	H	OH	H	OH	15.38 ± 2.76
254		H	H	OH	H	rutinose	89.56 ± 7.06
Dihydromyricetin (**255**)		OH	OH	OH	OH	OH	9.58 ± 1.82
Hesperetin (**256**)		H	OH	OCH_3	H	OH	20.16 ± 3.02
(+)-Catechin (**138**)		–	–	–	–	–	51.11 ± 5.92
Positive control Na_3VO_4	–	–	–	–	–	–	28.91 ± 2.78

Table 43. PTP1B inhibition by flavonoids tested by Xue et al (Xue et al. 2018).

Flavonoid	Structure	$R^{3'}$	$R^{4'}$	$R^{5'}$	R^7	IC_{50} (μM ± SD)
(-)-Broukanizol A (**257**)		OCH_3	OH	prenyl	OH	**20.00 ± 1.85**[a]
258		prenyl	OH	H	OH	27.20 ± 3.61[b]
Demethylbroussin (**259**)		H	OH	H	OH	NA
260		OH	OCH_3	H	OH	NA
261		OCH_3	OH	H	OCH_3	54.20 ± 5.38
(+)-Broukazinol A (**262**)		OCH_3	–	prenyl	–	**20.00 ± 1.85**[a]
263		prenyl	–	H	–	27.20 ± 3.61[b]
Tupichinol C (**264**)		H	–	H	–	NA
Broussoside F (**265**)		–	–	–	–	NA
Positive control Oleanolic acid	–	–	–	–	–	2.52 ± 0.22

[a]Mixture compounds **257**/**262**.
[b]Mixture compounds **259**/**263**. NA - Not active.

flavones, the most effective compound was galangin 3-methyl ether (**302**), with an IC_{50} value of 41.4 ± 1.4 μM. By comparing galangin 3-methyl ether (**302**) with galangin (**238**) (IC_{50} = 154.5 ± 8.9 μM), it seems that the replacement of the -OH group by a -OCH_3 group at 3-position of C ring is important for inhibition of the enzyme under study. Nevertheless, by comparing galangin 3-methyl ether (**302**) with quercetin 3-methyl ether (**300**), both with a -OCH_3 group at 3-position of C ring, it was possible to see that quercetin 3-methyl ether (**300**) was inactive at the maximum tested concentration. Thus, these results also suggest that beside the importance of the -OCH_3 at 3-position of C ring,

Table 44. PTP1B inhibition by flavonoids tested by Zhang et al (Zhang et al. 2018).

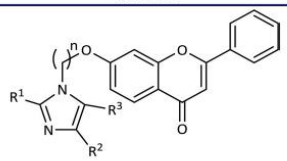
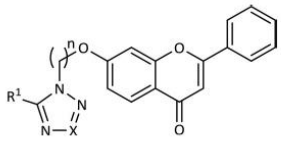
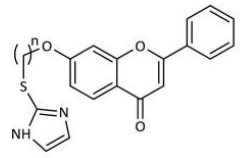
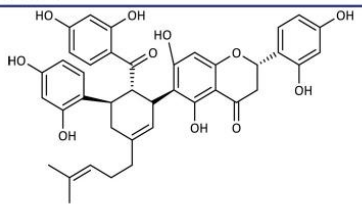
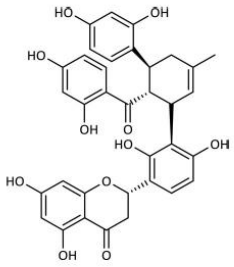
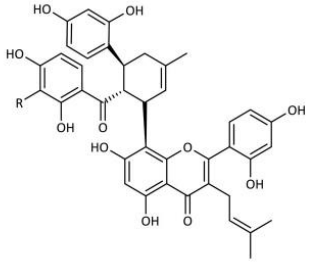
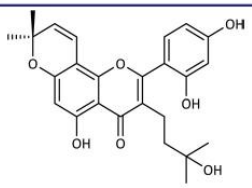
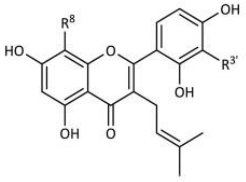
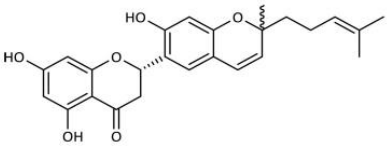
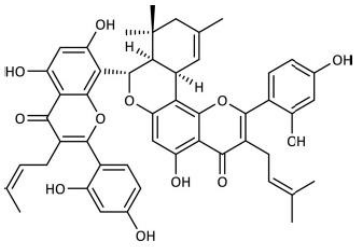
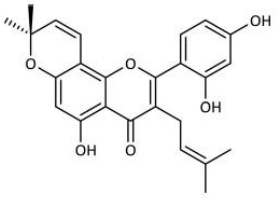
Flavonoid	Structure	n	X	R^1	R^2	R^3	IC_{50} (μM ± SD)
266		2	–	CH_3	H	NO_2	4.0 ± 1.7
267		4	–	CH_3	H	NO_2	6.9 ± 1.3
268		2	–	H	NO_2	H	5.0 ± 1.2
269		4	–	H	NO_2	H	7.0 ± 1.2
270		2	CH	H	–	–	**1.6 ± 0.9**
271		4	CH	H	–	–	3.6 ± 0.4
272		2	N	CH_3	–	–	7.9 ± 0.3
273		4	N	CH_3	–	–	15.1 ± 0.9
274		2	–	–	–	–	3.0 ± 0.04
275		4	–	–	–	–	3.9 ± 0.9

Table 45. PTP1B inhibition by flavonoids tested by Zhao et al (Zhao et al. 2018).

Flavonoid	Structure	R	$R^{3'}$	R^8	IC_{50} (μM ± SD)
Sanggenon G (**17**)		–	–	–	10.87 ± 1.09
Kwanon L (**18**)		–	–	–	21.67 ± 3.38
Moracenin B (**276**)		H	–	–	13.07 ± 1.74
Moracenin A (277)		prenyl	–	–	**4.04 ± 0.38**

(*continued*)

Table 45. Continued.

Flavonoid	Structure	R	$R^{3'}$	R^{8}	IC_{50} (μM ± SD)
Morusinol (**278**)		–	–	–	30.49 ± 2.49
Kwanon C (**152**)		–	H	prenyl	17.48 ± 2.52
Kwanon T (**279**)		–	prenyl	H	9.83 ± 0.36
Kwanon F* (**280/281**)		–	–	–	9.52 ± 0.46 9.68 ± 0.69
Kwanon M (**282**)		–	–	–	10.71 ± 2.41
Morusin (**283**)		–	–	–	19.63 ± 1.94
Positive control RK-682	–	–	–	–	13.27 ± 1.00

*Compounds **280/281** differ in the configuration at C-3'' (diastereomers).

the catechol group in B ring is not favorable for this specific biological activity.

The results obtained in the different research studies regarding the PTP1B inhibition by the most active flavonoids are summarized in Table 49.

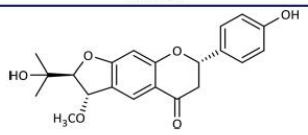
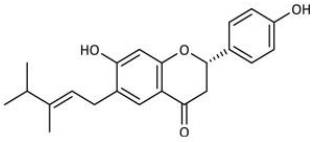
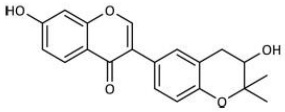
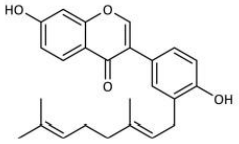
DPP-4 inhibitory effect of flavonoids

Methodologies used to evaluate the DPP-4 inhibitory activity of flavonoids

The various studies that are currently published on the inhibitory activity of flavonoids against DPP-4 also display a wide variability of experimental conditions. As mentioned before for *PTP1B*, this variability frequently leads to different results among the research studies under analysis, as different IC_{50} values for positive controls and flavonoids. Table 50 comprises all the experimental conditions found in the analyzed studies, namely the source and concentration of DPP-4, type and concentration of substrate, times of incubation applied before and after the addition of the substrate, temperature and pH.

The subclasses of flavonoids studied in the present review are: flavones, flavonols, isoflavones, flavans, isoflavans, flavanones, isoflavanones, anthocyanidins, and biflavonoids. The values of the results exhibited below are the ones presented by the authors of the research articles. As such, in some cases, the associated SD or SEM were not included as they were not originally available. For the evaluation of the inhibitory activity of flavonoids against the targets under

Table 46. PTP1B inhibition by flavonoids tested by Ren et al (Ren et al. 2019).

Flavonoid	Structure	IC_{50} (μM ± SD)
284		**10.3 ± 0.9**
Bavachin (**285**)		25.1 ± 1.6
Psoralenol (**286**)		19.7 ± 0.7
Corylifol A (**287**)		>60
Positive control RK-682	–	4.7 ± 0.6

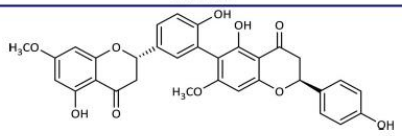
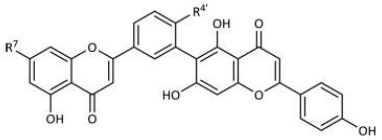
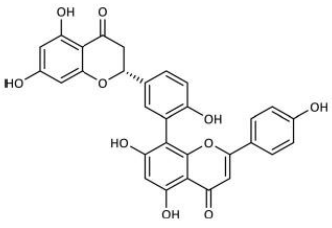
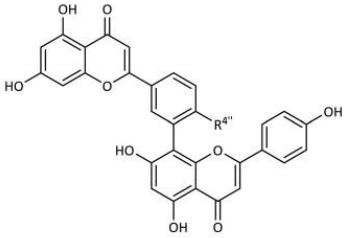
study, the present review was organized in the following order: flavonoids studied and establishment of the structure-activity relationship; tables presenting the corresponding flavonoid chemical structure and inhibitory activity; table presenting the summarized results of all the articles analyzed; and an integrated discussion of the results for the target under study.

Inhibitory activity of flavonoids against DPP-4

Eidenberger, Selg, and Krennhuber (2013) tested the DPP-4 inhibition by flavonoids glycosides isolated from *Psidium guajava* leaves (Table 51) in freshly obtained plasma from nondiabetic volunteers. The descending order of inhibitory activity of the tested compounds was the following: guaijaverin (**140**) (IC_{50} =0.086 ± 0.00851 μmol/mL) > peltatoside (**135**) (IC_{50} = 0.126 ± 0.0129 μmol/mL) > isoquercetin (**136**) (IC_{50} = 0.181 ± 0.171 μmol/mL) > hyperoside (**93**) (IC_{50} = 0.242 ± 0.0237 μmol/mL). By the obtained results it can be observed that the nature of the sugar at 3-position of C ring is relevant for the activity under study, since the presence of an arabinose at this position increased the DPP-4 inhibition more than an arabinofuranose, glucose or galactose.

The inhibition of DPP-4 by flavonoids isolated from citrus, berry, grape and soybean was tested (Table 52) (Fan

Table 47. PTP1B inhibition by flavonoids tested by Xu et al (Xu et al. 2019).

Flavonoid	Structure	$R^{4'}$	$R^{4''}$	R^{7}	IC_{50} (μM ± SD)
Uncinatabiflavone C 7-methyl ether (**288**)		–	–	–	7.7 ± 0.3
Robustaflavone 4′-methyl ether (**289**)		OCH_3	–	OH	9.2 ± 0.4
Robustaflavone 7-methyl ether (**290**)		OH	–	OCH_3	9.8 ± 0.5
291		–	–	–	16.1 ± 0.5
Amentoflavone (**142**)		–	OH	–	10.6 ± 0.3
Bilobetin (**292**)		–	OCH_3	–	14.6 ± 0.8

(*continued*)

Table 47. Continued.

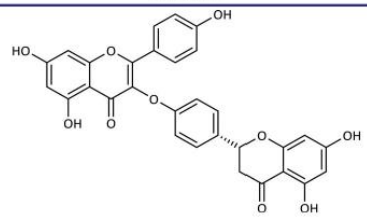
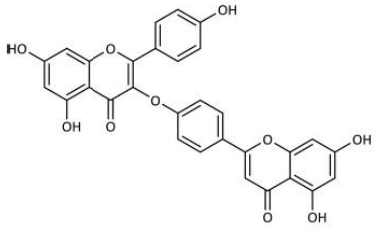
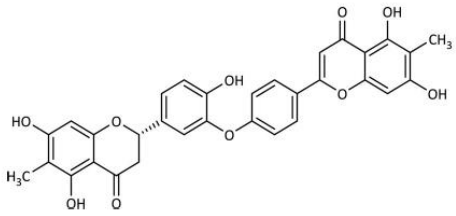
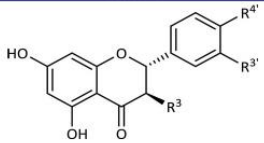
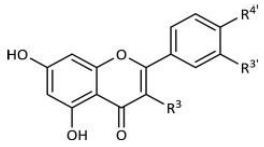
Flavonoid	Structure	$R^{4'}$	$R^{4''}$	R^{7}	IC_{50} (μM ± SD)
(2''S) Chrysocauloflavone I (293)		–	–	–	**5.5 ± 0.7**
Delicaflavone (**294**)		–	–	–	6.2 ± 0.5
295		–	–	–	**4.6 ± 0.5**
Positive control RK-682	–	–	–	–	3.1 ± 0.4

Table 48. PTP1B inhibition by flavonoids tested by Zhao et al (Zhao et al. 2019).

Flavonoid	Structure	R^{3}	$R^{3'}$	$R^{4'}$	IC_{50} (μM ± SD)
Pinocembrin (**108**)		H	H	H	NA
Taxifolin (**153**)		OH	OH	OH	NA
Dihydrokaempferol (**146**)		OH	H	OH	NA
3-*O*-Acetyltaxifolin (**296**)		$OCOCH_3$	OH	OH	NA
Pinobanksin (**297**)		OH	H	H	NA
3-Acetoxyhespertin (**298**)		$OCOCH_3$	OH	OCH_3	NA
Pinobanksin 3-acetate (**299**)		$OCOCH_3$	H	H	NA
Galangin (**238**)		OH	H	H	154.5 ± 8.9
Quercetin 3-methyl ether (**300**)		OCH_3	OH	OH	>50[a]
Quercetin 3,4′-dimethyl ether (**301**)		OCH_3	OH	OCH_3	NA
Galangin 3-methyl ether (**302**)		OCH_3	H	H	**41.4 ± 1.4**
Positive control RK-682	–	–	–	–	14.5 ± 0.2

NA – Not active.
[a]limited solubility at concentrations higher than 50 μM.

et al. 2013). Among the tested berry flavonoids [cyanidin (**303**), cyanidin 3-glucoside (**304**) and malvidin (**305**)], cyanidin 3-glucoside (**304**) was the most active, with an IC_{50} value of 0.42 ± 0.09 μM. Thus, by comparing this compound with cyanidin (**303**) (IC_{50} = 1.41 ± 0.25 μM), it was suggested that the replacement of the -OH by a glucose at 3-position of C ring increases the inhibitory activity. Considering the DPP-4 inhibition by flavones, it was found that the addition of an –OH at 3-position of C ring decreases the inhibitory activity, by comparing luteolin (**113**) (IC_{50} = 0.12 ± 0.01 μM) with quercetin (**3**) (IC_{50} = 2.92 ± 0.68 μM), and apigenin (**71**) (IC_{50} = 0.14 ± 0.02 μM) with kaempferol (**164**) (IC_{50} = 0.49 ± 0.02 μM). Besides that, by comparing quercetin (**3**) with kaempferol (**164**), it seems that the addition of an –OH group at 3′-position of B ring also has no beneficial effect for the intended biological activity. In addition, the glycosylation of flavones at 3-position of C ring reduces the inhibition of DPP-4 since rutin (**8**)

Table 49. Summary of the results obtained for the flavonoids with the best inhibitory activity against PTP1B, in the analyzed research studies.

Class	Most active flavonoid(s)	Inhibitory activity (IC_{50})	Type of inhibition	Positive control (IC_{50})	Relative coefficient to Positive control	Reference
Flavonols	Flavonoid **1**	4.3 μM	NT	Na_3VO_4 2 μM	0.47	(Chen et al. 2002)
	Quercetin (**3**)	28.12 μM		NM	–	(Li et al. 2005)
	Quercetin (**3**)	58.93 ± 6.69 μM		Ursolic acid 4.06 ± 0.20 μM	0.07	(Islam et al. 2013)
	Quercetin (**3**)	2.9 ± 0.12 μM		PTP1B inhibitor * 1.97 ± 0.5 μM	0.68	(Jiang et al. 2015)
	Kaempferol (**164**)	6.79 ± 0.22 μM		Oleanolic acid 8.35 ± 0.21 μM	1.23	(Qin et al. 2017)
	Flavonoid **235**	10 ± 1 μM	Mixed	Ursolic acid 7.1 ± 0.9 μM	0.71	(Proença et al. 2018)
	Myricetin (**251**):	3.53 ± 0.92 μM	NT	Na_3VO_4 28.91 ± 2.78 μM	Myricetin (**251**): 8.19	(Xu et al. 2018)
	Kaempferol (**164**)				Kaempferol (**164**): 7.38	
Flavones	Vitexin (**111**)	3.92 ± 0.36 μM 7.62 ± 0.21 μM	NT	Ursolic acid 5.99 ± 0.22 μM	0.79	(Choi, Islam, Ali, Kim, Kim, et al. 2014)
	Luteolin (**113**)	6.70 ± 0.03 μM		Ursolic acid 8.20 ± 0.55 μM	1.22	(Choi, Islam, Ali, Kim, Park, et al. 2014)
	Isorhamnetin-3-*O*-β-D-glucoside (**94**)	Isorhamnetin-3-*O*-β-D-glucoside (**94**):		Suramin	Isorhamnetin-3-*O*-β-D-glucoside (**94**):	(Cai, Zhao, and Tao 2015)
	Isorhamnetin-3-*O*-β-D-rutinoside (**120**)	1.16 ± 0.03 μM Isorhamnetin-3-*O*-β-D-rutinoside (**120**):		11 ± 1 μM	9.48 Isorhamnetin-3-*O*-β-D-rutinoside (**120**):	
		1.20 ± 0.05 μM			9.17	
	Licoflavone B (**128**)	15.62 μM		$NaVO_4$ 29.10 μM	1.86	(Guo et al. 2015)
	Isoquercetin (**136**)	17.49 ± 3.31 μg/mL		Oleanolic acid 1.17 ± 0.13 μg/mL	0.07	(Li et al. 2015)
	Afzelin (**7**)	12.16 ± 0.02 μM	Noncompetitive	RK-682 4.47 ± 0.03 μM	0.37	(Na et al. 2016)
	Quercetin 4′-*O*-β-D-glucoside (**176**)	0.92 ± 0.19 μM	Competitive	Ursolic acid 1.21 ± 0.18 μM	1.32	(Zhao et al. 2016)
	Kwanon C (**152**)	2.20 ± 0.83 μM	NT	Oleanolic acid 3.31 ± 0.02 μM	1.50	(Huang et al. 2017)
	Icariside II (**187**)	9.94 ± 0.15 μM	Noncompetitive	Ursolic acid 8.24 ± 0.30 μM	0.83	(Kim et al. 2017)
	Apigenin 7-*O*-β-D-glucuronide (**198**)	7.14 ± 1.75 μM	Mixed	Ursolic acid 9.43 ± 0.14 μM	1.32	(Nguyen et al. 2017)
	Flavonoid **269**	1.6 ± 0.9 μM	Competitive	NM	NM	(Zhang et al. 2018)
	Moracenin A (**276**)	4.04 ± 0.38 μM	NT	RK-682 13.27 ± 1.00 μM	3.28	(Zhao et al. 2018)
	Galangin 3-methyl ether (**301**)	41.4 ± 1.4 μM		RK682 14.5 ± 0.2 μM	0.35	(Zhao et al. 2019)
Isoflavones	2,3-Dihydroauriculatin (**15**)	2.6 ± 0.5 μM	NT	Ursolic acid 2.5 ± 0.2 μM	0.96	(Bae et al. 2006)
	Glisoflavone (**68**)	27.9 ± 1.4 μM	Mixed	RK-682 4.4 ± 0.1 μM	0.16	(Li et al. 2010)
	Flavonoid **73** Flavonoid **75**	Flavonoid **73**: 14.9 ± 1.6 μM Flavonoid **75**: 15.2 ± 0.9 μM	NT	Ursolic acid 3.6 ± 0.2 μM	Flavonoid **73**: 0.24 Flavonoid **75**: 0.24	(Nguyen et al. 2011)
				Ursolic acid 3.6 ± 0.2 μM		
	Erythraddison III (**87**)	4.6 ± 0.3 μM	Mixed	RK-682 4.4 ± 0.1 μM	0.78	(Nguyen et al. 2012)
	3-8″-Bisapigenin (**134**)	4.5 ± 0.1 μM	Mixed	RK-682: 4.5 ± 0.2 μM Ursolic acid: 3.4 ± 0.1 μM	RK-682: 1.00 Ursolic acid: 0.76	(Nguyen et al. 2015)
	Hultenin (**154**)	1.04 ± 0.16 μM	NT	Oleanolic acid 2.98 ± 0.35 μM	2.87	(Wang et al. 2015)
	Alpinumisoflavone (**26**)	11.16 ± 1.88 μM		Oleanolic acid 2.61 ± 0.59 μM	0.23	(Wu et al. 2015)

	6,8-Diprenylorobol (**166**)	2.4 ± 0.3 μM	Noncompetitive	Ursolic acid 15.5 ± 0.9 μM	6.46		(Wang et al. 2016)
	Mucusisoflavone B (**213**)	2.5 ± 0.2 μM		RK682 10.4 ± 1.6 μM	4.16		(Trinh, Jager, and Staerk 2017)
Flavanones	Sanggenon G(**17**)	1.6 ± 0.3 μM	Mixed	RK-682 4.5 ± 0.5 μM	2.81		(Cui et al. 2006)
	Abyssinone-IV (**22**)	16 ± 1.1 μM	NT	RK-682: 4.5 ± 0.5 μM Ursolic acid: 3.6 ± 0.2 μM	RK-682: 0.28 Ursolic acid: 0.23		(Na et al. 2006)
	Sigmoidin F (**32**) Sigmoidin A (**36**)	Sigmoidin F (**32**): 14.2 ± 1.7 μM Sigmoidin A (**36**): 14.4 ± 0.8 μM		RK-682: 4.5 ± 0.5 μM Ursolic acid: 3.6 ± 0.2 μM	**RK-682** Sigmoidin F (**32**): 0.32 Sigmoidin A (**36**): 0.25 **Ursolic acid** Sigmoidin F (**32**): 0.31 Sigmoidin A (**36**): 0.25		(Cui et al. 2007)
	Flavonoid **38** Flavonoid **41**	Flavonoid **38**: 13.9 ± 2.1 μM Flavonoid **41**: 14.9 ± 1.6 μM		RK-682: 4.7 ± 0.5 μM Ursolic acid: 3.6 ± 0.2 μM	**RK-682** Flavonoid **38**: 0.34 Flavonoid **41**: 0.32 **Ursolic acid** Flavonoid **38**: 0.26 Flavonoid **41**: 0.24		(Cui et al. 2008)
	Flavonoid **59** Flavonoid **61**	Flavonoid **59**: 15.2 ± 1.2 μM Flavonoid **61**: 16.1 ± 1.1 μM		RK-682 4.7 ± 0.5 μM	Flavonoid **59**: 0.31 Flavonoid **61**: 0.29		(Cui et al. 2010)
	Flavonoid **103** Flavonoid **107**	Flavonoid **107**: 2.37 ± 0.37 μM Flavonoid **103**: 2.40 ± 0.22 μM	Flavonoid **107**: Competitive	Ursolic acid: 3.20 ± 0.31 μM	Flavonoid **107**: 1.35 Flavonoid **103**: 1.33		(Sun et al. 2013)
	2′-Methoxykurarinone (**118**)	5.26 ± 0.24 μM	Noncompetitive	RK-682: 4.49 ± 0.15 μM	0.85		(Sasaki et al. 2014)
	Cudraflavanone D (**149**)	5.7 ± 1.5 μM		Ursolic acid 3.8 ± 0.4 μM	0.67		(Quang et al. 2015)
	Bonannione A (**172**)	14.0 ± 1.2 μM	NT	Oleanolic acid 2.6 ± 0.6 μM	0.19		(Zhang et al. 2016)
	Prunin (**184**)	17.5 ± 2.6 μM		Ursolic acid 5.4 ± 0.3 μM	0.31		(Jung et al. 2017)
	Bonannione A (**172**)	1.9 ± 0.1 μM	Mixed	$NaVO_4$ 32.6 ± 1.5 μM	17.16		(Song et al. 2017)
	Isosilybin B (**244**) Silybin A (**241**)	Isosilybin B (**244**): 1.37 ± 0.22 μM Silybin A (**241**): 1.54 ± 0.22 μM	Isosilybin B (**244**): Noncompetitive Silybin A (**241**): Noncompetitive	Isosilybin B (**244**): Ursolic acid 3.52 ± 0.10 μM	Isosilybin B (**244**): 2.57 Silybin A (**241**): 2.29		(Qin et al. 2018)
	Flavonoid **283** Flavonoid **294**	10.3 ± 0.9 μM 4.6 ± 0.5 μM	NT	4.7 ± 0.6 μM Ursolic acid 3.1 ± 0.4 μM	0.46 0.67		(Ren et al. 2019) (Xu et al. 2019)
Flavans	Flavonoid **56**	5.5 ± 0.3 μM	NT	RK-682: 4.5 ± 0.5 μM Ursolic acid: 3.6 ± 0.2 μM	RK-682: 0.82 Ursolic acid: 0.65		(Jang et al. 2008)
	Broukazinol A (**256/261**)	20.00 ± 1.85 μM		Oleanolic acid 2.52 ± 0.22 μM	0.13		(Xue et al. 2018)

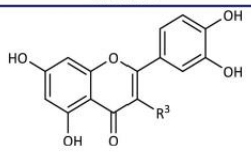
NM – Not mentioned; NT – Not tested.

Table 50. Experimental conditions applied in the research studies concerning the inhibition of DPP-4 by flavonoids.

DPP-4 (source, concentration)	Substrate	Substrate concentration	Preincubation of flavonoids with DPP-4	Time of enzymatic reaction	pH	Temperature (°C)	Positive control activity	Reference
Human, NM	Gly-Pro *p*-nitroanilide	0.86 mg/mL	3 min	20 min	7.0	37	P32/98 (hemifumarate) Ki = 130 nM	(Eidenberger, Selg, and Krennhuber 2013)
Porcine*, 1 ng/mL	Gly-Pro-amino methyl coumarin	NM	NM	30 min	NM	NM	Diprotin A $IC_{50} = 4.21 \pm 2.01$ μM	(Fan et al. 2013)
Porcine*, 0.075 U/nL	NM				8.0	26	Sitagliptin $IC_{50} = 0.05 \pm 0.01$ μM	(Bower et al. 2014)
Human, 17.3 mU/mL	Gly-Pro-amino methyl coumarin	4 mg/mL	10 min		7.5	25	Diprotin A $IC_{50} = 2.3$ μM	(Morikawa et al. 2015)
Porcine, 5.5 U/mL	Gly-Pro *p*-nitroanilide	0.75 mM	NM		8.6***	37	Linagliptin $IC_{50} = 0.14 \pm 0.03$ μM	(Zhao et al. 2016)
NM, NM	NM	NM			NM		Sitagliptin $IC_{50} = 24.51 \pm 1.01$ μg/mg	(Sarian et al. 2017)
NM, NM				NM		NM	Sitagliptin: 0.685 Saxagliptin: 0.708 Vildagliptin: 2.29	(Gupta et al. 2018)
NM, NM				30 min		37	Sitagliptin $IC_{50} = 0.071 \pm 0.005$ μM	(Kim et al. 2018)
Human, 150 U/mL	Gly-Pro *p*-nitroanilide	0.25 mM	10 min	60 min	8.0		Sitagliptin: $IC_{50} = 0.106 \pm 0.006$ μM Diprotin A: $IC_{50} = 37 \pm 3$ μM	(Proença, Freitas, Ribeiro, Tomé, Araújo, et al. 2019)
Human, 38 U/mL	Gly-Pro-amino methyl coumarin	0.125 mM					Sitagliptin: $IC_{50} = 0.064 \pm 0.005$ μM Diprotin A: $IC_{50} = 31 \pm 2$ μM	(Proença, Freitas, Ribeiro, Tomé, Araújo, et al. 2019)

NM - Not mentioned.
*It was followed the manufacturer's instructions from the DPP-4 Fluorometric Assay Kit (Abcam, Cambridge, UK).
**It was followed the manufacturer's instructions from the DPP-4 Inhibitor Assay Kit (Cayman, Michigan, USA).
***NaOH 10 M to stop the reaction.

Table 51. DPP-4 inhibition by flavonoids tested by Eidenberger et al (Eidenberger, Selg, and Krennhuber 2013).

Flavonoid	Structure	R^3	IC_{50} (μmol/mL ± SD)
Hyperoside (**93**)		galactose	0.242 ± 0.0237
Peltatoside (**135**)		arabinofuranose	0.126 ± 0.0129
Isoquercetin (**136**)		glucose	0.181 ± 0.171
Guaijaverin (**140**)		arabinose	**0.086 ± 0.00851**
Positive control P32/P98 hemifumarate	–	–	≈ 130 nM

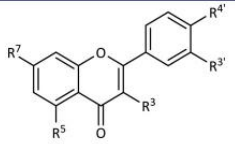
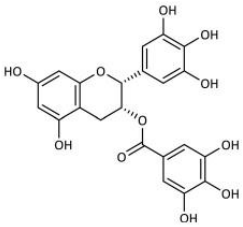
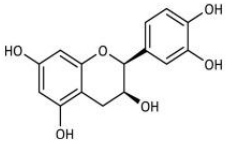
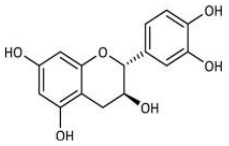
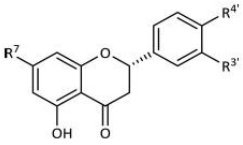
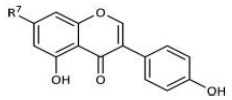
presented no activity at the highest tested concentration. The obtained results regarding the activity of flavanones, showed that naringenin (**181**) and hesperetin (**256**) were the most active compounds, with IC_{50} values of 0.24 ± 0.03 μM and 0.28 ± 0.07 μM, respectively. Taking this into account, it was observed that the substitution of a sugar by an –OH group at 7-position of A ring significantly increases the DPP-4 inhibition, as found by comparing naringenin (**181**) with naringin (**131**) (not active) and narirutin (**185**) (not active), and hesperetin (**256**) with hesperidin (**307**) (not active) and neohesperidin (**308**) (not active) . The same effect was observed for isoflavones since genistein (**121**) (IC_{50} = 0.48 ± 0.04 μM) was a better inhibitor than genistin (**309**) (not active).

Also, the replacement of the –OH for a $-OCH_3$ at 4′-position of B ring seems to decrease the DPP-4 inhibition, as eriocitrin (**306**), with an IC_{50} value of 10.36 ± 0.09 μM, was a better inhibitor than hesperidin (**307**), which was not active. The same effect was observed for isoflavones since genistein (**121**) (IC_{50} = 0.48 ± 0.04 μM) was a better inhibitor than genistin (**309**) (not active).

The ability of flavonoids isolated from culinary herbs to inhibit DPP-4 (Table 53) was tested by Bower et al (Bower et al. 2014). Flavonoids hispidulin (**310**) and cirismaritin (**311**) had similar IC_{50} values, 0.49 ± 0.1 μM and 0.43 ± 0.07 μM, respectively. This suggests that the replacement of an –OH by a $-OCH_3$ at 7-position of A ring has no effect in the inhibitory activity. In flavanones, the addition of an -OH group at 3′-position of B ring reduces the DPP-4 inhibition, as observed by comparing eriodictyol (**240**) (IC_{50} = 10.9 ± 0.4 μM) with naringenin (**181**) (IC_{50} = 2.5 ± 0.3 μM). Considering these results, it was suggested that flavones are better DPP-4 inhibitors than flavanones, highlighting the importance of the C2 = C3 double bond.

The DPP-4 inhibition by a series of glycosylated flavonoids isolated from flowers of *Helichrysum arenarium* (Table 54) was evaluated by Morikawa et al (Morikawa et al. 2015). Considering the tested flavanones, it was observed

Table 52. DPP-4 inhibition by flavonoids tested by Fan et al (Fan et al. 2013).

Flavonoid	Structure	R^3	$R^{3'}$	$R^{4'}$	R^5	$R^{5'}$	R^6	R^7	IC_{50} (μM ± SD)
Quercetin (**3**)		OH	OH	OH	OH	–	OH	–	2.92 ± 0.68
Rutin (**8**)		rutinose	OH	OH	OH	–	OH	–	NA
Apigenin (**71**)		H	H	OH	OH	–	OH	–	**0.14 ± 0.02**
Luteolin (**113**)		H	OH	OH	OH	–	OH	–	**0.12 ± 0.01**
Kaempferol (**164**)		OH	H	OH	OH	–	OH	–	0.49 ± 0.02
Flavone (**214**)		H	H	H	H	–	H	–	0.17 ± 0.01
Epigallocatechin gallate (**10**)		–	–	–	–		–	–	10.21 ± 0.75
(-)-Epicatechin (**137**)		–	–	–	–	–	–	–	NA
(+)-Catechin (**138**)		–	–	–	–	–	–	–	NA
Cyanidin (**303**)		OH	OH	–	–	H	–	–	1.41 ± 0.25
Cyanidin 3-glucoside (**304**)		glucose	OH	–	–	H	–	–	0.42 ± 0.09
Malvidin (**305**)		OH	OCH_3	–	–	OCH_3	–	–	1.41 ± 0.44
Naringin (**131**)		–	H	OH	–	–	–	neohesperidose	NA
Naringenin (**181**)		–	H	OH	–	–	–	OH	0.24 ± 0.03
Narirutin (**185**)		–	H	OH	–	–	–	rutinose	NA
Hesperetin (**256**)		–	OH	OCH_3	–	–	–	OH	0.28 ± 0.07
Eriocitrin (**306**)		–	OH	OH	–	–	–	rutinose	10.36 ± 0.09
Hesperidin (**307**)		–	OH	OCH_3	–	–	–	rutinose	NA
Neohesperidin (**308**)		–	OH	OCH_3	–	–	–	neohesperidose	NA
Genistein (**121**)		–	–	–	–	–	–	OH	0.48 ± 0.04
Genistin (**309**)		–	–	–	–	–	–	glucose	NA
Positive control Diprotin A	–	–	–	–	–	–	–	–	4.21 ± 2.01

NA – not active.

that these compounds were not effective inhibitors of the enzyme under study, since all of them presented an IC_{50} value higher than 100 μM. It seems that the lack of the C2 = C3 double bond is not beneficial for the inhibitory activity against DPP-4, by comparing, for example, prunin (**184**) with apigenin 7-*O*-*β*-D-glucoside (**197**) (IC_{50} = 62.7 μM). Regarding the activity of flavones, particularly the apigenin derivatives, it was possible to conclude that the presence of a gentiobiose at 7-position of A ring enhances the DPP-4 inhibition, as seen by comparing apigenin 7-*O*-*β*-D-gentiobioside (**322**) (IC_{50} = 32.0 μM) with apigenin 7-*O*-*β*-D-glucoside (**197**) (IC_{50} = 62.7 μM). For luteolin derivatives, cynaroside (**139**) and luteolin 3′-*O*-*β*-D-glucoside (**203**) presented IC_{50} values of 37.5 μM and > 100 μM, respectively, suggesting that the glucose is more favorable for the intended effect at 7-position of A ring than at 3′-position of B ring. In what concerns kaempferol derivatives, it was seen that addition of a glucose at 7-position of A ring significantly increases the DPP-4 inhibition, by comparing astraglin (**196**) (IC_{50} = > 100 μM) with kaempferol 3,7-di-*O*-*β*-D-glucoside (**328**) (IC_{50} = 36.8 μM). Regarding. kaempferol 3,7-di-*O*-*β*-D-glucoside (**328**) and kaempferol 3,4′-di-*O*-*β*-D-glucoside (**329**) (IC_{50} = 88.6 μM), it seems that the presence of a glucose is more important at 7-position of A ring than at 4′-position of B ring. Finally, considering quercetin derivatives, it was verified that addition of a glucose at 3′-position of B ring reduces the intended effect, since isoquercetin (**136**) (IC_{50} = 56.6 μM) was more active than

quercetin 3,3′-di-*O*-*β*-D-glucoside (**331**) (IC_{50} = 73.9 μM). Moreover, glucose at 3-position of C ring seems to increase DPP-4 inhibition more than rutinose, since rutin (**8**) presented an IC_{50} value higher than 100 μM, and isoquercetin (**136**) presented an IC_{50} value of 56.6 μM.

Zhao et al. (2016) studied the inhibitory activity of flavonoids from the leaves of *Smilax china* (Table 55) against DPP-4. Among the tested flavones, the best inhibitor found was kaempferol 7-*O*-α-L-rhamnoside (**175**), presenting an IC_{50} value of 20.81 ± 1.20 μM. Among the evaluated kaempferol derivatives, it can be observed that the presence of a rhamnose instead of an -OH group at 7-position of A ring increases the inhibition of DPP-4, by comparing for example kaempferol 7-*O*-α-L-rhamnoside (**175**) with kaempferol (**164**) (IC_{50} = 45.96 ± 1.52 μM). On the other hand, the replacement of a rhamnose by an -OH group at 3-position of C ring led to enhancement of the intended effect, as observed by comparing kaempferol (**164**) with afzelin (**7**) (IC_{50} > 100 μM). In addition, through comparison of kaempferide (**173**) (IC_{50} = > 100 μM) with kaempferol (**164**), it appears that the substitution of a -OCH_3 by an -OH group at 4′-position of B ring increase the inhibitory activity of flavonoids.

The inhibitory activity of a panel flavonoids against DPP-4 was evaluated by Sarian et al. (2017) (Table 56). By comparing norwogonin (**337**) (IC_{50} > 100 μM) with isoscutellarein (**339**) (IC_{50} = 22.23 ± 1.52 μM) and hypolaetin (**340**) (IC_{50} = 34.89 ± 7.44 μM), it was found that the addition of -OH groups at 3′- or/and at −4′-positions of B ring increase the inhibition of DPP-4. The same conclusion can be made by comparing chrysin (**236**), which presented no activity at the highest tested concentration, with quercetin (**3**) and kaempferol (**164**), both exhibiting IC_{50} values of 21.75 ± 5.81 μM and 45.93 ± 8.61 μM, respectively. In addition, it can be observed that the methoxylation and acetylation of flavones did not have a favorable effect for the inhibition of the enzyme under study.

Gupta et al. (2018) evaluated the inhibition of DPP-4 by citrus flavonoids (Table 57), and rutin (**8**) was the most active compound, with an IC_{50} value of 485 μM. Through the obtained results, it can be concluded that the presence of the C2 = C3 double bond increases the inhibitory effect, by comparing rutin (**8**) with eriocitrin (**311**) (IC_{50} = 3820 μM). In addition, it seems that the rhamnose instead of the -OH group at 3-position of C ring is advantageous for DPP-4 inhibition, since eriocitrin (**311**) was a better inhibitor than eriodictyol (**240**) (IC_{50} = 5700 μM). Also, among the tested flavanones, it was found that substitution of an -OH group for a -OCH_3 group at 4′-position of B ring almost does not produce a different effect in the activity the

Table 53. DPP-4 inhibition by flavonoids tested by Bower et al (Bower et al. 2014).

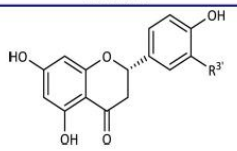
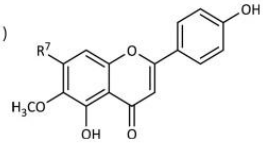
Flavonoid	Structure	$R^{3'}$	R^7	IC_{50} (μM ± SEM)
Naringenin (**181**)		H	–	2.5 ± 0.3
Eriodictyol (**240**)		OH	–	10.9 ± 0.4
Hispidulin (**310**)		–	OH	**0.49 ± 0.1**
Cirsimaritin (**311**)		–	OCH_3	**0.43 ± 0.07**
Positive control Sitagliptin	–	–	–	0.06 ± 0.03

Table 54. DPP-4 inhibition by flavonoids tested by Morikawa et al (Morikawa et al. 2015).

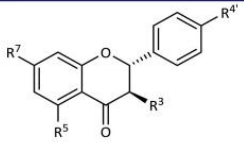
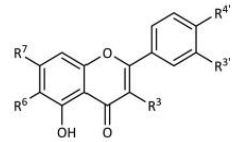
Flavonoid	Structure	R^3	$R^{3'}$	$R^{4'}$	R^5	R^6	R^7	IC_{50} (μM)
Prunin (**184**)		H	–	OH	OH	–	glucose	>100
2*S*-Helichrysin (**312**)		H	–	OH	glucose	–	H-	>100
2*R*-Helichrysin (**313**)		H	–	OH	glucose	–	H	>100
5,7-Di-*O*-*β*-glucosyl-(2*S*)-naringenin (**314**)		H	–	OH	glucose	–	glucose	>100
5,7-Di-*O*-*β*-glucosyl-(2*R*)-naringenin (**315**)		H	–	OH	glucose	–	glucose	>100
(2*S*) Arenariumoside I (**316**)		H	–	OH	glucosyl-(1-6)-glucose	–	OH	>100
(2*R*) Arenariumoside II (**317**)		H	–	OH	glucosyl-(1-6)-glucose	–	OH	>100
(2*S*) Arenariumoside IV (**318**)		H	–	glucose	glucose	–	OH	>100
Helicloside A (**319**)		OH	–	OH	glucose	–	OH	>100
Dihydrokaempferol 7-*O*-*β*-D-glucoside (**320**)		OH	–	OH	OH	–	glucose	>100
Rutin (**8**)		rutinose	OH	OH	–	H	OH	>100
Isoquercetin (**136**)		glucose	OH	OH	–	H	OH	56.6
Cynaroside (**139**)		H	OH	OH	–	H	glucose	37.5
Astraglin (**196**)		glucose	H	OH	–	H	OH	>100
Apigenin 7-*O*-*β*-D-glucoside (**197**)		H	H	OH	–	H	glucose	62.7
Luteolin 3′-*O*-*β*-D-glucoside (**203**)		H	glucose	OH	–	H	OH	>100
Apigenin 7-*O*-*β*-D-glucosiduronic methyl ester (**321**)		H	H	OH	–	H	glucosiduronic methyl ester	50.5
Apigenin 7-*O*-*β*-D-gentiobioside (**322**)		H	H	OH	–	H	gentiobiose	**32.0**
Apigenin 4′,7-di-*O*-*β*-D-glucoside (**323**)		H	H	glucose	–	H	glucose	>100
Scutellarein 7-*O*-*β*-D-gentiobioside (**324**)		H	H	OH	–	OH	gentiobiose	>100
6-Hydroxyluteolin 7-*O*-*β*-D-glucoside (**325**)		H	OH	OH	–	OH	glucose	60.3
326		H	OCH_3	OH	–	OH	glucose	73.2
Kaempferol 3-*O*-*β*-D-gentiobioside (**327**)		gentiobiose	H	OH	–	H	OH	58.0
Kaempferol 3,7-di-*O*-*β*-D-glucoside (**328**)		glucose	H	OH	–	H	glucose	36.8
Kaempferol 3,4′-di-*O*-*β*-D-glucoside (**329**)		glucose	H	glucose	–	H	OH	88.6
330		glucosyl-(1-3)-*β*-D-glucose	H	OH	–	H	OH	85.2
Quercetin 3,3′-di-*O*-*β*-D-glucoside (**331**)		glucose	glucose	OH	–	H	OH	73.9
Positive controls	–		–				–	0.0018
Alogliptin								2.3
Diprotin A								

Table 55. DPP-4 inhibition by flavonoids tested by Zhao et al (Zhao et al. 2016).

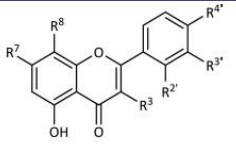
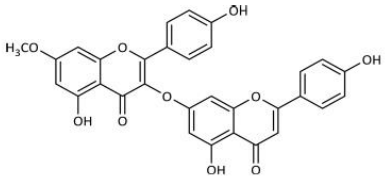
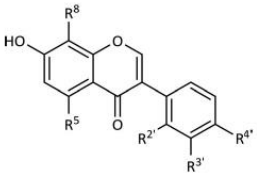
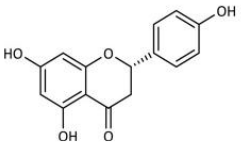
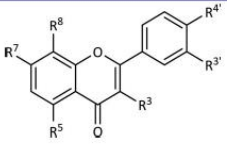
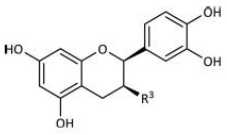
Flavonoid	Structure	$R^{2'}$	R^3	$R^{3'}$	$R^{4'}$	R^5	R^7	R^8	IC_{50} (μM ± SD)
Afzelin (**7**)		H	rhamnose	H	OH	–	OH	H	>100
Rutin (**8**)		H	rutinose	OH	OH	–	OH	H	32.93 ± 1.84
Kaempferitrin (**9**)		H	rhamnose	H	OH	–	rhamnose	H	>100
Vitexin (**111**)		H	H	H	OH	–	OH	glucose	33.12 ± 1.01
Kaempferol (**164**)		H	OH	H	OH	–	OH	H	45.96 ± 1.52
Kaempferide (**173**)		H	OH	H	OCH_3	–	OH	H	>100
Morin (**174**)		OH	OH	H	OH	–	OH	H	>100
Kaempferol 7-*O*-α-L-rhamnoside (**175**)		H	OH	H	OH	–	rhamnose	H	**20.81 ± 1.20**
Quercetin 4′-*O*-β-D-glucoside (**176**)		H	OH	OH	glucose	–	OH	H	>100
Lepidoside (**177**)		H	rhamnose	H	OH	–	xylose	H	43.61 ± 0.97
Bismilachinone (**178**)		–	–	–	–	–	–	–	>100
Puerarin (**132**)		H	–	H	OH	H	–	glucose	>100
Pratensein (**179**)		H	–	OH	OCH_3	OH	–	H	>100
Smilachinin (**180**)		glucose	–	H	OCH_3	OH	–	H	>100
Naringenin (**181**)		–	–	–	–	–	–	–	>100
Positive control Linagliptin	–	–	–	–	–	–	–	–	0.14 ± 0.03

Table 56. DPP-4 inhibition by flavonoids tested by Sarian et al. (2017).

Flavonoid	Structure	R^3	$R^{3'}$	$R^{4'}$	R^5	R^7	R^8	IC_{50} (μg/m) ± SEM)
Quercetin (**3**)		OH	OH	OH	OH	OH	H	**21.75 ± 5.81**
Kaempferol (**164**)		OH	H	OH	OH	OH	H	45.93 ± 8.61
Chrysin (**236**)		H	H	H	OH	OH	H	NA
Wogonin (**332**)		H	H	H	OH	OH	OCH_3	>100
Wogonin methyl ether (**333**)		H	H	H	OCH_3	OCH_3	OCH_3	>100
Wogonin acetate (**334**)		H	H	H	AcO	AcO	OCH_3	NA
Techtochrysin (**335**)		H	H	H	OH	OCH_3	H	>100
336		H	H	H	H	OCH_3	OH	>100
Norwogonin (**337**)		H	H	H	OH	OH	OH	>100
Norwogonin acetate (**338**)		H	H	H	AcO	AcO	AcO	>100
Isoscutellarein (**339**)		H	H	OH	OH	OH	OH	**22.23 ± 1.52**
Hypolaetin (**340**)		H	OH	OH	OH	OH	OH	34.89 ± 7.44
(-)-Epicatechin (**137**)		–	–	–	–	–	–	NA
(+)-Catechin (**138**)		–	–	–	–	–	–	NA
Positive control Sitagliptin	–	–	–	–	–	–	–	24.51 ± 1.01

NA – not active.

DPP-4 inhibition, as seen by comparing eriodictyol (**240**) (IC_{50} = 5700 μM) with hesperetin (**256**) (IC_{50} = 5700 μM), and eriocitrin (**311**) (IC_{50} = 3820 μM) with hesperidin (**307**) (IC_{50} = 3910 μM).

Kim et al. (2018) isolated flavonoids from the seeds of *Lens culinaris* (Table 58) and their capacity to inhibit DPP-4 was studied. The obtained results showed that flavonoid glycosides (compounds **341**, **342** and **343**) were better

Table 57. DPP-4 inhibition by flavonoids tested by Gupta et al. (2018).

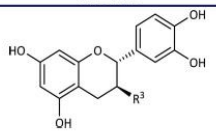
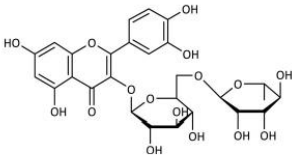
Flavonoid	Structure	$R^{3'}$	$R^{4'}$	R^{7}	IC_{50} (μM)
Rutin (8)		–	–	–	**485**
Naringin (**133**)		H	OH	neohesperidose	5440
Naringenin (**181**)		H	OH	OH	5500
Eriodictyol (**240**)		OH	OH	OH	5700
Hesperetin (**256**)		OH	OCH_3	OH	5700
Hesperidin (**307**)		OH	OCH_3	rutinose	3910
Eriocitrin (**311**)		OH	OH	rutinose	3820
Positive controls	–	–	–	–	0.685
Sitagliptin					0.708
Saxagliptin					2.29
Vildagliptin					

Table 58. DPP-4 inhibition by flavonoids tested by Kim et al (Kim et al. 2018).

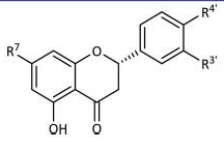
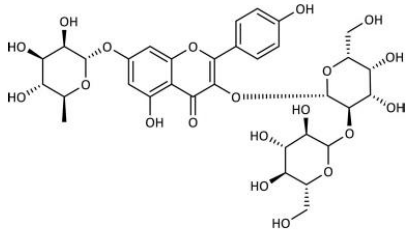
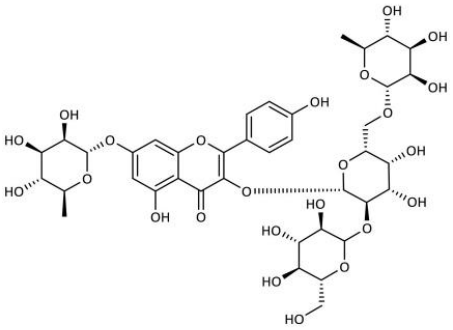
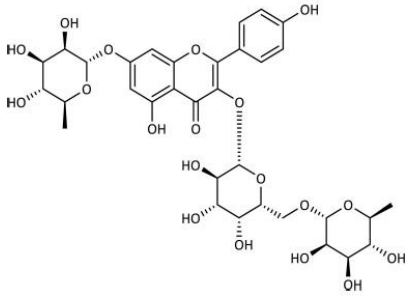
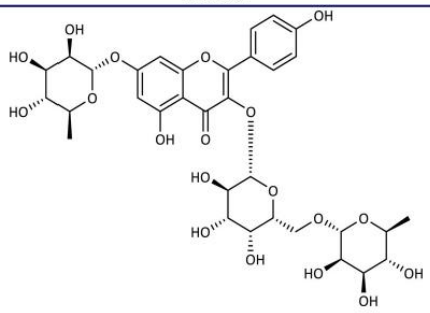
Flavonoid	Structure	IC_{50} (μM ± SD)
Kaempferol (**164**)		51.9 ± 4.83
341		**27.89 ± 1.29**
342		36.52 ± 0.78
343		37.0 ± 1.40
Positive control Sitagliptin	–	0.071 ± 0.005

Table 59. DPP-4 inhibition by flavonoids tested by Proença et al (Proença, Freitas, Ribeiro, Tomé, Araújo, et al. 2019).

Flavonoid	Structure	R^3	$R^{3'}$	$R^{4'}$	R^5	R^6	R^7	R^8	% Inhibition at 200 μM	% Inhibition at 100 μM	IC_{50} (μM ± SEM)
Flavone (**214**)		H	H	H	H	H	H	H	<20	NT	>200
215		H	OH	H	H	H	H	H	<20	NT	>200
216		H	H	OH	H	H	H	H	<20	NT	>200
217		H	OH	OH	H	H	H	H	42 ± 3	22 ± 2	>200
218		OH	OH	OH	H	H	H	H	47 ± 1	27 ± 1	>200
219		OH	OCH_3	OCH_3	H	H	H	H	<20	NT	>200
220		H	H	H	OH	H	H	H	<20	NT	>200
221		H	OH	H	OH	H	H	H	<20	NT	>200
222		H	H	OH	OH	H	H	H	23 ± 2	NT	>200
223		H	OH	OH	OH	H	H	H	28 ± 4	NT	>200
224		H	H	H	H	H	OH	H	28 ± 3	NT	>200
225		H	OH	H	H	H	OH	H	36 ± 3	NT	>200
126		H	H	OH	H	H	OH	H	47 ± 2	28 ± 1	>200
226		OH	OH	H	H	H	OH	H	38 ± 3	NT	>200
227		OH	H	OH	H	H	OH	H	44 ± 2	29 ± 1	>200
228		H	OH	OH	H	H	OH	H	47 ± 2	33 ± 2	>200
229		OH	OH	OH	H	H	OH	OH	34 ± 1	NT	>200
230		OH	OCH_3	H	H	H	OCH_3	H	<20	NT	>200
231		OH	H	OCH_3	H	H	OCH_3	H	<20	NT	>200
232		OH	OH	OH	H	H	OCH_3	OCH_3	48 ± 1	28 ± 1	>200
233		OH	OCH_3	OCH_3	H	H	OH	OH	**82 ± 1**	**60 ± 1**	**73 ± 2**
234		OH	OBn	OBn	H	H	OCH_3	OCH_3	41 ± 2	20 ± 1	>200
235		OH	OCH_3	OCH_3	H	H	OBn	OBn	42 ± 2	28 ± 1	>200
Quercetin (**3**)		OH	OH	OH	OH	H	OH	H	46 ± 2	26 ± 3	>200
Rutin (**8**)		rutinose	OH	OH	OH	H	OH	H	40 ± 2	22 ± 4	>200
Apigenin (**71**)		H	H	OH	OH	H	OH	H	44 ± 2	25 ± 1	>200
Luteolin (**113**)		H	OH	OH	OH	H	OH	H	45 ± 2	24 ± 2	>200
Kaempferol (**164**)		OH	H	OH	OH	H	OH	H	38 ± 1	NT	>200
Chrysin (**236**)		H	H	H	OH	H	OH	H	33 ± 4	NT	>200
Galangin (**237**)		OH	H	H	OH	H	OH	H	35 ± 4	NT	>200
Baicalein (**238**)		H	H	H	OH	OH	OH	H	43 ± 4	22 ± 2	>200
Acacetin (**239**)		H	H	OCH_3	OH	H	OH	H	<20	NT	>200
Hispidulin (**310**)		H	H	OH	OH	OCH_3	OH	H	46 ± 2	28 ± 1	>200
344		H	OH	H	OH	H	OH	H	40 ± 3	20 ± 1	>200
345		Cl	OH	OH	OH	H	OH	H	55 ± 2	36 ± 2	170 ± 10
346		H	OH	OH	OH	Cl	OH	H	41 ± 1	24 ± 2	>200
347		H	OH	OH	OH	H	OH	Cl	40 ± 1	24 ± 2	>200
348		Cl	OH	OH	OH	H	OH	Cl	55 ± 1	35 ± 1	171 ± 8
349		H	OH	OH	OH	Cl	OH	Cl	37 ± 1	NT	>200
Chrysoeriol (**350**)		H	OCH_3	OH	OH	H	OH	H	37 ± 1	NT	>200
351		H	OCH_3	OCH_3	OH	H	OH	H	28 ± 2	NT	>200
Taxifolin (**153**)		OH	OH	OH	OH	H	OH	H	<20	NT	>200
Naringenin (**181**)		H	H	OH	OH	H	OH	H	<20	NT	>200
Eriodictyol (**240**)		H	OH	OH	OH	H	OH	H	<20	NT	>200
Positive control	–	–	–	–	–	–	–	–	NT*	NT*	0.064 ± 0.005
Sitagliptin											31 ± 2
Diprotin A											

NT – Not tested.
*The highest tested concentration was 20 μM.

inhibitors than the non-glycoside flavonoid kaempferol (**164**) (IC_{50} = 51.9 ± 4.83 μM), being compound **341** the most active flavonoid, with an IC_{50} value of 27.89 ± 1.29. These data demonstrate that the substituent present at 3-position of C ring in compound **341** is more favorable for the intended effect than the substituents present in the other tested flavonoids.

In the work of the group of Proença, Freitas, Ribeiro, Tomé, Araújo, et al. (2019), the inhibition of human DPP-4 was evaluated for a large panel of flavonoids (Table 59) using in vitro and ex vivo models. Using the colorimetric method, the tested flavonoids did not show any inhibitory activity against DPP-4, at the highest tested concentration (200 μM), demonstrating that the fluorometric method is more sensitive. Using the last method, the most active flavonoid was compound **233** (IC_{50} = 73 ± 2 μM), a noncompetitive inhibitor. By comparing flavonoid **233** with flavonoid **229** (34 ± 1% of inhibition at 200 μM), it was observed that the substitution of the -OCH_3 groups by -OH groups at 3′- and 4′- positions of B ring significantly decreases the inhibition of DPP-4. In addition, it was possible to see that the presence of -OBn groups at 7- and 8-

Table 60. Summary of the results obtained for the flavonoids with best inhibitory activity against DPP-4, in the analyzed research studies.

Class	Most active flavonoid(s)	Inhibitory activity (IC_{50})	Type of inhibition	Positive control (IC_{50})	Relative coefficient to Positive control	Reference
Flavones	Guaijaverin (**140**)	0.086 ± 0.00851 μmol/mL	NT	P32/98 (hemifumarate) 130 nM	0.002	(Eidenberger, Selg, and Krennhuber 2013)
	Luteolin (**113**)	Luteolin (**113**): 0.12 ± 0.01 μM	Luteolin (**115**) and Apigenin (**73**): Noncompetitive	Diprotin A 4.21 ± 2.01 μM	Luteolin (**113**): 32.08	(Fan et al. 2013)
	Apigenin (**71**)	Apigenin (**71**): 0.14 ± 0.02 μM			Apigenin (**71**): 30.07	
	Hispidulin (**310**)	Hispidulin (**310**): 0.49 ± 0.1 μM	NT	Sitagliptin 0.06 ± 0.03 μM	Hispidulin (**310**): 0.12	(Bower et al. 2014)
	Cirsimaritin (**311**)	Cirsimaritin (**311**): 0.43 ± 0.07 μM			Cirsimaritin (**311**): 0.14	
	Rutin (**8**)	485 μM		Sitagliptin 0.685 μM	Sitagliptin: 0.001	(Gupta et al. 2018)
				Saxagliptin 0.708 μM	Saxagliptin: 0.001	
				Vildagliptin 2.29 μM	Vildagliptin: 0.005	
	Kaempferol 3-*O*-*β*-glucosyl-(1->2)-*β*-galactosyl-7-*O*-*α*-rhamnoside (**341**)	27.89 ± 1.29 μM		Sitagliptin: 0.071 ± 0.005 μM	0.003	(Kim et al. 2018)
Flavanones	Apigenin 7-*O*-*β*-D-gentiobioside (**322**)	32.0 μM		Alogliptin: 0.0018 μM	Alogliptin: 0.00006	(Morikawa et al. 2015)
				Diprotin A: 2.3 μM	Diprotin A: 0.07	
Flavonols	Kaempferol 7-*O*-*α*-L-rhamnoside (**175**)	20.81 ± 1.20 μM		Linagliptin 0.14 ± 0.03 μM	0.007	(Zhao et al. 2016)
	Quercetin (**3**)	Quercetin (**3**): 21.75 ± 5.81 μg/mg		Sitagliptin 24.51 ± 1.01 μg/mg	Quercetin (**3**): 1.13	(Sarian et al. 2017)
	Isoscutellarein (**339**)	Isoscutellarein (**339**): 22.23 ± 1.52 μg/mg			Isoscutellarein (**339**): 1.10	
	Flavonoid **233**	73 ± 2 μM	Noncompetitive	Sitagliptin: 0.064 ± 0.005 μM	Sitagliptin: 0.0009	(Proença, Freitas, Ribeiro, Tomé, Araújo, et al. 2019)
				Diprotin A: 31 ± 2 μM	Diprotin A: 0.42	

NM – Not mentioned.
NT – Not tested.

positions of A ring is not advantageous for the intended effect, by comparing compound **233** with compound **235** (42 ± 2% of inhibition at 200 μM).

Chlorinated flavonoids **345** and **348** presented IC_{50} values of 170 ± 10 μM and 171 ± 8 μM, respectively. The structures of compounds **345** and **348** are similar, and the only difference between them is that compound **348** exhibits an additional -Cl at 8-position of A ring. Thus, the presence of a -Cl substituent at 3-position of C ring seems to be important for the inhibition of the enzyme under study. Furthermore, the importance of this substituent at this position is emphasized by comparing flavonoid **345** with quercetin (**3**), since quercetin had an IC_{50} value higher than 200 μM. The tested flavanones taxifolin (**153**), naringenin (**181**) and eriodictyol (**240**) were not able to inhibit DPP-4, highlighting that the absence of the C2 = C3 double bond is not favorable for the intended effect.

The results obtained in the different research studies regarding the DPP-4 inhibition by the most active flavonoids were summarized in Table 60.

Discussion

Inhibition of PTP1B by flavonoids

This section consists of an interpretation of the above-mentioned results obtained in the analyzed publications. PTP1B plays an important role in the negative regulation of insulin transduction pathway and has emerged as a novel therapeutic strategy for the management of T2D. In the last years, many flavonoids, either synthetic or isolated from natural products, have been investigated concerning their capacity to inhibit PTP1B. From the analysis of the different research studies published on this field, some important structure-activity relationship conclusions can be drawn (Figure 6).

First, it was found that some flavonoid subclasses are more favorable for PTP1B inhibition, and in general, the descending order potencies is the following: flavones and flavonols > flavans > isoflavones > flavanones.

It was interesting to observe that the presence or addition of less polar and/or bulky substituents, such as -OCH_3, -OBn and prenyl groups, increase the ability of flavonoids to inhibit PTP1B. Interestingly, it appears that increasing lipophilicity is even more important in B ring. Starting on methoxylation, it was found that, in general, the presence of -OCH_3 groups at 2′-, 3′- or 4′- position of B ring or at 5-position of A ring is favorable for this specific biologic activity, especially when -OCH_3 groups are in replacement of -OH groups. In addition, it seems that the substitution of a -OH group for an -OCH_3 group at 3-position of C ring, slightly increase PTP1B inhibition. Prenylation also seems to play a crucial role for the inhibitory activity of flavonoids against this target. In fact, if more than one prenyl groups are present in the flavonoid's structure, it is better the capacity to inhibit PTP1B. The presence of prenyl groups enhance the inhibition of PTP1B, particularly in 2′-, 3′- or 5′-positions of B ring. Furthermore, prenyl groups in A ring, especially at 6- or 8- positions also improve the inhibitory effect. Moreover, it seems that prenylation is more significant for the intended effect than methoxylation, namely at 3′-position of B ring. Interestingly, flavonoids with prenyl groups in B ring are better inhibitors than flavonoids with prenyl groups in A ring. It was also found that -OBn groups are responsible for a significant increase in PTP inhibition, when present at 3′- and 4′-positions of B ring or at 7- and 8-positions of A ring.

Additionally, some studies revealed that the cyclization between an -OH group and a prenyl group to form 2,2-dimethyl pyrano ring is more favorable for the intended effect in A ring than in B ring. Moreover, the presence of a CF_3 group at 3′-position of B rig or the existence of -Cl substituents at 2′- and 4′-positions of the same ring appears to play a beneficial role for inhibition of PTP1B. Finally, it seems to be relevant to explore the role of a triazole moiety or long-chain alkyl in flavonoids, since they showed some potential for the enhancement of PTP1B inhibition.

On the contrary, glycosylation of flavonoids (in A, B or C rings) appears to decrease the inhibitory activity of flavonoids against PTP1B. However, among glycosylated flavonoids, the nature and the position of the sugar has different

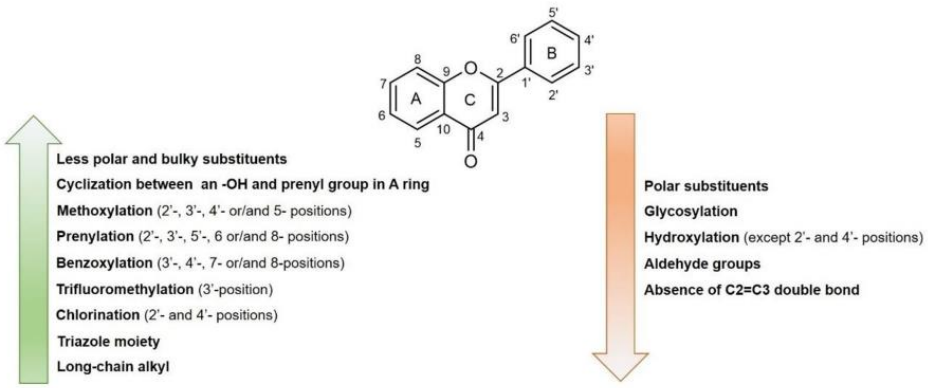


Figure 6. Chemical features of flavonoids that increase or decrease the inhibition of PTP1B.

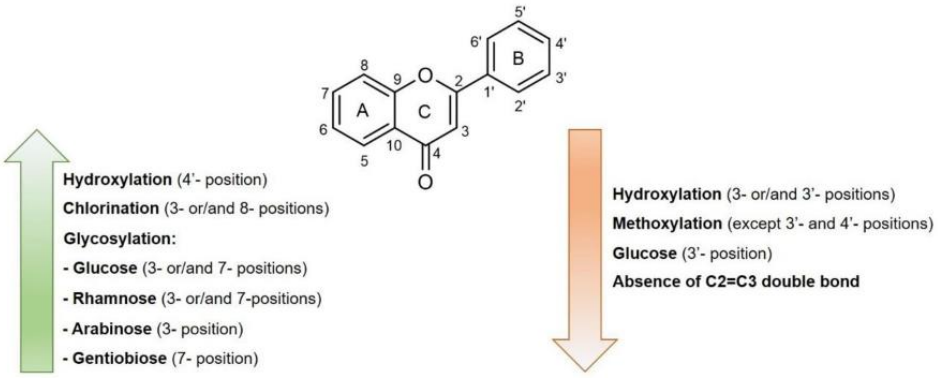


Figure 7. Chemical features of flavonoids that increase or decrease the inhibition of DPP-4.

contributions for the effect under study. For example, at 3-position of C ring, glucose is responsible for a higher PTP1B inhibition than galactose or arabinose at this same position. In addition, the presence of a glucose at 3-position of C ring increases the inhibition of PTP1B comparing with the presence of this sugar at 7-position of A ring. The presence of glucose at 4′-position of B ring improve the effect comparing with presence of rhamnose at 3-position C ring. At 7-position of A ring, glucose also seems to increase the inhibition of PTP1B, followed by rutinose and neohesperidose. The existence of a polar moiety in flavonoids, such as -OH groups, was found not to be favorable for the PTP1B inhibition. Interestingly, in specific cases, the presence of -OH groups seems to enhance the intended effect, but only at 2′- and −4′-positions of B ring. Despite some different conclusions obtained between different studies, in general, hydroxylation leads to a higher inhibition than glycosylation. Beside glycosylation and hydroxylation, also the presence of aldehyde groups reduces the inhibitory activity of flavonoids. Finally, the absence of the C2 = C3 double bond clearly decreases the PTP1B inhibition.

Inhibition of DPP-4 by flavonoids

This section consists of an interpretation of the above-mentioned results obtained in the analyzed publications. DPP-4 inhibitors are one of the most recent agents used for the treatment of T2D. Due to the possible adverse effects, namely cardiovascular complications, resulting from the use of the currently available DPP-4 inhibitors, novel molecules with promising inhibitory effect against DPP-4 are currently being tested. Some studies have been focused on the potential inhibition of this target by flavonoids, which have already shown antidiabetic properties. In this context, from the research studied published in the past few years, some observations were made regarding the structure-activity relationship (Figure 7).

It was found that the inhibitory activity of flavonoids against DPP-4 is highly dependent on the position of -OH groups in their structure. The presence of an –OH group at 3-position of C ring or at 3′-position of B ring appears to decrease the intended effect. On the other hand, the hydroxylation at 4′-position of B ring seems to increase the inhibition of DPP-4. Interestingly, some of the presented studies suggest that the replacement of the catechol in B ring (3′- and 4′-positions) by $-OCH_3$ groups increase this specific biological effect. Nevertheless, in general, the methoxylation and acetoxylation of flavonoids reduce DPP-4 inhibition. It was also observed that the presence of a -Cl substituent at 3-position of C ring and/or at 8-position of A ring plays a beneficial role in inhibiting DPP-4, especially in substitution of –OH groups.

Glycosylation of flavonoids seems to be favorable for the intended effect. In particular, the existence of glucose at 3-position of C ring or at 7-position of A ring increase the inhibitory activity, comparing with the presence of –OH groups at the mentioned positions. On the contrary, the presence of glucose at 3′-position of B ring seems to have the opposite effect. Like glucose, also the presence of rhamnose enhances the inhibition of DPP-4, especially at 3-position of C ring or at 7-position of A ring. It was also evidenced that the existence of arabinose at 3-position of C ring, results in a better inhibition comparing with the presence of arabinofuranose, galactose or even glucose, at this position. Regarding the 7-position of A ring, gentiobiose increase DPP-4 inhibition comparing with the presence of glucosiduronic acid or glucose. Finally, the absence of the C2 = C3 double bond significantly reduces the inhibition of the target under study.

Conclusion

The inhibition of the important T2D targets, PTP1B and DPP-4, by flavonoids was reviewed. The comparison of results is difficult due to the high variability of experimental conditions. In this sense, it was described the main experimental conditions applied, as well as the enzyme source and the type of substrate used in the analyzed research studies. Notwithstanding, it was analyzed the *in vitro* inhibitory activity of 302 flavonoids against PTP1B, and the inhibitory activity of 140 flavonoids against DPP-4. The *in vitro* experiments from current literature confirmed the potential of

flavonoids, both synthesized or isolated from natural products, in inhibiting the activity of the enzymes under study. The wide number of studied compounds enabled the establishment of a structure-activity relationship. Taking this potential role of flavonoids in inhibiting PTP1B and DPP-4 into account, future investigations should be focused on the development of novel flavonoid-based molecules with improved ability to inhibit these targets and to be used in the treatment of T2D.

Disclosure statement

No potential conflict of interest was reported by the authors.

Abbreviations

cAMP	cyclic adenosine monophosphate
DPP-4	dipeptidyl peptidase-4
EPAC2	exchange protein activated by $cAMP_2$
ER	endoplasmic reticulum
FAP	fibroblast activating protein
FDA	Food and Drug Administration
GAP	GTPase activating protein
GEP	cAMP-guanine nucleotide exchange factor
GIP	glucose-dependent insulinotropic polypeptide
GIPR	GIP receptor
GLP-1	glucagon-like peptide-1
GLP-1R	GLP-1 receptor
GLUT4	glucose transporter-4
GSV	GLUT4 storage vesicles
IR	insulin receptor
IRS	insulin receptor substrates
mTORC2	mammalian target of rapamycin complex 2
PC-1/3	pro-hormone convertase 1/3
PDK1	phosphatidylinositol-dependent kinase -1
PH	pleckstrin homology
PI3K	phosphatidylinositol-3-kinase
PIP_2	phosphatidylinositol 4,5-bisphosphate
PIP_3	phosphatidylinositol 3,4,5-triphosphate
PKA	protein kinase A
*p*NPP	*p*-nitrophenyl phosphate
PTB	phosphotyrosine binding
PTKs	protein tyrosine kinases
PTP1B	protein tyrosine phosphatase 1B
PTPs	protein tyrosine phosphatases
QPP	quiescent cell proline dipeptidase
SD	standard deviation
SEM	standard error of mean
SGLT2	sodium/glucose transporter 2
T2D	type 2 diabetes
TCPTP	T-cell protein tyrosine phosphatase

Funding

The work was supported by UIDB/50006/2020 with funding from Fundação para a Ciência e Tecnologia (FCT)/Ministério da Ciência, Tecnologia e Ensino Superior (MCTES) through national funds, and "Programa Operacional Competitividade e Internacionalização" (COMPETE) (POCI-01-0145-FEDER-029241). CP acknowledges FCT the financial support for the PhD grant (SFRH/BD/116005/2016), in the ambit of "QREN - POPH - Tipologia 4.1 - Formação Avançada", co-sponsored by Fundo Social Europeu (FSE) and by national funds of MCTES. DR and MF acknowledge the financial support from the European Union (FEDER funds through COMPETE) (POCI-01-0145-FEDER-029253 and POCI-01-0145-FEDER-029248, respectively).

ORCID

Carina Proença http://orcid.org/0000-0003-0859-6526
Daniela Ribeiro http://orcid.org/0000-0001-9733-7934
Marisa Freitas http://orcid.org/0000-0001-9114-9967
Félix Carvalho http://orcid.org/0000-0003-3858-3494
Eduarda Fernandes http://orcid.org/0000-0001-6424-0976

References

Abbas, M., F. Saeed, F. M. Anjum, M. Afzaal, T. Tufail, M. S. Bashir, A. Ishtiaq, S. Hussain, and H. A. R. a Suleria. 2017. Natural polyphenols: An overview. *International Journal of Food Properties* 20 (8):1689–99. doi: 10.1080/10942912.2016.1220393.

Abdelsalam, S. S., H. M. Korashy, A. Zeidan, and A. Agouni. 2019. The role of protein tyrosine phosphatase (PTP)-1B in cardiovascular disease and its interplay with insulin resistance. *Biomolecules* 9 (286):1–23. doi: 10.3390/biom9070286.

AdInsight. 2007. JTT 551. https://adisinsight.springer.com/drugs/800024307.

Ahrén, B. 2019. DPP-4 inhibition and the path to clinical proof. *Frontiers in Endocrinology* 10 (376):376– 18. doi: 10.3389/fendo.2019.00376.

Al-Ishaq, R. K., M. Abotaleb, P. Kubatka, K. Kajo, and D. Büsselberg. 2019. Flavonoids and their anti-diabetic effects: Cellular mechanisms and effects to improve blood sugar levels. *Biomolecules* 9 (9):430. doi: 10.3390/biom9090430.

Alfayez, O. M., A. R. Almutairi, A. Aldosari, and M. S. Al Yami. 2019. Update on cardiovascular safety of incretin-based therapy in adults with type 2 diabetes *mellitus*: A meta-analysis of cardiovascular outcome trials. *Canadian Journal of Diabetes* 43 (7):538–45. doi: 10.1016/j.jcjd.2019.04.003.

Alkhalidy, H., Y. Wang, and D. Liu. 2018. Dietary flavonoids in the prevention of T2D: An overview. *Nutrients* 10 (4):438– 3. doi: 10.3390/nu10040438.

Annunziata, G., M. Jiménez-García, X. Capó, D. Moranta, A. Arnone, G. C. Tenore, A. Sureda, and S. Tejada. 2020. Microencapsulation as a tool to counteract the typical low bioavailability of polyphenols in the management of diabetes. *Food and Chemical Toxicology: An International Journal Published for the British Industrial Biological Research Association* 139:111248 doi: 10.1016/j.fct.2020.111248.

Atmani, D., N. Chaher, D. Atmani, M. Berboucha, N. Debbache, and H. Boudaoud. 2009. Flavonoids in human health: From structure to biological activity. *Current Nutrition & Food Science* 5 (4):225–37. doi: 10.2174/157340109790218049.

Babu, P. V. A., D. Liu, and E. R. Gilbert. 2013. Recent advances in understanding the anti-diabetic actions of dietary flavonoids. *The Journal of Nutritional Biochemistry* 24 (11):1777–89. doi: 10.1016/j.jnutbio.2013.06.003.

Bae, E. Y., M. Na, D. Njamen, J. T. Mbafor, Z. T. Fomum, L. Cui, D. H. Choung, B. Y. Kim, W. K. Oh, and J. S. Ahn. 2006. Inhibition of protein tyrosine phosphatase 1B by prenylated isoflavonoids isolated from the stem bark of *Erythrina addisoniae*. *Planta Medica* 72 (10):945–8. doi: 10.1055/s-2006-946674.

Bakke, J., and F. G. Haj. 2015. Protein-tyrosine phosphatase 1B substrates and metabolic regulation. *Seminars in Cell & Developmental Biology* 37:58–65. doi: 10.1016/j.semcdb.2014.09.020.

Balentine, D. A., J. T. Dwyer, J. W. Erdman, Jr., M. G. Ferruzzi, P. C. Gaine, J. M. Harnly, and C. L. Kwik-Uribe. 2015. Recommendations on reporting requirements for flavonoids in research. *The American Journal of Clinical Nutrition* 101 (6):1113–25. doi: 10.3945/ajcn.113.071274.

Bento, J. L., N. D. Palmer, J. C. Mychaleckyj, L. A. Lange, C. D. Langefeld, S. S. Rich, B. I. Freedman, and D. W. Bowden. 2004. Association of protein tyrosine phosphatase 1B gene polymorphisms with type 2 diabetes. *Diabetes* 53 (11):3007–12. doi: 10.2337/diabetes.53.11.3007.

Boucher, J., A. Kleinridders, and C. R. Kahn. 2014. Insulin receptor signaling in normal and insulin-resistant states. *Cold Spring Harbor*

Perspectives in Biology 6 (1):a009191– 23. doi: 10.1101/cshperspect.a009191.

Bower, A. M., L. M. Real Hernandez, M. A. Berhow, and E. G. de Mejia. 2014. Bioactive compounds from culinary herbs inhibit a molecular target for type 2 diabetes management, dipeptidyl peptidase IV. *Journal of Agricultural and Food Chemistry* 62 (26):6147–58. doi: 10.1021/jf500639f.

Cahn, A., S. Cernea, and I. Raz. 2016. An update on DPP-4 inhibitors in the management of type 2 diabetes. *Expert Opinion on Emerging Drugs* 21 (4):409–19. doi: 10.1080/14728214.2016.1257608.

Cai, J., L. Zhao, and W. Tao. 2015. Potent protein tyrosine phosphatase 1B (PTP1B) inhibiting constituents from *Anoectochilus chapaensis* and molecular docking studies. *Pharmaceutical Biology* 53 (7):1030–4. doi: 10.3109/13880209.2014.957781.

Chen, M., K. Wang, Y. Zhang, M. Zhang, Y. Ma, H. Sun, Z. Jin, H. Zheng, H. Jiang, P. Yu, et al. 2019. New insights into the biological activities of *Chrysanthemum morifolium*: Natural flavonoids alleviate diabetes by targeting α-glucosidase and the PTP-1B signaling pathway . *European Journal of Medicinal Chemistry* 178:108–15. doi: 10.1016/j.ejmech.2019.05.083.

Chen, P. J., S. P. Cai, C. Huang, X. M. Meng, and J. Li. 2015. Protein tyrosine phosphatase 1B (PTP1B): A key regulator and therapeutic target in liver diseases. *Toxicology* 337:10–20. doi: 10.1016/j.tox.2015.08.006.

Chen, R. M., L. H. Hu, T. Y. An, J. Li, and Q. Shen. 2002. Natural PTP1B Inhibitors from *broussonetia papyrifera*. *Bioorganic & Medicinal Chemistry Letters* 12 (23):3387–90. doi: 10.1016/S0960-894X(02)00757-6.

Choi, J. S., M. N. Islam, M. Y. Ali, E. J. Kim, Y. M. Kim, and H. A. Jung. 2014. Effects of C-glycosylation on anti-diabetic, anti-Alzheimer's disease and anti-inflammatory potential of apigenin. *Food and Chemical Toxicology: An International Journal Published for the British Industrial Biological Research Association* 64:27–33. doi: 10.1016/j.fct.2013.11.020.

Choi, J. S., M. N. Islam, M. Y. Ali, Y. M. Kim, H. J. Park, H. S. Sohn, and H. A. Jung. 2014. The effects of C-glycosylation of luteolin on its antioxidant, anti-Alzheimer's disease, anti-diabetic, and anti-inflammatory activities. *Archives of Pharmacal Research* 37 (10):1354–63. doi: 10.1007/s12272-014-0351-3.

Cui, L., H. S. Lee, D. T. Ndinteh, J. T. Mbafor, Y. H. Kim, T. V. Le, P. H. Nguyen, and W. K. Oh. 2010. New prenylated flavanones from *Erythrina abyssinica* with protein tyrosine phosphatase 1B (PTP1B) inhibitory activity. *Planta Medica* 76 (7):713–8. doi: 10.1055/s-0029-1240682.

Cui, L., M. Na, H. Oh, E. Y. Bae, D. G. Jeong, S. E. Ryu, S. Kim, B. Y. Kim, W. K. Oh, and J. S. Ahn. 2006. Protein tyrosine phosphatase 1B inhibitors from *Morus* root bark. *Bioorganic & Medicinal Chemistry Letters* 16 (5):1426–9. doi: 10.1016/j.bmcl.2005.11.071.

Cui, L., D. T. Ndinteh, M. Na, P. T. Thuong, J. Silike-Muruumu, D. Njamen, J. T. Mbafor, Z. T. Fomum, J. S. Ahn, and W. K. Oh. 2007. Isoprenylated flavonoids from the stem bark of *Erythrina abyssinica*. *Journal of Natural Products* 70 (6):1039–42. doi: 10.1021/np060477+.

Cui, L., P. T. Thuong, H. S. Lee, D. T. Ndinteh, J. T. Mbafor, Z. T. Fomum, and W. K. Oh. 2008. Flavanones from the stem bark of *Erythrina abyssinica*. *Bioorganic & Medicinal Chemistry* 16 (24):10356–62. doi: 10.1016/j.bmc.2008.10.012.

De Felice, S. L. 1992. Nutraceuticals – opportunities in an emerging market. In *Scrip Magazine*.

De, S., S. Banerjee, S. K. A. Kumar, and P. Paira. 2019. Critical role of dipeptidyl peptidase IV: A therapeutic target for diabetes and cancer. *Mini Reviews in Medicinal Chemistry* 19 (2):88–97. doi: 10.2174/1389557518666180423112154.

Deacon, C. F. 2018. Peptide degradation and the role of DPP-4 inhibitors in the treatment of type 2 diabetes. *Peptides* 100:150–7. doi: 10.1016/j.peptides.2017.10.011.

Deacon, C. F. 2019. Physiology and pharmacology of DPP-4 in glucose homeostasis and the treatment of type 2 diabetes. *Frontiers in Endocrinology* 10 (80):1–14. doi: 10.3389/fendo.2019.00080.

Digenio, A., N. C. Pham, L. M. Watts, E. S. Morgan, S. W. Jung, B. F. Baker, R. S. Geary, and S. Bhanot. 2018. Antisense inhibition of protein tyrosine phosphatase 1B With IONIS-PTP-1BRx improves insulin sensitivity and reduces weight in overweight patients with Type 2 Diabetes . *Diabetes Care* 41 (4):807–14. doi: 10.2337/dc17-2132.

Drucker, D. J. 2006. The biology of incretin hormones. *Cell Metabolism* 3 (3):153–65. doi: 10.1016/j.cmet.2006.01.004.

Eidenberger, T., M. Selg, and K. Krennhuber. 2013. Inhibition of dipeptidyl peptidase activity by flavonol glycosides of guava (*Psidium guajava* L.): A key to the beneficial effects of guava in type II diabetes mellitus. *Fitoterapia* 89:74–9. doi: 10.1016/j.fitote.2013.05.015.

Elchebly, M., P. Payette, E. Michaliszyn, W. Cromlish, S. Collins, A. L. Loy, D. Normandin, A. Cheng, J. Himms-Hagen, C. C. Chan, et al. 1999. Increased insulin sensitivity and obesity resistance in mice lacking the protein tyrosine phosphatase-1B gene. *Science (New York, N.Y.)* 283 (5407):1544–8. doi: 10.1126/science.283.5407.1544.

Elgendy, I. Y., A. N. Mahmoud, A. F. Barakat, A. Y. Elgendy, M. Saad, A. Abuzaid, S. A. Wayangankar, and A. A. Bavry. 2017. Cardiovascular safety of dipeptidyl-peptidase IV inhibitors: A meta-analysis of placebo-controlled randomized trials. *American Journal of Cardiovascular Drugs: drugs, Devices, and Other Interventions* 17 (2):143–55. doi: 10.1007/s40256-016-0208-x.

Fan, J., M. H. Johnson, M. A. Lila, G. Yousef, and E. G. de Mejia. 2013. Berry and citrus phenolic compounds inhibit dipeptidyl peptidase IV: Implications in diabetes management. *Evidence-Based Complementary and Alternative Medicine* 2013:1–13. doi: 10.1155/2013/479505.

Farhang-Fallah, J., V. K. Randhawa, A. Nimnual, A. Klip, D. Bar-Sagi, and M. Rozakis-Adcock. 2002. The pleckstrin homology (PH) domain-interacting protein couples the insulin receptor substrate 1 PH domain to insulin signaling pathways leading to mitogenesis and GLUT4 translocation. *Molecular and Cellular Biology* 22 (20):7325–36. doi: 10.1128/mcb.22.20.7325-7336.2002.

Feldhammer, M., N. Uetani, D. Miranda-Saavedra, and M. L. Tremblay. 2013. PTP1B: A simple enzyme for a complex world. *Critical Reviews in Biochemistry and Molecular Biology* 48 (5):430–45. doi: 10.3109/10409238.2013.819830.

Ferreyra, M. L. F., S. Rius, and P. Casati. 2012. Flavonoids: Biosynthesis, biological functions, and biotechnological applications. *Frontiers in Plant Science* 3 (222):222– 15. doi: 10.3389/fpls.2012.00222.

Fiorentino, T. V., and G. Sesti. 2016. Lessons learned from cardiovascular outcome clinical trials with dipeptidyl peptidase 4 (DPP-4) inhibitors. *Endocrine* 53 (2):373–80. doi: 10.1007/s12020-015-0811-7.

Fueller, J., M. V. Egorov, K. A. Walther, O. Sabet, J. Mallah, M. Grabenbauer, and A. Kinkhabwala. 2015. Subcellular partitioning of protein tyrosine phosphatase 1B to the endoplasmic reticulum and mitochondria depends sensitively on the composition of its tail anchor. *PloS One* 10 (10):e0139429. doi: 10.1371/journal.pone.0139429.

Gall, M. G., and M. D. Gorrell. 2017. The multifunctional post-proline dipeptidyl peptidase, DPP9, in mice, cell biology and immunity. In *Pathophysiological aspects of proteases*, eds. S. Chakraborti and N. S. Dhalla, 23–45. Singapore: Springer Singapore.

Gallwitz, B. 2019. Clinical use of DPP-4 inhibitors. *Frontiers in Endocrinology* 10 (389):389– 10. doi: 10.3389/fendo.2019.00389.

Ghorbani, A., R. Rashidi, and R. Shafiee-Nick. 2019. Flavonoids for preserving pancreatic beta cell survival and function: A mechanistic review. *Biomedicine & Pharmacotherapy = Biomedecine & Pharmacotherapie* 111:947–57. doi: 10.1016/j.biopha.2018.12.127.

Gontijo, V. S., M. H. Dos Santos, and C. Viegas. Jr. 2017. Biological and chemical aspects of natural biflavonoids from plants: A brief review. *Mini Reviews in Medicinal Chemistry* 17 (10):834–62. doi: 10.2174/1389557517666161104130026.

Govers, R. 2014. Molecular mechanisms of GLUT4 regulation in adipocytes. *Diabetes & Metabolism* 40 (6):400–10. doi: 10.1016/j.diabet.2014.01.005.

Guo, Z., X. Niu, T. Xiao, J. Lu, W. Li, and Y. Zhao. 2015. Chemical profile and inhibition of α-glycosidase and protein tyrosine

phosphatase 1B (PTP1B) activities by flavonoids from licorice (*Glycyrrhiza uralensis Fisch*). *Journal of Functional Foods* 14:324–36. doi: 10.1016/j.jff.2014.12.003.

Gupta, A., G. A. Jacobson, J. R. Burgess, H. F. Jelinek, D. S. Nichols, C. K. Narkowicz, and H. A. Al-Aubaidy. 2018. Citrus bioflavonoids dipeptidyl peptidase-4 inhibition compared with gliptin antidiabetic medications. *Biochemical and Biophysical Research Communications* 503 (1):21–5. doi: 10.1016/j.bbrc.2018.04.156.

Haj, F. G., J. M. Zabolotny, Y. B. Kim, B. B. Kahn, and B. G. Neel. 2005. Liver-specific protein-tyrosine phosphatase 1B (PTP1B) re-expression alters glucose homeostasis of PTP1B-/-mice. *The Journal of Biological Chemistry* 280 (15):15038–46. doi: 10.1074/jbc.M413240200.

He, R-j, L.-F. Zeng, Y. He, and Z.-Y. Zhang. 2012. *New therapeutic strategies for type 2 diabetes: Small molecule approaches, Recent advances in PTP1B inhibitor development for the treatment of type 2 diabetes and obesity*. Cambridge, UK: Royal Society of Chemistry

He, R-j, and Z. Y. Zhang. 2016. *Protein tyrosine phosphatases in cancer, Current status of PTP-based therapeutics*. New York, USA: Springer Nature.

Huang, Q. H., C. Lei, P. P. Wang, J. Y. Li, J. Li, and A. J. Hou. 2017. Isoprenylated phenolic compounds with PTP1B inhibition from *Morus alba*. *Fitoterapia* 122:138–43. doi: 10.1016/j.fitote.2017.09.006.

Hussain, T., B. Tan, G. Murtaza, G. Liu, N. Rahu, M. Saleem Kalhoro, D. Hussain Kalhoro, T. O. Adebowale, M. Usman Mazhar, Z. U. Rehman, et al. 2020. Flavonoids and type 2 diabetes: Evidence of efficacy in clinical and animal studies and delivery strategies to enhance their therapeutic efficacy. *Pharmacological Research* 152: 104629. doi: 10.1016/j.phrs.2020.104629.

Islam, M. N., H. A. Jung, H. S. Sohn, H. M. Kim, and J. S. Choi. 2013. Potent α-glucosidase and protein tyrosine phosphatase 1B inhibitors from *Artemisia capillaris*. *Archives of Pharmacal Research* 36 (5): 542–52. doi: 10.1007/s12272-013-0069-7.

Ito, M., S. Fukuda, S. Sakata, H. Morinaga, and T. Ohta. 2014. Pharmacological effects of JTT-551, a novel protein tyrosine phosphatase 1B inhibitor, in diet-induced obesity mice. *Journal of Diabetes Research* 2014:1–7. doi: 10.1155/2014/680348.

Jaldin-Fincati, J. R., M. Pavarotti, S. Frendo-Cumbo, P. J. Bilan, and A. Klip. 2017. Update on GLUT4 vesicle traffic: A cornerstone of insulin action. *Trends in Endocrinology and Metabolism: TEM* 28 (8): 597–611. doi: 10.1016/j.tem.2017.05.002.

Jang, J.,. M. Na, P. T. Thuong, D. Njamen, J. T. Mbafor, Z. T. Fomum, E. R. Woo, and W. K. Oh. 2008. Prenylated flavonoids with PTP1B inhibitory activity from the root bark of *Erythrina mildbraedii*. *Chemical & Pharmaceutical Bulletin* 56 (1):85–8. doi: 10.1248/cpb.56.85.

Jeong, S. Y., P. H. Nguyen, B. T. Zhao, M. Y. Ali, J. S. Choi, B. S. Min, and M. H. Woo. 2015. Chemical constituents of *Euonymus alatus* (Thunb.) Sieb. and their PTP1B and α-glucosidase inhibitory activities. *Phytotherapy Research : PTR* 29 (10):1540–8. doi: 10.1002/ptr.5411.

Jiang, L., S. Numonov, K. Bobakulov, M. N. Qureshi, H. Zhao, and H. A. Aisa. 2015. Phytochemical profiling and evaluation of pharmacological activities of *Hypericum scabrum* L. *Molecules (Basel, Switzerland)* 20 (6):11257–71. doi: 10.3390/molecules200611257.

Jung, H. A., P. Paudel, S. H. Seong, B. S. Min, and J. S. Choi. 2017. Structure-related protein tyrosine phosphatase 1B inhibition by naringenin derivatives. *Bioorganic & Medicinal Chemistry Letters* 27 (11):2274–80. doi: 10.1016/j.bmcl.2017.04.054.

Kawser, H. M., D. A. Abdal, J. Han, Y. Yin, K. Kim, S. S. Kumar, G. Yang, H. Y. Choi, and S. G. Cho. 2016. Molecular mechanisms of the anti-obesity and anti-diabetic properties of flavonoids. *International Journal of Molecular Sciences* 17 (4):569–32. doi: 10.3390/ijms17040569.

Kennedy, B. P., and C. Ramachandran. 2000. Protein tyrosine phosphatase-1B in diabetes. *Biochemical Pharmacology* 60 (7):877–83. doi: 10.1016/S0006-2952(00)00305-1.

Kim, B. R., H. Y. Kim, I. Choi, J. B. Kim, C. H. Jin, and A. R. Han. 2018. DPP-IV inhibitory potentials of flavonol glycosides isolated from the seeds of *Lens culinaris*: In vitro and molecular docking analyses. *Molecules* 23 (8):1998–10. doi: 10.3390/molecules23081998.

Kim, D. H., H. A. Jung, H. S. Sohn, J. W. Kim, and J. S. Choi. 2017. Potential of icariin metabolites from *Epimedium koreanum Nakai* as antidiabetic therapeutic agents. *Molecules* 22 (6):986–14. doi: 10.3390/molecules22060986.

Klip, A., Y. Sun, T. T. Chiu, and K. P. Foley. 2014. Signal transduction meets vesicle traffic: The software and hardware of GLUT4 translocation. *American Journal of Physiology. Cell Physiology* 306 (10): C879–C86. doi: 10.1152/ajpcell.00069.2014.

Krishnan, N., C. A. Bonham, I. A. Rus, O. K. Shrestha, C. M. Gauss, A. Haque, A. Tocilj, L. Joshua-Tor, and N. K. Tonks. 2018. Harnessing insulin- and leptin-induced oxidation of PTP1B for therapeutic development. *Nature Communications* 9 (1):283. doi: 10.1038/s41467-017-02252-2.

Kumar, A., S. K. Bharti, and A. Kumar. 2017. Therapeutic molecules against type 2 diabetes: What we have and what are we expecting? *Pharmacological Reports : PR* 69 (5):959–70. doi: 10.1016/j.pharep.2017.04.003.

Kumar, G. S., R. Page, and W. Peti. 2020. The mode of action of the Protein tyrosine phosphatase 1B inhibitor Ertiprotafib. *PloS One* 15 (10):e0240044. doi: 10.1371/journal.pone.0240044.

Kumar, S., and A. K. Pandey. 2013. Chemistry and biological activities of flavonoids: An overview. *The Scientific World Journal* 2013:1–16. doi: 10.1155/2013/162750.

Kundu, A., P. Sardar, S. Ghosh, P. Patel, S. Chatterjee, and T. E. Meyer. 2016. Risk of heart failure with dipeptidyl peptidase-4 inhibitors in patients with type 2 diabetes mellitus: A meta-analysis of randomized controlled trials. *International Journal of Cardiology* 212:203–5. doi: 10.1016/j.ijcard.2016.03.016.

Li, J. L., L. X. Gao, F. W. Meng, C. L. Tang, R. J. Zhang, J. Y. Li, C. Luo, J. Li, and W. M. Zhao. 2015. PTP1B inhibitors from stems of *Angelica keiskei* (Ashitaba). *Bioorganic & Medicinal Chemistry Letters* 25 (10):2028–32. doi: 10.1016/j.bmcl.2015.04.003.

Li, L., S. Li, K. Deng, J. Liu, P. O. Vandvik, P. Zhao, L. Zhang, J. Shen, M. M. Bala, Z. N. Sohani, et al. 2016. Dipeptidyl peptidase-4 inhibitors and risk of heart failure in type 2 diabetes: Systematic review and meta-analysis of randomised and observational studies. *BMJ (Clinical Research ed.)* 352 (i610):i610– 17. doi: 10.1136/bmj.i610.

Li, S., W. Li, Y. Wang, Y. Asada, and K. Koike. 2010. Prenylflavonoids from *Glycyrrhiza uralensis* and their protein tyrosine phosphatase-1B inhibitory activities. *Bioorganic & Medicinal Chemistry Letters* 20 (18):5398–401. doi: 10.1016/j.bmcl.2010.07.110.

Li, X., L. Wang, and D. Shi. 2016. The design strategy of selective PTP1B inhibitors over TCPTP. *Bioorganic & Medicinal Chemistry* 24 (16):3343–52. doi: 10.1016/j.bmc.2016.06.035.

Li, Y. F., L. H. Hu, F. C. Lou, J. Li, and Q. Shen. 2005. PTP1B inhibitors from *Ardisia japonica*. *Journal of Asian Natural Products Research* 7 (1):13–8. doi: 10.1080/10286020310001596033.

Libianto, R., and E. I. Ekinci. 2019. New agents for the treatment of type 2 diabetes. *Critical Care Clinics* 35 (2):315–28. doi: 10.1016/j.ccc.2018.11.007.

Liu, Y.-J., J. Zhan, X.-L. Liu, Y. Wang, J. Ji, and Q.-Q. He. 2014. Dietary flavonoids intake and risk of type 2 diabetes: A meta-analysis of prospective cohort studies. *Clinical Nutrition (Edinburgh, Scotland)* 33 (1):59–63. doi: 10.1016/j.clnu.2013.03.011.

Luo, J., Q. Xu, B. Jiang, R. Zhang, X. Jia, X. Li, L. Wang, C. Guo, N. Wu, and D. Shi. 2018. Selectivity, cell permeability and oral availability studies of novel bromophenol derivative HPN as protein tyrosine phosphatase 1B inhibitor. *British Journal of Pharmacology* 175 (1):140–53. doi: 10.1111/bph.14080.

Miinea, C. P., H. Sano, S. Kane, E. Sano, M. Fukuda, J. Peränen, W. S. Lane, and G. E. Lienhard. 2005. AS160, the Akt substrate regulating GLUT4 translocation, has a functional Rab GTPase-activating protein domain. *The Biochemical Journal* 391 (Pt 1):87–93. doi: 10.1042/BJ20050887.

Molina-Vega, M., A. Munoz-Garach, J. C. Fernandez-Garcia, and F. J. Tinahones. 2018. The safety of DPP-4 inhibitor and SGLT2 inhibitor combination therapies. *Expert Opinion on Drug Safety* 17 (8): 815–24. doi: 10.1080/14740338.2018.1497158.

Monami, M., I. Dicembrini, and E. Mannucci. 2014. Dipeptidyl peptidase-4 inhibitors and heart failure: A meta-analysis of randomized clinical trials. *Nutrition, Metabolism, and Cardiovascular Diseases: NMCD* 24 (7):689–97. doi: 10.1016/j.numecd.2014.01.017.

Moradi-Marjaneh, R., M. Paseban, and A. Sahebkar. 2019. Natural products with SGLT2 inhibitory activity: Possibilities of application for the treatment of diabetes. *Phytotherapy Research: PTR* 33 (10): 2518–30. doi: 10.1002/ptr.6421.

Morikawa, T., K. Ninomiya, J. Akaki, N. Kakihara, H. Kuramoto, Y. Matsumoto, T. Hayakawa, O. Muraoka, L.-B. Wang, L.-J. Wu, et al. 2015. Dipeptidyl peptidase-IV inhibitory activity of dimeric dihydrochalcone glycosides from flowers of *Helichrysum arenarium*. *Journal of Natural Medicines* 69 (4):494–506. doi: 10.1007/s11418-015-0914-8.

Mulvihill, E. E., and D. J. Drucker. 2014. Pharmacology, physiology, and mechanisms of action of dipeptidyl peptidase-4 inhibitors. *Endocrine Reviews* 35 (6):992–1019. doi: 10.1210/er.2014-1035.

Na, B., P. H. Nguyen, B. T. Zhao, Q. H. Vo, B. S. Min, and M. H. Woo. 2016. Protein tyrosine phosphatase 1B (PTP1B) inhibitory activity and glucosidase inhibitory activity of compounds isolated from *Agrimonia pilosa*. *Pharmaceutical Biology* 54 (3):474–80. doi: 10.3109/13880209.2015.1048372.

Na, M., J. Jang, D. Njamen, J. T. Mbafor, Z. T. Fomum, B. Y. Kim, W. K. Oh, and J. S. Ahn. 2006. Protein tyrosine phosphatase-1B inhibitory activity of isoprenylated flavonoids isolated from *Erythrina mildbraedii*. *Journal of Natural Products* 69 (11):1572–6. doi: 10.1021/np0601861.

Nauck, M. A., and J. J. Meier. 2018. Incretin hormones: Their role in health and disease. *Diabetes, Obesity & Metabolism* 20 (Suppl 1): 5–21. doi: 10.1111/dom.13129.

Nguyen, D. H., U. M. Seo, B. T. Zhao, D. D. Le, S. H. Seong, J. S. Choi, B. S. Min, and M. H. Woo. 2017. Ellagitannin and flavonoid constituents from *Agrimonia pilosa* Ledeb. with their protein tyrosine phosphatase and acetylcholinesterase inhibitory activities. *Bioorganic Chemistry* 72:293–300. doi: 10.1016/j.bioorg.2017.04.017.

Nguyen, P. H., T. T. Dao, J. Kim, D. T. Phong, D. T. Ndinteh, J. T. Mbafor, and W. K. Oh. 2011. New 5-deoxyflavonoids and their inhibitory effects on protein tyrosine phosphatase 1B (PTP1B) activity. *Bioorganic & Medicinal Chemistry* 19 (11):3378–83. doi: 10.1016/j.bmc.2011.04.037.

Nguyen, P. H., D. J. Ji, Y. R. Han, J. S. Choi, D. Y. Rhyu, B. S. Min, and M. H. Woo. 2015. Selaginellin and biflavonoids as protein tyrosine phosphatase 1B inhibitors from *Selaginella tamariscina* and their glucose uptake stimulatory effects. *Bioorganic & Medicinal Chemistry* 23 (13):3730–7. doi: 10.1016/j.bmc.2015.04.007.

Nguyen, P. H., G. Sharma, T. T. Dao, M. N. Uddin, K. W. Kang, D. T. Ndinteh, J. T. Mbafor, and W. K. Oh. 2012. New prenylated isoflavonoids as protein tyrosine phosphatase 1B (PTP1B) inhibitors from *Erythrina addisoniae*. *Bioorganic & Medicinal Chemistry* 20 (21): 6459–64. doi: 10.1016/j.bmc.2012.08.024.

Nicolle, E., F. Souard, P. Faure, and A. Boumendjel. 2011. Flavonoids as promising lead compounds in type 2 diabetes mellitus: Molecules of interest and structure-activity relationship. *Current Medicinal Chemistry* 18 (17):2661–72. doi: 10.2174/092986711795933777.

Opinto, G., A. Natalicchio, and P. Marchetti. 2013. Physiology of incretins and loss of incretin effect in type 2 diabetes and obesity. *Archives of Physiology and Biochemistry* 119 (4):170–8. doi: 10.3109/13813455.2013.812664.

Panzhinskiy, E., J. Ren, and S. Nair. 2013. Pharmacological inhibition of protein tyrosine phosphatase 1B: A promising strategy for the treatment of obesity and type 2 diabetes mellitus. *Current Medicinal Chemistry* 20 (21):2609–25. doi: 10.2174/0929867311320210001.

Proença, C., M. Freitas, D. Ribeiro, E. F. T. Oliveira, J. L. C. Sousa, S. M. Tome, M. J. Ramos, A. M. S. Silva, P. A. Fernandes, and E. Fernandes. 2017. α-Glucosidase inhibition by flavonoids: An *in vitro* and *in silico* structure-activity relationship study. *Journal of Enzyme Inhibition and Medicinal Chemistry* 32 (1):1216–28. doi: 10.1080/14756366.2017.1368503.

Proença, C., M. Freitas, D. Ribeiro, J. L. C. Sousa, F. Carvalho, A. M. S. Silva, P. A. Fernandes, and E. Fernandes. 2018. Inhibition of protein tyrosine phosphatase 1B by flavonoids: A structure - activity relationship study. *Food and Chemical Toxicology: An International Journal Published for the British Industrial Biological Research Association* 111 (2018):474–81. doi: 10.1016/j.fct.2017.11.039.

Proença, C., M. Freitas, D. Ribeiro, S. M. Tomé, E. F. T. Oliveira, M. F. Viegas, A. N. Araújo, M. J. Ramos, A. M. S. Silva, P. A. Fernandes, et al. 2019. Evaluation of a flavonoids library for inhibition of pancreatic α-amylase towards a structure-activity relationship. *Journal of Enzyme Inhibition and Medicinal Chemistry* 34 (1): 577–88. doi: 10.1080/14756366.2018.1558221.

Proença, C., M. Freitas, D. Ribeiro, S. M. Tomé, A. N. Araújo, A. M. S. Silva, P. A. Fernandes, and E. Fernandes. 2019. The dipeptidyl peptidase-4 inhibitory effect of flavonoids is hindered in protein rich environments. *Food & Function* 10 (9):5718–31. doi: 10.1039/C9FO00722A.

Proença, C., A. Oliveira, M. Freitas, D. Ribeiro, J. L. C. Sousa, M. J. Ramos, A. M. S. Silva, P. A. Fernandes, and E. Fernandes. 2020. Structural specificity of flavonoids in the inhibition of human fructose 1,6-bisphosphatase. *Journal of Natural Products* 83 (5):1541–52. doi: 10.1021/acs.jnatprod.0c00014.

Qin, N., T. Sasaki, W. Li, J. Wang, X. Zhang, D. Li, Z. Li, M. Cheng, H. Hua, and K. Koike. 2018. Identification of flavonolignans from *Silybum marianum* seeds as allosteric protein tyrosine phosphatase 1B inhibitors. *Journal of Enzyme Inhibition and Medicinal Chemistry* 33 (1):1283–91. doi: 10.1080/14756366.2018.1497020.

Qin, N. B., C. C. Jia, J. Xu, D. H. Li, F. X. Xu, J. Bai, Z. L. Li, and H. M. Hua. 2017. New amides from seeds of *Silybum marianum* with potential antioxidant and antidiabetic activities. *Fitoterapia* 119: 83–9. doi: 10.1016/j.fitote.2017.04.008.

Quang, T. H., N. T. Ngan, C. S. Yoon, K. H. Cho, D. G. Kang, H. S. Lee, Y. C. Kim, and H. Oh. 2015. Protein tyrosine phosphatase 1B inhibitors from the roots of *Cudrania tricuspidata*. *Molecules (Basel, Switzerland)* 20 (6):11173–83. doi: 10.3390/molecules200611173.

Rehman, M. B., B. V. Tudrej, J. Soustre, M. Buisson, P. Archambault, D. Pouchain, H. Vaillant-Roussel, F. Gueyffier, J.-L. Faillie, M.-C. Perault-Pochat, et al. 2017. Efficacy and safety of DPP-4 inhibitors in patients with type 2 diabetes: Meta-analysis of placebo-controlled randomized clinical trials. *Diabetes & Metabolism* 43 (1):48–58. doi: 10.1016/j.diabet.2016.09.005.

Ren, L., L. Z. Li, J. Huang, L. Z. Huang, J. H. Li, Y. M. Li, and S. Y. Tang. 2020. New compounds from the seeds of *Psoralea corylifolia* with their protein tyrosine phosphatase 1B inhibitory activity. *Journal of Asian Natural Products Research* 22 (8):732–6. doi: 10.1080/10286020.2019.1621852.

Röhrborn, D., N. Wronkowitz, and J. Eckel. 2015. DPP4 in diabetes. *Frontiers in Immunology* 6 (386):386– 20. doi: 10.3389/fimmu.2015.00386.

RusznyÁK, S. T., and A. Szent-GyÖRgyi. 1936. Vitamin P: Flavonols as vitamins. *Nature* 138 (3479):27. doi: 10.1038/138027a0.

Salmeen, A., J. N. Andersen, M. P. Myers, N. K. Tonks, and D. Barford. 2000. Molecular basis for the dephosphorylation of the activation segment of the insulin receptor by protein tyrosine phosphatase 1B. *Molecular Cell* 6 (6):1401–12. doi: 10.1016/S1097-2765(00)00137-4.

Sano, M. 2019. Mechanism by which dipeptidyl peptidase-4 inhibitors increase the risk of heart failure and possible differences in heart failure risk. *Journal of Cardiology* 73 (1):28–32. doi: 10.1016/j.jjcc.2018.07.004.

Sarian, M. N., Q. U. Ahmed, S. Z. Mat So'ad, A. M. Alhassan, S. Murugesu, V. Perumal, S. N. A. Syed Mohamad, A. Khatib, and J. Latip. 2017. Antioxidant and antidiabetic effects of flavonoids: A structure-activity relationship based study. *BioMed Research International* 2017:1–14. doi: 10.1155/2017/8386065.

Sasaki, T., W. Li, K. Higai, T. H. Quang, Y. H. Kim, and K. Koike. 2014. Protein tyrosine phosphatase 1B inhibitory activity of lavandulyl flavonoids from roots of *Sophora flavescens*. *Planta Medica* 80 (07):557–60. doi: 10.1055/s-0034-1368400.

Scirica, B. M., D. L. Bhatt, E. Braunwald, P. G. Steg, J. Davidson, B. Hirshberg, P. Ohman, R. Frederich, S. D. Wiviott, E. B. Hoffman,

et al. 2013. Saxagliptin and cardiovascular outcomes in patients with type 2 diabetes mellitus. *New England Journal of Medicine* 369 (14): 1317–26. doi: 10.1056/NEJMoa1307684.

Seino, Y., M. Fukushima, and D. Yabe. 2010. GIP and GLP-1, the two incretin hormones: Similarities and differences. *Journal of Diabetes Investigation* 1 (1-2):8–23. doi: 10.1111/j.2040-1124.2010.00022.x.

Sesti, G., A. Avogaro, S. Belcastro, B. M. Bonora, M. Croci, G. Daniele, M. Dauriz, F. Dotta, C. Formichi, S. Frontoni, et al. 2019. Ten years of experience with DPP-4 inhibitors for the treatment of type 2 diabetes *mellitus*. *Acta Diabetologica* 56 (6):605–17. doi: 10.1007/s00592-018-1271-3.

Soares, J. M. D., A. E. B. Pereira Leal, J. C. Silva, J. R. G. S. Almeida, and H. P. de Oliveira. 2017. Influence of flavonoids on mechanism of modulation of insulin secretion. *Pharmacognosy Magazine* 13 (52):639–46. doi: 10.4103/pm.pm_87_17.

Song, Y. H., Z. Uddin, Y. M. Jin, Z. Li, M. J. Curtis-Long, K. D. Kim, J. K. Cho, and K. H. Park. 2017. Inhibition of protein tyrosine phosphatase (PTP1B) and α-glucosidase by geranylated flavonoids from *Paulownia tomentosa*. *Journal of Enzyme Inhibition and Medicinal Chemistry* 32 (1):1195–202. doi: 10.1080/14756366.2017.1368502.

Sugiyama, M., R. Banno, A. Mizoguchi, T. Tominaga, T. Tsunekawa, T. Onoue, D. Hagiwara, Y. Ito, Y. Morishita, S. Iwama, et al. 2017. PTP1B deficiency improves hypothalamic insulin sensitivity resulting in the attenuation of AgRP mRNA expression under high-fat diet conditions. *Biochemical and Biophysical Research Communications* 488 (1):116–21. doi: 10.1016/j.bbrc.2017.05.019.

Sun, C., C. Zhao, E. C. Guven, P. Paoli, J. Simal-Gandara, K. M. Ramkumar, S. Wang, F. Buleu, A. Pah, V. Turi, et al. 2020. Dietary polyphenols as antidiabetic agents: Advances and opportunities. *Food Frontiers* 1 (1):18–44. doi: 10.1002/fft2.15.

Sun, J., C. Qu, Y. Wang, H. Huang, M. Zhang, H. Li, Y. Zhang, Y. Wang, and W. Zou. 2016. PTP1B, a potential target of type 2 diabetes mellitus. *Molecular Biology* 05 (04):1–6. doi: 10.4172/2168-9547.1000174.

Sun, L. P., W. P. Ma, L. X. Gao, L. L. Yang, Y. C. Quan, J. Li, and H. R. Piao. 2013. Synthesis and characterization of 5,7-dihydroxyflavanone derivatives as novel protein tyrosine phosphatase 1B inhibitors. *Journal of Enzyme Inhibition and Medicinal Chemistry* 28 (6): 1199–204. doi: 10.3109/14756366.2012.723206.

Tamrakar, A. K., C. K. Maurya, and A. K. Rai. 2014. PTP1B inhibitors for type 2 diabetes treatment: A patent review (2011 - 2014). *Expert Opinion on Therapeutic Patents* 24 (10):1101–15. doi: 10.1517/13543776.2014.947268.

Tang, Y., X. Zhang, Z. Chen, W. Yin, G. Nan, J. Tian, F. Ye, and Z. Xiao. 2018. Novel benzamido derivatives as PTP1B inhibitors with anti-hyperglycemic and lipid-lowering efficacy. *Acta Pharmaceutica Sinica. B* 8 (6):919–32. doi: 10.1016/j.apsb.2018.05.001.

Teng, H., and L. Chen. 2019. Polyphenols and bioavailability: An update. *Critical Reviews in Food Science and Nutrition* 59 (13): 2040–51. doi: 10.1080/10408398.2018.1437023.

Thareja, S., S. Aggarwal, T. R. Bhardwaj, and M. Kumar. 2012. Protein tyrosine phosphatase 1B inhibitors: A molecular level legitimate approach for the management of diabetes mellitus. *Medicinal Research Reviews* 32 (3):459–517. doi: 10.1002/med.20219.

Trinh, B. T. D., A. K. Jager, and D. Staerk. 2017. High-resolution inhibition profiling combined with HPLC-HRMS-SPE-NMR for identification of PTP1B inhibitors from Vietnamese plants. *Molecules* 22 (7):1228– 12. doi: 10.3390/molecules22071228.

van Dam, R. M., N. Naidoo, and R. Landberg. 2013. Dietary flavonoids and the development of type 2 diabetes and cardiovascular diseases: Review of recent findings. *Current Opinion in Lipidology* 24 (1): 25–33. doi: 10.1097/MOL.0b013e32835bcdff.

Verma, S., R. M. Goldenberg, D. L. Bhatt, M. E. Farkouh, A. Quan, H. Teoh, K. A. Connelly, L. A. Leiter, and J. O. Friedrich. 2017. Dipeptidyl peptidase-4 inhibitors and the risk of heart failure: A systematic review and meta-analysis. *CMAJ Open* 5 (1):E152–E77. doi: 10.9778/cmajo.20160058.

Wang, M., B. W. Yu, M. H. Yu, L. X. Gao, J. Y. Li, H. Y. Wang, J. Li, and A. J. Hou. 2015. New isoprenylated phenolic compounds from *Morus laevigata*. *Chemistry & Biodiversity* 12 (6):937–45. doi: 10.1002/cbdv.201400210.

Wang, Y., H. J. Yuk, J. Y. Kim, D. W. Kim, Y. H. Song, X. F. Tan, M. J. Curtis-Long, and K. H. Park. 2016. Novel chromenedione derivatives displaying inhibition of protein tyrosine phosphatase 1B (PTP1B) from *Flemingia philippinensis*. *Bioorganic & Medicinal Chemistry Letters* 26 (2):318–21. doi: 10.1016/j.bmcl.2015.12.021.

Wu, L. Q., C. Lei, L. X. Gao, H. B. Liao, J. Y. Li, J. Li, and A. J. Hou. 2015. Isoprenylated flavonoids with PTP1B inhibition from *Ficus tikoua*. *Natural Product Communications* 10 (12):2105–7. doi: 10.1177/1934578X1501001223.

Xu, J., X. Wang, J. Yue, Y. Sun, X. Zhang, and Y. Zhao. 2018. Polyphenols from acorn leaves (*Quercus liaotungensis*) protect pancreatic beta cells and their inhibitory activity against α-glucosidase and protein tyrosine phosphatase 1B. *Molecules* 23 (9):2167– 12. doi: 10.3390/molecules23092167.

Xu, J., L. Yang, R. Wang, K. Zeng, B. Fan, and Z. Zhao. 2019. The biflavonoids as protein tyrosine phosphatase 1B inhibitors from *Selaginella uncinata* and their antihyperglycemic action. *Fitoterapia* 137 (104255):104255– 8. doi: 10.1016/j.fitote.2019.104255.

Xue, J. J., C. Lei, P. P. Wang, K. Y. Kim, J. Y. Li, J. Li, and A. J. Hou. 2018. Flavans and diphenylpropanes with PTP1B inhibition from *Broussonetia kazinoki*. *Fitoterapia* 130:37–42. doi: 10.1016/j.fitote.2018.08.001.

Yang, B., Y. Dong, F. Wang, and Y. Zhang. 2020. Nanoformulations to enhance the bioavailability and physiological functions of polyphenols. *Molecules* 25 (20):4613. doi: 10.3390/molecules25204613.

Yang, X., Y. Zhao, Q. Sun, Y. Yang, Y. Gao, W. Ge, J. Liu, X. Xu, D. Weng, S. Wang, et al. 2019. Adenine nucleotide-mediated regulation of hepatic PTP1B activity in mouse models of type 2 diabetes. *Diabetologia* 62 (11):2106–17. doi: 10.1007/s00125-019-04971-1.

Yip, S. C., S. Saha, and J. Chernoff. 2010. PTP1B: A double agent in metabolism and oncogenesis. *Trends in Biochemical Sciences* 35 (8): 442–9. doi: 10.1016/j.tibs.2010.03.004.

Zabolotny, J. M., F. G. Haj, Y. B. Kim, H. J. Kim, G. I. Shulman, J. K. Kim, B. G. Neel, and B. B. Kahn. 2004. Transgenic overexpression of protein-tyrosine phosphatase 1B in muscle causes insulin resistance, but overexpression with leukocyte antigen-related phosphatase does not additively impair insulin action. *The Journal of Biological Chemistry* 279 (23):24844–51. doi: 10.1074/jbc.M310688200.

Zhang, L., Y. Ge, H. M. Song, Q. M. Wang, and C. H. Zhou. 2018. Design, synthesis of novel azolyl flavonoids and their protein tyrosine phosphatase-1B inhibitory activities. *Bioorganic Chemistry* 80: 195–203. doi: 10.1016/j.bioorg.2018.06.008.

Zhang, L. B., C. Lei, L. X. Gao, J. Y. Li, J. Li, and A. J. Hou. 2016. Isoprenylated flavonoids with PTP1B inhibition from *Macaranga denticulata*. *Natural Products and Bioprospecting* 6 (1):25–30. doi: 10.1007/s13659-015-0082-2.

Zhao, B. T., D. D. Le, P. H. Nguyen, M. Y. Ali, J.-S. Choi, B. S. Min, H. M. Shin, H. I. Rhee, and M. H. Woo. 2016. PTP1B, α-glucosidase, and DPP-IV inhibitory effects for chromene derivatives from the leaves of *Smilax china* L. *Chemico-Biological Interactions* 253: 27–37. doi: 10.1016/j.cbi.2016.04.012.

Zhao, Y., L. Kjaerulff, K. T. Kongstad, A. M. Heskes, B. L. Møller, and D. Staerk. 2019. 2(5H)-Furanone sesquiterpenes from *Eremophila bignoniiflora*: High-resolution inhibition profiling and PTP1B inhibitory activity. *Phytochemistry* 166 (112054):112054. doi: 10.1016/j.phytochem.2019.112054.

Zhao, Y., K. T. Kongstad, A. K. Jager, J. Nielsen, and D. Staerk. 2018. Quadruple high-resolution α-glucosidase/α-amylase/PTP1B/radical scavenging profiling combined with high-performance liquid chromatography-high-resolution mass spectrometry-solid-phase extraction-nuclear magnetic resonance spectroscopy for identification of antidiabetic constituents in crude root bark of *Morus alba* L. *Journal of Chromatography. A* 1556:55–63. doi: 10.1016/j.chroma.2018.04.041.

Zhu, J., C. Chen, B. Zhang, and Q. Huang. 2020. The inhibitory effects of flavonoids on alpha-amylase and alpha-glucosidase. *Critical Reviews in Food Science and Nutrition* 60 (4):695–14. doi: 10.1080/10408398.2018.1548428.

I.2. General and specific objectives of the thesis

The main objective of this thesis was to evaluate the modulatory effect of a panel of structurally related flavonoids on enzymatic targets involved in the pathophysiology of hyperglycaemia in T2D. Through the establishment of an accurate structure-activity relationship for each target under study, we intend to contribute for the elucidation of the best chemical features that contribute for a better inhibitory effect of flavonoids. We expect to contribute for the development of safer and more effective treatments of T2D.

As specific objectives, we aimed to develop methodologies and evaluate a series of flavonoids in:

- The inhibitory activity on α-glucosidase.

- The inhibitory activity on α-amylase.

- The inhibitory activity on protein tyrosine phosphatase 1B (PTP1B).

- The inhibitory activity on dipeptidyl peptidase-4 (DPP-4).

- The inhibitory activity on fructose 1,6-bisohosphatase (FBPase).

- The inhibitory activity on sucrase-isomaltase (SI) using the Caco-2/TC7 cellular model as enzyme source.

CHAPTER II. ORIGINAL RESEARCH

II.1. α-Glucosidase inhibition by flavonoids: an *in vitro* and *in silico* structure-activity relationship study

Version of record from Journal of Enzyme Inhibition and Medicinal Chemistry

Copyright © (2017) with kind permission of Taylor & Francis

"A fixed version of a journal article that has been made available by Taylor & Francis, a publisher by formally and exclusively declaring the article 'published'."

JOURNAL OF ENZYME INHIBITION AND MEDICINAL CHEMISTRY, 2017
VOL. 32, NO. 1, 1216–1228
https://doi.org/10.1080/14756366.2017.1368503

Taylor & Francis
Taylor & Francis Group

RESEARCH PAPER

OPEN ACCESS Check for updates

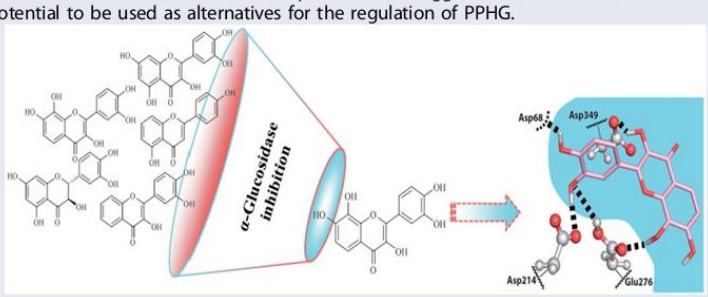
α-Glucosidase inhibition by flavonoids: an *in vitro* and *in silico* structure–activity relationship study

Carina Proença[a], Marisa Freitas[a], Daniela Ribeiro[a], Eduardo F. T. Oliveira[b], Joana L. C. Sousa[c], Sara M. Tomé[c], Maria J. Ramos[b], Artur M. S. Silva[c], Pedro A. Fernandes[b] and Eduarda Fernandes[a]

[a]UCIBIO, REQUIMTE, Laboratory of Applied Chemistry, Department of Chemical Sciences, Faculty of Pharmacy, University of Porto, Porto, Portugal; [b]UCIBIO, REQUIMTE, Faculty of Sciences, Department of Chemistry and Biochemistry, University of Porto, Porto, Portugal; [c]Department of Chemistry & QOPNA, University of Aveiro, Aveiro, Portugal

ABSTRACT

α-Glucosidase inhibitors are described as the most effective in reducing post-prandial hyperglycaemia (PPHG) from all available anti-diabetic drugs used in the management of type 2 diabetes *mellitus*. As flavonoids are promising modulators of this enzyme's activity, a panel of 44 flavonoids, organised in five groups, was screened for their inhibitory activity of α-glucosidase, based on *in vitro* structure–activity relationship studies. Inhibitory kinetic analysis and molecular docking calculations were also applied for selected compounds. A flavonoid with two catechol groups in A- and B-rings, together with a 3-OH group at C-ring, was the most active, presenting an IC_{50} much lower than the one found for the most widely prescribed α-glucosidase inhibitor, **acarbose**. The present work suggests that several of the studied flavonoids have the potential to be used as alternatives for the regulation of PPHG.



ARTICLE HISTORY
Received 31 May 2017
Revised 27 July 2017
Accepted 4 August 2017

KEYWORDS
Diabetes; flavonoids; α-glucosidase inhibition; *in vitro*; *in silico*

Introduction

Diabetes mellitus (DM) is one of the most significant public health concerns worldwide. According to the International Diabetes Federation, there are 415 million of adults with diabetes, probably reaching 642 million in 2040[1]. DM is a multifactorial metabolic disorder, characterised by chronic hyperglycaemia and can be primarily classified as type 1 (insulin dependent DM) and type 2 (non-insulin dependent DM)[2]. Type 2 DM is the most common form of DM, accounting for more than 90% of all diabetic patients, and results from the interaction between behavioural, environmental and genetic risk factors[3,4]. Diabetic patients are more vulnerable to various forms of both short- and long-term complications, such an increased risk of common infections and cancer, increasing the morbidity and mortality[4–6].

DM is characterised by absolute or relative deficiency in insulin secretion by pancreatic β-cells, increased insulin resistance and/or impairment of insulin action in target tissues[7–10]. Post-prandial hyperglycaemia (PPHG) is known as the plasma glucose value taken 1.5–2 h after a meal. The disequilibrium in the insulin regulatory system, culminates in high PPHG level (≥200 mg/dL) compared to individuals without type 2 DM (<140 mg/dL)[11]. Prolonged hyperglycaemia has been associated with several macro- and micro-vascular complications, e.g. nephropathy, retinopathy and cardiovascular disorders[11–13]. Therefore, the management of PPHG, in order to achieve blood glucose levels as close to normal as possible, is considered by the scientific community one of the major therapeutic strategies for type 2 DM treatment[14].

An effective control of hyperglycaemia in type 2 DM includes the retarding, regulation and/or inhibition of carbohydrate hydrolysing enzymes[15]. Among these, α-glucosidase, which is located in the brush border of the enterocytes of the jejunum, is the most important enzyme in carbohydrates digestion[16]. It catalyses the

CONTACT Eduarda Fernandes egracas@ff.up.pt UCIBIO, REQUIMTE, Laboratory of Applied Chemistry, Department of Chemical Sciences, Faculty of Pharmacy, University of Porto, Porto, Portugal; Pedro A. Fernandes pafernan@fc.up.pt UCIBIO, REQUIMTE, Faculty of Sciences, Department of Chemistry and Biochemistry, University of Porto, Porto, Portugal

Supplemental data for this article can be accessed here.

© 2017 The Author(s). Published by Informa UK Limited, trading as Taylor & Francis Group.
This is an Open Access article distributed under the terms of the Creative Commons Attribution License (http://creativecommons.org/licenses/by/4.0/), which permits unrestricted use, distribution, and reproduction in any medium, provided the original work is properly cited.

hydrolysis of 1,4-α bonds of the unabsorbed oligo- and disaccharides, and converts them into monosaccharides, namely, glucose, which are absorbed in the upper jejunum, resulting in hyperglycaemia[17,18]. Inhibitors of α-glucosidase can retard the decomposition and absorption of dietary carbohydrates by restricting the breakdown of linear or branched oligosaccharide units like α-limit dextrins, maltose and maltotriose to produce glucose, thereby preventing glucose absorption into blood stream and suppress the PPHG[19,20].

The use of α-glucosidase inhibitors started in the 1970s and the first related therapeutic agents for diabetes were approved in the 1990s[18]. Nowadays, several oral drugs are used such as voglibose, acarbose and miglitol to inhibit the α-glucosidase activity[20]. However, their use has been associated with several adverse effects such as abdominal distention, flatulence, diarrhoea and pneumatosis cystoides intestinalis[11]. Most of these side-effects occur when undigested carbohydrates are fermented by colonic bacteria[21,22]. The commonly used α-glucosidase inhibitors were also reported to be associated with rare adverse hepatic events[23]. Moreover, these drugs have low efficacy, with high IC_{50} values[24,25]. Thus, much effort has been undertaken to search for more effective and safer inhibitors.

Some flavonoids, such as morin[17], luteolin[26], baicalein[27], kaempferol[28] and apigenin[24], have been shown to exhibit inhibitory effects against α-glucosidase enzymes. Nevertheless, the information found in the literature is disperse and variable, probably due to the use of different enzyme concentrations (0.3–1.7 U/mL)[8,29,30], from different origins (e.g. yeast and rat intestinal α-glucosidase)[18,19,31,32], different substrates concentrations (1–20 mM)[19,30,33] and incubation time with the flavonoids (5 min–3 h)[8,26,28,29,34]. The discrepancies between the studies bring difficulties to their comparison and consequently the conclusions about the flavonoids efficacy against α-glucosidase activity.

The present study aims to establish a structure–activity relationship of a panel of flavonoids (Figure 1), divided in five groups, against α-glucosidase activity, covering a solid set of different structures. For this purpose, a microanalysis screening system was applied for testing the type of inhibition of the most active flavonoids from each group, and the positive control **acarbose**. Molecular docking calculations were also applied to complement the inhibitory activity studies and to predict the binding model of the selected flavonoids to the three-dimensional structure of α-glucosidase.

The overall obtained results constitute an important step for the establishment of the adequate and ideal chemical structure of flavonoids to target α-glucosidase and consequently, to manage type 2 DM.

Materials and methods

Chemicals

The following reagents were purchased from Sigma-Aldrich Co. LLC (St. Louis, MO): α-glucosidase from *Saccharomyces cerevisiae*, *p*-nitrophenyl-α-D-glucopyranoside (*p*NPG), DMSO, $NaHPO_4$, Na_2HPO_4, compounds **D3** (baicalein), **D4** (apigenin), **D6** (kaempferol), **D7** (luteolin), **D8** (quercetin), **D9** (morin), **D16** (acacetin), **D18** (rutin), **E1** (naringenin), **E2** (eriodictyol), **E3** (taxifolin) and **acarbose**. Compounds **A1**, **A2**, **A3**, **A4**, **A5**, **A6**, **B1**, **B2**, **B3**, **B4**, **C1**, **C2**, **C3**, **C4**, **C5**, **C6**, **C8**, **C9**, **D1** (chrysin), **D2** (galangin) and **D5** were obtained from Indofine Chemical Company, Inc. (Hillsborough, NJ). The flavonoids **C7**, **C10**, **C11**, **C12**, **C13**, **D10**, **D11**, **D12**, **D13**, **D14** and **D17** were synthesised as previously described[35–37]. For the enzymatic assays, flavonoids were dissolved in DMSO (the final concentration of DMSO in the reactional mixture was 4.76%).

In vitro *inhibition assay for α-glucosidase activity*

The α-glucosidase activity was measured using a method of Tadera et al.[31] slightly modified. The assay was carried out by monitoring the α-glucosidase-mediated transformation of the substrate *p*NPG into α-D-glucose and *p*-nitrophenol, at 405 nm. Briefly, in a 96-well plate, the enzyme (0.05 U/mL), dissolved in 100 mM phosphate buffer (pH 6.8), was pre-incubated at 37 °C for 5 min with the flavonoids (0–200 μM). In sequence, *p*NPG was added (600 μM) and incubated in the reaction mixture at 37 °C for 30 min. The enzymatic reaction was monitored spectrophotometrically, in a microplate reader (Synergy HT, BIO-TEK), by measuring the absorbance at 405 nm. The obtained values correspond to the slope measured between 5 and 20 min. The amount of DMSO used had no interference with the assay. Acarbose (0–2000 μM) was used as positive control. The obtained results represent at least three independent experiments.

Inhibitory kinetic analysis

The inhibitory kinetic analyses were performed for the most active flavonoids of each group (A–E): **A5** (0–62.5 μM), **B3** (0–50 μM), **C7** (0–5 μM), **D8** (quercetin) (0–12.5 μM), **D10** (0–18.75 μM), **E3** (taxifolin) (0–100 μM) and for the positive control, **acarbose** (0–2000 μM).

Briefly, the enzyme (0.05 U/mL), dissolved in 100 mM phosphate buffer (pH 6.8), was pre-incubated at 37 °C with the above mentioned flavonoids in a 96-well plate, for 5 min. In sequence, *p*NPG was added (300, 600 and 1200 μM) and incubated in the reaction mixture at 37 °C for 30 min.

The study of the inhibition type (competitive, uncompetitive, non-competitive or mixed) of the tested flavonoids was performed using the nonlinear regression Michaelis–Menten enzyme kinetics and the corresponding Lineweaver–Burk double reciprocal plots for each concentration of the inhibitor and substrate. The Ki values were calculated with GraphPad Software 6.0 by plotting the reciprocal of maximum velocity ($1/V_{max}$) (*y* axis) against the flavonoid concentrations (*x* axis) (Table 2)[38–40].

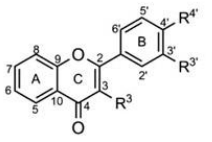
The type of inhibition parameters were all calculated with GraphPad Software 6.0. The obtained results represent at least three independent experiments.

Molecular docking

Homology modelling

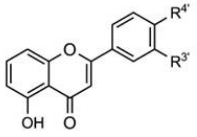
3D structures of *Saccharomyces cerevisiae* α-glucosidase (maltase, EC 3.2.1.20) are unavailable. There are, however, X-ray structures available for the isozyme isomaltase/α-methylglucosidase (EC 3.2.1.10). The isomaltase/α-methylglucosidase with the PDB[41] entry 3AJ7 has a high-resolution X-ray structure and a high sequence identity (72.51%) and sequence similarity score (0.54) with the *Saccharomyces cerevisiae* α-glucosidase MAL32 (UniProt entry P38158)[42].

We identified several differences between residues lining the binding pockets of α-glucosidase and isomaltase, such as the pairs Asp307/Glu204, Asp408/Glu411, Phe157/Tyr158, Thr215/Val216, Ala278/Gln279, Val303/Thr306 or Ala178/Cys179, respectively for α-glucosidase and isomaltase. Most of these differences involve very similar residues, but considering the differences in the size of the side chains (which can affect binding through stereochemical effects) and the high confidence entrusted by the extremely



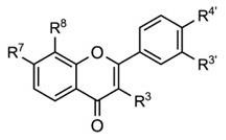
A1-6

A1: R^3= $R^{3'}$= $R^{4'}$= H (Flavone)
A2: R^3= H, $R^{3'}$= OH, $R^{4'}$= H
A3: R^3= $R^{3'}$= H, $R^{4'}$= OH
A4: R^3= H, $R^{3'}$= $R^{4'}$= OH
A5: R^3= $R^{3'}$= $R^{4'}$= OH
A6: R^3= OH, $R^{3'}$= $R^{4'}$= OMe



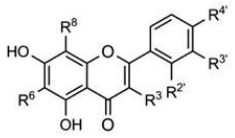
B1-4

B1: $R^{3'}$= $R^{4'}$= H
B2: $R^{3'}$= OH, $R^{4'}$= H
B3: $R^{3'}$= H, $R^{4'}$= OH
B4: $R^{3'}$= $R^{4'}$= OH



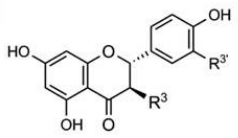
C1-13

C1: R^3= $R^{3'}$= $R^{4'}$= H, R^7= OH, R^8= H
C2: R^3= H, $R^{3'}$= OH, $R^{4'}$= H, R^7= OH, R^8= H
C3: R^3= $R^{3'}$= H, $R^{4'}$= R^7= OH, R^8= H
C4: R^3= $R^{3'}$= OH, $R^{4'}$= H, R^7= OH, R^8= H
C5: R^3= OH, $R^{3'}$= H, $R^{4'}$= R^7= OH, R^8= H
C6: R^3= H, $R^{3'}$= $R^{4'}$= R^7= OH, R^8= H
C7: R^3= $R^{3'}$= $R^{4'}$= R^7= R^8= OH
C8: R^3= OH, $R^{3'}$= OMe, $R^{4'}$= H, R^7= OMe, R^8= H
C9: R^3= OH, $R^{3'}$= H, $R^{4'}$= R^7= OMe, R^8= H
C10: R^3= $R^{3'}$= $R^{4'}$= OH, R^7= R^8= OMe
C11: R^3= OH, $R^{3'}$= $R^{4'}$= OMe, R^7= R^8= OH
C12: R^3= OH, $R^{3'}$= $R^{4'}$= OBn, R^7= R^8= OMe
C13: R^3= OH, $R^{3'}$= $R^{4'}$= OMe, R^7= R^8= OBn



D1-18

D1: $R^{2'}$= R^3= $R^{3'}$= $R^{4'}$= R^6= R^8= H (Chrysin)
D2: $R^{2'}$= H, R^3= OH, $R^{3'}$= $R^{4'}$= R^6= R^8= H (Galangin)
D3: $R^{2'}$= R^3= $R^{3'}$= $R^{4'}$= H, R^6= OH, R^8= H (Baicalein)
D4: $R^{2'}$= R^3= H, $R^{3'}$= OH, $R^{4'}$= R^6= R^8= H
D5: $R^{2'}$= R^3= $R^{3'}$= H, $R^{4'}$= OH, R^6= R^8= H (Apigenin)
D6: $R^{2'}$= H, R^3= OH, $R^{3'}$= H, $R^{4'}$= OH, R^6= R^8= H (Kaempferol)
D7: $R^{2'}$= R^3= H, $R^{3'}$= $R^{4'}$= OH, R^6= R^8= H (Luteolin)
D8: $R^{2'}$= H, R^3= $R^{3'}$= $R^{4'}$= OH, R^6= R^8= H (Quercetin)
D9: $R^{2'}$= R^3= OH, $R^{3'}$= H, $R^{4'}$= OH, R^6= R^8= H (Morin)
D10: $R^{2'}$= H, R^3= Cl, $R^{3'}$= $R^{4'}$= OH, R^6= R^8= H
D11: $R^{2'}$= R^3= H, $R^{3'}$= $R^{4'}$= OH, R^6= Cl, R^8= H
D12: $R^{2'}$= R^3= H, $R^{3'}$= $R^{4'}$= OH, R^6= H, R^8= Cl
D13: $R^{2'}$= H, R^3= Cl, $R^{3'}$= $R^{4'}$= OH, R^6= H, R^8= Cl
D14: $R^{2'}$= R^3= H, $R^{3'}$= $R^{4'}$= OH, R^6= R^8= Cl
D15: $R^{2'}$= R^3= H, $R^{3'}$= OMe, $R^{4'}$= OH, R^6= R^8= H (Chrysoeriol)
D16: $R^{2'}$= R^3= $R^{3'}$= H, $R^{4'}$= OMe, R^6= R^8= H (Acacetin)
D17: $R^{2'}$= R^3= H, $R^{3'}$= $R^{4'}$= OMe, R^6= R^8= H
D18: $R^{2'}$= H, R^3= rutinose, $R^{3'}$= $R^{4'}$= OH, R^6= R^8= H (Rutin)



E1-3

E1: R^3= $R^{3'}$= H
E2: R^3= H, $R^{3'}$= OH
E3: R^3= $R^{3'}$= OH

Figure 1. Chemical structures of the tested flavonoids.

favourable sequence identity, we opted to build a high accuracy homology model of α-glucosidase using isomaltase as template.

Using MAL32 target sequence and the structure with the PDB ID 3AJ7 as template, we built the α-glucosidase homology model in SWISS-MODEL[43] based on the target-template alignment using ProMod3. The resulting model has a Global Model Quality Estimation of 0.92 and a rmsd for 4452 atoms of 0.40 Å, which is excellent. Supplementary Figure S1 provides a summary of the homology modelling parameters and Supplementary Figure S2 the Ramachandran plot analysis of the homology model.

Docking protocol

The protonation states of the enzyme were predicted using the Protoss server[44]. Accordingly, His6, His97 and His251 were modelled in the charged form, Glu276 and Glu481 were modelled in the neutral form. All other residues were protonated according to their pK_a at pH 7.

The substrate α-maltose was modelled inside the binding pocket and subsequently, to remove potential clashes and relax the structure of the model, Molecular Mechanics minimisation followed by classical MD simulations were done. This protocol was

performed within the AMBER 12[45] suite using the ff99SB[46] force field for the protein and GLYCAM06[47] force field for maltose. The details for the energy minimisation and MD simulation are given in SI.

To validate the receptor for the docking protocol we extracted the last step from the MD simulation and re-docked the substrate α-maltose and also the inhibitor acarbose. Since the predicted binding modes, both for α-maltose and acarbose[48], behaved according to the expected catalytic binding mode and to the X-ray structure 3TOP, we proceeded to binding mode prediction of the most active flavonoids of each group (A–E).

AutoDock Vina[49] was used to generate binding poses using default parameters (see Supplementary Material for details), such as the exhaustiveness of the global search = 8 or the maximum number of output poses = 9. The search space was confined to a box of circa 15 × 20 × 17 centred on the site occupied by the second glucose in maltose. The receptor was treated as a rigid body and prepared using openbabel[50] for atom-typing and charge assignment using Gasteiger–Marsili charges[51]. Flavones atom-types and charges were attributed the same way.

Subsequently, the poses generated by AutoDock Vina were rescored using the scoring function ChemPLP, which is excellent for oligosaccharides[52]. We used the GOLD software[53] with the standard parameters for a "Rescoring Run" with local optimisation and selected the binding mode with the highest score.

Results

In vitro *inhibition assay for α-glucosidase activity*

The inhibitory effect of flavonoids against α-glucosidase activity is shown in Table 1. This effect was highly dependent on small variations of the flavonoids' structures. According to the flavonoids' structures, we divided the studied compounds into five groups (A–E).

Flavonoids of A group

From all the flavones from A group, flavone **A5** was noticeably the most effective, presenting an IC_{50} of 54 ± 3 μM. For the other tested compounds, it was not possible to achieve the IC_{50} value up to the concentrations of 100 μM (**A6**) or 200 μM (**A1**–**A4**). These results indicate that the presence of a 3-OH group in the C-ring is relevant for the inhibitory activity of flavonoids. Moreover, when comparing the flavonoid **A5** and the flavonoid **A6**, we may conclude that the replacement of the 3′,4′-$(OH)_2$, in the B-ring, by methoxy (–OMe) groups withdraws the inhibitory activity of compound **A5**.

Flavonoids of B group

From B group, flavone **B1** was the less active. Comparing the activities of **B1** (with a 5-OH in A-ring) and **A1** (without substitutions) it is shown that the presence or absence of 5-OH in A-ring, *per se*, is indifferent for the inhibitory activity. However, the 5-OH substitution in A-ring, together with the 4′-OH (**B3**) or 3′,4′-$(OH)_2$ (**B4**) in B-ring, increases the activity, comparing with the related compounds, from A group, which do not have 5-OH substitution.

Flavonoids of C group

C group has the most active flavonoid, **C7** with an IC_{50} = 7.6 ± 0.4 μM, which is almost 80 times lower than the IC_{50} of the positive control, **acarbose** (IC_{50} = 607 ± 56 μM). Comparing the flavones **C5** and **C4**, it is clear that the presence of –OH groups in the B-ring is more relevant in the 3′-position (**C4**, IC_{50} = 42 ± 4 μM) than in the 4′-position (**C5**, IC_{50} = 96 ± 10 μM). Flavone **C1**, with just one 7-OH group, did not achieve the IC_{50} value up to the maximum tested concentration (200 μM). However, adding another 3′-OH at the B-ring (**C2**) is enough to increase the inhibitory activity of the compound (IC_{50} = 53 ± 4 μM). In turn, increasing the complexity of the structure by the addition of a –OMe and/or a benzyloxy (–OBn) group (**C8**–**C13**) did not favour the activity.

Flavonoids of D group

In what concerns D group, the most effective compound was **D8** (quercetin) with an IC_{50} = 15 ± 3 μM. The substitution in 3-position of the C-ring seems to be advantageous for the intended activity, since **D7** (luteolin), with no substitution in 3-position, had a higher IC_{50} (46 ± 6 μM). Moreover, the relevance of the existence of a 3-OH substitution in the C-ring was evidenced by the low activity of **D18** (rutin), which had a rutinose in this position. In turn, the close IC_{50} values of **D8** (quercetin) and **D10** (IC_{50} = 21 ± 2 μM) indicate that the presence of a 3-OH group or a 3-Cl atom in the C-ring is indifferent for α-glucosidase inhibition. The relevance of the presence of a catechol moiety in the B-ring is shown by the different IC_{50} values found for **D7** (luteolin) (46 ± 6 μM), which have a catechol group in 3′,4′- positions, and the compounds **D5** (apigenin) (IC_{50} = 82 ± 6 μM) and **D4** (IC_{50} = 89 ± 3 μM), which had just one OH in the 4′- or 3′-positions, respectively. Similarly to the obtained results in C group, results of D group indicate that the methylation of the catechol arrangement in the B-ring (**D15**–**D17**) did not show any advantage for the studied activity.

Flavonoids of E group

Analysing the IC_{50} of flavonoids from E group, **E3** (taxifolin) had the best inhibitory activity. Nonetheless, its IC_{50} was approximately 200 μM, the maximum tested concentration.

Inhibitory kinetics analysis

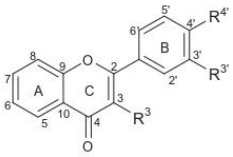
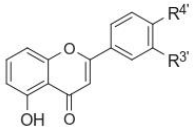
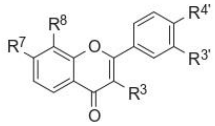
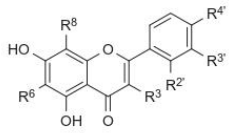
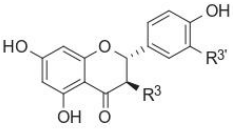
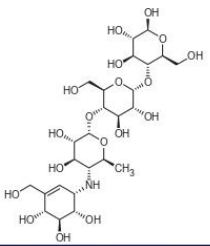
The type of inhibition of the most active flavonoids of each group (A–E), **A5**, **B3**, **C7**, **D8** (quercetin), **D10**, **E3** (taxifolin) and **acarbose** was deducted from the calculation of Km and maximum enzyme velocity (V_{max}). These parameters were obtained by the nonlinear regression Michaelis–Menten enzyme kinetics and complemented with Lineweaver–Burk double reciprocal plots. As observed in Figure 2, flavones **A5** (Figure 2(A)) and **B3** (Figure 2(B)) showed a mixed type inhibition. Concerning flavonoid **C7**, although the Figure 2(C) does not clearly differentiate between a mixed and a competitive inhibition type, the interception of the lines is close to the y axis, suggesting a competitive pattern. Flavonoid **D8** (quercetin) (Figure 2(D)) and the positive control **acarbose** (Figure 2(G)) have shown a competitive inhibition type. Flavones **D10** (Figure 2(E)) and **E3** (taxifolin) (Figure 2(F) presented a non-competitive inhibition type, since the K_m value remained constant and the V_{max} value decreased with increasing concentrations of the flavonoids.

The K_i values were calculated with GraphPad Software 6.0 by plotting the reciprocal of maximum velocity ($1/V_{max}$) (*y* axis) against the flavonoid concentrations (*x* axis) (Table 2).

Binding mode of the selected inhibitors/flavonoids

We have investigated the binding poses of a selection of inhibitors within the reactive pocket of the active site of

Table 1. Structures and *in vitro* α-glucosidase inhibition by the studied flavonoids (IC_{50} μM, mean ± SEM).

Compounds	Structure	$R^{2'}$	R^3	$R^{3'}$	$R^{4'}$	R^6	R^7	R^8	IC_{50} (μM)
A1 (Flavone)		–	H	H	H	–	–	–	<20%*200 μM[a]
A2		–	H	OH	H	–	–	–	<20%*200 μM[a]
A3		–	H	H	OH	–	–	–	<20%*200 μM[a]
A4		–	H	OH	OH	–	–	–	32 ± 4%*200 μM[a]
A5		–	OH	OH	OH	–	–	–	**54 ± 3**
A6		–	OH	OMe	OMe	–	–	–	<20%*100 μM[a]
B1		–	–	H	H	–	–	–	<20%*200 μM[a]
B2		–	–	OH	OH	–	–	–	31 ± 4%*200 μM[a]
B3		–	–	H	OH	–	–	–	**66 ± 2**
B4		–	–	OH	OH	–	–	–	**66 ± 7**
C1		–	H	H	H	–	OH	H	<20%*200 μM[a]
C2		–	H	OH	H	–	OH	H	53 ± 4
C3		–	H	H	OH	–	OH	H	≈200
C4		–	OH	OH	H	–	OH	H	42 ± 4
C5		–	OH	H	OH	–	OH	H	96 ± 10
C6		–	H	OH	OH	–	OH	H	95 ± 7
C7		–	OH	OH	OH	–	OH	OH	**7.6 ± 0.4**
C8		–	OH	OMe	H	–	OMe	H	22 ± 2%*100 μM[a]
C9		–	OH	H	OMe	–	OMe	H	<20%*200 μM[a]
C10		–	OH	OH	OH	–	OMe	OMe	86 ± 6
C11		–	OH	OMe	OMe	–	OH	OH	31 ± 3%*200 μM[a]
C12		–	OH	OBn	OBn	–	OMe	OMe	<20%*200 μM[a]
C13		–	OH	OMe	OMe	–	OBn	OBn	32 ± 3%*200 μM[a]
D1 (Chrysin)		H	H	H	H	H	–	H	<20%*50 μM[a]
D2 (Galangin)		H	OH	H	H	H	–	H	21 ± 3%*200 μM[a]
D3 (Baicalein)		H	H	H	H	OH	–	H	44 ± 3
D4		H	H	OH	H	H	–	H	89 ± 3
D5 (Apigenin)		H	H	H	OH	H	–	H	82 ± 6
D6 (Kaempferol)		H	OH	H	OH	H	–	H	32 ± 3
D7 (Luteolin)		H	H	OH	OH	H	–	H	46 ± 6
D8 (Quercetin)		H	OH	OH	OH	H	–	H	**15 ± 3**
D9 (Morin)		OH	OH	H	OH	H	–	H	32 ± 2
D10		H	Cl	OH	OH	H	–	H	21 ± 2
D11		H	H	OH	OH	Cl	–	H	≈200
D12		H	H	OH	OH	H	–	Cl	55 ± 2
D13		H	Cl	OH	OH	H	–	Cl	43 ± 3
D14		H	H	OH	OH	Cl	–	Cl	34 ± 3
D15 (Chrysoeriol)		H	H	OMe	OH	H	–	H	156 ± 5
D16 (Acacetin)		H	H	H	OMe	H	–	H	≈200
D17		H	H	OMe	OMe	H	–	H	<20%*200 μM[a]
D18 (Rutin)		H	Rutinose	OH	OH	H	–	H	<20%*200 μM[a]
E1 (Naringenin)		–	H	H	–	–	–	–	45 ± 3%*200 μM[a]
E2 (Eriodictyol)		–	H	OH	–	–	–	–	35 ± 4%*200 μM[a]
E3 (Taxifolin)		–	OH	OH	–	–	–	–	≈**200**
Positive control: **Acarbose**		–	–	–	–	–	–	–	607 ± 56

[a]Inhibitory activity (mean ± SEM %) at the highest tested concentration (in superscript).

Table 2. K_i values (mean ± SEM, μM) for the inhibition of yeast α-glucosidase by the selected flavonoids.

Flavonoid	Type of inhibition	K_i (μM)
A5	Mixed	41 ± 7
B3	Mixed	127 ± 9
C7	Competitive	6.5 ± 0.2
D8 (quercetin)	Competitive	6.8 ± 0.6
D10	Non-competitive	51 ± 6
E3 (taxifolin)	Non-competitive	347 ± 15
Positive control: **Acarbose**	Competitive	457 ± 11

α-glucosidase [**acarbose**, **A5**, **B3**, **C7**, **D8** (quercetin), **D10** and **E3** (taxifolin)]. It is important to realise that a few of them may bind in more than one sugar pocket, even predominantly in other sugar pockets that line the active site cavity (which were physiologically developed to bind the sugars of oligosaccharide chain tips), and in a lesser extent at the deeper, reactive pocket of the active site. However, for the purpose of drug discovery, the deep reactive pocket is by far the most relevant, because it is the one for which the drugs are always optimised to bind (an evidence of this is that all approved drugs for this target are described as competitive inhibitors). Therefore, it was the binding to this deep pocket that we explore in this section.

Acarbose

The predicted binding mode for **acarbose** in the homology model (Figure 3(A)) positions the first glucose of **acarbose** in the exact same site as the first glucose of the α-maltose substrate, which was used to build and refine the model. Thus, the first glucose of **acarbose** is placed in the deep reactive pocket with 2,3,4-$(OH)_3$ groups donating hydrogen bonds to Asp349 and Asp68. The oxygen atoms from these three hydroxyls accept hydrogen bonds from Arg212, His348 and Arg439. The single difference between **acarbose** first glucose and α-maltose is in the CH_2OH group, since in α-maltose the C-4 has sp^3 hybridisation while in **acarbose** the C-4 has sp^2 hybridisation. Therefore, the α-maltose CH_2OH group hydrogen bonds to both His111 and Asp214 while the same group in acarbose makes a single hydrogen bond with Asp68.

The nucleophilic Asp214 is placed below the acarbose C-1 carbon but does not accept any hydrogen bond from **acarbose**. Different to α-maltose binding, Glu276 donates one hydrogen bond to the *N*-glycosidic bond nitrogen and accepts one hydrogen bond from the 3-OH group of the second **acarbose** glucose.

To conclude, the first glucose, the *N*-glycosidic bond and the second glucose of **acarbose**, all occupy the same site as the substrate α-maltose and have a binding mode identical to α-maltose. This is compatible with a competitive mode of inhibition, which the Lineweaver-Burk double reciprocal plots of Figure 2(G) seem to corroborate.

Flavone A5

Flavones skeleton is quite different from the saccharides found in α-maltose and **acarbose**. Nevertheless, when we analyse the predicted binding poses for the most active compounds, we can observe similar interactions with binding pocket residues.

In the case of the most active compound of A group, **A5**, the catechol group in the B-ring and the OH substitution in the 3-position of the C ring, provide similar interactions to active site residues as found in α-maltose or **acarbose** (Figure 3(B)). The 3′,4′-$(OH)_2$ B-ring substitutions donate hydrogen bonds to Asp214 and the neutral Glu276 donates one hydrogen bond to B-ring 3′-OH. The OH in the 3-position of the C-ring donates a hydrogen bond to the conserved Asp349.

The B-ring binds in the small crevice of the active site pocket, occupying the same site as the first glucose of **acarbose** and α-maltose. The C-ring occupies a similar site to α-maltose second glucose, in the entrance of the deep small pocket, while the A-ring is exposed to the larger binding pocket.

The Lineweaver–Burk double reciprocal plots (Figure 2(A)) shows a mixed inhibition type. The binding mode described here for flavone **A5** corresponds to the competitive inhibition mode. We directed the binding mode prediction to the active site, where the natural substrates bind the first two sugar rings and did not explore all possible modes of interaction of flavones with α-glucosidase, as the interactions with the active site are the most relevant for drug design. However, given the large size of the active site and knowing that many natural substrates are oligosaccharides, it is possible that the inhibitors bind to the sites where the oligosaccharides sugar rings (other than the first two) bind. Therefore, we cannot exclude that flavone **A5** may bind with increased affinity to a different oligosaccharide site, which could interfere with substrate binding and explain the mixed inhibition type.

Flavone B3

When flavone **B3** binds the reactive region of the active site it is predicted to bind the A- and C- rings close to the catalytic Glu276 and the conserved Asp349, establishing strong hydrogen bonds with them (Figure 3(C)). However, **B3** does not insert into the deepest region of the catalytic pocket, formed by Asp349/Glu276/Asp214 triad (Asp214 is the nucleophilic residue), but instead in a larger, shallower region of the pocket bordered by hydrophobic residues (such as Phe157, Phe158, Phe177, Thr215 and Phe300) and polar residues (His245, His279, Glu304, Arg312 or Asp408). This binding mode is very similar to the one obtained for flavone **B1** (Figure 3(C)). The additional 3′-OH group of flavone **B3** might hydrogen bond His274, but it is not totally clear from our binding mode prediction.

Despite **B3** binding outside the small crevice formed by the catalytic residues, the predicted mode of binding would still be more compatible with a competitive mode of inhibition. The reason is **B3** C-ring binds exactly in the site of the α-maltose second glucose. The binding pose shown in Figure 3(C) will not allow for substrate binding, despite the fact that the data shown in Figure 2(B) seems to point to the opposite. As mentioned earlier, it is possible that the inhibitors bind to the sites where the oligosaccharides sugar rings (other than the first two) bind. These cases are less relevant than the one shown here for the actual purpose of drug discovery, but could allow for substrate binding even though interfering with the substrate pose.

Flavone C7

Comparing the inhibitory activity of **C1** and **C3** with **C6**, it seems that addition of –OH groups to the B-ring improves the inhibitory activity of group C flavonoids, with the 3′-OH substitution to have the greater impact on the inhibitory activity (Table 1). Flavone **C7** has both of these substitutions, plus three more –OH substitutions, one on the C-ring (3-OH) and two on the A-ring (7,8-$(OH)_2$).

The predicted binding mode for flavone **C7** in the active site region places the B-ring deep in the small crevice formed by the catalytic residues. Glu276 hydrogen bonds to 3′-OH, and 3′-OH

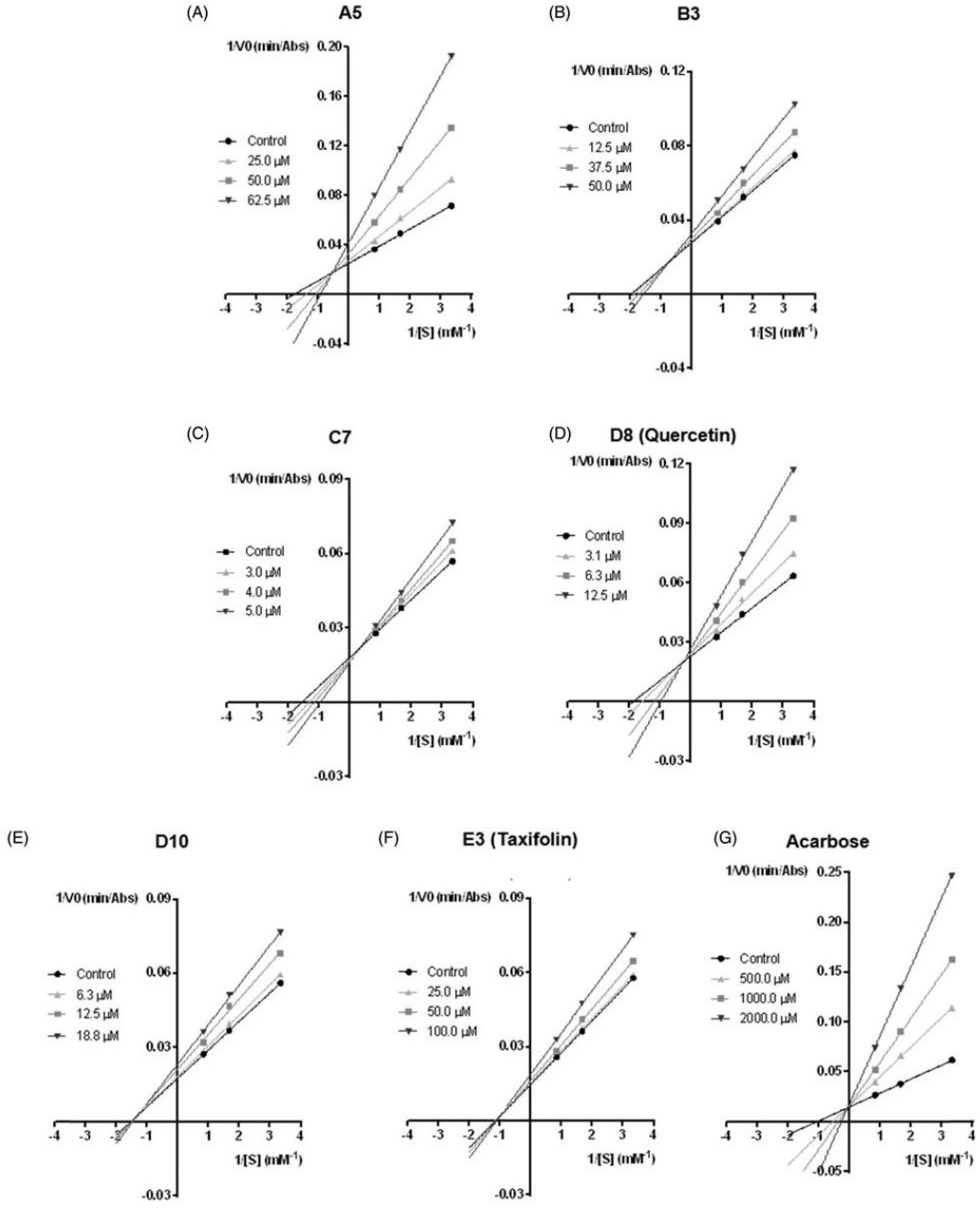


Figure 2. Lineweaver–Burk double reciprocal plots of α-glucosidase inhibition by **A5** (A), **B3** (B), **C7** (C), **D8** (quercetin) (D), **D10** (E), **E3** (taxifolin) (F) and **acarbose** (G).

donates a hydrogen bond to Asp214. 4′-OH group is even deeper in the small pocket and hydrogen bonds Asp68.

The C- and A-rings bind in the entrance of the small crevice, with C-ring 3-OH substitution hydrogen bonding Asp349. The A- and C-rings are placed around Glu276, and 8-OH group donates a hydrogen bond to Glu276. The 7-OH substitution is exposed to the larger binding pocket and no specific interactions with 8-OH group can be identified.

Considering this binding mode, the strong hydrogen bond interactions with active site amino acids are consistent with a very favourable binding affinity to the active site, indicating a competitive type of inhibition.

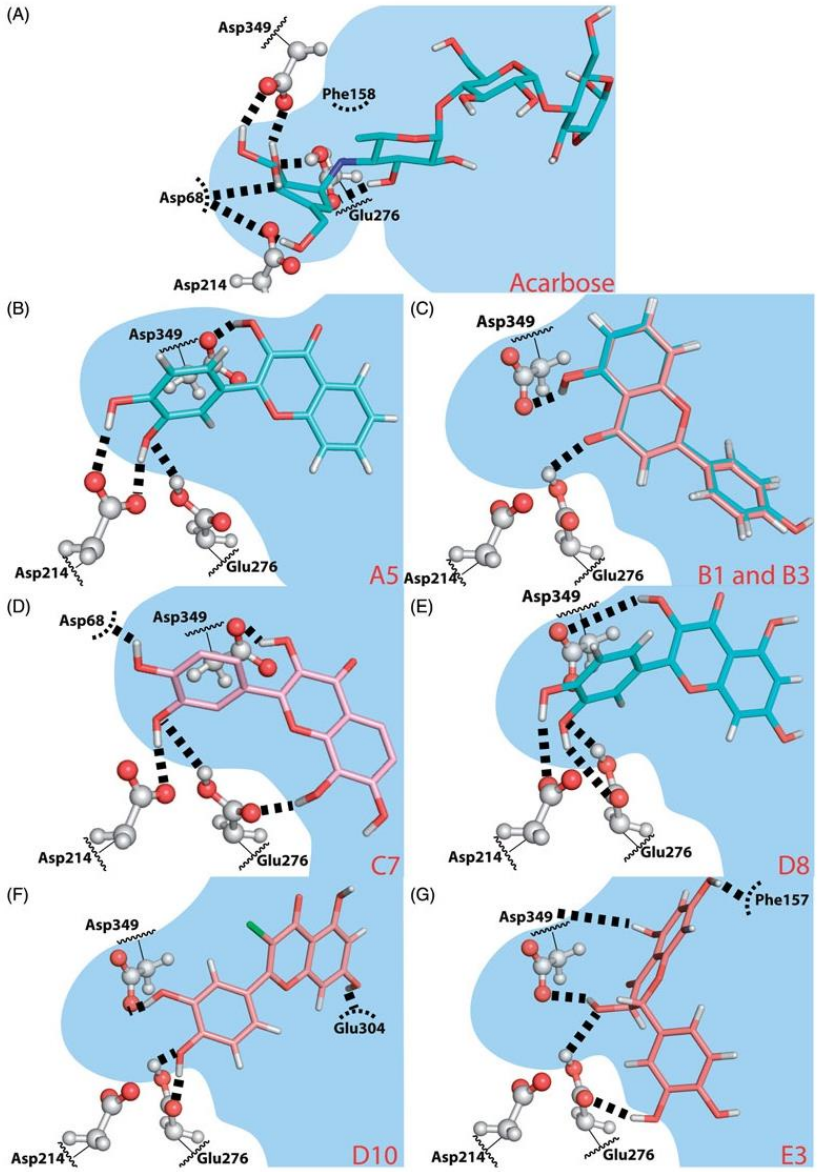


Figure 3. Predicted binding poses for **acarbose** (A) and flavones **A5** (B), **B1** and **B3** (C), **C7** (D), **D8** (quercetin) (E), **D10** (F) and **E3** (taxifolin) (G). Hydrogen bonds are represented by dashed lines. (B) **B1** is coloured salmon and **B3** light blue. The residues that establish the most relevant interactions are also shown. Asp214 and Glu276 are the catalytic residues that participate in the hydrolysis reaction. Asp349 is also a conserved residue.

Flavones D8 (quercetin) and D10

Figure 2 shows that flavone **D8** (quercetin) (Figure 2(D)) is a competitive inhibitor while the very similar **D10** (Figure 2(E)) is non-competitive. The predicted binding mode for flavones **D8** (quercetin) and **D10** brings the B-ring into the small reactive catalytic pocket formed by the Asp349/Glu276/Asp214 triad. The 3′-OH of flavone **D8** (quercetin) makes two hydrogen bonds with Glu276, while **D10**, which is slightly rotated, accepts one hydrogen bond from Asp214 and donates another to Asp349 (Figure 3(E,F)). The 4′-OH of flavone **D8** (quercetin) hydrogen bonds to Asp214 while 4′-OH from **D10** hydrogen bonds to Asp68. The crucial difference between **D8** (quercetin) and **D10** seems to be the C-ring substitution. The 3-OH group in flavone **D8** (quercetin) is able to hydrogen bond the conserved Asp349, while the hydrophobic 3-Cl-substitution in flavone **D10** cannot provide any specific interaction. The lack of this interaction makes **D10** to rotate and changes slightly the hydrogen bond pattern found for 3′,4′-$(OH)_2$ substitution.

The extensive hydrogen bonding with the deep reactive pocket of flavone **D8** (quercetin) is absolutely consistent with the competitive inhibition pattern seen in Figure 2(D). **D10**, in contrast, loses the hydrogen bonds with one of the Asp349/Glu276/Asp214

triad members (namely with Asp214), weakening the interaction with the deep reactive pocket, also very well in line with the non-competitive pattern shown in Figure 2(E). Therefore, extensive hydrogen bond with the Glu/Asp triad seems to be relevant to hold the inhibitors bound to the deep reactive pocket.

Flavanone E3 (taxifolin)

Flavanone **E3** (taxifolin) contains 3′,4′-$(OH)_2$ substitution in the B-ring, which were demonstrated to be important to drive the B-ring into the Glu276/Asp214/Asp349 triad pocket[32]. However, the lack of C2 = C3 double bound makes the B-ring to move out of the plane of the A- and C-rings, destroying the overall planarity of the compounds, which has a major impact in the binding properties. The predicted binding pose of **E3** (taxifolin) does not have the B-ring inserted in the small active site pocket. Instead, the entire flavanone moves to a larger, less deep pocket (Figure 3(G)). This result is consistent with the non-competitive mode of inhibition determined through the Lineweaver–Burk double reciprocal plots of Figure 2(F). The B-ring binds a hydrophobic pocket formed by Phe157, Leu176, Phe177, Thr215, Leu218, Ala278 and Phe300, and with 3′-OH hydrogen bonding to Glu276. The 5-OH of A-ring hydrogen bonds to the backbone of Asp349 and 7-OH of the same ring hydrogen bonds to the Phe157 backbone.

Discussion

In this work, we explored a panel of flavonoids, covering a solid set of different structures, tested in the same model, under the same experimental conditions, which enabled us to draw relevant conclusions about the relationship structure *versus* activity.

Many of the studied flavonoids offer a promising alternative for the management of PPHG, presenting an $IC_{50} \leq 200\,\mu M$, much lower than the one found for **acarbose** ($607 \pm 56\,\mu M$), the positive control.

We started our study by testing a flavone without –OH groups (**A1**), which was not able to inhibit α-glucosidase. We also tested flavonoids **A2**, **A3** and **A4**, and all of them showed low or no inhibitory activity. From A group, the most active flavonoid was **A5**, which has a 3-OH in the C-ring and presented an IC_{50} of $54 \pm 3\,\mu M$. The replacement of the –OH groups of the catechol in B-ring by –OMe groups (**A6**) decreased the inhibitory activity of the flavonoid.

The importance of the –OH groups position was also highlighted when A5, with OH groups at 3-position of C-ring and at 3′- and 4′- positions of B-ring, was tested, because the obtained IC_{50} was lower than the one obtained for A5, with –OH groups at 5 position of A-ring and at 3′- and 4′- positions of B-ring.

We followed our rationale of increasing the complexity of the structure, by the addition of a catechol group in the A-ring. The most effective compound was **C7**, studied here for the first time, with an $IC_{50} = 7.6 \pm 0.4\,\mu M$. The presence of two catechol groups distributed in the A and B rings, together with a 3-OH group in the C-ring, seems to be the more favourable structure for the inhibition of the enzyme. In fact, and as it can be seen in Table 1, the other related compounds (**C1**–**C6**) that differ from **C7** by the lack of an –OH group in some positions, have considerable weaker activities. Gao et al.[27] corroborate our results showing that **B1** and **C1** have no activity against α-glucosidase catalytic activity. In the present study, we observed that the addition of a catechol group to the B-ring in both compounds increased their activity, the –OH group in 5-position of the A-ring (**B4**) being better than in 7-position (**C6**) ($IC_{50} = 66 \pm 7\,\mu M$ and $IC_{50} = 95 \pm 7\,\mu M$, respectively). The obtained results also have shown that, as mentioned by Gao and co-workers[27], baicalein has a favourable structure for the intended effect, as observed in the present study for the same flavonoid [**D3** (baicalein)], which presents an IC_{50} of $44 \pm 3\,\mu M$. Nevertheless, and corroborating our results, the activity increased substantially with the hydroxylation at the B-ring. In addition, comparing the results obtained for **C4** and **C5** it is possible to infer that the presence of the –OH group at the 3′-position (**C4**) is more relevant than at the 4′-position (**C5**) of the B-ring, as **C4** is more active than **C5**. In turn, with the basic structure studied by Gao et al.[54] (5,6,7-trihydroxyflavone), only the 4′-hydroxylation of the B-ring enhanced the inhibitory activity of the 5,6,7-trihydroxyflavone. We can also conclude from the obtained results that the addition of hydrophobic and bulky substituents in the flavonoid structure decreases its activity, as it was possible to see in flavonoids that possess –OMe and/or –OBn groups (**C8**–**C13**).

We also tested another group of flavonoids, based on chrysin (**D1**) structure, in the D group. Once again, our results are in agreement with Gao et al.[54], since chrysin had no inhibitory effect against α-glucosidase activity. Hydroxylation at 4′-position of the B-ring of chrysin (**D1**), giving apigenin (**D5**), increased the activity reaching an $IC_{50} = 82 \pm 6\,\mu M$. With this basic structure, the presence of an –OH group at 3′- (**D4**) or 4′- (**D5**) positions of the B-ring seems to be indifferent for the inhibitory activity.

It has been postulated that –OH groups in the B-ring are favourable for the inhibitory activity of the compounds[16,31,32]. Zeng et al.[24] compared the activity of morin and myricetin and concluded that myricetin, that has three –OH groups at the 3′-, 4′- and 5′-positions of the B-ring, was more potent than morin that has only two –OH groups at 2′- and 4′-positions. Comparing **D6** (kaempferol) and **D8** (quercetin) or **D5** (apigenin) and **D7** (luteolin), it is possible to conclude that the presence of the catechol group in the B-ring increased considerably the activity of the flavonoids. Additionally, our results indicate that **D8** (quercetin) is a stronger inhibitor when compared with **D9** (morin). These findings clearly demonstrate that the *ortho* –OH groups might be responsible for the higher inhibitory effect, which seems to promote the interaction between α-glucosidase and flavonoids, while the *meta*-position of –OH groups decreases the electron cloud density of band I resulting in a lower inhibitory activity[24,32]. Comparing the activity of **D8** (quercetin) ($IC_{50} = 15 \pm 3\,\mu M$) and **D7** (luteolin) ($IC_{50} = 46 \pm 6\,\mu M$), we can conclude that the presence of a 3-OH group in the C-ring increases the ability to inhibit α-glucosidase. This result is corroborated by Nicolle et al.[55] and Xu[32] who suggested that the 3-OH in the C-ring may have the ability to make flavonoids bind into the binding pocket of yeast α-glucosidase properly to maintain a high inhibitory activity.

It is currently accepted that modification of any of the –OH groups in the A-ring diminishes the α-glucosidase inhibitory effects of flavonoids[27,56–58]. From the D group analysis, it becomes clear that **D3** (baicalein), which has –OH groups at 5-, 6- and 7-positions of A-ring, is more effective than **D2** (galangin) and **D1** (chrysin), with only –OH groups at 5- and 7-positions. These results are in agreement with Gao et al.[27], that studied parent compounds of baicalein and reported that removal of any –OH group from the 5-, 6- and 7-positions led to a dramatic loss of the inhibitory potency. Moreover, here we concluded that the 5-hydroxylation at the A-ring is important for the intended effect, since the IC_{50} of **D6** (kaempferol) is almost three times lower than the IC_{50} of **C5**. Wang et al.[56] results validate this finding, as compounds that bear one acetyl group at the 5-position of the A-ring of chrysin almost induce the disappearance of the flavonoids' inhibitory activity. It is known that hydrogen bonding is a crucial factor for the interactions between the enzyme and its substrates and

for the conformation and orientation of the inhibitors in the active site[8]. Kumar et al.[57] showed that a 5-OH group of the A-ring acts as a hydrogen bond donor and consequently enhances the inhibitory activity of the flavonoid.

Our results illustrate that the presence of a 3-OH group in the C-ring is also relevant, evidenced by the lowest IC_{50} of **D5** (apigenin) and **D8** (quercetin) when compared with **D6** (kaempferol) and **D7** (luteolin), respectively. Accordingly, Silva et al.[25], also compared the effect of luteolin and quercetin and suggested that 3-hydroxylation of the C-ring increases the inhibitory activity against α-glucosidase. Furthermore, Xu[32] gathered information about the interaction of flavonoids with α-glucosidase, analysed with Autodock, and reported that the 3′,4′-$(OH)_2$ groups of the B-ring together with a 3-OH group in the C-ring are crucial for the inhibitory effect of flavonoids.

In the panel of flavonoids in this work, we tested a series of chlorinated flavonoids (**D10**–**D14**) for the first time. It has been postulated that under diabetic conditions, the inflammatory process is exacerbated and consequently there is an excessive production of reactive species, namely, HOCl[59]. It is currently known the reactivity of flavonoids with HOCl in order to form stable mono and dichlorinated products[36]. Our group has recently shown that chlorinated flavonoids were more efficient than their parent compounds in modulate human neutrophils' activities, foreseeing a potential anti-inflammatory activity[36]. These results raised our attention to these promising compounds, exploring here for the first time, their inhibitory effect against α-glucosidase. The chlorinated flavonoid **D10** was one of the most active compounds tested in this work, presenting an IC_{50} similar to the one obtained for **D8** (quercetin). Moreover, comparing compounds **D10** and **D8** (quercetin) it is possible to conclude that the substitution of a 3-OH group or a 3-Cl atom at the C-ring is almost indifferent for the inhibitory effect. In contrast, the results obtained with **D18** (rutin), reveal that the addition of a larger group, in this case rutinose, at the 3-position of the C-ring, weakens the activity of the flavonoid[16].

Following the order of potency of the chlorinated flavonoids, it is possible to see that the second most effective compound was flavonoid **D14**, with –Cl atoms at 6 and 8 positions of the A-ring. However, when we have only one –Cl atom at 6 (**D11**) or 8 (**D12**) position of the A-ring, the inhibition of the enzyme decreased considerably.

We also tested a group of methoxylated compounds (**D15**–**D17**), and, corroborating the results obtained in A and C groups, the inhibitory effect on α-glucosidase was reduced by the introduction of an –OMe group, independently of the ring. According to the literature, the contribution of –OMe groups to the inhibitory effect of flavonoids depends on the basic structure of the flavonoid and/or with the type of substrate used[60]. Azuma et al.[60] indicated that the α-glucosidase inhibition was enhanced by the presence of 5-OMe groups at the A-ring, and at 3′-, 4′-positions of the B-ring, when compared with quercetin. In turn, Gao et al.[54] reported that, in contrast to –OH, the –OMe group substitution on the B-ring of 5,6,7-trihydroxyflavone was unfavourable for the activity.

It is known that the C2 = C3 double bond of flavonoids is crucial for their anti-inflammatory activity[37,61,62]. Analysing E group and comparing the inhibitory effect with some flavonoids of D group, namely, **D5** (apigenin) with **E1** (naringenin), **D7** (luteolin) with **E2** (eriodictyol), **D8** (quercetin) with **E3** (taxifolin), it is clear that the lack of C2 = C3 double bond weakens the flavonoids activity. This finding is in agreement with other reports about this issue[31,57]. Xiao et al.[15] reported that the C2 = C3 double bond increases the π-conjugation of the bond linking the B and C rings, which favours near-planarity of the two rings. It is known that the molecules with near-planar structure easily enter the hydrophobic pockets in enzymes and subsequently can increase their inhibitory effect.

Once defined the effectiveness of the tested flavonoids, it was our aim to evaluate the type of α-glucosidase inhibition of the most active flavonoids from each group (A–E): **A5**, **B3**, **C7**, **D8** (quercetin) and **E3** (taxifolin). We also analysed the chlorinated flavonoid **D10**, since it was one of the most effective compounds, presenting an IC_{50} value similar to the one found for **D8** (quercetin). Lineweaver–Burk double reciprocal plots were employed to investigate the inhibition kinetics of the tested compounds against α-glucosidase activity. As observed in Figure 2, flavonoids **A5** (Figure 2(A)) and **B3** (Figure 2(B)) presented a mixed inhibition type (K_m value increased and V_{max} value decreased), which means that binding of the substrate or the inhibitor affects their enzyme binding affinity. In the mixed type inhibition, the inhibitor did not bind to the enzyme in the active site and both inhibitor and substrate can simultaneously be attached to the enzyme. However, the binding affinity for the substrate is decreased when the inhibitor is present. Concerning flavonoid **C7**, Figure 2(C) cannot clearly differentiate between a mixed and a competitive inhibition type. However, the interception of lines is close to the *y* axis. Moreover, the result obtained by docking calculations for flavone **C7** suggested that the binding pose prediction was directed to the active site. Considering the *in vitro* and docking studies, the results indicate that **C7** presents a competitive inhibition type. Flavonoid **D8** (quercetin) (Figure 2(D)) and **acarbose** (Figure 2(G)) are also competitive inhibitors, since the K_m value increased and the V_{max} value remained constant. As shown in Figure 2, flavonoids **D10** (Figure 2(E)) and **E3** (taxifolin) (Figure 2(F)) are non-competitive inhibitors (K_m value remained constant and V_{max} value decreased), which means that they can bind with equal affinity to both the free enzyme and the enzyme–substrate complex. In this inhibitory mechanism, the inhibitor binds to the enzyme at a site that is distinct from the substrate binding site (active site of the enzyme). A non-competitive inhibitor binds to an enzyme whether the substrate is at low or high concentrations[63–67]. To the best of our knowledge, this is the first report stating the type of inhibition for the mentioned flavonoids, except for **D8** (quercetin), which was already reported as a mixed type inhibitor[16,31,32].

In what concerns **acarbose**, we verified a competitive inhibition type, as observed by the studies of Kim et al.[68] and Lopez et al.[69]. Interestingly, Son et al.[70] referred that this compound has a mixed type of inhibition.

The K_i values can also be a useful tool to compare the activity of the compounds, being reflective of the binding affinity of the inhibitor for the enzyme. The tested flavonoids presented the following order of Ki values: **C7** < **D8** (quercetin) < **A5** < **D10** < **B3** < **E3** (taxifolin). These results show that flavonoid **C7**, followed by **D8** (quercetin), exhibit the strongest affinity for the enzyme.

Flavones **A5**, **D8** (quercetin) and **C7** share very similar interactions with the active site and mimic interactions found between the first glucose of **acarbose** and the active site pocket. Moreover, the predicted mode of binding can rationalise the trends found across the series of studied flavonoids, namely the importance of 3-hydroxylation in the C-ring and the catechol group in the B-ring. The 3-OH substitution provides a hydrogen bond to Asp349, while the catechol in the B-ring hydrogen bonds Asp68, Asp214 and Glu276. Similarly, the inhibitor **acarbose** presents hydrogen bond interactions with the same active site amino acids.

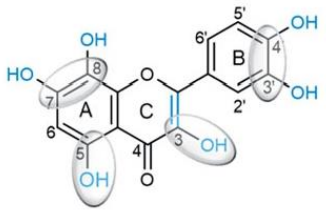


Figure 4. Potential flavonoids 'substitution pattern that contributes to increase the α-glucosidase inhibition.

Conclusions

Our results have shown that adequately substituted flavonoids are effective α-glucosidase inhibitors. The flavonoid structure, the position and number of OH groups are determinant factors for the intended effect. The most active flavonoids were **C7** and **D8** (quercetin), which indicates that hydoxylations at 5- and 7- or 8-positions of the A-ring, at 3′ and 4′-positions of the B-ring and at 3-position of the C-ring, as well as the C2 = C3 double bond in the C-ring, are critical for the inhibitory activity of flavonoids (Figure 4). The results obtained in this study provide a series of potentially effective flavonoids that can be used as alternatives to the commonly administrated α-glucosidase inhibitors in the DM therapeutics.

Disclosure statement

The authors report no conflicts of interest.

Funding

The authors acknowledge the financial support from National funds [Fundação para a Ciência e Tecnologia and Ministério da Educação e Ciência (FCT/MEC)] and European Union funds [Fundo Europeu de Desenvolvimento Regional (FEDER)] under the program PT2020 (PT2020 UID/MULTI/04378/2013 - POCI/01/0145/FEDER/007728), the framework of QREN (NORTE-01-0145-FEDER-000024), and Programa Operacional Competitividade e Internacionalização (COMPETE). Carina Proença acknowledges FCT the financial support for the PhD grant (SFRH/BD/116005/2016), in the ambit of "QREN - POPH - Tipologia 4.1 - Formação Avançada", co-sponsored by Fundo Social Europeu (FSE) and by national funds of Ministério da Ciência, Tecnologia e Ensino Superior (MCTES). Daniela Ribeiro acknowledges FEDER, through COMPETE and FCT, the financial support for the Post-doc grant in the ambit of the project PTDC/QEQ-QAN/1742/2014 - POCI-01-0145-FEDER-016530.

ORCID

Eduarda Fernandes http://orcid.org/0000-0001-6424-0976

References

1. International Diabetes Federation. IDF Diabetes Atlas, 2015. Available from: http://www.diabetesatlas.org/.
2. Salsali A, Nathan M. A review of types 1 and 2 diabetes mellitus and their treatment with insulin. Am J Ther 2006;13:349–61.
3. Wilke T, Boettger B, Berg B, et al. Epidemiology of urinary tract infections in type 2 diabetes mellitus patients: an analysis based on a large sample of 456,586 German T2DM patients. J Diabetes Complicat 2015;29:1015–23.
4. Olokoba AB, Obateru OA, Olokoba LB. Type 2 diabetes mellitus: a review of current trends. Oman Med J 2012;27:269–73.
5. Muller LM, Gorter KJ, Hak E, et al. Increased risk of common infections in patients with type 1 and type 2 diabetes *mellitus*. Clin Infect Dis 2005;41:281–8.
6. Garg SK, Maurer H, Reed K, Selagamsetty R. Diabetes and cancer: two diseases with obesity as a common risk factor. Diabetes Obes Metab 2014;16:97–110.
7. Taylor SI, Accili D, Imai Y. Insulin resistance or insulin deficiency. Which is the primary cause of NIDDM? Diabetes 1994;43:735–40.
8. Cheng N, Yi WB, Wang QQ, et al. Synthesis and α-glucosidase inhibitory activity of chrysin, diosmetin, apigenin, and luteolin derivatives. Chin Chem Lett 2014;25:1094–8.
9. Pereira DF, Cazarolli LH, Lavado C, et al. Effects of flavonoids on α-glucosidase activity: potential targets for glucose homeostasis. Nutrition 2011;27:1161–7.
10. Kawser HM, Abdal DA, Han J, et al. Molecular mechanisms of the anti-obesity and anti-diabetic properties of flavonoids. Int J Mol Sci 2016;17:569–132.
11. Sudhir R, Mohan V. Postprandial hyperglycemia in patients with type 2 diabetes mellitus. Treat Endocrinol 2002;1:105–16.
12. Leiter LA, Ceriello A, Davidson JA, et al. Postprandial glucose regulation: new data and new implications. Clin Ther 2005;27(Suppl B):S42–S56.
13. Ceriello A, Davidson J, Hanefeld M, et al. Postprandial hyperglycaemia and cardiovascular complications of diabetes: an update. Nutr Metab Cardiovasc Dis 2006;16:453–6.
14. Ceriello A, Genovese S. Atherogenicity of postprandial hyperglycemia and lipotoxicity. Rev Endocr Metab Disord 2016;17:111–16.
15. Xiao JB, Hogger P. Dietary polyphenols and type 2 diabetes: current insights and future perspectives. Curr Med Chem 2015;22:23–38.
16. Li YQ, Zhou FC, Gao F, et al. Comparative evaluation of quercetin, isoquercetin and rutin as inhibitors of alpha-glucosidase. J Agric Food Chem 2009;57:11463–8.
17. Zeng L, Zhang G, Liao Y, Gong D. Inhibitory mechanism of morin on α-glucosidase and its anti-glycation properties. Food Funct 2016;7:3953–63.
18. Hakamata W, Kurihara M, Okuda H, et al. Design and screening strategies for alpha-glucosidase inhibitors based on enzymological information. Curr Top Med Chem 2009;9:3–12.
19. Priscilla DH, Roy D, Suresh A, et al. Naringenin inhibits α-glucosidase activity: a promising strategy for the regulation of postprandial hyperglycemia in high fat diet fed streptozotocin induced diabetic rats. Chem Biol Interact 2014;210:77–85.
20. Joshi SR, Standl E, Tong N, et al. Therapeutic potential of α-glucosidase inhibitors in type 2 diabetes *mellitus*: an evidence-based review. Expert Opin Pharmacother 2015;16:1959–81.
21. Derosa G, Maffioli P. α-Glucosidase inhibitors and their use in clinical practice. Arch Med Sci 2012;8:899–906.
22. Lebovitz HE. Alpha-glucosidase inhibitors. Endocrinol Metab Clin North Am 1997;26:539–51.
23. Zhang L, Chen Q, Li L, et al. Alpha-glucosidase inhibitors and hepatotoxicity in type 2 diabetes: a systematic review and meta-analysis. Sci Rep 2016;6:32649–18.

24. Zeng L, Zhang G, Lin S, Gong D. Inhibitory mechanism of apigenin on α-glucosidase and synergy analysis of flavonoids. J Agric Food Chem 2016;64:6939–49.
25. Silva EL, Lobo JF, Vinther JM, et al. High-resolution α-glucosidase inhibition profiling combined with HPLC-HRMS-SPE-NMR for identification of antidiabetic compounds in *Eremanthus crotonoides* (*Asteraceae*). Molecules 2016;21:782.
26. Yan J, Zhang G, Pan J, Wang Y. α-Glucosidase inhibition by luteolin: kinetics, interaction and molecular docking. Int J Biol Macromol 2014;64:213–23.
27. Gao H, Nishioka T, Kawabata J, Kasai T. Structure-activity relationships for alpha-glucosidase inhibition of baicalein, 5,6,7-trihydroxyflavone: the effect of A-ring substitution. Biosci Biotechnol Biochem 2004;68:369–75.
28. Na B, Nguyen PH, Zhao BT, et al. Protein tyrosine phosphatase 1B (PTP1B) inhibitory activity and glucosidase inhibitory activity of compounds isolated from *Agrimonia pilosa*. Pharm Biol 2016;54:474–80.
29. Kim JS, Kwon CS, Son KH. Inhibition of alpha-glucosidase and amylase by luteolin, a flavonoid. Biosci Biotechnol Biochem 2000;64:2458–61.
30. Kang S, Park JY, Choi H, Kim J. α-Glucosidase inhibitory activities of myricetin in animal models of diabetes mellitus. Food Sci Biotechnol 2015;24:1897–900.
31. Tadera K, Minami Y, Takamatsu K, Matsuoka T. Inhibition of alpha-glucosidase and alpha-amylase by flavonoids. J Nutr Sci Vitaminol 2006;52:149–53.
32. Xu H. Inhibition kinetics of flavonoids on yeast α-glucosidase merged with docking simulations. Protein Pept Lett 2010;17:1270–9.
33. Abdullah NH, Salim F, Ahmad R. Chemical constituents of Malaysian *U. cordata* var. *ferruginea* and their *in vitro* α-glucosidase inhibitory activities. Molecules 2016;21:525.
34. Meng Y, Su A, Yuan S, et al. Evaluation of total flavonoids, myricetin, and quercetin from *Hovenia dulcis* Thunb. as inhibitors of alpha-amylase and alpha-glucosidase. Plants Food Hum Nutr 2016;71:444–9.
35. Sousa JLC, Proença C, Freitas M, et al. New polyhydroxylated flavon-3-ols and 3-hydroxy-2-styrylchromones: synthesis and ROS/RNS scavenging activities. Eur J Med Chem 2016;119:250–9.
36. Freitas M, Ribeiro D, Tome SM, et al. Synthesis of chlorinated flavonoids with anti-inflammatory and pro-apoptotic activities in human neutrophils. Eur J Med Chem 2014;86:153–64.
37. Ribeiro D, Freitas M, Tome SM, et al. Modulation of human neutrophils' oxidative burst by flavonoids. Eur J Med Chem 2013;67:280–92.
38. Das D. Biochemistry. 8th ed. Kolkata, India: Academic Publishers, 1993:89–111.
39. Banerjee S. Inhibition of mackerel (*Scomber scombrus*) muscle lipoxygenase by green tea polyphenols. Food Res Int 2006;39:486–91.
40. Nelson DL, Cox MM. Enzyme kinetics as an approach to understanding mechanism. In: Lehninger principles of biochemistry. 6th ed. New York: W. H. Freeman & Co.; 2014:P200–12.
41. Berman HM, Westbrook J, Feng Z, et al. The Protein Data Bank. Nucleic Acids Res 2000;28:235–42.
42. Consortium TU. UniProt: a hub for protein information. Nucleic Acids Res 2015;43:D204–12.
43. Benkert P, Biasini M, Schwede T. Toward the estimation of the absolute quality of individual protein structure models. Bioinformatics 2011;27:343–50.
44. Bietz S, Urbaczek S, Schulz B, Rarey M. Protoss: a holistic approach to predict tautomers and protonation states in protein-ligand complexes. J Cheminform 2014;6:1–12.
45. Case DA, Darden TA, Cheatham TE, et al. AMBER 12. University of California, San Francisco; 2012.
46. Hornak V, Abel R, Okur A, et al. Comparison of multiple Amber force fields and development of improved protein backbone parameters. Proteins 2006;65:712–25.
47. Kirschner KN, Yongye AB, Tschampel SM, et al. GLYCAM06: a generalizable biomolecular force field. Carbohydrates. J Comput Chem 2008;29:622–55.
48. Yamamoto K, Miyake H, Kusunoki M, Osaki S. Steric hindrance by 2 amino acid residues determines the substrate specificity of isomaltase from *Saccharomyces cerevisiae*. J Biosci Bioeng 2011;112:545–50.
49. Trott O, Olson AJ. AutoDock Vina: improving the speed and accuracy of docking with a new scoring function, efficient optimization, and multithreading. J Comput Chem 2010;31:455–61.
50. O'Boyle NM, Morley C, Hutchison GR. Pybel: a Python wrapper for the OpenBabel cheminformatics toolkit. Chem Cent J 2008;2:1–7.
51. Gasteiger J, Marsili M. Iterative partial equalization of orbital electronegativity – a rapid access to atomic charges. Tetrahedron 1980;36:3219–28.
52. Eldridge MD, Murray CW, Auton TR, et al. Empirical scoring functions: I. The development of a fast empirical scoring function to estimate the binding affinity of ligands in receptor complexes. J Comput Aided Mol Des 1997;11:425–45.
53. Jones G, Willett P, Glen RC, et al. Development and validation of a genetic algorithm for flexible docking. J Mol Biol 1997;267:727–48.
54. Gao H, Kawabata J. Importance of the B ring and its substitution on the α-glucosidase inhibitory activity of baicalein, 5,6,7-trihydroxyflavone. Biosci Biotechnol Biochem 2004;68:1858–64.
55. Nicolle E, Souard F, Faure P, Boumendjel A. Flavonoids as promising lead compounds in type 2 diabetes *mellitus*: molecules of interest and structure-activity relationship. Curr Med Chem 2011;18:2661–72.
56. Wang QQ, Cheng N, Yi WB, et al. Synthesis, nitric oxide release, and α-glucosidase inhibition of nitric oxide donating apigenin and chrysin derivatives. Bioorg Med Chem 2014;22:1515–21.
57. Kumar V, Kumar S, Rani P. Pharmacophore modeling and 3D-QSAR studies on flavonoids as α-glucosidase inhibitors. Der Pharma Chem 2010;2:324–35.
58. Gu C, Zhang H, Putri CY, Ng K. Evaluation of α-amylase and α-glucosidase inhibitory activity of flavonoids. Int J Food Nutr Sci 2015;2:1–6.
59. Kaneto H, Katakami N, Matsuhisa M, Matsuoka TA. Role of reactive oxygen species in the progression of type 2 diabetes and atherosclerosis. Mediat Inflamm 2010;2010:1–11.
60. Azuma T, Kayano S, Matsumura Y, et al. Antimutagenic and α-glucosidase inhibitory effects of constituents from *Kaempferia parviflora*. Food Chem 2011;125:471–5.
61. Ribeiro D, Freitas M, Lima JL, Fernandes E. Proinflammatory pathways: the modulation by flavonoids. Med Res Rev 2015;35:877–936.
62. Ribeiro D, Freitas M, Tome SM, et al. Flavonoids inhibit COX-1 and COX-2 enzymes and cytokine/chemokine production in human whole blood. Inflammation 2015;38:858–70.
63. Ault A. An introduction to enzyme kinetics. J Chem Educ 1974;51:381–6.

64. Hüttl R, Frank N. Enzymatic kinetic determinations. In: Encyclopedia of analytical chemistry. New York: John Wiley & Sons, Ltd; 2006.
65. Kakkar T, Pak Y, Mayersohn M. Evaluation of a minimal experimental design for determination of enzyme kinetic parameters and inhibition mechanism. J Pharmacol Exp Ther 2000;293:861–9.
66. Ochs RS. Understanding Enzyme Inhibition. J Chem Educ 2000;77:1453–6.
67. Waldrop GL. A qualitative approach to enzyme inhibition. Biochem Mol Biol Educ 2009;37:11–15.
68. Kim M, Lee S, Lee H, et al. Comparative study of the inhibition of α-glucosidase, α-amylase, and cyclomaltodextrin glucanosyltransferase by acarbose, isoacarbose, and acarviosine–glucose. Arch Biochem Biophys 1999;371:277–83.
69. Lopez D, Cherigo L, Spadafora C, et al. Phytochemical composition, antiparasitic and α-glucosidase inhibition activities from *Pelliciera rhizophorae*. Chem Cent J 2015; 9:1–11.
70. Son HU, Lee SH. Comparison of α-glucosidase inhibition by *Cudrania tricuspidata* according to harvesting time. Biomed Rep 2013;1:624–8.

II.2. Evaluation of a flavonoids library for inhibition of pancreatic α-amylase towards a structure-activity relationship

Version of record from Journal of Enzyme Inhibition and Medicinal Chemistry

Copyright © (2019) with kind permission of Taylor & Francis

"A fixed version of a journal article that has been made available by Taylor & Francis, a publisher by formally and exclusively declaring the article 'published'."

JOURNAL OF ENZYME INHIBITION AND MEDICINAL CHEMISTRY
2019, VOL. 34, NO. 1, 577–588
https://doi.org/10.1080/14756366.2018.1558221

Taylor & Francis
Taylor & Francis Group

RESEARCH PAPER

OPEN ACCESS Check for updates

Evaluation of a flavonoids library for inhibition of pancreatic α-amylase towards a structure–activity relationship

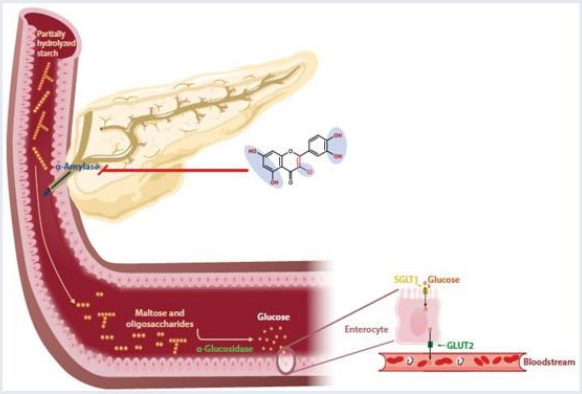
Carina Proença[a], Marisa Freitas[a], Daniela Ribeiro[a], Sara M. Tomé[b], Eduardo F. T. Oliveira[c], Matilde F. Viegas[c], Alberto N. Araújo[a], Maria J. Ramos[c], Artur M. S. Silva[b], Pedro A. Fernandes[c] and Eduarda Fernandes[a]

[a]LAQV, REQUIMTE, Laboratory of Applied Chemistry, Department of Chemical Sciences, Faculty of Pharmacy, University of Porto, Porto, Portugal; [b]Department of Chemistry and QOPNA, University of Aveiro, Aveiro, Portugal; [c]UCIBIO, REQUIMTE, Department of Chemistry and Biochemistry, Faculty of Sciences, University of Porto, Porto, Portugal

ABSTRACT

α-Amylase has been considered an important therapeutic target for the management of type 2 diabetes *mellitus* (T2DM), decreasing postprandial hyperglycaemia (PPHG). In the present work, a panel of 40 structurally related flavonoids was tested, concerning their ability to inhibit α-amylase activity, using a microanalysis screening system, an inhibitory kinetic analysis and molecular docking calculations. From the obtained results, it was possible to observe that the flavone with a -Cl ion at 3-position of C-ring, an –OH group at 3′- and 4′- positions of B-ring and at 5- and 7- positions of A-ring and the C2 = C3 double bond, was the most active tested flavonoid, through competitive inhibition. In conclusion, some of the tested flavonoids have shown promising inhibition of α-amylase and may be considered as possible alternatives to the modulation of T2DM.

GRAPHICAL ABSTRACT



ARTICLE HISTORY
Received 26 September 2018
Revised 4 December 2018
Accepted 6 December 2018

KEYWORDS
α-Amylase inhibition; diabetes; docking; flavonoids; *in vitro*

Introduction

α-1,4-Glucan-4-glucanohydrolases (EC 3.2.1.1.), belonging to the family 13 of glycoside hydrolases (GH) and found in saliva and pancreatic juice, are known by the common name of α-amylase[1,2]. Both are isozymes expressed respectively from genes AMY1 and AMY2 and are composed of 496 amino acid residues in a single polypeptide chain, presenting a 97% identity of the amino acids sequence and a 92% similarity of the residues in the catalytic domains[3–5]. They have three different domains (A, B and C) and a common calcium-binding site that stabilizes the interface between the central A domain and the variable B domain[6,7]. The catalytic triad (Asp, Asp, Glu) is present in the A domain and the active site is located in a long cleft between the carboxyl end of both A and B domains. The C domain consists of a β-sheet structure linked to the A domain by a simple polypeptide chain[5].

CONTACT Eduarda Fernandes egracas@ff.up.pt LAQV, REQUIMTE, Laboratory of Applied Chemistry, Department of Chemical Sciences, Faculty of Pharmacy, University of Porto, Rua de Jorge Viterbo Ferreira no. 228, 4050-313 Porto, Portugal; Pedro A. Fernandes pafernan@fc.up.pt UCIBIO, REQUIMTE, Department of Chemistry and Biochemistry, Rua do Campo Alegre, w/n, 4169-007 Porto, Portugal

Supplemental data for this article can be accessed here.

© 2019 The Author(s). Published by Informa UK Limited, trading as Taylor & Francis Group.
This is an Open Access article distributed under the terms of the Creative Commons Attribution License (http://creativecommons.org/licenses/by/4.0/), which permits unrestricted use, distribution, and reproduction in any medium, provided the original work is properly cited.

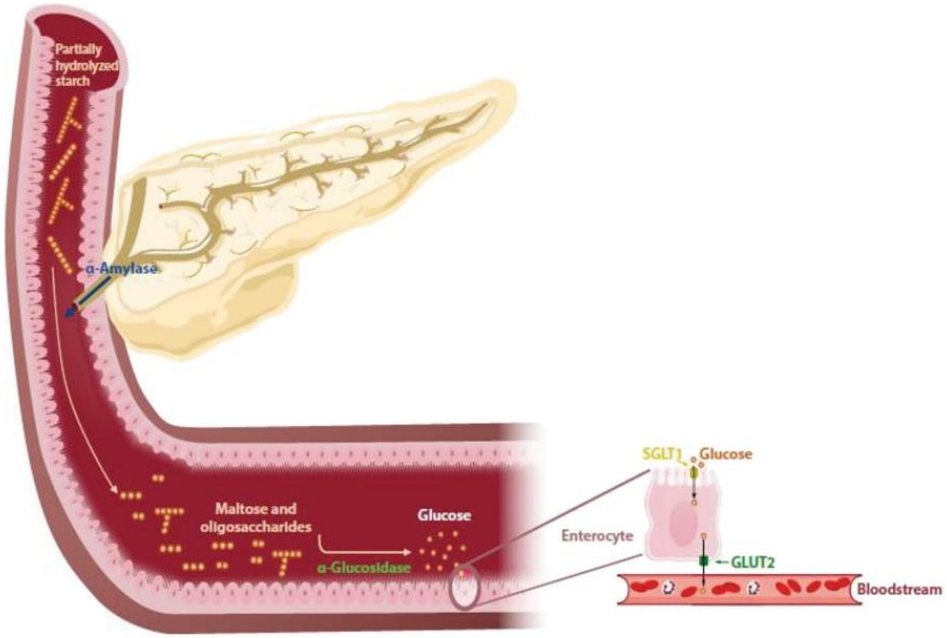


Figure 1. Schematic representation of the pancreatic α-amylase and α-glucosidase activity. After a meal, α-amylase synthesized in pancreas and released in the duodenum, catalyzes the hydrolysis of α-1,4 glycosidic linkages in partially hydrolyzed starch (amylopectin and amylose). From this reaction, intermediate unbranched, such as maltose and maltotriose, and branched (α-limit dextrins) oligosaccharides are formed. α-Glucosidase present in the brush border of the intestinal epithelium (enterocytes) is responsible for the final step of carbohydrates digestion, prior to their absorption. This enzyme converts the disaccharides and oligosaccharides into glucose, which is then transported by sodium/glucose co-transporter 1 (SGLT1) from the intestinal lumen to the cytosol of enterocytes. In turn, glucose transporter 2 (GLUT2), found in the basolateral membrane of enterocytes, transports glucose from cytosol to blood via facilitated diffusion.

α-Amylase catalyzes the initial hydrolysis of starch and other carbohydrate polymers into shorter oligosaccharides through cleavage of α-1,4- bonds[5,7,8]. The salivary isozyme provides an initial partial cleavage into shorter oligomers (10–30%)[7]. Once these partially digested saccharides reach the gut, they are extensively hydrolyzed by the α-amylase synthesized in the pancreas and excreted in the lumen into smaller oligosaccharides, such as maltose, maltotriose and α-limit dextrins (Figure 1)[3]. These sugars are finally broken down into glucose by the intestinal brush border α-glucosidases, which is in turn absorbed from the intestinal mucosa into the portal blood, by means of the glucose transporter (GLUT2) and sodium-glucose co-transporter 1 (SGLT1), leading to postprandial hyperglycaemia (PPHG)[2]. Impaired regulation of PPHG constitutes a common feature in type 2 diabetes *mellitus* (T2DM), the most prevalent form of diabetes, accounting for about 90% of all diabetes cases[2,9,10].

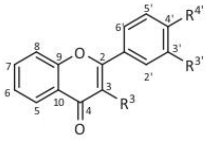
The pancreatic α-amylase activity has been targeted for inhibition by means of the so-called starch blockers in order to mitigate PPHG[1,3]. Acarbose is the most widely prescribed α-amylase inhibitor, and in spite of its efficiency in the control of PPHG, the administration of this drug is associated with gastrointestinal adverse effects in diabetic patients, namely abdominal distention, flatulence and diarrhoea[11]. Thus, the search and development of new effective and safer agents, able to control glucose levels is of high importance for the management of T2DM[12].

In the last few years, the activity of flavonoids has been studied even up to clinical trials concerning the modulation of diabetes in humans[13,14]. Promising inhibitory potential against important targets related with the T2DM pathophysiology was evidenced regarding the inhibition of isolated enzymes such as α-glucosidase[15] and protein tyrosine phosphatase 1B (PTP1B)[16]. Some bibliographic reviews compile the obtained results of the antidiabetic activity of flavonoids[17–20]. Further isolated studies also describe flavonoids as α-amylase inhibitors, such as apigenin[21,22], luteolin[21,23], kaempferol[21,22], naringenin[21], quercetin[21,22,24,25], myricetin[21,22,25], chrysin[22] and baicalein[21,22]. Nevertheless, significant differences in the experimental conditions among studies, such as the source and concentrations of enzyme and substrate and the different incubation times applied, turn difficult the establishment of a reliable structure-activity relationship. To fill this gap, a panel of 40 structurally related flavonoids (Figure 2), most of them studied for the first time, was assessed regarding their inhibitory activity against α-amylase. This study comprehends an *in vitro* microanalysis screening system, modelling of kinetics inhibition and an *in silico* molecular docking analysis.

Materials and methods

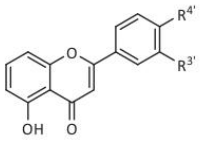
Chemicals

α-Amylase from porcine pancreas, 2-chloro-4-nitrophenyl-α-D-maltotrioside (CNPG3), **acarbose**, DMSO, $NaHPO_4$, Na_2HPO_4, flavonoids **D3** (baicalein), **D4** (apigenin), **D6** (kaempferol), **D7** (luteolin), **D8** (quercetin), **D9** (myricetin), **D10** (morin), **D17** (acacetin), **D19** (rutin), **E1** (naringenin), **E2** (eriodictyol) and **E3** (taxifolin) were obtained from Sigma-Aldrich Co. LLC (St. Louis, MO). The following flavonoids were obtained from Indofine Chemical Company, Inc. (Hillsborough, NJ): **A1**, **A2**, **A3**, **A4**, **A5**, **A6**, **B1**, **B2**, **B3**, **B4**, **C1**, **C2**, **C3**, **C4**, **C5**, **C6**, **C7**, **C8**, **D1** (chrysin), **D2** (galangin) and **D5**. The



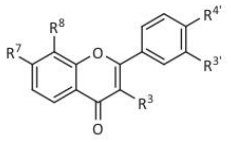
A1-6

A1: R^3= $R^{3'}$= $R^{4'}$= H (Flavone)
A2: R^3= H, $R^{3'}$= OH, $R^{4'}$= H
A3: R^3= $R^{3'}$= H, $R^{4'}$= OH
A4: R^3= H, $R^{3'}$= $R^{4'}$= OH
A5: R^3= $R^{3'}$= $R^{4'}$= OH
A6: R^3= OH, $R^{3'}$= $R^{4'}$= OMe



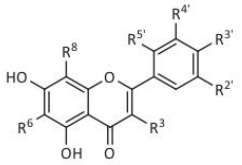
B1-4

B1: $R^{3'}$= $R^{4'}$= H
B2: $R^{3'}$= OH, $R^{4'}$= H
B3: $R^{3'}$= H, $R^{4'}$= OH
B4: $R^{3'}$= $R^{4'}$= OH



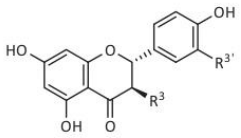
C1-8

C1: R^3= $R^{3'}$= $R^{4'}$= H, R^7= OH, R^8= H
C2: R^3= H, $R^{3'}$= OH, $R^{4'}$= H, R^7= OH, R^8= H
C3: R^3= $R^{3'}$= H, $R^{4'}$= R^7= OH, R^8= H
C4: R^3= $R^{3'}$= OH, $R^{4'}$= H, R^7= OH, R^8= H
C5: R^3= OH, $R^{3'}$= H, $R^{4'}$= R^7= OH, R^8= H
C6: R^3= H, $R^{3'}$= $R^{4'}$= R^7= OH, R^8= H
C7: R^3= OH, $R^{3'}$= OMe, $R^{4'}$= H, R^7= OMe, R^8= H
C8: R^3= OH, $R^{3'}$= H, $R^{4'}$= R^7= OMe, R^8= H



D1-19

D1: $R^{2'}$= R^3= $R^{3'}$= $R^{4'}$= $R^{5'}$= R^6= R^8= H (Chrysin)
D2: $R^{2'}$= H, R^3= OH, $R^{3'}$= $R^{4'}$= $R^{5'}$= R^6= R^8= H (Galangin)
D3: $R^{2'}$= R^3= $R^{3'}$= $R^{4'}$= H, $R^{5'}$= R^6= OH, R^8= H (Baicalein)
D4: $R^{2'}$= R^3= H, $R^{3'}$= OH, $R^{4'}$= $R^{5'}$= R^6= R^8= H
D5: $R^{2'}$= R^3= $R^{3'}$= H, $R^{4'}$= OH, $R^{5'}$= R^6= R^8= H (Apigenin)
D6: $R^{2'}$= H, R^3= OH, $R^{3'}$= H, $R^{4'}$= OH, $R^{5'}$= R^6= R^8= H (Kaempferol)
D7: $R^{2'}$= R^3= H, $R^{3'}$= $R^{4'}$= OH, $R^{5'}$= R^6= R^8= H (Luteolin)
D8: $R^{2'}$= H, R^3= $R^{3'}$= $R^{4'}$= OH, $R^{5'}$= R^6= R^8= H (Quercetin)
D9: $R^{2'}$= R^3= OH, $R^{3'}$= H, $R^{4'}$= OH, $R^{5'}$= R^6= R^8= H (Morin)
D10: $R^{2'}$= H, R^3= Cl, $R^{3'}$= $R^{4'}$= OH, $R^{5'}$= R^6= R^8= H
D11: $R^{2'}$= R^3= H, $R^{3'}$= $R^{4'}$= OH, $R^{5'}$= H, R^6= Cl, R^8= H
D12: $R^{2'}$= R^3= H, $R^{3'}$= $R^{4'}$= OH, $R^{5'}$= R^6= H, R^8= Cl
D13: $R^{2'}$= H, R^3= Cl, $R^{3'}$= $R^{4'}$= OH, $R^{5'}$= R^6= H, R^8= Cl
D14: $R^{2'}$= R^3= H, $R^{3'}$= $R^{4'}$= OH, $R^{5'}$= H, R^6= R^8= Cl
D15: $R^{2'}$= R^3= H, $R^{3'}$= OMe, $R^{4'}$= OH, $R^{5'}$= R^6= R^8= H (Chrysoeriol)
D16: $R^{2'}$= R^3= $R^{3'}$= H, $R^{4'}$= OMe, $R^{5'}$= R^6= R^8= H (Acacetin)
D17: $R^{2'}$= R^3= $R^{3'}$= H, $R^{4'}$= OH, $R^{5'}$= H, R^6= OMe, $R^{8'}$= H (Hispidulin)
D18: $R^{2'}$= R^3= H, $R^{3'}$= $R^{4'}$= OMe, $R^{5'}$= R^6= R^8= H
D19: $R^{2'}$= H, R^3= rutinose, $R^{3'}$= $R^{4'}$= OH, $R^{5'}$= R^6= R^8= H (Rutin)



E1-3

E1: R^3= $R^{3'}$= H (Naringenin)
E2: R^3= H, $R^{3'}$= OH (Eriodictyol)
E3: R^3= $R^{3'}$= OH (Taxifolin)

Figure 2. Chemical structures of the studied flavonoids.

flavonoids **D11**, **D12**, **D13**, **D14**, **D15, D16**and **D18** were synthesized according to previous companion papers[26,27].

In vitro *pancreatic α-amylase inhibition assay*

The evaluation of inhibitory effect on α-amylase activity was based on the method described by Trinh et al.[28], with slight modifications. In each assay, the α-amylase mediated hydrolysis of the substrate CNPG3 into 2-chloro-nitrophenol (CNP), 2-chloro-4-nitrophenyl-α-D-maltoside (CNPG2), maltotriose and glucose was monitored. The initial rate of CNP generation, measured spectrophotometrically at 405 nm, is proportional to the concentration of α-amylase present. In brief, in a 96-well plate, the enzyme (0.2 U/mL), dissolved in 20 mM phosphate buffer (20 mM Na_2HPO_4

and 7 mM NaCl, pH 6.8) was exposed to the flavonoids under study (0–200 μM), dissolved in DMSO [final concentration of DMSO of 4.5% (*v/v*)]. After an incubation time of 10 min, at 37 °C, the reaction was started by the addition of CNPG3 (0.5 mM), dissolved in 20 mM phosphate buffer (pH 6.8) and monitored along 30 min, at 37 °C, in a microplate reader (Synergy HT, BIO-TEK), with the wavelength set to 405 nm. The concentration of α-amylase and the tested flavonoids was determined before the addition of the substrate. Increasing absorbance values obtained within the 5 to 30 min interval (slope) served for the calculation of catalytic rates and the results in the form of inhibition percentages, representing at least three independent experiments. **Acarbose** (0–16 μM) was used as positive control. The amount of DMSO used did not interfere with the assay. The results of the *in vitro* inhibitory activity of flavonoids against the pancreatic α-amylase activity are expressed as mean ± standard error of mean (SEM). Statistical comparison between the active flavonoids was estimated by applying the one-way analysis of variance (ANOVA). Differences were considered to be significant at p values lower than 0.05. All the statistical analysis were performed using GraphPad Prism™ (version 7.0; GraphPad Software).

Inhibitory kinetics of α-amylase

The estimation of kinetic parameters and prediction of the actual mechanism of inhibition was performed by means of Microsoft Office Excel™ spreadsheets and using the Solver supplement add-in, according to Bezerra et al.[29] and Dias et al.[30]. Therefore, the kinetics of conversion of CNPG3 by α-amylase in each microplate well was fitted by nonlinear least squares regression[31] using the general model for enzymatic reactions translated by the Equation (1), and each one of its simplifications regarding the different types of inhibition:

$$v_{inic} = \frac{V_{máx}(S)}{K_m\left(1+\frac{I}{K_{ic}}\right)+(S)\left(1+\frac{I}{K_{iu}}\right)} \quad (1)$$

where v_{inic} and V_{max} represent respectively the initial velocity of formation of absorbing CNP in μmol/min and the maximum achievable velocity when for the 0.2 U/mL of enzyme used all catalytic sites are saturated by the substrate, S is the CNPG3 concentration in mM, K_m is the Michaelis–Menten constant in mM and K_{ic}, K_{iu} are the constants for competitive and uncompetitive inhibition processes expressed in μM^{-1}.

To study the enzyme kinetics, nonlinear regression was applied to the nontransformed data for the most active flavonoids of each group: **B4** (0–200 μM), **C5** (0–100 μM), **D11** (0–100 μM) and **acarbose** (0–2 μM). For each concentration of inhibitor, three concentrations of the substrate CNPG3 were tested: 0.25, 0.5 and 1 mM. The obtained results represent at least three independent experiments.

For each tested condition, the best guesses for equation parameters were thrown by Solver tool after iterative minimization of the sum of squared residuals between the experimental values of V_{max} and the corresponding counterparts estimated according to each model used. Hence, the values obtained for the parameters of the simplest model (without inhibition) were used as initial values, proceeding to competitive inhibition, noncompetitive inhibition, uncompetitive inhibition and finishing with the more complex model, mixed inhibition. The actual mechanism of inhibition was established after comparison and discrimination between the models with a different number of parameters applying the extra sum-of-square F test[32] and the Akaike information criterion (AIC) test[33].

The jackknife procedure was applied to determinate the error of the kinetic constant values. It consisted of the calculation of standard deviation of all estimates guessed by Solver when each experimental data point was in turn drawn from the initial set[34].

Molecular docking analysis

Seventeen entries in the Protein Data Bank (PDB) correspond to *Sus Scrofa* α-amylase (E.C. 3.2.1.1.). From these, it was chosen the PDB entry 1HX0[35] corresponding to the highest resolution X-ray structure (1.38). This structure was co-crystalized with a trisaccharide inhibitor K2, derived from acarbose after α-amylase cleaved one glucose unit at the reducing end. The crystal structure shown two α-1,4-linked K2 molecules, condensed *in situ*. The K2 unit bound at the active site was used to compare the binding mode of the tested flavonoids and as a template to model the substrate for receptor minimization and conformational sampling.

The protonation states of the enzyme were predicted using the Protoss server[36]. Accordingly, Glu233 and Glu390 were modelled in the neutral form and His101, His201 and His215 were modelled in the positively charged for, with both side chain nitrogen atoms protonated. All other residues were protonated according to their p*K*a, at pH = 7.

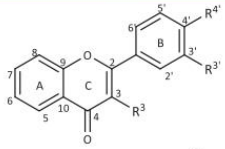
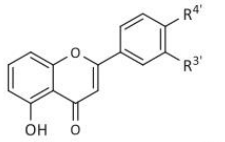
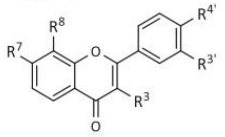
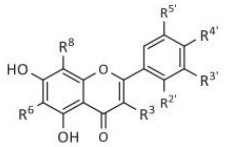
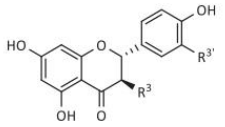
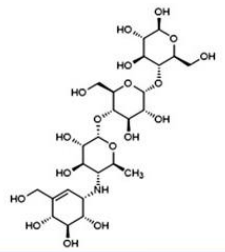
From the hexasaccharide compound present in 1HXO (resultant of two α-1,4-linked K2 molecules), the substrate maltohexose was modelled. On this system, Molecular Mechanics minimization was performed, followed by 20 ns of classical molecular dynamics (MD) simulation to sample receptor conformations. This protocol was performed within the AMBER 12 suite[37] using the ff99SB[38] force field for the protein and GLYCAM06[39] force field for maltohexose. Further details for the energy minimization and MD simulation can be found in Supporting Information.

To choose and validate the conformation of the receptor for the docking protocol several receptor conformations were evaluated: the X-ray conformation, the conformation of the receptor minimized with maltohexose and four representative conformations of the clustered MD simulation. The suitability of each conformation was assessed by evaluating if the docking of the inhibitor acarbose in the active site reproduced the X-ray conformation and how well the ranking of the tested flavonoids with the lowest IC_{50} was reproduced. The conformation of the receptor with the best performance was obtained after 3.3 ns of simulation.

The binding mode of the selected flavonoids was predicted by means of the AutoDock Vina[40]. The binding poses were generated using default parameters (see Supporting Information for details), such as the exhaustiveness of the global search (8) or the maximum number of output poses (9). The search space was confined to a box of 19 Å × 12 Å × 17 Å centered on the site occupied by the glycosidic oxygen between the –1 and –2 glucose units of maltohexose. The receptor was treated as a rigid body and prepared using openbabel[41] for atom-typing and charge assignment using Gasteiger–Marsili charges[42]. The atom-types and charges for the tested flavonoids were attributed the same way.

Subsequently, the poses predicted by AutoDock Vina for each flavonoid were scored using the scoring function GoldScore within the GOLD software suite[43], using the standard parameters for a "Rescoring Run" with local optimization.

Table 1. Inhibitory activity of flavonoids against porcine pancreatic α-amylase (IC_{50}, μM ± SEM).

Compound	Structure	$R^{2\prime}$	R^3	$R^{3\prime}$	$R^{4\prime}$	$R^{5\prime}$	R^6	R^7	R^8	IC_{50} (μM) or Inhibition (%)
A1 (Flavone)		–	H	H	H	–	–	–	–	<20%^{200} μM*
A2		–	H	OH	H	–	–	–	–	<20%^{200} μM*
A3		–	H	H	OH	–	–	–	–	<20%^{200} μM*
A4		–	H	OH	OH	–	–	–	–	46 ± 2%^{200} μM*
A5		–	OH	OH	OH	–	–	–	–	31 ± 3%^{200} μM*
A6		–	OH	OMe	OMe	–	–	–	–	<20%^{200} μM*
B1		–	–	H	H	–	–	–	–	<2%^{200} μM*
B2		–	–	OH	H	–	–	–	–	<20%^{200} μM*
B3		–	–	H	OH	–	–	–	–	<20%^{200} μM*
B4		–	–	OH	OH	–	–	–	–	148 ± 5 μM$^{(a,h)}$
C1		–	H	H	H	–	–	OH	H	<20%^{200} μM*
C2		–	H	OH	H	–	–	OH	H	28 ± 3%^{200} μM*
C3		–	H	H	OH	–	–	OH	H	36 ± 3%^{200} μM*
C4		–	OH	OH	H	–	–	OH	H	34 ± 3%^{200} μM*
C5		–	OH	H	OH	–	–	OH	H	59 ± 4 μM$^{(b,c)}$
C6		–	H	OH	OH	–	–	OH	H	131 ± 1 μM$^{(a,d)}$
C7		–	OH	OMe	H	–	–	OMe	H	< 20 %^{200} μM*
C8		–	OH	H	OMe	–	–	OMe	H	< 20%^{100} μM*
D1 (Chrysin)		H	H	H	H	H	H	–	H	22 ± 3%^{200} μM*
D2 (Galangin)		H	OH	H	H	H	H	–	H	< 20%^{200} μM*
D3 (Baicalein)		H	H	H	H	H	OH	–	H	< 20 %^{200} μM*
D4		H	H	OH	H	H	H	–	H	≈ 200 μM$^{(e)}$
D5 (Apigenin)		H	H	H	OH	H	H	–	H	122 ± 7 μM$^{(a,f)}$
D6 (Kaempferol)		H	OH	H	OH	H	H	–	H	118 ± 7 μM$^{(a,f)}$
D7 (Luteolin)		H	H	OH	OH	H	H	–	H	78 ± 3 μM$^{(b,g)}$
D8 (Quercetin)		H	OH	OH	OH	H	H	–	H	138 ± 5 μM$^{(a)}$
D9 (Myricetin)		H	OH	OH	OH	OH	H	–	H	107 ± 6 μM$^{(d,f)}$
D10 (Morin)		OH	OH	H	OH	H	H	–	H	23 ± 1 %^{200} μM*
D11		H	Cl	OH	OH	H	H	–	H	44 ± 3 μM$^{(c)}$
D12		H	H	OH	OH	H	Cl	–	H	≈ 200 μM$^{(e)}$
D13		H	H	OH	OH	H	H	–	Cl	173 ± 5 μM$^{(e,h)}$
D14		H	Cl	OH	OH	H	H	–	Cl	82 ± 4 μM$^{(g)}$
D15		H	H	OH	OH	H	Cl	–	Cl	98 ± 3 μM$^{(f)}$
D16 (Chrysoeriol)		H	H	OMe	OH	H	H	–	H	192 ± 7 μM$^{(e)}$
D17 (Acacetin)		H	H	H	OMe	H	H	–	H	<20%^{200} μM*
D18		H	H	OMe	OMe	H	H	–	H	33 ± 3 %^{200} μM*
D19 (Rutin)		H	Rutinose	OH	OH	H	H	–	H	<20%^{200} μM*
E1 (Naringenin)		–	H	H	–	–	–	–	–	<20%^{200} μM*
E2 (Eriodictyol)		–	H	OH	–	–	–	–	–	<20%^{200} μM*
E3 (Taxifolin)		–	OH	OH	–	–	–	–	–	<20%^{200} μM*
Positive control: Acarbose		–	–	–	–	–	–	–	–	1.3 ± 0.2 μM$^{(i)}$

*Inhibition (mean, % ± SEM) at the highest tested concentration (in superscript), at the assay conditions.
The IC_{50} with different lowercase superscript letters are significantly different from each other ($p < 0.05$).

Results

In vitro pancreatic α-amylase inhibition assay

The tested flavonoids were divided into five groups (A–E), according to their substitution pattern. The substitution pattern of flavonoids from the A group differs at 3-position of the C-ring and at 3′- and 4′-positions of the B-ring; flavones from B group have an –OH group at 5-position of the A-ring and different substitutions at 3′- and 4′-positions of the B-ring; flavonoids from C group show –OH, –OMe and/or –OBn groups at 3-position of the C-ring, at 3′- and 4′-positions of the B-ring and at 7- and 8-position of the A-ring; flavonoids from D group present –OH substitutions at 5- and 7- positions of the A-ring and also present –OH, –OMe and/or –Cl substitutions at 3-position of the C-ring, at 2′-, 3′-, 4′- and 5′-positions of the B-ring and at 6- and 8-positions of the A-ring; flavanones from E group have –OH groups at 5- and 7-positions of the A-ring and their substitution pattern differs in the presence or absence of –OH groups at 3′- and 4′-positions of the B-ring (Table 1).

No relevant inhibitory activities were observed, up to the highest tested concentration (200 μM), for the flavones belonging to A group with different substitutions in 3-position of C-ring and in 3′- and 4′-positions of B-ring.

For flavones of B group, with an –OH group at 5-position of A-ring and different substitutions in 3′- and 4′-positions of B-ring, the most effective was **B4,** presenting an IC_{50} value of 148 ± 5 μM. This result demonstrates that the presence of the catechol group at B-ring translated in a relatively slight increase of the inhibitory effect over α-amylase catalysis when compared to the other flavones of this group. The presence of an –OH group at 5-position of A-ring also seems to contribute to such effect, since flavone **B4** was more active than flavone **A4** (also with 3′- and 4′–OH in B-ring, but without 5–OH in A-ring).

From C group, which includes flavonoids with different substitutions at 3-position of C-ring, at 3′ and 4′ positions of B-ring and at 7 and 8 positions of A-ring, the most active flavonoid was compound **C5**, tested here for the first time, with an IC_{50} value of 59 ± 4 μM. It seems that the presence of –OH groups at 3-position of C-ring, at 4′-position of B-ring and at 7-position of A-ring, is accompanied by a significant inhibitory effect on α-amylase. On the other hand, the presence of -OMe groups in the flavonoid scaffold (**C7**, **C8**) did not bring any advantage for the intended effect, since the initial conversion rates of the CNPG3 substrates remained unchanged even for the highest tested concentration (200 μM).

All members of D group have –OH groups at 5- and 7-positions of A-ring and the substitution pattern varies according to the presence or absence of –Cl ions, –OH and –OMe groups in their structure. The most effective flavonoid found was the chlorinated flavone **D11**, with an IC_{50} value of 44 ± 3 μM. Thus, the presence of a –Cl ion at 3-position of C-ring, as well as the presence of a catechol in B-ring and –OH groups at 5- and 7-positions of A-ring, showed to be crucial for the inhibition of α-amylase activity. Comparing flavonoid **D11** with **D8** (quercetin) (IC_{50}= 138 ± 5 μM), it is clear that the substitution of the Cl- ion for an OH-group at 3-position of C-ring results in a significant decrease of the corresponding inhibitory activity. It was also observed that the presence of a -OMe group at 3′- position of B-ring [**D16** (chrysoeriol)] slightly improves the ability to inhibit α-amylase activity (IC_{50}= 192 ± 7 μM), comparing with **D17** (acacetin), which presents a -OMe group at 4′-position of B-ring. An increase of the number of -OMe groups in the structure of flavonoids is not favourable for the intended effect, as it can be concluded from a comparison of **D16** (chrysoeriol) with **D18**, the later with an extra -OMe group at 4′-position of B-ring. A glycosylated flavonoid, **D19** (rutin), was also tested, but no activity was found up to the highest tested concentration (200 μM).

Table 2. Type of inhibition and V_{max}, K_m, K_{ic}, and K_{iu} values ± SD (μM) for the inhibition of α-amylase by the selected flavonoids.

Compound	Type of inhibition	V_{max} (μmol/min)	K_m (mM)	K_{ic} (μM)	K_{iu} (μM)
B4	Competitive	12.0 ± 0.6	1.2 ± 0.1	132 ± 15	–
C5	Competitive	10.5 ± 0.9	1.0 ± 0.1	71 ± 7	–
D11	Competitive	15 ± 4	1.1 ± 0.4	21 ± 3	–
Positive control:					
Acarbose	Mixed	12.0 ± 0.9	0.9 ± 0.1	6 ± 3	0.71 ± 0.09

The studied flavanones of E group, **E1** (naringenin), **E2** (eriodictyol) and **E3** (taxifolin) were not able to inhibit α-amylase activity, at the maximum tested concentration (200 μM). These results demonstrate that the presence of C2 = C3 double bond is very relevant for the intended effect.

Inhibitory kinetics of α-amylase

In accordance with the described results, the most effective flavonoids of B, C and D groups, **B4**, **C5** and **D11**, respectively, and the positive control, **acarbose**, were henceforth selected for their type of inhibition calculation. No flavonoids from A and E group were tested, due to their lack of inhibitory activity.

By comparing the sum of the square errors values among the different enzyme inhibition models and, for models with different number of parameters, applying the extra sum-of-square *F* test and the AIC test, it was possible to select the best model (without inhibition, competitive inhibition, noncompetitive inhibition, uncompetitive inhibition or mixed inhibition). In that sense, the model with the lowest sum of the square error value corresponds to the best kinetic model. The comparison between models with a different number of parameters can be done by comparing the extra sum-of-square *F* test, at the desired level of probability (f 0.95): if the $-f$ value is superior to 0, the more complex model should be applied. The Akaike test was also used to discriminate the different enzyme inhibition models, with a different number of parameters: the model with the lower corrected AIC (AIC_c) score is the model more likely to be correct.

By the obtained results, it was possible to conclude that **acarbose** [see Supporting Information, Figures 1(S)–5(S)] is a mixed-type inhibitor, and flavonoids **B4** [see Supporting Information, Figures 6(S)–10(S)], **C5** [see Supporting Information, Figures 11(S)–15(S)] and **D11** are competitive inhibitors [see Supporting Information, Figures 16(S)–20(S)].

After the definition of the best model, it was possible to summarize the kinetic constants values (V_{max}, K_m, K_{ic} and/or K_{iu}) (Table 2). The tested compounds presented the following order of K_{ic} values: **B4**>**C5**>**D11**>**acarbose**.

Molecular docking analysis

Binding mode of the selected inhibitors

Once evidenced the inhibition mechanism through experimental data and calculations using Solver supplement of Microsoft Excel Office™, it was predicted the binding pose of flavonoids within the active site of α-amylase. Special attention is given to **B4**, **C5** and **D11** derivatives, the ones exhibiting a higher inhibitory effect in their groups.

The binding pocket of α-amylase is usually divided in –1 to N subpockets, each one creating a particular environment around each sugar ring. The innermost subpocket is numbered as –1

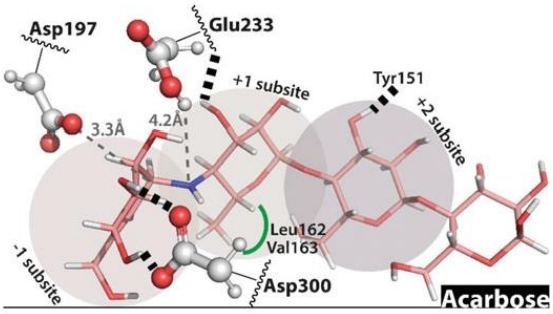


Figure 3. Predicted binding mode for **acarbose**. Hydrogen bonds are represented by dashed lines and hydrophobic interactions by green lines. The distances between the catalytic residues Asp197 and Glu233 and the anomeric carbon/N-glycosidic bond are represented by dashed gray lines.

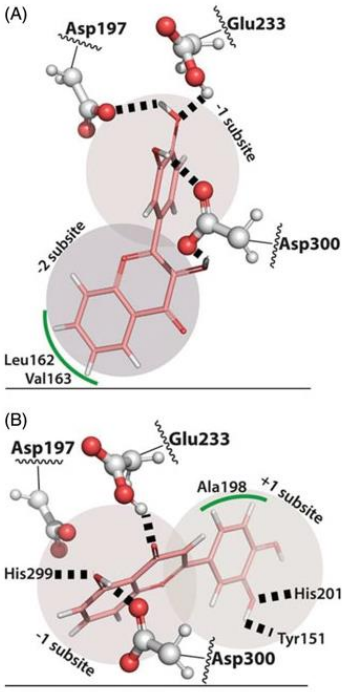


Figure 4. (A) Predicted binding mode of flavonoid **A5**, occupying the –2 and –1 subsites with the more hydrophobic A-ring on the –2 subsite interacting with Leu162 and Val163. (B) The predicted binding mode for **B4** shows the C-ring carbonyl and A-ring hydroxyl hydrogen bonded to the catalytic residues Glu233, Asp300 and His299.

subpocket and is immediately followed the +1 subpocket while the glycosidic bond to be cleaved stays positioned in-between the sugars and also in-between the –1 and +1 subpockets. The next subpockets are numbered +2, +3, etc. An even deeper subpocket (–2) can be occupied by inhibitors, but generally not by natural substrates.

We started by evaluating the accuracy of our Molecular Docking Protocol. For this purpose, we performed a docking assay using the crystal structure of alpha-amylase complexed with acarbose (*Bacillus subtilis,* PDB structure 1UA7, and resolution 2.21 Å). We deleted the acarbose hexasaccharide from the 1UA7 PDB file and re-docked it into the active site, following the protocol described in the methods, using the same parameters, except for the size of the box (which was, in this case, 21.75 × 22.50 × 22.50 Å). The top-ranking solution of the docking assay displayed a very similar pose to that of acarbose in the crystallographic structure [see Supporting Information, Figure 21(S)]. Root mean square deviation (RMSD) analysis of the heavy atoms in the docking solution concurs with visual inspection, with a very low heavy-atom RMSD value of 0.482 Å, confirming that the used protocol has significant predictive power.

The study started with the prediction of the binding mode of acarbose, which in the chosen receptor perfectly reproduces the binding interactions of the substrate maltohexose seen in the MD simulation (Figure 3). This was expected, as it was a condition that we imposed to choose the receptor conformation for the docking calculations. The hydroxymethyl conduritol ring of acarbose accommodates to the acarviosine moiety bound to the –1 and +1 subpockets while the two farthest glucose units extend from the +2 subpocket to onwards. In such conformation, this non-hydrolyzable *N*-glycosidic bond stays moderately distant from the general acid Glu233 (4.2 Å), but the nucleophilic Asp197 is only at 3.3 Å from the anomeric carbon, Asp300 is hydrogen bonded to the 2-hydroxyl and 3-hydroxyl groups of the glucose unit of the –1 subpocket. An additional hydrogen bond is established between the hydroxymethyl group and Asp197.

The most relevant interaction between the glucose unit in the +1 subpocket and the receptor seems to be the hydrophobic interaction between its methyl group and a hydrophobic pocket formed by Leu162 and Val163, and a hydrogen bond between the 3–OH and the backbone of Glu233. For the glucose unit at the +2 subpocket, the most relevant interaction seems to be a hydrogen bond between the 3–OH group and the side-chain of Tyr151. The glucose unit at the +3 subpocket is completely exposed to the solvent and does not interact meaningfully with the receptor.

Among flavonoids from A group, which carry substitutions at the 3-position of C-ring and at 3′- and 4′-positions of B-ring, a clear trend is observed: from flavonoids **A1** to **A5**, the –OH groups at 3-position of C-ring and at 3′-position of B-ring establish hydrogen bonds with Asp300, while the –OH group at 4′-position of B-ring establishes hydrogen bonds with Asp197, with this hydrogen bonding network being optimized in flavonoid **A5**.

Therefore, flavonoids **A1** to **A5** bind the active site with the B-ring oriented towards the catalytic triad (Asp197, Asp300, Glu233), occupying a site equivalent to the –1 subpocket of the K2 inhibitor in the PDB structure 1HXO[35], while the A- and C-rings are pointing outwards occupying the binding site cleft equivalent to the –2 subpocket, which is a pocket not usually occupied by the natural substrate, located in the opposite direction in relation to the +1 subpocket.

For the less substituted **A1** to **A3** flavonoids, the described set of hydrogen bond interactions is not optimized and as such, they do not bind so deep in the active site. Instead, aromatic stacking interactions are observed between the A- and C-rings and Trp58, and between the B-ring and Tyr62.

When two –OH groups are added to B-ring (flavonoids **A4** and **A5**) the hydrogen bonds with the catalytic triad are optimized and these flavonoids bind deeper in the active site, hydrogen bonding with Asp197, Glu233 and Asp300, which might explain the higher inhibitory activity observed for these two flavones within A group [Figure 4(A)].

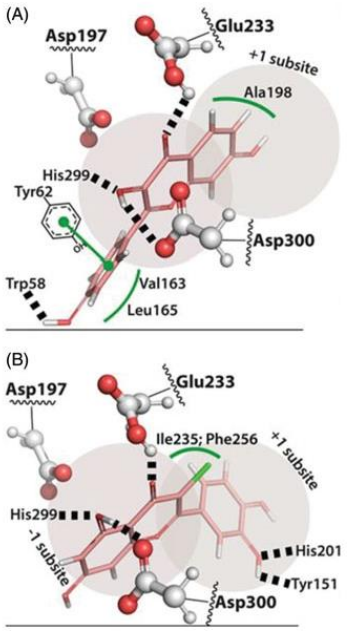


Figure 5. (A) The binding mode predicted for **C5** shows the C-ring carbonyl and –OH group interacting with the active site residues in a similar way as in **B4**. This requires the B-ring to be placed in the –1/–2 subsites, stabilized mostly by hydrophobic interactions with Tyr62, Val163 and Leu165. (B)The best tested inhibitor, flavonoid **D11**, and flavonoid **B4** binds very similarly to α-amylase. The most important difference seems to come from the 3–Cl substitution that interacts with Ile235 and Phe256.

The steric hindrance introduced by methoxylation at 3′- and 4′-positions of B-ring (flavonoid **A6**), flips the binding pose, placing instead the A- and C-rings in the –1 subpocket. This allows the –OH group at 3-position of C-ring to establish a hydrogen bond with Asp300 and Glu233.

As evidenced before, within B group of structurally related flavonoids, the best inhibitor is **B4** with an IC_{50} value of 148 ± 5 μM. This compound shares with **A4** and **A5** the same hydroxyl substituents in the B-ring, but an additional –OH group at 5-position of the A-ring, which jointly promotes a stabilized conformation and an increase of the inhibition of α-amylase activity.

Looking at the pose predictions, it is clear that the C-ring carbonyl and the –OH group at the A-ring, promote the positioning of the A- and C-rings close to the catalytic triad. The orientation of the flavonoid, however, depends on the substitutions present in the B-ring [Figure 4(B)].

The two –OH substitutions present in the B-ring of flavonoid **B4** increase the hydrophilicity of the catechol, which seems to distinguish **B4** from the rest of the group. This allows the B-ring to occupy the +1 subpocket, with His201 hydrogen bonding the oxygen of the –OH group at 3′ position of B-ring, while that same –OH group makes a hydrogen bond with the oxygen of the Tyr151 hydroxyl [Figure 4(B)]. This orientation is unlike **B1** and **B2**, where the more hydrophobic B-ring binds the –2 subpockets, in the more hydrophobic region formed by Val163 and Leu165. Despite positioning the A- and C-ring between the catalytic triad, as the other flavonoids, this different orientation of the A- and C-ring of **B4**, seems to optimize the hydrogen-bonding network around the active site. Namely, the –OH group in the 5-position of A-ring establishes a hydrogen bond with Asp300 and to His299, while the C-ring carbonyl is hydrogen bonded to Glu233.

In turn, from C group, the 3–OH substitution present in C-ring of flavonoids **C4** and **C5** gives rise to a substructural motif of adjoined hydroxyl and carbonyl groups, similarly to the one found in the B group. On the latter, a C-ring carbonyl group adjoined by a –OH group at 4-position of A-ring allows the positioning of A- and C-rings within the catalytic triad. Therefore, the C-ring carbonyl and 3–OH substitution in **C4** and **C5** flavonoids also promotes the placing of the A- and C-rings within the catalytic triad, with the hydrogen of the –OH group at 3-position of C-ring bonded to Asp300 and to His299, and with the Glu233 hydrogen bonding the carbonyl group [Figure 5(A)]. These positions of the carbonyl and –OH groups, exactly as in **B4,** and the same hydrogen-bonding network, are observed between these groups and the active site. This also means that **C4** and **C5** are bound in a flipped orientation when compared to flavonoid **B4**. Thus, these flavonoids occupy the subpockets +2 to –1, with the –OH group at 7-position of A-ring in the –1 subpocket, while the B-ring binds in the other side of the active site cleft, with the B-ring facing the more hydrophobic side of the substrate cleft characterized by Val163, Leu165 and Tyr62 (+2 subpocket). The B-ring establishes aromatic stacking interactions with Tyr62 and in the case of flavonoid **C5**, the 3′–OH substitution is hydrogen bonded to the backbone of Trp58. Moving this –OH substitution to 3′-position of B-ring, as in **C4**, leads to the breakage of the hydrogen bond with Trp58 and leaves the –OH at 3′-position of B-ring more exposed to the solvent, lowering the inhibitory activity of **C4**.

The absence of an –OH group at 3-position of C-ring, as in **C6**, and the presence of an –OH substitution in the 3′ position of B-ring, define a completely different mode of interaction. In **C6**, the lack of hydrogen bond donors in the C-ring precludes the binding within the catalytic triad. Instead, B-ring binds the catalytic triad with the two –OH substitutions hydrogen bonding Asp300, while Glu233 hydrogen bonds the 3′–OH (+1 subpocket). In this binding mode, the A- and C-rings occupy the site of the substrate cleft corresponding to the –1 and –2 subpockets of the leaving maltose, with the hydrogen of the –OH at 7-position of A-ring bonding Glu240.

In what concerns D group, the binding mode of **D11**, the flavonoid with the higher inhibitory activity, is almost identical to **B4**. The C-ring carbonyl group adjoined by the –OH group of A-ring allow the binding of A- and C-rings within the catalytic triad, establishing the same hydrogen bonding network with the active site residues Asp300, His299 and Glu233 (subpocket +1). This also means that B-ring of flavonoid **D11** binds in the same site as the B-ring of flavonoid **B4** and, like **B4**, His201 hydrogen bonds the –OH group at 3′-position of B-ring, while the 3′–OH hydrogen bonds Tyr151 (subpocket –1). On the other hand, the –OH group at 7-position of A-ring seems to establish no specific interactions, while the –Cl ion at 3-position of C-ring fills the cavity formed by Ile235 and Phe256 and hydrogen bonds the backbone of Ile234 [Figure 5(B)].

A similar binding mode is predicted when the –Cl ion at 3-position of C-ring of flavonoid **D11** is substituted by an -H or –OH group (**D7** and **D8**, respectively), but the inhibitory activity is decreased by two-fold and three-fold, respectively. The lower shape complementarity of **D7** and the resistance of binding the more electronegative oxygen in the pocket formed by Ile235 and Phe256 for flavonoid **D8** might explain the decreased inhibitory activity.

It is interesting to compare **D11** with **D14**, which bears an additional –Cl substitution at 8-position of A-ring. The binding mode of **D14** is exactly the same as **D11**, thus the 8–Cl substitution binds in the hydrophobic pocket formed by Leu162, Val163 and Leu165. Despite the increased shape complementarity, the IC_{50} value increased by twofold. Perhaps a similar sized but more hydrophobic group in this position would be advantageous.

Methoxylation of the B-ring in **D16**, **D17** and **D18** flipped the mode of binding, when compared to **D11**, and disrupted the interactions with the active site triad.

Among flavonoids of the E group, it was possible to observe that exchanging the sp^2 C2 carbon on the C-ring for a sp^3 carbon, has a dramatic effect on the inhibitory efficiency when compared to **D5**, **D7** and **D8**. The predicted mode of binding is the same for the three flavonoids, with the A- and C-rings occupying the +3 and +2 subpockets, while the B-ring occupies the +1 subpocket and hydrogen bonds Asp197. These three flavonoids clearly cannot occupy the subpockets +1 and −1 simultaneously to maximize the interaction with the catalytic triad, thus cannot inhibit α-amylase.

Discussion

The search for safer, specific and effective hypoglycaemic agents has been a concern of the scientific community. As a major player in the route leading to the assimilation of polysaccharides, the enzyme α-amylase plays an important role in controlling the postprandial blood glucose levels, thus being an interesting therapeutic target forT2DM. It was previously shown that the molecular models for the human and porcine pancreatic α-amylases are extremely similar[44], which enables the use of a porcine pancreatic α-amylase surrogate in microanalysis screening of novel α-amylase inhibitors [see Supporting Information, Figure 22(S), showing the superposition of the human and porcine enzymes].

In the present work, we tested the inhibition of pancreatic α-amylase activity by a panel of 40 flavonoids, that were divided among five groups (A–E) according to the respective parent structure scaffolds, with –OH, –OMe and/or –Cl substitutions, in order to elucidate a rationale for structure-activity relationship. The kinetic analysis, inhibitory mechanism determination and the corresponding molecular docking calculations were also applied, in order to explain the binding model of the most effective flavonoid of each group and the positive control, **acarbose**, regarding the three-dimensional structure of the α-amylase catalytic site. The obtained results clearly show that α-amylase inhibition by flavonoids varies with the nature, number and position of the substituents present in the derivative flavonoids' structure. From the studied flavonoids, the most effective compound found was the chlorinated flavone **D11**.

In what concerns the A group, the tested flavonoids (**A1**–**A6**) present low or no ability to inhibit α-amylase up to the highest tested concentration, 200 μM. Comparing the flavone **A1** with **A2**, **A3**, **A4** and **A5**, it is clear that addition of –OH groups at 3-position of C-ring and at 3′- and/or at 4′-positions of B-ring lead to no effect against the α-amylase activity. In addition, the substitution of –OH groups by –OMe groups at 3′-and 4′-positions of B-ring (**A6**) also did not lead to any effect for the inhibitory activity of α-amylase.

The most active flavonoid of B group was **B4** (IC_{50}= 148 ± 5 μM). Thus, the presence of a catechol group in B-ring, together with the –OH group at 5-position of A-ring, seems distinctive features for inhibitory activity, especially if a comparison is made with those derivatives without –OH groups in B-ring (**B1**) or with just one –OH group at 3′- or 4′-positions of B-ring (**B2** and **B3**, respectively). In addition, by comparing **A5** with **B4**, it can be noticed that the –OH group seems to be more favourable at 5-position of A-ring than at 3-position of C-ring for the intended activity. This is in accordance to previous studies showing that the hydroxylation of A- (at 5- and 7-positions) and B-rings (at 3′- and 4′-positions) of flavonoids improve their inhibitory effect against this enzyme[4,45–47].

The most effective flavonoid from the C group was **C5** (IC_{50}= 59 ± 4 μM), which was tested here for the first time. Taking into account the obtained result, it is possible to conclude that the presence of an –OH group at 3-position of C-ring, at 4′-position of B-ring and at 7-position of A-ring are advantageous for the inhibitory effect. Accordingly, it was previously reported, through the study of various structurally-related flavonoids, that the hydroxylation at 4′-position of B-ring and at 7-position of A-ring in flavonoids' scaffold is relevant for their inhibitory activity against α-amylase[4,21,45–48]. The importance of the presence of an –OH group at 4′-position in B-ring is also highlighted by comparing **C5** with **C4** (–OH group at 3′-position of the B-ring), since flavonoid **C4** presented low activity up to 200 μM, the highest tested concentration. The relevance of the presence of an –OH group at 3-position of C-ring together with an OH group at 4′-position of B-ring for the inhibition of α-amylase, is highlighted by the lack of inhibitory activity of **C3**, when compared with **C5**.

Concerning the studied methoxylated flavonoids, **C7** and **C8**, both presented no inhibitory activity against α-amylase, corroborating the idea that the inhibitory activity of flavonoids against α-amylase is not favoured through methoxyl substitution. Accordingly, it was previously described in *in vitro* studies that the methylation and methoxylation in the structure of flavonoids reduce the inhibitory activity towards α-amylase[45,46,48].

In D group we found the most active compound of this work, flavone **D11**, with a –Cl ion at 3-position of C-ring, a –OH group at 3′ and 4′-positions of B-ring and at 5- and 7-positions of A-ring, presenting an IC_{50} value = 44 ± 3 μM. Chlorinated flavonoids were previously reported by our research group as potent anti-inflammatory agents due to their ability to suppress mechanisms engaged at the onset and progression of inflammation[27,49]. Since both oxidative stress and inflammation play a key role in the pathogenesis of insulin resistance and dysfunction of β-cells[50], we selected these promising chlorinated flavonoids and studied their effectiveness as α-amylase inhibitors. In addition, these flavonoids already proved to be effective compounds in the inhibition of α-glucosidase[15] and PTP1B[16]. Comparing flavones **D11** and **D8** (quercetin) (IC_{50} = 138 ± 5 μM), it is possible to conclude that the substitution of the –Cl ion by an –OH group, at 3-position of C-ring, significantly decreased the α-amylase inhibition. Moreover, the removal of the –Cl ion from 3-position of C-ring also led to a decrease of the inhibitory activity of flavonoids, as it is possible to verify by comparing **D11** with **D7** (luteolin) (IC_{50} = 78 ± 3 μM). Furthermore, the addition of an –OH group at 3-position of C-ring [**D8** (quercetin)] significantly decreased the inhibitory activity towards α-amylase (138 ± 5 μM). The comparison of flavone **D11** with **D14** show that addition of a –Cl ion at 8-position of A-ring, led to a two-fold increase of the IC_{50} value (82 ± 4 μM). Thus, the presence of a –Cl ion at 3-position of the C-ring is especially advantageous for the ability of flavonoids to inhibit α-amylase activity.

Through the comparison of the results obtained for flavone **D9** (myricetin) (IC_{50} = 107 ± 6 μM) and **D8** (quercetin) (IC_{50} = 138 ± 5 μM), it was possible to observe that the addition of an –OH group at 5′-position of B-ring slightly enhanced α-amylase inhibition. The results of the present work are in accordance with those reported by Meng et al.[25] and Tadera et al.[21], who also studied the α-amylase inhibition by quercetin and myricetin and found that myricetin was slightly more effective than quercetin.

By comparing **D7** (luteolin) (IC_{50}= 78 ± 3 μM) and **D8** (quercetin) (IC50 = 138 ± 5 μM), it was also possible to conclude that the addition of an –OH group at 3-position of C-ring decreased the flavonoids' inhibitory activity towards α-amylase. The obtained results are in agreement with the study of Tadera et al.[21], who also tested the mentioned flavonoids. In the study of Kim et al.[23], the authors also observed that luteolin was an effective α-amylase inhibitor.

Comparing methoxylated flavonoids with their parent hydroxylated flavonoids, it is possible to conclude that the presence of

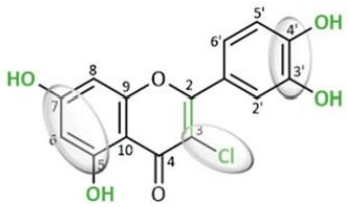


Figure 6. Potential substitution pattern of flavonoids contributing to the improvement of α-amylase inhibition.

–OMe groups decrease α-amylase inhibition, as it can be seen comparing flavone **D16** (chrysoeriol) and **D18** with **D7** (luteolin), and **D17** (acacetin) with **D5** (apigenin). These results are in agreement with previous studies found in literature[45–48,51].

A glycosylated flavonoid was also tested, **D19** (rutin), and the presence of a sugar in the flavonoid structure did not favour its ability to inhibit α-amylase activity. In this sense, the obtained results showed that the substitution of an –OH group [**D8** (quercetin)] by a rutinose [**D19** (rutin)] at 3-position of C-ring reduced the α-amylase inhibition by flavonoids. Accordingly, it was previously described in the literature that the glycosylation of flavonoids decreases their inhibitory effect against α-amylase, possibly due to the increasing molecular size and polarity, and to the nonplanar structure[45,46,48]. In addition, this conclusion is in agreement with the study of Li et al.[24], who tested the interaction between quercetin, rutin and isoquercetin with α-amylase, and found that the binding affinity of quercetin to the enzyme is higher when compared to rutin.

The flavanones from E group did not inhibit α-amylase, up to the highest tested concentration (200 μM). Comparing **E1** (naringenin) with **D5** (apigenin), **E2** (eriodictyol) with **D7** (luteolin) and **E3** (taxifolin) with **D8** (quercetin), it was observed that the lack of the C2 = C3 double bond did not favour the intended effect. This conclusion is in agreement with Tadera et al.,[21] who observed that naringenin was not able to inhibit porcine pancreatic α-amylase activity, at the highest tested concentration of 0.5 mM. It is well known that the C2 = C3 double bond allows an easier entry of the molecules into the hydrophobic pockets of α-amylase since the presence of this double bond favours the near-planarity of flavonoids[4,45,46,48].

Acarbose is a pseudotetrasaccharide produced by *Actinoplanes* sp. fermentation and its structure comprises a hydroxymethyl conduritol residue α-(1,4) linked to a 4-amino-4,6-dideoxyglucose which is, in turn, α-(1,4) linked to maltose[52,53]. It is the most widely prescribed α-glucosidase and α-amylase inhibitor. However, it was previously shown that only a mild inhibition of pancreatic α-amylase is recommended in order to avoid gastrointestinal side-effects as a result of excessive bacterial fermentation of carbohydrates in colon[11], that has been shown as a limiting factor for T2DM treatment, in some countries[11]. In the present work, the IC_{50} values found for the tested flavonoids were higher than the IC_{50} value found for acarbose, which is 1.3 ± 0.2 μM. The mild pancreatic α-amylase inhibition prevents the abnormal bacterial fermentation of carbohydrates in the colon and consequent gastrointestinal adverse effects, such as abdominal distention, flatulence and diarrhea[11]. Moreover, it was previously shown by our research group that, in general, the tested flavonoids were more effective concerning the inhibition of α-glucosidase than the inhibition of α-amylase[15]. As such, the obtained results suggest that flavonoids could be promising α-amylase inhibitors and cause less gastrointestinal side-effects. Interestingly, it was found that the combination of baicalein or apigenin with acarbose showed additive inhibition of α-amylase at lower concentrations and antagonistic inhibition at higher concentrations. On the other hand, the combination of baicalein with acarbose synergistically inhibits α-glucosidase and lowers HGPP[54].

After the study of α-amylase inhibition by flavonoids, we selected the most active flavonoid of each group (**B4**, **C5** and **D11**) and the positive control, **acarbose**, to test their type of inhibition.

It was described that the discrimination between mechanisms of enzymatic inhibition based on linear transformation of Michaelis–Menten equation is less accurate than the use of the nonlinear regression, since the transformation can also mask the variability inherent to kinetic data[29,30]. By the same reason, modelling on the means of repeated experiments instead of using individual data can also lead to misinterpreted mechanisms. In that sense, for the enzyme kinetic analysis, it was used the nonlinear regression to determine kinetic parameters and the type of inhibition of the most active flavonoids of each group. For this purpose, it was applied the Solver supplement of Microsoft Office Excel™. By means of iterative guesses for variables in each model equation, Solver was asked to minimize the sum of squared residuals between individual raw experimental results and the corresponding values generated by the model.

In accordance, kinetic analysis consisted in the sequential fitting of available models (without inhibition, competitive inhibition, noncompetitive inhibition, uncompetitive inhibition and mixed inhibition), and in the estimation of the kinetic constants (parameters) values. It was possible to observe by the analysis of the sum of the square errors values from the different models, and by the application of F-test and AIC test, that **acarbose** presents a mixed-type inhibition [see Supporting Information, Figures 1(S)–5(S)], and flavonoids **B4** [see Supporting Information, Figures 6(S)–10(S)], **C5** (see Supporting Information, Figures 11(S)–15(S)) and **D11** [see Supporting Information, Figures 16(S)–20(S)] present a competitive inhibition. Accordingly, Kim et al.[55] and Yoon and Robyt,[52] also described acarbose as a mixed type inhibitor of α-amylase. To the best of our knowledge, the inhibition type of flavonoids **B4**, **C5** and **D11** were studied here for the first time.

Once defined the best kinetic model for **acarbose** and for flavonoids **B4**, **C5** and **D11**, the kinetic constants were estimated: V_{max}, K_m, K_{ic} and K_{iu}. The calculation of the Ki value is considered a useful tool to compare the potency of inhibitors. The K_{ic} values of the selected compounds demonstrated the following order: **B4**>**C5**>**D11**>**acarbose**. This means that, as expected, **acarbose** has the highest binding affinity to α-amylase, followed by flavonoids **D11**, **C5** and **B4**.

The prediction of the binding mode of the most active flavonoids towards α-amylase in each group showed that one of the most important aspects shared by them is a motif bearing a carbonyl group next to a –OH group. This allows the carbonyl group to accept a hydrogen bond from Glu233 and the –OH group to donate a hydrogen bond to Asp300 in the region between the –1 subpocket and +1 subpocket. The interactions with these groups can be further enhanced with a hydrogen bond between His299 and the -OH group.

The relative positioning of the -OH and carbonyl groups determine, to a great extent, the orientation of the flavonoid. Thus, the flavonoid part on the side of the carbonyl will be preferably oriented towards the +1 subpocket, while the part on the -OH side will be preferably oriented towards the –1 subpocket.

Hydrophobic groups seem to be more tolerated on the –1/–2 subpockets than on the +1/+2 subpockets, where they can interact with Tyr62, Leu162, Val163 and Leu165. Hydrophobic groups on the +1/+2 subpockets, on the other hand, can establish hydrogen bonds with Tyr151 and His201.

Halogen substitutions or hydrophobic groups might be used next to the carbonyl to explore the interaction with Ile235 and Phe256, as the best flavonoid tested herein shows.

Conclusion

In the present study, the inhibition of pancreatic α-amylase by a panel of 40 flavonoids (A–E groups) was tested, in order to establish an accurate structure-activity relationship. For that purpose, the kinetic analysis, the inhibitory mechanism determination and the corresponding molecular docking calculations were applied, to explain the binding model of the most effective flavonoid of each group to the three-dimensional structure of α-amylase catalytic site. Thus, from the obtained results, it may be concluded that α-amylase inhibition by flavonoids is strongly dependent on the nature and position of the substituents. The most effective flavonoid was the chlorinated flavone **D11**. As such, the presence of an –OH group at 5- and 7-positions of A-ring and in the 3′- and 4′-positions of B-ring, and the presence of a –Cl ion at 3-position of C-ring, as well as the C2 = C3 double bond, have shown to be favourable for the intended effect (Figure 6). This flavonoid presented a competitive type of inhibition. The promising α-amylase inhibitory activity of some of the studied flavonoids should be deeply explored allowing these compounds to be considered as possible alternatives for the management of PPHG and consequently T2DM.

Disclosure statement

No potential conflict of interest was reported by the authors.

Funding

This work was financed by FEDER–Fundo Europeu de Desenvolvimento Regional through the COMPETE 2020–Operacional Programme for Competitiveness and Internationalisation (POCI), and by Portuguese funds through FCT–Fundação para a Ciência e a Tecnologia in the framework of the project POCI-01–0145-FEDER-029241. Carina Proença acknowledges FCT the financial support for the PhD grant [SFRH/BD/116005/2016], in the ambit of "QREN–POPH–Tipologia 4.1–FormaçãoAvançada", co-sponsored by Fundo Social Europeu (FSE) and by national funds of Ministério da Ciência, Tecnologia e Ensino Superior (MCTES).

ORCID

Carina Proença https://orcid.org/0000-0003-0859-6526
Marisa Freitas https://orcid.org/0000-0001-9114-9967
Daniela Ribeiro https://orcid.org/0000-0001-9733-7934
Sara M. Tomé http://orcid.org/0000-0002-9021-2909
Eduardo F. T. Oliveira https://orcid.org/0000-0003-4637-2099
Matilde F. Viegas https://orcid.org/0000-0002-4472-9691
Alberto N. Araújo http://orcid.org/0000-0001-5348-4924
Maria J. Ramos http://orcid.org/0000-0002-7554-8324
Artur M. S. Silva http://orcid.org/0000-0003-2861-8286
Pedro A. Fernandes http://orcid.org/0000-0003-2748-4722
Eduarda Fernandes http://orcid.org/0000-0001-6424-0976

References

1. Butterworth PJ, Warren FJ, Ellis PR. Human α-amylase and starch digestion: an interesting marriage. Starch–Stärke 2011;63:395–405.
2. Patel H, Royall PG, Gaisford S, et al. Structural and enzyme kinetic studies of retrograded starch: inhibition of α-amylase and consequences for intestinal digestion of starch. Carbohydr Polym 2017;164:154–61.
3. Brayer GD, Sidhu G, Maurus R, et al. Subsite mapping of the human pancreatic α-amylase active site through structural, kinetic, and mutagenesis techniques. Biochemistry 2000;39:4778–91.
4. Lo Piparo E, Scheib H, Frei N, et al. Flavonoids for controlling starch digestion: structural requirements for inhibiting human α-amylase. J Med Chem 2008;51:3555–61.
5. Sales PM, Souza PM, Simeoni LA, et al. A-amylase inhibitors: a review of raw material and isolated compounds from plant source. J Pharm Pharm Sci 2012;15:141–83.
6. Liu D, Gao H, Tang W, Nie S. Plant non-starch polysaccharides that inhibit key enzymes linked to type 2 diabetes mellitus. Ann N Y Acad Sci 2017;1401:28–36.
7. Martinez-Gonzalez AI, Diaz-Sanchez AG, Rosa LA, et al. Polyphenolic compounds and digestive enzymes: *in vitro* non-covalent interactions. Molecules 2017;22:1–24.
8. Janecek S, Svensson B, MacGregor EA. α-Amylase: an enzyme specificity found in various families of glycoside hydrolases. Cell Mol Life Sci 2014;71:1149–70.
9. International Diabetes Federation. IDF Diabetes Atlas. In IDF Diabetes Atlas. 8th ed. 2017. Available from: http://diabetesatlas.org/IDF_Diabetes_Atlas_8e_interactive_EN/
10. American Diabetes Association. Classification and diagnosis of diabetes: standards of medical care in diabetes–2018. Diabetes Care 2018;41:S13–S27.
11. Etxeberria U, de la Garza AL, Campion J, et al. Antidiabetic effects of natural plant extracts via inhibition of carbohydrate hydrolysis enzymes with emphasis on pancreatic alpha amylase. Expert Opin Ther Targets 2012;16:269–97.
12. Kahn SE, Cooper ME, Del Prato S. Pathophysiology and treatment of type 2 diabetes: perspectives on the past, present, and future. Lancet 2014;383:1068–83.
13. Wedick NM, Pan A, Cassidy A, et al. Dietary flavonoid intakes and risk of type 2 diabetes in US men and women. Am J Clin Nutr 2012;95:925–33.
14. Liao X, Wang X, Li H, et al. Sodium-glucose cotransporter 2 (SGLT2) inhibitor increases circulating zinc-α2-glycoprotein levels in patients with type 2 diabetes. Sci Rep 2016;6:1–12.
15. Proenca C, Freitas M, Ribeiro D, et al. α-Glucosidase inhibition by flavonoids: an *in vitro* and *in silico* structure–activity relationship study. J Enzyme Inhib Med Chem 2017;32:1216–28.
16. Proenca C, Freitas M, Ribeiro D, et al. Inhibition of protein tyrosine phosphatase 1B by flavonoids: a structure–activity relationship study. Food Chem Toxicol 2018;111:474–81.
17. Nicolle E, Souard F, Faure P, Boumendjel A. Flavonoids as promising lead compounds in type 2 diabetes mellitus: molecules of interest and structure–activity relationship. Curr Med Chem 2011;18:2661–72.
18. Vinayagam R, Xu B. Antidiabetic properties of dietary flavonoids: a cellular mechanism review. Nutr Metab 2015;12:1–20.
19. Xiao JB, Hogger P. Dietary polyphenols and type 2 diabetes: current insights and future perspectives. Curr Med Chem 2015;22:23–38.
20. Kawser HM, Abdal DA, Han J, et al. Molecular mechanisms of the anti-obesity and anti-diabetic properties of flavonoids. Int J Mol Sci 2016;17:569–32.

21. Tadera K, Minami Y, Takamatsu K, Matsuoka T. Inhibition of alpha-glucosidase and alpha-amylase by flavonoids. J Nutr Sci Vitaminol 2006;52:149–53.
22. Gu C, Zhang H, Putri CY, Ng K. Evaluation of α-amylase and α-glucosidase inhibitory activity of flavonoids. Int J Food Nutr Sci 2015;2:1–6.
23. Kim JS, Kwon CS, Son KH. Inhibition of alpha-glucosidase and amylase by luteolin, a flavonoid. Biosci Biotechnol Biochem 2000;64:2458–61.
24. Li Y, Gao F, Gao F, et al. Study on the interaction between 3 flavonoid compounds and α-amylase by fluorescence spectroscopy and enzymatic kinetics. J Food Sci 2009;74: C199–203.
25. Meng Y, Su A, Yuan S, et al. Evaluation of total flavonoids, myricetin, and quercetin from *Hovenia dulcis* thunb. as inhibitors of α-amylase and α-glucosidase. Plant Foods Hum Nutr 2016;71:444–9.
26. Ribeiro D, Freitas M, Tome SM, et al. Modulation of human neutrophils' oxidative burst by flavonoids. Eur J Med Chem 2013;67:280–92.
27. Freitas M, Ribeiro D, Tome SM, et al. Synthesis of chlorinated flavonoids with anti-inflammatory and pro-apoptotic activities in human neutrophils. Eur J Med Chem 2014;86:153–64.
28. Trinh BTD, Staerk D, Jäger AK. Screening for potential α-glucosidase and α-amylase inhibitory constituents from selected Vietnamese plants used to treat type 2 diabetes. J Ethnopharmacol 2016;186:189–95.
29. Bezerra RMF, Fraga I, Dias AA. Utilization of integrated Michaelis–Menten equations for enzyme inhibition diagnosis and determination of kinetic constants using Solver supplement of Microsoft Office Excel. Comput Methods Programs Biomed 2013;109:26–31.
30. Dias AA, Pinto PA, Fraga I, Bezerra RMF. Diagnosis of enzyme inhibition using Excel Solver: a combined dry and wet laboratory exercise. J Chem Educ 2014;91:1017–21.
31. Motulsky H, Christopoulos A, Fitting models to biological data using linear and nonlinear regression: a pratical guide to curve fitting. New York: Oxford University Press; 2004.
32. Burguillo FJ, Wright AJ, Bardsley WG. Use of the F test for determining the degree of enzyme-kinetic and ligand-binding data. A Monte Carlo simulation study. Biochem J 1983; 211:23–34.
33. Yamaoka K, Nakagawa T, Uno T. Application of Akaike's information criterion (AIC) in the evaluation of linear pharmacokinetic equations. J Pharmacokinet Biopharm 1978;6: 165–75.
34. Naes T, Isakson T, Fearn T, Davies T, A user-friendly guide to multivariate calibration and classification. Chichester: NIR Publications; 2002.
35. Qian M, Nahoum V, Bonicel J, et al. Enzyme-catalyzed condensation reaction in a mammalian alpha-amylase. High-resolution structural analysis of an enzyme-inhibitor complex. Biochemistry 2001;40:7700–9.
36. Bietz S, Urbaczek S, Schulz B, Rarey M. Protoss: a holistic approach to predict tautomers and protonation states in protein-ligand complexes. J Cheminform 2014; 6:1–12.
37. Case DA, Darden TA, Cheatham TE, et al. Amber 12. In. Amber 12. San Francisco: University of California; 2012.
38. Hornak V, Abel R, Okur A, et al. Comparison of multiple amber force fields and development of improved protein backbone parameters. Proteins 2006;65:712–25.
39. Kirschner KN, Yongye AB, Tschampel SM, et al. Glycam06: a generalizable biomolecular force field. J Comput Chem 2008;29:622–55.
40. Trott O, Olson AJ. Autodock vina: improving the speed and accuracy of docking with a new scoring function, efficient optimization, and multithreading. J Comput Chem 2010;31: 455–61.
41. O'Boyle NM, Morley C, Hutchison GR. Pybel: a python wrapper for the openbabel cheminformatics toolkit. Chem Cent J 2008;2:5–7.
42. Gasteiger J, Marsili M. Iterative partial equalization of orbital electronegativity–a rapid access to atomic charges. Tetrahedron 1980;36:3219–28.
43. Jones G, Willett P, Glen RC, et al. Development and validation of a genetic algorithm for flexible docking. J Mol Biol 1997;267:727–48.
44. Qian M, Spinelli S, Driguez H, Payan F. Structure of a pancreatic α-amylase bound to a substrate analogue at 2.03 a resolution. Protein Sci 2008;6:2285–96.
45. Cao H, Chen X. Structures required of flavonoids for inhibiting digestive enzymes. Anticancer Agents Med Chem 2012; 12:929–39.
46. Xiao J, Ni X, Kai G, Chen X. A review on structure–activity relationship of dietary polyphenols inhibiting α-amylase. Crit Rev Food Sci Nutr 2013;53:497–506.
47. Gonzales GB, Smagghe G, Grootaert C, et al. Flavonoid interactions during digestion, absorption, distribution and metabolism: a sequential structure–activity/property relationship-based approach in the study of bioavailability and bioactivity. Drug Metab Rev 2015;47:175–90.
48. Xu W, Shao R, Xiao J. Is there consistency between the binding affinity and inhibitory potential of natural polyphenols as α-amylase inhibitors? Crit Rev Food Sci Nutr 2016;56: 1630–9.
49. Proença C, Ribeiro D, Soares T, et al. Chlorinated flavonoids modulate the inflammatory process in human blood. Inflammation 2017;40:1155–65.
50. Pitocco D, Tesauro M, Alessandro R, et al. Oxidative stress in diabetes: implications for vascular and other complications. Int J Mol Sci 2013;14:21525–50.
51. Asghari B, Salehi P, Sonboli A, Nejad Ebrahimi S. Flavonoids from *salvia chloroleuca* with α-amylase and α-glucosidase inhibitory effect. Iran J Pharm Res 2015;14:609–15.
52. Yoon S-H, Robyt JF. Study of the inhibition of four alpha amylases by acarbose and its 4iv-α-maltohexaosyl and 4iv-α-maltododecaosyl analogues. Carbohydr Res 2003;338:1969–80.
53. Rosak C, Mertes G. Critical evaluation of the role of acarbose in the treatment of diabetes: patient considerations. Diabetes Metab Syndr Obes 2012;5:357–67.
54. Zhang BW, Li X, Sun WL, et al. Dietary flavonoids and acarbose synergistically inhibit α-glucosidase and lower postprandial blood glucose. J Agric Food Chem 2017;65: 8319–30.
55. Kim M, Lee S, Lee H, et al. Comparative study of the inhibition of α-glucosidase, α-amylase, and cyclomaltodextrin glucanosyltransferase by acarbose, isoacarbose, and acarviosine–glucose. Arch Biochem Biophys 1999;371: 277–83.

II.3. Inhibition of protein tyrosine phosphatase 1B by flavonoids: a structure-activity relationship study

Version of record from Food and Chemical Toxicology

Copyright © (2018) with kind permission of Elsevier

Food and Chemical Toxicology 111 (2018) 474–481

Contents lists available at ScienceDirect

Food and Chemical Toxicology

journal homepage: www.elsevier.com/locate/foodchemtox

Inhibition of protein tyrosine phosphatase 1B by flavonoids: A structure - activity relationship study

Carina Proença[a], Marisa Freitas[a], Daniela Ribeiro[a], Joana L.C. Sousa[b], Félix Carvalho[c, **], Artur M.S. Silva[b], Pedro A. Fernandes[d], Eduarda Fernandes[a,*]

[a] UCIBIO, REQUIMTE, Laboratory of Applied Chemistry, Department of Chemical Sciences, Faculty of Pharmacy, University of Porto, 4050-313 Porto, Portugal
[b] Department of Chemistry & QOPNA, University of Aveiro, 3810-193 Aveiro, Portugal
[c] UCIBIO, REQUIMTE, Laboratory of Toxicology, Department of Biological Sciences, Faculty of Pharmacy, University of Porto, 4050-313 Porto, Portugal
[d] UCIBIO, REQUIMTE, Department of Chemistry and Biochemistry, Faculty of Sciences, University of Porto, 4169-007 Porto, Portugal

ARTICLE INFO

Keywords:
Diabetes *mellitus*
PTP1B inhibition
Flavonoids
Enzymatic inhibition type

ABSTRACT

The classical non-transmembrane protein tyrosine phosphatase 1B (PTP1B) has emerged as a key negative regulator of insulin signaling pathways that leads to insulin resistance, turning this enzyme a promising therapeutic target in the management of type 2 diabetes *mellitus* (T2DM). In the present work, the *in vitro* inhibitory activity of a panel of structurally related flavonoids, for recombinant human PTP1B was studied and the type of inhibition of the most active compounds further evaluated. The majority of the studied flavonoids was tested in this work for the first time, including flavonoid **C13**, which was the most potent inhibitor. It was observed that the ability to inhibit PTP1B depends on the nature, position and number of substituents in the flavonoid structure, as the presence of both 7- and 8-OBn groups in the A ring, together with the presence of both 3′ and 4′-OMe groups in the B ring and the 3-OH group in the C ring; these substituents increase the flavonoids' ability to inhibit PTP1B. In conclusion, some of the tested flavonoids seem to be promising PTP1B inhibitors and potential effective agents in the management of T2DM, by increasing insulin sensitivity.

1. Introduction

According to the International Diabetes Federation (IDF) (International Diabetes Federation, 2015), Diabetes *mellitus* (DM) is an important public health problem that affected 415 million people worldwide in 2015, and it is estimated that this number will increase to 642 million people in 2040. Type 2 DM (T2DM) represents the much more prevalent form of DM, accounting for 90–95% of the diabetes cases, and it is characterized by the combination of insulin action resistance and an inadequate compensatory insulin secretory response (American Diabetes Association, 2011). The development of new effective antidiabetic agents is therefore a permanent concern for the scientific community.

The classical non-transmembrane protein tyrosine phosphatase 1B (PTP1B) has emerged as a key negative regulator of insulin signaling pathways that leads to insulin resistance, turning this enzyme into a promising therapeutic target in the management of T2DM (Kennedy and Ramachandran, 2000; Feldhammer et al., 2013; Panzhinskiy et al., 2013; Qian et al., 2016). In brief, the binding of insulin to the α-subunits of its receptor leads to autophosphorylation of the β-subunits and the tyrosine phosphorylation of insulin receptor substrates (IRS). Phosphorylated IRS proteins serve as docking proteins for other secondary messengers, leading to the activation of protein kinase B (PKB), also known as Akt. The net effect of this pathway is to produce a translocation of the glucose transporter 4 (GLUT4) from cytoplasmic vesicles to the cell membrane in order to facilitate glucose transport (Fig. 1) (Youngren, 2007; Boucher et al., 2014; Bakke and Haj, 2015; Wang et al., 2015a). PTP1B is involved in the dephosphorylation and concomitantly inactivation of the insulin receptor (IR) and IRS, leading to the attenuation of the insulin signal. Thus, any changes in the expression levels or activity of this enzyme relative to IR can affect insulin signaling and contribute to the insulin resistance observed in T2DM

ABBREVIATIONS: DM, Diabetes *mellitus*; GLUT4, glucose transporter 4; IR, insulin receptor; IRS, insulin receptor substrates; Km, Michaelis constant; PKB, protein kinase B; *p*NPP, *p*-nitrophenyl phosphate; PTP1B, Protein tyrosine phosphatase 1B; Vmax, maximum velocity

* Corresponding author. UCIBIO, REQUIMTE, Laboratory of Applied Chemistry, Department of Chemical Sciences, Faculty of Pharmacy, University of Porto, Rua de Jorge Viterbo Ferreira n.º 228, 4050-313 Porto, Portugal.
** Corresponding author. UCIBIO, REQUIMTE, Laboratory of Toxicology, Department of Biological Sciences, Faculty of Pharmacy, University of Porto, Rua de Jorge Viterbo Ferreira n.º 228, 4050-313 Porto, Portugal.
E-mail addresses: felixdc@ff.up.pt (F. Carvalho), egracas@ff.up.pt (E. Fernandes).

https://doi.org/10.1016/j.fct.2017.11.039
Received 21 September 2017; Received in revised form 5 November 2017; Accepted 19 November 2017
Available online 22 November 2017
0278-6915/ © 2017 Elsevier Ltd. All rights reserved.

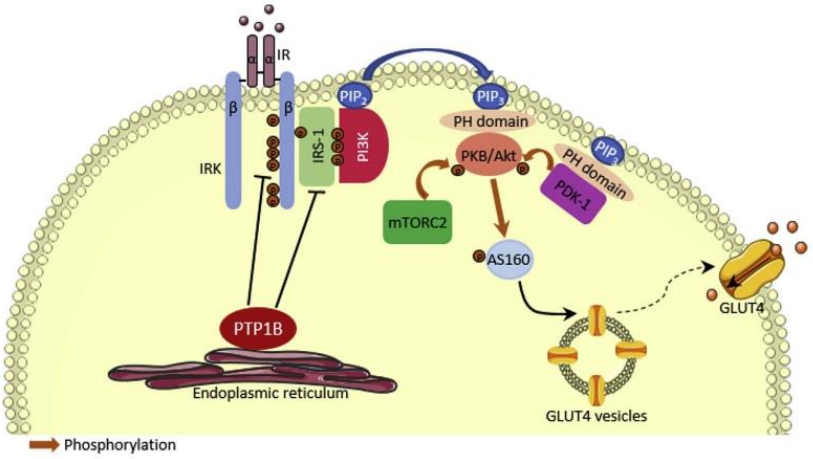


Fig. 1. Negative regulation of insulin signaling pathway by PTP1B.
Insulin binding to the extracellular α-subunit of its receptor induces the activation of insulin receptor (IR) through autophosphorylation. Tyrosine phosphorylation of insulin receptor substrates (IRS) promotes binding to phosphatidylinositol-3-kinase (PI3K). PI3K converts phosphatidylinositol 4,5-bisphosphate (PIP_2) to the lipid second messenger phosphatidylinositol 3,4,5-triphosphate (PIP_3), inducing the recruitment of 3-phosphoinositide dependent protein kinase-1 (PDK-1) to the plasma membrane, which phosphorylates the protein kinase B (PKB) (also known as Akt) at Thr308. PH domain is required for the recruitment of PKB/Akt and PDK-1 to the plasma membrane through high affinity binding to PIP3. The PKB-pThr308 increases the mechanistic (or mammalian) target of rapamycin complex 2 (mTORC2) activity, which in turn phosphorylates PKB at Ser473, thereby fully activating PKB. PKB phosphorylates PKB substrate of 160 kDa (AS160), facilitating translocation of glucose transporter 4 (GLUT4) from intracellular storage vesicles to plasma membrane and the consequent glucose uptake in cell. The endoplasmic reticulum-bounded protein tyrosine phosphatase (PTP1B) dephosphorylates IR, causing its deactivation. This process leads to the prevention of the PI3K and PKB activation and therefore the translocation of GLUT4 does not occur, causing a decrease of glucose transport into the cell.

(Kennedy and Ramachandran, 2000; Feldhammer et al., 2013; Panzhinskiy et al., 2013; Tamrakar et al., 2011–2014; Wang et al., 2015b; Sun et al., 2016). It was also described that PTP1B overexpression is closely related to a large number of diseases: liver disorders (Chen et al., 2015), obesity, cardiovascular complications, inflammation, endoplasmic reticulum (ER) stress and prostate and breast cancer (Feldhammer et al., 2013). Taking the above rationale into account, inhibition of PTP1B may modulate T2DM (and be potentially useful in the treatment of PTP1B related diseases), being an outstanding target for the treatment of this epidemic disease (Zhang and Lee, 2003; Zhang and Zhang, 2007). A large number of PTP1B inhibitors have been studied, the development of novel highly effective, selective and safe compounds still remains a challenge.

Flavonoids are phenolic compounds widely distributed in the Plant Kingdom and are important components of the human diet. The basic structural feature of flavonoids is a 2-phenyl-benzo-γ-pyrane nucleus consisting of two benzene rings (A and B rings) linked by a pyran heterocyclic ring (C ring) (Ribeiro et al., 2015a). Some flavonoids have already been described as inhibitors of PTP1B activity, such as morin (Paoli et al., 2013), quercetin (Jiang et al., 2015), luteolin (Choi et al., 2014a), apigenin (Choi et al., 2014b) and kaempferol (Paoli et al., 2013; Na et al., 2016). The main aim of the present work is to test a diversified panel of flavonoids (Fig. 2), with different types of substituents in different positions, including flavonoids that were never studied in what concerns their PTP1B inhibitory activity, establishing an accurate structure - activity relationship. For that purpose, an *in vitro* microanalysis screening system was used to test the panel of flavonoids. The type of inhibition of the most active flavonoids was also evaluated.

2. Material and methods

2.1. Chemicals

The following reagents were purchased from Sigma-Aldrich Co. LLC (St. Louis, USA): PTP1B (human recombinant), *p*-nitrophenyl phosphate (*p*NPP), dimethylsulfoxide (DMSO), citric acid, dithiotheritol (DTT), ethylenediaminetetraacetic acid (EDTA), compounds **D3** (baicalein), **D4** (apigenin), **D5** (kaempferol), **D6** (luteolin), **D7** (quercetin), **D8** (morin), **D9** (acacetin), **D10** (rutin), **E1** (naringenin), **E2** (eriodictyol), **E3** (taxifolin) and ursolic acid. Compounds **A1**, **A2**, **A3**, **A4**, **A5**, **A6**, **B1**, **B2**, **B3**, **B4**, **C1**, **C2**, **C3**, **C4**, **C5**, **C6**, **C8**, **C9**, **D1** (chrysin) and **D2** (galangin) were obtained from Indofine Chemical Company, Inc. (Stryker Lane Hillsborough, USA). Flavonoids **C7**, **C10**, **C11**, **C12** and **C13** were synthesized as previously described (Sousa et al., 2016). Sodium chloride (NaCl) was purchased from VWR Chemicals (Carnaxide, Portugal).

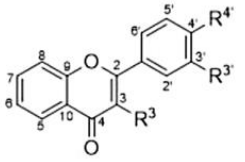
2.2. In vitro assay for PTP1B inhibitory activity

The PTP1B-catalyzed hydrolysis of the substrate, *p*NPP, was measured by monitoring the absorbance of the product *p*-nitrophenolate, at 405 nm. The assay was carried out in a 96-well microplate according to Nguyen et al. (2015), with some modifications. Briefly, to each well were added the enzyme (4 μg/mL), dissolved in a 50 mM citrate buffer (pH 6.0) [0.1 M NaCl, 1 mM EDTA and 1 mM DTT] and the flavonoids under study (0–200 μM) dissolved in DMSO [final concentration of 10% (v/v)]. After an incubation of 5 min at 37 °C, *p*NPP (2 mM) was added to the reaction mixture and incubated for 30 min at 37 °C. The enzymatic reaction was monitored in a microplate reader (Synergy HT, BIOTEK), through the measurement of the absorbance at 405 nm. Obtained values correspond to the slope measured between 5 and 20 min. The quantity of DMSO used did not interfere with the assay. **Ursolic acid** was used as positive control (0–20 μM). The results were expressed as the percentage of inhibition of PTP1B activity. The obtained results represent at least three independent experiments.

2.3. Inhibitory kinetic study

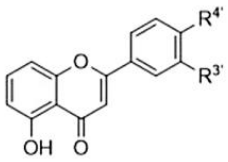
The inhibitory kinetic analysis was performed for the most active flavonoid from C and D group, **C13** (6.25–15.63 μM) and morin (**D8**) (25–50 μM), and for the positive control, **ursolic acid**, (5–15 μM).

Briefly, the enzyme (4 μg/mL), dissolved in 50 mM citrate buffer (pH 6.0), was pre-incubated during 5 min at 37 °C with the selected compounds. Then, *p*NPP (1 mM, 2 mM and 4 mM) was added and incubated in the reaction mixture for 30 min at 37 °C. Obtained values correspond to the slope measured between 5 and 20 min, at 405 nm. The study of the inhibition type (competitive, uncompetitive, non-competitive or mixed type inhibition) of the selected compounds was made using the nonlinear regression Michaelis - Menten enzymatic kinetics and the corresponding Lineweaver - Burk for each tested concentration of substrate and inhibitor. The obtained results represent at least four independent experiments.



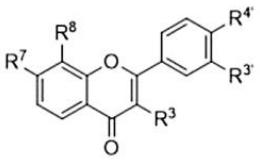
A1-6

A1: R^3= $R^{3'}$= $R^{4'}$= H (flavone)
A2: R^3= H, $R^{3'}$= OH, $R^{4'}$= H
A3: R^3= $R^{3'}$= H, $R^{4'}$= OH
A4: R^3= H, $R^{3'}$= $R^{4'}$= OH
A5: R^3= $R^{3'}$= $R^{4'}$= OH
A6: R^3= OH, $R^{3'}$= $R^{4'}$= OMe



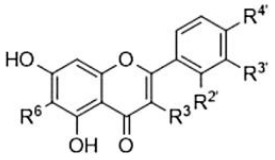
B1-4

B1: $R^{3'}$= $R^{4'}$= H
B2: $R^{3'}$= OH, $R^{4'}$= H
B3: $R^{3'}$= H, $R^{4'}$= OH
B4: $R^{3'}$= $R^{4'}$= OH



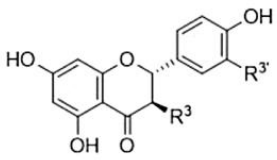
C1-13

C1: R^3= $R^{3'}$= $R^{4'}$= H, R^7= OH, R^8= H
C2: R^3= H, $R^{3'}$= OH, $R^{4'}$= H, R^7= OH, R^8= H
C3: R^3= $R^{3'}$= H, $R^{4'}$= R^7= OH, R^8= H
C4: R^3= $R^{3'}$= OH, $R^{4'}$= H, R^7= OH, R^8= H
C5: R^3= OH, $R^{3'}$= H, $R^{4'}$= R^7= OH, R^8= H
C6: R^3= H, $R^{3'}$= $R^{4'}$= R^7= OH, R^8= H
C7: R^3= $R^{3'}$= $R^{4'}$= R^7= R^8= OH
C8: R^3= OH, $R^{3'}$= OMe, $R^{4'}$= H, R^7= OMe, R^8= H
C9: R^3= OH, $R^{3'}$= H, $R^{4'}$= R^7= OMe, R^8= H
C10: R^3= $R^{3'}$= $R^{4'}$= OH, R^7= R^8= OMe
C11: R^3= OH, $R^{3'}$= $R^{4'}$= OMe, R^7= R^8= OH
C12: R^3= OH, $R^{3'}$= $R^{4'}$= OBn, R^7= R^8= OMe
C13: R^3= OH, $R^{3'}$= $R^{4'}$= OMe, R^7= R^8= OBn



D1-18

D1: $R^{2'}$= R^3= $R^{3'}$= $R^{4'}$= R^6= H (chrysin)
D2: $R^{2'}$= H, R^3= OH, $R^{3'}$= $R^{4'}$= R^6= H (galangin)
D3: $R^{2'}$= R^3= $R^{3'}$= $R^{4'}$= H, R^6= OH (baicalein)
D4: $R^{2'}$= R^3= $R^{3'}$= H, $R^{4'}$= OH, R^6= H (apigenin)
D5: $R^{2'}$= H, R^3= OH, $R^{3'}$= H, $R^{4'}$= OH, R^6= H (kaempferol)
D6: $R^{2'}$= R^3= H, $R^{3'}$= $R^{4'}$= OH, R^6= H (luteolin)
D7: $R^{2'}$= H, R^3= $R^{3'}$= $R^{4'}$= OH, R^6= H (quercetin)
D8: $R^{2'}$= R^3= OH, $R^{3'}$= H, $R^{4'}$= OH, R^6= H (morin)
D9: $R^{2'}$= R^3= $R^{3'}$= H, $R^{4'}$= OMe, R^6= H (acacetin)
D10: $R^{2'}$= H, R^3= rutinose, $R^{3'}$= $R^{4'}$= OH, R^6= H (rutin)



E1-3

E1: R^3= $R^{3'}$= H
E2: R^3= H, $R^{3'}$= OH
E3: R^3= $R^{3'}$= OH (taxifolin)

Fig. 2. Chemical structures of the tested flavonoids.

2.4. Statistical analysis

All the statistical treatments were performed using GraphPad Prism™ (version 7.0; GraphPad Software). Results of the *in vitro* assay for the PTP1B inhibitory activity are expressed as mean ± standard error of the mean (SEM). Statistical comparison between the active compounds was estimated using the one-way analysis of variance (ANOVA). Differences were considered to be significant at p values lower than 0.05.

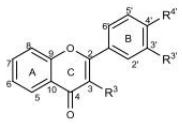
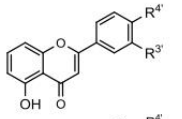
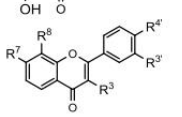
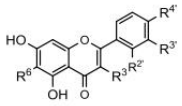
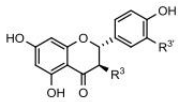
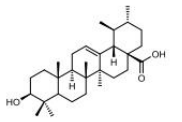
3. Results

3.1. In vitro inhibition assay for PTP1B activity

The studied flavonoids were divided into five groups (A - E) (Table 1), according to their structures.

In group A, based on the structure of flavone (**A1**), the studied flavonoids presented no or low activity up to the highest tested concentration (200 μM). From the tested flavonoids in group B, all presenting a 5-OH group in A ring, it was observed that the presence of a 4′-OH group in B ring slightly improved PTP1B inhibition. In

Table 1
Structure and *in vitro* PTP1B inhibitory activity of the tested flavonoids (IC_{50} μM ± SEM or % inhibition at the highest tested concentration).

Compound	Structure	$R^{2'}$	R^3	$R^{3'}$	$R^{4'}$	R^6	R^7	R^8	IC_{50} (μM) or % inhibition at the highest tested concentration
A1 (Flavone)		–	H	H	H	–	–	–	< 20% [200 μM *]
A2		–	H	OH	H	–	–	–	< 20% [200 μM *]
A3		–	H	H	OH	–	–	–	< 20% [200 μM *]
A4		–	H	OH	OH	–	–	–	27 ± 4% [200 μM *]
A5		–	OH	OH	OH	–	–	–	< 20% [200 μM *]
A6		–	OH	OMe	OMe	–	–	–	< 20% [100 μM *]
B1		–	–	H	H	–	–	–	29 ± 1% [200 μM *]
B2		–	–	OH	H	–	–	–	39 ± 5% [200 μM *]
B3		–	–	H	OH	–	–	–	184 ± 13 [(a)]
B4		–	–	OH	OH	–	–	–	< 20% [200 μM *]
C1		–	H	H	H	–	OH	H	< 20% [200 μM *]
C2		–	H	OH	H	–	OH	H	< 20% [200 μM *]
C3		–	H	H	OH	–	OH	H	< 20% [200 μM *]
C4		–	OH	OH	H	–	OH	H	153 ± 16 [(a)]
C5		–	OH	H	OH	–	OH	H	< 20% [200 μM *]
C6		–	H	OH	OH	–	OH	H	< 20% [200 μM *]
C7		–	OH	OH	OH	–	OH	OH	36 ± 3% [200 μM *]
C8		–	OH	OMe	H	–	OMe	H	27 ± 6% [100 μM *]
C9		–	OH	H	OMe	–	OMe	H	182 ± 15 [(a)]
C10		–	OH	OH	OH	–	OMe	OMe	< 20% [200 μM *]
C11		–	OH	OMe	OMe	–	OH	OH	< 20% [200 μM *]
C12		–	OH	OBn	OBn	–	OMe	OMe	16 ± 2 [(b)]
C13		–	OH	OMe	OMe	–	OBn	OBn	10 ± 1 [(c)]
D1 (Chrysin)		H	H	H	H	H	–	–	182 ± 1 [(a)]
D2 (Galangin)		H	OH	H	H	H	–	–	< 20% [200 μM *]
D3 (Baicalein)		H	H	H	H	OH	–	–	< 20% [200 μM *]
D4 (Apigenin)		H	H	H	OH	H	–	–	159 ± 20 [(a)]
D5 (Kaempferol)		H	OH	H	OH	H	–	–	< 20% [200 μM *]
D6 (Luteolin)		H	H	OH	OH	H	–	–	< 20% [200 μM *]
D7 (Quercetin)		H	OH	OH	OH	H	–	–	26 ± 1% [200 μM *]
D8 (Morin)		OH	OH	H	OH	H	–	–	37 ± 3 [(d)]
D9 (Acacetin)		H	H	H	OMe	H	–	–	91 ± 7 [(e)]
D10 (Rutin)		H	Rutinose	OH	OH	H	–	–	< 20% [200 μM *]
E1 (Naringenin)		–	H	H	–	–	–	–	< 20% [200 μM *]
E2 (Eriodictyol)		–	H	OH	–	–	–	–	< 20% [200 μM *]
E3 (Taxifolin)		–	OH	OH	–	–	–	–	< 20% [200 μM *]
Positive control: **Ursolic acid**		–	–	–	–	–	–	–	7.1 ± 0.9 [(c)]

*– Inhibition (mean % ± SEM) at the highest tested concentration (in superscript) at the assay conditions. The IC_{50} with different lowercase superscript letters are significantly different from each other ($p < 0.05$).

accordance, flavonoid **B3** was the most potent (IC_{50} = 184 ± 13 μM). It was not possible to determine the IC_{50} values of flavonoids **B1**, **B2** and **B4** up to 200 μM, the highest tested concentration.

Group C has the two most potent flavonoids, **C13** and **C12**, with IC_{50} values of 10 ± 1 μM and 16 ± 2 μM, respectively. Of note, the IC_{50} of the compound **C13** did not significantly differ from the IC_{50} of **ursolic acid**, the positive control (7.1 ± 0.9 μM). These results indicate that less polar substituents, -OBn and -OMe groups, increase the ability of flavonoids to inhibit PTP1B. In what concerns the other flavonoids from C group, with exception of flavonoids **C4** (IC_{50} = 153 ± 16 μM) and **C9** (IC_{50} = 182 ± 15 μM), it was not possible to determine the IC_{50} values up to the highest tested concentration, 200 μM.

From group D, the most potent compound was morin (**D8**) with an IC_{50} of 37 ± 3 μM. Comparing morin (**D8**) with kaempferol (**D5**), which presented no effect up to the highest tested concentration, 200 μM, it is clear that the lack of a 2′-OH group in B ring decreased considerably the inhibitory effect of the flavonoids. In what concerns flavonoid with-OMe groups, and comparing acacetin (D9) with apigenin (D4), presenting IC_{50} values of 91 ± 7 and 159 ± 20 μM, respectively, we can conclude that the substitution of a 4′-OH group by a

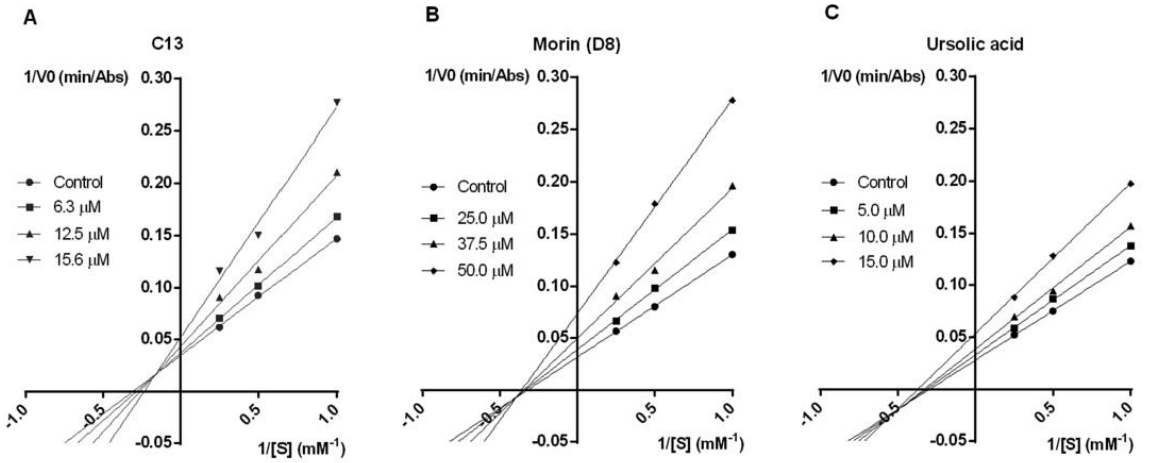


Fig. 3. Lineweaver-Burk double reciprocal plots of PTP1B inhibition by flavonoids **C13** (A), morin (**D8**) (B) and the positive control, **ursolic acid** (C).

4′-OMe group in B ring increased the PTP1B inhibition.

Analysing the activity of flavonoids from E group, it was possible to conclude that the lack of C2 = C3 double bond weakened the flavonoids' activity, since naringenin (**E1**), eriodictyol (**E2**) and taxifolin (**E3**) did not inhibit PTP1B activity.

3.2. Inhibitory kinetic study

Flavonoid **C13**, morin (**D8**) and **ursolic acid** were selected for the study of their type of inhibition (Fig. 3). Flavonoid **C13** and the positive control, **ursolic acid**, presented a mixed type of inhibition, since the Michaelis constant (Km) increased, while the maximum velocity (Vmax) decreased (Fig. 3A and C). Concerning the type of inhibition of morin (**D8**), the Km value remained constant and the Vmax value decreased, attesting a non-competitive inhibition type (Fig. 3B).

The inhibitory constant (Ki) values of the selected compounds were also determined. Flavonoid **C13**, morin (**D8**) and **ursolic acid** presented Ki values of 24 ± 5 μM, 60 ± 9 μM and 23 ± 4 μM respectively (Table 2).

4. Discussion

In the physiological environment, phosphorylation states are orchestrated by two dynamic and opposing groups of enzymes: protein tyrosine kinases (PTKs), which catalyse tyrosine phosphorylation, and protein tyrosine phosphatases (PTPs), which are responsible for dephosphorylation (Feldhammer et al., 2013; Zhang and Lee, 2003). The mechanism of phosphorylation/dephosphorylation of protein tyrosine residues, named protein tyrosine phosphorylation, is implicated in the control of fundamental cellular processes including cell growth, differentiation, proliferation, migration, apoptosis, metabolism, gene transcription, ion-channel activity, immune response, and bone development (Chen et al., 2015). The dysregulation of protein tyrosine phosphorylation is often associated to a large number of diseases, including diabetes, cancer, autoimmune, and neurodegenerative diseases (Chen et al., 2015; Zhang, 1998).

Table 2
Ki values ± SEM (μM) for the inhibition of human recombinant PTP1B.

Flavonoid	Type of inhibition	Ki (μM)
C13	Mixed	24 ± 5
Morin	Non-competitive	60 ± 9
Ursolic acid	Mixed	23 ± 4

PTP1B is the founding member of PTPs superfamily. It is the major non-transmembrane PTP in human tissues (Thareja et al., 2012), encoded by the *Ptpn1* gene, which is ubiquitously expressed in all tissues (Panzhinskiy et al., 2013). PTP1B is composed by an N-terminal catalytic domain, two proline-rich motifs and a C-terminal hydrophobic region, that anchors the protein to the cytoplasmic face of endoplasmic reticulum (ER) and promotes the ability to access substrates (Bakke and Haj, 2015; Lessard et al., 2010). Despite its physiological functions, PTP1B overproduction is responsible for the development of many diseases, including T2DM, obesity (Tamrakar et al., 2011–2014; Zhang and Lee, 2003; Thareja et al., 2012; Lee and Wang, 2007), cancer (Lessard et al., 2010; Yip et al., 2010), cardiovascular (Thiebaut et al., 2016), and liver (Chen et al., 2015) diseases. The establishment of PTP1B as a potential target in the treatment of T2DM was first reported in 1999 (Elchebly et al., 1999). At the present, only ertiprotafib and trodusquemine reached clinical trials as selective inhibitors of PTP1B (Erbe et al., 2005; Lantz et al., 2010; Song et al., 2016). Trodusquemine is still in phase 2 clinical trials (Cho, 2013; Qin et al., 2015; Smith et al., 2017). However, phase 2 of clinical trials for ertiprotafib was discontinued due to its lack of clinical efficacy and undesirable side effects (Nguyen et al., 2013). It was found that ertiprotafib did not behave as a simple competitive inhibitor since the inhibition followed a time-dependent and irreversible mechanism. It was observed high inhibition at lower PTP1B levels and later time points (van Huijsduijnen et al., 2002; Vintonyak et al., 2009). Moreover, the therapeutic activity of ertiprotafib is not specific, involving other mechanisms besides the inhibition of PTP1B, such as the activation of peroxisome proliferator-activated receptor (PPAR)-α and PPAR-γ (Erbe et al., 2005). Thus, the discovery and development of more effective and safer PTP1B inhibitors still is a topic of great interest among the scientific community.

In the present study, we explored the PTP1B inhibitory activity of a panel of flavonoids, tested under the same experimental conditions, in order to establish an accurate structure - activity relationship. The PTP1B inhibitory activity of the majority of the studied flavonoids was tested in the present work for the first time. The enzymatic activity of PTP1B was determined by measuring the hydrolysis of the colourless substrate *p*NPP into *p*-nitrophenolate, which can be quantified spectrophotometrically at 405 nm. The results reported in the literature about the effect of flavonoids against PTP1B activity are disperse and sometimes contradictory. These differences are mainly related with the experimental conditions where various concentrations of PTP1B (Paoli

et al., 2013; Jiang et al., 2015; Guo et al., 2015) and substrate, pNPP (Jiang et al., 2015; Guo et al., 2015; Islam et al., 2013), can be found and lead to different ranges of IC_{50} values. Moreover, the authors usually study a small number of flavonoids, which does not allow the establishment of an accurate structure-activity relationship. The screening method developed and applied in the present study offers a good opportunity to provide data in a more harmonized form. In addition, a large number of studies has been performed using end-point measurements with addition of sodium hydroxide (NaOH) or potassium hydroxide (KOH), to provide highest sensibility to the reaction, through the highest possible photometric readout. Nevertheless, the change of pH can also change the absorbance of the tested phytochemicals in the microplate wells, giving false positive or false negative results (Tahtah et al., 2016). Thus, in this work, we tested the potential inhibition of this enzyme by flavonoids in rate measurements, without change of pH, to obtain values as close to reality as possible.

Some of the tested flavonoids showed to be effective inhibitors of PTP1B, presenting IC_{50} values comparable to the positive control, **ursolic acid**. Compound **C13** (IC_{50} = 10 ± 1 μM), tested here for the first time, was the most effective inhibitor of PTP1B activity.

From A group, we verified that flavone (**A1**), without substituents, was not able to inhibit PTP1B. The addition of OH-groups at positions 3, 3′and/or 4′in B ring of the flavone structure did not provide a higher PTP1B inhibition, as it was possible to confirm by testing flavonoids **A2**, **A3**, **A4** and **A5**, since all of them showed none or low activity, up to 200 μM. The presence of a 3-OH group in C ring and of both 3′- and 4′-OMe groups in B ring (**A6**) also did not contribute to increase the ability to inhibit PTP1B. Interestingly, Nguyen et al. (2011), referred that the significant activity of flavonoids could be attributed to the presence of -OMe groups in B ring. However, the authors studied flavonoids with prenyl groups and without the C2=C3 double bond, which do not allow a direct comparison with the flavonoids tested in the present work.

Comparing flavonoids **A3**, which presents no inhibitory activity, and **B3**, with an IC_{50} of 184 ± 13 μM, we can conclude that the addition of a 5-OH group in A ring seems to slightly increase the PTP1B inhibition. To the best of our knowledge, flavonoids of B group were tested in the present work for the first time. Analysing the obtained results, we can conclude that among the tested flavonoids with a 5-OH group in A ring, the presence of another 4′-OH group in B ring seems to be slightly favourable for the PTP1B inhibition, as flavonoid **B3** was the most active of this group.

Group C has the most active flavonoids, namely **C13**, with an IC_{50} of 10 ± 1 μM, followed by **C12**, with an IC_{50} of 16 ± 2 μM, which were tested here for the first time. These results reinforce the idea that the presence of -OBn groups together with -OMe groups in the flavonoid structure significantly increases PTP1B inhibition. This observation is in agreement with those of Quang et al. (2015), who suggested that the presence of less polar substituents on the flavonoid structure are usually beneficial to the inhibitory activity against PTP1B, while the addition of polar groups, such as -OH, may decrease their ability to inhibit PTP1B. For example, the replacement of -OMe and -OBn groups (**C13**) by -OH groups (**C7**) drastically decreased the activity to 36 ± 3%, at the highest tested concentration, 200 μM.

Concerning flavonoid **C8**, it was not possible to determine the IC_{50} up to the highest tested concentration (100 μM). The change of the -OMe group in B ring from position 3' (**C8**) to position 4' (**C9**) seemed to slightly improve the PTP1B inhibition. In what concerns flavonoids with only -OH groups in their structure (**C1 - C5**), compound **C4** was the most active, indicating that 3-OH group in C ring and 3′-OH group in B ring favour the activity. Flavonoid **C3** did not show ability to inhibit PTP1B activity, which corroborates the results of the study of Guo et al. (2015), who tested flavonoids isolated from licorice (*Glycyrrhiza uralensis* Fish).

The most active flavonoid of D group was morin (**D8**), with an IC_{50} of 37 ± 3 μM, suggesting that the presence of -OH groups at 3 position of C ring, at 5 and 7 positions of A ring, and at 2′ and 4' positions of B ring favours the PTP1B inhibition. This result is in agreement with Paoli et al. (2013), that reported that morin is an effective inhibitor of PTP1B, presenting an IC_{50} value of 15 ± 0.8 μM. The difference of IC_{50} values between the present work and the study of Paoli et al. (2013). may be due to the use of KOH to stop the enzymatic reaction by these researchers. As it was also shown by the results obtained in the present work, Paoli et al. (2013). also demonstrated that morin was a better inhibitor than baicalein (**D3**), kaempferol (**D5**), luteolin (**D6**), quercetin (**D7**) and naringenin (**E1**).

In the work of Choi et al. (2014b) both apigenin and quercetin were effective inhibitors of PTP1B. Interestingly, in our work, apigenin (**D4**) presented an IC_{50} value of 159 ± 20 μM and it was not possible to achieve an IC_{50} value for quercetin (**D7**), at the maximum tested concentration (26 ± 1% of inhibition at 200 μM). Other works also demonstrated that quercetin (**D7**) was an effective PTP1B inhibitor (Jiang et al., 2015; Islam et al., 2013; Chen et al., 2002). These differences can be explained by the application of different experimental conditions, namely by the addition of NaOH to stop the reaction as well as the use of different concentrations of enzyme or substrate.

Concerning acacetin (**D9**), with a 4′-OMe group in B ring, it was possible to observe that the substitution of the 4′-OMe group by a 4′-OH group in B ring significantly decreased the PTP1B inhibition, as it is possible to see by comparing it with apigenin (**D4**). We also tested rutin (**D10**), which was not able to inhibit PTP1B, this result being in agreement with the study of Li et al. (2005). who tested compounds isolated from the plant *Ardisia japonica*, showing that the presence of a rutinose in the 3 position of C ring did not contribute for the increase of PTP1B inhibition.

It has been postulated that the double C2=C3 bond on flavonoids plays an important role in their anti-inflammatory activity (Ribeiro et al., 2013, 2015b). In the present work we also studied a group of flavonoids without the double bond at C2=C3: naringenin (**E1**), eriodictyol (**E2**) and taxifolin (**E3**). Making a comparison of their activities with their correspondent flavonoids from D group: naringenin (**E1**) with apigenin (**D4**), eriodictyol (**E2**) with luteolin (**D6**), and taxifolin (**E3**) with quercetin (**D7**), we can conclude that the absence of the double C2=C3 bond did not bring any advantage to the PTP1B inhibition.

Once defined the inhibitory activity of flavonoids, we studied the type of inhibition of the most active flavonoids **C13**, morin (**D8**) and the positive control, **ursolic acid**. The type of inhibition of the selected compounds against PTP1B activity was studied applying the Lineweaver - Burk plots. The Km value is the substrate concentration needed to achieve a half-maximum of the enzyme velocity, being the intersection of the lines in the x axis equal to −1 /Km. The Vmax value corresponds to the number of substrate molecules each enzyme site can convert to product, per unit of time (enzyme saturation), being the intersection of the lines in the y axis equal to 1/Vmax (Waldrop, 2009). As observed in Fig. 3A, flavonoid **C13** presented a mixed type of inhibition, since the Km value increased while the Vmax decreased. This means that both inhibitor and substrate can be attached to the enzyme, being the inhibitor attached out of the active site of PTP1B. In this inhibition type, the enzyme's binding activity is affected by the binding of the substrate or inhibitor. Despite the intensive research of flavonoids as potential PTP1B inhibitors, among the panel of flavonoids studied in the present work, to the best of our knowledge, morin (**D8**) was the only flavonoid studied before concerning its inhibition type (Paoli et al., 2013). As shown in Fig. 3B, the Km value remained constant while the Vmax value decreased, attesting a non-competitive inhibition type for morin (**D8**). This result means that the inhibitor can bind with equal affinity to both the free enzyme and substrate - enzyme complex. In this model, the inhibition is not surmountable by increasing substrate concentration. The non-competitive type of inhibition of morin (**D8**) was in agreement with the study of Paoli et al. (2013). As it was obtained for flavonoid **C13**, the positive control **ursolic acid**, also presented a mixed type of inhibition. As observed in Fig. 3C, the Km value increased while the Vmax value decreased. This result is in

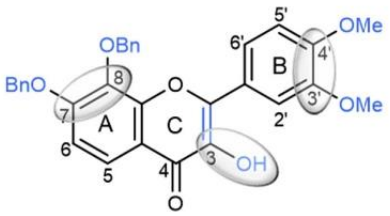


Fig. 4. Potential pattern substitution of flavonoids that contributes to increase PTP1B inhibition.

agreement with other authors who described **ursolic acid** as a competitive inhibitor (Choi et al., 2015; Na et al., 2006; Zhang et al., 2006).

The Ki values can also be a useful tool to compare the activity of the compounds, being reflective of the binding affinity of the inhibitor for the enzyme. Concerning the Ki values, flavonoid **C13**, morin (**D8**) and **ursolic acid** presented Ki values of 24 ± 5, 60 ± 9 and 23 ± 4 μM, respectively (Table 2). The obtained results suggest that the binding affinity of flavonoid **C13** and **ursolic acid** to the enzyme is similar. On the other hand, flavonoid **C13** has higher affinity to bind the enzyme than morin (**D8**).

5. Conclusion

In this work some promising flavonoids scaffolds were found as potential effective PTP1B inhibitors for the treatment of T2DM. The obtained results clearly show that the nature, position, and number of substituents present in the flavonoid scaffold are determinant for the inhibition of PTP1B activity. The majority of the flavonoids were here studied for the first time, including the most effective one, flavonoid **C13** (Fig. 4) that presented a mixed type of inhibition. These preliminary results prompt us to follow our rational using other cellular *in vitro* models and then test the most promising compound(s) in diabetes *in vivo* models. In the light of these preliminary results, we strongly hope that this compound(s) will increase insulin sensitivity resulting in a rise of the glucose transport into cells.

Conflicts of interest

The authors have declared no conflicts of interest.

Acknowledgments

The authors acknowledge the financial support from National funds [*Fundação para a Ciência e Tecnologia and Ministério da Educação e Ciência* (FCT/MEC)] and European Union funds [*Fundo Europeu de Desenvolvimento Regional* (FEDER)] under the program PT2020 (PT2020 UID/MULTI/04378/2013 - POCI/01/0145/FEDER/007728; QOPNA research unit FCT UID/QUI/00062/2013), the framework of QREN (NORTE-01-0145-FEDER-000024), and *Programa Operacional Competitividade e Internacionalização* (COMPETE) (PTDC/QEQ-QAN/1742/2014 – POCI-01-0145-FEDER-016530). Carina Proença acknowledges FCT the financial support for the PhD grant (SFRH/BD/116005/2016), in the ambit of "QREN - POPH - Tipologia 4.1 - Formação Avançada", co-sponsored by *Fundo Social Europeu* (FSE) and by national funds of *Ministério da Ciência, Tecnologia e Ensino Superior* (MCTES).

Transparency document

Transparency document related to this article can be found online at http://dx.doi.org/10.1016/j.fct.2017.11.039.

References

American Diabetes Association, 2011. Diagnosis and classification of diabetes mellitus. Diabetes Care 34, S62–S69.
Bakke, J., Haj, F.G., 2015. Protein-tyrosine phosphatase 1B substrates and metabolic regulation. Semin. Cell Dev. Biol. 37, 58–65.
Boucher, J., Kleinridders, A., Kahn, C.R., 2014. Insulin receptor signaling in normal and insulin-resistant states. Cold Spring Harb. Perspect. Biol. 6, 1–23.
Chen, R.M., Hu, L.H., An, T.Y., Li, J., Shen, Q., 2002. Natural PTP1B inhibitors from *Broussonetia papyrifera*. Bioorg Med. Chem. Lett. 12, 3387–3390.
Chen, P.J., Cai, S.P., Huang, C., Meng, X.M., Li, J., 2015. Protein tyrosine phosphatase 1B (PTP1B): a key regulator and therapeutic target in liver diseases. Toxicology 337, 10–20.
Cho, H., 2013. Protein tyrosine phosphatase 1B (PTP1B) and obesity. Vitam. Horm. 91, 405–424.
Choi, J.S., Islam, M.N., Ali, M.Y., Kim, Y.M., Park, H.J., Sohn, H.S., et al., 2014a. The effects of C-glycosylation of luteolin on its antioxidant, anti-Alzheimer's disease, anti-diabetic, and anti-inflammatory activities. Arch. Pharm. Res. 37, 1354–1363.
Choi, J.S., Islam, M.N., Ali, M.Y., Kim, E.J., Kim, Y.M., Jung, H.A., 2014b. Effects of C-glycosylation on anti-diabetic, anti-Alzheimer's disease and anti-inflammatory potential of apigenin. Food Chem. Toxicol. 64, 27–33.
Choi, J.S., Ali, M.Y., Jung, H.A., Oh, S.H., Choi, R.J., Kim, E.J., 2015. Protein tyrosine phosphatase 1B inhibitory activity of alkaloids from *Rhizoma Coptidis* and their molecular docking studies. J. Ethnopharmacol. 171, 28–36.
Elchebly, M., Payette, P., Michaliszyn, E., Cromlish, W., Collins, S., Loy, A.L., et al., 1999. Increased insulin sensitivity and obesity resistance in mice lacking the protein tyrosine phosphatase-1B gene. Science 283, 1544–1548.
Erbe, D.V., Wang, S., Zhang, Y.L., Harding, K., Kung, L., Tam, M., et al., 2005. Ertiprotafib improves glycemic control and lowers lipids via multiple mechanisms. Mol. Pharmacol. 67, 69–77.
Feldhammer, M., Uetani, N., Miranda-Saavedra, D., Tremblay, M.L., 2013. PTP1B: a simple enzyme for a complex world. Crit. Rev. Biochem. Mol. Biol. 48, 430–445.
Guo, Z., Niu, X., Xiao, T., Lu, J., Li, W., Zhao, Y., 2015. Chemical profile and inhibition of α-glycosidase and protein tyrosine phosphatase 1B (PTP1B) activities by flavonoids from licorice (*Glycyrrhiza uralensis* Fisch). J. Funct. Foods 14, 324–336.
International Diabetes Federation. IDF Diabetes Atlas, 2015. Available from: http://www.diabetesatlas.org/across-the-globe.html.
Islam, M.N., Jung, H.A., Sohn, H.S., Kim, H.M., Choi, J.S., 2013. Potent alpha-glucosidase and protein tyrosine phosphatase 1B inhibitors from *Artemisia capillaris*. Arch. Pharm. Res. 36, 542–552.
Jiang, L., Numonov, S., Bobakulov, K., Qureshi, M.N., Zhao, H., Aisa, H.A., 2015. Phytochemical profiling and evaluation of pharmacological activities of *Hypericum scabrum* L. Molecules 20, 11257–11271.
Kennedy, B.P., Ramachandran, C., 2000. Protein tyrosine phosphatase-1B in diabetes. Biochem. Pharmacol. 60, 877–883.
Lantz, K.A., Hart, S.G., Planey, S.L., Roitman, M.F., Ruiz-White, I.A., Wolfe, H.R., et al., 2010. Inhibition of PTP1B by trodusquemine (MSI-1436) causes fat-specific weight loss in diet-induced obese mice. Obesity 18, 1516–1523.
Lee, S., Wang, Q., 2007. Recent development of small molecular specific inhibitor of protein tyrosine phosphatase 1B. Med. Res. Rev. 27, 553–573.
Lessard, L., Stuible, M., Tremblay, M.L., 2010. The two faces of PTP1B in cancer. Biochim. Biophys. Acta 1804, 613–619.
Li, Y.F., Hu, L.H., Lou, F.C., Li, J., Shen, Q., 2005. PTP1B inhibitors from *Ardisia japonica*. J. Asian Nat. Prod. Res. 7, 13–18.
Na, M., Yang, S., He, L., Oh, H., Kim, B.S., Oh, W.K., et al., 2006. Inhibition of protein tyrosine phosphatase 1B by ursane-type triterpenes isolated from *Symplocos paniculata*. Planta Med. 72, 261–263.
Na, B., Nguyen, P.H., Zhao, B.T., Vo, Q.H., Min, B.S., Woo, M.H., 2016. Protein tyrosine phosphatase 1B (PTP1B) inhibitory activity and glucosidase inhibitory activity of compounds isolated from *Agrimonia pilosa*. Pharm. Biol. 54, 474–480.
Nguyen, P.H., Dao, T.T., Kim, J., Phong, D.T., Ndinteh, D.T., Mbafor, J.T., et al., 2011. New 5-deoxyflavonoids and their inhibitory effects on protein tyrosine phosphatase 1B (PTP1B) activity. Bioorg Med. Chem. 19, 3378–3383.
Nguyen, L.K., Matallanas, D., Croucher, D.R., von Kriegsheim, A., Kholodenko, B.N., 2013. Signalling by protein phosphatases and drug development: a systems-centred view. Febs J. 280, 751–765.
Nguyen, P.H., Ji, D.J., Han, Y.R., Choi, J.S., Rhyu, D.Y., Min, B.S., et al., 2015. Selaginellin and biflavonoids as protein tyrosine phosphatase 1B inhibitors from *Selaginella tamariscina* and their glucose uptake stimulatory effects. Bioorg Med. Chem. 23, 3730–3737.
Panzhinskiy, E., Ren, J., Nair, S., 2013. Pharmacological inhibition of protein tyrosine phosphatase 1B: a promising strategy for the treatment of obesity and type 2 diabetes mellitus. Curr. Med. Chem. 20, 2609–2625.
Paoli, P., Cirri, P., Caselli, A., Ranaldi, F., Bruschi, G., Santi, A., et al., 2013. The insulin-mimetic effect of morin: a promising molecule in diabetes treatment. Biochim. Biophys. Acta 1830, 3102–3111.
Qian, S., Zhang, M., He, Y., Wang, W., Liu, S., 2016. Recent advances in the development of protein tyrosine phosphatase 1B inhibitors for type 2 diabetes. Future Med. Chem. 8, 1239–1258.
Qin, Z., Pandey, N.R., Zhou, X., Stewart, C.A., Hari, A., Huang, H., et al., 2015. Functional properties of claramine: a novel PTP1B inhibitor and insulin-mimetic compound. Biochem. Biophys. Res. Commun. 458, 21–27.
Quang, T.H., Ngan, N.T., Yoon, C.S., Cho, K.H., Kang, D.G., Lee, H.S., et al., 2015. Protein tyrosine phosphatase 1B inhibitors from the roots of *Cudrania tricuspidata*. Molecules 20, 11173–11183.

Ribeiro, D., Freitas, M., Tome, S.M., Silva, A.M., Porto, G., Fernandes, E., 2013. Modulation of human neutrophils' oxidative burst by flavonoids. Eur. J. Med. Chem. 67, 280–292.
Ribeiro, D., Freitas, M., Lima, J.L., Fernandes, E., 2015a. Proinflammatory pathways: the modulation by flavonoids. Med. Res. Rev. 35, 877–936.
Ribeiro, D., Freitas, M., Tome, S.M., Silva, A.M., Laufer, S., Lima, J.L., et al., 2015b. Flavonoids inhibit COX-1 and COX-2 enzymes and cytokine/chemokine production in human whole blood. Inflammation 38, 858–870.
Smith, A.M., Maguire-Nguyen, K.K., Rando, T.A., Zasloff, M.A., Strange, K.B., Yin, V.P., 2017. The protein tyrosine phosphatase 1B inhibitor MSI-1436 stimulates regeneration of heart and multiple other tissues. npg Regen. Med. 4, 1–10.
Song, G.J., Jung, M., Kim, J.H., Park, H., Rahman, M.H., Zhang, S., et al., 2016. A novel role for protein tyrosine phosphatase 1B as a positive regulator of neuroinflammation. J. Neuroinflammation 13, 1–14.
Sousa, J.L.C., Proença, C., Freitas, M., Fernandes, E., Silva, A.M.S., 2016. New polyhydroxylated flavon-3-ols and 3-hydroxy-2-styrylchromones: synthesis and ROS/RNS scavenging activities. Eur. J. Med. Chem. 119, 250–259.
Sun, J., Qu, C., Wang, Y., Huang, H., Zhang, M., Li, H., et al., 2016. PTP1B, a potential target of type 2 diabetes mellitus. Mol. Biol. 5, 1–6.
Tahtah, Y., Wubshet, S.G., Kongstad, K.T., Heskes, A.M., Pateraki, I., Moller, B.L., et al., 2016. High-resolution PTP1B inhibition profiling combined with high-performance liquid chromatography-high-resolution mass spectrometry-solid-phase extraction-nuclear magnetic resonance spectroscopy: proof-of-concept and antidiabetic constituents in crude extract of *Eremophila lucida*. Fitoterapia 110, 52–58.
Tamrakar, A.K., Maurya, C.K., Rai, A.K., 2011-2014. PTP1B inhibitors for type 2 diabetes treatment: a patent review. Expert Opin. Ther. Pat. 2014 (24), 1101–1115.
Thareja, S., Aggarwal, S., Bhardwaj, T.R., Kumar, M., 2012. Protein tyrosine phosphatase 1B inhibitors: a molecular level legitimate approach for the management of diabetes mellitus. Med. Res. Rev. 32, 459–517.
Thiebaut, P.A., Besnier, M., Gomez, E., Richard, V., 2016. Role of protein tyrosine phosphatase 1B in cardiovascular diseases. J. Mol. Cell Cardiol. 101, 50–57.
van Huijsduijnen, R.H., Bombrun, A., Swinnen, D., 2002. Selecting protein tyrosine phosphatases as drug targets. Drug Discov. Today 7, 1013–1019.
Vintonyak, V.V., Antonchick, A.P., Rauh, D., Waldmann, H., 2009. The therapeutic potential of phosphatase inhibitors. Curr. Opin. Chem. Biol. 13, 272–283.
Waldrop, G.L., 2009. A qualitative approach to enzyme inhibition. Biochem. Mol. Biol. Educ. 37, 11–15.
Wang, L.J., Jiang, B., Wu, N., Wang, S.Y., Shi, D.Y., 2015a. Small molecules as potent protein tyrosine phosphatase 1B (PTP1B) inhibitors documented in patents from 2009 to 2013. Mini Rev. Med. Chem. 15, 104–122.
Wang, L.J., Jiang, B., Wu, N., Wang, S.Y., Shi, D.Y., 2015b. Natural and semisynthetic protein tyrosine phosphatase 1B (PTP1B) inhibitors as anti-diabetic agents. RSC Adv. 5, 48822–48834.
Yip, S.C., Saha, S., Chernoff, J., 2010. PTP1B: a double agent in metabolism and oncogenesis. Trends Biochem. Sci. 35, 442–449.
Youngren, J.F., 2007. Regulation of insulin receptor function. Cel. Mol. Life Sci. 64, 873–891.
Zhang, Z.Y., 1998. Protein-tyrosine phosphatases: biological function, structural characteristics, and mechanism of catalysis. Crit. Rev. Biochem. Mol. Biol. 33, 1–52.
Zhang, Z.Y., Lee, S.Y., 2003. PTP1B inhibitors as potential therapeutics in the treatment of type 2 diabetes and obesity. Expert Opin. Investig. Drugs 12, 223–233.
Zhang, S., Zhang, Z.Y., 2007. PTP1B as a drug target: recent developments in PTP1B inhibitor discovery. Drug Discov. Today 12, 373–381.
Zhang, W., Hong, D., Zhou, Y., Zhang, Y., Shen, Q., Li J-y, et al., 2006. Ursolic acid and its derivative inhibit protein tyrosine phosphatase 1B, enhancing insulin receptor phosphorylation and stimulating glucose uptake. Biochim. Biophys. Acta 1760, 1505–1512.

II.4. The dipeptidyl peptidase-4 inhibitory effect of flavonoids is hindered in protein rich environments

Version of record from Food & Function

Copyright © (2019) with kind permission of Royal Society of Chemistry

Food & Function

PAPER



Cite this: *Food Funct.*, 2019, **10**, 5718

The dipeptidyl peptidase-4 inhibitory effect of flavonoids is hindered in protein rich environments†

Carina Proença,[a] Marisa Freitas,[a] Daniela Ribeiro,[a] Sara M. Tomé,[b] Alberto N. Araújo,[a] Artur M. S. Silva,[b] Pedro A. Fernandes[c] and Eduarda Fernandes*[a]

Received 8th April 2019,
Accepted 18th July 2019

DOI: 10.1039/c9fo00722a

rsc.li/food-function

Dipeptidyl peptidase-4 (DPP-4) inhibitors present a unique approach for the management of type 2 diabetes (T2D). In the present study, the inhibition of DPP-4 was evaluated for a large panel of flavonoids, important components of the human diet, using *in vitro* and *ex vivo* models. The activity of the isolated enzyme was assayed *in vitro*. Subsequently, the most active flavonoids were tested *ex vivo* in human whole blood and plasma. In this study, contrary to the *in vitro* fluorometric tests, flavonoids did not show inhibitory activity against DPP-4. Due to the discrepancy in the results between the *in vitro* and *ex vivo* approaches, plasma protein binding values were determined, presenting values from 43.9 to 100.0%. This work provides a new insight into the inhibitory activity for DPP-4, based on the flavonoid scaffold. Additionally, the obtained results showed that the inhibitory effect of flavonoids against DPP-4 was hindered in protein rich environments, like that occurring in blood, and indicated the need for experimental refinement in drug discovery for blood targets.

1. Introduction

According to the International Diabetes Federation (IDF), diabetes mellitus currently affects over 425 million adults worldwide.[1] Particularly, type 2 diabetes (T2D) is responsible for about 90 to 95% of all cases of diabetes and is characterized by chronic hyperglycaemia as a result of a progressive loss of insulin secretion by pancreatic β-cells, commonly in the background of insulin resistance.[1]

Traditional antidiabetic agents, such as sulfonylureas and thiazolidinediones, have been associated with several adverse effects. For this reason, the search for new, safer, and effective antidiabetic drugs has resulted in the development of new classes of therapeutic agents. Dipeptidyl peptidase-4 (DPP-4) inhibitors are among the most recently developed antidiabetic drugs, targeting fasting and postprandial blood glucose and reducing hypoglycaemia risk.[2,3]

The DPP-4 family has the following members: DPP-4, DPP-6, DPP-8, DPP-9, DPP-10 and fibroblast activation protein (FAP).[4,5] DPP-4 and FAP are membrane-bound cell surface proteases and also have soluble forms, DPP-8 and DPP-9 are intracellular proteases, and DPP-6 and DPP-10 are non-enzymatic and membrane-bound proteins.[5] DPP-4 (EC 3.4.14.5), also known as CD26, is the most well-characterized member of the DPP-4 family. DPP-4 is a 766 amino acid glycoprotein and a type II transmembrane protein with a typical α/β hydrolase fold, consisting of the following domains: a short cytoplasmic domain, a transmembrane domain, and an extracellular domain, which can be further separated by a highly glycosylated region, a cysteine-rich region and a catalytic region (Fig. 1).[3,6]

DPP-4, as a member of the type II transmembrane proteins, has a typical signal peptide, which is required for the targeting to the endoplasmic reticulum and translocation across the cell membrane, and serves as a membrane anchor. The circulating or soluble form of DPP-4, without the cytoplasmic domain and the transmembrane region, is cleaved off the membrane by matrix metalloproteases (MMPs), a process known as shedding (Fig. 1). Since DPP-4 is shedded from the cell membrane, with intact enzymatic activity and cysteine-rich regions, it can exert

[a]*LAQV, REQUIMTE, Laboratory of Applied Chemistry, Department of Chemical Sciences, Faculty of Pharmacy, University of Porto, 4050-313 Porto, Portugal. E-mail: egracas@ff.up.pt*
[b]*QOPNA and LAQV, REQUIMTE, Department of Chemistry, University of Aveiro, 3810-193 Aveiro, Portugal*
[c]*UCIBIO, REQUIMTE, Department of Chemistry and Biochemistry, Faculty of Sciences, University of Porto, 4169-007 Porto, Portugal*

†Electronic supplementary information (ESI) available. See DOI: 10.1039/c9fo00722a

This journal is © The Royal Society of Chemistry 2019

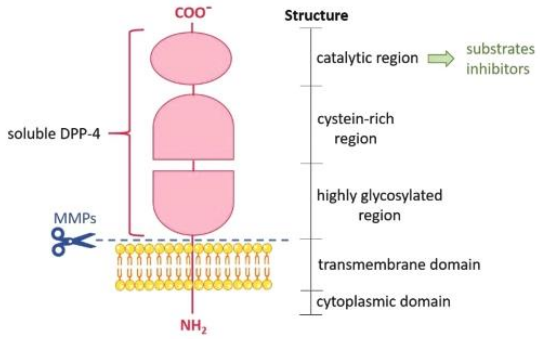


Fig. 1 Schematic representation of the dipeptidyl peptidase-4 (DPP-4) monomer bound to the cell membrane (adapted from ref. 6 and 9). The vertical black bar on the right represents the DPP-4 primary structure with the indication of the different domains and regions. Substrates or inhibitors (in green) interact with the catalytic region of the enzyme structure. Shedding of DPP-4 from the cell membrane by matrix metalloproteinases (MMPs) is indicated by a scissor symbol in blue.

biological functions in a paracrine or endocrine manner.[6] DPP-4 with catalytic activity is liberated from the plasma membrane, originating a soluble circulating form (727 amino acids), without the intracellular tail and the transmembrane regions, which accounts for a high DPP-4 activity in human plasma.[7]

This enzyme is expressed in multiple cell types and tissues, namely the epithelial cells in the liver, gut, uterus and kidneys; endothelial cells; fibroblasts and leukocyte subsets. The soluble circulating form of DPP-4 is present in serum, seminal fluid, saliva, kidneys, liver and bile.[5,8]

Besides its important role in T2D, DPP-4 is also important in immune cell activation, the release of soluble DPP-4 being increased upon tumour necrosis factor (TNF)-α and insulin stimulation. In fact, there is clear evidence that increased circulating levels of soluble DPP-4 is associated with several hallmarks of diabetes and obesity, including insulin resistance, increased body mass index (BMI) and adipocyte hypertrophy.[6] The biological activities of this enzyme, namely its role in glucose homeostasis and immune response, are associated with the interactions with the extracellular part of DPP-4. The catalytic domain contains a catalytic triad (Ser, Asp, and His), which is responsible for the inactivation of glucose-dependent insulinotropic polypeptide (GIP) and glucagon like peptide-1 (GLP-1) (also known as incretin hormones) by removing their N-terminal dipeptide.[9,10] GIP is a 42-amino acid hormone secreted by K cells in the upper small intestine, while GLP-1 is a 31-amino acid hormone produced from proglucagon and secreted by L cells in the lower intestine (ileum) and colon.[11,12] After glucose ingestion, both hormones exert their insulinotropic effect, through binding to specific receptors in pancreatic β cells, the GIP receptor (GIPR) and the GLP-1 receptor (GLP-1R). Then, adenylate cyclase activation is triggered and translated by increased levels of cytoplasmic cyclic adenosine monophosphate (cAMP), and enhanced exocytosis of insulin-containing granules (Fig. 2) in a concentration-dependent manner.[11] These two DPP-4 substrates, GIP and GLP-1, account for about 60% of postprandial insulin secretion.[4]

GIP and GLP-1 rapidly undergo proteolytic degradation by DPP-4 in plasma, which cleaves the two NH2-terminal amino acids of these hormones and inactivates their insulinotropic effects.[11] It was shown that DPP-4 inactivates not only incretins but also several cytokines, chemokines and neuropeptides

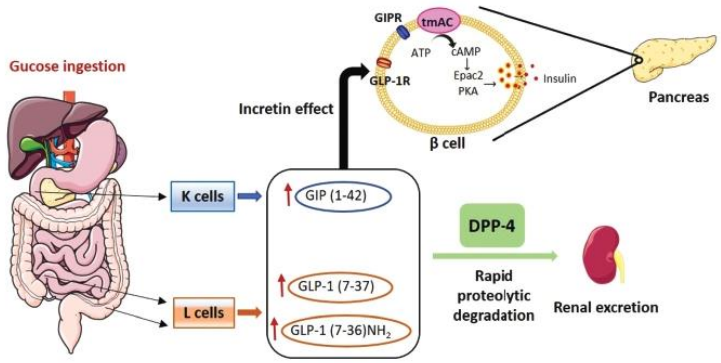


Fig. 2 Metabolic pathway of dipeptidyl peptidase-4 (DPP-4). Incretin hormones, glucose-insulinotropic polypeptide (GIP) and glucagon like peptide-1 (GLP-1), are released after a meal or oral glucose ingestion. GIP is secreted from K cells present in the duodenum and proximal jejunum, and GLP-1 is secreted from L cells present in the ileum and colon. Binding of GIP and GLP-1 to their receptors, GIPR and GLP-1R, in pancreatic β cells, results in an increase of cyclic adenosine monophosphate (cAMP) catalyzed by transmembrane adenylyl cyclase (tmAC). cAMP activates the guanine nucleotide exchange factor (Epac2) and protein kinase A (PKA) in order to potentiate glucose-stimulated insulin secretion. This process enhances the exocytosis of insulin-containing granules and consequent secretion of insulin in a glucose-dependent manner. GIP and GLP-1 have short half-lives since they are rapidly degraded by the proteolytic enzyme DPP-4, which decreases their insulinotropic effects. The inactivated GIP and GLP-1 are excreted through the kidneys.

This journal is © The Royal Society of Chemistry 2019

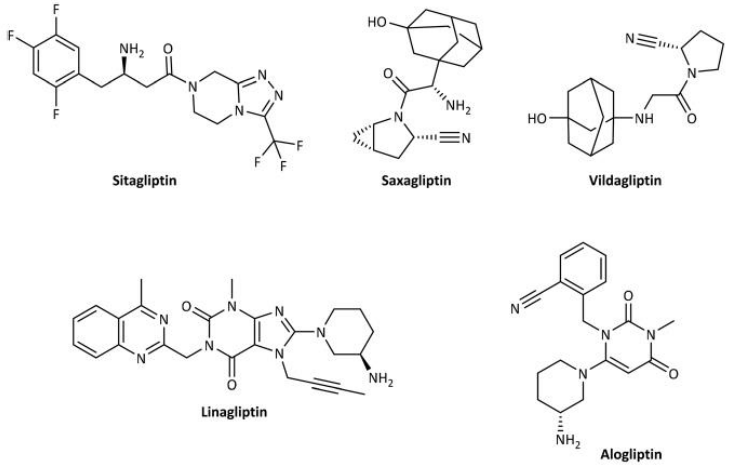


Fig. 3 Chemical structures of DPP-4 inhibitors applied in the treatment of T2D.

associated with inflammation and vascular function. In that sense, DPP-4 is an important target in the management of T2D and for preventing inflammatory reactions in diabetic patients.[8,10,13]

DPP-4 inhibitors globally available for the treatment of T2D include sitagliptin, saxagliptin, vildagliptin, linagliptin and alogliptin[3,14,15] (Fig. 3). Their use in therapeutics is beneficial in the early stages and throughout T2D as evidenced by a previous study where sitagliptin and vildagliptin lowered HbA1c levels in patients with longstanding T2D for more than 10 years.[16] Nonetheless, an increased hospitalization risk was found due to heart failure in subjects treated with saxagliptin and alogliptin without previous history of heart failure and in patients with existing cardiovascular disease.[2,17] Other adverse findings include increased risk of nasopharyngitis, headaches and urinary tract infections.[18] Moreover, all diabetic patients initiating treatment with DPP-4 inhibitors should be monitored for hypersensitivity and skin disorders. Kidney (in the case of treatment with sitagliptin) and liver (in the case of treatment with vildagliptin) functions also require careful monitoring.[19]

In view of the metabolic importance, disease morbidity and adverse effects of the inhibitors used in therapeutics, the search for new effective and safer DPP-4 inhibitors remains a hot scientific topic.[20,21] Flavonoids, a numerous group of phenolic compounds widely found in nature, have been recognized as promising lead compounds for the management of T2D.[22–27] Some flavonoids, such as luteolin,[28] apigenin,[28,29] rutin,[30] kaempferol[28,31] and naringin,[32] have already been evaluated in this context. However, the use of DPP-4 from different sources (human or porcine) and the use of different methods (luminescence, fluorometric or colorimetric) hampers the systematic comparison of results among studies. Aiming to contribute to a clearer view, this work looks over a panel of 45 flavonoids, divided according to their structural features into five groups (A–E) (Fig. 4), where their ability to inhibit human DPP-4 was assessed, based on *in vitro* colorimetric and fluorometric methods, using the isolated recombinant human enzyme. The study of this large panel of flavonoids allowed the establishment of an accurate and adequate structure–activity relationship and the selection of the most active flavonoid for the determination of its type of inhibition. The activity of selected flavonoids was also tested in human whole blood and plasma to confirm their potential as DPP-4 inhibitors. The affinity of flavonoids for plasma proteins was also studied.

2. Materials and methods

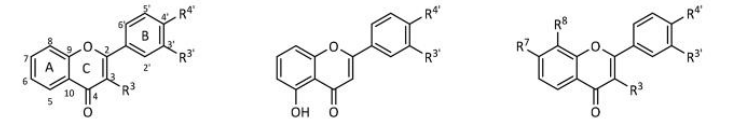
2.1. Materials

The following products were purchased from Sigma-Aldrich Co. LLC (St Louis, MO): DPP-4 enzyme (human recombinant), Gly-Pro *p*-nitroanilide hydrochloride (GPPN), Trizma® base, hydrochloric acid (HCl), dimethyl sulfoxide (DMSO), Dulbecco's phosphate buffered saline, without calcium chloride and magnesium (PBS), sitagliptin phosphate monohydrate, flavonoids **D3** (baicalein), **D4** (apigenin), **D6** (kaempferol), **D7** (luteolin), **D8** (quercetin), **D9** (morin), **D15** (chrysoeriol), **D16** (acacetin), **D17** (hispidulin), **D19** (rutin), **E1** (naringenin), **E2** (eriodictyol) and **E3** (taxifolin). Flavonoids **A1–A6**, **B1–B4**, **C1–C6**, **C8**, **C9**, **D1** (chrysin), **D2** (galangin) and **D5** were obtained from Indofine Chemical Company, Inc. (Hillsborough, NJ). H-Gly-Pro-7-amido-4-methylcoumarin hydrobromide (GP-AMC) was purchased from Bachem (Bubendorf, Switzerland). Diprotin A was purchased from Enzo Life Sciences. Flavonoids **C7**, **C10–C13**, **D10–D14** and **D18** were synthesized as previously described.[33,34]

2.2. *In vitro* inhibition of DPP-4 activity

2.2.1. Colorimetric method. The colorimetric assay for the study of the inhibitory effect of flavonoids against DPP-4 activity was based on a method described by Parmar *et al.*,[32]

 This journal is © The Royal Society of Chemistry 2019



A1-6

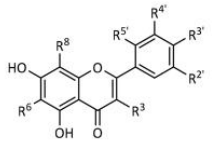
A1: R^3= $R^{3'}$= $R^{4'}$= H (Flavone)
A2: R^3= H, $R^{3'}$= OH, $R^{4'}$= H
A3: R^3= $R^{3'}$= H, $R^{4'}$= OH
A4: R^3= H, $R^{3'}$= $R^{4'}$= OH
A5: R^3= $R^{3'}$= $R^{4'}$= OH
A6: R^3= OH, $R^{3'}$= $R^{4'}$= OMe

B1-4

B1: $R^{3'}$= $R^{4'}$= H
B2: $R^{3'}$= OH, $R^{4'}$= H
B3: $R^{3'}$= H, $R^{4'}$= OH
B4: $R^{3'}$= $R^{4'}$= OH

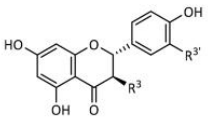
C1-13

C1: R^3= $R^{3'}$= $R^{4'}$= H, R^7= OH, R^8= H
C2: R^3= H, $R^{3'}$= OH, $R^{4'}$= H, R^7= OH, R^8= H
C3: R^3= $R^{3'}$= H, $R^{4'}$= R^7= OH, R^8= H
C4: R^3= $R^{3'}$= OH, $R^{4'}$= H, R^7= OH, R^8= H
C5: R^3= OH, $R^{3'}$= H, $R^{4'}$= R^7= OH, R^8= H
C6: R^3= H, $R^{3'}$= $R^{4'}$= R^7= OH, R^8= H
C7: R^3= $R^{3'}$= $R^{4'}$= R^7= R^8= OH
C8: R^3= OH, $R^{3'}$= OMe, $R^{4'}$= H, R^7= OMe, R^8= H
C9: R^3= OH, $R^{3'}$= H, $R^{4'}$= R^7= OMe, R^8= H
C10: R^3= $R^{3'}$= $R^{4'}$= OH, R^7= R^8= OMe
C11: R^3= OH, $R^{3'}$= $R^{4'}$= OMe, R^7= R^8= OH
C12: R^3= OH, $R^{3'}$= $R^{4'}$= OBn, R^7= R^8= OMe
C13: R^3= OH, $R^{3'}$= $R^{4'}$= OMe, R^7= R^8= OBn



D1-19

D1: $R^{2'}$= R^3= $R^{3'}$= $R^{4'}$= $R^{5'}$= R^6= R^8= H (Chrysin)
D2: $R^{2'}$= H, R^3= OH, $R^{3'}$= $R^{4'}$= $R^{5'}$= R^6= R^8= H (Galangin)
D3: $R^{2'}$= R^3= $R^{3'}$= $R^{4'}$= $R^{5'}$= H, R^6= OH, R^8= H (Baicalein)
D4: $R^{2'}$= R^3= H, $R^{3'}$= OH, $R^{4'}$= $R^{5'}$= R^6= R^8= H
D5: $R^{2'}$= R^3= $R^{3'}$= H, $R^{4'}$= OH, $R^{5'}$= R^6= R^8= H (Apigenin)
D6: $R^{2'}$= H, R^3= OH, $R^{3'}$= H, $R^{4'}$= OH, $R^{5'}$= R^6= R^8= H (Kaempferol)
D7: $R^{2'}$= R^3= H, $R^{3'}$= $R^{4'}$= OH, $R^{5'}$= R^6= R^8= H (Luteolin)
D8: $R^{2'}$= H, R^3= $R^{3'}$= $R^{4'}$= OH, $R^{5'}$= R^6= R^8= H (Quercetin)
D9: $R^{2'}$= R^3= OH, $R^{3'}$= H, $R^{4'}$= OH, $R^{5'}$= R^6= R^8= H (Morin)
D10: $R^{2'}$= H, R^3= Cl, $R^{3'}$= $R^{4'}$= OH, $R^{5'}$= R^6= R^8= H
D11: $R^{2'}$= R^3= H, $R^{3'}$= $R^{4'}$= OH, $R^{5'}$= H, R^6= Cl, R^8= H
D12: $R^{2'}$= R^3= H, $R^{3'}$= $R^{4'}$= OH, $R^{5'}$= R^6= H, R^8= Cl
D13: $R^{2'}$= H, R^3= Cl, $R^{3'}$= $R^{4'}$= OH, $R^{5'}$= R^6= H, R^8= Cl
D14: $R^{2'}$= R^3= H, $R^{3'}$= $R^{4'}$= OH, $R^{5'}$= H, R^6= R^8= Cl
D15: $R^{2'}$= R^3= H, $R^{3'}$= OMe, $R^{4'}$= OH, $R^{5'}$= R^6= R^8= H (Chrysoeriol)
D16: $R^{2'}$= R^3= $R^{3'}$= H, $R^{4'}$= OMe, $R^{5'}$= R^6= R^8= H (Acacetin)
D17: $R^{2'}$= R^3= $R^{3'}$= H, $R^{4'}$= OH, $R^{5'}$= H, R^6= OMe, $R^{8'}$= H (Hispidulin)
D18: $R^{2'}$= R^3= H, $R^{3'}$= $R^{4'}$= OMe, $R^{5'}$= R^6= R^8= H
D19: $R^{2'}$= H, R^3= rutinose, $R^{3'}$= $R^{4'}$= OH, $R^{5'}$= R^6= R^8= H (Rutin)



E1-3

E1: R^3= $R^{3'}$= H
E2: R^3= H, $R^{3'}$= OH
E3: R^3= $R^{3'}$= OH

Fig. 4 Chemical structures of the tested flavonoids.

with slight modifications. The assay was carried out by monitoring the DPP-4 mediated cleavage of the substrate GPPN to release *p*-nitroanilide, at 405 nm. Briefly, in a 96-well microplate, DPP-4 (150 U mL^{-1}), dissolved in Tris-HCl (50 mM, pH 8.0), was pre-incubated at 37 °C, for 10 min, with the tested flavonoids (0–200 μM) dissolved in DMSO [final concentration of 9.1% (v/v)]. Subsequently, GPPN (0.25 mM), dissolved in Tris-HCl (50 mM, pH 8.0), was added. Kinetic readings were initiated immediately after the addition of GPPN and maintained for 60 min, at 37 °C. The enzymatic reaction was monitored using a microplate reader (Synergy HT, BIO-TEK), by measuring the absorbance at 405 nm. The concentrations of DPP-4 and of the tested flavonoids refer to those attained before the addition of the substrate. The amount of DMSO used had no interference in the assay. The effects are expressed as the % inhibition of DPP-4 activity, calculated using the slope of the enzymatic reaction between 5 and 60 min. Sitagliptin (0–0.8 μM) and diprotin A (0–500 μM) were used as positive controls. The obtained results represent at least three independent experiments.

2.2.2. Fluorometric method. The fluorometric assay for the study of the inhibitory effect of flavonoids against DPP-4

activity was based on a method described by Morikawa *et al.*,[30] with slight modifications. The assay was carried out by monitoring the DPP-4 mediated cleavage of the non-fluorescent substrate GP-AMC to release a fluorescent product, 7-amino-4-methylcoumarin (AMC) (λ_{ex} = 360 nm/λ_{em} = 460 nm). Briefly, in a 96-well microplate, DPP-4 (38 U mL^{-1}), dissolved in Tris-HCl (50 mM, pH 8.0), was pre-incubated at 37 °C, for 10 min, with the tested flavonoids (0–200 μM), dissolved in DMSO [final concentration of 9.1% (v/v)]. Subsequently, GP-AMC (0.125 mM), dissolved in Tris-HCl (50 mM, pH 8.0), was added. Photoluminescence readings were initiated immediately after the addition of GP-AMC and lasted for 60 min, at 37 °C. The enzymatic reaction was monitored using a microplate reader (Synergy HT, BIO-TEK), by measuring the fluorescence at excitation and emission wavelengths of 360 ± 40 and 460 ± 40 nm, respectively. The concentrations of DPP-4 and of the tested flavonoids refer to those attained before the addition of the substrate. The amount of DMSO used had no interference in the assay. The effects are expressed as the % inhibition of DPP-4 activity, calculated using the slope of the enzymatic reaction between 5 and 60 min. Sitagliptin (0–0.8 μM) and diprotin A (0–250 μM) were used as positive controls. The obtained results represent at least three independent experiments.

2.3. Inhibition kinetic analysis

The estimation of kinetic parameters and prediction of the type of inhibition were performed using Microsoft® Office Excel software with the Solver supplement, as described previously.[35,36] Using this methodology, the kinetic conversion of the substrate GP-AMC by DPP-4 in each microplate well was fitted by nonlinear least squares regression[37] by applying eqn (1), which translates the general model for enzymatic reactions, and each one of its simplifications considering the different types of inhibition:

$$V_{inic} = \frac{V_{max}(S)}{K_m\left(1 + \frac{|I|}{K_{ic}}\right) + (S)\left(1 + \frac{|I|}{K_{iu}}\right)} \quad (1)$$

where V_{inic} and V_{max} represent the initial velocity of formation of AMC in RFU min^{-1} and the maximum achievable velocity when 38 U mL^{-1} of enzyme used is saturated by the substrate, respectively, S is the GP-AMC concentration in mM, K_m is the Michaelis Menten constant in mM and K_{ic} and K_{iu} are the constants for competitive and uncompetitive inhibition processes expressed in μM^{-1}.

The inhibition kinetic analysis was performed for the most active flavonoid tested in the fluorometric method, **C11** (0–150 μM), and for the positive controls, sitagliptin (0–0.2 μM) and diprotin A (0–125 μM). For each concentration of these inhibitors, three concentrations of the substrate GP-AMC (0.0625, 0.125 and 0.25 mM) were tested. The obtained results represent at least five independent experiments.

For each tested condition, the best indications for equation parameters were obtained using the Solver supplement after iterative minimization of the sum of squared residuals between the experimental values of V_{max} and the corresponding counterparts estimated according to each model used. Hence, the values obtained for the parameters of the simplest model (without inhibition) were used as initial values, proceeding to competitive inhibition, noncompetitive inhibition, uncompetitive inhibition and finishing with a more complex model, mixed inhibition types. The mechanism of inhibition was established after comparison and discrimination between the models with different numbers of parameters applying the extra sum-of-squares F test[38] and the Akaike information criterion (AIC) test.[39]

The error of the kinetic constant values was determined using the Jackknife procedure, which consists of the calculation of standard deviation of all estimated kinetic values obtained by Solver when each experimental data point was in turn drawn from the initial set.[40] The precision of the procedure was estimated through the analysis of variance (ANOVA) (one factor).[41]

2.4. *Ex vivo* inhibition of DPP-4 activity

2.4.1. Human whole blood. Following informed consent, venous blood was collected from healthy human volunteers by antecubital venepuncture, into heparinized vacuum tubes. The assessment of DPP-4 inhibition in human whole blood was performed by monitoring the DPP-4 mediated cleavage of the non-fluorescent substrate GP-AMC to release a fluorescent product, AMC (λ_{ex} = 360 nm/λ_{em} = 460 nm). This methodology was developed and tested under different experimental conditions: different dilutions and volumes of human whole blood, different concentrations of the substrate and different times of incubation. The following most favourable experimental conditions were selected to perform the assays: human blood was diluted 1 : 3 (in PBS), placed in 1.5 mL microtubes with the tested flavonoids (0–200 μM) [dissolved in PBS/DMSO (1 : 1), to obtain a final DMSO concentration of 5% (v/v)], and incubated at 37 °C, for 30 min. The samples were then centrifuged at 3000*g* for 15 min, at room temperature. After centrifugation, the supernatants were collected and placed in a 96-well microplate with Tris-HCl (50 mM, pH 8.0) buffer and the substrate GP-AMC (0.125 mM) dissolved in Tris-HCl (50 mM, pH 8.0). Photoluminescence readings were initiated immediately after the addition of GP-AMC and during 60 min. The enzymatic reaction was monitored using a microplate reader (Synergy HT, BIO-TEK), by measuring the fluorescence at excitation and emission wavelengths of 360 ± 40 and 460 ± 40 nm, respectively. The amount of DMSO used had no interference in the assay. The concentrations of the tested flavonoids refer to those attained before the addition of the substrate. The effects are expressed as the % inhibition of DPP-4 activity, calculated using the slope of the enzymatic reaction between 5 and 60 min. Sitagliptin (0–1 μM) and diprotin A (0–500 μM) were used as positive controls. The obtained results represent, at least, three independent experiments.

2.4.2. Human plasma. Following informed consent, venous blood was collected from healthy human volunteers by antecubital venepuncture, into heparinized vacuum tubes, and

 This journal is © The Royal Society of Chemistry 2019

centrifuged at 3000*g* for 15 min, at room temperature, to obtain plasma. This methodology was developed and tested under different experimental conditions: different dilutions and volumes of human plasma, different concentrations of the substrate and different times of incubation. Following the most favourable experimental conditions, the human plasma was placed in a 48-well microplate with PBS and the tested flavonoids (0–200 μM) [dissolved in PBS/DMSO (1 : 1) to obtain a final DMSO concentration of 5% (v/v)] and incubated at 37 °C, for 30 min. Part of this reaction mixture was placed in a 96-well microplate with Tris-HCl (50 mM, pH 8.0) and the substrate GP-AMC (0.0625 mM), dissolved in Tris-HCl (50 mM, pH 8.0). The enzymatic reaction was monitored using a microplate reader (Synergy HT, BIO-TEK), by measuring the fluorescence at excitation and emission wavelengths of 360 ± 40 and 460 ± 40 nm, respectively. The amount of DMSO used had no interference in the assay. The concentrations of the tested flavonoids refer to those attained at the first incubation time. The effects are expressed as the % inhibition of DPP-4 activity, calculated using the slope of the enzymatic reaction between 5 and 60 min. Sitagliptin (0–1 μM) and diprotin A (0–500 μM) were used as positive controls. The obtained results represent at least three independent experiments.

2.5. Binding of flavonoids to plasma proteins

The plasma protein binding (PPB) values were predicted using PreADMET®, a web-based application providing prediction of drug-likeness and absorption–distribution–metabolism–excretion (ADME)/toxicological data.[42]

2.6. Live subject statement

All experiments were performed in accordance with the Portuguese Guideline "DGS nº 015/2013 de 03/10/2013" and experiments were approved by the Joint Ethics Committee at the University Hospital Center of Porto (CHUP/ICBAS). Informed consents were obtained from human participants of this study.

2.7. Statistical analysis

Statistical comparisons among the tested compounds, in which it was possible to determine the IC_{50}, were performed applying the one-way ANOVA. Differences were considered to be significant at p values lower than 0.05. All the statistical analyses were performed using GraphPad Prism™ (version 7.0; GraphPad Software).

3. Results

3.1. *In vitro* inhibition of DPP-4 activity

3.1.1. Colorimetric method. Using the colorimetric method, the tested flavonoids (from groups A to E) did not show any inhibitory activity against DPP-4, up to the highest tested concentration, 200 μM. The positive controls sitagliptin and diprotin A presented IC_{50} values of 0.106 ± 0.006 μM and 37 ± 3 μM, respectively.

3.1.2. Fluorometric method. Using the fluorometric method, the most active flavonoid was flavonoid **C11**, with an IC_{50} value of 73 ± 2 μM, followed by chlorinated flavonoids **D11** (IC_{50} = 170 ± 10 μM) and **D14** (IC_{50} = 171 ± 8 μM). The results obtained for the most active flavonoid suggest that the presence of –OH groups at 3-position of the C-ring and at 7- and 8-positions of the A-ring, together with the presence of –OMe groups at 3′- and 4′-positions of the B-ring, is favourable for the inhibition of DPP-4, in comparison with the other tested flavonoids. The positive controls sitagliptin and diprotin A presented IC_{50} values of 0.064 ± 0.005 μM and 31 ± 2 μM, respectively (Table 1).

3.2. Inhibition kinetic analysis

The most active flavonoid, **C11**, found using the fluorometric assay, together with the positive controls sitagliptin and diprotin A, was selected to determine the type of inhibition.

Through the comparison between the sum of squared error (SSE) values of the different enzyme inhibition models and applying the extra sum-of-squares F test and the AIC test for models with different numbers of parameters, it was possible to select the best kinetic model (without inhibition, competitive inhibition, noncompetitive inhibition, uncompetitive inhibition and mixed inhibition) (see the ESI†).

From the analysis of the obtained results, flavonoid **C11** was classified as a noncompetitive inhibitor, and the positive controls, sitagliptin and diprotin A, as competitive inhibitors.

After the selection of the best kinetic model for the tested compounds, it was possible to summarize the kinetic constant parameters for each tested compound: K_m, V_{max}, K_{ic} and/or K_{iu} (Table 2).

The analysis by one factor ANOVA enabled the conclusion that the adopted procedure had a precision better than 0.785; 0.902 and 0.530 ΔAbs/min for flavonoid **C11**, sitagliptin and diprotin A respectively, as calculated from the within-groups mean square. The ANOVA also showed F values of 131.91, 108.80 and 378.58 for flavonoid **C11**, sitagliptin and diprotin A respectively, corresponding to a p value inferior to 0.05 (one-tail probability), as a consequence of its significant effect on the enzymatic activity.

3.3. *Ex vivo* inhibition of DPP-4 activity

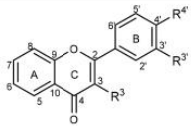
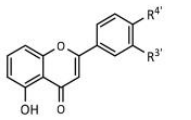
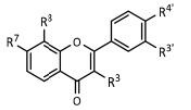
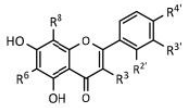
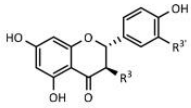
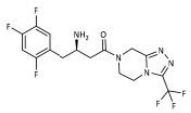
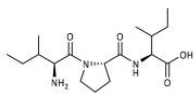
3.3.1. Human whole blood. Flavonoids incubated in a reaction mixture with human whole blood did not inhibit DPP-4 activity, at the highest tested concentration (200 μM). The positive controls sitagliptin and diprotin A presented IC_{50} values of 0.20 ± 0.02 μM and 128 ± 7 μM, respectively (Table 3).

3.3.2. Human plasma. Flavonoids tested in human plasma did not inhibit DPP-4 activity, at the highest tested concentration (200 μM). The positive controls sitagliptin and diprotin A presented IC_{50} values of 0.18 ± 0.01 μM and 124 ± 4 μM, respectively (Table 3).

3.4. Binding of flavonoids to plasma proteins

From the obtained results, it can be observed that PPB values of the tested flavonoids vary from 43.9% [for **D19** (rutin)] to

Table 1 Inhibition of human DPP-4 by the flavonoids under study and the positive controls, applying the fluorometric method

Compound	Structure	$R^{2'}$	R^3	$R^{3'}$	$R^{4'}$	R^6	R^7	R^8	Fluorometric method: Inhibition (%) at 200 μM (mean ± SEM)	Fluorometric method: Inhibition (%) at 100 μM (mean ± SEM)	Fluorometric method: IC_{50} (μM) (mean ± SEM)
A1 (flavone)		—	H	H	H	—	—	—	<20	—	—
A2		—	H	OH	H	—	—	—	<20	—	—
A3		—	H	H	OH	—	—	—	<20	—	—
A4		—	H	OH	OH	—	—	—	42 ± 3	22 ± 2	—
A5		—	OH	OH	OH	—	—	—	47 ± 1	27 ± 1	—
A6		—	OH	OMe	OMe	—	—	—	<20	—	—
B1		—	—	H	H	—	—	—	<20	—	—
B2		—	—	OH	H	—	—	—	<20	—	—
B3		—	—	H	OH	—	—	—	23 ± 2	—	—
B4		—	—	OH	OH	—	—	—	28 ± 4	—	—
C1		—	H	H	H	—	OH	H	28 ± 3	—	—
C2		—	H	OH	H	—	OH	H	36 ± 3	—	—
C3		—	H	H	OH	—	OH	H	47 ± 2	28 ± 1	—
C4		—	OH	OH	H	—	OH	H	38 ± 3	—	—
C5		—	OH	H	OH	—	OH	H	44 ± 2	29 ± 1	—
C6		—	H	OH	OH	—	OH	H	47 ± 2	33 ± 2	—
C7		—	OH	OH	OH	—	OH	OH	34 ± 1	—	—
C8		—	OH	OMe	H	—	OMe	H	<20	—	—
C9		—	OH	H	OMe	—	OMe	H	<20	—	—
C10		—	OH	OH	OH	—	OMe	OMe	48 ± 1	28 ± 1	—
C11		—	OH	OMe	OMe	—	OH	OH	**82 ± 1**	**60 ± 1**	**73 ± 2**[c]
C12		—	OH	OBn	OBn	—	OMe	OMe	41 ± 2	20 ± 1	—
C13		—	OH	OMe	OMe	—	OBn	OBn	42 ± 2	28 ± 1	—
D1 (chrysin)		H	H	H	H	H	—	H	33 ± 4	—	—
D2 (galangin)		H	OH	H	H	H	—	H	35 ± 4	—	—
D3 (baicalein)		H	H	H	H	OH	—	H	43 ± 4	22 ± 2	—
D4		H	H	OH	H	H	—	H	28 ± 2	—	—
D5 (apigenin)		H	H	H	OH	H	—	H	44 ± 2	25 ± 1	—
D6 (kaempferol)		H	OH	H	OH	H	—	H	38 ± 1	—	—
D7 (luteolin)		H	H	OH	OH	H	—	H	45 ± 2	24 ± 2	—
D8 (quercetin)		H	OH	OH	OH	H	—	H	46 ± 2	26 ± 3	—
D9 (morin)		OH	OH	H	OH	H	—	H	37 ± 4	—	—
D10		H	Cl	OH	OH	H	—	H	40 ± 3	20 ± 1	—
D11		H	H	OH	OH	Cl	—	H	55 ± 2	36 ± 2	170 ± 10[d]
D12		H	H	OH	OH	H	—	Cl	41 ± 1	24 ± 2	—
D13		H	Cl	OH	OH	H	—	Cl	40 ± 1	24 ± 2	—
D14		H	H	OH	OH	Cl	—	Cl	55 ± 1	35 ± 1	171 ± 8[d]
D15 (chrysoeriol)		H	H	OMe	OH	H	—	H	37 ± 1	—	—
D16 (acacetin)		H	H	H	OMe	H	—	H	<20	—	—
D17 (hispidulin)		H	H	H	OH	OMe	—	H	46 ± 2	28 ± 1	—
D18		H	H	OMe	OMe	H	—	H	47 ± 2	29 ± 3	—
D19 (rutin)		H	Rutinose	OH	OH	H	—	H	40 ± 2	22 ± 4	—
E1 (naringenin)		—	H	H	—	—	—	—	<20	—	—
E2 (eriodictyol)		—	H	OH	—	—	—	—	<20	—	—
E3 (taxifolin)		—	OH	OH	—	—	—	—	<20	—	—
Positive control: **sitagliptin**		—	—	—	—	—	—	—	—	—	0.064 ± 0.005[e]
Positive control: **diprotin A**		—	—	—	—	—	—	—	—	—	31 ± 2[b]

The IC_{50} values with different lowercase superscript letters are significantly different from each other ($p < 0.05$).

 This journal is © The Royal Society of Chemistry 2019

Table 2 Type of inhibition of flavonoid **C11**, sitagliptin and diprotin A and respective kinetic parameters values: K_m, V_{max}, K_{ic} and/or K_{iu} (mean ± SD)

Compound	Type of inhibition	K_m (mM)	V_{max} (RFU min^{-1})	K_{ic} (μM)	K_{iu} (μM)
C11	Noncompetitive	0.075 ± 0.003	20.1 ± 0.2	76.3 ± 0.9	76.3 ± 0.9
Sitagliptin	Competitive	0.080 ± 0.001	19.8 ± 0.1	0.0243 ± 0.0003	—
Diprotin A	Competitive	0.091 ± 0.001	22.1 ± 0.1	14.9 ± 0.1	—

Table 3 Inhibition of DPP-4 activity by the positive controls sitagliptin and diprotin A and by the flavonoids under study in the human blood assay and in the human plasma assay

Compound	Human blood assay IC_{50} (μM ± SEM)	Human plasma assay IC_{50} (μM ± SEM)
A4, A5, B3, B4, C1–C7, C10–C13, D1 (chrysin)–**D15** (chrysoeriol), **D17**–(hispidulin) **D19** (rutin)	<20%$^{200\ \mu M*}$	<20%$^{200\ \mu M*}$
Sitagliptin	0.20 ± 0.02$^{(a)}$	0.18 ± 0.01$^{(a)}$
Diprotin A	128 ± 7$^{(b)}$	124 ± 4$^{(b)}$

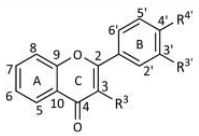
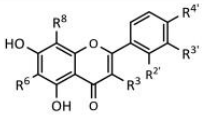
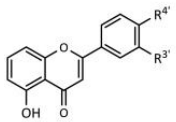
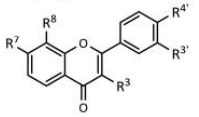
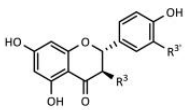
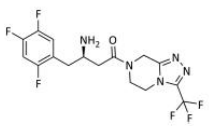
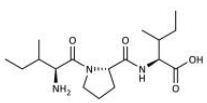
* % of inhibition at the highest tested concentration (in superscript). The IC_{50} values with different lowercase superscript letters are significantly different from each other ($p < 0.05$).

100.0% [for **E1** (naringenin) and **E2** (eriodictyol)]. The flavonoids that have shown higher inhibitory activity against DPP-4 in the assay with the isolated human recombinant enzyme (fluorometric method), **C11**, **D11** and **D14**, presented PPB values of 80.0%, 90.7% and 91.4%, respectively. The positive controls sitagliptin and diprotin A exhibited PPB values of 54.3% and 43.6%, respectively (Table 4).

4. Discussion

DPP-4 inhibitors have become an established therapy for the improvement of glycaemic control and do not usually cause hypoglycaemia and weight gain, being considered relatively safe, and several guidelines place these inhibitors ahead of

Table 4 Plasma protein binding (PPB) values for the flavonoids under study

Compound	Structure	Plasma protein binding (%)	Compound	Structure	Plasma protein binding (%)
A1 (flavone)		92.5	**D1** (chrysin)		95.1
A2		96.4	**D2** (galangin)		88.1
A3		95.3	**D3** (baicalein)		99.0
A4		97.9	**D4**		97.9
A5		88.7	**D5** (apigenin)		97.2
A6		84.1	**D6** (kaempferol)		89.6
			D7 (luteolin)		99.7
B1		95.2	**D8** (quercetin)		93.2
B2		98.0	**D9** (morin)		91.6
B3		97.2	**D10**		95.4
B4		99.5	**D11**		90.7
			D12		89.8
			D13		94.0
C1		92.6	**D14**		91.4
C2		95.6	**D15** (chrysoeriol)		90.9
C3		94.8	**D16** (acacetin)		90.9
C4		87.1	**D17** (hispidulin)		91.6
C5		85.3	**D18**		87.8
C6		97.4	**D19** (rutin)		43.9
C7		90.5			
C8		84.4			
C9		83.9	**E1** (naringenin)		100.0
C10		80.8	**E2** (eriodictyol)		100.0
C11		80.0	**E3** (taxifolin)		95.2
C12		90.9			
C13		91.3			
Positive control: **sitagliptin**		54.3	Positive control: **diprotin A**		43.6

sulfonylureas.[7,21] However, as described above, there are several adverse effects observed in T2D patients treated with DPP-4 inhibitors, including higher vulnerability to upper respiratory tract infection, urinary tract infection, nasopharyngitis and headache.[43] Moreover, an increased risk of hospitalization for heart failure was observed with the use of DPP-4 inhibitors.[2,17]

For these reasons, the search for effective and safer DPP-4 inhibitors has been a subject of interest among the scientific community. Flavonoids have been recognized as potential alternative drugs for a large number of diseases, including T2D.[44] In fact, flavonoids have already been described as effective inhibitors of important targets related to T2D physiopathology, including α-amylase,[27] α-glucosidase,[25,45] protein tyrosine phosphatase 1B (PTP1B),[26] DPP-4, sodium-glucose cotransporter 2 (SGLT2),[46] among others.[22,47–49]

It was described that flavonoids from natural products and crude herbal extracts rich in these phenolic compounds were found to be promising DPP-4 inhibitors, serving as useful clues for the development of new antidiabetic agents.[20,21]

In this work, the DPP-4 inhibition by a panel of 45 flavonoids, divided into 5 groups (A–E), was tested, establishing, whenever possible, an accurate structure–activity relationship. For this purpose, the inhibitory activity of flavonoids against human isolated DPP-4 was studied, using colorimetric and fluorometric methods. DPP-4 inhibition in human blood and in human plasma was also tested for the most active flavonoids.

For the evaluation of the DPP-4 inhibition by flavonoids, colorimetric and fluorometric methods were applied. These methods are the most commonly applied methods in the study of DPP-4 inhibition by various classes of compounds, including flavonoids. According to the work of Matheeussen *et al.*,[50] in which the DPP-4 activity was studied using colorimetric, fluorescent and luminescent substrates, the fluorometric substrates presented about 10-fold higher sensitivity compared to the colorimetric assay. Accordingly, when the colorimetric method was applied in the present study, it was observed that the tested flavonoids did not show any ability to inhibit DPP-4 activity, at the highest tested concentration (200 μM). In turn, using the fluorometric method, it was possible to verify that some flavonoids presented an inhibitory effect against DPP-4. In addition, the IC_{50} values of the positive controls sitagliptin and diprotin A were lower in the fluorometric method, in comparison with those in the colorimetric method. Moreover, Matheeussen *et al.*[50] advised the use of fluorometric assays namely when the available volume of biological samples is limited and when the DPP-4 inhibition must be measured in samples after the treatment with an inhibitor. For all these reasons, the fluorometric method was subsequently applied for the evaluation of the DPP-4 inhibition in human whole blood and in human plasma.

In the scientific literature, the differences in the experimental conditions, such as the origin of the DPP-4, the detection methods, the concentrations of the enzyme and substrate, and the incubation times, lead to differences in the obtained results among different studies. Furthermore, as remarked by Lacroix *et al.*,[51] most studies that evaluated the *in vitro* activity of synthetic molecules or natural compounds on DPP-4 have been performed using human or porcine enzymes. It is noteworthy that the comparison of the kinetic parameters and the inhibition patterns of these two enzymes is sparse and shows contradictory results. For example, in the work of Lacroix *et al.*,[51] it was found that, in general, the porcine DPP-4 is inhibited with higher potency by protein-derived peptides than the human DPP-4. In fact, although among mammalian species the enzyme sequence is highly conserved, the human and porcine DPP-4 are not identical, presenting an overall sequence identity of 88%.[51]

In what concerns the study of the inhibition by flavonoids from the A group, it was observed that flavonoids **A5** and **A4** have similar levels of DPP-4 inhibition. By the obtained results it can be concluded that the presence of –OH groups at C-3′ and C-4′ of the B-ring slightly favours the DPP-4 inhibition. In the work of Fan *et al.*,[28] the unsubstituted flavone was described as an effective inhibitor of DPP-4, presenting an IC_{50} value of 0.17 ± 0.01 μM. However, porcine DPP-4 was used and the method was based on a luminescent detection.[28] In contrast, using a fluorometric assay, and human recombinant DPP-4, the compound **A1** (flavone) did not show any inhibitory activity.

The tested flavonoids from B and E groups presented low or no inhibitory activity against DPP-4, at the highest tested concentration, 200 μM. In what respects the flavonoids from the E group, this result highlights that the absence of the C2═C3 double bond is not favourable for the intended effect. In the study of Zhao *et al.*,[31] naringenin also did not inhibit DPP-4. In addition, in the study of Bower *et al.*,[52] eriodictyol showed high inhibitory activity against DPP-4. In the work of Bower *et al.*,[52] extracts from rosemary and Mexican oregano, rich in flavonoids, were the most potent DPP-4 inhibitors. The flavonoids cirsimaritin, hispidulin and naringenin were isolated from these extracts and, interestingly, were found to be potent inhibitors of DPP-4, with IC_{50} values similar to those obtained for the extracts. As mentioned above, it can be concluded that the source of the enzyme, the type of the substrate and the different times of incubation applied have a great influence on the final results.

As described above, in the C group the most effective flavonoid was found, **C11** (IC_{50} = 73 ± 2 μM), which was tested here for the first time, concerning its inhibitory activity against DPP-4. It also can be observed, by comparing flavonoid **C11** with flavonoid **C7**, that the substitution of the –OMe groups by –OH groups, at C-3′ and C-4′ of the B-ring, significantly decreases the ability of flavonoids to inhibit DPP-4. Moreover, comparing flavonoids **C11** with **C13**, it was possible to observe that the presence of –OBn groups at C-7 and C-8 of the A-ring is not advantageous for the intended effect, when compared to the presence of –OMe groups at these positions.

Concerning the D group, the most effective compounds, with similar activities, were the chlorinated flavonoids **D11** and **D14**. Chlorinated flavonoids have already been described

 This journal is © The Royal Society of Chemistry 2019

as anti-inflammatory agents by our research group.[33] Taking into account the role of inflammation in the development of T2D, these compounds constitute an important feature in the modulation of this disease. The structures of flavonoids **D11** and **D14** are similar, and the only difference between both compounds is that flavonoid **D14** presents an additional 8-Cl substituent at the A-ring, and flavonoid **D11** does not present substituents at this position. In addition, it can also be seen by comparing flavonoids **D11** and **D8** (quercetin) that the lack of the 3-Cl substituent at the A-ring does not favour the inhibition of the enzyme under study, due to the lower IC_{50} found for quercetin. Interestingly, quercetin was reported as an effective DPP-4 inhibitor in different studies, with IC_{50} values of approximately 2.92 ± 0.68 μM [28] and 70 ± 19 μM.[49] As mentioned above, the differences in the experimental conditions, such as different sources of DPP-4 enzymes, and different detection methods can explain the divergence in the results.[28,49]

In the study of Fan *et al.*,[28] besides the inhibitory activities of flavone and quercetin against DPP-4, luteolin, apigenin, kaempferol, naringenin and rutin were also tested. All these flavonoids presented effective DPP-4 inhibition, except rutin, which did not inhibit the enzyme under study.[28] DPP-4 inhibition by rutin was also tested by Morikawa *et al.*,[30] and once again, it presented no activity, at 100 μM, the maximum tested concentration. Accordingly, in the present work flavonoid **D19** (rutin) presented no inhibition at the highest tested concentration (200 μM). On the other hand, in the study of Zhao *et al.*,[31] rutin was able to inhibit DPP-4, with an IC_{50} value of 32.93 ± 1.84 μM. However, in the referred work, porcine kidney DPP-4 was used in the colorimetric assay with the GPPN substrate, which may justify the obtained results.

In the studies of Sarian *et al.*[49] and Zhao *et al.*,[31] kaempferol was an effective inhibitor of DPP-4, with IC_{50} values of 45.93 ± 8.61 μg mg^{-1} and 45.96 ± 1.52 μM respectively, contrary to what was observed in the present assay. In the study of Sarian *et al.*,[49] the source of DPP-4 was not clarified and the activity of flavonoids was studied using a DPP-4 inhibitory assay kit. Zhao and co-workers used the porcine kidney DPP-4 and the substrate GPPN.[31] Once again, the different experimental conditions could promote the achievement of different results. In the present work, flavonoid **D1** (chrysin) presented low inhibitory activity against DPP-4. Sarian and colleagues[49] also reported no activity of chrysin against DPP-4. Similar results were found for flavonoid **D9** (morin), which had low inhibitory activity at the highest tested concentration, in the present study. These results are corroborated by the study of Zhao *et al.*,[31] where no inhibitory activity of morin against DPP-4 was found.

In this work, it was not possible to determine the IC_{50} value for flavonoid **D17** (hispidulin). Bower *et al.*,[52] who used porcine DPP-4 and a DPP-4 inhibitory assay kit to evaluate the flavonoid activity, found an IC_{50} value of 0.49 ± 0.1 μM for this flavonoid. On the other hand, Marques *et al.*[53] showed that hispidulin inhibited the enzyme by 15% but only at a concentration as high as 15 mM. In this last work, porcine DPP-4 and a fluorometric method were used with the substrate GP-AMC. Sodium acetate (pH 4.0) was also used to stop the reaction.[53] It is described that alterations in the pH levels of the reaction mixture, followed by the end-point measurement, can give false positive results, so the continuous measurement of the signal during the entire incubation time (without pH changes) should be preferentially performed.[54]

The type of inhibition of the most active flavonoid, **C11**, and of the positive controls sitagliptin and diprotin A was also determined. Since the linear transformations of the Michaelis–Menten equation, such as Lineweaver–Burk double-reciprocal transformation, can distort experimental errors, the determination of the type of inhibition was performed using the nonlinear regression with the Solver supplement of Microsoft® Office Excel.[36] The best model found for flavonoid **C11** was the noncompetitive model. This result indicates that flavonoid **C11** can bind to both the free enzyme and the enzyme–substrate complex.[55] The best model for sitagliptin and diprotin A was the competitive model, in which the inhibitor competes with the substrate for binding to the active site of the enzyme.[56] This result is in accordance with the previously reported inhibition type for sitagliptin[57–59] and diprotin A.[60,61] Since Ki is an indicator of the binding affinity of the inhibitor to the enzyme, the expected and obtained order of the inhibitor dissociation constant of enzyme-inhibitor, K_{ic}, was as follows: **C11** > diprotin A > sitagliptin.

In the present study, the flavonoids tested in the *in vitro* assay with the isolated human DPP-4, which presented an inhibitory activity against DPP-4 above 20%, at 200 μM, and the positive controls, sitagliptin and diprotin A, were also tested against DPP-4 in human whole blood and human plasma. These two models are more complex and better resemble the physiological system, including the protein binding of the tested compounds. The selected method was fluorescence-based assay, with the substrate GP-AMC.

Since Gly-Pro-containing fluorogenic substrates also detect other members of the DPP-4 family, the inhibitory activity of sitagliptin, a highly selective and potent DPP-4 inhibitor used in the treatment of T2D, was studied to confirm that the Gly-Pro liberating activity is mainly attributed to DPP-4 and not to other unidentified factors.[5,50] Diprotin A, which was also tested in the present work, is also a selective DPP-4 inhibitor but it is not used as an antidiabetic agent. Both compounds confirmed the DPP-4 selectivity of this model. Additionally, the IC_{50} values of sitagliptin and diprotin A remained almost the same, irrespective of the use of whole blood or plasma (Table 3), validating both fluids for the assay. On the other hand, the tested flavonoids, at the highest tested concentration (200 μM), did not show any inhibitory activity against DPP-4, in any of the human *ex vivo* models used in the present work.

The higher IC_{50} values obtained for sitagliptin and diprotin A in the human whole blood and plasma methods, compared to the IC_{50} values of these compounds obtained in the fluorometric method, using the isolated human enzyme, as well as the lack of effect of the tested flavonoids, can be explained by the possible binding of these compounds to the plasma pro-

teins. In fact, sitagliptin binding to plasma proteins is reported to be about 38%.[62,63] It was also described that a large number of flavonoids and their metabolites circulate in the bloodstream mostly bound to human serum albumin (HSA).[64–73]

In vivo, drugs can bound to proteins and lipids in plasma [termed plasma protein binding (PPB)] and to proteins and lipids in tissues or unbound and diffuse to the blood and tissues.[74] The major drug-binding proteins in plasma are HSA, α1-acid glycoprotein (AAG) and lipoproteins.[73] In particular, the levels of HSA and AAG are high enough to enable the binding of a broad variety of drugs with enough affinity to affect their bioactivity.[75] HSA is a 66.6 kDa globular protein and is the most abundant protein in human plasma (4.5% of human blood weight) with a relatively constant concentration (around 600 μM), being one of the most important carriers of endogenous and exogenous compounds present in the human body.[73,75] As the most abundant plasma protein, HSA is the most widely explored protein in what concerns the ligand–biological molecule interaction model. Its role in the transportation of drugs and other small molecules is of utmost importance, since it serves as an indicator of the bioavailability of many biologically active compounds.[76–78] For this reason, the possible binding of the tested flavonoids and the positive controls sitagliptin and diprotin A to plasma proteins was studied in the present work. To perform this study, the web-based application PreADMET was used, which predicts ADME data of chemical compounds and builds a drug-like library using the *in silico* method, from the early step of drug discovery. As expected, the tested flavonoids presented PPB values from 43.9% [for **D19** (rutin)] to 100.0% [for **E1** (naringenin) and **E2** (eriodictyol)]. In general, a drug is considered highly bound to plasma proteins when the bound fraction exceeds 90% of the total drug concentration.[79] The obtained results explain the loss of the inhibitory activity of flavonoids against DPP-4 in human *ex vivo* models, since in most cases only free drug molecules interact with the therapeutic target to produce efficacy.[73–75,80] The PPB values obtained for flavonoids **D8** (quercetin) and **D17** (acacetin) and the positive control sitagliptin are similar to the ones found in the literature.[62,81,82] In general, the major conclusions found through the obtained results are that the presence of a –OH group at 3-position of the C-ring decreases the binding affinity of flavonoids for plasma proteins. Moreover, by comparing flavonoids **D7** (luteolin) and **D19** (rutin), it can be concluded that the glycosylation of flavonoids significantly reduces the PPB values. Accordingly, in the work of Xiao *et al.*,[83] it was also possible to observe that the addition of a 3-OH substituent at the C-ring decreased the binding affinity for plasma proteins [common rat plasma proteins (CRPP)], by comparing luteolin with quercetin. Furthermore, in the same work, it was also possible to verify a decreased affinity for CRPP after glycosylation, which may be due to the increase in molecular size and polarity and transfer to the non-planar structure.[83] In fact, PPB optimization is very useful in the development of DPP-4 inhibitors, since during the development of these drugs, these values should be considered to obtain the desired efficacy.

On the other hand, the effectiveness of *Pilea microphylla* (L.)[84] and *Pueraria tuberosa*[85] extracts, both rich in flavonoids, in inhibiting DPP-4 was already tested in diabetic Swiss albino mice and Charles Foster rats, respectively. In both studies, it was concluded that the administered extracts led to a decrease in plasma DPP-4 specific activity.[84,85] Thus, it is possible that competition between complex mixture components of plant extracts for albumin binding sites may increase the free concentration of flavonoids to DPP-4 inhibitory levels, though this theory still needs to be experimentally confirmed.

5. Conclusions

DPP-4 inhibitors are a relatively new class of antidiabetic drugs. These inhibitors preserve incretin hormones GLP-1 and GIP and promote postprandial insulin secretion. In the present work, a panel of 45 structurally related flavonoids was studied concerning their ability to inhibit the DPP-4 activity. This study was based on *in vitro* fluorometric and colorimetric methods using the human isolated enzyme. The fluorometric method was revealed to be more sensitive and was applied in the evaluation of DPP-4 activity in the *ex vivo* method, using human blood and plasma. The most effective flavonoid found using human isolated DPP-4, flavonoid **C11**, displayed no inhibitory activity in the *ex vivo* method, probably due to its high affinity for plasma proteins, notably HSA. These results will certainly contribute to the synthesis and development of new flavonoid scaffolds, with promising DPP-4 inhibitory activity and lower affinity for plasma proteins.

Conflicts of interest

There are no conflicts to declare.

Acknowledgements

The work was supported by UID/QUI/50006/2019 with funding from FCT/MCTES through national funds and "Programa Operacional Competitividade e Internacionalização" (COMPETE) (POCI-01-0145-FEDER-029241). Carina Proença acknowledges the financial support by FCT for the PhD grant (SFRH/BD/116005/2016), in the ambit of "QREN - POPH - Tipologia 4.1 - Formação Avançada", co-sponsored by Fundo Social Europeu (FSE) and by national funds of Ministério da Ciência, Tecnologia e Ensino Superior (MCTES).

References

1 International Diabetes Federation, *IDF Diabetes Atlas*, 2017, http://diabetesatlas.org/IDF_Diabetes_Atlas_8e_interactive_EN/.

2 E. Bonora and M. Cigolini, DPP-4 inhibitors and cardiovascular disease in type 2 diabetes mellitus. Expectations,

 This journal is © The Royal Society of Chemistry 2019

observations and perspectives, *Nutr., Metab. Cardiovasc. Dis.*, 2016, **26**, 273–284.
3 A. Cahn, S. Cernea and I. Raz, An update on DPP-4 inhibitors in the management of type 2 diabetes, *Expert Opin. Emerging Drugs*, 2016, **21**, 409–419.
4 R. Han, X. Wang, W. Bachovchin, Z. Zukowska and J. W. Osborn, Inhibition of dipeptidyl peptidase 8/9 impairs preadipocyte differentiation, *Sci. Rep.*, 2015, **5**, 12348.
5 M. G. Gall and M. D. Gorrell, in *Pathophysiological Aspects of Proteases*, ed. S. Chakraborti and N. S. Dhalla, Springer Singapore, Singapore, 2017, pp. 23–45, DOI: 10.1007/978-981-10-6141-7_2.
6 D. Röhrborn, N. Wronkowitz and J. Eckel, DPP4 in diabetes, *Front. Immunol.*, 2015, **6**, 1–20.
7 E. E. Mulvihill and D. J. Drucker, Pharmacology, physiology, and mechanisms of action of dipeptidyl peptidase-4 inhibitors, *Endocr. Rev.*, 2014, **35**, 992–1019.
8 J. Zhong, Q. Gong, A. Goud, S. Srinivasamaharaj and S. Rajagopalan, Recent advances in dipeptidyl-peptidase-4 inhibition therapy: lessons from the bench and clinical trials, *J. Diabetes Res.*, 2015, **2015**, 1–14.
9 A. M. Lambeir, C. Durinx, S. Scharpe and I. De Meester, Dipeptidyl-peptidase IV from bench to bedside: an update on structural properties, functions, and clinical aspects of the enzyme DPP IV, *Crit. Rev. Clin. Lab. Sci.*, 2003, **40**, 209–294.
10 W. S. d. S. Júnior, A. F. d. Godoy-Matos and L. G. Kraemer-Aguiar, Dipeptidyl peptidase 4: a new link between diabetes mellitus and atherosclerosis?, *BioMed Res. Int.*, 2015, **2015**, 1–10.
11 Y. Seino, M. Fukushima and D. Yabe, GIP and GLP-1, the two incretin hormones: similarities and differences, *J. Diabetes Invest.*, 2010, **1**, 8–23.
12 T. Wang, X. Ma, T. Tang, K. Higuchi, D. Peng, R. Zhang, M. Chen, J. Yan, S. Wang, D. Yan, Z. He, F. Jiang, Y. Bao, W. Jia, K. Ishida and C. Hu, The effect of glucose-dependent insulinotropic polypeptide (GIP) variants on visceral fat accumulation in Han Chinese populations, *Nutr. Diabetes*, 2017, **7**, 1–6.
13 M. Long, L. Cai, W. Li, L. Zhang, S. Guo, R. Zhang, Y. Zheng, X. Liu, M. Wang, X. Zhou, H. Wang, X. Li, L. Li, Z. Zhu, G. Yang and H. Zheng, DPP-4 inhibitors improve diabetic wound healing via direct and indirect promotion of epithelial-mesenchymal transition and reduction of scarring, *Diabetes*, 2018, **67**, 518–531.
14 C. F. Deacon and H. E. Lebovitz, Comparative review of dipeptidyl peptidase-4 inhibitors and sulphonylureas, *Diabetes, Obes. Metab.*, 2016, **18**, 333–347.
15 S. K. Sharma, A. Panneerselvam, K. P. Singh, G. Parmar, P. Gadge and O. C. Swami, Teneligliptin in management of type 2 diabetes mellitus, *Diabetes, Metab. Syndr. Obes.: Targets Ther.*, 2016, **9**, 251–260.
16 K. V. Kumar and A. K. Gupta, Clinical audit of patients using DPP4 inhibitors in longstanding type 2 diabetes, *Diabetes, Metab. Syndr. Obes.: Targets Ther.*, 2015, **9**, 277–279.
17 L. Li, S. Li, K. Deng, J. Liu, P. O. Vandvik, P. Zhao, L. Zhang, J. Shen, M. M. Bala, Z. N. Sohani, E. Wong, J. W. Busse, S. Ebrahim, G. Malaga, L. P. Rios, Y. Wang, Q. Chen, G. H. Guyatt and X. Sun, Dipeptidyl peptidase-4 inhibitors and risk of heart failure in type 2 diabetes: systematic review and meta-analysis of randomised and observational studies, *Br. Med. J.*, 2016, **352**, i610.
18 V. Gupta and S. Kalra, Choosing a gliptin, *Indian J. Endocrinol. Metab.*, 2011, **15**, 298–308.
19 T. Karagiannis, P. Boura and A. Tsapas, Safety of dipeptidyl peptidase 4 inhibitors: a perspective review, *Ther. Adv. Drug Saf.*, 2014, **5**, 138–146.
20 Y. Gao, Y. Zhang, J. Zhu, B. Li, Z. Li, W. Zhu, J. Shi, Q. Jia and Y. Li, Recent progress in natural products as DPP-4 inhibitors, *Future Med. Chem.*, 2015, **7**, 1079–1089.
21 A.-K. Singh, R. Jatwa, A. Purohit and H. Ram, Synthetic and phytocompounds based dipeptidyl peptidase-IV (DPP-IV) inhibitors for therapeutics of diabetes, *J. Asian Nat. Prod. Res.*, 2017, **19**, 1036–1045.
22 E. Nicolle, F. Souard, P. Faure and A. Boumendjel, Flavonoids as promising lead compounds in type 2 diabetes mellitus: molecules of interest and structure-activity relationship, *Curr. Med. Chem.*, 2011, **18**, 2661–2672.
23 J. Liu, Y. Huan, C. Li, M. Liu and Z. Shen, Establishment of a selective evaluation method for DPP4 inhibitors based on recombinant human DPP8 and DPP9 proteins, *Acta Pharm. Sin. B*, 2014, **4**, 135–140.
24 H. M. Eid and P. S. Haddad, The antidiabetic potential of quercetin: underlying mechanisms, *Curr. Med. Chem.*, 2017, **24**, 355–364.
25 C. Proenca, M. Freitas, D. Ribeiro, E. F. T. Oliveira, J. L. C. Sousa, S. M. Tome, M. J. Ramos, A. M. S. Silva, P. A. Fernandes and E. Fernandes, α-Glucosidase inhibition by flavonoids: an *in vitro* and *in silico* structure-activity relationship study, *J. Enzyme Inhib. Med. Chem.*, 2017, **32**, 1216–1228.
26 C. Proenca, M. Freitas, D. Ribeiro, J. L. C. Sousa, F. Carvalho, A. M. S. Silva, P. A. Fernandes and E. Fernandes, Inhibition of protein tyrosine phosphatase 1B by flavonoids: a structure - activity relationship study, *Food Chem. Toxicol.*, 2018, **111**, 474–481.
27 C. Proença, M. Freitas, D. Ribeiro, S. Tomé, E. Oliveira, M. Viegas, A. Araujo, M. J. Ramos, A. Silva, P. Fernandes and E. Fernandes, Evaluation of a flavonoids library for inhibition of pancreatic α-amylase towards a structure-activity relationship, *J. Enzyme Inhib. Med. Chem.*, 2019, **34**, 577–588.
28 J. Fan, M. H. Johnson, M. A. Lila, G. Yousef and E. G. de Mejia, Berry and citrus phenolic compounds inhibit dipeptidyl peptidase IV: implications in diabetes management, *Evid. Based Complement. Alternat. Med.*, 2013, **2013**, 13.
29 K. Jagan, M. K. Radika, E. Priyadarshini and C. V. Anuradha, A study on the inhibitory potential of DPP-IV enzyme by apigenin through *in silico* and *in vivo* approaches, *Res. J. Recent Sci.*, 2015, **4**, 22–29.

This journal is © The Royal Society of Chemistry 2019

30 T. Morikawa, K. Ninomiya, J. Akaki, N. Kakihara, H. Kuramoto, Y. Matsumoto, T. Hayakawa, O. Muraoka, L.-B. Wang, L.-J. Wu, S. Nakamura, M. Yoshikawa and H. Matsuda, Dipeptidyl peptidase-IV inhibitory activity of dimeric dihydrochalcone glycosides from flowers of *Helichrysum arenarium*, *J. Nat. Med.*, 2015, **69**, 494–506.

31 B. T. Zhao, D. D. Le, P. H. Nguyen, M. Y. Ali, J.-S. Choi, B. S. Min, H. M. Shin, H. I. Rhee and M. H. Woo, PTP1B, α-glucosidase, and DPP-IV inhibitory effects for chromene derivatives from the leaves of *Smilax china* L, *Chem.-Biol. Interact.*, 2016, **253**, 27–37.

32 H. S. Parmar, P. Jain, D. S. Chauhan, M. K. Bhinchar, V. Munjal, M. Yusuf, K. Choube, A. Tawani, V. Tiwari, E. Manivannan and A. Kumar, DPP-IV inhibitory potential of naringin: an in silico, in vitro and in vivo study, *Diabetes Res. Clin. Pract.*, 2012, **97**, 105–111.

33 M. Freitas, D. Ribeiro, S. M. Tome, A. M. Silva and E. Fernandes, Synthesis of chlorinated flavonoids with anti-inflammatory and pro-apoptotic activities in human neutrophils, *Eur. J. Med. Chem.*, 2014, **86**, 153–164.

34 J. L. C. Sousa, C. Proença, M. Freitas, E. Fernandes and A. M. S. Silva, New polyhydroxylated flavon-3-ols and 3-hydroxy-2-styrylchromones: synthesis and ROS/RNS scavenging activities, *Eur. J. Med. Chem.*, 2016, **119**, 250–259.

35 R. M. F. Bezerra, I. Fraga and A. A. Dias, Utilization of integrated Michaelis–Menten equations for enzyme inhibition diagnosis and determination of kinetic constants using Solver supplement of Microsoft Office Excel, *Comput. Methods Programs Biomed.*, 2013, **109**, 26–31.

36 A. A. Dias, P. A. Pinto, I. Fraga and R. M. F. Bezerra, Diagnosis of enzyme inhibition using Excel Solver: a combined dry and wet laboratory exercise, *J. Chem. Educ.*, 2014, **91**, 1017–1021.

37 H. Motulsky and A. Christopoulos, *Fitting models to biological data using linear and nonlinear regression: a pratical guide to curve fitting*, Oxford University Press, New York, 2004.

38 F. J. Burguillo, A. J. Wright and W. G. Bardsley, Use of the F test for determining the degree of enzyme-kinetic and ligand-binding data. A Monte Carlo simulation study, *Biochem. J.*, 1983, **211**, 23–34.

39 K. Yamaoka, T. Nakagawa and T. Uno, Application of Akaike's information criterion (AIC) in the evaluation of linear pharmacokinetic equations, *J. Pharmacokinet. Biopharm.*, 1978, **6**, 165–175.

40 T. Naes, T. Isaksson, T. Fearn and T. Davies, *A user-friendly guide to multivariate calibration and classification*, NIR Publications, Chichester, 2002.

41 J. N. Miller, J. C. Miller and R. D. Miller, *Statistics and chemometrics for Analytical Chemistry*, Pearson, London, 7th edn, 2017.

42 PreADMET, https://preadmet.bmdrc.kr/adme/.

43 R. Pathak and M. B. Bridgeman, Dipeptidyl peptidase-4 (DPP-4) inhibitors in the management of diabetes, *P&T*, 2010, **35**, 509–513.

44 D. Ribeiro, M. Freitas, J. L. Lima and E. Fernandes, Proinflammatory pathways: the modulation by flavonoids, *Med. Res. Rev.*, 2015, **35**, 877–936.

45 J. Zhu, C. Chen, B. Zhang and Q. Huang, The inhibitory effects of flavonoids on alpha-amylase and alpha-glucosidase, *Crit. Rev. Food Sci. Nutr.*, 2019, 1–14, DOI: 10.1080/10408398.2018.1548428.

46 O. Kwon, P. Eck, S. Chen, C. P. Corpe, J.-H. Lee, M. Kruhlak and M. Levine, Inhibition of the intestinal glucose transporter GLUT2 by flavonoids, *FASEB J.*, 2007, **21**, 366–377.

47 R. Vinayagam and B. Xu, Antidiabetic properties of dietary flavonoids: a cellular mechanism review, *Nutr. Metab.*, 2015, **12**, 1–20.

48 H. M. Kawser, D. A. Abdal, J. Han, Y. Yin, K. Kim, S. S. Kumar, G. Yang, H. Y. Choi and S. G. Cho, Molecular mechanisms of the anti-obesity and anti-diabetic properties of flavonoids, *Int. J. Mol. Sci.*, 2016, **17**, 1–32.

49 M. N. Sarian, Q. U. Ahmed, S. Z. Mat So'ad, A. M. Alhassan, S. Murugesu, V. Perumal, S. N. A. Syed Mohamad, A. Khatib and J. Latip, Antioxidant and antidiabetic effects of flavonoids: a structure-activity relationship based study, *BioMed Res. Int.*, 2017, **2017**, 1–14.

50 V. Matheeussen, A.-M. Lambeir, W. Jungraithmayr, N. Gomez, K. Mc Entee, P. Van der Veken, S. Scharpé and I. De Meester, Method comparison of dipeptidyl peptidase IV activity assays and their application in biological samples containing reversible inhibitors, *Clin. Chim. Acta*, 2012, **413**, 456–462.

51 I. M. Lacroix and E. C. Li-Chan, Comparison of the susceptibility of porcine and human dipeptidyl-peptidase IV to inhibition by protein-derived peptides, *Peptides*, 2015, **69**, 19–25.

52 A. M. Bower, L. M. Real Hernandez, M. A. Berhow and E. G. de Mejia, Bioactive compounds from culinary herbs inhibit a molecular target for type 2 diabetes management, dipeptidyl peptidase IV, *J. Agric. Food Chem.*, 2014, **62**, 6147–6158.

53 M. R. Marques, C. Stüker, N. Kichik, T. Tarragó, E. Giralt, A. F. Morel and I. I. Dalcol, Flavonoids with prolyl oligopeptidase inhibitory activity isolated from *Scutellaria racemosa* Pers, *Fitoterapia*, 2010, **81**, 552–556.

54 Y. Tahtah, S. G. Wubshet, K. T. Kongstad, A. M. Heskes, I. Pateraki, B. L. Moller, A. K. Jager and D. Staerk, High-resolution PTP1B inhibition profiling combined with high-performance liquid chromatography-high-resolution mass spectrometry-solid-phase extraction-nuclear magnetic resonance spectroscopy: proof-of-concept and antidiabetic constituents in crude extract of *Eremophila lucida*, *Fitoterapia*, 2016, **110**, 52–58.

55 R. Hüttl and N. Frank, in *Encyclopedia of Analytical Chemistry*, ed. R. A. Meyers, John Wiley & Sons, Ltd, Chichester, 2006, DOI: 10.1002/9780470027318.a5706.pub2.

56 G. L. Waldrop, A qualitative approach to enzyme inhibition, *Biochem. Mol. Biol. Educ.*, 2009, **37**, 11–15.

 This journal is © The Royal Society of Chemistry 2019

57 S. Miller and E. L. St Onge, Sitagliptin: a dipeptidyl peptidase IV inhibitor for the treatment of type 2 diabetes, *Ann. Pharmacother.*, 2006, **40**, 1336–1343.

58 C. F. Deacon, Dipeptidyl peptidase 4 inhibition with sitagliptin: a new therapy for type 2 diabetes, *Expert Opin. Invest. Drugs*, 2007, **16**, 533–545.

59 P. Berger Joel, R. SinhaRoy, A. Pocai, M. Kelly Theresa, G. Scapin, Y.-D. Gao, D. Pryor Kelly Ann, K. Wu Joseph, J. Eiermann George, S. Xu Shiyao, X. Zhang, A. Tatosian Daniel, E. Weber Ann, A. Thornberry Nancy and D. Carr Richard, A comparative study of the binding properties, dipeptidyl peptidase-4 (DPP-4) inhibitory activity and glucose-lowering efficacy of the DPP-4 inhibitors alogliptin, linagliptin, saxagliptin, sitagliptin and vildagliptin in mice, *Endocrinol., Diabetes Metab.*, 2017, **1**, 1–8.

60 J. Rahfeld, M. Schierhorn, B. Hartrodt, K. Neubert and J. Heins, Are diprotin A (Ile-Pro-Ile) and diprotin B (Val-Pro-Leu) inhibitors or substrates of dipeptidyl peptidase IV?, *Biochim. Biophys. Acta*, 1991, **1076**, 314–316.

61 K. Augustyns, P. Van der Veken, K. Senten and A. Haemers, The therapeutic potential of inhibitors of dipeptidyl peptidase IV (DPP IV) and related proline-specific dipeptidyl aminopeptidases, *Curr. Med. Chem.*, 2005, **12**, 971–998.

62 European Medicines Agency, Januvia: EPAR - scientific discussion, https://www.ema.europa.eu/documents/scientific-discussion/januvia-epar-scientific-discussion_en.pdf.

63 T. A. Sonia and C. P. Sharma, in *Oral Delivery of Insulin*, ed. T. A. Sonia and C. P. Sharma, Woodhead Publishing, 2014, pp. 1–57, DOI: 10.1533/9781908818683.1.

64 O. Dangles, C. Dufour, C. Manach, C. Morand and C. Remesy, Binding of flavonoids to plasma proteins, *Methods Enzymol.*, 2001, **335**, 319–333.

65 C. Dufour and O. Dangles, Flavonoid–serum albumin complexation: determination of binding constants and binding sites by fluorescence spectroscopy, *Biochim. Biophys. Acta, Gen. Subj.*, 2005, **1721**, 164–173.

66 M. I. Kaldas, U. K. Walle, H. van der Woude, J. M. McMillan and T. Walle, Covalent binding of the flavonoid quercetin to human serum albumin, *J. Agric. Food Chem.*, 2005, **53**, 4194–4197.

67 M. X. Xie, X. Y. Xu and Y. D. Wang, Interaction between hesperetin and human serum albumin revealed by spectroscopic methods, *Biochim. Biophys. Acta*, 2005, **1724**, 215–224.

68 H. G. Mahesha, S. A. Singh, N. Srinivasan and A. G. A. Rao, A spectroscopic study of the interaction of isoflavones with human serum albumin, *FEBS J.*, 2006, **273**, 451–467.

69 C. Qin, M. X. Xie and Y. Liu, Characterization of the myricetin-human serum albumin complex by spectroscopic and molecular modeling approaches, *Biomacromolecules*, 2007, **8**, 2182–2189.

70 A. Bolli, M. Marino, G. Rimbach, G. Fanali, M. Fasano and P. Ascenzi, Flavonoid binding to human serum albumin, *Biochem. Biophys. Res. Commun.*, 2010, **398**, 444–449.

71 B. Zhang, T. Chen, Z. Chen, M. Wang, D. Zheng, J. Wu, X. Jiang and X. Li, Synthesis and anti-hyperglycemic activity of hesperidin derivatives, *Bioorg. Med. Chem. Lett.*, 2012, **22**, 7194–7197.

72 C.-Z. Lin, M. Hu, A.-Z. Wu and C.-C. Zhu, Investigation on the differences of four flavonoids with similar structure binding to human serum albumin, *J. Pharm. Anal.*, 2014, **4**, 392–398.

73 Q. Jiao, R. Wang, Y. Jiang and B. Liu, Study on the interaction between active components from traditional Chinese medicine and plasma proteins, *Chem. Cent. J.*, 2018, **12**, 1–20.

74 D. A. Smith, L. Di and E. H. Kerns, The effect of plasma protein binding on in vivo efficacy: misconceptions in drug discovery, *Nat. Rev. Drug Discovery*, 2010, **9**, 929.

75 G. L. Trainor, The importance of plasma protein binding in drug discovery, *Expert Opin. Drug Discovery*, 2007, **2**, 51–64.

76 D. E. Epps, T. J. Raub, V. Caiolfa, A. Chiari and M. Zamai, Determination of the affinity of drugs toward serum albumin by measurement of the quenching of the intrinsic tryptophan fluorescence of the protein, *J. Pharm. Pharmacol.*, 1999, **51**, 41–48.

77 G. Zhang, L. Wang and J. Pan, Probing the binding of the flavonoid diosmetin to human serum albumin by multi-spectroscopic techniques, *J. Agric. Food Chem.*, 2012, **60**, 2721–2729.

78 M. T. Larsen, M. Kuhlmann, M. L. Hvam and K. A. Howard, Albumin-based drug delivery: harnessing nature to cure disease, *Mol. Cell. Ther.*, 2016, **4**, 1–12.

79 P. Ascenzi, G. Fanali, M. Fasano, V. Pallottini and V. Trezza, Clinical relevance of drug binding to plasma proteins, *J. Mol. Struct.*, 2014, **1077**, 4–13.

80 N. A. Kratochwil, W. Huber, F. Müller, M. Kansy and P. R. Gerber, Predicting plasma protein binding of drugs: a new approach, *Biochem. Pharmacol.*, 2002, **64**, 1355–1374.

81 D. W. Boulton, U. K. Walle and T. Walle, Extensive binding of the bioflavonoid quercetin to human plasma proteins, *J. Pharm. Pharmacol.*, 1998, **50**, 243–249.

82 S.-B. Kim, T. Lee, H. S. Lee, C. K. Song, H.-J. Cho, D.-D. Kim, H.-J. Maeng and I.-S. Yoon, Development and validation of a highly sensitive LC–MS/MS method for the determination of acacetin in human plasma and its application to a protein binding study, *Arch. Pharmacal Res.*, 2016, **39**, 213–220.

83 J. Xiao, H. Cao, T. Chen, F. Yang, C. Liu and X. Xu, Molecular property-binding affinity relationship of flavonoids for common rat plasma proteins in vitro, *Biochimie*, 2011, **93**, 134–140.

84 P. Bansal, P. Paul, J. Mudgal, P. G. Nayak, S. T. Pannakal, K. I. Priyadarsini and M. K. Unnikrishnan, Antidiabetic, antihyperlipidemic and antioxidant effects of the flavonoid rich fraction of *Pilea microphyll*a (L.) in high fat diet/streptozotocin-induced diabetes in mice, *Exp. Toxicol. Pathol.*, 2012, **64**, 651–658.

85 S. Srivastava, P. Shree and Y. B. Tripathi, Active phytochemicals of *Pueraria tuberosa* for DPP-IV inhibition: in silico and experimental approach, *J. Diabetes Metab. Disord.*, 2017, **16**, 1–9.

This journal is © The Royal Society of Chemistry 2019

II.5. Structural specificity of flavonoids in the inhibition of human fructose 1,6-bisphosphatase

Reprinted with permission from Journal of Natural Products

Copyright © (2020) American Chemical Society (ACS) Publications

JOURNAL OF NATURAL PRODUCTS

pubs.acs.org/jnp Article

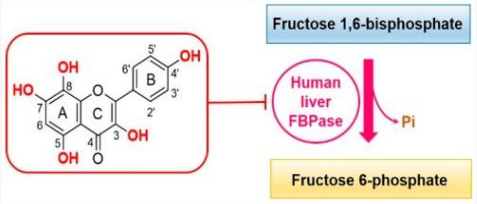
Structural Specificity of Flavonoids in the Inhibition of Human Fructose 1,6-Bisphosphatase

Carina Proença, Ana Oliveira, Marisa Freitas, Daniela Ribeiro, Joana L. C. Sousa, Maria J. Ramos, Artur M. S. Silva, Pedro A. Fernandes, and Eduarda Fernandes*

Cite This: J. Nat. Prod. 2020, 83, 1541−1552 Read Online

ACCESS | Metrics & More | Article Recommendations | Supporting Information

ABSTRACT: Liver fructose 1,6-bisphosphatase (FBPase) is a recognized regulatory enzyme of the gluconeogenesis pathway, which has emerged as a valid target to control gluconeogenesis-mediated overproduction of glucose. As such, the management of diabetes with FBPase inhibitors represents a potential alternative for the currently used antidiabetic agents. In this study, the FBPase inhibition of a panel of 55 structurally related flavonoids was tested, through a microanalysis screening system. Then, a subset of seven active inhibitors and their close chemical relatives were further evaluated by molecular dynamics (MD) simulations using a linear interaction energy (LIE) approach. The results obtained showed that **D14** (herbacetin) was the most potent inhibitor, suggesting that the presence of −OH groups at the C-3, C-4′, C-5, C-7, and C-8 positions, as well as the double bond between C-2 and C-3 and the 4-oxo function at the pyrone ring, are favorable for the intended effect. Furthermore, **D14** (herbacetin) is stabilized by a strong interaction with the Glu30 side chain and the Thr24 backbone of FBPase. This is the first investigation studying the in vitro inhibitory effect of a panel of flavonoids against human liver FBPase, thus representing a potentially important step for the search and design of novel inhibitors of this enzyme.

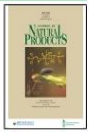


The two major pathways for endogenous glucose production (EGP) are gluconeogenesis and glycogenolysis. Gluconeogenesis is of special relevance during long periods of fasting and starvation, accounting for about 50% of EGP after an overnight fast, reaching about 90% EGP after 40 h of fasting. In type 2 diabetes (T2D) patients, the increased EGP mostly occurs through the gluconeogenesis pathway, while the glycogenolysis remains unaffected.[1] Gluconeogenesis is the primary process for EGP in the liver and produces glucose from noncarbohydrate precursors, namely, glycerol, the carbon skeleton of amino acids and lactate (Figure 1). Fructose 1,6-bisphosphatase (FBPase) remains as one of the key regulatory enzymes of gluconeogenesis and represents a potential target for T2D therapy, while the inhibition of other enzymes acting on gluconeogenesis, such as phosphoenolpyruvate (PEP) carboxykinase and glucose 6-phosphatase (G6Pase), has shown several drawbacks and limitations, with multiple side effects, such as disruption of mitochondrial redox state and hepatic steatosis.[2]

FBPase (EC 3.1.3.11) catalyzes the hydrolysis of fructose 1,6-bisphosphate to fructose 6-phosphate and inorganic phosphate (P_i), in the presence of divalent cations, such as manganese and magnesium, acting as a rate-limiting enzyme in the gluconeogenesis pathway (Figure 1).[1,3−5] Two isoforms of FBPase, encoded by two genes, have been found in mammals: liver FBPase (FBP1), which is found in the liver (hepatocytes) and kidney (proximal tubules cells); and muscle FBPase (FBP2), which is expressed in muscle tissue (cardiomyocytes and smooth muscle cells).[6] The muscle isoform is also encoded in neurons and in cells that predominantly express the liver FBPase (e.g., in the liver itself).[7] These two isoforms of FBPase represent about 77% of amino acid similarity and nearly complete identity in the active site.[1,5] The liver isoform of FBPase, located in the cytoplasm, has a critical role in the maintenance of the glucose levels and is the main source of de novo synthesis of glucose (gluconeogenesis). In the kidney, FBPase constitutes a minor source of de novo synthesis of glucose, except in extreme fasting periods and/or in diabetic patients.[1,5]

The X-ray crystal structure of human liver FBPase revealed that it possesses four identical polypeptide chains, each with 337 amino acid residues. This cytosolic enzyme is represented as a tetramer with four identical subunits, each comprising a substrate-binding site, a magnesium-binding site (within the substrate site), and an allosteric regulatory binding site. The intracellular activity of FBPase is synergistically regulated by the inhibitors fructose 2,6-bisphosphate, which binds at the substrate site (competitive inhibitor), and adenosine 5′-

Received: January 7, 2020
Published: May 4, 2020



ACS Publications © 2020 American Chemical Society and American Society of Pharmacognosy

https://dx.doi.org/10.1021/acs.jnatprod.0c00014
J. Nat. Prod. 2020, 83, 1541−1552

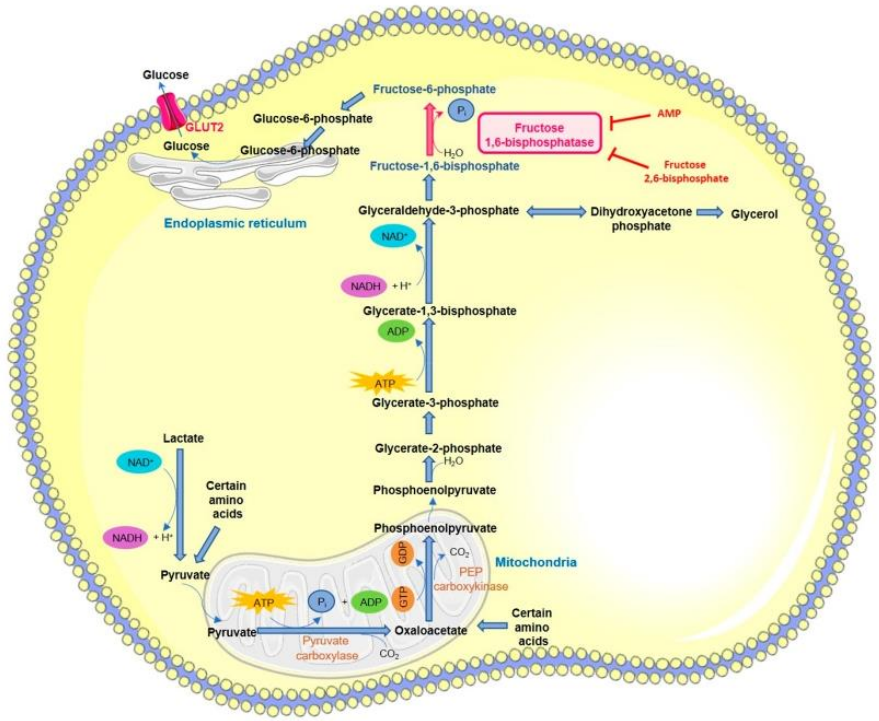


Figure 1. Gluconeogenesis process. The major substrates for this metabolic pathway are certain amino acids (derived from muscle, e.g., alanine), lactate (produced in the muscles and red blood cells), and glycerol (formed from the degradation of triacylglycerols). The gluconeogenesis reactions catalyzed by pyruvate carboxylase and PEP carboxykinase occur within the mitochondria. In turn, the reaction catalyzed by glucose-6-phosphatase takes place in the endoplasmic reticulum. The reaction catalyzed by fructose 1,6-bisphosphatase (FBPase) occurs in the cytoplasm, with its intracellular activity regulated by the competitive inhibitor fructose 2,6-bisphoshate and the allosteric inhibitor AMP. ADP, adenosine diphosphate; AMP, adenosine 5′-monophosphate; ATP, adenosine triphosphate; GDP, guanosine diphosphate; GLUT2, glucose transporter 2; GTP, guanosine triphosphate; NAD^+, nicotinamide adenine dinucleotide; NADH, reduced nicotinamide adenine dinucleotide; PEP, phosphoenolpyruvate; P_i, inorganic phosphate.

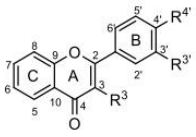
monophosphate (AMP), which binds at the allosteric site (noncompetitive inhibitor).[1,2,8−10] It is known that fructose 2,6-bisphosphate is the major physiological regulator of FBPase, since the AMP intracellular levels are generally maintained within a narrow range.[2] Recently, a new allosteric binding site was found, differing from both the active binding site and the AMP binding site. According to kinetic studies, the inhibition of this recently identified site is characterized as noncompetitive (e.g., inhibitor OC252).[1]

High glucose levels in healthy individuals induce an increase in the expression of the FBPase competitive inhibitor, fructose 2,6-bisphosphate, which is regulated by the increased production of insulin. As T2D is characterized by the combination of insulin deficiency and insulin resistance, excessive hepatic glucose output represents a key factor leading to fasting hyperglycemia and significantly contributes to postprandial hyperglycemia in T2D patients.[4,11,12] It was found that FBPase levels in the liver are elevated in insulin-resistant and insulin-deficient animal models of diabetes.[10] FBPase inhibition has revealed a reduced risk of side effects such as hypoglycemia (due to the compensatory stimulation of glycogenolysis during inhibition of gluconeogenesis), lacticemia, and/or hyperlipidemia, as suggested by the near-normal biochemical and clinical parameters of adults with FBPase deficiency, a rare autosomal recessive genetic disorder.[1,2] Moreover, it was observed that the inhibition of FBPase in animal models of T2D lowers hepatic glucose production without causing hypoglycemia.[13] As such, these observations highlight the importance of this enzyme as a target in the control of blood glucose.[10]

Among several classes of known FBPase inhibitors, the phosphonic acid-containing thiazoles and AMP mimetic MB07803, a prodrug of MB07729, has advanced to a phase II clinical trial.[10,13,14] However, the development of competitive inhibitors is restricted due to several reasons, namely, the highly hydrophilic nature of the FBPase active site and the difficulty of designing suitable carbohydrate phosphate mimetics that can bind with higher affinity and compete with the high fructose 1,6-bisphosphate levels (resultant from FBPase inhibition). As such, a major effort has been focused on the design of AMP binding site inhibitors (noncompetitive inhibitors).[1,2,11,15]

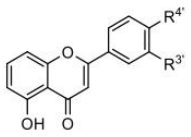
Flavonoids, a class of phenolic secondary metabolites in plants with the basic structure of $C_6-C_3-C_6$, are among the most well-studied derived natural products, due to their recognized biological activities, including their potential antidiabetic activity.[16−25] However, there are few studies reported in the literature concerning the inhibitory activity of flavonoids against liver FBPase in diabetic rats or mice.[26−31] The present study intends to fill this gap by evaluating, for the first time, the effect of 55 structurally related flavonoids (Figure 2) on the inhibition

https://dx.doi.org/10.1021/acs.jnatprod.0c00014
J. Nat. Prod. 2020, 83, 1541−1552



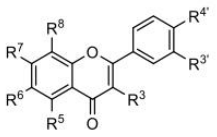
A1-6

A1: R^3= $R^{3'}$= $R^{4'}$= H (flavone)
A2: R^3= H, $R^{3'}$= OH, $R^{4'}$= H
A3: R^3= $R^{3'}$= H, $R^{4'}$= OH
A4: R^3= H, $R^{3'}$= $R^{4'}$= OH
A5: R^3= $R^{3'}$= $R^{4'}$= OH
A6: R^3= OH, $R^{3'}$= $R^{4'}$= OMe



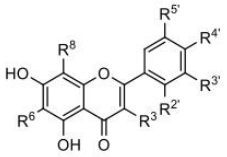
B1-4

B1: $R^{3'}$= $R^{4'}$= H
B2: $R^{3'}$= OH, $R^{4'}$= H
B3: $R^{3'}$= H, $R^{4'}$= OH
B4: $R^{3'}$= $R^{4'}$= OH



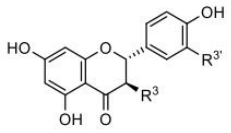
C1-16

C1: R^3= $R^{3'}$= $R^{4'}$= R^5= R^6 = H, R^7= OH, R^8= H
C2: R^3= H, $R^{3'}$= OH, $R^{4'}$= R^5= R^6= H, R^7= OH, R^8= H
C3: R^3= $R^{3'}$= H, $R^{4'}$= OH, R^5= R^6= H, R^7= OH, R^8= H
C4: R^3= $R^{3'}$= OH, $R^{4'}$= R^5= R^6 = H, R^7= OH, R^8= H
C5: R^3= OH, $R^{3'}$= H, $R^{4'}$= OH, R^5= R^6= H, R^7= OH, R^8= H
C6: R^3= H, $R^{3'}$= $R^{4'}$= OH, R^5= R^6= H, R^7= OH, R^8= H
C7: R^3= $R^{3'}$= $R^{4'}$= OH, R^5= R^6= H, R^7= R^8= OH
C8: R^3= $R^{3'}$= $R^{4'}$= H, R^5= R^6= OH, R^7= OMe, R^8= H
C9: R^3= $R^{3'}$= $R^{4'}$= H, R^5= R^6= R^7= OMe, R^8= H
C10: R^3= $R^{3'}$= $R^{4'}$= H, R^5= R^6= OH, R^7= glucuronide, R^8= H (baicalin)
C11: R^3= OH, $R^{3'}$= OMe, $R^{4'}$= R^5= R^6= H, R^7= OMe, R^8= H
C12: R^3= OH, $R^{3'}$= H, $R^{4'}$= OMe, R^5= R^6= H, R^7= OMe, R^8= H
C13: R^3= $R^{3'}$= $R^{4'}$= OH, R^5= R^6= H, R^7= R^8= OMe
C14: R^3= OH, $R^{3'}$= $R^{4'}$= OMe, R^5= R^6= H, R^7= R^8= OH
C15: R^3= OH, $R^{3'}$= $R^{4'}$= OBn, R^5= R^6= H, R^7= R^8= OMe
C16: R^3= OH, $R^{3'}$= $R^{4'}$= OMe, R^5= R^6= H, R^7= R^8= OBn



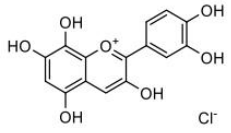
D1-25

D1: $R^{2'}$= R^3= $R^{3'}$= $R^{4'}$= $R^{5'}$= R^6= R^8= H (chrysin)
D2: $R^{2'}$= H, R^3= OH, $R^{3'}$= $R^{4'}$= $R^{5'}$= R^6= R^8= H (galangin)
D3: $R^{2'}$= R^3= $R^{3'}$= $R^{4'}$= $R^{5'}$= H, R^6= OH, R^8= H (baicalein)
D4: $R^{2'}$= R^3= H, $R^{3'}$= OH, $R^{4'}$= $R^{5'}$= R^6= R^8= H
D5: $R^{2'}$= R^3= $R^{3'}$= H, $R^{4'}$= OH, $R^{5'}$= R^6= R^8= H (apigenin)
D6: $R^{2'}$= H, R^3= OH, $R^{3'}$= H, $R^{4'}$= OH, $R^{5'}$= R^6= R^8= H (kaempferol)
D7: $R^{2'}$= R^3= H, $R^{3'}$= $R^{4'}$= OH, $R^{5'}$= R^6= R^8= H (luteolin)
D8: $R^{2'}$= R^3= $R^{3'}$= H, $R^{4'}$= OH, $R^{5'}$= H, R^6= OH, R^8= H (scutellarein)
D9: $R^{2'}$= H, R^3= $R^{3'}$= $R^{4'}$= OH, $R^{5'}$= R^6= R^8= H (quercetin)
D10: $R^{2'}$= H, R^3= $R^{3'}$= $R^{4'}$= $R^{5'}$= OH, R^6= R^8= H (myricetin)
D11: $R^{2'}$= R^3= OH, $R^{3'}$= H, $R^{4'}$= OH, $R^{5'}$= R^6= R^8= H (morin)
D12: $R^{2'}$= H, R^3= $R^{3'}$= $R^{4'}$= OH, $R^{5'}$= H, R^6= OH, R^8= H (quercetagetin)
D13: $R^{2'}$= R^3= $R^{3'}$= $R^{4'}$= H, R^5= OH, R^6= H, R^7= R^8= OH (norwogonin)
D14: $R^{2'}$= H, R^3= OH, $R^{3'}$= H, $R^{4'}$= R^5= OH, R^6= H, R^7= R^8= OH (herbacetin)
D15: $R^{2'}$= H, R^3= $R^{3'}$= $R^{4'}$= OH, $R^{5'}$= R^6= H, R^8= OH (gossypetin)
D16: $R^{2'}$= H, R^3= Cl, $R^{3'}$= $R^{4'}$= OH, $R^{5'}$= R^6= R^8= H
D17: $R^{2'}$= R^3= H, $R^{3'}$= $R^{4'}$= OH, $R^{5'}$= H, R^6= Cl, R^8= H
D18: $R^{2'}$= R^3= H, $R^{3'}$= $R^{4'}$= OH, $R^{5'}$= R^6= H, R^8= Cl
D19: $R^{2'}$= H, R^3= Cl, $R^{3'}$= $R^{4'}$= OH, $R^{5'}$= R^6= H, R^8= Cl
D20: $R^{2'}$= H, R^3= Cl, $R^{3'}$= $R^{4'}$= OH, $R^{5'}$= H, R^6= R^8= Cl
D21: $R^{2'}$= R^3= H, $R^{3'}$= OMe, $R^{4'}$= OH, $R^{5'}$= R^6= R^8= H (chrysoeriol)
D22: $R^{2'}$= R^3= $R^{3'}$= H, $R^{4'}$= OMe, $R^{5'}$= R^6= R^8= H (acacetin)
D23: $R^{2'}$= R^3= H, $R^{3'}$= $R^{4'}$= OMe, $R^{5'}$= R^6= R^8= H
D24: $R^{2'}$= H, R^3= rutinose, $R^{3'}$= $R^{4'}$= OH, $R^{5'}$= R^6= R^8= H
D25: $R^{2'}$= H, R^3= $R^{3'}$= $R^{4'}$= OH, $R^{5'}$= R^6= H, R^8= glucoside (gossypin)



E1-3

E1: R^3= $R^{3'}$= H (naringenin)
E2: R^3= H, $R^{3'}$= OH (eriodictyol)
E3: R^3= $R^{3'}$= OH (taxifolin)



F1: gossypetinidin chloride

Figure 2. Chemical structures of the studied flavonoids.

of isolated human FBPase. Moreover, this work investigated the molecular basis of the FBPase inhibition by flavonoids, through molecular dynamics (MD).

■ RESULTS AND DISCUSSION

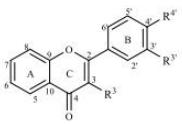
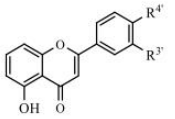
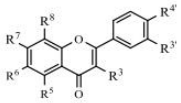
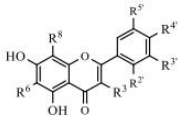
In Vitro Human Liver FBPase Inhibition Assay. The flavonoids under study were divided into five different groups (A–E), according to their substitution pattern (Table 1). This is the first time that the inhibitory activity of a panel of flavonoids has been tested against the isolated human liver FBPase.

For the assessment of the inhibitory activity of flavonoids, a fluorescent-based FBPase inhibitor screening kit was used, followed by the evaluation of the most active flavonoids and their close parent compounds by MD simulations using a linear interaction energy (LIE) approach.

From all the tested flavonoids, four from group D showed a significant inhibitory activity of FBPase, **D3** (baicalein), **D8** (scutellarein), **D14** (herbacetin), and **D15** (gossypetin), with $IC_{50} = 29 \pm 3\ \mu M$, $38.2 \pm 0.4\ \mu M$, $8.7 \pm 0.7\ \mu M$, and $24 \pm 2\ \mu M$, respectively. The most active flavonoid found was **D14**

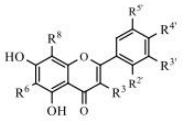
https://dx.doi.org/10.1021/acs.jnatprod.0c00014
J. Nat. Prod. 2020. 83. 1541−1552

Table 1. Inhibitory Activity of Tested Flavonoids against Human Liver FBPase[a]

compound	structure	$R^{2'}$	R^3	$R^{3'}$	$R^{4'}$	R^5	$R^{5'}$	R^6	R^7	R^8	% inhibition* or IC_{50} (μM) (mean ± SEM)
A1 (flavone)		-	H	H	H	-	-	-	-	-	< 20 %
A2		-	H	OH	H	-	-	-	-	-	< 20 %
A3		-	H	H	OH	-	-	-	-	-	< 20 %
A4		-	H	OH	OH	-	-	-	-	-	25 ± 2 %
A5		-	OH	OH	OH	-	-	-	-	-	20 ± 3 %
A6		-	OH	OMe	OMe	-	-	-	-	-	< 20 %
B1		-	-	H	H	-	-	-	-	-	< 20 %
B2		-	-	OH	H	-	-	-	-	-	< 20 %
B3		-	-	H	OH	-	-	-	-	-	< 20 %
B4		-	-	OH	OH	-	-	-	-	-	< 20 %
C1		-	H	H	H	H	-	H	OH	H	< 20 %
C2		-	H	OH	H	H	-	H	OH	H	< 20 %
C3		-	H	H	OH	H	-	H	OH	H	< 20 %
C4		-	OH	OH	H	H	-	H	OH	H	< 20 %
C5		-	OH	H	OH	H	-	H	OH	H	< 20 %
C6		-	H	OH	OH	H	-	H	OH	H	< 20 %
C7		-	OH	OH	OH	H	-	H	OH	OH	< 20 %
C8 (baicalein 7-methyl ether)		-	H	H	H	OH	-	OH	OMe	H	46 ± 3 %
C9 (baicalein trimethyl ether)		-	H	H	H	OMe	-	OMe	OMe	H	< 20 %
C10 (baicalin)		-	H	H	H	OH	-	OH	glucuronide	H	< 20 %
C11		-	OH	OMe	H	H	-	H	OMe	H	< 20 %
C12		-	OH	H	OMe	H	-	H	OMe	H	< 20 %
C13		-	OH	OH	OH	H	-	H	OMe	OMe	< 20 %
C14		-	OH	OMe	OMe	H	-	H	OH	OH	33 ± 1 %
C15		-	OH	OBn	OBn	H	-	H	OMe	OMe	< 20 %
C16		-	OH	OMe	OMe	H	-	H	OBn	OBn	< 20 %
D1 (chrysin)		H	H	H	H	-	H	H	-	H	< 20 %
D2 (galangin)		H	OH	H	H	-	H	H	-	H	< 20 %

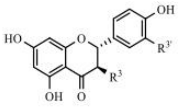
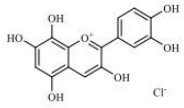
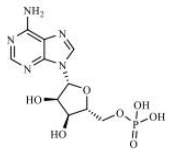
https://dx.doi.org/10.1021/acs.jnatprod.0c00014
J. Nat. Prod. 2020, 83, 1541−1552

Table 1. continued

compound	structure	$R^{2'}$	R^3	$R^{3'}$	$R^{4'}$	R^5	$R^{5'}$	R^6	R^7	R^8	% inhibition* or IC_{50} (μM) (mean ± SEM)
D3 (baicalein)		H	H	H	H	-	H	OH	-	H	**29 ± 3 μM** [a,c]
D4		H	H	OH	H	-	H	H	-	H	< 20 %
D5 (apigenin)		H	H	H	OH	-	H	H	-	H	< 20 %
D6 (kaempferol)		H	OH	H	OH	-	H	H	-	H	< 20 %
D7 (luteolin)		H	H	OH	OH	-	H	H	-	H	22 ± 2 %
D8 (scutellarein)		H	H	H	OH	-	H	OH	-	H	**38.2 ± 0.4 μM** [a]
D9 (quercetin)		H	OH	OH	OH	-	H	H	-	H	< 20 %
D10 (myricetin)		H	OH	OH	OH	-	OH	H	-	H	< 20 %
D11 (morin)		OH	OH	H	OH	-	H	H	-	H	< 20 %
D12 (quercetagetin)		H	OH	OH	OH	-	H	OH	-	H	37 ± 4 %
D13 (norwogonin)		H	H	H	H	-	H	H	-	OH	< 20 %
D14 (herbacetin)		H	OH	H	OH	-	H	H	-	OH	**8.7 ± 0.7 μM** [b]
D15 (gossypetin)		H	OH	OH	OH	-	H	H	-	OH	**24 ± 2 μM** [c]
D16		H	Cl	OH	OH	-	H	H	-	H	< 20 %
D17		H	H	OH	OH	-	H	Cl	-	H	< 20 %
D18		H	H	OH	OH	-	H	H	-	Cl	< 20 %
D19		H	Cl	OH	OH	-	H	H	-	Cl	< 20 %
D20		H	H	OH	OH	-	H	Cl	-	Cl	< 20 %
D21 (chrysoeriol)		H	H	OMe	OH	-	H	H	-	H	< 20 %
D22 (acacetin)		H	H	H	OMe	-	H	H	-	H	< 20 %
D23		H	H	OMe	OMe	-	H	H	-	H	< 20 %
D24 (rutin)		H	rutinose	OH	OH	-	H	H	-	H	< 20 %
D25 (gossypin)		H	OH	OH	OH	-	H	H	-	glucose	< 20 %

https://dx.doi.org/10.1021/acs.jnatprod.0c00014
J. Nat. Prod. 2020, 83, 1541−1552

Table 1. continued

compound	structure	$R^{2'}$	R^3	$R^{3'}$	$R^{4'}$	R^5	$R^{5'}$	R^6	R^7	R^8	% inhibition* or IC_{50} (μM) (mean ± SEM)
E1 (naringenin)		-	H	H	-	-	-	-	-	-	< 20 %
E2 (eriodictyol)		-	H	OH	-	-	-	-	-	-	< 20 %
E3 (taxifolin)		-	OH	OH	-	-	-	-	-	-	< 20 %
F1 (gossypetinidin chloride)		-	-	-	-	-	-	-	-	-	46 ± 1 %
Positive control: **AMP**		-	-	-	-	-	-	-	-	-	**2.6 ± 0.2 μM** [d]

[a]*Inhibition (mean,% ± SEM) at the highest tested concentration, 200 μM. Same superscript letters indicate that the IC_{50} values are not statistically different ($p > 0.05$), and different superscript letters indicate that the IC_{50} values are statistically different from each other ($p < 0.05$).

(herbacetin), IC_{50} = 8.7 ± 0.7 μM. The positive control, AMP, exhibited an IC_{50} value of 2.6 ± 0.2 μM (Table 1).

Herbacetin, a natural flavonoid found in flaxseed and other plants, has already been shown to protect against the harmful effects of chronic high-fat diet consumption (associated with insulin resistance) due to its anti-hyperglycaemic and anti-hyperlipidemic activities through the regulation of hepatic lipid metabolizing and lipid-regulating enzymes.[32] Moreover, the potential of herbacetin for the management of T2D has been acknowledged, through interaction with the targets aldose reductase and insulin receptor.[33] Interestingly, flaxseed has already been described as a potential anti-inflammatory agent, and the ingestion of flaxseed oil or flaxseed supplementation reduced glucose levels and glycosylated hemoglobin concentration, as well as increased insulin sensitivity in humans.[34,35] As mentioned above, in addition to **D14** (herbacetin), **D3** (baicalein), **D8** (scutellarein), and **D15** (gossypetin) were among the most active FBPase inhibitors. Baicalein is known as an important component of the Chinese plant *Scutellaria baicalensis*. This plant is a member of the mint family and is used in Chinese and Japanese medicine. Baicalein has already demonstrated antitumor, anti-inflammatory, antioxidant, and antidiabetic properties, among others.[36] Scutellarein is found in the perennial herb *Scutellaria lateriflora*. The high bioavailability of scutellarein has been attributed to its improved solubility compared with scutellarin. Scutellarin has been used in China since 1984 for the treatment of acute cerebral infarction and paralysis induced by cerebrovascular diseases such as hypertension, cerebral thrombosis, and cerebral hemorrhage. In fact, scutellarin is mainly absorbed in the form of its hydrolyzed product scutellarein, which might be the real bioactive component that can be found in the body.[37,38] Regarding gossypetin, this compound is usually found in the flowers and the calyces of *Hibiscus sabdariffa*. This plant has been used traditionally as a sedative and for the treatment of nervous disorders. Besides anxiolytic and antidepressant activities of gossypetin, this flavonoid is also associated with antimicrobial, antiatherosclerotic, and anti-inflammatory effects.[39,40]

Concerning flavonoids from groups A and B, no significant FBPase inhibition was found up to the highest tested concentration of 200 μM (less than 20% inhibition).

Regarding group C, only two of the tested flavonoids presented inhibitory activity against FBPase, at the maximum tested concentration (200 μM): **C8** (baicalein 7-methyl ether) and **C14**: with inhibition percentages of 46 ± 3% and 33 ± 1%, respectively.

Regarding flavonoids from group D, the most effective compound was flavonoid **D14** (herbacetin), with an IC_{50} = 8.7 ± 0.7 μM. **D14** presents −OH groups at C-3 of ring C, at C-4′ of ring B, and at C-5, C-7, and C-8 of ring A. The addition of a OH-3′ group at ring B led to a reduction of about 3-fold of the inhibitory activity of flavonoids, as it can be seen through comparison of **D14** (herbacetin) with **D15** (gossypetin). Comparing **D25** (gossypin) and **C10** (baicalin), with **D15** (gossypetin) and **D3** (baicalein), respectively, it was possible to verify that the 7-glycosylation at ring A decreases the FBPase inhibition. In fact, both **D15** (gossypetin) and **D3** (baicalein) were among the most active compounds, both being trihydroxylated in ring A.

In flavonoids with no substituents in rings B and C, the location of the −OH group at C-6 affected their activity. When comparing **D3** (baicalein) with **D1** (chrysin), the latter was not active up to the highest tested concentration (200 μM). Additionally, comparing **D3** (baicalein) with **D8** (scutellarein), it can be concluded that the addition of a OH-4′ group in ring B led to a slight increase in the IC_{50} value. Moreover, the addition of hydroxy groups at C-3 of ring C and at C-3′ of ring B, besides the presence of an OH-4′ group in ring B [**D12** (quercetagetin)], decreased even more the inhibition of the liver enzyme by flavonoids: **D3** (baicalein) (IC_{50} = 29 ± 3 μM) > **D8**

https://dx.doi.org/10.1021/acs.jnatprod.0c00014
J. Nat. Prod. 2020, 83, 1541−1552

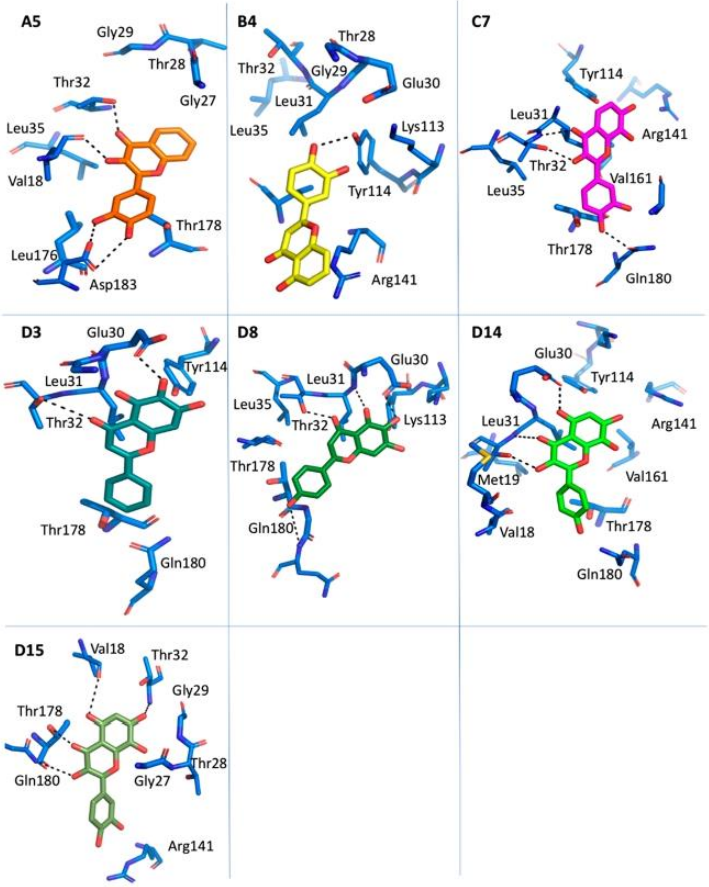


Figure 3. Predominant interactions observed along the MD trajectories for the selected flavonoids. Hydrogen bonds are labeled with a dashed line.

(scutellarein) (IC_{50} = 38.2 ± 0.4 μM) > **D12** (quercetagetin) (inhibition of 37 ± 4% at 200 μM). In the present work, flavonoids **D9** (quercetin), **D11** (morin), and **D24** (rutin) showed no ability to inhibit FBPase. Contrary to what has been reported in previous studies, morin[30] and rutin[26] decreased the FBPase activity in streptozotocin-induced diabetic rats, while the FBPase reduction by quercetin was observed in alloxan-induced T2D mice.[29] These differences may be attributed to the source of the enzyme, since the present work was focused on the direct inhibition of the human liver FBPase.

Furthermore, the methoxylation and glycosylation of **D3** (baicalein) was not favorable for the effect under study, as seen from comparing **D3** (baicalein) with **C8** (baicalein 7-methyl ether), **C9** (baicalein trimethyl ether), and **C10** (baicalin).

Chlorinated flavonoids (**D16**–**D20**) did not inhibit human liver FBPase up to the maximum tested concentration of 200 μM. However, in previous works our research group have demonstrated their promising activities against α-amylase[41] and α-glucosidase.[23] These results highlight the importance of finding a detailed potential antidiabetic mechanism of action of each flavonoid and, in this way, the possible finding of a specific target-directed therapeutic.

In the flavanone group (group E), the compounds **E1**–**E3**, without the double bond between C-2 and C-3, were not able to inhibit FBPase; likewise, their parent compounds **D5** (apigenin), **D7** (luteolin), and **D9** (quercetin) that have this double bond did not inhibit FBPase. Thus, it seems this feature does not favor the FBPase inhibition.

Finally, anthocyanin **F1** (gossypetinidin chloride) exhibited an inhibition of only 46 ± 1%, at the maximum tested concentration. When comparing **F1** (gossypetinidin chloride) with **D15** (gossypetin), it is clear the C-4 carbonyl group at the pyrone ring (ring C) in the last one is important for the inhibition of FBPase.

Molecular Determinants of Flavonoid Binding to the Human Liver FBPase. The flavonoid series evaluated contained 55 compounds with reported data on FBPase inhibition. Each of the 55 flavonoids was docked in the allosteric cavity of FBPase. After an in-depth analysis, it was realized that the docking results did not discriminate between active and inactive compounds. In this preliminary docking study, the ligands were docked close to the N-terminal, and the loop regions were delimited by residues 23–31 and 176–182. As observed in other enzymes, these regions might display high flexibility to accommodate the allosteric ligands. As the docking was performed with a rigid receptor, such effects could not be captured. Flexible receptor docking might represent an alternative, but the extent of reorganization of the receptor provided by the method is often insufficient. Therefore, it was decided to study instead the binding of a subset of compounds

https://dx.doi.org/10.1021/acs.jnatprod.0c00014
J. Nat. Prod. 2020, 83, 1541−1552

Table 2. Persistent Hydrogen Bonds between Each Inhibitor and the Receptor, in Terms of Percentage of Time Held[a]

	enzyme residue										
flavonoid	Val 18	Gly 29	Glu 30	Leu 31	Thr 32	Tyr 114	Thr 178	Gln 180	Asp 183	**ΔG_{bind} Kcal/mol**	**IC_{50} (μM) or % inhibition at 200 μM**
A5	47%				96%				99%	-2.70	20 ± 3 %
B4						30%				-0.42	< 20 %
C7		41%			91%			27%		-0.87	< 20 %
D3 (baicalein)		0	33%		53%					-4.17	29 ± 3 μM
D8 (scutellarein)		66%	96%	69%	93%			35%		-2.36	38.2 ± 0.4 μM
D14 (herbacetin)			99%	54%	82%					-13.1	8.7 ± 0.7 μM
D15 (gossypetin)	28%				61%		25%	35%		-1.17	24 ± 2 μM

[a]Only hydrogen bonds with a lifetime larger than 25% are shown. Binding free energies (ΔG_{bind}) calculated with MD-LIE for the selected active and nonactive inhibitors are also shown. The calculations used α and β parameters of 0.16 and 0.5.

that included the marginally active compound **A5**, the active compounds **D3** (baicalein), **D8** (scutellarein), **D14** (herbacetin), and **D15** (gossypetin), and the structurally close, but inactive, analogues of the latter, **B4** and **C7**, through a much more accurate, and computational-intensive, MD and LIE approach.

The compounds were selected to map the key interactions between the ligands and the enzyme and to rationalize the importance of the substituents at each position. The experimental results showed that at least three −OH groups are present in all active inhibitors. From groups A and B, the only compounds that met this property were **A5** and **B4** since they have the same substituents in ring A, but differ at the C-3 and C-5 positions. While **A5** (<20% inhibition) has an OH-3 in ring C, B4 has an OH-5 functionality, also adjacent to a C-4 C═O, but in ring A. In contrast, **C7** was inactive, but **D15** (gossypetin) was active, with an IC_{50} value of 24 ± 2 μM, even though these two compounds only differ by the presence of an OH-5 in ring A.

MD simulations showed that there were no significant rearrangements of the allosteric pocket, but a rearrangement on the binding pose of compounds **B4** and **C7** was found instead, which was not captured in the docking calculations (Figure S1, Supporting Information), confirming the need for MD calculations in this system. In all complexes simulated, the root-mean-square fluctuations of residues 7 to 32 displayed smaller values when compared with the apo enzyme, which showed a rigidification of the loop due to the inhibitor binding.

The MD simulations revealed that it takes approximately 20 ns for the ligands and its surroundings to adopt their definitive binding pose (Figures S2 and S3, Supporting Information). The binding poses are shown in Figure 3. A map of the interactions that hold for at least 25% of the analyzed time is shown in Table 2.

The results showed that six out of the seven evaluated compounds form a H-bond with the Thr32 during more than 50% of the time analyzed.

The nonactive ligands **B4** and **C7** did not form strong interactions with the protein. Compound **B4** even lost contact with Thr32 as observed for all other compounds in the set examined. This ligand did not form any stable interaction during the trajectory, forming short-lived interactions with many residues in the pocket instead. The longest-lived interaction occurred between the OH-3 in ring B and the Tyr114 side chain, but only during 30% of the simulation time. Consistently, LIE calculation identified **B4** as the compound with less affinity, with a binding free energy (ΔG_{bind}) of −0.42 kcal/mol.

Compound **C7** was stabilized through interactions with Thr32, Gly29, and Gln180 only. The predicted LIE for this compound was in line with the observed interactions, showing higher affinity than **B4** (−0.87 kcal/mol).

In the case of **A5**, the interactions with Thr178 and Gln180 were lost. The MD simulations revealed an interaction between the C-3′ and C-4′ catechol moiety of ring B and Asp183, during the whole trajectory. The absence of substituents in ring A and, as a consequence, its reduced volume (when compared with the ligands in the other groups) allowed flavonoid **A5** to explore less surface-exposed regions in the pocket. The LIE calculations predicted a ΔG_{bind} of −2.7 kcal/mol, making it a better ligand than **C7** and **B4**. In fact, this value seems to be overestimated and is the only one that lies out of the general experimental trend.

Flavonoids **D3** (baicalein), **D8** (scutellarein), **D14** (herbacetin), and **D15** (gossypetin) were found to be the most active inhibitors, all interacting all Thr32 and Glu30. **D8** (scutellarein) and **D14** (herbacetin), but not **D3** (baicalein), also interacted strongly with Leu31. In all cases, the side chain of Glu30 rotated during the MD simulation to allow the establishment of interactions with the flavonoids and seemed to display an important role in its inhibitory effect. In fact, the longer the ligands interacted with Glu30, the more favorable were the predicted binding free energies (see Table 2).

The ΔG_{bind} for **D8** (scutellarein) and **D14** (herbacetin) was calculated to be −2.36 and −13.1 kcal/mol. The value for **D3** (baicalein) was −4.1 kcal/mol. These results are consistent with the in vitro assays conducted, which show that **D14** (herbacetin) is by far the inhibitor with the most potent affinity and that **D3**

https://dx.doi.org/10.1021/acs.jnatprod.0c00014
J. Nat. Prod. 2020, 83, 1541−1552

(baicalein) and **D8** (scutellarein) have similar effects. The LIE results also show the affinities of **D3** (baicalein) and **D8** (scutellarein) to be similar, **D14** (herbacetin) being much more favorable.

Flavonoid **D15** (gossypetin) displayed an alternative set of contacts involving Val18, Thr32, Thr178, and Gln180. The predicted ΔG_{bind} (−1.17 kcal/mol) was less favorable than the other compounds in the group, but more favorable than **B4** and **C7**.

The calculated LIE binding free energy values, despite being semiquantitative in nature, correlate very well with the experimental results [except for **D15** (gossypetin)], showing that the predicted binding poses are mostly correct and reliable. The results suggested that three −OH groups, at the C-5, C-7, and C-8, and/or C-3′ and C-4′ positions, in ring A or B are needed to stabilize the loops that are delimited by the residues 23 to 31 and 176 to 182. MD simulations pinpoint the relevance of the H-bond established between the C-4 carbonyl group and the backbone amine of Thr32. In fact, all the active compounds interact with this residue during more than 50% of the trajectory. This key interaction is also present in several X-ray structures, including the one used in this study. The MD simulations also showed that the active compounds **D3** (baicalein), **D8** (scutellarein), and **D14** (herbacetin) form an important H-bond between the substituents in ring C and the Glu30 side chain, which reorients itself to establish such interaction. These results, together with the LIE free energy predictions, suggest that Glu30 may be relevant for the inhibition of the enzyme. The simulations revealed an interaction between the hydroxy groups of ring B for **A5** and the Asp183 during the whole trajectory calculated. The absence of substituents in ring A and, as a consequence, its reduced volume, when compared with the ligands in the other groups, allowed the compound to explore less surface-exposed regions in the pocket. In fact, Glu30 and Asp183 display similar chemical properties, and this alternative interaction may justify the marginal inhibition of the enzyme by **A5**.

The search and development of novel and specific hypoglycemic agents represents an area of high interest among the scientific community. Particularly, inhibition of liver FBPase is considered a new valid approach for the treatment of T2D. Nowadays there is no pharmacological treatment that directly acts on the reduction of the gluconeogenesis process,[1] but it has been reported that the flavonoids rutin,[26] diosmin,[27] biochanin A,[28] morin,[30] and hesperetin[31] are able to decrease FBPase activity in streptozotocin-induced diabetic rats. In accordance, the inhibition of FBPase by quercetin,[29] performed in alloxan-induced diabetic mice, led to a reduction in EGP.

Despite the promising activity of these naturally occurring flavonoids, care should be taken with the interpretation of the present results, because in humans, the absorption of flavonoids depends on their physicochemical properties such as molecular size, configuration, lipophilicity, solubility, pK_a, and pharmacokinetic properties.[42] After ingestion, flavonoids suffer extensive metabolism, with absorption occurring in both the small and large intestine.[43] In particular, the absorption of flavonoid glycosides requires hydrolysis of sugar conjugates or a specific active transport mechanism in the intestine. In the lumen of the small intestine, lactase phlorizin hydrolase (LPH) hydrolyzes flavonoid glycosides into their respective aglycones. Alternatively, the glycosides can be directly transported into the epithelium through epithelial transporters, such as sodium-glucose transport proteins, with subsequent hydrolyzation by intracellular β-glucosidases.[43] The production of smaller compounds facilitates their entry into the bloodstream. Once in the bloodstream, flavonoids undergo phase I metabolism by cytochrome P450 monooxygenases and phase II metabolism by conjugation enzymes, such as glucuronosyltransferases (UGTs), sulfotransferases, and catechol-*O*-methyltransferases (COMTs), in the liver with additional glucuronidation, sulfation, or methylation.[43,44] In general, it is difficult to compare plasma levels of flavonoids found in different studies mainly due to the variability of the studied population and supplementation methods. Nevertheless, despite the ingestion of flavonoids in mg/day, they are found in human plasma in the range of μM.[45] It is expected that the application of nanotechnology, such as the use of liposomes as carriers, may increase solubility and stability of phytochemicals, enhancing their absorption and bioavailability, protect them from premature degradation, and therefore increase their circulation time.[46,47]

Concluding Remarks. For the first time, the inhibitory activities of flavonoids against isolated human liver FBPase have been investigated. For this evaluation, a total of 55 flavonoids (groups A−F) were tested, applying a kinetic analysis. Moreover, a subset of seven compounds among four different groups in this flavonoid series was evaluated by LIE free energy calculations. The results showed that FBPase inhibition depends on the nature and position of the substituents present. Following this rationale, it was concluded that the hydroxylation of the flavonoid structure, particularly in ring A, is important for the enhancement of inhibitory activity when compared with methoxylation, benzyloxylation, chlorination, or glycosylation. The most effective flavonoid found was **D14** (herbacetin), and the most important structural features for FBPase inhibition are the presence of −OH groups at C-3 of ring C, at C-4′ of ring B, and at C-5, C-7, and C-8 of ring A, as well as the double bond between C-2 and C-3 and a C-4 carbonyl function at the pyrone ring (Figure 4). This flavonoid is found in flaxseed, a functional

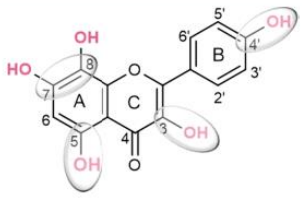


Figure 4. Potential flavonoid substituents that contribute to increase FBPase inhibition.

food that has already shown anti-inflammatory and antidiabetic effects. This work significantly contributes to the study of the direct inhibition of isolated human FBPase by flavonoids and sheds light on a better understanding of the flavonoid substituents and their FBPase interactions. The most promising flavonoids found here may constitute a valuable model for the search and design of new scaffolds toward T2D management, via FBPase inhibition.

■ EXPERIMENTAL SECTION

Chemicals. The PicoProbe fructose-1,6-bisphosphatase inhibitor screening kit was obtained from BioVision, Inc. (Milpitas, CA, USA). The following flavonoids were obtained from Indofine Chemical Company, Inc. (Hillsborough, NJ, USA): **A1**, **A2**, **A3**, **A4**, **A5**, **A6**, **B1**, **B2**, **B3**, **B4**, **C1**, **C2**, **C3**, **C4**, **C5**, **C6**, **C11**, **C12**, **D1** (chrysin), and **D2**

https://dx.doi.org/10.1021/acs.jnatprod.0c00014
J. Nat. Prod. 2020, 83, 1541−1552

(galangin). Flavonoids **C8** (baicalein 7-methyl ether), **C9** (baicalein trimethyl ether), **C10** (baicalin), **D8** (scutellarein), **D12** (quercetagetin), **D13** (norwogonin), **D15** (gossypetin), and **F1** (gossypetinidin chloride) were obtained from Extrasynthese (Genay, France). Dimethyl sulfoxide (DMSO), AMP, and flavonoids **D3** (baicalein), **D5** (apigenin), **D6** (kaempferol), **D7** (luteolin), **D9** (quercetin), **D10** (myricetin), **D11** (morin), **D14** (herbacetin), **D22** (acacetin), **D24** (rutin), **D25** (gossypin), **E1** (naringenin), **E2** (eriodictyol), and **E3** (taxifolin) were obtained from Sigma-Aldrich, Inc. (St. Louis, MO, USA). Finally, the following flavonoids were synthesized according to previous companion papers:[48,49] **C7**, **C13**, **C14**, **C15**, **C16**, **D4**, **D16**, **D17**, **D18**, **D19**, **D20**, **D21** (chrysoeriol), and **D23**.

In Vitro Human Liver FBPase Inhibition Assay. The inhibitory activity of the flavonoids under study against human liver FBPase—the protein product of FBP1 gene—was tested using a PicoProbe fructose-1,6-bisphosphatase inhibitor screening kit, according to the manufacturer's instructions. In this kit, human FBPase hydrolyzes fructose 1,6-bisphosphate to fructose 6-phosphate, which oxidizes and reacts with a fluorogenic probe, which is detected at $\lambda_{Em/Ex}$ = 535/587 nm. Briefly, the FBPase enzyme was exposed to the flavonoids under study (0−200 μM, dissolved in DMSO) in a 96-well plate. After 5 min of incubation at 37 °C, the reaction was started by the addition of the "reaction mix preparation" and monitored for 20 min at 37 °C in a microplate reader (Cytation 3 Imaging Reader, BioTek) ($\lambda_{Em/Ex}$ = 535/587 nm). AMP (0−10 μM) was used as positive control. The amount of DMSO used [0.1% (v/v)] did not interfere with the assay. The difference between the fluorescence values obtained at 4 min and at 14 min served for the calculation of catalytic rates. Each result of FBPase inhibition by the tested flavonoids is expressed as % of inhibition ± standard error of the mean (SEM). All statistical analysis was performed using GraphPad Prism. Statistical comparison among the active flavonoids was estimated by applying one-way analysis of variance (ANOVA). Differences were considered to be significant at p values lower than 0.05. Each study corresponds to at least three independent experiments.

In Silico Approach to Determine the Molecular Determinants of the FBPase Inhibition. Molecular docking was applied initially to predict the binding mode of the series of 55 flavonoids to the human FBPase. The chain A of the X-ray structure with the Protein Data Bank (PDB) ID 5Q0C[50] was selected to perform the calculations. Although this is not the structure with the highest resolution available, it is, as far as we are aware, the only complete structure of human FBPase available to date and was solved at 2.4 Å resolution. The side chain protonation states were predicted with propka3.1.[51] Accordingly, to the propka3.1 results, the Asp119 residue was modeled as neutral, with all other residues modeled in the same protonation states that they have in water at a pH of 7.5. The series of ligands were modeled with MarvinSketch (version 19.9) from the Chemaxon package and then optimized in 3D using the same software.[52] Docking calculations were performed using the GOLD software. Altogether 100 poses per ligand were generated using the genetic algorithm search parameters, with the Chemscore scoring function implemented in the software. Full flexibility for the ligand was considered, which included the flipping of amide bonds.[53] A cavity with a 15 Å radius centered on the CD1 atom of Leu31 was defined to perform the binding search. The 100 binding poses were then clustered by similarity, and the representative structure of each cluster was inspected visually.

The binding cavity is located on a loop region comprising residues 8 to 30 and 176 to 182. Anticipating that the flexibility of the binding cavity may play a crucial role for the allosteric binding, MD simulations and LIE calculations were carried out on a subset of seven compounds. The selected compounds were **A5**, **B4**, **C7**, **D3** (baicalein), **D8** (scutellarein), **D14** (herbacetin), and **D15** (gossypetin). The calculations were carried out to better understand the molecular basis of the affinity of the compounds and the role of the flavonoid substituents. The MD simulations were performed using the Amber18 package, and the calculations were done using AmberTools 14 following the LIEW protocol described in the A24 tutorial.[54] Thus, for each of the compounds referred to above, two systems were prepared: an enzyme-ligand complex and a ligand in solution. A system with the apo protein in water was also modeled.

Briefly, each system was parametrized using the ff14SB force field parameters for the protein[55] and the gaff force field for the organic molecules.[56,57] The simulations began with a short minimization and equilibration of the respective system, followed by 20 ns of MD production in the NVT ensemble at 300 K. Snapshots of the systems were saved in intervals of 20 ps. Simulations were performed with a 9 Å cutoff for short-range nonbonding interactions, and the long-range electrostatic interactions were treated with the particle-mesh Ewald summation method. Bonds to hydrogen atoms were constrained by the SHAKE method,[58] and an integration time step of 2 fs was used. The snapshots recorded during the simulation trajectories were analyzed with the cpptraj module implemented in the Amber package. The energetic calculations were carried out using a LIE approach on the snapshots recorded in the interval of 10 to 20 ns of MD simulations, in each starting system. Calculations were carried out with the lie.pl program in AmberTools14, employing the three-trajectory approach.[59]

■ ASSOCIATED CONTENT

Supporting Information

The Supporting Information is available free of charge at https://pubs.acs.org/doi/10.1021/acs.jnatprod.0c00014.

Predicted binding modes of the selected flavonoids (**A5**, **B4**, **C7**, **D3**, **D8**, **D14**, and **D15**), obtained by molecular docking calculations; stability and flexibility of the protein backbone and the ligand during the 20 ns trajectory calculated for each of the complexes; estimated energy of binding of selected compounds (**A5**, **B4**, **C7**, **D3**, **D8**, **D14**, and **D15**) to the allosteric cavity of the FBPase enzyme (PDF)

■ AUTHOR INFORMATION

Corresponding Author

Eduarda Fernandes − *LAQV, REQUIMTE, Laboratory of Applied Chemistry, Department of Chemical Sciences, Faculty of Pharmacy, University of Porto, 4050-313 Porto, Portugal;* orcid.org/0000-0001-6424-0976; Phone: +351 220428675; Email: egracas@ff.up.pt

Authors

Carina Proença − *LAQV, REQUIMTE, Laboratory of Applied Chemistry, Department of Chemical Sciences, Faculty of Pharmacy, University of Porto, 4050-313 Porto, Portugal*

Ana Oliveira − *UCIBIO, REQUIMTE, Department of Chemistry and Biochemistry, Faculty of Sciences, University of Porto, 4169-007 Porto, Portugal*

Marisa Freitas − *LAQV, REQUIMTE, Laboratory of Applied Chemistry, Department of Chemical Sciences, Faculty of Pharmacy, University of Porto, 4050-313 Porto, Portugal*

Daniela Ribeiro − *LAQV, REQUIMTE, Laboratory of Applied Chemistry, Department of Chemical Sciences, Faculty of Pharmacy, University of Porto, 4050-313 Porto, Portugal*

Joana L. C. Sousa − *LAQV-REQUIMTE & QOPNA, Department of Chemistry, University of Aveiro, 3810-193 Aveiro, Portugal*

Maria J. Ramos − *UCIBIO, REQUIMTE, Department of Chemistry and Biochemistry, Faculty of Sciences, University of Porto, 4169-007 Porto, Portugal;* orcid.org/0000-0002-7554-8324

Artur M. S. Silva − *LAQV-REQUIMTE & QOPNA, Department of Chemistry, University of Aveiro, 3810-193 Aveiro, Portugal;* orcid.org/0000-0003-2861-8286

https://dx.doi.org/10.1021/acs.jnatprod.0c00014
J. Nat. Prod. 2020, 83, 1541−1552

Pedro A. Fernandes − *UCIBIO, REQUIMTE, Department of Chemistry and Biochemistry, Faculty of Sciences, University of Porto, 4169-007 Porto, Portugal;* orcid.org/0000-0003-2748-4722

Complete contact information is available at: https://pubs.acs.org/10.1021/acs.jnatprod.0c00014

Notes

The authors declare no competing financial interest.

■ ACKNOWLEDGMENTS

The work was supported by UIDB/50006/2020 with funding from FCT/MCTES through national funds, and "Programa Operacional Competitividade e Internacionalização" (COMPETE) (POCI-01-0145-FEDER-029241) as well as by UID/QUI/062/2019. C.P. acknowledges FCT for the financial support for the Ph.D. grant (SFRH/BD/116005/2016), in the ambit of "QREN - POPH - Tipologia 4.1 - Formação Avançada", cosponsored by Fundo Social Europeu (FSE) and by national funds of Ministério da Ciência, Tecnologia e Ensino Superior (MCTES). D.R. and M.F. acknowledge the financial support from the European Union [FEDER funds through the Operational Competitiveness Program (COMPETE)] (POCI-01-0145-FEDER-029253 and POCI-01-0145-FEDER-029248, respectively). We acknowledge that the results of this research have been achieved using the PRACE Research Infrastructure resources of Marenostrum IV in Spain.

■ REFERENCES

(1) Kaur, R.; Dahiya, L.; Kumar, M. *Eur. J. Med. Chem.* **2017**, *141*, 473−505.
(2) van Poelje, P. D.; Potter, S. C.; Erion, M. D. In *Diabetes - Perspectives in Drug Therapy*; Schwanstecher, M., Ed.; Springer Berlin Heidelberg: Berlin, Heidelberg, 2011; pp 279−301.
(3) Kitas, E.; Mohr, P.; Kuhn, B.; Hebeisen, P.; Wessel, H. P.; Haap, W.; Ruf, A.; Benz, J.; Joseph, C.; Huber, W.; Sanchez, R. A.; Paehler, A.; Benardeau, A.; Gubler, M.; Schott, B.; Tozzo, E. *Bioorg. Med. Chem. Lett.* **2010**, *20*, 594−599.
(4) Bie, J.; Liu, S.; Zhou, J.; Xu, B.; Shen, Z. *Bioorg. Med. Chem.* **2014**, *22*, 1850−1862.
(5) Kerru, N.; Singh-Pillay, A.; Awolade, P.; Singh, P. *Eur. J. Med. Chem.* **2018**, *152*, 436−488.
(6) Droppelmann, C. A.; Saez, D. E.; Asenjo, J. L.; Yanez, A. J.; Garcia-Rocha, M.; Concha, I. I.; Grez, M.; Guinovart, J. J.; Slebe, J. C. *Biochem. J.* **2015**, *472*, 225−237.
(7) Barciszewski, J.; Wisniewski, J.; Kolodziejczyk, R.; Jaskolski, M.; Rakus, D.; Dzugaj, A. *Acta Cryst. D Struct. Biol.* **2016**, *72*, 536−550.
(8) Choe, J.-Y.; Nelson, S. W.; Arienti, K. L.; Axe, F. U.; Collins, T. L.; Jones, T. K.; Kimmich, R. D. A.; Newman, M. J.; Norvell, K.; Ripka, W. C.; Romano, S. J.; Short, K. M.; Slee, D. H.; Fromm, H. J.; Honzatko, R. B. *J. Biol. Chem.* **2003**, *278*, 51176−51183.
(9) Agius, L. *Best Pract. Res. Clin. Endocrinol. Metab.* **2007**, *21*, 587−605.
(10) Bie, J.; Liu, S.; Li, Z.; Mu, Y.; Xu, B.; Shen, Z. *Eur. J. Med. Chem.* **2015**, *90*, 394−405.
(11) Heng, S.; Harris, K. M.; Kantrowitz, E. R. *Eur. J. Med. Chem.* **2010**, *45*, 1478−1484.
(12) Tayyem, R. F.; Zalloum, H. M.; Elmaghrabi, M. R.; Yousef, A. M.; Mubarak, M. S. *Eur. J. Med. Chem.* **2012**, *56*, 70−95.
(13) Chikara, G.; Sharma, P. K.; Dwivedi, P.; Charan, J.; Ambwani, S.; Singh, S. *Indian J. Clin. Biochem.* **2018**, *33*, 121−131.
(14) U.S. National Library of Medicine Safety, tolerability, and efficacy study of MB07803 administered to patients with type 2 diabetes mellitus. https://www.clinicaltrials.gov/ct2/results?cond=&term=mbo7803&cntry=&state=&city=&dist=.
(15) Han, X.; Huang, Y.; Zhang, R.; Xiao, S.; Zhu, S.; Qin, N.; Hong, Z.; Wei, L.; Feng, J.; Ren, Y.; Feng, L.; Wan, J. *Spectrochim. Acta, Part A* **2016**, *165*, 155−160.
(16) Nicolle, E.; Souard, F.; Faure, P.; Boumendjel, A. *Curr. Med. Chem.* **2011**, *18*, 2661−2672.
(17) Babu, P. V. A.; Liu, D.; Gilbert, E. R. *J. Nutr. Biochem.* **2013**, *24*, 1777−1789.
(18) Wenzel, U. *Curr. Opin. Pharmacol.* **2013**, *13*, 864−868.
(19) Xiao, J. B.; Hogger, P. *Curr. Med. Chem.* **2014**, *22*, 23−38.
(20) Vinayagam, R.; Xu, B. *Nutr. Metab.* **2015**, *12*, 1−20.
(21) Kawser, H. M.; Abdal, D. A.; Han, J.; Yin, Y.; Kim, K.; Kumar, S. S.; Yang, G.; Choi, H. Y.; Cho, S. G. *Int. J. Mol. Sci.* **2016**, *17*, 1−32.
(22) Eid, H. M.; Haddad, P. S. *Curr. Med. Chem.* **2017**, *24*, 355−364.
(23) Proença, C.; Freitas, M.; Ribeiro, D.; Oliveira, E. F. T.; Sousa, J. L. C.; Tome, S. M.; Ramos, M. J.; Silva, A. M. S.; Fernandes, P. A.; Fernandes, E. *J. Enzyme Inhib. Med. Chem.* **2017**, *32*, 1216−1228.
(24) Zhang, B. W.; Li, X.; Sun, W. L.; Xing, Y.; Xiu, Z. L.; Zhuang, C. L.; Dong, Y. S. *J. Agric. Food Chem.* **2017**, *65*, 8319−8330.
(25) Proença, C.; Freitas, M.; Ribeiro, D.; Sousa, J. L. C.; Carvalho, F.; Silva, A. M. S.; Fernandes, P. A.; Fernandes, E. *Food Chem. Toxicol.* **2018**, *111*, 474−481.
(26) Prince, P. S. M.; Kamalakkannan, N. *J. Biochem. Mol. Toxicol.* **2006**, *20*, 96−102.
(27) Pari, L.; Srinivasan, S. *Biomed. Pharmacother.* **2010**, *64*, 477−481.
(28) Harini, R.; Ezhumalai, M.; Pugalendi, K. V. *Eur. J. Pharmacol.* **2012**, *676*, 89−94.
(29) Alam, M. M.; Meerza, D.; Naseem, I. *Life Sci.* **2014**, *109*, 8−14.
(30) Vanitha, P.; Uma, C.; Suganya, N.; Bhakkiyalakshmi, E.; Suriyanarayanan, S.; Gunasekaran, P.; Sivasubramanian, S.; Ramkumar, K. M. *Environ. Toxicol. Pharmacol.* **2014**, *37*, 326−335.
(31) Jayaraman, R.; Subramani, S.; Sheik Abdullah, S. H.; Udaiyar, M. *Biomed. Pharmacother.* **2018**, *97*, 98−106.
(32) Veeramani, C.; Alsaif, M. A.; Al-Numair, K. S. *Chem.-Biol. Interact.* **2018**, *288*, 49−56.
(33) Singh, P.; Singh, V. K.; Singh, A. K. *Bioinformation* **2019**, *15*, 179−188.
(34) Rhee, Y.; Brunt, A. *Nutr. J.* **2011**, *10*, 10−44.
(35) Kajla, P.; Sharma, A.; Sood, D. R. *J. Food Sci. Technol.* **2015**, *52*, 1857−1871.
(36) Donald, G.; Hertzer, K.; Eibl, G. *Curr. Drug Targets* **2012**, *13*, 1772−1776.
(37) Tang, H.; Tang, Y.; Li, N.; Shi, Q.; Guo, J.; Shang, E.; Duan, J.-a. *Pharmacol., Biochem. Behav.* **2014**, *118*, 51−59.
(38) Shi, X.; Chen, G.; Liu, X.; Qiu, Y.; Yang, S.; Zhang, Y.; Fang, X.; Zhang, C.; Liu, X. *Int. J. Mol. Med.* **2015**, *35*, 31−38.
(39) Dwi Antika, L.; Kim, Y.-H.; Kang, M.-K.; Park, S.-H.; Lee, E.-J.; Choi, Y.-J.; Kang, Y.-H. *J. Funct. Foods* **2016**, *24*, 390−402.
(40) Gulsheen; Kumar, A.; Sharma, A. *J. Biol. Act. Prod. Nat.* **2019**, *9*, 205−214.
(41) Proença, C.; Freitas, M.; Ribeiro, D.; Tomé, S.; Oliveira, E.; Viegas, M.; Araujo, A.; Ramos, M. J.; Silva, A.; Fernandes, P.; Fernandes, E. *J. Enzyme Inhib. Med. Chem.* **2019**, *34*, 577−588.
(42) Kumar, S.; Pandey, A. K. *Sci. World J.* **2013**, *2013*, 1−16.
(43) Cassidy, A.; Minihane, A.-M. *Am. J. Clin. Nutr.* **2017**, *105*, 10−22.
(44) Ribeiro, D.; Proenca, C.; Rocha, S.; Lima, J.; Carvalho, F.; Fernandes, E.; Freitas, M. *Curr. Med. Chem.* **2018**, *25*, 3374−3412.
(45) Manach, C.; Donovan, J. L. *Free Radic. Res.* **2004**, *38*, 771−785.
(46) Mignet, N.; Seguin, J.; Chabot, G. G. *Pharmaceutics* **2013**, *5*, 457−471.
(47) Wang, S.; Su, R.; Nie, S.; Sun, M.; Zhang, J.; Wu, D.; Moustaid-Moussa, N. *J. Nutr. Biochem.* **2014**, *25*, 363−376.
(48) Freitas, M.; Ribeiro, D.; Tome, S. M.; Silva, A. M.; Fernandes, E. *Eur. J. Med. Chem.* **2014**, *86*, 153−164.
(49) Sousa, J. L. C.; Proença, C.; Freitas, M.; Fernandes, E.; Silva, A. M. S. *Eur. J. Med. Chem.* **2016**, *119*, 250−259.
(50) Ruf, A.; Joseph, C.; Alker, A.; Banner, D.; Tetaz, T.; Benz, J.; Kuhn, B.; Rudolph, M. B.; Yang, H.; Shao, C.; Burley, S. K. 5Q0C:

Human liver fructose-1,6-bisphosphatase 1 (fructose 1,6-bisphosphate 1-phosphatase, E.C.3.1.3.11) complexed with the allosteric inhibitor 1-(5-bromo-1,3-thiazol-2-yl)-3-[5-(4-methoxyphenyl)thiophen-2-yl]-sulfonylurea and with fructose-2,6-diphosphate, **2017**, DOI: 10.2210/pdb5Q0C/pdb.

(51) Olsson, M. H.; Sondergaard, C. R.; Rostkowski, M.; Jensen, J. H. *J. Chem. Theory Comput.* **2011**, *7*, 525−537.

(52) Axon, C. MarvinSketch. http://www.chemaxon.com.

(53) Jones, G.; Willett, P.; Glen, R. C.; Leach, A. R.; Taylor, R. *J. Mol. Biol.* **1997**, *267*, 727−748.

(54) Case, D. A.; Ben-Shalom, I. Y.; Brozell, S. R.; Cerutti, D. S.; Cheatham, I. D. E.; Cruzeiro, V. W. D.; Darden, T. A.; Duke, R. E.; Ghoreishi, D.; Gilson, M. K.; Gohlke, H.; Goetz, A. W.; Greene, D.; Harris, R.; Homeyer, N.; Izadi, S.; Kovalenko, A.; Kurtzman, T.; Lee, T. S.; LeGrand, S.; Li, P.; Lin, C.; Liu, J.; Luchko, T.; Luo, R.; Mermelstein, D. J.; Merz, K. M.; Miao, Y.; Monard, G.; Nguyen, C.; Nguyen, H.; Omelyan, I.; Onufriev, A.; Pan, F.; Qi, R.; Roe, D. R.; Roitberg, A.; Sagui, C.; Schott-Verdugo, S.; Shen, J.; Simmerling, C. L.; Smith, J.; Salomon-Ferrer, R.; Swails, J.; Walker, R. C.; Wang, J.; Wei, H.; Wolf, R. M.; Wu, X.; Xiao, L.; York, D. M.; Kollman, P. A. *AMBER 2018*; University of California: San Francisco, 2018.

(55) Maier, J. A.; Martinez, C.; Kasavajhala, K.; Wickstrom, L.; Hauser, K. E.; Simmerling, C. *J. Chem. Theory Comput.* **2015**, *11*, 3696−3713.

(56) Wang, J.; Wolf, R. M.; Caldwell, J. W.; Kollman, P. A.; Case, D. A. *J. Comput. Chem.* **2004**, *25*, 1157−1174.

(57) Wang, J.; Wang, W.; Kollman, P. A.; Case, D. A. *J. Mol. Graphics Modell.* **2006**, *25*, 247−260.

(58) Ryckaert, J.-P.; Ciccotti, G.; Berendsen, H. J. C. *J. Comput. Phys.* **1977**, *23*, 327−341.

(59) Case, D. A.; Babin, V.; Berryman, J. T.; Betz, R. M.; Cai, Q.; Cerutti, D. S.; Cheatham, I. T. E.; Darden, T. A.; Duke, R. E.; Gohlke, H.; Goetz, A. W.; Gusarov, S.; Homeyer, N.; Janowski, P.; Kaus, J.; Kolossváry, I.; Kovalenko, A.; Lee, T. S.; LeGrand, S.; Luchko, T.; Luo, R.; Madej, B.; Merz, K. M.; Paesani, F.; Roe, D. R.; Roitberg, A.; Sagui, C.; Salomon-Ferrer, R.; Seabra, G.; Simmerling, C. L.; Smith, W.; Swails, J.; Walker, R. C.; Wang, J.; Wolf, R. M.; Wu, X.; Kollman, P. A. *AmberTools14*; University of California: San Francisco, 2014.

https://dx.doi.org/10.1021/acs.jnatprod.0c00014
J. Nat. Prod. 2020, 83, 1541−1552

II.6. Development of a human sucrase-isomaltase (α-glucosidase) *in vitro* assay in Caco-2/TC7 cells, and proof of concept with the inhibitory activity of flavonoids

Manuscript submitted for publication

Development of a human sucrase-isomaltase (α-glucosidase) *in vitro* assay in Caco-2/TC7 cells, and proof of concept with the inhibitory activity of flavonoids

Carina Proença[a], Ana T. Rufino[a], José Miguel P. Ferreira de Oliveira[a], Pedro A. Fernandes[b], Artur M. S. Silva[c], Eduarda Fernandes[a,*]

[a]LAQV, REQUIMTE, Laboratory of Applied Chemistry, Department of Chemical Sciences, Faculty of Pharmacy, University of Porto, 4050-313 Porto, Portugal.

[b]UCIBIO, REQUIMTE, Department of Chemistry and Biochemistry, Faculty of Sciences, University of Porto, 4169-007 Porto, Portugal

[c]LAQV, REQUIMTE, Department of Chemistry, University of Aveiro, 3810-193 Aveiro, Portugal

* Corresponding author:

Eduarda Fernandes, PharmD; PhD

LAQV, REQUIMTE, Laboratory of Applied Chemistry

Department of Chemical Sciences

Faculty of Pharmacy, University of Porto

Rua de Jorge Viterbo Ferreira n.º 228, 4050-313 Porto, Portugal

Phone: +351 220428675

Email: egracas@ff.up.pt

Abstract

Type 2 diabetes (T2D) is the most common form of diabetes, and the number of people with this metabolic disease is steadily rising worldwide. From the available antidiabetic agents, α-glucosidase inhibitors are the most effective at reducing postprandial hyperglycaemia (PPHG). However, most of the studies have used the more readily available rat intestinal preparations or yeast α-glucosidase as the enzyme source in the experiments, so it cannot be assumed that the inhibition of those hydrolases and human enzyme will be equivalent. The present study evaluates the inhibitory activity of a selected group of flavonoids against human sucrase-isomaltase (SI), the α-glucosidase found in Caco-2/TC7 cells, following methodological optimization using the physiological substrates sucrose and maltose, and a synthetic substrate, *p*-nitrophenyl-α-D-glucopyranoside (*p*NPG). It was verified that the method using sucrose or maltose as substrate is specific for the evaluation of the brush-border SI enzyme. The flavonoids under study had, in general, a similar inhibitory activity against sucrase and maltase. On the contrary, the tested flavonoids were not effective in inhibiting SI, when using *p*NPG as substrate. Hydroxylation of flavonoids at C-3 of the C ring, at C-3'- and C-4' of the B ring, and at C-7 and C-8 of the A ring, exhibited an enhanced inhibition of human SI. These phenolic compounds deserve further exploration as alternatives to the currently available α-glucosidase inhibitors. Most importantly, this study clearly demonstrates that the non-clinical in vitro studies applied in the evaluation of α-glucosidase activity should use the human source rather than surrogates of α-glucosidase.

Keywords: Type 2 diabetes; sucrase-isomaltase inhibition; phenolic compounds; flavonoids; Caco-2/TC7 cells.

1. Introduction

Starch is one of the main sources of glucose for humans, being initially hydrolysed into oligosaccharides through cleavage of α-1,4-bonds by salivary and pancreatic α-1,4-glucan-4-glucanohydrolases, commonly known as α-amylase (EC 3.2.1.1.) (1, 2). The starch oligosaccharides such as maltose, maltotriose and α-limit dextrins, are finally broken down into glucose by the intestinal brush-border α-glucosidases (3). The produced glucose is in turn absorbed at the intestinal mucosa into the portal blood by the glucose transporter (GLUT)2 and the sodium-glucose co-transporter 1 (SGLT1), leading to postprandial hyperglycaemia (PPHG). Impaired control of PPHG is a common feature of the type 2 diabetes (TD2) , which is the most prevalent form of diabetes, representing around 90 % of all the diabetes cases (2, 4, 5).

Treatment of T2D through regulation of PPHG consists on retarding the absorption of glucose by inhibiting carbohydrate hydrolysing enzymes, using α-glucosidase inhibitors as antidiabetic agents (6). The α-glucosidase activity is associated with two small intestinal membrane-bound enzymes, sucrase-isomaltase (SI) (EC 3.2.1.48 and 3.2.1.10) and maltase-glucoamylase (MGAM) (EC 3.2.1.20 and 3.2.1.3), both belonging to the glycoside hydrolase family 31 (GH31), according to the Carbohydrate Active Enzymes database (CAZy) (7, 8). Human SI and MGAM have duplicated catalytic domains: the N-terminal membrane proximal domain (ntSI and ntMGAM) and the C-terminal luminal domain (ctSI and ctMGAM). The domains are anchored to the brush-border membrane of the small intestine through an *O*-glycosylated stalk stemming from the *N*-terminal domain (7). Both α-glucosidases are differently expressed along the small intestine. MGAM is increasingly expressed across the intestine, presenting the highest expression levels in the distal ileum (≈ 2 % of the intestinal brush border membrane proteins), while SI is mostly expressed in the jejunum, with lower expression towards the proximal and distal ends of the intestine (≈ 8 - 10 % of the intestinal brush border proteins) (9). The MGAM complex accounts for the total glucoamylase activity, about 20 % of the maltase activity and a lesser amount of the isomaltase activity. MGAM has a preference for α-1,4-glycosidic linkages and efficiently hydrolyses increasing lengths, up to glucohexose. In turn, α-1,6-glycosidic bonds are cleaved at only 2 % of the rate of α-1,4-glycosidic bonds. Additionally, there is some α-1,2- and α-1,3- hydrolysing activity, although sucrose is not hydrolysed (7, 9-11). Regarding the SI complex , its effect accounts for nearly 80 % of the overall intestinal maltase activity and almost all sucrase activity existing in the intestine, being one of the most abundant proteins present in the brush border membrane (9). In that sense, SI can efficiently hydrolyse α-1,4- , α-1,6-, and α-1,2-glycosidic linkages, also presenting some hydrolysing activity for α-1,3-glycosidic bonds (7, 9-11).

T2D patients typically present increased levels of SI, which can increase the rate of sugar absorption and exacerbate hyperglycaemia, making this α-glucosidase an important target (12). As specified above, α-glucosidase inhibitors are the most effective in reducing PPHG, and the most prescribed α-glucosidase inhibitor used for the management of T2D is acarbose. These agents, which also inhibit α-amylase, were widely used in therapy and have been associated with gastrointestinal adverse effects, namely flatulence, diarrhoea and abdominal pain (13). As acarbose also inhibits the salivary and pancreatic α-amylase activities, unabsorbed polysaccharides in the intestine are broken down by enterobacteria leading to increased colonic gas production. Therefore, symptoms like flatulence and abdominal bloating scores are likely to be higher after acarbose administration, affecting about 50 % of diabetic patients who use this agent (14, 15). These effects can lead to treatment non-adherence and consequent treatment failure. For these reasons, the search and development of novel α-glucosidase inhibitors that can be used in the treatment of T2D has been considered a hot topic of research (6).

As α-glucosidase enzymes are present in enterocytes, Caco-2 (Cancer coli-2) cell line is the most widely used cellular model to study SI. Moreover, MGAM is not present in those cells, which increases the SI specificity of this cell model (16). Caco-2 was originally established from a human colorectal adenocarcinoma by Jorgen Fogh. Early studies revealed that differentiated Caco-2 cells express numerous morphological and functional properties of small intestine enterocytes (16). When seeded on semi-permeable membranes and after long-term culture, Caco-2 cells develop apical-basal polarity and undergo differentiation. During this *in vitro* process, a continuous monolayer held by tight junctions is formed, which mimics the intestinal barrier. Thus, these cells have become a popular surrogate for human intestinal epithelium. Nevertheless, the Caco-2 cell line has been shown to be heterogeneous, as confirmed by highly variable solute transport properties and permeability (16). TC7 clone, obtained from the late passage of the parental Caco-2 cell line, has reduced heterogeneity, compared with Caco-2 cells. In the Caco-2/TC7 cellular model, the brush border hydrolase SI has shown to exhibit higher expression than the parental ones, at similar levels to the ones found in human jejunum, and the SI gene sequence was confirmed to be identical to the SI gene sequence in normal enterocytes from human biopsies (12, 16).

Flavonoids are heterocyclic phenolic compounds widely distributed in nature, being secondary metabolites of plants. These compounds share the basic chemical structure of a common three ring moiety (A, B and C rings) with 15 carbon atoms (C_6-C_3-C_6). Flavonoids have several recognized biological activities (17), including antidiabetic activity (18). In fact, a large number of studies has been focused on the study of the inhibition of α-amylase and

α-glucosidase by flavonoids (6, 19-22). However, most of the studies have used the more readily available rat intestinal preparations or yeast α-glucosidase as the enzyme source in the experiments, so it cannot be assumed that the inhibition of those hydrolases and human enzyme will be equivalent, especially when comparing yeast and human enzyme(12, 23, 24). In fact, the sequential identity between rat and human enzyme is 75 %, while the sequential similarity is 84 %. The identity between human and yeast enzyme is more difficult to estimate due to their large difference in size. The human SI has 18426 residues and yeast α-glucosidase has only 584 residues. Comparing the sucrase domain of SI with the yeast enzyme, the sequential identity is 28 % and the sequential similarity is 52 %. Regarding the isomaltase domain of SI, the sequential identity/similarity is lower (21 %/40 %) (25). Taking that into account, it is expected that the experimental results will be more transferable from the rat enzyme to the human enzyme than from the yeast to the human enzyme, although even the rat enzyme still shows notable differences comparing with the human SI. Thus, the purpose of this work is to evaluate the ability of a group of selected flavonoids, with effective inhibitory activity against yeast α-glucosidase (19), (Figure 1) to inhibit SI using the Caco-2/TC7 cell line as human source of α-glucosidase.

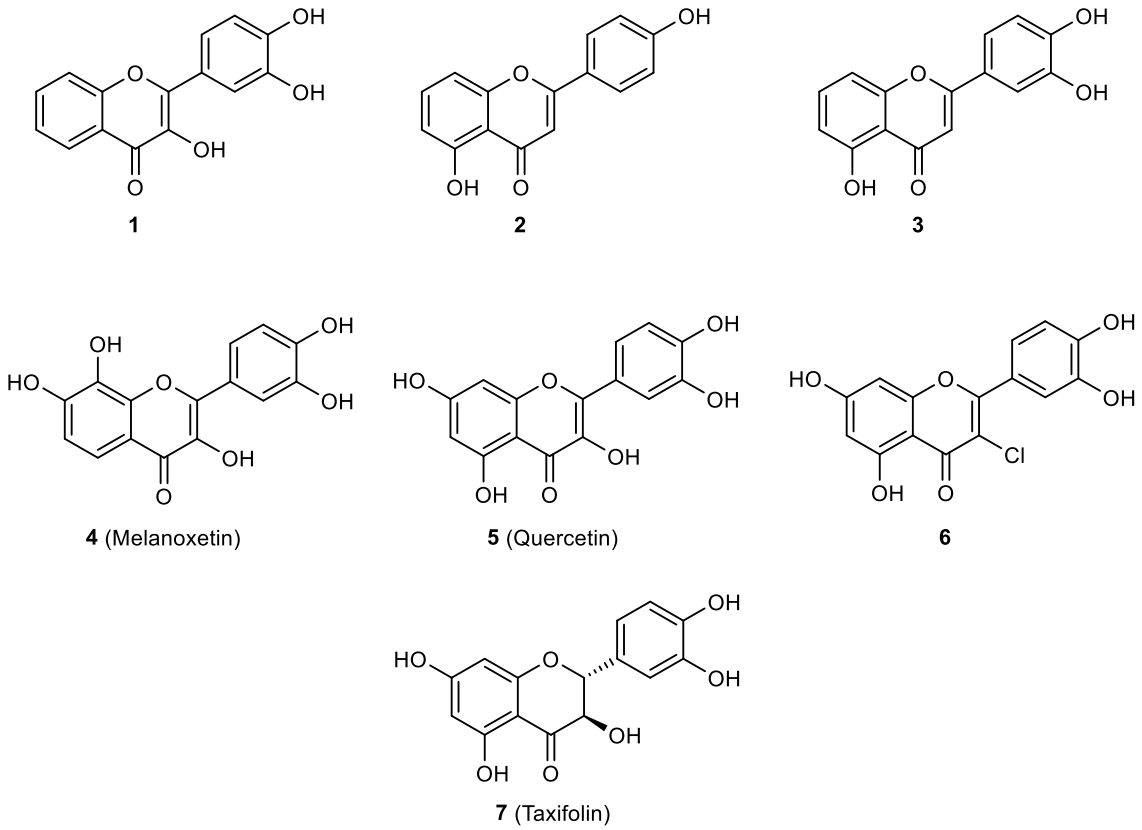


Figure 1: Chemical structure of the studied flavonoids.

2. Materials and Methods

2.1. Chemicals

Acarbose, bromophenol blue, dimethyl sulfoxide (DMSO), Dulbecco's phosphate buffered saline (DPBS), glycerol, MEM non-essential amino acid solution, maltose, 2-mercaptoethanol, miglitol, mouse anti human β-actin antibody (AC-15), *p*-nitrophenyl-α-D-glucopyranoside (*p*NPG), penicillin-streptomycin solution, sodium phosphate monobasic, sodium phosphate dibasic, protease inhibitor cocktail powder, trypsin-EDTA solution, 3-(4,5-dimethylthiazol-2-yl)-2,5-diphenyltetrazolium salt (MTT), sodium dodecyl sulphate (SDS), voglibose, flavonoids **5** (quercetin) and **7** (taxifolin), Trizma base, and the mouse monoclonal anti-β-actin antibody, were obtained from Sigma-Aldrich (St. Louis, MO, USA). Amplex® Red glucose/glucose oxidase assay kit; Dulbecco's modified Eagle's medium (DMEM) high glucose GlutaMAX™ supplement; DMEM (high glucose, no glutamine, no phenol red); heat inactivated fetal bovine serum (FBS); L-glutamine; and sucrose were obtained from Thermo Fisher Scientific (Waltham, MA, USA). The mouse monoclonal antibody sucrase-isomaltase (A-12) was obtained from Santa Cruz Biotechnology (Dallas, TX, USA). Flavonoids **1**, **2** and **3** were obtained from Indofine Chemical Company, Inc. (Hillsborough, NJ). The enhanced chemiluminescence (ECL) reagent was obtained from BioRad (Hercules, CA, USA). Flavonoids **4** (melanoxetin) and **6** were synthesized as previously described (26, 27).

2.2. Cell culture

The human epithelial colorectal adenocarcinoma cell line Caco-2/TC7 was a kind gift by Prof. Sophie Thenet, Centre de Recherche Saint-Antoine, Équipe Microbiote, Intestin et Inflammation, Paris, France. This cell line was cultured in standard medium DMEM high glucose Glutamax™, supplemented with 20 % (v/v) heat-inactivated foetal bovine serum (FBS), 1 % (v/v) non-essential amino acids and 1 % penicillin-streptomycin.

2.3. Growth culture conditions of Caco-2/TC7 cells

Cells were routinely cultured at a density of 7.5 x 10^5 cells per 75 cm^2 culture flask in the standard medium mentioned above, and were maintained in an incubator at 37 °C with 5 % CO_2. Medium was changed every 48 h, and when 80 % confluence was reached the cells were subcultured by detaching with 0.25 % trypsin/EDTA. Caco-2/TC7 cells were allowed to fully differentiate for 21 days. After 21 days, cells were washed 3 times with cold DPBS

and then scraped in 1 mL of 10 mM phosphate buffer (pH 7.0) containing protease inhibitors. Cells were stored at -80 °C until required.

On the day of the assay, a cell extract was prepared according to Pyner *et al* (12): cell lysates were thawed and passed 10 times through a 21G needle syringe. Cells were centrifuged at 200 *g* for 5 min at 4 °C and the supernatant was used for the assay, to access human SI as the enzyme source. To determine the protein content of the cell lysate, the Bradford assay was performed (28).

2.4. Cell viability: MTT colorimetric assay

The MTT assay, based on the reduction of MTT to formazan, was performed to investigate Caco-2/TC7 cellular metabolic activity when treated with flavonoids under study.

Briefly, cells were plated in 48-well plates at a density of 1 x 10^4 cells per well in DMEM (no phenol red) and incubated at 37 °C with 5 % CO_2. After 24 h, different concentrations of flavonoids (0 - 100 µM) were added to each well and cells were incubated for 24 h. Then, MTT at 0.5 mg/mL in DPBS was added to each well, followed by 2 h incubation at 37 °C with 5 % CO_2. Subsequently, the resulting purple crystals of formazan were solubilized with 200 µL of DMSO in each well. After an incubation of 30 min with shaking at room temperature, the absorbance of the corresponding solution, which is directly proportional to the number of living cells, was measured using a microplate reader (Synergy HT, BIO-TEK) at 570 nm. In all the subsequent assays, flavonoids were used at concentrations resulting in cell viabilities of at least 80 % of MTT reduction, which were considered essentially non-cytotoxic concentrations.

2.5. Cell samples preparation and Western blot analysis

Western blot (WB) analysis was performed to demonstrate the presence of the SI in the cell line used in the study. To prepare cell extracts for WB analysis, Caco-2/TC7 cells were treated as described in section 2.3. Protein concentration was determined by the Bradford method and cell lysates were denaturated in sample buffer [0.5 M Tris-HCl, pH=6.8, 2 % (v/v) sodium dodecyl sulphate, 10 % glycerol, 25 % (v/v) 2-mercaptoethanol and bromophenol blue]. Thereafter, equivalent amounts of protein were separated by 10 % (v/v) SDS-PAGE followed by Western blotting. In order to examine the protein levels of SI, polyvinylidene fluoride (PVDF) membranes were incubated overnight at 4 °C with the primary antibody mouse monoclonal anti human SI (1:1000). Mouse anti-human actin monoclonal antibody was used to detect actin as loading control. Immune complexes were

detected with the ECL reagent and the bands were analysed using CLIQS Gel Image Analysis Software, from TotalLab (Newcastle, UK). Results were normalized by calculating the ratio between the intensities of the bands corresponding to the protein of interest and the protein used as a loading control.

2.6. Sucrase and maltase inhibitory activity - glucose oxidase assay

Samples of Caco-2/TC7 cell extract in 10 mM phosphate buffer (pH 7.0) were used as the enzyme source. To exclude a potential direct interference with Amplex® Red, flavonoids at maximum concentration (as evaluated by MTT assay) were added to cell extracts containing 100 µM glucose and compared with a control with no flavonoid added.

For the evaluation of the inhibitory activity, sucrase- and maltase- catalysed hydrolysis of sucrose and maltose, respectively, was measured by monitoring glucose as the final reaction product. The enzymatic assay was optimized considering the time of incubation, the protein concentration, and the substrate concentration.

The assay was carried out in a 96-well microplate, according to Pyner et al (12), with modifications. Briefly, cell extracts corresponding to 86 µg of total protein and each tested flavonoid were added to each well, and DMSO final concentration was 4 % (v/v). After an incubation period of 5 min at 37 °C, sucrose (76 mM) or maltose (1 mM) was added to the reaction mixture and incubated for 30 min at 37 °C in a thermoshaker incubator (MS-100, Labgene Scientific SA). After this time, the release of glucose was determined using an Amplex® Red glucose/glucose oxidase assay kit, according to the manufacturer's instructions. Since peroxidase- and glucose oxidase-mediated reactions can be coupled, the release of glucose by any glucosidase can be measured. In this assay, glucose oxidase catalyses the conversion of D-glucose to D-gluconolactone and H_2O_2. In the presence of horseradish peroxidase, H_2O_2 then reacts with the Amplex® Red reagent (10-acetyl-3,7-dihydroxyphenoxazine) to form resorufin, a red-fluorescent oxidation product ($\lambda_{Ex}/\lambda_{Em}$ = 530/590 nm). This determination was monitored in a microplate reader (Cytation 3, Imaging Reader, BioTek). Acarbose, voglibose and miglitol were used as positive controls. The amount of DMSO used did not interfere with the assay.

2.7. Sucrase-isomaltase inhibitory activity using *p*NPG as substrate

The assay was carried out by monitoring the SI-mediated transformation of the substrate *p*NPG into α-D-glucose and *p*-nitrophenol, at 405 nm. The enzymatic assay was optimized considering the time of incubation (0 - 60 min), total protein added (0 - 1333 µg), and

substrate concentration (0 - 10 mM). Briefly, depending on the protein concentration, cell extract was diluted with 10 mM phosphate buffer (pH 7.0) and 330 µg of total protein were added to each well of a 96-microplate. Then, flavonoids were added to the corresponding wells and DMSO final concentration was 4% (v/v).

2.8. Statistical analysis

Each result of sucrase or maltase, or SI inhibition by the tested flavonoids was expressed as % of inhibition ± standard error of the mean (SEM), as shown in the following equation:

$$\% \text{ Inhibition} = 100 \times \left[1 - \frac{(S_{sample} - S_{blank})}{(S_{control} - S_{blank})}\right]$$

S_{sample} - Analytical signal obtained with inhibitor.

$S_{control}$ - Analytical signal obtained without inhibitor.

S_{blank} - Analytical signal obtained without inhibitor and without substrate.

Statistical analyses were performed using GraphPad Prism™ (version 7.0; GraphPad Software). The results of the *in vitro* inhibitory activity of flavonoids against the SI activity are expressed as mean ± standard error of mean (SEM). Statistical comparison between the active flavonoids was estimated by applying one-way analysis of variance (ANOVA). Each study corresponds to at least four independent experiments ($n \geq 4$).

3. Results

3.1. Cell viability: MTT colorimetric assay

The MTT assay was used to quantitatively determine the cellular viability or metabolic activity in Caco-2/TC7 treated with flavonoids under study. The concentration of flavonoids that allowed an absorbance reading of at least 80 % of MTT reduction (cell viability compared to control) was 25 µM for compounds **1** and **4** (melanoxetin), 100 µM for compounds **2** and **7** (taxifolin), 6.25 µM for compound **3**, and 50 µM for compounds **5** (quercetin) and **6** (Figure 2).

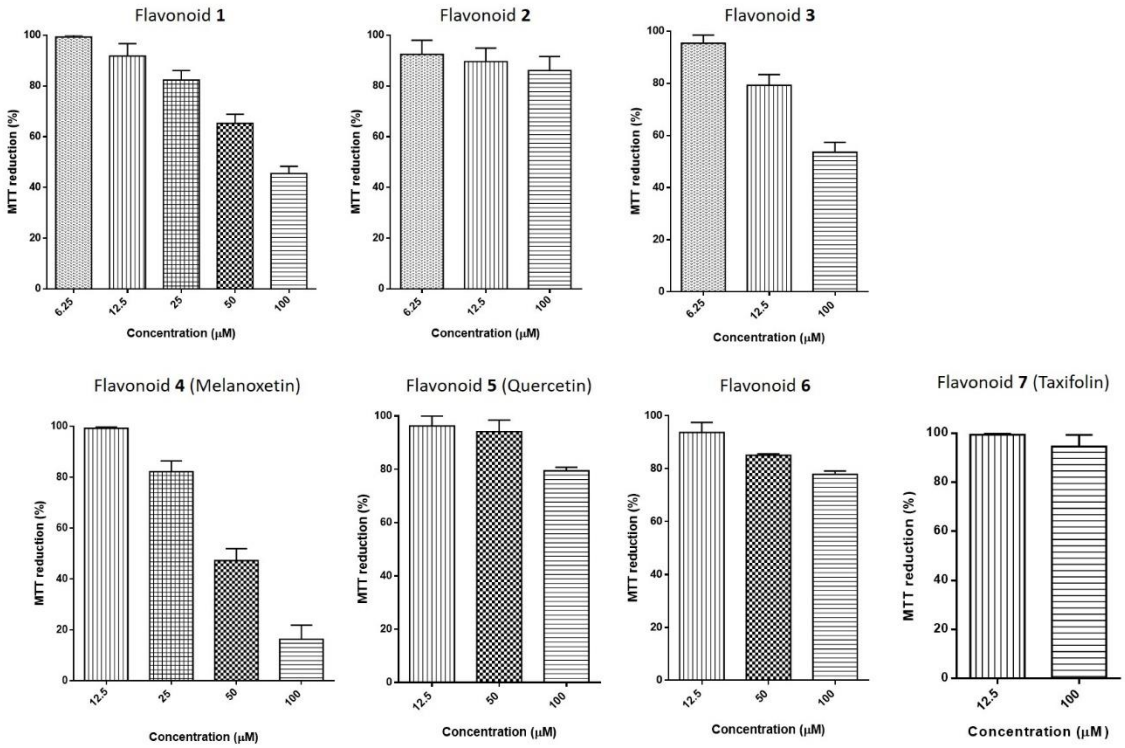


Figure 2: Viability (ability to reduce MTT) of Caco-2/TC7 cells treated with different concentrations of flavonoids.

3.2. Western blot analysis

In order to proceed to the detection of human SI in Caco-2 cellular line in the experimental conditions, the presence of this α-glucosidase was confirmed in lysates after 21 days of differentiation (Figure 3).

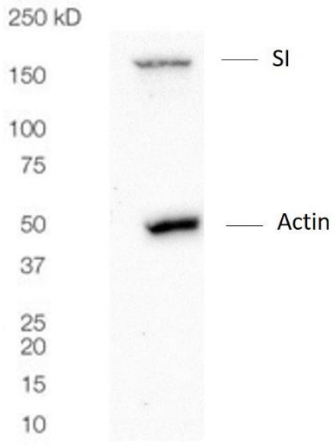


Figure 3: Detection of human sucrase-isomaltase (SI) enzyme by western blot. Western blot shows a lysate of Caco-2/TC7 cell line after 21 days differentiation. A specific band was detected for SI at approximately 150 kDa (as indicated). The experiment was conducted under reducing conditions using phosphate buffer as a solvent of cell lysates. β-Actin band was detected at around 50kDa and was used as a loading control.

3.3. Sucrase and maltase inhibitory activity - glucose oxidase assay

One of the main goals of the present study was to optimize an assay to evaluate the inhibition of SI by flavonoids, using Caco-2/TC-7 cell extracts as a source of the human enzyme. The enzymatic assay was optimized considering three major parameters: the time of incubation, protein concentration, and substrate concentration (Figure 4). Regarding the obtained results, the final experimental conditions selected were 30 min of incubation time for both sucrase and maltase activities, with a final total protein mass of 86 μg. Lastly, the final concentration selected for sucrose and maltose was 76 mM and 1 mM, respectively. The physiological conditions prevailing in the cell, such as pH and temperature, must be taken as standards for the mammalian enzymes, but moderate deviations produce only minor activity decrease. As such, the enzyme reactions were performed at 37 °C, the optimum temperature (29). The pH value selected was 7.0, since the optimum pH range for SI was reported to be 6 - 7, and the optimum curves in enzyme assays have a broader maximum so there is no considerable reduction of the enzyme activity (30). These assays allow the continuous monitoring of enzymatic catalysis. The reaction rate is derived from the initial segment of the reaction curve, which typically follows a linear relationship. (29).

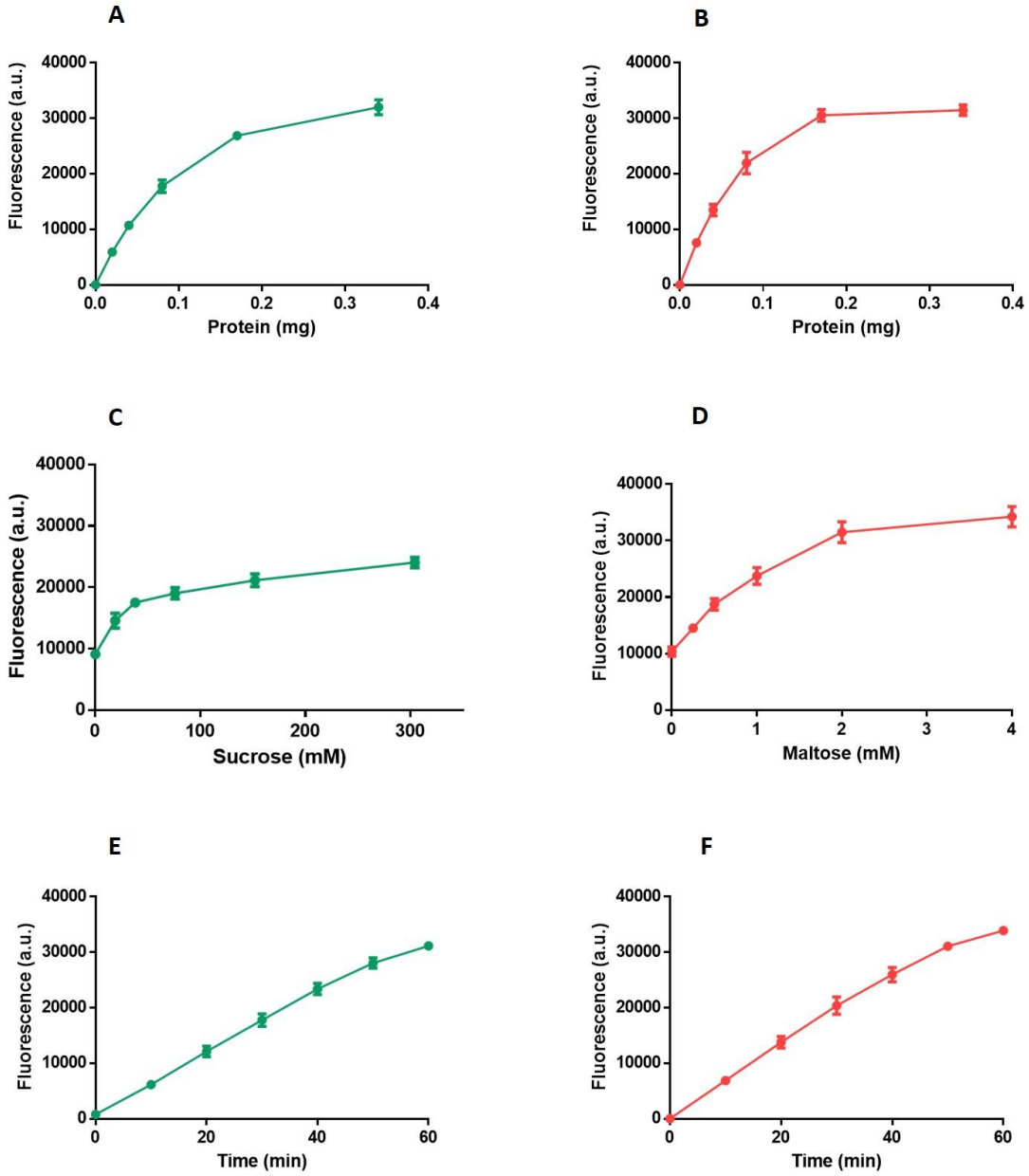
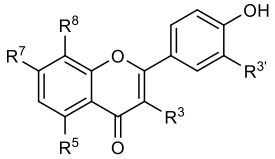
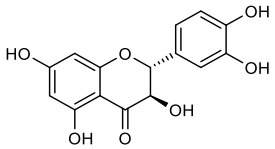
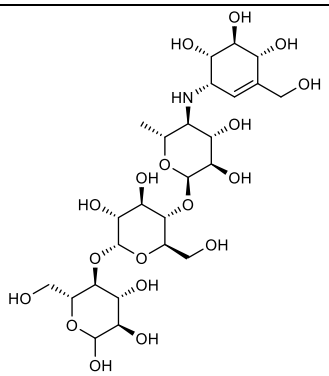
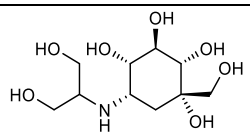
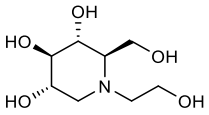


Figure 4: Optimization of assay parameters in Caco-2/TC7 cell extracts, using sucrose (green) and maltose (red) as substrates: dependence of the obtained fluorescence signal on the added protein [A] [B], added substrate [C] [D] and time [E] [F].

After the optimization of assay conditions, the evaluation of the inhibitory activity of flavonoids against SI was performed. For this purpose, an enzyme-linked fluorimetric assay based on glucose oxidase to assess glucose concentration was used. Firstly, the interference of the tested compounds with the assay was studied, using 100 μM of glucose in the presence or absence of different concentrations of flavonoids, considering the results obtained in the MTT colorimetric assay. Following these exclusion principles, flavonoids were tested at the following maximum concentrations: 3.13 μM for compounds **1**, **4** (melanoxetin) and **5**

(quercetin); 6.25 µM for compounds **3**, **6** and **7** (taxifolin); and 100 µM for compound **2**. The highest concentrations used for positive controls, namely acarbose (50 µM), voglibose (3.13 µM) and miglitol (25 µM) did not interfere with the assay.

Table 1: Inhibitory activity of the selected flavonoids and positive controls against human sucrase and maltase (IC_{50} ± SEM or % inhibition ± SEM).

Compound	Structure	R³	R³'	R⁵	R⁷	R⁸	IC_{50} (µM) ± SEM or Inhibition (%) ± SEM	
							Sucrose	Maltose
1		OH	OH	H	H	H	42 ± 3 % *	42 ± 2 % *
2		H	H	OH	H	H	< 20 % **	< 20 % **
3		H	OH	OH	H	H	3.8 ± 0.5	6.0 ± 0.6
4 (Melanoxetin)		OH	OH	H	OH	OH	**2.2 ± 0.2**	**2.5 ± 0.2**
5 (Quercetin)		OH	OH	OH	OH	H	3.1 ± 0.3	43 ± 3 % *
6		Cl	OH	OH	OH	H	46 ± 2 %***	6.1 ± 0.4
7 (Taxifolin)		-	-	-	-	-	37 ± 4 % ***	39 ± 3 % ***
Acarbose		-	-	-	-	-	4.2 ± 0.2	9.5 ± 0.9
Voglibose		-	-	-	-	-	0.32 ± 0.04	0.43 ± 0.07
Miglitol		-	-	-	-	-	1.1 ± 0.2	6.3 ± 0.8

Inhibition (mean, % ± SEM), under the assay conditions, at the highest tested concentration: *3.13 µM), **100 µM, ***6.25 µM.

3.4. Sucrase-isomaltase inhibitory activity using *p*NPG as substrate

The substrate *p*NPG is used in most of the enzyme reactions where the yeast α-glucosidase activity is studied (22, 31). For this reason, in the present work, the evaluation of the human α-glucosidase SI activity was also made using this substrate, in order to compare the activity in different sources of enzyme, as well as to observe the differences in the inhibitory activity of flavonoids and positive controls using physiological and synthetic substrates. During the initial optimization stage of the assay using *p*NPG as substrate, the incubation time, protein mass and substrate concentration were carefully investigated (Figure 5). Regarding the obtained results, the final experimental conditions selected were 30 min of assay time. The final mass selected of total protein used was 330 μg. Finally, the final concentration selected for the substrate *p*NPG was 2.5 mM.

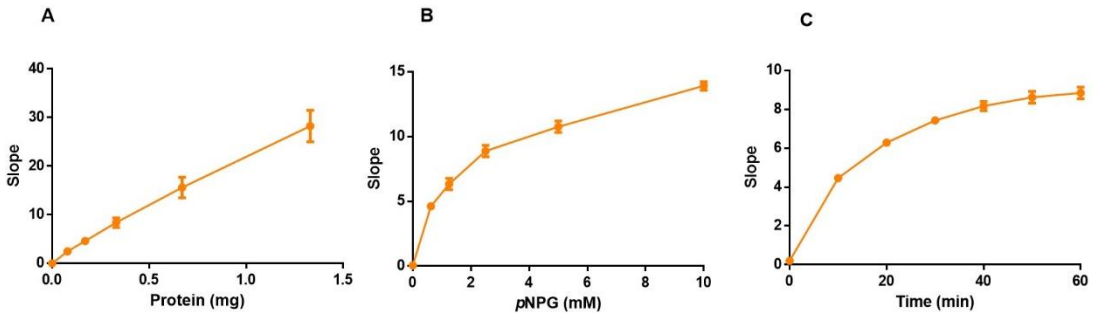


Figure 5: Optimization of assay parameters in Caco-2/TC7 cell-free extracts, using pNPG as substrate: dependence of the obtained absorbance signal on added protein [A], added substrate [B] and time [C].

After the optimization of the assay conditions, the evaluation of the inhibitory activity of flavonoids against SI with this method was tested. The highest tested concentration for each flavonoid, considering the results obtained in the MTT colorimetric assay, as well as the maximum concentration used for positive controls did not interfere with the assay. The tested flavonoids did not show any ability to inhibit SI, when using *p*NPG as substrate (Table 2).

Table 2: Inhibitory activity of the selected flavonoids and positive controls against human sucrase-isomaltase (IC_{50} ± SEM or % inhibition ± SEM).

Compound	IC_{50} (μM) ± SEM or Inhibition (%) ± SEM
1	< 20 %
2	< 20 %
3	< 20 %
4 (Melanoxetin)	< 20 %
5 (Quercetin)	< 20 %
6	< 20 %
7 (Taxifolin)	< 20 %
Acarbose	23.4 ± 0.6
Voglibose	0.49 ± 0.05
Miglitol	7.1 ± 0.6

4. Discussion

The long-term inhibitory effect of α-glucosidase inhibitors contributes to reduce the level of glycated haemoglobin (HbA1c) in diabetic patients, which results in a significant reduction in the incidence of chronic vascular complications such as micro- and macrovascular disease (32). Currently, there is an urgent need for the discovery and development of new α-glucosidase inhibitors, due to the significant gastrointestinal side effects elicited by the conventional inhibitors used in T2D treatment. These effects include, flatulence (78 % of patients) and diarrhoea (14 % of patients), which lead to treatment non-adherence and consequently treatment failure (33). In the past few years, resulting from the search for safer and more effective inhibitors, available flavonoids have been evaluated concerning their capacity to inhibit α-glucosidase (19).

The most common assay that has been applied to study the *in vitro* α-glucosidase inhibitory effect of flavonoids is a spectrophotometric method based on the measurement of the yellow-coloured *p*-nitrophenol release from *p*NPG. Most of the available literature has been based on the study of the inhibition of α-glucosidase from *Saccharomyces cerevisiae* (22, 31). In the present work, the Caco-2/TC7 cellular model was used to determine the inhibitory activity of flavonoids against α-glucosidase. The TC7 clone, isolated from a late passage of Caco-2 line, was already described to comprise a more homogeneous cell population with more developed intercellular junctions. Moreover, in Caco-2/TC7 cells, the brush-border-associated SI showed a higher expression, being present at similar levels as those found in human jejunum (16). It was also previously confirmed that the sequence of SI in Caco-2/TC7 cellular model is identical to human tissue SI (12). In this work, we used

the western blot technique to identify specifically the human SI from cell extracts. It was observed that SI, our protein of interest, is significantly expressed in the sample, prepared in the same conditions used for the inhibitory assays.

Subsequently, the optimization of experimental conditions and the evaluation of the inhibitory activity of a group of flavonoids against SI was performed. The initial optimization is crucial, since enzymatic reactions depend on various factors besides pH, temperature, and ionic strength. In fact, concentrations of all assay components, as well as the time of reaction, are of great importance (29). Fluorometric methods are more sensitive than colorimetric methods, and this was observed by comparing the methods using maltose and sucrose with the method using *p*NPG. The aim of any enzymatic assay is to observe the time-dependent formation of the product, following a linear reaction course from the catalysed reaction. Unlike the other components involved in the enzyme reaction, the amount of added enzyme should be as low as possible, meaning that only catalytic amounts are necessary, as postulated from the fundamental Michaelis-Menten equation. There is no general rule for the reaction time, except that it must be within the area of the linear progression of the reaction rate, since nonlinear phase will yield inaccurate results (29).

Taking the above rationale into account, we started to optimize the method using the protein of our cellular model extract and the sucrose or maltose as substrates. The formed product, i.e. glucose, was detected by the glucose oxidase/peroxidase fluorimetric assay, as fluorimetry is more sensitive (about 100-fold) than absorbance measurements (29). It is known that the glucose oxidase/peroxidase assay is a coupled enzymatic assay commonly used to measure glucose levels, more specifically for quantification of α-glucosidase activity. Nevertheless, this method is susceptible to numerous interferences. As the glucose oxidase/peroxidase method involves the use of two oxidases and redox reaction mechanisms, any compounds that can inhibit the two enzymes or react with the reaction intermediates will cause interference (34, 35). In that sense, for published literature data on the study of α-glucosidase inhibition by flavonoids using the glucose oxidase/peroxidase method, it should be taken into consideration the presence of false positives. For this reason, it was crucial to study the degree of interference of flavonoids before the application of the measurement of α-glucosidase inhibitory activity. In order to rule out false positive results, we studied the interference of the studied flavonoids with this method, starting by testing the highest concentration of these flavonoids that allows at least 80 % of cell viability, as measured by the MTT assay, and found that most of them have a significant interference with the method at the higher concentrations tested. Once determined the non-interfering concentrations, we studied the inhibitory activity of flavonoids against SI, applying the glucose oxidase/peroxidase method. Since SI has affinity for sucrose and

maltose, both disaccharides were used as physiological substrates of the enzyme (10). In this respect, the higher affinity for α-1,4-glycosidic bond, present in maltose but not in sucrose, is reflected on the sucrose (76 mM) and maltose (1 mM) concentrations used in the experimental conditions. From α-glucosidases expressed in normal enterocytes, MGAM and SI, Caco-2 only expresses SI (36). Sucrase activity arises solely from the sucrase subunit of SI, but this enzyme also includes the hydrolytic activities of MGAM, being a good representative complex cellular model for the study of α-glucosidase activity, and consequently for the study of carbohydrates' hydrolysis (7, 9, 36). In literature, flavonoids have so far been tested as inhibitors of yeast or rat α-glucosidases as enzyme source. Quercetin was previously reported to reduce the activity of sucrase and maltase in *in vitro* and *in vivo* studies, as well as the yeast α-glucosidase (22, 37-39). Taxifolin has also shown promising inhibitory activity against α-glucosidase from *Saccharomyces cerevisiae* (40). To the best of our knowledge, this is the first study that investigates the effects of flavonoids on the activity of human SI. In fact, these flavonoids were selected due to their potential α-glucosidase inhibitory activity on *Saccharomyces cerevisiae* enzyme, from our previous study (19). As it can be observed by the obtained results, using sucrose and maltose as substrate, flavonoid **4** (melanoxetin) was the best inhibitor when compared to the other flavonoids under study. Interestingly, this compound was also the most active flavonoid in our previous work, where the yeast enzyme was used (19). Flavonoid **4** (melanoxetin) was a better inhibitor than acarbose, using both substrates, and also than miglitol using maltose as substrate. When using sucrose as substrate (α-1,-2-glycosidic linkage), it is possible to establish a relation between the number of -OH groups in the flavonoids structure and the capacity to inhibit the SI. Thus, by comparing flavonoid **4** (melanoxetin) (IC_{50} = 2.2 ± 0.2 μM) with flavonoids **1** (42 ± 3 % inhibition at 3.13 μM) and **2** (less than 20 % inhibition at 100 μM), it is possible to conclude that the flavonoids with lower number of -OH groups have a lower capacity to inhibit SI. Moreover, by comparing flavonoid **4** (melanoxetin) with **5** (quercetin) (IC_{50} = 3.1 ± 0.3 μM), the replacement of an -OH group from C-8 to C-5 of the A ring seems to slightly reduce the inhibitory activity. Besides that, the substitution of an -OH group by a -Cl substituent, as well as the absence of the C2=C3 double bond, appears to decrease the effect under study, by comparing **5** (quercetin) with compounds **6** (46 ± 2 % at 6.25 μM) and **7** (taxifolin) (37 ± 4 % of inhibition at 6.25 μM), respectively. Similar conclusions can be drawn when using maltose (α-1,4-glycosidic linkage) as substrate. Of note, although MGAM is absent from Caco-2/TC7 cells, SI provides the majority of the maltase and isomaltase activities in the human intestinal brush border (41). Interestingly, the inhibitory activity of each tested compound was maintained or was slightly decreased by comparing the assay applying sucrose or maltose. For example, the IC_{50} value of

compound **3** went from 3.8 ± 0.5 μM to 6.0 ± 0.6 μM, and all positive controls also increased their IC_{50} values when the assay using maltose was performed.

We proceeded our study by testing the inhibitory activity of flavonoids against SI, using the chromogenic *p*NPG as substrate. According to the literature, ntSI substrate specificity for maltose and *p*NPG, and their specificity constants (K_{cat}/k_m) were determined as 19 ± 4 and 13 ± 1 $s^{-1}{\cdot}mM^{-1}$, respectively (7). In addition, the substrate *p*NPG was reported to be more efficiently cleaved and tightly bound to ntSI (1.3 ± 0.1 mM) because its K_m is about 10-fold smaller than that of ntMGAM (12.1 ± 1.0 mM). Comparing the obtained IC_{50} values for the tested positive controls, it was found that acarbose, using *p*NPG, had an IC_{50} value approximately 5.5-fold higher (23.4 ± 0.6 μM) than the one obtained when using sucrose and about 2.5-fold higher than the one obtained using maltose. Regarding voglibose, the IC_{50} values were similar when performing the assays with *p*NPG, sucrose, or maltose. In what concerns miglitol, the IC_{50} value found with *p*NPG as substrate (7.1 ± 0.6 μM) was 6.5 higher than the one found using sucrose, and similar to the one when using maltose. Interestingly, applying the inhibition of SI using *p*NPG, at the conditions of the assay, flavonoids did not show any inhibitory activity at the highest tested concentrations. It is important to highlight that the flavonoids under study did not interfere with this assay at the maximum concentration which provides at least 80 % of cell viability in Caco-2/TC7 model. It is possible that the concentrations used were too low to inhibit SI with the experimental conditions applied.

5. Conclusion

For the first time, a group of 7 flavonoids were evaluated regarding their ability to inhibit human SI. The inhibitory activity of these compounds against yeast α-glucosidase was previously studied. When using sucrose and maltose with human SI, it was possible to observe that the obtained IC_{50} values were considerably different than those obtained when studying the yeast enzyme. However, the most active flavonoid was the same in both studies (flavonoid **4**), revealing that the presence of -OH groups at C-3 of C ring, at C-3' and C-4' of B ring, as well as at C-7 and C-8 of A ring are important for increasing the effect under study. Interestingly, when human SI was used with *p*NPG, the tested flavonoids were not effective at the highest tested concentration. We believe that the present work significantly contributes to the study of inhibition of human SI by flavonoids and provides a better understanding on the chemical features of flavonoids which modulates the mentioned hydrolysing enzyme activity. The most promising flavonoid found in this work might constitute an alternative to the available α-glucosidase inhibitors used as oral antidiabetic

drugs, although more studies should be performed. Flavonoid **4** (melanoxetin) might also be a valuable model for the design and development of new scaffolds toward T2D management, via α-glucosidase inhibition.

Last, but not least, this study clearly demonstrates that the non-clinical in vitro studies applied in the evaluation of α-glucosidase activity should use the human SI rather than rat intestinal preparations or yeast α-glucosidase surrogate enzyme.

Acknowledgements

This work received financial support from PT national funds (FCT/MCTES, Fundação para a Ciência e Tecnologia and Ministério da Ciência, Tecnologia e Ensino Superior) through the project UIDB/50006/2020, and from the European Union (FEDER funds through the Operational Competitiveness Program (COMPETE2020) POCI-01-0145-FEDER-029241). CP acknowledge FCT (Fundação para a Ciência e Tecnologia) and ESF (European Social Fund) through POCH (Programa Operacional Capital Humano) for his/her PhD grant ref. SFRH/BD/116005/2016. JMPFO thanks FCT (Fundação para a Ciência e Tecnologia) for funding through program DL 57/2016 – Norma transitória (ref. SFRH/BPD/74868/2010).

Declaration of interest statement

No potential conflict of interest was reported by the authors.

References

1. Butterworth PJ, Warren FJ, Ellis PR. Human α-amylase and starch digestion: an interesting marriage. Starch - Stärke. 2011;63(7):395-405.

2. Patel H, Royall PG, Gaisford S, Williams GR, Edwards CH, Warren FJ, et al. Structural and enzyme kinetic studies of retrograded starch: inhibition of α-amylase and consequences for intestinal digestion of starch. Carbohydr Polym. 2017;164(2017):154-61.

3. Brayer GD, Sidhu G, Maurus R, Rydberg EH, Braun C, Wang Y, et al. Subsite mapping of the human pancreatic α-amylase active site through structural, kinetic, and mutagenesis techniques. Biochemistry. 2000;39(16):4778-91.

4. American Diabetes Association. 2. Classification and diagnosis of diabetes: standards of medical care in diabetes - 2018. Diabetes Care. 2018;41(Supplement 1):S13-S27.

5. International Diabetes Federation. IDF Diabetes Atlas. 2019.

6. Zhu J, Chen C, Zhang B, Huang Q. The inhibitory effects of flavonoids on alpha-amylase and alpha-glucosidase. Crit Rev Food Sci Nutr. 2019:1-14.

7. Sim L, Willemsma C, Mohan S, Naim HY, Pinto BM, Rose DR. Structural basis for substrate selectivity in human maltase-glucoamylase and sucrase-isomaltase N-terminal domains. J Biol Chem. 2010;285(23):17763-70.

8. Gericke B, Schecker N, Amiri M, Naim HY. Structure-function analysis of human sucrase-isomaltase identifies key residues required for catalytic activity. J Biol Chem. 2017;292(26):11070-8.

9. Elferink H, Bruekers JPJ, Veeneman GH, Boltje TJ. A comprehensive overview of substrate specificity of glycoside hydrolases and transporters in the small intestine. Cel Mol Life Sci. 2020;77(23):4799-826.

10. Jones K, Sim L, Mohan S, Kumarasamy J, Liu H, Avery S, et al. Mapping the intestinal alpha-glucogenic enzyme specificities of starch digesting maltase-glucoamylase and sucrase-isomaltase. Bioorg Med Chem. 2011;19(13):3929-34.

11. Williamson G. Possible effects of dietary polyphenols on sugar absorption and digestion. Mol Nutr Food Res. 2013;57(1):48-57.

12. Pyner A, Nyambe-Silavwe H, Williamson G. Inhibition of human and rat sucrase and maltase activities to assess antiglycemic potential: optimization of the assay using acarbose and polyphenols. J Agric Food Chem. 2017;65(39):8643-51.

13. Derosa G, Maffioli P. α-Glucosidase inhibitors and their use in clinical practice. Arch Med Sci. 2012;8(5):899-906.

14. Schmeltz L, Metzger B. 6.19 - Diabetes/Syndrome X. In: Taylor JB, Triggle DJ, editors. Comprehensive Medicinal Chemistry II. Oxford: Elsevier; 2007. p. 417-58.

15. Aoki K, Muraoka T, Ito Y, Togashi Y, Terauchi Y. Comparison of adverse gastrointestinal effects of acarbose and miglitol in healthy men: a crossover study. Intern Med. 2010;49(12):1085-7.

16. Turco L, Catone T, Caloni F, Consiglio ED, Testai E, Stammati A. Caco-2/TC7 cell line characterization for intestinal absorption: how reliable is this in vitro model for the prediction of the oral dose fraction absorbed in human? Toxicol In Vitro. 2011;25(1):13-20.

17. Jucá MM, Cysne Filho FMS, de Almeida JC, Mesquita DDS, Barriga JRM, Dias KCF, et al. Flavonoids: biological activities and therapeutic potential. Nat Prod Res. 2020;34(5):692-705.

18. Alkhalidy H, Wang Y, Liu D. Dietary flavonoids in the prevention of T2D: an overview. Nutrients. 2018;10(438):1-33.

19. Proença C, Freitas M, Ribeiro D, Oliveira EFT, Sousa JLC, Tome SM, et al. α-Glucosidase inhibition by flavonoids: an *in vitro* and *in silico* structure-activity relationship study. J Enzyme Inhib Med Chem. 2017;32(1):1216-28.

20. Takahama U, Hirota S. Interactions of flavonoids with α-amylase and starch slowing down its digestion. Food Funct. 2018;9(2):677-87.

21. Proença C, Freitas M, Ribeiro D, Tomé S, Oliveira E, Viegas M, et al. Evaluation of a flavonoids library for inhibition of pancreatic α-amylase towards a structure-activity relationship. J Enzyme Inhib Med Chem. 2019;34(1):577-88.

22. Şöhretoğlu D, Sari S. Flavonoids as alpha-glucosidase inhibitors: mechanistic approaches merged with enzyme kinetics and molecular modelling. Phytochem Rev. 2020;19(5):1081-92.

23. Zhang H, Wang G, Beta T, Dong J. Inhibitory properties of aqueous ethanol extracts of propolis on alpha-glucosidase. Evid Based Complement Alternat Med. 2015;2015(587383):1-7.

24. Van Beers EH, Büller HA, Grand RJ, Einerhand AWC, Dekker J. Intestinal brush border glycohydrolases: structure, function, and development. Crit Rev Biochem Mol Biol. 1995;30(3):197-262.

25. EMBOSS Matcher. Pairwise Sequence Alignment [Available from: https://www.ebi.ac.uk/Tools/psa/emboss_matcher/#].

26. Sousa JLC, Proença C, Freitas M, Fernandes E, Silva AMS. New polyhydroxylated flavon-3-ols and 3-hydroxy-2-styrylchromones: synthesis and ROS/RNS scavenging activities. Eur J Med Chem. 2016;119:250-9.

27. Freitas M, Ribeiro D, Tome SM, Silva AM, Fernandes E. Synthesis of chlorinated flavonoids with anti-inflammatory and pro-apoptotic activities in human neutrophils. Eur J Med Chem. 2014;86(2014):153-64.

28. Bradford MM. A rapid and sensitive method for the quantitation of microgram quantities of protein utilizing the principle of protein-dye binding. Anal Biochem. 1976;72:248-54.

29. Bisswanger H. Enzyme assays. Perspectives in Science. 2014;1(1):41-55.

30. Schomburg D, Salzmann M. Sucrose alpha-glucosidase. In: Schomburg D, Salzmann M, editors. Enzyme Handbook 4: Class 3: Hydrolases. Berlin, Heidelberg: Springer Berlin Heidelberg; 1991. p. 285-9.

31. Proença C, Ribeiro D, Freitas M, Fernandes E. Flavonoids as potential agents in the management of type 2 diabetes through the modulation of α-amylase and α-glucosidase activity: a review. Crit Rev Food Sci Nutr. 2021 (in press). DOI: 10.1080/10408398.2020.1862755.

32. Kim S-J. Chapter 21 - Herbal Chrysanthemi Flos, Oxidative Damage and Protection against Diabetic Complications. In: Preedy VR, editor. Diabetes: Oxidative Stress and Dietary Antioxidants. San Diego: Academic Press; 2014. p. 201-11.

33. Hossain MA, Pervin R. Chapter 34 - Current Antidiabetic Drugs: Review of Their Efficacy and Safety. In: Bagchi D, Nair S, editors. Nutritional and Therapeutic Interventions for Diabetes and Metabolic Syndrome (Second Edition): Academic Press; 2018. p. 455-73.

34. Xu H, Leng X, Wang M, Zhang G. Glucose measurement in the presence of tea polyphenols. Food Analytical Methods. 2012;5(5):1027-32.

35. Wong AI, Huang D. Assessment of the degree of interference of polyphenolic compounds on glucose oxidation/peroxidase assay. J Agric Food Chem. 2014;62(20):4571-6.

36. Cheng M-W, Chegeni M, Kim K-H, Zhang G, Benmoussa M, Quezada-Calvillo R, et al. Different sucrose-isomaltase response of Caco-2 cells to glucose and maltose suggests dietary maltose sensing. J Clin Biochem Nutr. 2014;54(1):55-60.

37. Li H, Song F, Xing J, Tsao R, Liu Z, Liu S. Screening and structural characterization of α-glucosidase inhibitors from Hawthorn Leaf flavonoids extract by ultrafiltration LC-DAD-MSn and SORI-CID FTICR MS. J Am Soc Mass Spectrom. 2009;20(8):1496-503.

38. Pereira DF, Cazarolli LH, Lavado C, Mengatto V, Figueiredo MS, Guedes A, et al. Effects of flavonoids on α-glucosidase activity: potential targets for glucose homeostasis. Nutrition. 2011;27(11-12):1161-7.

39. He C, Liu X, Jiang Z, Geng S, Ma H, Liu B. Interaction Mechanism of Flavonoids and alpha-Glucosidase: Experimental and Molecular Modelling Studies. Foods (Basel, Switzerland). 2019;8(355):1-9.

40. Liu J, Wang X, Geng S, Liu B, Liang G. Inhibitory mechanism of taxifolin against α-glucosidase based on spectrofluorimetry and molecular docking. Nat Prod Commun. 2017;12(11):1725-8

41. Van Beers EH, Büller HA, Grand RJ, Einerhand AW, Dekker J. Intestinal brush border glycohydrolases: structure, function, and development. Crit Rev Biochem Mol Biol. 1995;30(3):197-262.

CHAPTER III. DISCUSSION AND CONCLUSIONS

III.1. Integrated discussion

The terms “diabetes” and “mellitus” derived from Greek language. “Diabetes” means “a passer through, a siphon”, while “mellitus” means “sweet”. It is believed that Greeks, specifically Aretaeus, entitled this disease such way due to the high urine proportions produced by diabetic patients which attracted flies and bees. This disease has a long history, reaching back into antiquity (around 3000 years ago), and despite its huge impact until now, there is still no cure for any type of diabetes (1). Diabetes (all forms) and its complications have contributed extremely to the burden of mortality and disability worldwide. Diabetic patients are at high risk to develop a number of serious and life-threatening complications that, if not well managed, can lead to frequent hospital admissions and premature death (2). In fact, according to World Health Organization (WHO), diabetes was the 9th leading cause of death in 2019 (3). Moreover, International Diabetes Federation (IDF) stated that 10 % of global health expenditure goes to diabetes, corresponding to about 760 billion US dollars (4). People living with diabetes are also at increased risk of developing other diseases, namely cardiovascular and cerebrovascular diseases, cataracts, erectile dysfunction, and non-alcoholic fatty liver disease (5). In addition, it was found that diabetes or uncontrolled diabetes is considered a risk factor for a rapid progression and bad prognosis of patients with severe acute respiratory syndrome coronavirus 2 (SARS-CoV-2), the pathogen of coronavirus disease 2019 (COVID-19), a newly identified illness which has spread rapidly around the globe in 2020 (6-8). In fact, besides to the well-known adverse effects associated to the currently available antidiabetic agents, it was also described that sodium-glucose cotransporter (SGLT)2 inhibitors, GLP-1 receptor agonists, pioglitazone, and even insulin and metformin might induce an over-expression of the angiotensin converting enzyme-2 (ACE2). To the current knowledge, ACE2 is highly expressed in the lungs and pancreas, and represents a receptor of SARS-CoV-2 for invading target cells. In sequence of the endocytosis of the virus complex, ACE2 is downregulated. Thus, the above-mentioned antidiabetic drugs may theoretically increase ACE2 availability in respiratory tract, promoting SARS-CoV-2 infection (6, 9, 10).

In addition to this, several available antidiabetic drugs have demonstrated possible severe adverse effects, which can lead to patient incompliance and consequent treatment failure (11).

Taking all into consideration, there is an urgent need of develop new antidiabetic agents, with improved safety and efficacy. Natural products, and in particular plant-based products,

have been used toward the alleviation of disease conditions for centuries. Such products have been employed as templates for the synthesis of new drugs (12, 13). Among these compounds, flavonoids represent an important class of specialized plant metabolites that are ubiquitously found in human daily consumed fruits, vegetables, nuts, cocoa, tea, grain seeds, and herbs (14). In a restricted and specific sense, the term "flavonoid" is used for those compounds with a C_6-C_3-C_6 carbon framework exhibiting the structure of a chromane or that of a chromene. Flavonoids play a wide range of physiological end ecological roles in plants, as ultraviolet(UV)-B protectants, pigments that attract pollinators, phytoalexins, signalling molecules, and regulators of auxin transport and fertility (15, 16). It is well-known that these compounds have multiple positive health effects, including antidiabetic activity (15, 17). The antidiabetic activity of flavonoids comprises the regulation of carbohydrate digestion, insulin signalling, insulin secretion, glucose uptake, and adipose deposition. Furthermore, they target several molecules that are involved in the regulation of different pathways, such as improving β-cells proliferation, promoting insulin secretion, reducing apoptosis, and decreasing glucose levels by regulating glucose metabolism in the liver (14).

Among the antidiabetic drugs currently available, there is a class responsible for the inhibition of the carbohydrate hydrolysing enzymes α-glucosidases, maltase-glucoamylase (MGAM) and sucrase-isomaltase (SI), which also inhibit α-amylase. The first step of starch digestion is performed by salivary and pancreatic α-amylase, resulting in the production of linear glucose oligomers and branched α-limit dextrins. The α-amylase degradation products are further hydrolysed into free glucose by MGAM and SI. The Nt subunit of both α-glucosidases attaches these enzymes complexes to the apical membrane of small intestine enterocytes through an *O*-glycosylated stalk domain (18). The α-glucosidase inhibitors act as antidiabetic drug class, competing with oligosaccharides for binding the α-glucosidase enzymes in the brush border of the small intestine. This process delays the rate of digestion of ingested carbohydrates and thus reduces postprandial hyperglycaemia (PPHG). Due to its proven efficacy, many international guidelines recommend the use of α-glucosidase inhibitors as first-line alternative to metformin or in combination with sulfonylureas, metformin or insulin (19). However, they are responsible for common problems of flatulence, abdominal discomfort, and diarrhoea, as result of the fermentation of unabsorbed carbohydrates. For instance, although acarbose is the most prescribed α-glucosidase inhibitor, it is unpopular in United Kingdom, which reflects the aforementioned poor tolerability (20). In the continuous search of novel effective and safer α-glucosidase and α-amylase inhibitors, we started our studies by evaluating the inhibitory activity of a panel of flavonoids against α-glucosidase (EC 3.2.1.20) and establishing a structure-activity relationship. Many of the tested compounds were tested for the first time. It was found that the -OH group at 3-positionof C ring, the catechol group in B ring, at 3'- and 4- positions,

as well as the presence of a catechol group at A ring, at 7- and 8-positions of A ring, contribute significantly for the inhibition of α-glucosidase. The presence of C2-C3 double bond is also of special relevance for the increase of the effect under study. The most active compound (**1**) (IC_{50} = 7.6 ± 0.4 μM) (Figure 1) presented a competitive mechanism of inhibition, competing with the substrate for the same active binding site on the enzyme. The predicted binding mode of this flavonoid places the B ring deep in the small crevice formed by the catalytic residues. In this sense, Glu276 hydrogen bonds to OH- group from 3'-position of B ring, while this -OH group donates a hydrogen bond to Asp214. The -OH group at 4'-position of B ring is even deeper in the small pocket and hydrogen bonds Asp68. In turn, the A and C rings bind in the entrance of the small crevice, with the -OH group of C ring hydrogen bonding Asp349. Those rings are placed around Glu276, and the -OH group at 8-position of A ring donate a hydrogen bond to Glu276, while the -OH at 7-position is exposed to the larger binding pocket. Considering this binding mode, the strong hydrogen bond interactions with active site amino acids are consistent with a competitive type of inhibition.

As the targets α-glucosidase and α-amylase work together in the carbohydrate digestion, the subsequent work was performed by evaluating the inhibition of panel of flavonoids against pancreatic α-amylase (EC 3.2.1.1). The most effective tested inhibitor was flavonoid **2** (IC_{50} = 44 ± 3 μM) (Figure 1), demonstrating that the -Cl substituent at 3-position of C ring, the catechol group at 3'- and 4'-positions of B ring, as well as the presence of -OH groups at 5- and 7-positions of A ring favour the inhibition of α-amylase. The presence of the C2-C3 double bond is also important for the inhibition of the enzyme under study. Flavonoid **2** presented a competitive type of inhibition. Considering the interactions of this compound with α-amylase, it seems that the carbonyl group in C ring adjoined by the -OH group at 5- positions of A ring allow the binding of C and A rings within the catalytic triad, establishing the same hydrogen bonding network with the active sites residues Glu233, Asp300 and His299. In turn, His201 hydrogen bonds the -OH at 3'-position of B ring, while the same -OH group makes a hydrogen bond with Tyr151. On the other hand, the -OH group at 7-position of A ring seems to establish no specific interactions, while the -Cl substituent at 3-position of C ring fills the cavity formed by Ile235 and Phe256 and hydrogen bonds the backbone of Ile234. Interestingly, it was previously shown that only a mild inhibition of pancreatic α-amylase is recommended in order to avoid gastrointestinal adverse effects as a result of excessive bacterial fermentation of carbohydrates in colon (21). In this sense, it appears that the effect of flavonoid **2** could be valuable, since this compound inhibited more efficiently α-glucosidase, with an IC_{50} of 21 ± 2 μM, in a competitive manner. Another remark is the fact that α-glucosidase inhibitors are poorly absorbed, acting locally and strategically in the brush border of enterocytes (22). In this case, the limited absorption of

hydrophilic molecules can be advantageous for the inhibition of carbohydrate hydrolysing enzymes.

Another target studied in this thesis was protein tyrosine phosphatase 1B (PTP1B). This enzyme is a soluble non-transmembrane and cytosolic tyrosine-specific phosphatase, being widely expressed. The hydrophobic sequence of PTP1B is an endoplasmic reticulum (ER) anchoring domain that tethers the protein to the cytosolic face of ER allowing access to a wide range of intracellular targets (23-25). PTP1B has raised much attention in the recent years due to its ability to attenuate insulin signalling and it is currently regarded as a potential therapeutic target in type 2 diabetes (T2D), metabolic syndrome and obesity. Insulin is secreted from pancreatic β-cells and is known as a major regulator of glucose homeostasis by triggering an integrated and complex signalling network. Insulin exerts its action by binding to its receptor, which undergoes autophosphorylation on tyrosine residues, triggering the downstream signalling response (26, 27). The activity of insulin receptor is controlled through the balance between its tyrosine phosphorylation and dephosphorylation, being mostly negatively regulated by PTP1B. Differing to other insulin sensitizing strategies, the inhibition of PTP1B activity was described to improve glucose metabolism and enhance insulin response without increasing lipid metabolism and causing lipid accumulation in liver. These effects represent an advantage when compared with some other antidiabetic agents, preventing side effects such as body weight gain and liver steatosis (27, 28). A large number of potential PTP1B inhibitors has been studied, although the development of novel highly effective, selective and safe small compounds still remains a challenge, as none of the studied inhibitors made their way through phase II of the clinical trials yet (27, 29). For this reason, in the present thesis, a panel of flavonoids was evaluated concerning their capacity to inhibit human PTP1B (EC 3.1.3.48). Considering the obtained results, it was possible to conclude that the most active compound was flavonoid **3**, with an IC_{50} value of 10 ± 1 μM. After the establishment of the structure-activity relationship, it was observed that the presence of nonpolar substituents increases the PTP1B inhibition, since the presence of -OCH_3 groups at 3'-and 4'-positions of B ring and of -OBn groups at 7- and 8-positions of A ring, was very favourable for the intended effect. In addition, it seems that the presence of an -OH group at 3-position of C ring has a beneficial role for the inhibition of the target under study. Flavonoid **3** showed to bind either to the free enzyme or the enzyme substrate complex, resulting in a mixture of competitive and uncompetitive inhibition (30, 31). Inhibition by targeting the catalytic domain of PTP1B results in the inhibition of other family members, in particular with T cell protein tyrosine phosphatase (TC-PTP) (94 % of similarity on the catalytic site), which may lead to undesirable side effects. To overcome this challenge, several approaches were used among which included the use of inhibitors designed to bind not only to the catalytic site but to an allosteric site or

other sites. Such approach provides a potent inhibitor with enhanced selectivity towards PTP1B over other PTPs (27, 32). In this sense, being flavonoid **3** a mixed-type inhibitor might be an advantage for its use as a good PTP1B inhibitor. Moreover, this phenolic compound is mostly a nonpolar molecule, which can facilitate its cellular permeability.

In the fourth work of this thesis, it was studied the inhibitory activity of flavonoids against another T2D therapeutic target, dipeptidyl peptidase-4 (DPP-4) (EC 3.4.14.5). DPP-4, also known as CD26, is an ubiquitous protein, which exists as a cell membrane-bound enzyme and is secreted to the blood circulation after cleavage, to act as a soluble enzymatic protein (33, 34). It was in the 1990s that it was discovered that the enzyme DPP-4 inactivates the incretin hormones glucagon-like peptide-1 (GLP-1) and glucose-dependent insulinotropic polypeptide (GIP). In that way, the inhibition of DPP-4 results in raised levels of the two mentioned incretin hormones, which in turn leads to a decrease of glucose in circulation through stimulation of insulin secretion from the pancreatic β-cells and inhibition of glucagon secretion from the pancreatic α-cells (34, 35). In addition, the use of DPP-4 inhibitors slows gastric emptying and acts on the brain to promote satiety. It is known that the incretin effect is reduced in T2D patients, possibly due to the effect of incretins on insulin secretion or/and a decreased secretion of GLP-1 (36). They are among the classes of antidiabetic agents most recently made available for the treatment of T2D (37). Five of the DPP-4 inhibitors available for management of T2D (sitagliptin, vildagliptin, alogliptin, saxagliptin and linagliptin) were approved and entered in the market between 2006 and 2013 (34). DPP-4 inhibitors currently constitute approximately 50 % of the market share of oral hypoglycaemic agents (33).

Several studies have focused on the role of DPP-4 inhibitors in the development of infections, particularly with sitagliptin. It is believed that the administration of sitagliptin reduces the levels of pro-inflammatory markers such as interleukin-6 (IL-6) and tumour necrosis factor-α (TNF-α). It is also currently known that patients with COVID-19 showed significantly high levels of IL-6, which is associated with an increased risk of respiratory failure. In addition, human DPP-4 has been identified as a functional receptor for the spike protein of the coronavirus which caused the Middle East Respiratory Syndrome (MERS), since the antibodies directed against DPP-4 inhibited MERS-CoV infection. Considering the similarity among MERS-CoV and the other coronaviruses, it has been speculated that DPP-4 might also be a functional SARS-CoV receptor. Despite this, to date, there are no direct links between DPP-4 and Covid-19 epidemic (whose gateway is ACE2) so more studies must be carried on (38, 39).

With the purpose to address concerns over the cardiovascular safety of new glucose-lowering agents (including DPP-4 inhibitors), the US Food and Drug Administration (FDA)

introduced large prospective postmarketing cardiovascular outcome trials (CVOTs). Overall, DPP-4 inhibitors have shown good tolerability and a good safety profile at a convenient dosing. Furthermore, as a second-class antidiabetic drug, the combination therapy of DPP-4 inhibitors with metformin demonstrated high cost/benefit ratio (40). However, an association of some members of this antidiabetic class with more hospitalization for heart failure, as well as with higher risk of pancreatitis, cannot be excluded (41). In fact, FDA has issued a warning since 2016 and recommends discontinuation in patients who develop heart failure, for alogliptin, saxagliptin and sitagliptin (42, 43). Additionally, a label indicating an acute pancreatitis risk has been added to all DPP-4 inhibitors (44). Other side effects associated with the use of DPP-4 inhibitors are increased risk of some infections, headache, increased risk of inflammatory bowel disease, severe joint pain, among others (37, 42, 45). The adverse effects of currently available DPP-4 inhibitors severely hinder their clinical applications, and there is a clinical demand for novel molecules with the ability to inhibit DPP-4 from synthetic and natural sources, with fewer side effects (46). Thus, the inhibitory activity of a panel of flavonoids against human DPP-4 was evaluated. For this purpose, a colorimetric and fluorometric assay were performed. The fluorometric method has shown to be more sensitive than the colorimetric one since that in the colorimetric assay, none of the tested flavonoids was able to reduce DPP-4 activity. This conclusion is in agreement with a previous study that compared different assays for the evaluation of this enzyme activity (47). In the fluorometric method with the isolated human enzyme, it was found that the most active flavonoid was compound **4** (Figure 1), with an IC_{50} value of 73 ± 2 μM. After establishing the structure-activity relationship, it was observed that the presence of an -OH group at 3-position of C ring, and at 7- and 8-positions of A ring, together with the presence of a $-OCH_3$ group at 3'- and 4'-positions of B ring, increased the DPP-4 inhibitory activity comparing with the other tested flavonoids. Flavonoid **4** presented a noncompetitive mechanism of inhibition, which indicates that the inhibitor binds to an allosteric site of the enzyme Flavonoids presenting more than 20 % of DPP-4 inhibition of DPP-4 activity in this assay were subsequently tested in human plasma and whole blood. Interestingly, the flavonoids under study did not inhibit the enzyme (less than 20 % of inhibition), possibly due to their binding to plasma proteins, specially to albumin and α1-acid glycoprotein. The results obtained in this work may contribute to the synthesis and development of new flavonoids with potential DPP-4 inhibitory activity, and with lower affinity to plasma proteins.

The fifth work of this thesis was focused on the inhibitory activity of flavonoids against fructose 1,6-bisphosphatase (FBPase) (EC 3.1.3.11). FBPase is responsible for the catalysis of the hydrolysis of fructose 1,6-bisphosphate to fructose 6-phosphate and inorganic phosphate in the presence of divalent metal cations, and constitutes a key enzyme of

gluconeogenesis (48-50). Two isoforms of FBPase are expressed: the liver and the muscle isozymes. The liver isoform (encoded by gene FBP1) is mainly expressed in gluconeogenic organs, where its role is to regulate glucose synthesis from noncarbohydrates. The muscle isoform (encoded by gene FBP2) is expressed ubiquitously, and it is involved cell cycle regulation and apoptosis (48, 50). There are two distinct states, depending on different ligands binding to the enzyme: the active state (R form) and the inactive (T form) conformational state (51). The liver FBPase activity is regulated by fructose 2,6-bisphosphate which inhibits the enzyme synergistically with adenosine 5'-monophosphate (AMP) (48, 50, 52). Fructose 2,6-bisphosphate binds to the active site and inhibits catalysis competitively, while AMP binds to the allosteric site and converts the enzyme from the active R state to the inactive T state (51).

In individuals without T2D, when blood glucose levels are high, there is a corresponding increase in the production of fructose 2,6-bisphosphate. In T2D, the enzymatic control of gluconeogenesis is compromised, resulting in the excessive production of glucose. Since the increase in cellular concentrations of fructose 2,6-bisphosphate is hormonally regulated by increased insulin concentration, in T2D the stimulation of this inhibitor production is compromised, since there is an insulin deficiency and/or resistance (53). It has been previously demonstrated that liver FBPase plays an important role in the control of glucose levels since this enzyme in liver is increased in insulin-resistant and insulin-deficient animal models of diabetes. Moreover, it was shown that inhibitors of liver FBPase are able to reduce hepatic glucose production and to decrease blood glucose levels in diabetic animal models. For this reason, inhibition of FBPase may become a new strategy for the development of novel antidiabetic agents (54, 55). Up to date, several pharmaceutical companies and academic laboratories have focused on the development of FBPase inhibitors, although none of them have advanced phase II clinical trial (55, 56).

In this work, a panel of flavonoids was tested for the first time, regarding their capacity to inhibit human FBPase. After the establishment of the structure-activity relationship, it was interesting to observe that the presence of three -OH groups in A ring was responsible for an increase of the inhibition of the enzyme under study. Therefore, this chemical feature was explored by testing the FBPase inhibition of some of these flavonoids. It was observed that the most promising flavonoid was compound **5** (herbacetin) (Figure 1), which presented an IC_{50} value of 8.7 ± 0.7 μM. Thus, the presence of -OH groups at 5-, 7- and 8-positions of A ring was crucial for the effect under study, together with the presence of an -OH group at 3-position of C ring and at 4'-position of B ring. The double bond between C2 and C3, together with the 4-oxo function at the pyrone ring are also important for the intended effect. After the evaluation of flavonoid **5** (herbacetin) by molecular dynamics

(MD) stimulations using a linear interaction energy (LIE) approach, it was verified that this compound is stabilized by a strong interaction with the Glu30 side chain and the Thr24 backbone of FBPase. On the other side, the absence of -OH groups in A ring and consequently a reduced volume, when compared with the ligands in the other groups, allowed the flavonoids to explore less surface-exposed regions in the pocket. This work significantly contributes to the study of the direct inhibition of human isolated FBPase by flavonoids and provides a better understanding of the flavonoid substituents and their FBPase interactions. The most promising flavonoids found in this work may constitute a valuable model for the design of novel scaffolds with potential use in T2D management through FBPase inhibition.

In the sixth and last work of this thesis, the SI (EC 3.2.1.48 and 3.2.1.10) inhibition by flavonoids was studied based on the obtained results from the first study. Thus, the best inhibitors of α-glucosidase (EC 3.2.1.20) found in the first work were evaluated concerning their inhibitory activity against SI. SI, as mentioned above, is an integral intestinal membrane α-glucosidase that hydrolyses the final step of carbohydrate digestion by breaking disaccharides and oligosaccharides in absorbable glucose and other monosaccharides. SI possesses two homologous functional subunits (sucrase and isomaltase) that both belong to the glycoside hydrolase family 31 (GH31) and differ in substrate specificity (57). As already described, a possible strategy to control the rate of free glucose released from the digestion of starch is to inhibit the hydrolytic activity of salivary and pancreatic α-amylase, and preferentially, inhibit the intestinal α-glucosidases (MGAM and SI) where glucose is actually generated. It was previously shown that a variety of chemical compounds, either derived from chemical synthesis or from natural sources, have an inhibitory activity effect on mammalian α-glucosidases (18). Clinically available α-glucosidase inhibitors are highly effective in reducing PPHG, but are associated with several gastrointestinal side effects, which can lead to medication incompliance (58). For inhibition of SI inhibition by flavonoids, the Caco-2/TC7 cellular model was selected as enzyme source. Caco-2 cells are able to differentiate in long-term culture (21 days) and to polarize, forming a continuous monolayer with tight junctions, mimicking the intestinal barrier. Thus, these cells have become a popular surrogate for human intestinal epithelium although Caco-2 cell line has been shown to be heterogenous and highly dependent on culture conditions. With the purpose to reduce the heterogeneity of the Caco-2 cell line, several clones have been isolated, including TC7 clone obtained from late passage of the parental Caco-2 cell line. Caco-2/Tc7 cellular model consists of a more homogenous population with the most representative functions of the small intestine enterocytes, with more developed intercellular junctions. Additionally, in TC7 brush-border-associated hydrolase SI exhibited higher expression, at levels similar to the one in human jejunum (59). Of the small intestinal

α-glucosidases, Caco-2 cells only express SI. Nevertheless, SI includes of MGAM and is, thus, a good representative complex for human α-glucosidase activity (60). In the present work, the flavonoids were tested using the physiological substrates maltose and sucrose, and the synthetic substrate 4-nitrophenyl α-D-glucuronide (*p*NPG). The most active compound was flavonoid **1** (Figure 1), with an IC_{50} value of 2.2 ± 0.2 μM and 2.5 ± 0.2 μM for sucrose and maltose, respectively. Interestingly, flavonoid **1** was also the best inhibitor of yeast α-glucosidase (first work). The tested flavonoids were not able to inhibit SI, when using *p*NPG as substrate, possibly due to the low tested concentrations of flavonoids or because *p*NPG binds in a different site of the enzyme comparing with sucrose and maltose, and thus preventing the binding of flavonoids to SI. Taking into account the obtained results, it should be highlighted the promising inhibitory activity of flavonoid **1** against SI, and its potential to be used as possible alternative of the currently available α-glucosidase inhibitors, should be explored.

Combining and integrating all the works developed under this thesis, it can be concluded that, for each target under study, different chemical features of flavonoids are required to increase their inhibitory activity. It is clear that a pattern of action of flavonoids was found, targeting different pathways for the management of T2D. In Figure 1 the structure of the most promising flavonoid for the inhibition of yeast and human α-glucosidase, α-amylase, PTP1B, DPP-4 and FBPase is represented.

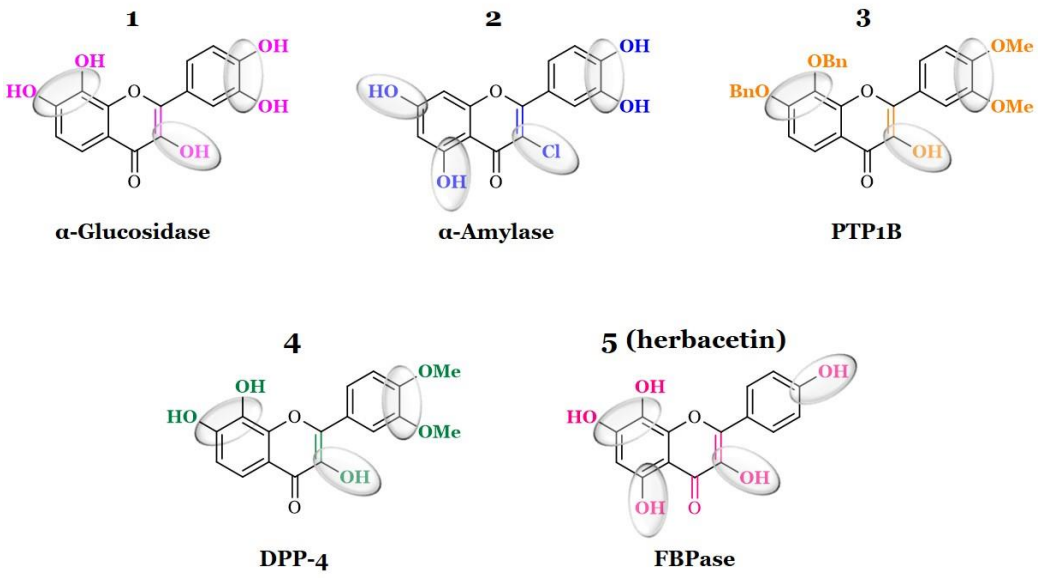


Figure 1: Substitution pattern of the flavonoid that presented the best inhibitory activity against α-glucosidase, α-amylase, PTP1B, DPP-4 and FBPase.

The common chemical feature in the best inhibitors of each target is the presence of the C2-C3 double bond, but substituents in A, B and C rings for an increase of inhibition differ according to the enzyme under study. To the best of our knowledge, flavonoids 1, 2, 3 e 4 were not tested before regarding their capacity to inhibit α-glucosidase, α-amylase, PTP1B, DPP-4 and FBPase. Overall, these flavonoids may represent good templates or alternatives in the search and design of new safe and effective molecules with potential to treat T2D.

We finish the thesis with the hope of having contributed to a better understanding of the structure-activity relationship of inhibitory activity of flavonoids on already established or promising therapeutic targets of T2D (α-glucosidase, α-amylase, PTP1B, DPP-4 and FBPase), but also certain that more studies are required before the application of flavonoids for medical purposes.

III.2. Conclusions

From the results obtained in the course of the performed studies it may be concluded that:

- The chemical features of flavonoids clearly influence the modulation of all targets under study:

- Concerning the inhibitory activity of flavonoids against α-glucosidase, it was found that the presence of the C2-C3 double bond and of -OH groups at 3-position of C ring, at 3'- and 4'-positions of B ring, as well as at 7- and 8-positions of A ring, are favourable for the intended effect;

- The presence of a Cl- substituent at 3-position of C ring, together with -OH groups at 3'-and 4'-positions of B ring and at 5- and 7-positions of A ring, and the C2-C3 double bond, are responsible for the increase of the α-amylase inhibition by flavonoids;

- For the inhibition of PTP1B by flavonoids the best chemical pattern is: OH- group at 3-position of C ring, -OCH_3 groups at 3'- and 4'-positions of B ring, and -OBn groups at 7- and 8-positions of A ring, together with the presence of the C2-C3 double bond;

- A flavonoid with double bond between C2 and C3, -OH groups at 3-position of C ring and at 7- and 8-positions of A ring, together with -OCH_3 groups at 3'- and 4'-positions of B ring, has promising DPP-4 inhibitory effect. However, its activity is hindered in human plasma and blood, so additional studies must be performed for the development of novel effective flavonoid-based molecules with lower binding affinity for plasma proteins.

- Regarding the FBPase inhibition by flavonoids, the best inhibitor was herbacetin, a flavonoid present in flaxseed, demonstrating that the hydroxylation at 3-position of C ring, at 4'-position of B ring and, specially, at 5-, 7- and 8-positions of A ring has a favourable role in the target inhibition. The presence of the C2-C3 double bond and the 4-oxo function at the pyrone ring also contribute for the higher inhibition of flavonoids.

- Finally, concerning the ability of a group of flavonoids to inhibit SI (from Caco-2/TC7 cell line), it was found that the most active compound was the same obtained in the first work, using both sucrose and maltose as substrates. Thus, the presence of -OH groups at 3-position of C ring, at 3'- and 4'-positions of B ring, as well as at 7- and 8-positions of A ring is responsible for increasing the inhibitory activity against SI.

III.3. Future perspectives

The results obtained in the different studies of this thesis provide new data indicating the high potential of flavonoids to act in different targets involved in the development of hyperglycaemia in T2D. In order to continue the work achieved for this thesis, further proof of concept studies must be performed. It is well known that to discover, validate and optimize novel therapeutics for their safe use in humans, the use of animal models is absolutely necessary. Thus, the development of *in vivo* studies in diabetic rodent models treated with the most promising flavonoids is one of our further goals to evidence the antidiabetic effect of these phenolic compounds.

Another aspect to be taken into consideration is the poor solubility and low permeability of flavonoids, resulting in a reduction of their bioavailability and bioactivity. In the last few years, nanotechnological systems have been developed for use as carriers to improve the delivery of bioactive compounds and thus obtain a higher bioavailability (61). In fact, previous studies in phyto-derived bioactive compounds that have been loaded into nanoparticles for oral delivery in diabetic animal models led to improved stability, bioavailability, and sustained antidiabetic effects (62, 63). Following this rationale, we intend to continue our studies on the most promising antidiabetic flavonoids found in the present thesis, performing their nanoencapsulation using suitable nanocarriers, polymers and encapsulation techniques. The study of the expected enhanced bioavailability and therapeutic effectiveness of encapsulated flavonoids over their non-encapsulated form will then be subsequently studied *in vivo*.

III.4. References

1. Karamanou M, Protogerou A, Tsoucalas G, Androutsos G, Poulakou-Rebelakou E. Milestones in the history of diabetes mellitus: The main contributors. World J Diabetes. 2016;7(1):1-7.

2. Zheng Y, Ley SH, Hu FB. Global aetiology and epidemiology of type 2 diabetes mellitus and its complications. Nat Rev Endocrinol. 2018;14(2):88-98.

3. World Health Organization. The top 10 causes of death 2020 [Available from: https://www.who.int/news-room/fact-sheets/detail/the-top-10-causes-of-death].

4. International Diabetes Federation. IDF Diabetes Atlas 9th edition. 2019.

5. Deshpande AD, Harris-Hayes M, Schootman M. Epidemiology of diabetes and diabetes-related complications. Phys Ther. 2008;88(11):1254-64.

6. Ceriello A, Stoian AP, Rizzo M. COVID-19 and diabetes management: What should be considered? Diabetes Res Clin Pract. 2020;163(108151):1-3.

7. Singh AK, Gupta R, Ghosh A, Misra A. Diabetes in COVID-19: Prevalence, pathophysiology, prognosis and practical considerations. Diabetes & Metabolic Syndrome: Clinical Research & Reviews. 2020;14(4):303-10.

8. Guo W, Li M, Dong Y, Zhou H, Zhang Z, Tian C, et al. Diabetes is a risk factor for the progression and prognosis of COVID-19. Diabetes Metab Res Rev. 2020;e3319:1-7.

9. Ursini F, Ciaffi J, Landini MP, Meliconi R. COVID-19 and diabetes: Is metformin a friend or foe? Diabetes Res Clin Pract. 2020;164(108167):1-2.

10. Chee YJ, Ng SJH, Yeoh E. Diabetic ketoacidosis precipitated by Covid-19 in a patient with newly diagnosed diabetes mellitus. Diabetes Res Clin Pract. 2020;164(108166):1-2.

11. Chaudhury A, Duvoor C, Reddy Dendi VS, Kraleti S, Chada A, Ravilla R, et al. Clinical review of antidiabetic drugs: implications for type 2 diabetes mellitus management. Front Endocrinol (Lausanne). 2017;8(6):1-12.

12. Rios JL, Francini F, Schinella GR. Natural products for the treatment of type 2 diabetes mellitus. Planta Med. 2015;81(12-13):975-94.

13. DeCorte BL. Underexplored opportunities for natural products in drug discovery. J Med Chem. 2016;59(20):9295-304.

14. Al-Ishaq RK, Abotaleb M, Kubatka P, Kajo K, Büsselberg D. Flavonoids and their anti-diabetic effects: cellular mechanisms and effects to improve blood sugar levels. Biomolecules. 2019;9(430):1-35.

15. Panche AN, Diwan AD, Chandra SR. Flavonoids: an overview. J Nutr Sci. 2016;5(e47):1-15.

16. Yonekura-Sakakibara K, Higashi Y, Nakabayashi R. The origin and evolution of plant flavonoid metabolism. Front Plant Sci. 2019;10(943):1-16.

17. Vinayagam R, Xu B. Antidiabetic properties of dietary flavonoids: a cellular mechanism review. Nutr Metab. 2015;12(60):1-20.

18. Simsek M, Quezada-Calvillo R, Ferruzzi MG, Nichols BL, Hamaker BR. Dietary phenolic compounds selectively inhibit the individual subunits of maltase-glucoamylase and sucrase-isomaltase with the potential of modulating glucose release. J Agric Food Chem. 2015;63(15):3873-9.

19. Joshi SR, Standl E, Tong N, Shah P, Kalra S, Rathod R. Therapeutic potential of α-glucosidase inhibitors in type 2 diabetes mellitus: an evidence-based review. Expert Opin Pharmacother. 2015;16(13):1959-81.

20. Krentz AJ. Chapter 33 - Evolution of glucose-lowering drugs for type 2 diabetes: a new era of cardioprotection. In: Bagchi D, Nair S, editors. Nutritional and Therapeutic Interventions for Diabetes and Metabolic Syndrome (Second Edition): Academic Press; 2018. p. 431-54.

21. Etxeberria U, de la Garza AL, Campion J, Martinez JA, Milagro FI. Antidiabetic effects of natural plant extracts via inhibition of carbohydrate hydrolysis enzymes with emphasis on pancreatic alpha amylase. Expert Opin Ther Targets. 2012;16(3):269-97.

22. Li X, Liu ZQ. Chapter 7 - Pharmacogenetic factors that affect drug metabolism and efficacy in type 2 diabetes mellitus. In: Xie W, editor. Drug Metabolism in Diseases. Boston: Academic Press; 2017. p. 157-79.

23. Feldhammer M, Uetani N, Miranda-Saavedra D, Tremblay ML. PTP1B: a simple enzyme for a complex world. Crit Rev Biochem Mol Biol. 2013;48(5):430-45.

24. Qian S, Zhang M, He Y, Wang W, Liu S. Recent advances in the development of protein tyrosine phosphatase 1B inhibitors for type 2 diabetes. Future Med Chem. 2016;8(11):1239-58.

25. Chen PJ, Cai SP, Huang C, Meng XM, Li J. Protein tyrosine phosphatase 1B (PTP1B): a key regulator and therapeutic target in liver diseases. Toxicology. 2015;337(2015):10-20.

26. Bakke J, Haj FG. Protein-tyrosine phosphatase 1B substrates and metabolic regulation. Semin Cell Dev Biol. 2015;37(2015):58-65.

27. Abdelsalam SS, Korashy HM, Zeidan A, Agouni A. The role of protein tyrosine phosphatase (PTP)-1B in cardiovascular disease and its interplay with insulin resistance. Biomolecules. 2019;9(286):1-23.

28. Thareja S, Aggarwal S, Bhardwaj TR, Kumar M. Protein tyrosine phosphatase 1B inhibitors: a molecular level legitimate approach for the management of diabetes mellitus. Med Res Rev. 2012;32(3):459-517.

29. Hussain H, Green IR, Abbas G, Adekenov SM, Hussain W, Ali I. Protein tyrosine phosphatase 1B (PTP1B) inhibitors as potential anti-diabetes agents: patent review (2015-2018). Expert Opin Ther Pat. 2019;29(9):689-702.

30. Ramsay RR, Tipton KF. Assessment of enzyme inhibition: a review with examples from the development of monoamine oxidase and cholinesterase inhibitory drugs. Molecules. 2017;22(1192):1-46.

31. Robin T, Reuveni S, Urbakh M. Single-molecule theory of enzymatic inhibition. Nat Commun. 2018;9(779):1-9.

32. Jin T, Yu H, Huang X-F. Selective binding modes and allosteric inhibitory effects of lupane triterpenes on protein tyrosine phosphatase 1B. Sci Rep. 2016;6(20766):1-14.

33. Bae EJ. DPP-4 inhibitors in diabetic complications: role of DPP-4 beyond glucose control. Arch Pharm Res. 2016;39(8):1114-28.

34. Ahrén B. DPP-4 inhibition and the path to clinical proof. Front Endocrinol (Lausanne). 2019;10(376):1-18.

35. Dowarah J, Singh VP. Anti-diabetic drugs recent approaches and advancements. Bioorg Med Chem. 2020;28(2020):1-78.

36. Cahn A, Cernea S, Raz I. An update on DPP-4 inhibitors in the management of type 2 diabetes. Expert Opin Emerg Drugs. 2016;21(4):409-19.

37. Bonora E, Cigolini M. DPP-4 inhibitors and cardiovascular disease in type 2 diabetes mellitus. Expectations, observations and perspectives. Nutr Metab Cardiovasc Dis. 2016;26(4):273-84.

38. Bouhanick B, Cracowski JL, Faillie JL. Diabetes and COVID-19. Therapie. 2020;75(4):327-33.

39. Du H, Wang DW, Chen C. The potential effects of DPP-4 inhibitors on cardiovascular system in COVID-19 patients. J Cell Mol Med. 2020;24(18):10274-8.

40. Deng X, Tavallaie MS, Sun R, Wang J, Cai Q, Shen J, et al. Drug discovery approaches targeting the incretin pathway. Bioorg Chem. 2020;99:(103810):1-13.

41. Bailey CJ, Day C. The future of new drugs for diabetes management. Diabetes Res Clin Pract. 2019;155(107785):1-27.

42. Makrilakis K. The Role of DPP-4 Inhibitors in the Treatment Algorithm of Type 2 Diabetes Mellitus: When to Select, What to Expect. Int J Environ Res Public Health. 2019;16(2720):1-20.

43. Taylor OM, Lam C. The effect of dipeptidyl peptidase-4 inhibitors on macrovascular and microvascular complications of diabetes mellitus: a systematic review. Curr Ther Res Clin Exp. 2020;93(100596):1-10.

44. Gallwitz B. Clinical use of DPP-4 inhibitors. Front Endocrinol. 2019;10(389):1-10.

45. Ceriello A, Genovese S. Atherogenicity of postprandial hyperglycemia and lipotoxicity. Rev Endocr Metab Disord. 2016;17(1):111-6.

46. Lin SR, Chang CH, Tsai MJ, Cheng H, Chen JC, Leong MK, et al. The perceptions of natural compounds against dipeptidyl peptidase 4 in diabetes: from in silico to in vivo. Ther Adv Chronic Dis. 2019;10:1-16.

47. Matheeussen V, Lambeir A-M, Jungraithmayr W, Gomez N, Mc Entee K, Van der Veken P, et al. Method comparison of dipeptidyl peptidase IV activity assays and their application in biological samples containing reversible inhibitors. Clin Chim Acta. 2012;413(3):456-62.

48. Barciszewski J, Wisniewski J, Kolodziejczyk R, Jaskolski M, Rakus D, Dzugaj A. T-to-R switch of muscle fructose-1,6-bisphosphatase involves fundamental changes of secondary and quaternary structure. Acta Cryst D Struct Biol. 2016;72(Pt 4):536-50.

49. Droppelmann CA, Saez DE, Asenjo JL, Yanez AJ, Garcia-Rocha M, Concha, II, et al. A new level of regulation in gluconeogenesis: metabolic state modulates the intracellular localization of aldolase B and its interaction with liver fructose-1,6-bisphosphatase. Biochem J. 2015;472(2):225-37.

50. Gizak A, Duda P, Wisniewski J, Rakus D. Fructose-1,6-bisphosphatase: From a glucose metabolism enzyme to multifaceted regulator of a cell fate. Adv Biol Regul. 2019;72:41-50.

51. Han X, Huang Y, Zhang R, Xiao S, Zhu S, Qin N, et al. New insight into the binding modes of TNP-AMP to human liver fructose-1,6-bisphosphatase. Spectrochim Acta A Mol Biomol Spectrosc. 2016;165:155-60.

52. Gao Y, Shen L, Honzatko RB. Central cavity of fructose-1,6-bisphosphatase and the evolution of AMP/fructose 2,6-bisphosphate synergism in eukaryotic organisms. J Biol Chem. 2014;289(12):8450-61.

53. Heng S, Harris KM, Kantrowitz ER. Designing inhibitors against fructose 1,6-bisphosphatase: exploring natural products for novel inhibitor scaffolds. Eur J Med Chem. 2010;45(4):1478-84.

54. Bie J, Liu S, Zhou J, Xu B, Shen Z. Design, synthesis and biological evaluation of 7-nitro-1H-indole-2-carboxylic acid derivatives as allosteric inhibitors of fructose-1,6-bisphosphatase. Bioorg Med Chem. 2014;22(6):1850-62.

55. Bie J, Liu S, Li Z, Mu Y, Xu B, Shen Z. Discovery of novel indole derivatives as allosteric inhibitors of fructose-1,6-bisphosphatase. Eur J Med Chem. 2015;90:394-405.

56. Kaur R, Dahiya L, Kumar M. Fructose-1,6-bisphosphatase inhibitors: a new valid approach for management of type 2 diabetes mellitus. Eur J Med Chem. 2017;141(Supplement C):473-505.

57. Gericke B, Schecker N, Amiri M, Naim HY. Structure-function analysis of human sucrase-isomaltase identifies key residues required for catalytic activity. J Biol Chem. 2017;292(26):11070-8.

58. Rosak C, Mertes G. Critical evaluation of the role of acarbose in the treatment of diabetes: patient considerations. Diabetes Metab Syndr Obes. 2012;5:357-67.

59. Turco L, Catone T, Caloni F, Consiglio ED, Testai E, Stammati A. Caco-2/TC7 cell line characterization for intestinal absorption: how reliable is this in vitro model for the prediction of the oral dose fraction absorbed in human? Toxicol In Vitro. 2011;25(1):13-20.

60. Cheng N, Yi WB, Wang QQ, Peng SM, Zou XQ. Synthesis and α-glucosidase inhibitory activity of chrysin, diosmetin, apigenin, and luteolin derivatives. Chinese Chem Lett. 2014;25(7):1094-8.

61. Song X, Gan K, Qin S, Chen L, Liu X, Chen T, et al. Preparation and characterization of general-purpose gelatin-based co-loading flavonoids nano-core structure. Sci Rep. 2019;9(6365):1-11.

62. Ganesan P, Arulselvan P, Choi DK. Phytobioactive compound-based nanodelivery systems for the treatment of type 2 diabetes mellitus - current status. International journal of nanomedicine. 2017;12:1097-111.

63. Hussain T, Tan B, Murtaza G, Liu G, Rahu N, Saleem Kalhoro M, et al. Flavonoids and type 2 diabetes: Evidence of efficacy in clinical and animal studies and delivery strategies to enhance their therapeutic efficacy. Pharmacol Res. 2020;152(104629):1-17.